ČESKÁ KARDIOLOGICKÁ SPOLEČNOST

XXXIII. VÝROČNÍ SJEZD ČESKÉ KARDIOLOGICKÉ SPOLEČNOSTI

TO NEJLEPŠÍ Z ČESKÉ KARDIOLOGIE ZA ROK 2024

Nejlepší původní české práce publikované v roce 2024

Tato sekce prezentuje každoročně na výročním sjezdu ČKS **nejlepší původní vědecké práce členů ČKS**, vzniklé na pracovištích v ČR a publikované v předchozím kalendářním roce v mezinárodních časopisech s impakt faktorem >2,0. Tři nejlepší jsou rovněž **oceněny výborem ČKS**. Práce jsou řazeny dle IF.

Podmínky:

- Práce musí být publikována v časopise s impakt faktorem > 2,0 v průběhu posledního kalendářního roku před sjezdem ČKS, na který je přihlášena
- Práce musí vzniknout na pracovišti v České republice
- Prvním autorem musí být člen ČKS
- Musí jít o původní práci, prezentující vlastní výzkumné výsledky (nemůže se jednat o přehledný článek, editorial, abstrakt ani o kasuistiku)
- Nemůže se jednat ani o práci vzniklou v zahraničí (např. při studijním pobytu českého lékaře)
- Současně s přihlášením práce je autor povinen zaslat do sekretariátu ČKS e–mailem PDF verzi originálního článku s přihlášenou prací. Bez tohoto textu „in extenso" nemůže být práce přijata.

Luca Monzo et al.

Circulating beta-hydroxybutyrate levels in advanced heart failure with reduced ejection fraction: Determinants and prognostic impact

European Journal of Heart Failure
Impact Factor: 16,9

rejstřík

ESC European Society of Cardiology

European Journal of Heart Failure (2024) **26**, 1931–1940
doi:10.1002/ejhf.3324

RESEARCH ARTICLE

Circulating beta-hydroxybutyrate levels in advanced heart failure with reduced ejection fraction: Determinants and prognostic impact

Luca Monzo[1,2], Jan Kovar[1], Barry A. Borlaug[3], Jan Benes[1], Martin Kotrc[1], Katerina Kroupova[1], Antonin Jabor[1], Janka Franekova[1], and Vojtech Melenovsky[1]*

[1]Institute for Clinical and Experimental Medicine (IKEM), Prague, Czech Republic; [2]Université de Lorraine, Centre d'Investigations Cliniques Plurithématique 1433 and Inserm U1116, CHRU Nancy, FCRIN INI-CRCT (Cardiovascular and Renal Clinical Trialists), Nancy, France; and [3]Department of Cardiovascular Diseases, Mayo Clinic, Rochester, MN, USA

Received 29 January 2024; revised 16 May 2024; accepted 20 May 2024; online publish-ahead-of-print 10 June 2024

Aims Patients with heart failure (HF) display metabolic alterations, including heightened ketogenesis, resulting in increased beta-hydroxybutyrate (β-OHB) formation. We aimed to investigate the determinants and prognostic impact of circulating β-OHB levels in patients with advanced HF and reduced ejection fraction (HFrEF).

Methods and results A total of 867 patients with advanced HFrEF (age 57 ± 11 years, 83% male, 45% diabetic, 60% New York Heart Association class III), underwent clinical and echocardiographic examination, circulating metabolite assessment, and right heart catheterization ($n = 383$). The median β-OHB level was 64 (interquartile range [IQR] 33–161) μmol/L (normal 0–74 μmol/L). β-OHB levels correlated with increased markers of lipolysis (free fatty acids [FFA]), higher natriuretic peptides, worse pulmonary haemodynamics, and lower humoral regulators of ketogenesis (insulin/glucagon ratio). During a median follow-up of 1126 (IQR 410–1781) days, there were 512 composite events, including 324 deaths, 81 left ventricular assist device implantations and 107 urgent cardiac transplantations. In univariable Cox regression, increased β-OHB levels (T3 vs. T1: hazard ratio [HR] 1.39, 95% confidence interval [CI] 1.13–1.72, $p = 0.002$) and elevated FFA levels (T3 vs. T1: HR 1.39, 95% CI 1.09–1.79, $p = 0.008$) were both predictors of a worse prognosis. In multivariable Cox analysis evaluating the simultaneous associations of FFA and β-OHB levels with outcomes, only FFA levels remained significantly associated with adverse outcomes.

Conclusions In patients with advanced HFrEF, increased plasma β-OHB correlate with FFA levels, worse right ventricular function, greater neurohormonal activation and other markers of HF severity. The association between plasma β-OHB and adverse outcomes is eliminated after accounting for FFA levels, suggesting that increased β-OHB is a consequence reflecting heightened lipolytic state, rather than a cause of worsening HF.

*Corresponding author. Department of Cardiology, Institute for Clinical and Experimental Medicine–IKEM, 140 21 Prague, Czech Republic. Tel: +420 739 528029, Fax: +420 261 362986, Email: vojtech.melenovsky@ikem.cz

Graphical Abstract

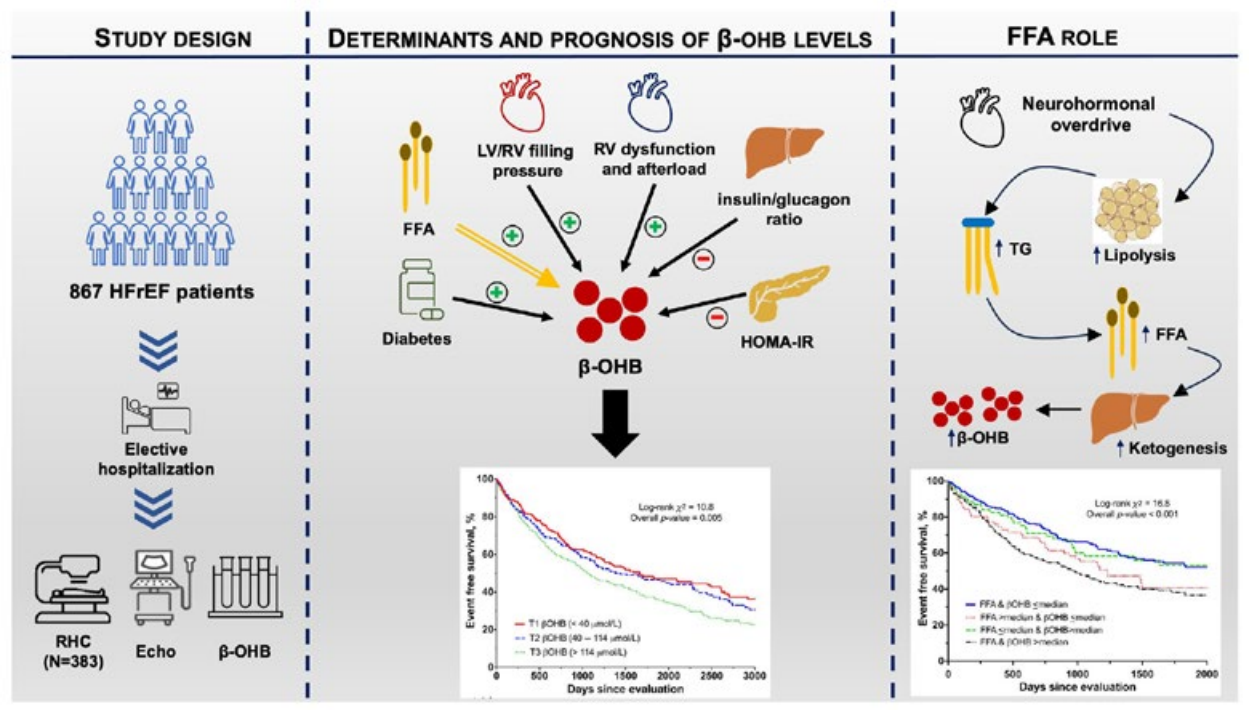

Summary of the study design and key findings. In the central panel, (+) and (−) means that the variable is directly or inversely associated with beta-hydroxybutyrate (β-OHB) levels, respectively. The gold arrow means that free fatty acid (FFA) levels are the only variable that remained associated with β-OHB levels in the multivariable model. HFrEF, heart failure with reduced ejection fraction; HOMA-IR, homeostasis model assessment of insulin resistance; LV, left ventricular; RHC, right heart catheterization; RV, right ventricular; TG, triglycerides. Parts of the figure were created using Biorender.com.

Keywords Ketone bodies • Free fatty acid • Cardiovascular disease • Prognosis • Heart failure • Beta-hydroxybutyrate

Introduction

Metabolism of the failing heart is characterized by decreased flexibility and efficiency of substrate consumption, with a switch from the preferred utilization of free fatty acids (FFA) towards glucose and alternative energy sources, such as ketone bodies (KB).[1,2] With heightened catabolism or starvation, there is increased lipolytic activity and increased KB formation in the liver through the conversion of free fatty acids (FFA).[3,4] Beta-hydroxybutyrate (β-OHB) is the most stable and abundant KB in the circulation.

Experimental and human observations suggest that the metabolic shift towards increased KB utilization in the heart may be an adaptive process with potentially beneficial effects in patients with heart failure (HF), mainly through the provision of an ancillary fuel in a setting of decreased mitochondrial function.[4] Indeed, KB provide more energy per metabolized carbon than glucose, and require less oxygen than free fatty acids for ATP generation.[5] Ketone bodies have also signalling role and act through pathways that improve cell survival and attenuate inflammation.[4] Exogenous administration of β-OHB has beneficial cardiovascular haemodynamic effects and prevents adverse cardiac remodelling in experimental models.[6] Notably, recent studies suggested that sodium–glucose cotransporter 2 (SGLT2) inhibitors may partly exert their benefit on the cardiovascular system via the elevation of circulating β-OHB.[7–9]

On the other hand, studies in patients with chronic HF have shown a positive association between elevated KB level and both disease severity[10,11] and adverse prognosis.[12,13] Similarly, KB elevations predicted worse outcomes in patients with decompensated HF,[14] in patients after myocardial infarction,[15] and on chronic haemodialysis,[16] as well as in the general population.[17] The determinants of ketogenesis in patients with HF are poorly understood, and it remains unclear whether ketonaemia is an aggravating cause or an adaptive consequence in advanced HF. In this study, we aimed

to investigate the determinants and prognostic impact of circulating β-OHB levels in patients with advanced HF and reduced ejection fraction (HFrEF).

Methods

Study population

The study retrospectively evaluated patients with chronic (>6 months) symptomatic HFrEF (left ventricular ejection fraction ≤40%) electively hospitalized for consideration of advanced therapies at the Institute for Clinical and Experimental Medicine (IKEM) in Prague (Czech Republic) from January 2008 to December 2016. Patients with acute ischaemia, uncontrolled cardiac arrhythmia, haemodynamic instability needing inotropes or mechanical circulatory support, reversible cardiac dysfunction, active malignancy, endocrine disease, chronic or acute infection were excluded. Patients with hypervolaemia on admission (based on clinical examination) were enrolled into the study after diuresis and reaching normovolaemia (central venous pressure <10 mmHg), if possible. The local ethics committee approved the protocol. All patients signed informed consent with the procedures and with participation in this research study.

Study protocol

After signing informed consent, patients underwent history review, physical examination, echocardiography, electrocardiogram, Minnesota Living with Heart Failure Questionnaire (MLHFQ), blood sampling with circulating metabolite assessment. Some patients underwent right heart catheterization and body composition assessment by skinfolds method, if clinically indicated as part of the diagnostic work-up or for research purposes. All investigations were performed in a post-absorptive state following an overnight fasting.

Blood samples were consistently collected from a peripheral vein between 6 and 7 a.m., immediately chilled on ice, and centrifuged within 20 min at a force of 800 × *g* at a temperature of 4°C. Plasma was collected, distributed into aliquots, and frozen at −80°C. β-OHB concentration was analysed instead of total KB, since it is the most abundant ketone in the bloodstream[3] and has a key role in human metabolism and cellular signalling.[18] β-OHB (normal value: 0–74 μmol/L, coefficient of variation [CV, intra-assay] 5%) and FFA (normal value: men: 0.1–0.6 mmol/L, women: 0.1–0.45 mmol/L, CV [intra-assay] 1.5%) were measured using a commercially available enzymatic assays (Autokit 3-HB and NEFA-HR, Wako Chemicals, Richmond, VA, USA). The homeostasis model assessment of insulin resistance (HOMA-IR) was calculated using the formula: [glucose (nmol/L) × insulin (μU/ml)/22.5].[19] Fasting glucose ≥126 mg/dl or the use of antidiabetic medications defined diabetes mellitus. Insulin concentration was determined using Insulin IRMA kit (Beckman Coulter, Prague, Czech Republic; normal value: 2.1–22.0 mIU/L, CV [intra-assay] 4%) and glucagon using Glucagon RIA kit (Millipore, Billerica, MA, USA; normal value [fasting]: 50–150 pg/ml, CV [intra-assay] 4–7%). Estimated glomerular filtration rate (eGFR) was calculated by the Chronic Kidney Disease Epidemiology Collaboration (CKD-EPI) equation.[20]

Right heart catheterization was performed in a subgroup ($n = 383$) according to current recommendations[21] using a 7 Fr balloon-tipped triple-lumen Swan–Ganz catheter (Braun Melsungen AG, Melsungen, Germany) inserted via the right internal jugular vein. Pressure waveforms were recorded and annotated by an invasive haemodynamic module (Mac-Lab, GE Healthcare, Chicago, IL, USA).

Bicipital, tricipital, subscapular and supra iliac skinfold measurements were performed in 322 patients to assess the body composition using a Lange adipometer, with a constant pressure of 10 g/mm^2 on the contact surface and accuracy of 1 mm, with a 0–65 mm scale.[19] Body density values were calculated using the older adults-specific equation of Durnin and Womersley (DWE),[22] and converted into fat percentage by using the Siri equation: body fat percentage = ([4.95/DWE] − 4.50) × 100.[19]

Data analysis

Data are shown as mean ± standard deviation or median (25th–75th interquartile range [IQR]) for continuous variables (according to distribution) and total count with proportion (%) for categorical variables. One-way ANOVA and Kruskal–Wallis tests were used to compare continuous variables between groups depending on the normality of the distribution, and the χ^2 test was used for categorical variables. Normality was assessed using the Shapiro–Wilk test. To assess the association of each variable with β-OHB plasma concentrations, separate multiple linear regression analyses adjusted for sex and age were conducted and Spearman's ρ was calculated. Univariable and multivariable (adjusted for age, sex, body mass index, MLHFQ score, diabetes, eGFR, HF medical treatment, left ventricular ejection fraction, and ischaemic HF etiology) Cox proportional hazards regression were used to the association of β-OHB and FFA plasma concentrations with the adverse outcome, defined as a combined endpoint of death, urgent transplantation, or left ventricular assist device (LVAD) implantation without heart transplantation. Kaplan–Meier curves with the log-rank statistics were used to illustrate the outcome. A p-value < 0.05 was considered statistically significant. All analyses were performed using JMP pro 17.0 statistical software (SAS Institute, Inc., Cary, NC, USA).

Results

Baseline characteristics

A total of 867 consecutive patients referred for advanced HF therapy evaluation (cardiac device implantation, cardiac transplantation or LVAD implantation) in our centre were enrolled. Median β-OHB level was 64 (IQR 33–161) μmol/L (for normal ranges see *Methods*). Based on the distribution in the overall population, β-OHB tertiles were created with cut-offs of: 1st tertile (T1): <40 μmol/L ($n = 278$); 2nd tertile (T2): 40–114 μmol/L ($n = 279$) and 3rd tertile (T3): >114 μmol/L ($n = 288$). Patients in the highest β-OHB tertile were older, with a higher body mass index, were more congested (increased right atrial [RA] pressure and brain natriuretic peptide [BNP]), had worse kidney function and more severe right ventricular (RV) dysfunction (higher RA/pulmonary artery wedge pressure [PAWP] ratio). From a metabolic perspective, patients with higher β-OHB were more likely to have diabetes, accompanied by increased markers of lipolysis (FFA) and significant alterations in humoral regulators of liver ketogenesis (insulin/glucagon ratio) (*Table 1*).

Table 1 Baseline characteristics according to beta-hydroxybutyrate plasma concentration tertiles

Variables	Tertile 1 (β-OHB <40 μmol/L)	Tertile 2 (β-OHB 40–114 μmol/L)	Tertile 3 (β-OHB >114 μmol/L)	*p*-value
Clinical characteristics				
Age, years	55 ± 11	57 ± 11	60 ± 11	<0.001
Female sex, *n* (%)	45 (16)	43 (15)	58 (20)	0.278
Body mass index, kg/m^2	27.0 ± 4.9	28.2 ± 5.2	28.3 ± 5.1	0.004
Body fat (skinfold method), %	25.4 ± 10.6	26.2 ± 9.6	23.8 ± 9.9	0.197
NYHA class (II/III/IV), *n* (%)	98 (35)/157 (57)/23 (8)	89 (32)/176 (63)/14 (5)	86 (29)/176 (61)/26 (9)	0.429
MLHFQ score	43.8 ± 22.2	41.8 ± 21.6	42.6 ± 23.0	0.641
HF ischaemic aetiology, *n* (%)	129 (47)	135 (50)	153 (54)	0.284
HF duration, years	8.4 [4.6–13.5]	8.6 [5.2–14.4]	9.6 [5.9–16.7]	0.023
Diabetes mellitus, *n* (%)	92 (33)	124 (44)	163 (57)	<0.001
Laboratory values				
Haemoglobin, g/L	142 ± 18	141 ± 16	139 ± 18	0.079
Sodium, mmol/L	139 ± 3	138 ± 4	139 ± 4	0.609
Potassium, mmol/L	4.4 ± 0.4	4.3 ± 0.4	4.3 ± 0.5	0.005
eGFR, ml/min/1.73 m^2	72 ± 21	70 ± 22	65 ± 23	0.001
HbA_{1c}, mmol/mol	44 [39–49]	45 [41–50]	47 [41–59]	<0.001
HOMA-IR index	2.2 [1.4–4.2]	2.4 [1.4–4.3]	2.2 [1.2–3.7]	0.378
Insulin/glucagon ratio	0.10 [0.06–0.17]	0.10 [0.06–0.16]	0.08 [0.05–0.12]	<0.001
Insulin, mIU/L	8.91 [5.97–16.22]	9.89 [5.84–15.75]	8.32 [4.72–12.67]	0.009
Glucagon, pg/ml	103.5 ± 45.9	109.3 ± 44.5	111.1 ± 55.7	0.154
BNP, ng/L	401 [150–906]	450 [212–1019]	620 [268–1301]	<0.001
Free fatty acids, mmol/L	0.39 ± 0.26	0.57 ± 0.22	0.72 ± 0.28	<0.001
Echocardiography				
LV end-diastolic diameter, mm	69 ± 9	71 ± 10	69 ± 9	0.012
LV ejection fraction, %	24 ± 6	23 ± 6	24 ± 6	0.200
E/Em ratio	15 ± 8	15 ± 7	16 ± 9	0.348
TAPSE, mm	16 ± 5	16 ± 5	16 ± 6	0.895
Mitral regurgitation (0–2 grade/3–4 grade), *n* (%)	162 (58)/115 (42)	140 (50)/138 (50)	140 (50)/141 (50)	0.072
Tricuspid regurgitation (0–2 grade/3–4 grade), *n* (%)	222 (80)/56 (20)	207 (75)/70 (25)	204 (72)/78 (28)	0.107
Haemodynamics				
RA pressure, mmHg	8.5 ± 5.5	9.9 ± 5.9	10.9 ± 6.0	0.007
RA/PAWP ratio	0.38 ± 0.20	0.41 ± 0.26	0.46 ± 0.22	0.026
Mean PA pressure, mmHg	32.5 ± 11.5	34.8 ± 12.0	35.9 ± 11.9	0.073
PCWP, mmHg	22.3 ± 8.5	23.6 ± 9.1	23.4 ± 8.4	0.376
Cardiac output, L/min	3.9 ± 1.2	3.8 ± 0.9	3.8 ± 1.1	0.844
PVR, WU	2.4 [1.7–4.0]	2.6 [1.9–4.0]	2.9 [2.1–4.8]	0.080
Systolic blood pressure, mmHg	115 ± 17	116 ± 20	118 ± 20	0.153
Diastolic blood pressure, mmHg	72 ± 10	74 ± 11	73 ± 12	0.159
Heart rate, bpm	75 ± 14	75 ± 15	77 ± 15	0.149
Treatment, *n* (%)				
Furosemide	241 (87)	253 (91)	257 (89)	0.317
ACEi or ARB	217 (78)	217 (78)	230 (80)	0.852
MRA	217 (78)	217 (78)	214 (74)	0.444
Beta-blocker	245 (88)	243 (87)	255 (89)	0.899
OAD/insulin	71 (25)/19 (7)	89 (32)/35 (12)	107 (37)/55 (19)	0.001
Devices (ICD/CRT)	163 (60)/85 (32)	165 (62)/88 (33)	153 (56)/87 (32)	0.905

ACEi, angiotensin-converting enzyme inhibitor; ARB, angiotensin receptor blocker; BNP, brain natriuretic peptide; β-OHB, beta-hydroxybutyrate; CRT, cardiac resynchronization therapy; eGFR, estimated glomerular filtration rate; HbA_{1c}, glycated haemoglobin; HF, heart failure; HOMA-IR, homeostasis model assessment of insulin resistance; ICD, implantable cardioverter-defibrillator; LV, left ventricular; MLHFQ, Minnesota Living with Heart Failure Questionnaire; MRA, mineralocorticoid receptor antagonist; NYHA, New York Heart Association; OAD, oral antidiabetic drugs; PA, pulmonary artery; PCWP, pulmonary capillary wedge pressure; PVR, pulmonary vascular resistance; RA, right atrial; TAPSE, tricuspid annular plane systolic excursion; WU, Wood units.

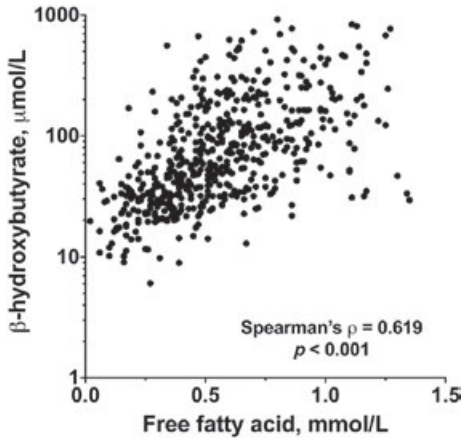

Figure 1 Correlation between beta-hydroxybutyrate levels and free fatty acid levels.

Determinants of beta-hydroxybutyrate plasma concentrations

At univariable regression analysis, β-OHB plasma concentration was strongly and directly correlated with FFA levels (β ± standard error [SE] = 1.708 ± 0.120; Spearman's $\rho = 0.619$, all $p < 0.001$), reflecting surplus delivery into the liver (*Figure 1*). Similarly, BNP (β ± SE = 0.197 ± 0.029; Spearman's $\rho = 0.192$, all $p < 0.001$), which act as a lipolytic hormone in the adipose tissue, showed a significant direct correlation with β-OHB levels. Higher RV afterload (mean pulmonary artery pressure: β ± SE = 0.016 ± 0.004, Spearman's $\rho = 0.181$; pulmonary vascular resistance: β ± SE = 0.357 ± 0.083, Spearman's $\rho = 0.187$; all $p < 0.001$), left ventricular filling pressure (PAWP: β ± SE = 0.014 ± 0.006, $p = 0.015$; Spearman's $\rho = 0.107$, $p = 0.036$), and RV filling pressure (RA pressure: β ± SE = 0.037 ± 0.008; Spearman's $\rho = 0.227$, all $p < 0.001$) were all positively associated with β-OHB levels. RA/PAWP ratio (β ± SE = 0.648 ± 0.216, $p = 0.003$; Spearman's $\rho = 0.190$, $p < 0.001$), a marker of RV failure, was also positively correlated with β-OHB levels (*Figure 2*). From a metabolic viewpoint, insulin/glucagon ratio (β ± SE = −1.231 ± 0.043; Spearman's $\rho = -0.185$, all $p < 0.001$) and HOMA-IR (β ± SE = −0.105 ± 0.042, $p = 0.012$; Spearman's $\rho = -0.068$, $p = 0.082$) were inversely associated with β-OHB concentrations, while diabetic status (β ± SE = 0.177 ± 0.034; Spearman's $\rho = 0.215$, all $p < 0.001$) and insulin use (β ± SE = 0.191 ± 0.051; Spearman's $\rho = 0.150$, $p < 0.001$) were positively associated. In multivariable regression analysis, FFA concentrations remained the only independent predictor of β-OHB plasma concentrations (*Table 2*).

Outcomes

During a median follow-up of 1126 (IQR 410–1781) days, there were 512 composite events including 324 deaths, 81 LVAD implantations and 107 urgent cardiac transplantations. In Kaplan–Meier plots, the risk of the composite outcome increased with increasing β-OHB (log-rank $\chi^2 = 10.8$, overall $p = 0.005$) and FFA (log-rank $\chi^2 = 8.9$, overall $p = 0.011$) levels (*Figure 3*). Univariable Cox regression analysis showed that patients in the highest tertile of β-OHB had an increased risk of adverse clinical events compared to those in the lowest tertile (T3 vs. T1: hazard ratio [HR] 1.39, 95% confidence interval [CI] 1.13–1.72, $p = 0.002$). Patients with elevated FFA concentration also displayed an increased risk of the composite outcome (T3 vs. T1: HR 1.39, 95% CI 1.09–1.79, $p = 0.008$) (online supplementary *Figure S1*). Notably, the association between higher FFA levels and the increased risk of clinical events was not significantly influenced by β-OHB levels, as showed by Cox regression analysis (FFA levels >median and β-OHB levels ≤median vs. FFA and β-OHB levels >median: HR 0.86, 95% CI 0.60–1.22, $p = 0.404$) and in Kaplan–Meier plots (*Figure 4*). Sensitivity analysis using as endpoint a composite of death or urgent cardiac transplantation (i.e. excluding LVAD implantation to avoid potential referral bias to our tertiary centre) showed results similar to the primary analysis (β-OHB, T3 vs. T1: HR 1.61, 95% CI 1.27–2.03, $p < 0.001$; FFA, T3 vs. T1: HR 1.52, 95% CI 1.16–2.00, $p = 0.003$).

In the multivariable Cox analysis evaluating the simultaneous associations of FFA and β-OHB levels with adverse clinical events, only FFA levels remained significantly associated with the composite outcome, both as continuous variables (β-OHB, log-rank $\chi^2 = 0.57$, $p = 0.447$; FFA, log-rank $\chi^2 = 10.9$, $p < 0.001$) and, even if more borderline likely due to the reduced sample size, according to tertiles (β-OHB, T3 vs. T1: HR 1.31, 95% CI 0.96–1.78, $p = 0.084$; FFA, T3 vs. T1: HR 1.39, 95% CI 1.01–1.92, $p = 0.048$) (online supplementary *Figure S1*).

Discussion

We explored the determinants and the prognostic impact of β-OHB in patients with advanced HFrEF. We demonstrated a close relationship between β-OHB levels and neurohumoral activation, worse haemodynamic, and more impaired RV function. Notably, we observed a direct association between β-OHB levels and an increased risk of clinical events in patients with advanced HFrEF. However, the association between β-OHB levels and adverse outcome was no longer evident after accounting for FFA concentrations, which were also associated with an increased risk (*Graphical Abstract*).

Altered myocardial use of energy-providing substrates and impaired metabolic flexibility are the key features of HF-related metabolic derangement.[23–25] In patients with HFrEF, myocardial β-OHB oxidation rate is significantly increased,[26] with a linear β-OHB uptake in proportion to the delivery and with no upper threshold.[10] Based on experimental studies, the increased reliance on KB of the failing heart has been postulated to be an adaptive process,[27] aiming to provide the energy-starved myocardium with an extra source of substrate to decrease its energy deficit and support its contractile function.[28] It is therefore quite surprising that several recent observational studies[11,13,29] found a negative association between circulating β-OHB and survival in HF. Our findings reveal a more intricate connection between β-OHB and HF prognosis and enrich the existing literature, clarifying the ongoing

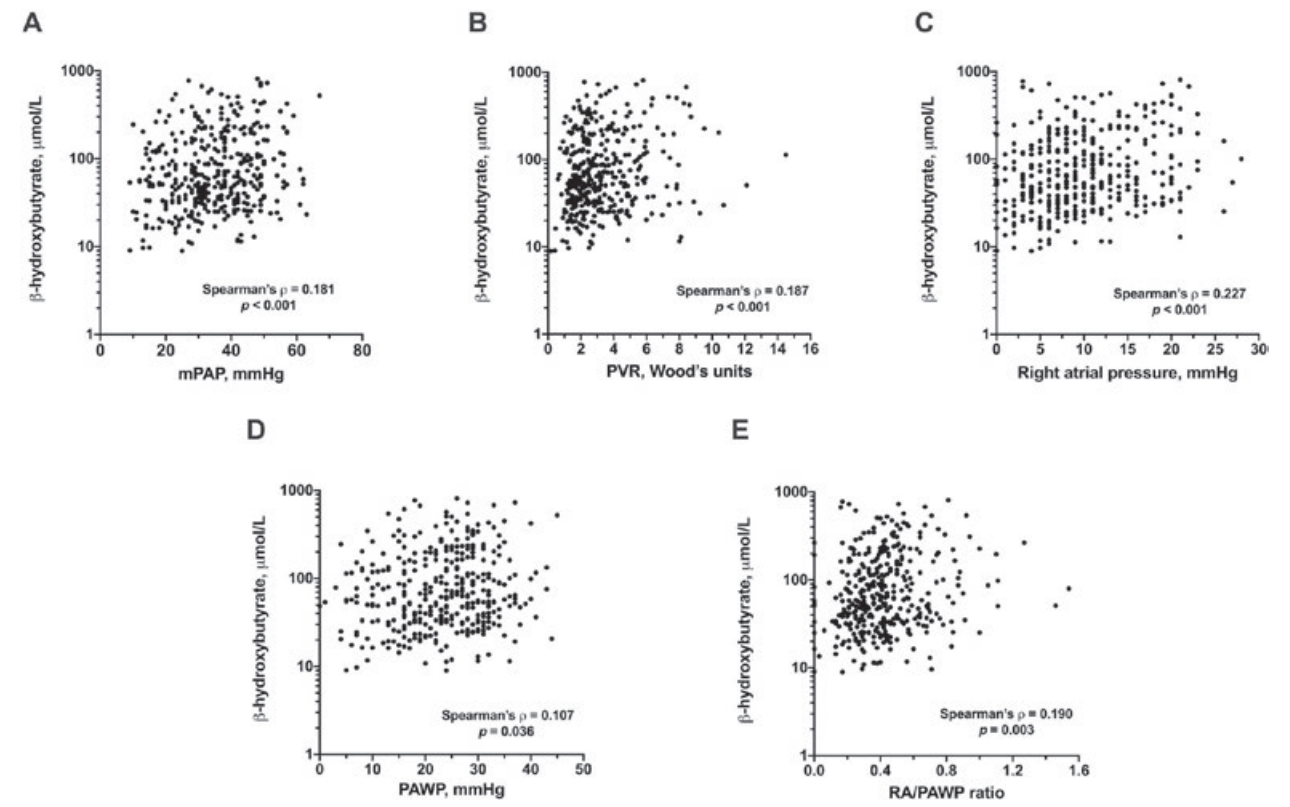

Figure 2 Correlation between beta-hydroxybutyrate levels and (*A*) mean pulmonary artery pressure (mPAP), (*B*) pulmonary vascular resistance (PVR), (*C*) right atrial (RA) pressure, (*D*) pulmonary artery wedge pressure (PAWP), (*E*) RA/PAWP ratio.

debate about the prognostic value of KB in HF.[12,13] Specifically, we demonstrated that the increase in circulating β-OHB likely reflects the severity of HF and the lipolytic overdrive triggered by the heightened neurohormonal activation. Therefore, the preference for using KB as a substrate in the failing heart might primarily stem from the increased availability of β-OHB and its cardiac uptake through concentration-dependent zero-order kinetics.[10]

Determinants of beta-hydroxybutyrate levels in the heart failure population

The amount of circulating β-OHB is affected by several factors. Increased β-OHB production secondary to a heightened hepatic delivery of β-OHB precursors, namely FFA, can be consequential to an increase in lipolytic hormones, or from either an absolute or a relative deficiency of insulin signalling in adipose tissue, as in diabetes. Liver ketogenesis is also activated by low insulin and increased glucagon, as during starvation.[3] Additionally, β-OHB level is influenced by the net rate of peripheral tissue utilization and the extent of renal reabsorption.[4]

Our study demonstrates that β-OHB level in advanced HF is primarily influenced by neurohumoral activation and the rate of lipolysis, along with the presence of diabetes,[30] while renal function is less relevant. Notably, we found that β-OHB concentration was inversely associated with insulin/glucagon ratio, an important regulator of liver ketogenesis, and directly with markers of insulin resistance (i.e. HOMA-IR). In addition, we showed a significant association between elevated β-OHB levels and worse haemodynamic status, namely increased RA pressure, pulmonary pressure, PVR, and PAWP. β-OHB level was also inversely associated with RV function (i.e. RA/PAWP ratio), suggesting that systemic catabolism associated with ventricular failure may be reflected by β-OHB.[19]

The elevation of KB in HF is likely a consequence of increased release of FFA from adipose tissue and the subsequent overload of hepatocytes with beta-oxidation byproducts, which are then converted into β-OHB in order to provide an additional source of energy for other organs. The HF-related neurohormonal overdrive, characterized by elevated levels of catecholamines, angiotensin II and natriuretic peptides, results in heightened activation of adipocyte lipolysis,[31,32] leading in turn to a rise in both circulating FFA and β-OHB. Consistently, high glycerol concentrations were observed in the adipose interstitial fluid of HF patients, indicating the high breakdown activity of triglycerides in this condition.[32] Direct *in-vivo* measurements documented that lipolytic actions of BNP are not attenuated even in patients with advanced HF, and BNP-driven lipolysis has been implicated in the development of cardiac cachexia.[19,33]

The link between increased lipolysis, ketone production, and low body weight was recently documented even in the general population.[34] Not only HF, but also other stress or catabolic

Table 2 Age- and sex-adjusted and multivariable linear regression analyses on plasma concentration of beta-hydroxybutyrate

Variables	Age- and sex-adjusted		Multivariable[a]	
	Standardized β ± SE	*p*-value	Standardized β ± SE	*p*-value
Clinical characteristics				
Body mass index, kg/m^2	0.016 ± 0.007	0.014		
Body fat (skinfold method), %	−0.006 ± 0.006	0.331		
NYHA class I–IV	0.065 ± 0.057	0.253		
MLHFQ score	−0.001 ± 0.002	0.906		
HF ischaemic aetiology (yes vs. no)	−0.041 ± 0.039	0.288		
HF duration, years	0.050 ± 0.041	0.226		
Diabetes mellitus (yes vs. no)	0.177 ± 0.034	<0.001	–	–
Laboratory values				
Haemoglobin, g/L	−0.002 ± 0.002	0.193		
eGFR, ml/min/1.73 m^2	−0.002 ± 0.002	0.203		
HbA_{1c}, mmol/mol	0.741 ± 0.138	<0.001	0.342 ± 0.377	0.365
HOMA-IR index	−0.105 ± 0.042	0.012		
Insulin, mIU/L	−0.008 ± 0.002	<0.001	–	–
Glucagon, pg/ml	0.001 ± 0.001	0.048		
Insulin/glucagon ratio	−1.231 ± 0.043	<0.001	−0.137 ± 0.101	0.174
BNP, ng/L	0.197 ± 0.029	<0.001	0.062 ± 0.087	0.478
Free fatty acids, mmol/L	1.708 ± 0.120	<0.001	1.384 ± 0.264	<0.001
Echocardiography				
LV end-diastolic diameter, mm	0.010 ± 0.004	0.010		
LV ejection fraction, %	−0.002 ± 0.006	0.716		
E/Em ratio	0.006 ± 0.005	0.261		
Haemodynamics				
RA pressure, mmHg	0.037 ± 0.008	<0.001	0.022 ± 0.015	0.146
PA mean pressure, mmHg	0.016 ± 0.004	<0.001	−0.001 ± 0.008	0.985
PA wedge pressure, mmHg	0.014 ± 0.006	0.015		
RA/PA wedge pressure ratio	0.648 ± 0.216	0.003	–	–
Cardiac output, L/min	−0.053 ± 0.047	0.266		
PVR, WU	0.357 ± 0.083	<0.001	–	–
Treatment (yes vs. no)				
ACEi or ARB use	−0.019 ± 0.041	0.635		
MRA use	0.019 ± 0.040	0.624		
Beta-blocker use	0.023 ± 0.053	0.659		
Insulin use	0.191 ± 0.051	<0.001	0.082 ± 0.139	0.768

ACEi, angiotensin-converting enzyme inhibitor; ARB, angiotensin receptor blocker; BNP, brain natriuretic peptide; eGFR, estimated glomerular filtration rate; HbA_{1c}, glycated haemoglobin; HF, heart failure; HOMA-IR, homeostasis model assessment of insulin resistance; MLHFQ, Minnesota Living with Heart Failure Questionnaire; LV, left ventricular; MRA, mineralocorticoid receptor antagonist; NYHA, New York Heart Association; PA, pulmonary artery; PVR, pulmonary vascular resistance; RA, right atrial; SE, standard error; WU, Wood units.

[a]In the multivariable model, dashes stand for variables not tested because of possible collinearity, meanwhile empty rows mean that variables were not tested because not strongly statistically significant (i.e. $p < 0.001$) in the adjusted univariate analysis.

situations, such as ST-elevation myocardial infarction,[15] or chronic dialysis,[16] are also associated with an increased blood level of KB, likely as a direct consequence of the sympathetic stress response, systemic catecholamine surge and FFA release.[15]

Beta-hydroxybutyrate levels and prognosis in the heart failure population

In patients with HFrEF, increasing circulating KB are associated with worse prognosis.[13,24,35] Our study demonstrates that FFA, the precursors of KB, are also independent predictor of adverse outcome, replacing KB in the multivariate model. Although we cannot draw definitive explanations for this finding from observational data, we can offer some potential insights. Enhanced ketogenesis in HF seems mainly driven by neurohormonal activation, as previously demonstrated by the positive association between HF severity and β-OHB levels,[24] being in turn just the mirror of a worse clinical status. This could also be supported by an association between β-OHB levels and worsen cardiac and pulmonary haemodynamics and higher BNP in the present study. High KB levels in HF can also reflects enhanced triglyceride metabolism, and

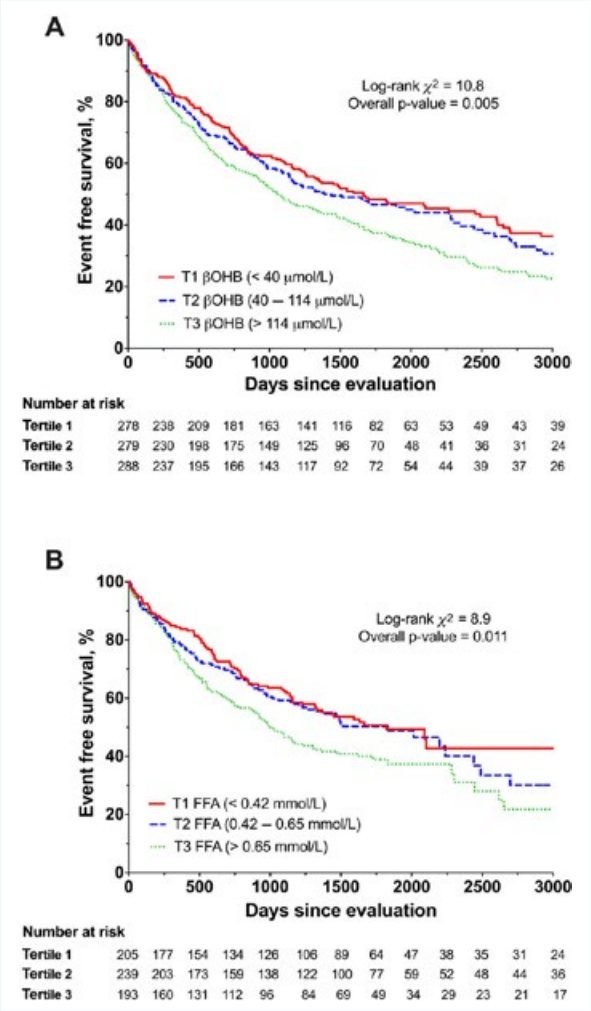

Figure 3 Kaplan–Meier curves for the composite outcome of death, urgent transplantation, or left ventricular assist device implantation without heart transplantation stratified by (*A*) beta-hydroxybutyrate (β-OHB) level tertiles and (*B*) free fatty acid (FFA) level tertiles.

consequent FFA production. As the last product of this metabolic cascade, β-OHB may represent a surrogate marker for heightened triglyceride mobilization and FFA flux.[34]

Previous observations reported that circulating FFA were associated with several comorbidities including coronary heart disease, hypertension, diabetes mellitus and atrial fibrillation that increase the risk for HF,[36] but also adverse outcomes such as sudden cardiac death and increased cardiovascular mortality.[37,38] From a mechanistic perspective, high FFA levels and their consequent preferential use as a metabolic substrate may reduce myocardial energy efficiency, through the uncoupling of mitochondrial proteins, and alter insulin signalling pathways and tissue insulin sensitivity.[39] Moreover, the imbalance between FFA uptake and oxidation may results in intracellular accumulation of toxic lipid species that drive the cardiac lipotoxicity.[40] Finally, FFA have been involved in several cellular pathways causing endothelial dysfunction and apoptosis,

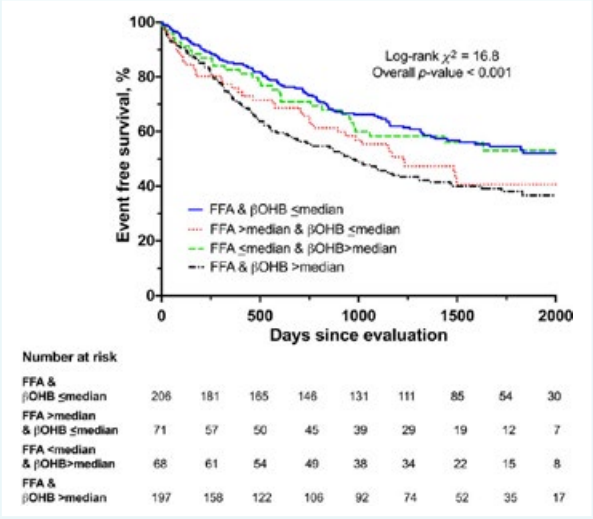

Figure 4 Kaplan–Meier curves for the composite outcome of death, urgent transplantation, or left ventricular assist device implantation without heart transplantation stratified by beta-hydroxybutyrate (β-OHB) and free fatty acid (FFA) levels above or below/equal the median.

playing a key role in accelerated atherosclerosis.[41] Altogether, these effects may provide biological plausibility for the observed increased risk of adverse outcomes in HF patients with higher FFA concentrations.

Strengths and limitations

The strengths of this study are its unparalleled sample size and depth of phenotyping, including invasive haemodynamics, anthropometry, and metabolic hormones, making it the most comprehensive cohort to date exploring the determinants and prognostic impact of β-OHB in HFrEF. The study has also inherent limitations. Due to its observational design, it is not possible to establish a causal link to the results obtained. Patients were referred or enrolled in a single tertiary centre, leading to a selection bias. We measured plasma FFA and β-OHB at a single time point. Whether repeated measures and evaluation of trajectories of change in FFA and β-OHB over time may have provided stronger associations with clinical outcomes is unknown. Our population mainly comprises middle-age, male Caucasian individuals with advanced HFrEF, which could limit the generalization of these findings to other HF populations, such as HFpEF. We did not directly measure peripheral lipolysis, therefore hypothesis related to this were speculative. Due to the period of observation, the study population was not treated with SGLT2 inhibitors; consequently, it is not possible to provide any insights about their effect on KB metabolism. The lack of granularity in our mortality outcome data prevents us from specifically analysing cardiovascular deaths and excluding other causes of death not exclusively related to HF conditions. Finally, our analysis was based on absolute levels of metabolites, but measurements of metabolite flux (i.e. appearance and disappearance over time) would provide more definitive answers.[34]

Conclusions

In patients with advanced HFrEF, both β-OHB and FFA levels were directly associated with an increased risk of clinical events, including death, urgent transplantation, or LVAD implantation. Notably, the association between plasma β-OHB and adverse outcomes vanishes upon accounting for FFA levels, suggesting that β-OHB might merely reflects a heightened lipolytic state induced by neurohormonal overdrive due to a worse clinical status, as demonstrated by the direct association between KB level and worse haemodynamic parameters, RV dysfunction and BNP.

Supplementary Information

Additional supporting information may be found online in the Supporting Information section at the end of the article.

Funding

This work was supported by the Ministry of Health of the Czech Republic through grant AZV NU22-02-00161 and the conceptual development of research organization ("Institute for Clinical and Experimental Medicine - IKEM, IN 00023001"). Additional support was provided by the project "National Institute for Research of Metabolic and Cardiovascular Diseases" of the Czech Republic (Programme EXCELES, ID Project No. LX22NPO5104), funded by the European Union - Next Generation EU.
Conflict of interest: none declared.

References

1. Dávila-Román VG, Vedala G, Herrero P, de las Fuentes L, Rogers JG, Kelly DP, *et al.* Altered myocardial fatty acid and glucose metabolism in idiopathic dilated cardiomyopathy. *J Am Coll Cardiol* 2002;**40**:271–277. https://doi.org/10.1016/S0735-1097(02)01967-8
2. Lopaschuk GD, Ussher JR. Evolving concepts of myocardial energy metabolism: More than just fats and carbohydrates. *Circ Res* 2016;**119**:1173–1176. https://doi.org/10.1161/CIRCRESAHA.116.310078
3. Cahill GF Jr. Fuel metabolism in starvation. *Annu Rev Nutr* 2006;**26**:1–22. https://doi.org/10.1146/annurev.nutr.26.061505.111258
4. Matsuura TR, Puchalska P, Crawford PA, Kelly DP. Ketones and the heart: Metabolic principles and therapeutic implications. *Circ Res* 2023;**132**:882–898. https://doi.org/10.1161/CIRCRESAHA.123.321872
5. Selvaraj S, Kelly DP, Margulies KB. Implications of altered ketone metabolism and therapeutic ketosis in heart failure. *Circulation* 2020;**141**:1800–1812. https://doi.org/10.1161/CIRCULATIONAHA.119.045033
6. Takahara S, Soni S, Maayah ZH, Ferdaoussi M, Dyck JRB. Ketone therapy for heart failure: Current evidence for clinical use. *Cardiovasc Res* 2022;**118**:977–987. https://doi.org/10.1093/cvr/cvab068
7. Selvaraj S, Fu Z, Jones P, Kwee LC, Windsor SL, Ilkayeva O, *et al.*; DEFINE-HF Investigators. Metabolomic profiling of the effects of dapagliflozin in heart failure with reduced ejection fraction: DEFINE-HF. *Circulation* 2022;**146**:808–818. https://doi.org/10.1161/CIRCULATIONAHA.122.060402
8. Kim SR, Lee SG, Kim SH, Kim JH, Choi E, Cho W, *et al.* SGLT2 inhibition modulates NLRP3 inflammasome activity via ketones and insulin in diabetes with cardiovascular disease. *Nat Commun* 2020;**11**:2127. https://doi.org/10.1038/s41467-020-15983-6
9. Monzo L, Melenovsky V. Letter by Monzo and Melenovsky regarding article, "Metabolomic profiling of the effects of dapagliflozin in heart failure with reduced ejection fraction: DEFINE-HF". *Circulation* 2023;**147**:920–921. https://doi.org/10.1161/CIRCULATIONAHA.122.061155
10. Monzo L, Sedlacek K, Hromanikova K, Tomanova L, Borlaug BA, Jabor A, *et al.* Myocardial ketone body utilization in patients with heart failure: The impact of oral ketone ester. *Metabolism* 2021;**115**:154452. https://doi.org/10.1016/j.metabol.2020.154452
11. Yokokawa T, Sugano Y, Shimouchi A, Shibata A, Jinno N, Nagai T, *et al.* Exhaled acetone concentration is related to hemodynamic severity in patients with non-ischemic chronic heart failure. *Circ J* 2016;**80**:1178–1186. https://doi.org/10.1253/circj.CJ-16-0011
12. Christensen KH, Nielsen RR, Schou M, Gustafsson I, Jorsal A, Flyvbjerg A, *et al.* Circulating 3-hydroxy butyrate predicts mortality in patients with chronic heart failure with reduced ejection fraction. *ESC Heart Fail* 2024;**11**:837–845. https://doi.org/10.1002/ehf2.14476
13. Marcondes-Braga FG, Batista GL, Gutz IG, Saldiva PH, Mangini S, Issa VS, *et al.* Impact of exhaled breath acetone in the prognosis of patients with heart failure with reduced ejection fraction (HFrEF). One year of clinical follow-up. *PLoS One* 2016;**11**:e0168790. https://doi.org/10.1371/journal.pone.0168790
14. Stryeck S, Gastrager M, Degoricija V, Trbusic M, Potocnjak I, Radulovic B, *et al.* Serum concentrations of citrate, tyrosine, 2- and 3- hydroxybutyrate are associated with increased 3-month mortality in acute heart failure patients. *Sci Rep* 2019;**9**:6743. https://doi.org/10.1038/s41598-019-42937-w
15. de Koning MLY, Westenbrink BD, Assa S, Garcia E, Connelly MA, van Veldhuisen DJ, *et al.* Association of circulating ketone bodies with functional outcomes after ST-segment elevation myocardial infarction. *J Am Coll Cardiol* 2021;**78**:1421–1432. https://doi.org/10.1016/j.jacc.2021.07.054
16. Obokata M, Negishi K, Sunaga H, Ishida H, Ito K, Ogawa T, *et al.* Association between circulating ketone bodies and worse outcomes in hemodialysis patients. *J Am Heart Assoc* 2017;**6**:e006885. https://doi.org/10.1161/JAHA.117.006885
17. Shemesh E, Chevli PA, Islam T, German CA, Otvos J, Yeboah J, *et al.* Circulating ketone bodies and cardiovascular outcomes: The MESA study. *Eur Heart J* 2023;**44**:1636–1646. https://doi.org/10.1093/eurheartj/ehad087
18. Cotter DG, Schugar RC, Crawford PA. Ketone body metabolism and cardiovascular disease. *Am J Physiol Heart Circ Physiol* 2013;**304**:H1060–H1076. https://doi.org/10.1152/ajpheart.00646.2012
19. Melenovsky V, Kotrc M, Borlaug BA, Marek T, Kovar J, Malek I, *et al.* Relationships between right ventricular function, body composition, and prognosis in advanced heart failure. *J Am Coll Cardiol* 2013;**62**:1660–1670. https://doi.org/10.1016/j.jacc.2013.06.046
20. Levey AS, Stevens LA, Schmid CH, Zhang YL, Castro AF 3rd, Feldman HI, *et al.*; CKD-EPI (Chronic Kidney Disease Epidemiology Collaboration). A new equation to estimate glomerular filtration rate. *Ann Intern Med*. 2009;**150**(9):604–612. https://https://doi.org/10.7326/0003-4819-150-9-200905050-00006
21. Rosenkranz S, Preston IR. Right heart catheterisation: Best practice and pitfalls in pulmonary hypertension. *Eur Respir Rev* 2015;**24**:642–652. https://doi.org/10.1183/16000617.0062-2015
22. Durnin JV, Womersley J. Body fat assessed from total body density and its estimation from skinfold thickness: Measurements on 481 men and women aged from 16 to 72 years. *Br J Nutr* 1974;**32**:77–97. https://doi.org/10.1079/BJN19740060
23. Byrne NJ, Levasseur J, Sung MM, Masson G, Boisvenue J, Young ME, *et al.* Normalization of cardiac substrate utilization and left ventricular hypertrophy precede functional recovery in heart failure regression. *Cardiovasc Res* 2016;**110**:249–257. https://doi.org/10.1093/cvr/cvw051
24. Lommi J, Kupari M, Koskinen P, Naveri H, Leinonen H, Pulkki K, *et al.* Blood ketone bodies in congestive heart failure. *J Am Coll Cardiol* 1996;**28**:665–672. https://doi.org/10.1016/0735-1097(96)00214-8
25. Zhang L, Jaswal JS, Ussher JR, Sankaralingam S, Wagg C, Zaugg M, *et al.* Cardiac insulin-resistance and decreased mitochondrial energy production precede the development of systolic heart failure after pressure-overload hypertrophy. *Circ Heart Fail* 2013;**6**:1039–1048. https://doi.org/10.1161/CIRCHEARTFAILURE.112.000228
26. Bedi KC Jr, Snyder NW, Brandimarto J, Aziz M, Mesaros C, Worth AJ, *et al.* Evidence for intramyocardial disruption of lipid metabolism and increased myocardial ketone utilization in advanced human heart failure. *Circulation* 2016;**133**:706–716. https://doi.org/10.1161/CIRCULATIONAHA.115.017545
27. Horton JL, Davidson MT, Kurishima C, Vega RB, Powers JC, Matsuura TR, *et al.* The failing heart utilizes 3-hydroxybutyrate as a metabolic stress defense. *JCI Insight* 2019;**4**:e124079. https://doi.org/10.1172/jci.insight.124079
28. Ho KL, Zhang L, Wagg C, Al Batran R, Gopal K, Levasseur J, *et al.* Increased ketone body oxidation provides additional energy for the failing heart without improving cardiac efficiency. *Cardiovasc Res* 2019;**115**:1606–1616. https://doi.org/10.1093/cvr/cvz045
29. Niezen S, Connelly MA, Hirsch C, Kizer JR, Benitez ME, Minchenberg S, *et al.* Elevated plasma levels of ketone bodies are associated with all-cause mortality and incidence of heart failure in older adults: The CHS. *J Am Heart Assoc* 2023;**12**:e029960. https://doi.org/10.1161/JAHA.123.029960
30. Melenovsky V, Kotrc M, Polak J, Pelikanova T, Bendlova B, Cahova M, *et al.* Availability of energetic substrates and exercise performance in heart failure with or without diabetes. *Eur J Heart Fail* 2012;**14**:754–763. https://doi.org/10.1093/eurjhf/hfs080
31. Kintscher U, Foryst-Ludwig A, Haemmerle G, Zechner R. The role of adipose triglyceride lipase and cytosolic lipolysis in cardiac function and heart failure. *Cell Rep Med* 2020;**1**:100001. https://doi.org/10.1016/j.xcrm.2020.100001

32. Polak J, Kotrc M, Wedellova Z, Jabor A, Malek I, Kautzner J, *et al.* Lipolytic effects of B-type natriuretic peptide 1-32 in adipose tissue of heart failure patients compared with healthy controls. *J Am Coll Cardiol* 2011;**58**:1119–1125. https://doi.org/10.1016/j.jacc.2011.05.042
33. Janovska P, Melenovsky V, Svobodova M, Havlenova T, Kratochvilova H, Haluzik M, *et al.* Dysregulation of epicardial adipose tissue in cachexia due to heart failure: The role of natriuretic peptides and cardiolipin. *J Cachexia Sarcopenia Muscle* 2020;**11**:1614–1627. https://doi.org/10.1002/jcsm.12631
34. Johansen MO, Afzal S, Vedel-Krogh S, Nielsen SF, Smith GD, Nordestgaard BG. From plasma triglycerides to triglyceride metabolism: Effects on mortality in the Copenhagen General Population Study. *Eur Heart J* 2023;**44**:4174–4182. https://doi.org/10.1093/eurheartj/ehad330
35. Marcondes-Braga FG, Gioli-Pereira L, Bernardez-Pereira S, Batista GL, Mangini S, Issa VS, *et al.* Exhaled breath acetone for predicting cardiac and overall mortality in chronic heart failure patients. *ESC Heart Fail* 2020;**7**:1744–1752. https://doi.org/10.1002/ehf2.12736
36. Djousse L, Benkeser D, Arnold A, Kizer JR, Zieman SJ, Lemaitre RN, *et al.* Plasma free fatty acids and risk of heart failure: The Cardiovascular Health Study. *Circ Heart Fail* 2013;**6**:964–969. https://doi.org/10.1161/CIRCHEARTFAILURE.113.000521
37. Miedema MD, Maziarz M, Biggs ML, Zieman SJ, Kizer JR, Ix JH, *et al.* Plasma-free fatty acids, fatty acid-binding protein 4, and mortality in older adults (from the Cardiovascular Health Study). *Am J Cardiol* 2014;**114**:843–848. https://doi.org/10.1016/j.amjcard.2014.06.012
38. Pilz S, Scharnagl H, Tiran B, Wellnitz B, Seelhorst U, Boehm BO, *et al.* Elevated plasma free fatty acids predict sudden cardiac death: A 6.85-year follow-up of 3315 patients after coronary angiography. *Eur Heart J* 2007;**28**:2763–2769. https://doi.org/10.1093/eurheartj/ehm343
39. Han L, Liu J, Zhu L, Tan F, Qin Y, Huang H, *et al.* Free fatty acid can induce cardiac dysfunction and alter insulin signaling pathways in the heart. *Lipids Health Dis* 2018;**17**:185. https://doi.org/10.1186/s12944-018-0834-1
40. Bertero E, Maack C. Metabolic remodelling in heart failure. *Nat Rev Cardiol* 2018;**15**:457–470. https://doi.org/10.1038/s41569-018-0044-6
41. Oram JF, Bornfeldt KE. Direct effects of long-chain non-esterified fatty acids on vascular cells and their relevance to macrovascular complications of diabetes. *Front Biosci* 2004;**9**:1240–1253. https://doi.org/10.2741/1300

P. Ošťádal et al.

Extracorporeal membrane oxygenation in the therapy of cardiogenic shock: 1-year outcomes of the multicentre, randomized ECMO-CS trial

CIRCULATION
Impact Factor: 37,8

‹ rejstřík

ESC European Society of Cardiology

European Journal of Heart Failure (2024)
doi:10.1002/ejhf.3398

RESEARCH ARTICLE

Extracorporeal membrane oxygenation in the therapy of cardiogenic shock: 1-year outcomes of the multicentre, randomized ECMO-CS trial

Petr Ostadal[1]*, Richard Rokyta[2], Jiri Karasek[3,4], Andreas Kruger[5], Dagmar Vondrakova[1], Marek Janotka[5], Jan Naar[5], Jana Smalcova[6], Marketa Hubatova[6], Milan Hromadka[2], Stefan Volovar[2], Miroslava Seyfrydova[2], Ales Linhart[6], and Jan Belohlavek[6], for the ECMO-CS Investigators

[1]Department of Cardiology, Second Faculty of Medicine, Charles University and Motol University Hospital, Prague, Czech Republic; [2]Department of Cardiology, University Hospital and Faculty of Medicine Pilsen, Charles University, Pilsen, Czech Republic; [3]Hospital Liberec, Liberec, Czech Republic; [4]Department of Emergency Medicine, Second Faculty of Medicine, Charles University and Motol University Hospital, Prague, Czech Republic; [5]Department of Cardiology, Na Homolce Hospital, Prague, Czech Republic; and [6]2nd Department of Medicine – Department of Cardiovascular Medicine, First Faculty of Medicine, Charles University and General University Hospital, Prague, Czech Republic

Received 25 February 2024; revised 29 June 2024; accepted 10 July 2024

Aims Among patients with cardiogenic shock, immediate initiation of extracorporeal membrane oxygenation (ECMO) did not demonstrate any benefit at 30 days. The present study evaluated 1-year clinical outcomes of the Extracorporeal Membrane Oxygenation in the therapy of Cardiogenic Shock (ECMO-CS) trial.

Methods and results The ECMO-CS trial randomized 117 patients with severe or rapidly progressing cardiogenic shock to immediate initiation of ECMO or early conservative strategy. The primary endpoint for this analysis was 1-year all-cause mortality. Secondary endpoints included a composite of death, resuscitated cardiac arrest or implantation of another mechanical circulatory support device, duration of mechanical ventilation, and the length of intensive care unit (ICU) and hospital stays. In addition, an unplanned post-hoc subgroup analysis was performed. At 1 year, all-cause death occurred in 40 of 58 (69.0%) patients in the ECMO arm and in 40 of 59 (67.8%) in the early conservative arm (hazard ratio [HR] 1.02, 95% confidence interval [CI] 0.66–1.58; $p = 0.93$). The composite endpoint occurred in 43 (74.1%) patients in the ECMO group and in 47 (79.7%) patients in the early conservative group (HR 0.83, 95% CI 0.55–1.25; $p = 0.29$). The durations of mechanical ventilation, ICU stay and hospital stay were comparable between groups. Significant interaction with treatment strategy and 1-year mortality was observed in subgroups according to baseline mean arterial pressure (MAP) indicating lower mortality in the subgroup with low baseline MAP (<63 mmHg: HR 0.58, 95% CI 0.29–1.16; $p_{interaction} = 0.017$).

Conclusions Among patients with severe or rapidly progressing cardiogenic shock, immediate initiation of ECMO did not improve clinical outcomes at 1 year compared to the early conservative strategy. However, immediate ECMO initiation might be beneficial in patients with advanced haemodynamic compromise.

Keywords Clinical trial • Cardiogenic shock • Therapy • Extracorporeal membrane oxygenation

*Corresponding author. Department of Cardiology, Second Faculty of Medicine, Charles University and Motol University Hospital, V Uvalu 84, 15006 Prague, Czech Republic. Tel: +420 224 434901, Email: ostadal.petr@gmail.com

Introduction

Cardiogenic shock is a critical condition caused by primary cardiac dysfunction resulting in inadequate cardiac output with tissue hypoperfusion.[1] Despite advances and developments in acute cardiovascular and intensive care, mortality rates for cardiogenic shock remain high.[2,3] During past years, mechanical circulatory support (MCS), especially veno-arterial extracorporeal membrane oxygenation (ECMO), has been increasingly used to restore total circulatory output, increase blood pressure, and improve tissue perfusion in these patients. Initiation of MCS became standard therapeutic strategy recommended by guidelines from the European Society of Cardiology (class IIa recommendation)[1] and the American Heart Association, American College of Cardiology and Heart Failure Society of America (class IIb recommendation).[4] These recommendations were based almost exclusively on findings from observational studies (level of evidence C).[1,4]

Recently, four randomized clinical trials and their meta-analysis reported that early initiation of ECMO in patients with cardiogenic shock did not improve clinical outcomes, including all-cause mortality at 30 days.[5–9] However, longer observation is needed to carefully evaluate the effect of ECMO in cardiogenic shock, considering that many patients remain hospitalized 30 days after the index event and that early haemodynamic improvement, similar to ischaemic or bleeding complications associated with the use of ECMO, may impact long-term outcome.[6] To date, long-term results from multicentre randomized trials comparing ECMO and standard care in cardiogenic shock have not been available. Therefore, we present 1-year pre-defined follow-up of the Extracorporeal Membrane Oxygenation in the therapy of Cardiogenic Shock (ECMO-CS) trial. In addition, an unplanned post-hoc subgroup analysis was performed.

Methods

Study overview

The ECMO-CS trial was an investigator-initiated, multicentre randomized trial conducted at four experienced centres in the Czech Republic. All patients provided informed written consent to participate in the study. If patient's status did not permit a written informed consent, it was provided retrospectively after improvement of their clinical condition. If a patient died, remained unconscious, or experienced significant brain dysfunction, informed consent was obtained from the patient's next of kin. If informed consent was not obtained, all acquired data were removed from the database and not used in the analysis. The authors confirm the accuracy and completeness of the data and for the fidelity of the trial to the protocol. The ECMO-CS trial was supported by a grant from the Czech Health Research Council (No. 15-27994A) and was registered at ClinicalTrials.gov (NCT02301819).

Study design and endpoints

The trial design and protocol were published previously.[6,10] Briefly, patients fulfilling the inclusion criteria for severe or rapidly progressing cardiogenic shock of various aetiologies (online supplementary *Tables S1* and *S2*) were randomly assigned to immediate initiation of ECMO or to an early conservative strategy. Importantly, in the early conservative arm, ECMO could be used in case of conservative therapy failure and further haemodynamic worsening with elevation in serum lactate level by 3 mmol/L compared with the lowest value during the past 24 h.[6,10] Thirty-day results of the trial were published previously.[6] The primary endpoint for this analysis was 1-year all-cause mortality. Secondary endpoints included a composite of death from any cause, resuscitated cardiac arrest and implementation of another MCS device, duration of mechanical ventilation, and the length of intensive care unit (ICU) and hospital stays. Furthermore, a post-hoc subgroup analysis was performed, including subgroups according to age, sex, presentation with ST-elevation myocardial infarction, percutaneous coronary intervention for the index event, baseline mean arterial pressure, left ventricular ejection fraction, lactate level, and vasoactive-inotropic score.

Statistical analysis

Sample size determination was based on the assumption of the incidence of the primary outcome (composite of death from any cause, resuscitated cardiac arrest and implementation of another type of MCS device at 30 days) and was published previously.[6] Analyses were performed according to the intention-to-treat principle and included data from all patients and for all events that occurred from the time of randomization up to 1 year. Categorical variables are expressed as percentages and compared using Pearson's chi-squared test or Fisher's exact test. Continuous variables are presented as median (interquartile range [IQR]) and compared using the *t*-test or Mann–Whitney test as appropriate. Time to death was analysed using the Kaplan–Meier method and compared using the log-rank test. Calculation of 95% confidence intervals (CIs) for point estimates of endpoint occurrence probability was based on the cumulative risk function (or logarithmic transformation of the survival function). Hazard ratios (HRs) with corresponding 95% CIs were calculated using a Cox proportional hazard model with Efron approximation for tie holding. Odds ratios (OR) with corresponding 95% CIs were calculated using Baptista–Pike test. Due to the potential for type 1 error in multiple comparisons, findings for the secondary outcomes and subgroup analyses should be interpreted as exploratory. The analysis was performed using SPSS version 28 (IBM Corporation, Armonk, NY, USA), R version 4.2.1 (R Foundation for Statistical Computing, Vienna, Austria) and Prism 8 (GraphPad Inc., San Diego, CA, USA). Hypotheses were tested at a significance level of 5% (i.e. differences with $p < 0.05$ were considered to be statistically significant).

Results

Patients

Between September 2014 and January 2022, 122 patients were randomly assigned to one of two groups: immediate ECMO, or early conservative therapy. After excluding five patients due to the absence of informed consent (all of them died and informed consent could not be obtained from the next of kin), 58 subjects were included in the immediate ECMO group and 59 in the early conservative therapy group, for whom 1-year data were available for all (online supplementary *Figure S1*). The baseline characteristics of the two study groups at the time of randomization were balanced (*Table 1*).

Table 1 Baseline characteristics

Characteristic	All ($n = 117$)	ECMO ($n = 58$)	Early conservative ($n = 59$)
Sex, *n* (%)			
Male	86 (73.5)	43 (74.1)	43 (72.9)
Female	31 (26.5)	15 (25.9)	16 (27.1)
Age, years, median (IQR)	66 (59–73)	67 (60–74)	65 (58–71)
Medical history, *n* (%)			
Chronic coronary syndrome	39 (34.2)	21 (37.5)	18 (31.0)
Chronic heart failure	27 (23.7)	14 (25.0)	13 (22.4)
Dilated cardiomyopathy	15 (13.3)	6 (10.9)	9 (15.5)
Chronic renal failure	16 (14.2)	7 (12.5)	9 (15.8)
Peripheral artery disease	10 (8.8)	3 (5.5)	7 (11.9)
Hypertension	73 (64.0)	35 (62.5)	38 (65.5)
Diabetes	37 (32.5)	16 (28.6)	21 (36.2)
Current smoker	41 (36.9)	14 (25.9)	27 (47.4)
Clinical parameters at randomization, median (IQR)			
Blood lactate, mmol/L	5.0 (3.2–8.0)	5.3 (3.1–8.4)	4.7 (3.3–7.4)
Systolic blood pressure, mmHg	85.0 (80.0–100.0)	84.0 (80.0–95.0)	89.0 (79.5–105.0)
Mean arterial pressure, mmHg	63.3 (55.3–72.0)	63.3 (56.7–68.7)	64.5 (54.3–75.3)
Heart rate, bpm	102.0 (84.0–120.0)	110.0 (86.5–130.0)	100.0 (82.0–110.0)
Therapy at randomization			
Intra-aortic balloon pump, *n* (%)	15 (13.3)	6 (10.9)	9 (15.5)
Mechanical ventilation, *n* (%)	81 (72.3)	41 (74.5)	40 (70.2)
Renal replacement therapy, *n* (%)	7 (6.2)	4 (7.3)	3 (5.2)
Norepinephrine, *n* (%)	100 (85.5)	50 (86.2)	50 (84.7)
Norepinephrine dose, µg/kg/min, median (IQR)	0.50 (0.23–1.24)	0.48 (0.23–1.36)	0.50 (0.27–1.19)
Epinephrine, *n* (%)	4 (3.4)	1 (1.7)	3 (5.1)
Epinephrine dose, µg/kg/min, median (IQR)	0.26 (0.14–0.80)	0.21 (0.21–0.21)	0.30 (0.07–1.30)
Dobutamine, *n* (%)	64 (54.7)	31 (53.4)	33 (55.9)
Dobutamine dose, µg/kg/min, median (IQR)	5.1 (4.9–8.0)	6.1 (5.0–9.7)	5.1 (4.7–7.6)
Milrinone, *n* (%)	38 (32.5)	22 (37.9)	16 (27.1)
Milrinone dose, µg/kg/min, median (IQR)	0.40 (0.30–0.50)	0.40 (0.30–0.50)	0.40 (0.37–0.51)
Vasopressin, *n* (%)	41 (35.0)	19 (32.8)	22 (37.3)
Vasopressin dose, U/kg/min, median (IQR)	0.0017 (0.0010–0.0025)	0.0020 (0.0010–0.0030)	0.0017 (0.0012–0.0022)
Levosimendan, *n* (%)	32 (29.4)	20 (37.0)	12 (21.8)
Vasoactive-inotropic score, median (IQR)	61.0 (30.0–124.0)	59.9 (32.8–121.5)	61.0 (28.0–124.9)
Cause of cardiogenic shock, *n* (%)			
ST-elevation myocardial infarction	59 (50.4)	30 (51.7)	29 (49.2)
Non-ST-elevation myocardial infarction	14 (12.0)	7 (12.1)	7 (11.9)
Decompensation of chronic heart failure	27 (23.1)	14 (24.1)	13 (22.0)
Mechanical complications of myocardial infarction	3 (2.6)	1 (1.7)	2 (3.4)
Aortic stenosis	9 (7.7)	5 (8.6)	4 (6.8)
Mitral regurgitation	4 (3.4)	1 (1.7)	3 (5.1)
Myocarditis	1 (0.9)	–	1 (1.7)

ECMO, extracorporeal membrane oxygenation; IQR, interquartile range.

Endpoints

At 1 year, death from any cause occurred in 40 of 58 (69.0%) patients in the ECMO arm and in 40 of 59 (67.8%) in the early conservative arm (HR 1.02, 95% CI 0.66–1.58; $p = 0.93$) (*Figure 1*, *Table 2*). The major cause of death was refractory shock followed by multi-organ failure in both groups (online supplementary *Table S3*). All survivors had good neurological outcome. The composite endpoint of death from any cause, resuscitated cardiac arrest, and implantation of another MCS device occurred in 43 (74.1%) patients in the immediate ECMO group and 47 (79.7%) in the early conservative group (HR 0.83, 95% CI 0.55–1.25; $p = 0.29$ (*Figure 2*, *Table 2*). Resuscitated cardiac arrest occurred in 6 (10.3%) patients in the immediate ECMO group and 8 (13.6%) in the early conservative group (OR 0.74, 95% CI 0.23–2.42) (*Table 2*). In the immediate ECMO group, fewer patients required another MCS device (11 [19.0%] vs. 29 [49.2%]; OR 0.28, 95% CI 0.13–0.64) (*Table 1*). The another MCS in the ECMO arm was intra-aortic balloon pump in four cases, two patients received Impella (Abiomed, Danvers, MA, USA) and two patients received

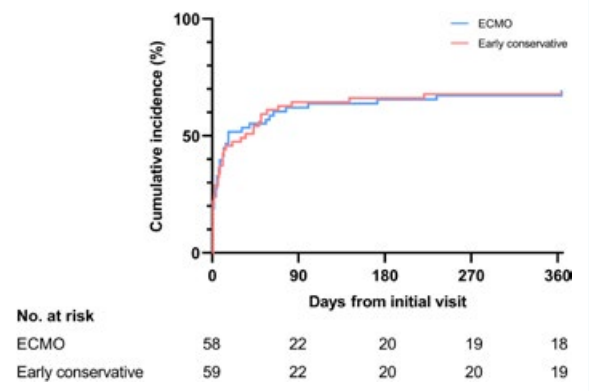

Figure 1 Cumulative incidence of all-cause death. ECMO, extracorporeal membrane oxygenation.

Table 2 Incidence of the composite endpoint and individual components of the composite endpoint

Endpoint	ECMO ($n = 58$)	Conservative ($n = 59$)	HR/OR (95% CI)
Death	40 (69.0)	40 (67.8)	1.02 (0.66–1.58)
Another mechanical circulatory support	11 (19.0)	29 (49.2)	0.28 (0.13–0.64)
Resuscitated cardiac arrest	6 (10.3)	8 (13.6)	0.74 (0.23–2.42)
Composite of death from any cause, implantation of another mechanical circulatory support, resuscitated cardiac arrest	43 (74.1)	47 (79.7)	0.83 (0.55–1.25)

Data are presented as *n* (%).
CI, confidence interval; ECMO, extracorporeal membrane oxygenation; HR, hazard ratio; OR, odds ratio.

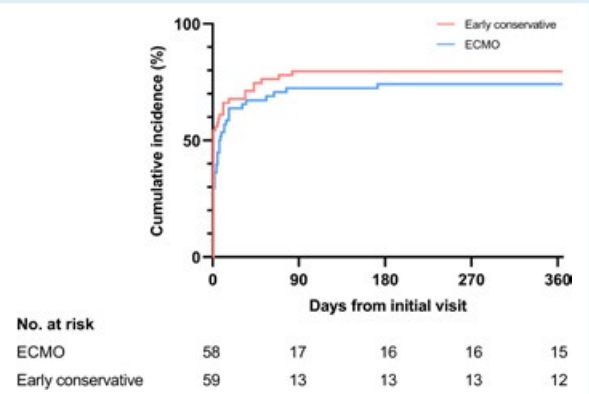

Figure 2 Cumulative incidence of the composite endpoint (all-cause death, resuscitated circulatory arrest, implantation of another mechanical circulatory support device). ECMO, extracorporeal membrane oxygenation.

short-term surgical mechanical left ventricular support (CentriMag, Abbott Laboratories, Abbott Park, IL, USA) – all these devices were implanted to unload the left ventricle; three patients were bridged to long-term mechanical support implantation (HeartMate, Abbott Laboratories, Abbott Park, IL, USA). In the early conservative arm, 23 patients required ECMO, three individuals received balloon pump and one subject received Impella in addition to ECMO for unloading, four patients had Impella alone and in three patients was implanted long-term left ventricular support HeartMate (one of them was on ECMO). From the 40 deaths in the early conservative arm, 19 occurred in patients with MCS.

The median duration of mechanical ventilation was 6 days (IQR 1–18 days) in the ECMO arm and 6 days (IQR 1–21 days) in the early conservative arm ($p = 0.66$) (online supplementary *Figure S2*). The median duration of ICU stay was 13 days (IQR 3–29 days) in the ECMO arm and 11 days (IQR 3–30 days) in the early conservative arm ($p = 0.62$) (online supplementary *Figure S3*). The median length of hospital stay was 17 days (IQR 3–31 days) in the ECMO arm and 11 days (IQR 3–41 days) in the early conservative arm ($p = 0.80$) (online supplementary *Figure S4*).

Three patients in the ECMO arm experienced stroke, all of them died (two from refractory shock, one from multi-organ failure); none stroke was observed in the early conservative arm. Renal replacement therapy was needed in 16 of 58 (27.6%) patients in the ECMO arm (12 of them died) and in 10 of 59 (16.9%) patients in the early conservative arm (8 of them died).

Subgroup analysis

Relative risks for 1-year all-cause mortality were consistent across subgroups according to age, sex, presentation with ST-elevation myocardial infarction, percutaneous coronary intervention for index event, left ventricular ejection fraction, lactate level and vasoactive-inotropic score. Significant interaction with treatment strategy and 1-year mortality was observed in subgroups according to baseline mean arterial pressure (<63 mmHg: HR 0.58, 95% CI 0.29–1.16 vs. ≥63 mmHg: HR 1.74, 95% CI 0.93–3.23; $p_{interaction} = 0.017$; median baseline mean arterial pressure in the ECMO-CS trial was 63 mmHg) (*Figure 3*). The interaction was even more pronounced in subgroups according to baseline mean arterial pressure of 60 mmHg (online supplementary *Figure S5*). Those with mean arterial pressure <63 mmHg had a comparable (numerically higher) vasoactive-inotropic score as subjects with a mean arterial pressure ≥63 mmHg (66 [IQR 36–144] vs. 51 [IQR 24–113]; $p = 0.12$) (online supplementary *Figure S6*) and similar pattern was observed for inotropic score (7.1 [IQR 4.7–9.6] vs. 5.0 [IQR 4.2–8.0], $p = 0.13$).

Discussion

In a 1-year follow-up of the randomized ECMO-CS trial, we report three key findings. First, among patients with rapidly progressing or severe cardiogenic shock, immediate initiation of ECMO did not improve 1-year clinical outcomes. Second, long-term all-cause mortality of cardiogenic shock remains very high and markedly

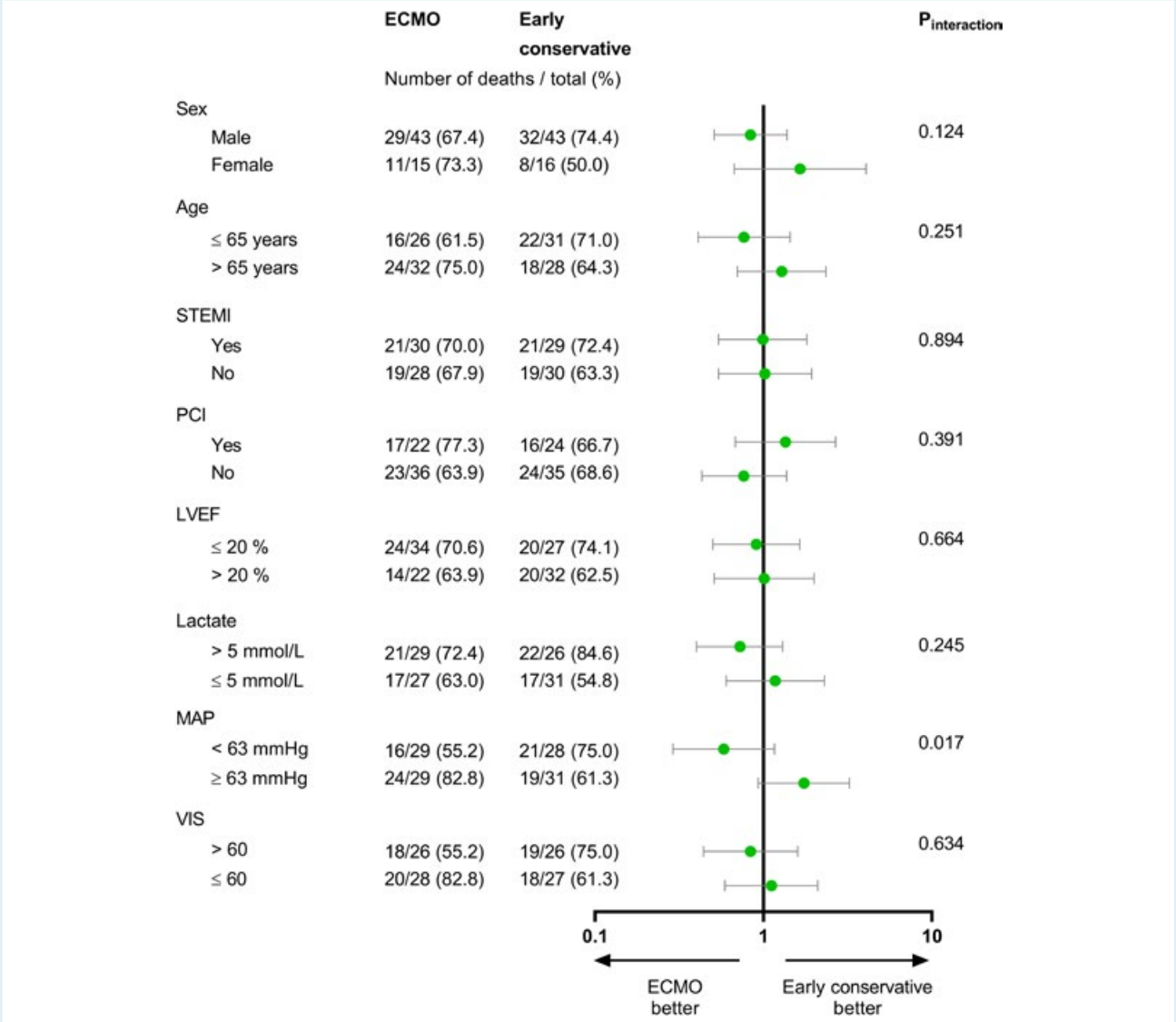

Figure 3 Relative risk for 1-year all-cause death in subgroups. ECMO, extracorporeal membrane oxygenation; LVEF, left ventricular ejection fraction; MAP, mean arterial pressure; PCI, percutaneous coronary intervention; STEMI, ST-elevation myocardial infarction; VIS, vasoactive inotropic score.

higher than 30-day mortality. Third, patients with persistent severe hypotension on inotropes and vasopressors may benefit from early implementation of ECMO.

The potential benefit from early ECMO implementation in cardiogenic shock was recently addressed in four randomized controlled trials. The first was the small, single-centre, ExtraCorporeal Life Support for acute myocardial infarction complicated by cardiogenic shock (ECLS-SHOCK I) trial, including 42 patients with acute myocardial infarction, most of them after successful resuscitation for cardiac arrest (90–100%).[5] The second was the present ECMO-CS trial, with 117 patients with cardiogenic shock of various aetiologies excluding patients after cardiac arrest.[6] The third was the Testing the Value of Novel Strategy and Its Cost Efficacy in Order to Improve the Poor Outcomes in Cardiogenic Shock (EURO SHOCK) trial, which was terminated early after enrolment of 35 patients with acute myocardial infarction (49% after resuscitation).[7] The fourth and, to date, the largest, Extracorporeal Life Support in Cardiogenic Shock (ECLS-SHOCK II) trial, included 417 patients with acute myocardial infarction, 78% of whom after resuscitation for cardiac arrest.[8] Neutral effect on 30-day outcomes was observed in all above trials and confirmed in the individual patient data meta-analysis (exclusively including subjects with acute myocardial infarction-related cardiogenic shock).[5–9] However, in the ECMO-CS trial, a substantial proportion of patients remained hospitalized at 30 days, partly on mechanical ventilation with uncertain prognosis and, therefore, longer-term follow-up is justified to evaluate the clinical outcomes.[6] Importantly, whereas the 30-day mortality in the

ECMO-CS trial was 49% (and 47% in the meta-analysis),[6,9] at 1 year, mortality increased to 68% with numerous deaths after 30 days. Of note, 91% of all deaths occurred within 90 days and 96% in 180 days; this observation may be useful for planning future clinical trials focused on MCS in cardiogenic shock.

Current evidence regarding the long-term effect of MCS in patients with cardiogenic shock from randomized controlled trials is limited. Consistent with results from the present study, Lackermair *et al.*,[11] in the ECLS-SHOCK I trial, did not observe significant difference in 1-year survival with and without ECMO. However, long-term mortality in that trial was very low (19–38%) compared to our study, as well as with the recent large trials in cardiac arrest survivors, and even lower than the 30-day mortality reported in other randomized trials with ECMO in cardiogenic shock.[6–8,11–13] On the other hand, the long-term mortality rate in the present study (68%) is greater than that from the Hypothermia During ECMO (HYPO-ECMO) trial[14] and registries,[15] indicating that the ECMO-CS cohort was extremely sick, which can be explained by the enrolment of subjects with cardiogenic shock of various aetiologies including decompensated chronic heart failure and therapy with higher doses of vasopressors that was required for enrolment. Comparable long-term mortality to the ECMO-CS trial was also observed in the recent Danish–German Cardiogenic Shock (DanGer Shock) trial.[16]

In contrast to other three studies comparing ECMO and standard care, patients who underwent resuscitation for cardiac arrest were not eligible for the ECMO-CS trial. The reason for exclusion of cardiac arrest survivors in the ECMO-CS trial included differences in haemodynamic profile, guideline-recommended therapy and, particularly, cause of death compared with other patients with cardiogenic shock.[17,18] Comatose cardiac arrest survivors were also excluded in the DanGer Shock trial, currently the only study that demonstrates benefit of MCS (Impella) in acute myocardial infarction-related cardiogenic shock.[16]

In the ECMO-CS trial, downstream use of ECMO in the conservative arm was permitted in case of failure of conservative therapy and further haemodynamic worsening defined per protocol as elevation of blood lactate level by 3 mmol/L. In fact, a substantial proportion of patients in the early conservative arm (39%) received ECMO later in the course of the treatment. Therefore, the results of the ECMO-CS trial should be interpreted as a comparison of immediate ECMO with an early conservative strategy, not as a comparison of ECMO versus no ECMO. It is noteworthy that despite the use of ECMO was not recommended in the conservative arms of the EURO SHOCK and ECLS-SHOCK II trials, 6% and 12% of patients respectively, also received ECMO in these studies and also other types of MCS in the ECLS-SHOCK II trial.[7,8]

Subgroup analysis suggested a significant interaction between treatment strategy and 1-year mortality in subgroups according to baseline blood pressure. It is important to note that at the time of baseline mean arterial pressure measurement, all patients were already treated with inotropes and vasopressors based on the inclusion criteria. Subjects with a baseline mean arterial pressure <63 mmHg had a better chance to benefit from an early ECMO strategy compared to those with higher mean arterial pressure. Mean arterial pressure is significantly associated with severity of shock and prognosis,[19] implying that patients with more advanced cardiogenic shock at presentation might benefit from early ECMO. Moreover, a numerically higher vasoactive-inotropic score or inotropic score in patients with lower mean arterial pressure indicates that the reason for low blood pressure was not inadequate conservative therapy. Based on this hypothesis-generated finding, severe hypotension despite conservative therapy with inotropes and vasopressors might help to identify patients who may benefit from ECMO. This observation in the ECMO-CS study where cardiac arrest survivors have been excluded may contrast with the ECLS-SHOCK II population, where the majority of patients suffered cardiac arrest before being diagnosed with cardiogenic shock and therefore their hypotension might have been caused by post-resuscitation syndrome, rather than primary cardiac dysfunction. And, consequently, a chance for ECMO to improve outcome in post-resuscitation syndrome may substantially differ resulting in no benefit in any of the subgroups in the ECLS-SHOCK II trial.[8] On the other hand, Moller *et al.*[16] in the DanGer Shock trial report similar observation in subgroup analysis as in the present study – benefit from Impella in patients with baseline mean arterial pressure ≤63 mmHg and no benefit in subjects with mean arterial pressure >63 mmHg.

Our study had several limitations. First, all participants were Caucasian, given that the trial recruited participants exclusively in the Czech Republic, which may limit the generalizability of our results to other racial or ethnic groups. There was also no upper age limit for enrolment but exclusion criteria included life expectancy <1 year. Second, the trial was designed and the sample size was calculated to find a difference in a composite primary outcome at 30 days. Therefore, all other results must be considered exploratory, including analysis of secondary outcomes and, especially, the post-hoc subgroup analysis. Third, as mentioned above, the trial did not compare ECMO with conservative therapy but immediate ECMO with an early conservative strategy permitting 'bailout' ECMO implementation in case of failure of conservative treatment and further haemodynamic worsening. The results should, therefore, be interpreted accordingly. Moreover, the baseline arterial pressure and inotrope/vasopressor doses correspond with the status at randomization. Unfortunately, the time from onset of symptoms or onset of shock was not recorded and was not included in the inclusion/exclusion criteria. The ECMO-CS trial also randomized patients who were transferred from other hospitals or departments because of cardiogenic shock. Therefore, we cannot identify subjects where ECMO was used as 'salvage' therapy and 'early implantation' refers to the time from presentation. Fourth, the trial was unblinded and the endpoints were not adjudicated. Finally, inclusion criteria were based on shock severity defined by intensity of vasoactive therapy, haemodynamic or metabolic parameters, and the evidence of cardiac pump failure, not on specific aetiologies. However, exclusion criteria included several specific conditions that may cause or influence cardiogenic shock, including high suspicion of pulmonary embolism, cardiac tamponade, bradycardia, tachycardia, aortic regurgitation, or obstructive hypertrophic cardiomyopathy. Moreover, as mentioned above, those who survived cardiac arrest were also excluded.

Therefore, our results cannot be generalized to all aetiologies of shock and to all concomitant conditions.

In conclusion, among patients with severe or rapidly progressing cardiogenic shock, immediate initiation of ECMO did not improve clinical outcomes at 1 year compared with early conservative strategy. However, an early ECMO strategy may be beneficial in patients with severe shock despite conservative therapy with inotropes and vasopressors.

Supplementary Information

Additional supporting information may be found online in the Supporting Information section at the end of the article.

Funding

The ECMO-CS study was supported by a grant from the Czech Health Research Council No. 15-27994A. The present analysis was co-funded by the Charles University in Prague, Cooperatio Cardiovascular Sciences.

Conflict of interest: P.O. has received speaker's honoraria from Abiomed, Edwards, Fresenius and Getinge. J.B. has received speaker's honoraria from Abiomed, Getinge and Resuscitec. All other authors have nothing to disclose.

References

1. McDonagh TA, Metra M, Adamo M, Gardner RS, Baumbach A, Böhm M, *et al.* 2021 ESC Guidelines for the diagnosis and treatment of acute and chronic heart failure: Developed by the Task Force for the diagnosis and treatment of acute and chronic heart failure of the European Society of Cardiology (ESC). With the special contribution of the Heart Failure Association (HFA) of the ESC. *Eur J Heart Fail* 2022;**24**:4–131. https://doi.org/10.1002/ejhf.2333
2. Thiele H, Akin I, Sandri M, de Waha-Thiele S, Meyer-Saraei R, Fuernau G, *et al.*; CULPRIT-SHOCK Investigators. One-year outcomes after PCI strategies in cardiogenic shock. *N Engl J Med* 2018;**379**:1699–1710. https://doi.org/10.1056/NEJMoa1808788
3. Thiele H, Akin I, Sandri M, Fuernau G, de Waha S, Meyer-Saraei R, *et al.*; CULPRIT-SHOCK Investigators. PCI strategies in patients with acute myocardial infarction and cardiogenic shock. *N Engl J Med* 2017;**377**:2419–2432. https://doi.org/10.1056/NEJMoa1710261
4. Heidenreich PA, Bozkurt B, Aguilar D, Allen LA, Byun JJ, Colvin MM, *et al.* 2022 AHA/ACC/HFSA Guideline for the management of heart failure: A report of the American College of Cardiology/American Heart Association Joint Committee on Clinical Practice Guidelines. *Circulation* 2022;**145**:e895–e1032. https://doi.org/10.1161/CIR.0000000000001063
5. Brunner S, Guenther SPW, Lackermair K, Peterss S, Orban M, Boulesteix AL, *et al.* Extracorporeal life support in cardiogenic shock complicating acute myocardial infarction. *J Am Coll Cardiol* 2019;**73**:2355–2357. https://doi.org/10.1016/j.jacc.2019.02.044
6. Ostadal P, Rokyta R, Karasek J, Kruger A, Vondrakova D, Janotka M, *et al.*; ECMO-CS Investigators. Extracorporeal membrane oxygenation in the therapy of cardiogenic shock: Results of the ECMO-CS randomized clinical trial. *Circulation* 2023;**147**:454–464. https://doi.org/10.1161/CIRCULATIONAHA.122.062949
7. Banning AS, Sabate M, Orban M, Gracey J, López-Sobrino T, Massberg S, *et al.* Venoarterial extracorporeal membrane oxygenation or standard care in patients with cardiogenic shock complicating acute myocardial infarction: The multicentre, randomised EURO SHOCK trial. *EuroIntervention* 2023;**19**:482–492. https://doi.org/10.4244/EIJ-D-23-00204
8. Thiele H, Zeymer U, Akin I, Behnes M, Rassaf T, Mahabadi AA, *et al.*; ECLS-SHOCK Investigators. Extracorporeal life support in infarct-related cardiogenic shock. *N Engl J Med* 2023;**389**:1286–1297. https://doi.org/10.1056/NEJMoa2307227
9. Zeymer U, Freund A, Hochadel M, Ostadal P, Belohlavek J, Rokyta R, *et al.* Venoarterial extracorporeal membrane oxygenation in patients with infarct-related cardiogenic shock: An individual patient data meta-analysis of randomised trials. *Lancet* 2023;**402**:1338–1346. https://doi.org/10.1016/S0140-6736(23)01607-0
10. Ostadal P, Rokyta R, Kruger A, Vondrakova D, Janotka M, Smíd O, *et al.* Extra corporeal membrane oxygenation in the therapy of cardiogenic shock (ECMO-CS): Rationale and design of the multicenter randomized trial. *Eur J Heart Fail* 2017;**19**:124–127. https://doi.org/10.1002/ejhf.857
11. Lackermair K, Brunner S, Orban M, Peterss S, Orban M, Theiss HD, *et al.* Outcome of patients treated with extracorporeal life support in cardiogenic shock complicating acute myocardial infarction: 1-year result from the ECLS-SHOCK study. *Clin Res Cardiol* 2021;**110**:1412–1420. https://doi.org/10.1007/s00392-020-01778-8
12. Lemkes JS, Janssens GN, van der Hoeven NW, Jewbali LSD, Dubois EA, Meuwissen MM, *et al.* Coronary angiography after cardiac arrest without ST segment elevation: One-year outcomes of the COACT randomized clinical trial. *JAMA Cardiol* 2020;**5**:1358–1365. https://doi.org/10.1001/jamacardio.2020.3670
13. Dankiewicz J, Cronberg T, Lilja G, Jakobsen JC, Levin H, Ullén S, *et al.*; TTM2 Trial Investigators. Hypothermia versus normothermia after out-of-hospital cardiac arrest. *N Engl J Med* 2021;**384**:2283–2294. https://doi.org/10.1056/NEJMoa2100591
14. Levy B, Girerd N, Amour J, Besnier E, Nesseler N, Helms J, *et al.*; HYPO-ECMO Trial Group and the International ECMO Network (ECMONet). Effect of moderate hypothermia vs normothermia on 30-day mortality in patients with cardiogenic shock receiving venoarterial extracorporeal membrane oxygenation: A randomized clinical trial. *JAMA* 2022;**327**:442–453. https://doi.org/10.1001/jama.2021.24776
15. Sterling LH, Fernando SM, Talarico R, Qureshi D, van Diepen S, Herridge MS, *et al.* Long-term outcomes of cardiogenic shock complicating myocardial infarction. *J Am Coll Cardiol* 2023;**82**:985–995. https://doi.org/10.1016/j.jacc.2023.06.026
16. Moller JE, Engstrom T, Jensen LO, Eiskjær H, Mangner N, Polzin A, *et al.*; DanGer Shock Investigators. Microaxial flow pump or standard care in infarct-related cardiogenic shock. *N Engl J Med* 2024;**390**:1382–1393. https://doi.org/10.1056/NEJMoa2312572
17. Josiassen J, Lerche Helgestad OK, Moller JE, Kjaergaard J, Hoejgaard HF, Schmidt H, *et al.* Hemodynamic and metabolic recovery in acute myocardial infarction-related cardiogenic shock is more rapid among patients presenting with out-of-hospital cardiac arrest. *PLoS One* 2020;**15**:e0244294. https://doi.org/10.1371/journal.pone.0244294
18. Nolan JP, Sandroni C, Bottiger BW, Cariou A, Cronberg T, Friberg H, *et al.* European Resuscitation Council and European Society of Intensive Care Medicine Guidelines 2021: Post-resuscitation care. *Resuscitation* 2021;**161**:220–269. https://doi.org/10.1016/j.resuscitation.2021.02.012
19. Burstein B, Tabi M, Barsness GW, Bell MR, Kashani K, Jentzer JC. Association between mean arterial pressure during the first 24 hours and hospital mortality in patients with cardiogenic shock. *Crit Care* 2020;**24**:513. https://doi.org/10.1186/s13054-020-03217-6

D. Rob et al.

Effect of intra-arrest transport, extracorporeal cardiopulmonary resuscitation and immediate invasive assessment in refractory out-of-hospital cardiac arrest: a long-term follow-up of the Prague OHCA trial

Critical Care
Impact Factor: 8,8

rejstřík

Critical Care

RESEARCH

Open Access

Effect of intra-arrest transport, extracorporeal cardiopulmonary resuscitation and immediate invasive assessment in refractory out-of-hospital cardiac arrest: a long-term follow-up of the Prague OHCA trial

Daniel Rob[1], Klaudia Farkasovska[1], Marketa Kreckova[1], Ondrej Smid[1], Petra Kavalkova[1], Jaromir Macoun[2], Michal Huptych[3], Petra Havrankova[4], Juraj Gallo[4], Jan Pudil[1], Milan Dusik[1], Stepan Havranek[1], Ales Linhart[1] and Jan Belohlavek[1*]

Abstract

Background Randomized data evaluating the impact of the extracorporeal cardiopulmonary resuscitation (ECPR) approach on long-term clinical outcomes in patients with refractory out-of-hospital cardiac arrest (OHCA) are lacking. The objective of this follow-up study was to assess the long-term clinical outcomes of the ECPR-based versus CCPR approach.

Methods The Prague OHCA trial was a single-center, randomized, open-label trial. Patients with witnessed refractory OHCA of presumed cardiac origin, without return of spontaneous circulation, were randomized during ongoing resuscitation on scene to conventional CPR (CCPR) or an ECPR-based approach (intra-arrest transport, ECPR if ROSC is not achieved prehospital and immediate invasive assessment).

Results From March 2013 to October 2020, 264 patients were randomized during ongoing resuscitation on scene, and 256 patients were enrolled. Long-term follow-up was performed 5.3 (interquartile range 3.8–7.2) years after initial randomization and was completed in 255 of 256 patients (99.6%). In total, 34/123 (27.6%) patients in the ECPR-based group and 26/132 (19.7%) in the CCPR group were alive (log-rank $P = 0.01$). There were no significant differences between the treatment groups in the neurological outcome, survival after hospital discharge, risk of hospitalization, major cardiovascular events and quality of life. Of long-term survivors, 1/34 (2.9%) in the ECPR-based arm and 1/26 (3.8%) in the CCPR arm had poor neurological outcome (both patients had a cerebral performance category score of 3).

Conclusions Among patients with refractory OHCA, the ECPR-based approach significantly improved long-term survival. There were no differences in the neurological outcome, major cardiovascular events and quality of life between the groups, but the trial was possibly underpowered to detect a clinically relevant difference in these outcomes.

*Correspondence:
Jan Belohlavek
jan.belohlavek@vfn.cz
Full list of author information is available at the end of the article

Trial registration ClinicalTrials.gov Identifier: NCT01511666, Registered 19 January 2012.

Keywords Out-of-hospital cardiac arrest, Extracorporeal membrane oxygenation, Extracorporeal cardiopulmonary resuscitation, Long-term, Quality of life

Background

Out-of-hospital cardiac arrest (OHCA) is a leading cause of death in Western countries. Despite extensive efforts to improve OHCA outcomes, the survival rate of hospital discharge remains low, averaging approximately 8% [1]. Most resuscitated OHCA patients do not respond to conventional cardiopulmonary resuscitation (CCPR) and fail to achieve a return of spontaneous circulation (ROSC) [2, 3]. In this context the use of veno-arterial extracorporeal membrane oxygenation (VA ECMO) during ongoing resuscitation, a technique known as extracorporeal cardiopulmonary resuscitation (ECPR), could be a promising intervention in selected patients with refractory OHCA [2–5].

Two single-center, randomized trials (ARREST and Prague OHCA) have presented results suggesting the survival benefit of advanced logistics and ECPR over CCPR at 30 and 180 days [2, 3, 6, 7]. However, in the Prague OHCA trial, ECPR-based approach did not significantly improve survival with neurologically favorable outcome at 180 days compared with CCPR and the trial was possibly underpowered to detect a clinically relevant difference for this outcome [2]. A multicenter, randomized trial (INCEPTION) showed no survival difference between ECPR and CCPR approaches for refractory OHCA at 30 and 180 days post-cardiac arrest [8]. These divergent findings may be attributed to several factors, including variations in system organization, the presence or absence of standardized protocols, different intervals from cardiac arrest to ECPR, case volume and post-resuscitation care. Most importantly, they stress the need for further research as ECPR is resource-intensive, posing significant challenges for prehospital and hospital systems.

Evidence from observational retrospective studies suggests good long-term survival and encouraging but impaired quality of life (QoL) in ECPR patients [5, 9, 10]. However, no randomized data are available on long-term clinical outcomes of the ECPR-based approach in patients with refractory OHCA.

Therefore, we conducted a long-term follow-up of the Prague OHCA trial to assess differences in clinical outcomes between the ECPR-based approach and CCPR and to analyze QoL in long-term survivors.

Methods

Study design

The Prague OHCA study was a single-center, prospective, open-label, randomized clinical trial that compared an ECPR-based approach (including early intra-arrest transport, ECPR if ROSC is not achieved prehospital and immediate invasive assessment and therapy) to a CCPR in patients with refractory OHCA: the trial design and results of up to 180 days after OHCA have been published previously [2, 7, 11]. The long-term follow-up of patients was planned and prospectively conducted, but there was no prespecified follow-up statistical analysis plan in the original study protocol and present study is a secondary analysis of RCT [11].

The study was approved by the Institutional Review Board of the General University Hospital and First Faculty of Medicine, Charles University, Prague (192/11 S-IV). Each participant's legal representative was informed of the study enrollment and asked for written informed consent as soon as possible. All patients who regained normal neurological function were asked to provide written permission to use their data. Consent requirements were waived for patients who died at the scene and never reached the hospital and those without known legal representatives. Additional ethical approval was obtained for the long-term follow-up (100/21 S-IV). The trial complied with the Declaration of Helsinki and is registered at www.clinicaltrials.gov (ClinicalTrials.gov Identifier: NCT01511666).

Participants

Adults aged 18–65 years receiving ongoing resuscitation for witnessed OHCA of presumed cardiac etiology were eligible for enrollment in the trial, given that they had received a minimum of 5 min of advanced cardiac life support without ROSC and when the ECPR team was available at the cardiac center. Patients who had unwitnessed cardiac arrest or presumed noncardiac cause, had suspected or confirmed pregnancy, attained ROSC within 5 min during initial resuscitation, regained consciousness, had obvious lifelimiting comorbidities, bleeding diathesis, known do-not resuscitate order, or known prearrest cerebral performance category (CPC) 3 or greater were excluded [2, 11, 12].

Randomization and masking

Between March 1, 2013, and October 25, 2020, 264 patients were randomized and 256 enrolled in the study to the ECPR-based arm or CCPR arm using a web-based secured randomization system that assigned patient numbers and intervention groups before hospitalization during ongoing CPR in the field [2]. Randomization into the standard strategy or invasive strategy group was based on 4 strata (men ≤ 45 years, men > 45 years, women ≤ 45 years, women > 45 years), with block size of 8. The block size was not disclosed to research personnel [2]. Functional assessments during follow-up were conducted by qualified evaluators who were blinded to group allocation.

Long-term follow-up

The follow-up of the present study includes all participants of the original study and initiates at the start of the index event (cardiac arrest) for all patients. All survivors of the index hospitalization were invited to the planned follow-up, including routine outpatient visits to the Heart Failure Center of the General University Hospital in Prague. The schedule for all visits at the outpatient clinic was initially set for 180 days after the index event and continued every six months thereafter. Additional visits were arranged as necessary, based on the patient's clinical status. All-cause mortality and events were determined based on follow-up data and hospital records and confirmed by mortality data from the Czech Central Insurance Database. Any clinical event was verified by hospital or general practitioner records. Long-term follow-up was performed by a cardiologist, a neurologist and a study nurse, either in the outpatient clinic or by telephone. Neurologic outcome during the follow-up was assessed by a neurologist masked to treatment allocation using CPC scores [12]. The CPC scale ranges from 1 to 5, with 1 representing good cerebral performance or minor disability, 2 moderate disability, 3 severe disability, 4 coma or vegetative state and 5 brain death. In addition, a structured interview was done with a functional status questionnaire (the EQ5D5L, www.euroqol.org) and a modified Rankin scale (mRS) with a study nurse masked to treatment allocation. The modified Rankin scale ranges from 0 to 6, with 0 indicating no symptoms, 1 no clinically significant disability, 2 slight disability, 3 moderate disability, 4 moderately severe disability, 5 severe disability and 6 death [13].

Intention-to-treat, crossovers, as-treated, per protocol population

During the trial, crossovers from the CCPR strategy to the ECPR-based strategy (and vice versa) occurred [2]. In the CCPR to ECPR-based strategy, the decision was made based on the request of an emergency physician. At least two additional unsuccessful defibrillations were required after randomization before the cardiac center coordinator accepted a crossover. The crossover from ECPR to the CCPR strategy was accepted when continuing care with invasive measures was deemed futile. All crossovers occurred during the initial CPR phase (no late crossovers transpired).

The primary analysis of the current study endpoints is done according to the randomization group, and data from patients who crossed over were analyzed by the original group assignment respecting the intention-to-treat principle. The as-treated analysis is a post hoc analysis that pooled all randomized patients according to their treatment allocation after the accepted crossover. The per-protocol analysis is a post hoc analysis that includes only those patients who completed the treatment originally allocated (excluding all crossovers). Some 20/256 patients (7.8%) were crossed over (11 crossovers from the CCPR group to the ECPR-based group and 9 from the ECPR-based group to the CCPR group). Details about crossovers appear in the original report [2].

Study endpoints

The primary outcome of the long-term follow-up was survival. The secondary outcome was neurological outcome assessed by CPC [12] (a CPC of 1–2 was considered a good neurological outcome and a CPC of 3–5 a poor neurological outcome) and mRS scores (a mRS score of 0–3 was regarded as a good outcome and a score of 4–6 a poor outcome) [13]. Further exploratory outcomes included the occurrence of major events after discharge (all-cause death, all-cause hospitalization, all-cause cardiovascular hospitalization, myocardial infarction, stroke, hospitalization for heart failure and ventricular arrhythmias), assessment of symptoms of heart failure using the New York Heart Association (NYHA) classification and QoL using the EQ5D5L (www.euroqol.org) questionnaire and the EQ visual analog scale.

Statistical analysis

Data were analyzed according to the intention-to-treat principle, with an additional analysis according to the as-treated and per-protocol principle for the primary and secondary outcome. All exploratory outcomes were analyzed according to the intention-to-treat principle only. Sample size determination of the original study was computed for the 180-day outcomes [11]; there was no formal power analysis for the long-term follow-up. Differences in survival rates were assessed using the Kaplan–Meier estimator with the log-rank test. To compare the treatment arms other endpoints were evaluated by the χ2test

or the exact Barnard method for binary endpoints. Differences in EQ visual analogue scale were assessed using Welch's t-test. For the construction of 95% confidence intervals and corresponding p-values of rehospitalizations, the test of relative risk was employed. A two-sided $P < 0.05$ was considered statistically significant. Statistical analyses were performed using the R (R Core Team, 2021) software, version 4.2.3 [14].

Results

Patients and follow-up

From March 2013 to October 2020, 264 patients were randomized during ongoing resuscitation on scene, and 256 (97%) were eligible for the final analysis. Data on screening, randomization, crossovers, 30-day, 180-day, 1-year, 2-year and long-term survival are displayed in Fig. 1. The median long-term follow-up was 5.3 years

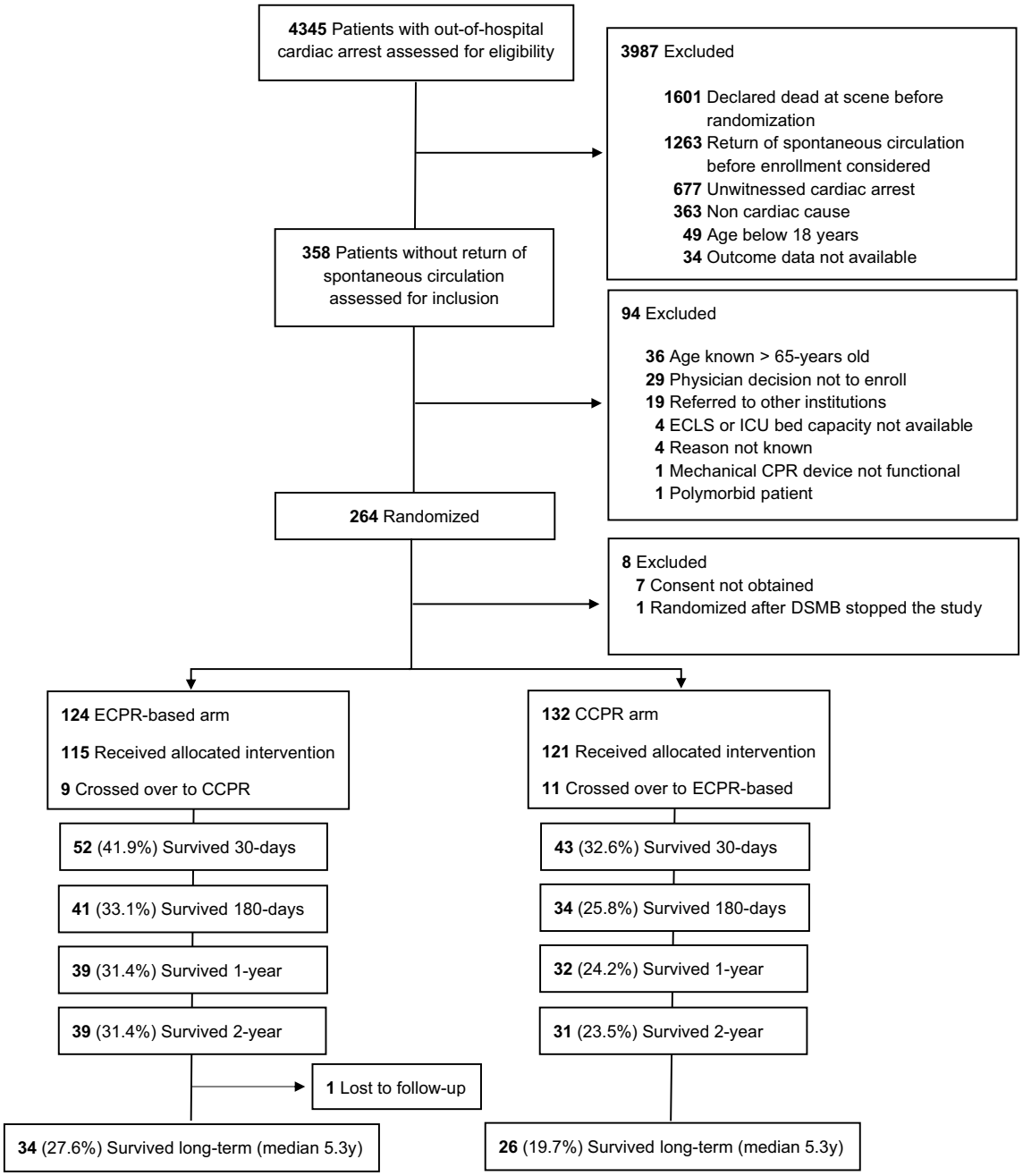

Fig. 1 Trial profile. *CCPR* conventional cardiopulmonary resuscitation, *CPR* cardiopulmonary resuscitation, *ECPR* extracorporeal cardiopulmonary resuscitation

(interquartile range, IQR 3.8–7.2 years) after initial randomization and was completed in 255 of 256 patients (99.6%). The last follow-up visit was performed on 23 May 2023, > 10 years after the randomization of the first patient on 12 May 2013.

Baseline and cardiac arrest characteristics

Baseline characteristics, published previously [2], were well balanced between treatment groups. The median age at randomization was 59 years (IQR 48–66) in the ECPR-based group and 57 years (IQR 47–65) in the CCPR group; 82% of patients in the ECPR-based and 83% in the CCPR group were men. Ventricular fibrillation was the most common initial rhythm (72/124 patients (58%) in the ECPR group and 84/132 (64%) in the CCPR group) [2]. Patients were randomized during ongoing CPR after a median of 24 min (min) (IQR 21–30) in the ECPR-based group and 26 min (IQR 19–31) in the CCPR strategy group after the collapse [2].

Long-term survival

In the intention-to-treat population, 34/123 patients (27.6%) in the ECPR-based group and 26/132 patients (19.7%) in the CCPR group were alive at the last follow-up (log-rank $P=0.01$) (Fig. 2A).

For the per-protocol population, 34/114 patients (29.8%) in the ECPR-based group and 22/121 patients (18.2%) in the CCPR group were alive at the last follow-up (log-rank $P=0.008$) (Fig. 2B).

For the as-treated population 38/125 patients (30.4%) in the ECPR-based group and 22/130 patients (16.9%) in the CCPR group were alive at the last follow-up (log-rank $P<0.001$) (Fig. 2C).

Long-term neurological outcome

In the intention-to-treat population, no significant differences were observed between the treatment groups in the CPC and mRS categories (Table 1). A good neurological outcome (CPC 1 or 2) occurred in 33/123 patients (26.8%) in the ECPR-based group and 25/132 patients (18.9%) in the CCPR group (RR 0.90, CI 0.79–1.03, $P=0.13$). Similar results were found for the mRS category (Table 1).

Among long-term survivors, only 1/34 patients (2.9%) in the ECPR-based group and 1/26 patients (3.8%) in the CCPR group had a poor neurological outcome (both with CPC scores = 3) (Table 1). The evolution of neurological outcome results assessed by CPC between 30-day, 180-day, and the last follow-up for ECPR-based and CCPR group is depicted in Fig. 3A–C. The numbers of patients in each CPC category at 30-day, 180-days, 1-year, 2-year, and the last follow-up are described in Additional file 1: Table S1.

For the per-protocol population, a good neurological outcome (CPC 1 or 2) occurred in 33/114 patients (28.9%) in the ECPR-based group and 21/121 patients (17.4%) in the CCPR group (RR 0.86, CI 0.75–0.99, $P=0.035$). Similar findings were observed for the mRS category (Additional file 1: Table S2).

In the as-treated population, a good neurological outcome (CPC 1 or 2) occurred in 37/125 patients (29.6%) in the ECPR-based group and 21/130 patients (16.2%) in the CCPR group (RR 0.84, CI 0.73–0.96, $P=0.007$). Similar findings were observed for the mRS category (Additional file 1: Table S3).

Long-term risk of events and rehospitalization

During the follow-up, 39/123 patients (31.7%) in the ECPR-based group and 30/132 (22.7%) in the CCPR group were discharged from the hospital or long-term hospital facilities after the index event ($P=0.11$) (median time to discharge 19.5 days, IQR 12.5–32 days). Of these, 4/39 (10.3%) patients in the ECPR-based group and 6/30 (20%) in the CCPR group died during the follow-up (relative risk 0.51 [0.16–1.66], $P=0.26$). Detailed causes of death are provided in the Additional file 1: Table S4. At least one rehospitalization occurred in 30/39 patients (76.9%) in the ECPR-based group and 18/30 (60%) in the CCPR group (relative risk, RR 1.28 [95%CI 0.91–1.8], $P=0.15$). At least one cardiovascular rehospitalization occurred in 25/39 patients (64.1%) in the ECPR-based group and 15/30 (50%) in the CCPR group (RR 1.28

(See figure on next page.)

Fig. 2 **A** Kaplan–Meier plot showing cumulative patient survival from index cardiac arrest to last follow-up for the intention-to-treat population. *CCPR* conventional cardiopulmonary resuscitation, *ECPR* extracorporeal cardiopulmonary resuscitation. **B** Kaplan–Meier plot showing cumulative patient survival from index cardiac arrest to last follow-up for the per-protocol population. *The per-protocol analysis is a post hoc analysis that includes only those patients who completed the treatment originally allocated (excluding all crossovers, 20/256 patients (7.8%) were crossed over, 11 crossovers from the CCPR group to the ECPR-based group and 9 from the ECPR-based group to the CCPR group). *CCPR* conventional cardiopulmonary resuscitation, *ECPR* extracorporeal cardiopulmonary resuscitation. **C** Kaplan–Meier plot showing cumulative patient survival from index cardiac arrest to last follow-up for the as-treated population. *The as-treated analysis is a post hoc analysis that pooled all randomized patients according to their treatment allocation after the accepted crossover (20/256 patients (7.8%) were crossed over, 11 crossovers from the CCPR group to the ECPR-based group and 9 from the ECPR-based group to the CCPR group). *CCPR* conventional cardiopulmonary resuscitation, *ECPR* extracorporeal cardiopulmonary resuscitation

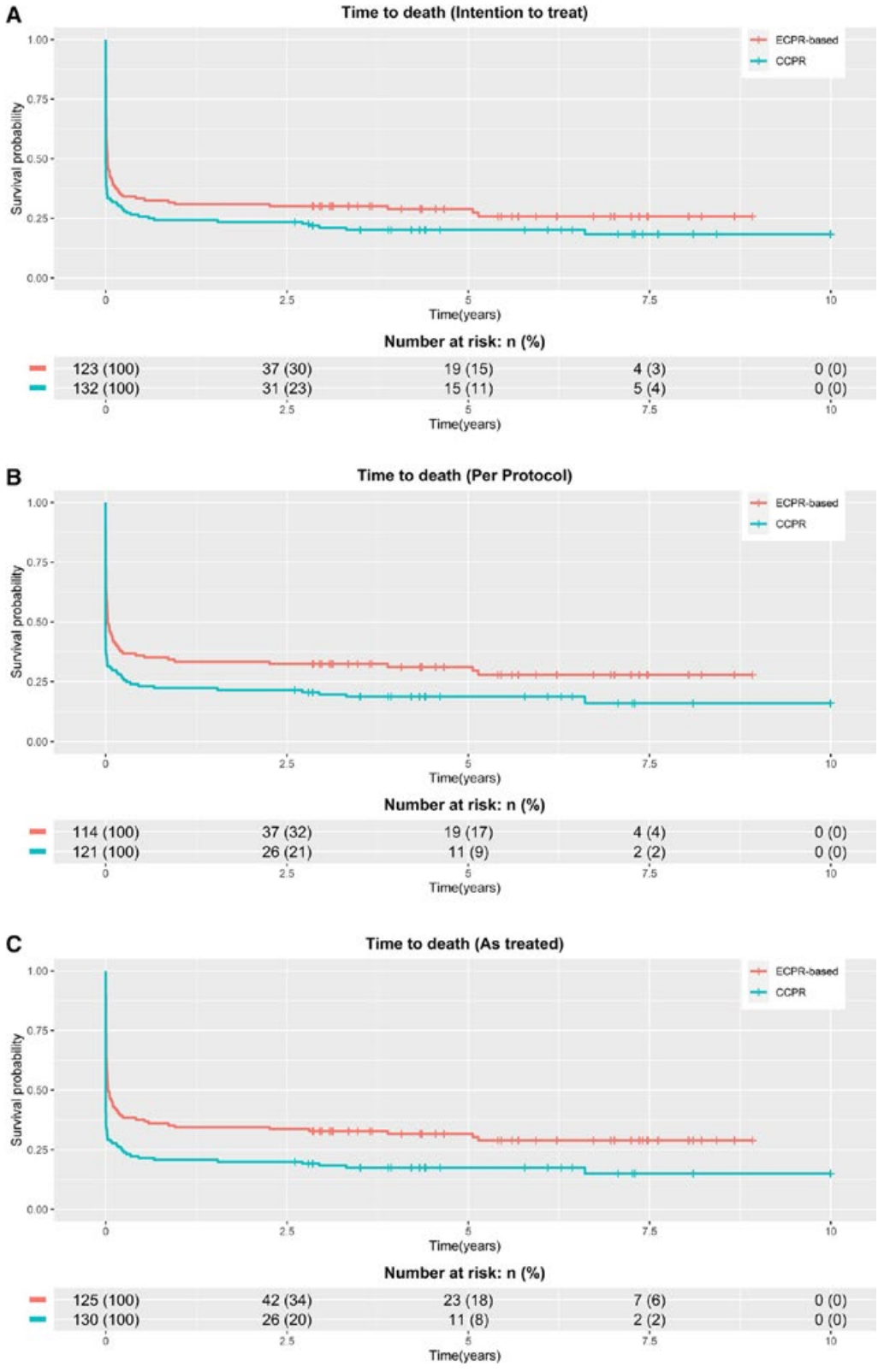

Fig. 2 (See legend on previous page.)

Table 1 Neurological outcome of patients assessed by CPC and mRS at the last follow-up (median 5.3 years, IQR 3.8–7.2 years), by treatment groups, intention-to-treat analysis

CPC category	ECPR-based ($n=123$)	CCPR ($n=132$)	*P* value*
1	30 (24.4%)	25 (18.9%)	0.133
2	3 (2.4%)	0	
3	1 (0.8%)	1 (0.8%)	
4	0	0	
5	89 (72.4%)	106 (80.3%)	
mRS category			P value*
0	2 (1.6%)	6 (4.5%)	0.133
1	17 (13.8%)	12 (9.1%)	
2	12 (9.8%)	7 (5.3%)	
3	2 (1.6%)	0	
4	1 (0.8%)	0	
5	0	1 (0.8%)	
6	89 (72.4%)	106 (80.3%)	

CCPR conventional cardiopulmonary resuscitation, *CPC* cerebral performance category, *ECPR* extracorporeal cardiopulmonary resuscitation, *mRS* modified Rankin scale

*The *P*-value testing was conducted for CPC 1–2 versus CPC 3–5 and mRS 0–3 versus 4–6

[95%CI 0.84–1.97], $P=0.26$). The frequency of major cardiovascular events, presented in Table 2, was low in both groups. Most of these rehospitalizations were attributable to staged cardiovascular procedures, and details are provided in Additional file 1: Table S5.

Functional status and quality of life

Among long-term survivors, 57/60 (95%) were in NYHA class I or II (94.1% in the ECPR-based group and 96.1% in the CCPR group, $P=0.74$). Details of the health profile assessed by the EQ-5D-5L are summarized in Table 3. There were no significant differences in QoL between the two treatment groups. The mean EQ-VAS value was 71.0 (± 19.9) in the ECPR-based group and 76.3 (± 18.3) in the CCPR group ($P=0.30$).

Discussion

In this long-term follow-up to a randomized controlled trial, an ECPR-based approach to refractory OHCA was associated with a significant survival benefit compared to CCPR. The survival benefit was observed in the intention-to-treat, per-protocol and as-treated populations. The importance of this finding is underlined because most patients in this cohort are middle-aged adults (the median age in the ECPR-based group was 59 years) with prolonged resuscitations. Moreover, our data suggest that the ECPR-based approach as a resource-intensive method translates into long-term benefits.

In terms of neurological outcomes, in both the CPC and mRS assessments, our study did not identify a significant difference between the study groups in the intention-to-treat analysis. This finding is consistent with the results observed at the 180-day mark [2]. However, it is important to note that the trial may have been underpowered to detect a clinically relevant difference. In contrast to the intention-to-treat analysis, both the per-protocol and as-treated analyses of neurological outcomes demonstrated a benefit of the ECPR-based strategy over CCPR. Nevertheless, these findings should be interpreted cautiously as they are hypothesis-generating only. A larger RCT to address neurological outcomes associated with the ECPR-based and CCPR strategies, including an assessment of minimal or no neurological impairment, is imperative.

Limited data are available on long-term outcomes in the refractory OHCA population [9, 10]. A retrospective observational analysis of patients who received ECPR for refractory ventricular fibrillation from Minnesota showed a 27% survival at 1 year, close to our results with a 1-year survival of 31% in the ECPR-based group [9]. Another retrospective analysis of the consecutive in-hospital cardiac arrest and OHCA cases treated with ECPR from Germany also showed 31% survival at 1 year [10]. The Minnesota analysis focused on survival and compared OHCA survivors to patients with heart failure who received heart transplantation or a left ventricular assist device and did not provide data on neurological outcome and QoL [9].

Another important finding is comparable survival between the ECPR-based and CCPR groups after discharge home from the hospital or long-term hospital facilities. This finding aligns with data from a Danish retrospective observational study showing similar survival rates between OHCA survivors treated with CCPR or mechanical circulatory support devices after hospital discharge [15]. Findings from our and the Danish study also suggest that overall long-term survival after discharge (90% in our ECPR-based group and 89% in the Danish study) is comparable to that seen in patients with short time to ROSC, who have the highest chance of in-hospital survival.

An additional noteworthy result of this study is that only two long-term survivors exhibited advanced neurological impairment with no difference between the ECPR-based and CCPR groups. However, these patients regained consciousness but remained dependent on long-term care. This result has several important implications. First, it suggests that severe neurological impairment is rare in refractory OHCA survivors after 180 days. Secondly, it underscores the significance of long-term survival as a relevant endpoint for follow-up. Our results

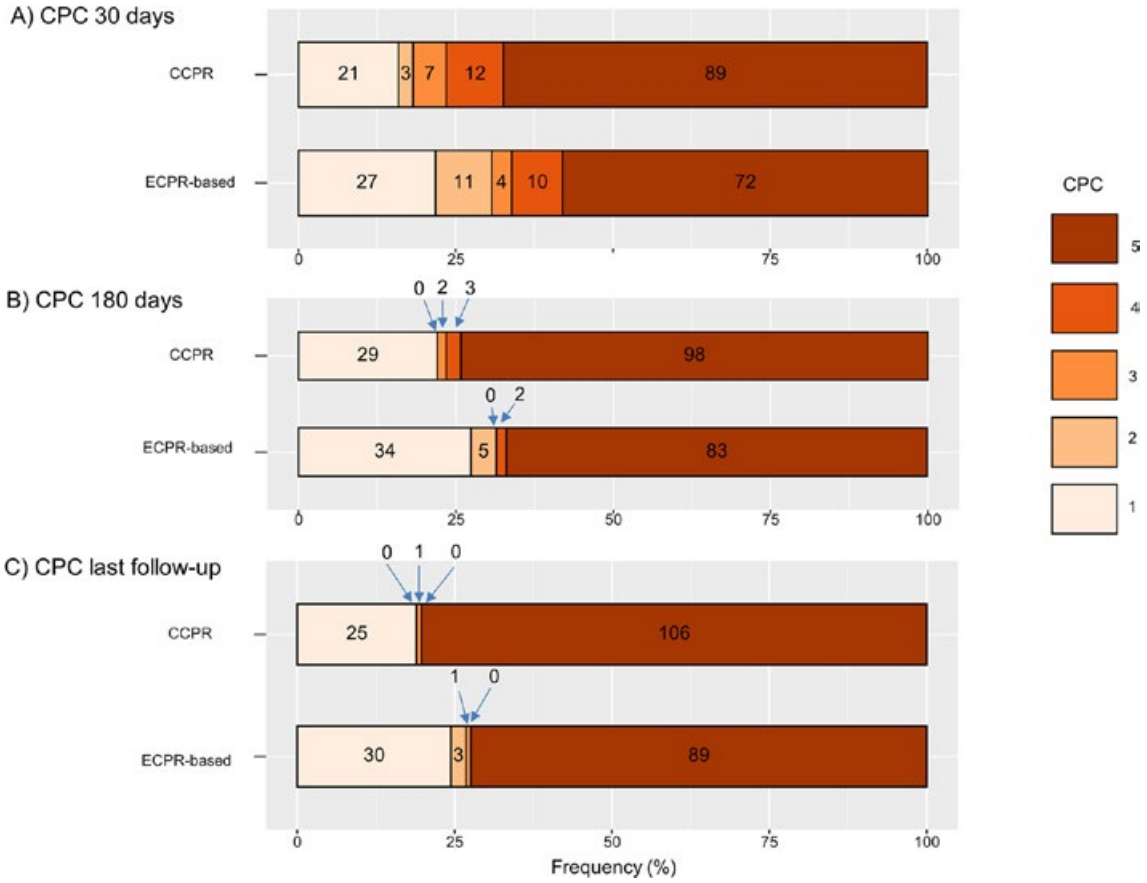

Fig. 3 Neurological outcome results assessed by CPC at 30-day (**A**), 180-day (**B**) and the last-follow-up (median 5.3 years, IQR 3.8–7.2 years) (**C**) for CCPR group and ECPR-based group. *CCPR* conventional cardiopulmonary resuscitation, *CPC* cerebral performance category, *ECPR* extracorporeal cardiopulmonary resuscitation

Table 2 Clinical events after index hospitalization during follow-up among patients discharged home from the hospital or long-term facility, by treatment groups, intention-to-treat analysis

Event	ECPR-based ($n=39$)	CCPR ($n=30$)	Relative risk (95% CI)	*P* value
All-cause death	4 (10.3%)	6 (20%)	0.51 [0.16–1.66]	0.26
All-cause hospitalization	30 (76.9%)	18 (60%)	1.28 [0.91–1.8]	0.15
All-cause cardiovascular hospitalizations	25 (64.1%)	15 (50%)	1.28 [0.84–1.97]	0.26
Myocardial infarction	1 (2.6%)	1 (3.3%)	NA	0.91
Stroke	0	1 (3.3%)	NA	0.34
Heart failure hospitalization	2 (5.1%)	3 (10%)	NA	0.57
Hospitalization for ventricular arrhythmia	1 (2.6%)	3 (10%)	NA	0.22

CCPR conventional cardiopulmonary resuscitation, *ECPR* extracorporeal cardiopulmonary resuscitation

are supported by observational studies [10, 15] and a randomized trial [16] reporting good neurological outcomes in most OHCA survivors.

Contrary to these findings from European centers, an observational study from South Korea [17] reported a high proportion of severe neurological impairment in OHCA survivors treated with CCPR at 1 year (34% of patients with a CPC score of 3 or 4). These poor neurological outcomes in the South Korean study were probably caused by low rates (36%) of bystander CPR and an initial shockable rhythm (15%). Our results are derived from a selected refractory OHCA population with high rates of bystander CPR (99%) and initial shockable rhythms (60%) and are therefore not generalizable to

Table 3 EQ-5D results, numbers and percentages of patients reporting problems in different dimensions at the last follow-up (median 5.3 years, IQR 3.8–7.2 years), by treatment groups, intention-to-treat analysis

EQ5D dimension	ECPR-based ($n=34$)	CCPR ($n=26$)	*P* value*
Mobility			
Level 1	21 (61.7%)	17 (65.4%)	
Level 2	6 (17.6%)	3 (11.5%)	1
Level 3	4 (11.8%)	3 (11.5%)	
Level 4	3 (8.8%)	3 (11.5%)	
Level 5	0	0	
Self-Care			
Level 1	28 (82.3%)	21 (80.8%)	
Level 2	3 (8.8%)	2 (7.7%)	0.79
Level 3	2 (5.9%)	2 (7.7%)	
Level 4	1 (2.9%)	1 (3.8%)	
Level 5	0	0	
Usual activity			
Level 1	25 (73.5%)	21 (80.8%)	
Level 2	3 (8.8%)	0	0.96
Level 3	3 (8.8%)	4 (15.4%)	
Level 4	3 (8.8%)	1 (3.8%)	
Level 5	0	0	
Pain/discomfort			
Level 1	18 (52.9%)	17 (65.4%)	
Level 2	10 (29.4%)	7 (26.9%)	0.34
Level 3	4 (11.8%)	2 (7.7%)	
Level 4	2 (5.9%)	0	
Level 5	0	0	
Anxiety/depression			
Level 1	24 (70.6%)	22 (84.6%)	
Level 2	7 (20.6%)	2 (7.7%)	0.96
Level 3	3 (8.8%)	2 (7.7%)	
Level 4	0	0	
Level 5	0	0	

CCPR conventional cardiopulmonary resuscitation, *ECPR* extracorporeal cardiopulmonary resuscitation

*The *P*-value testing was conducted for Level 1 + 2 versus Level 3 + 4 + 5

OHCA all-comers. Moreover, decisions regarding prognostication and withdrawal of life-sustaining therapy in patients with severe neurological impairment may differ substantially between centers, countries and regions, which may influence these results.

Moreover, few studies with limited sample sizes provided insights into the long-term neurological outcome evolution after OHCA [17–19]. Significant changes in the neurological outcome were observed between 1 and 6 months, with almost no changes occurring after 6 months, except for death. Our study confirms these findings in a randomized refractory OHCA population. However, further research in a larger population is needed as neurological recovery and outcome evolution have important consequences for long-term care decisions and outcome selection in future clinical studies. The commonly used 1-month outcomes in OHCA trials are too short to assess the effects of interventions in this population and a longer primary follow-up is needed [17–19].

Long-term follow-up data on patients discharged home after the index event in our study revealed a high number of rehospitalizations. Although the total number of major adverse cardiovascular events was relatively low, the high number of hospitalizations following discharge deserves attention. We found no study focusing on the risk of cardiovascular events and admission to hospital in OHCA survivors. However, this finding is not surprising, given that many OHCA patients have comorbidities [2, 20] and severe coronary artery disease as the underlying cause [21, 22]. Larger studies are needed to confirm our findings, but proper follow-up for this vulnerable patient cohort must be emphasized. A structured treatment program is necessary after discharge to manage the long-term sequelae of critical illness [9] and should be part of the standard care in all specialized OHCA centers.

A minority of studies reported QoL in the refractory OHCA population [10]. Our data show that a substantial proportion of patients who survived refractory OHCA experience difficulties in daily activities, but the overall QoL assessed by the EQ5D-5L and EQ-VAS show moderate to good QoL in most survivors. Additionally, our results indicate similar QoL in refractory OHCA survivors regardless of the initial treatment strategy. The observational study from Germany also revealed encouraging but impaired QoL in a small group of ECPR recipients [10]. However, a meaningful comparison with our data are not possible as the German study used a different measurement of QoL (i.e., the SF-36 health survey). Our results, with a mean EQ-VAS of 71.0 in the ECPR-based group and 76.3 in the CCPR group, are similar to EQ-VAS results reported in a large TTM2 study (mean EQ-VAS was 74 in the hypothermia group and 75 in the normothermia group) [16].

The limitations of our analysis include those of the primary trial [2]. First, the study was performed in a single high-volume OHCA center experienced in ECMO and ECPR management, restricting the generalizability of our results. Second, the sample size was small, limiting its power. Third, the study design allowed for crossover, which, although occurring at a low rate of 7.5%, may have impacted the results. Fourth, the long-term follow-up has been prospectively conducted but statistical analysis plan was not predefined in the original study protocol, and this is a secondary analysis. Finally, the as-treated and

per-protocol analyses should be considered as hypothesis-generating only.

Conclusions

Among patients with refractory OHCA, the ECPR-based approach significantly improved long-term survival. There were no differences in the neurological outcome, major cardiovascular events and quality of life between the groups but the trial was possibly underpowered to detect a clinically relevant difference in these outcomes. Only a small percentage of long-term survivors experienced severe adverse neurological outcomes. In addition, details from the follow-up reveal many survivors are rehospitalized and encounter difficulties in daily life but their overall QoL is moderate to good. These results highlight the need for comprehensive follow-up for the refractory OHCA population.

Abbreviations

CCPR	Conventional cardiopulmonary resuscitation
CPC	Cerebral performance category
ECMO	Extracorporeal membrane oxygenation
ECPR	Extracorporeal cardiopulmonary resuscitation
mRS	Modified Rankin scale
NYHA	New York Heart Association
OHCA	Out-of-hospital cardiac arrest
QoL	Quality of life

Supplementary Information

The online version contains supplementary material available at https://doi.org/10.1186/s13054-024-04901-7.

Additional file 1: Supplementary Tables S1–S5.

Acknowledgements

The authors express their gratitude to the Prague Emergency Medical Service teams and the coronary care unit, the catheterization laboratory and heart failure clinic teams of the 2nd Department of Internal Medicine, Cardiovascular Medicine, General University Hospital in Prague, for their efforts in providing quality care.

Author contributions

DR was involved in the conceptualization, data curation, formal analysis, funding acquisition, investigation, methodology, project administration, resources, validation, visualization, writing—original draft. KF contributed to the data curation, investigation, validation, visualization, writing—original draft. MK assisted in the investigation, project administration, validation, visualization, writing—review and editing. OS performed the investigation, project administration, visualization, writing—original draft. PK was involved in the data curation, investigation, project administration, visualization, writing—original draft. JM contributed to the data curation, formal analysis, methodology, validation, visualization, writing—original draft. MH contributed to the formal analysis, methodology, validation, visualization, writing—review and editing. PH was involved in the investigation, visualization, writing—review and editing. JG contributed to the investigation, visualization, writing—review and editing. JP was involved in the data curation, investigation, visualization, writing—review and editing. MD assisted in the data curation, investigation, visualization, writing—review and editing. SH performed the data curation, investigation, visualization, writing—review and editing. AL contributed to the conceptualization, supervision, visualization, writing—review and editing. JB was involved in the conceptualization, formal analysis, funding acquisition, investigation, methodology, project administration, resources, supervision, visualization, writing—original draft.

Funding

This study was supported by MH CZ–DRO-VFN00064165, General University Hospital in Prague and the Charles University Research program "Cooperatio – Intensive Care Medicine."

Availability of data and materials

The datasets used and analyzed in this study are available from the corresponding author upon reasonable request.

Declarations

Ethics approval and consent to participate

The study was approved by the Institutional Review Board of the General University Hospital and First Faculty of Medicine, Charles University, Prague. Each participant's legal representative was informed of the study enrollment and asked for written informed consent as soon as possible. All patients who regained normal neurological function were asked to provide written permission to use their data. Consent requirements were waived for patients who died at the scene and never reached the hospital and those without known legal representatives. The trial complied with the Declaration of Helsinki and is registered at www.clinicaltrials.gov (ClinicalTrials.gov Identifier: NCT01511666).

Competing interests

The corresponding author (JB) has received lecture honoraria from the Abiomed, Getinge, Xenios, Resuscitec, Novartis, Astra-Zeneca, Boegringer-Ingelheim. DR has received lecture honoraria from the Abiomed and Resuscitec. The remaining authors report no conflict of interest.

Author details

[1]2nd Department of Medicine, Department of Cardiovascular Medicine, First Faculty of Medicine, Charles University in Prague and General University Hospital in Prague, U Nemocnice 2, 128 00 Prague 2, Czech Republic. [2]Department of Probability and Mathematical Statistics, Faculty of Mathematics and Physics, Charles University in Prague, Prague, Czech Republic. [3]Czech Institute of Informatics, Robotics and Cybernetics (CIIRC), Czech Technical University in Prague, Prague, Czech Republic. [4]Department of Neurology, First Faculty of Medicine, Charles University in Prague and General University Hospital, Prague, Czech Republic.

Received: 8 February 2024 Accepted: 3 April 2024
Published online: 16 April 2024

References

1. Gräsner JT, Herlitz J, Tjelmeland IB, Wnent J, Masterson S, Lilja G, et al. European resuscitation council guidelines: epidemiology of cardiac arrest in Europe. Resuscitation. 2021;161:61–79.
2. Belohlavek J, Smalcova J, Rob D, Franek O, Smid O, Pokorna M, et al. Effect of intra-arrest transport, extracorporeal cardiopulmonary resuscitation, and immediate invasive assessment and treatment on functional neurologic outcome in refractory out-of-hospital cardiac arrest: a randomized clinical trial. JAMA. 2022;327(8):737–47.
3. Yannopoulos D, Bartos J, Raveendran G, Walser E, Connett J, Murray TA, et al. Advanced reperfusion strategies for patients with out-of-hospital cardiac arrest and refractory ventricular fibrillation (ARREST): a phase 2, single centre, open-label, randomised controlled trial. Lancet. 2020;396(10265):1807–16.
4. Lunz D, Calabrò L, Belliato M, Contri E, Broman LM, Scandroglio AM, et al. Extracorporeal membrane oxygenation for refractory cardiac arrest: a retrospective multicenter study. Intensive Care Med. 2020;46:973–82.
5. Abrams D, MacLaren G, Lorusso R, Price S, Yannopoulos D, Vercaemst L, et al. Extracorporeal cardiopulmonary resuscitation in adults: evidence and implications. Intensive Care Med. 2022;48(1):1–15.
6. Belohlavek J, Yannopoulos D, Smalcova J, Rob D, Bartos J, Huptych M, et al. Intraarrest transport, extracorporeal cardiopulmonary resuscitation,

and early invasive management in refractory out-of-hospital cardiac arrest: an individual patient data pooled analysis of two randomised trials. EClinicalMedicine 2023;59.
7. Rob D, Smalcova J, Smid O, Kral A, Kovarnik T, Zemanek D, et al. Extracorporeal versus conventional cardiopulmonary resuscitation for refractory out-of-hospital cardiac arrest: a secondary analysis of the Prague OHCA trial. Crit Care. 2022;26(1):1–9.
8. Suverein MM, Delnoij TS, Lorusso R, Brandon Bravo Bruinsma GJ, Otterspoor L, Elzo Kraemer CV, et al. Early extracorporeal CPR for refractory out-of-hospital cardiac arrest. N Engl J Med. 2023;388(4):299–309.
9. Alexy T, Kalra R, Kosmopoulos M, Bartos JA, Elliott A, Gutierrez Bernal A, et al. Initial hospital length of stay and long-term survival of patients successfully resuscitated using extracorporeal cardiopulmonary resuscitation for refractory out-of-hospital cardiac arrest. Eur Heart J Acute Cardiovasc Care. 2023;12(3):175–83.
10. Spangenberg T, Schewel J, Dreher A, Meincke F, Bahlmann E, van der Schalk H, et al. Health related quality of life after extracorporeal cardiopulmonary resuscitation in refractory cardiac arrest. Resuscitation. 2018;127:73–8.
11. Belohlavek J, Kucera K, Jarkovsky J, Franek O, Pokorna M, Danda J, et al. Hyperinvasive approach to out-of-hospital cardiac arrest using mechanical chest compression device, prehospital intraarrest cooling, extracorporeal life support and early invasive assessment compared to standard of care. A randomized parallel groups comparative study proposal. J Transl Med. 2012;10(1):1–13.
12. Jennett B, Bond M. Assessment of outcome after severe brain damage: a practical scale. Lancet. 1975;305(7905):480–4.
13. Van Swieten JC, Koudstaal PJ, Visser MC, Schouten HJ, Van Gijn J. Interobserver agreement for the assessment of handicap in stroke patients. Stroke. 1988;19(5):604–7.
14. R Core Team. R (2023): A language and environment for statistical computing. R Foundation for Statistical Computing, Vienna, Austria. URL https://www.R-project.org/.
15. Mørk SR, Bøtker MT, Christensen S, Tang M, Terkelsen CJ. Survival and neurological outcome after out-of-hospital cardiac arrest treated with and without mechanical circulatory support. Resuscitation plus. 2022;10:100230.
16. Dankiewicz J, Cronberg T, Lilja G, Jakobsen JC, Levin H, Ullén S, et al. Hypothermia versus normothermia after out-of-hospital cardiac arrest. N Engl J Med. 2021;384(24):2283–94.
17. Kim YJ, Ahn S, Sohn CH, Seo DW, Lee YS, Lee JH, et al. Long-term neurological outcomes in patients after out-of-hospital cardiac arrest. Resuscitation. 2016;101:1–5.
18. Lim C, Verfaellie M, Schnyer D, Lafleche G, Alexander MP. Recovery, long-term cognitive outcome and quality of life following out-of-hospital cardiac arrest. J Rehabil Med. 2014;46(7):691.
19. Raina KD, Rittenberger JC, Holm MB, Callaway CW. Functional outcomes: one year after a cardiac arrest. BioMed Res Int 2015;2015.
20. Andrew E, Nehme Z, Bernard S, Smith K. The influence of comorbidity on survival and long-term outcomes after out-of-hospital cardiac arrest. Resuscitation. 2017;110:42–7.
21. Yannopoulos D, Bartos JA, Raveendran G, Conterato M, Frascone RJ, Trembley A, et al. Coronary artery disease in patients with out-of-hospital refractory ventricular fibrillation cardiac arrest. J Am Coll Cardiol. 2017;70(9):1109–17.
22. Rob D, Kavalkova P, Smalcova J, Kral A, Kovarnik T, Zemanek D, et al. Coronary angiography and percutaneous coronary intervention in cardiac arrest patients without return of spontaneous circulation. Resuscitation. 2022;175:133–41.

Publisher's Note

P. Wohlfahrt et al.

Development and validation of a prognostic score integrating remote heart failure symptoms and clinical variables in mortality risk prediction after myocardial infarction: the PragueMi score

European Journal of Preventive Cardiology
Impact Factor: 8,6

‹ rejstřík

ESC European Society of Cardiology

European Journal of Preventive Cardiology (2024) **31**, 1713–1720
https://doi.org/10.1093/eurjpc/zwae114

FULL RESEARCH PAPER
Coronary artery disease

Development and validation of a prognostic score integrating remote heart failure symptoms and clinical variables in mortality risk prediction after myocardial infarction: the PragueMi score

Peter Wohlfahrt [1,2]*, Dominik Jenča[3,4], Vojtěch Melenovský[3], Josef Stehlik[5], Jolana Mrázková[6], Marek Šramko[2,3], Martin Kotrč[3], Michael Želízko[3], Věra Adámková[1], Jan Piťha[3], and Josef Kautzner [3,7]

[1]Department of Preventive Cardiology, Institute for Clinical and Experimental Medicine, Videnska 1958/9, Prague 140 21, Czech Republic; [2]First Medical School, Charles University, Katerinska 1660/32, Prague 120 00, Czech Republic; [3]Department of Cardiology, Institute for Clinical and Experimental Medicine (IKEM), Prague, Czech Republic; [4]Third Medical School, Charles University, Prague, Czech Republic; [5]Division of Cardiovascular Medicine, University of Utah School of Medicine, Salt Lake City, UT, USA; [6]Experimental Medicine Centre, Institute for Clinical and Experimental Medicine (IKEM), Prague, Czech Republic; and [7]Medical and Dentistry School, Palacký University, Olomouc, Czech Republic

Received 2 January 2024; revised 17 February 2024; accepted 11 March 2024; online publish-ahead-of-print 18 March 2024

See the editorial comment for this article 'Being a cardiologist looking in the mirror of prognosis assessment: who am I, a wizard or a mathematician?', by P. Agostoni *et al.*, https://doi.org/10.1093/eurjpc/zwae127.

Aims While heart failure (HF) symptoms are associated with adverse prognosis after myocardial infarction (MI), they are not routinely used for patients' stratification. The primary objective of this study was to develop and validate a score to predict mortality risk after MI, combining remotely recorded HF symptoms and clinical risk factors, and to compare it against the guideline-recommended Global Registry of Acute Coronary Events (GRACE) score.

Methods and results A cohort study design using prospectively collected data from consecutive patients hospitalized for MI at a large tertiary heart centre between June 2017 and September 2022 was used. Data from 1135 patients (aged 64 ± 12 years, 26.7% women), were split into derivation (70%) and validation cohort (30%). Components of the 23-item Kansas City Cardiomyopathy Questionnaire and clinical variables were used as possible predictors. The best model included the following variables: age, HF history, admission creatinine and heart rate, ejection fraction at hospital discharge, and HF symptoms 1 month after discharge including walking impairment, leg swelling, and change in HF symptoms. Based on these variables, the PragueMi score was developed. In the validation cohort, the PragueMi score showed superior discrimination to the GRACE score for 6 months [the area under the receiver operating curve (AUC) 90.1, 95% confidence interval (CI) 81.8–98.4 vs. 77.4, 95% CI 62.2–92.5, $P = 0.04$) and 1-year risk prediction (AUC 89.7, 95% CI 83.5–96.0 vs. 76.2, 95% CI 64.7–87.7, $P = 0.004$).

Conclusion The PragueMi score combining HF symptoms and clinical variables performs better than the currently recommended GRACE score.

Lay summary

- The prognosis of patients after myocardial infarction is heterogeneous. Thus, risk stratification is needed to identify and intervene patients at increased risk. While heart failure (HF) symptoms are associated with adverse prognosis, they are not used for patients' stratification.
- We have developed and internally validated the PragueMi score, which integrates clinical risk factors at the time of hospitalization and HF symptoms determined remotely by a questionnaire 1 month after hospital discharge.
- PragueMi score was able to better stratify patients' risk as compared with the currently recommended Global Registry of Acute Coronary Events score.

* Corresponding author. Tel: +420 739 777 242, Email: wohlfp@gmail.com

Graphical Abstract

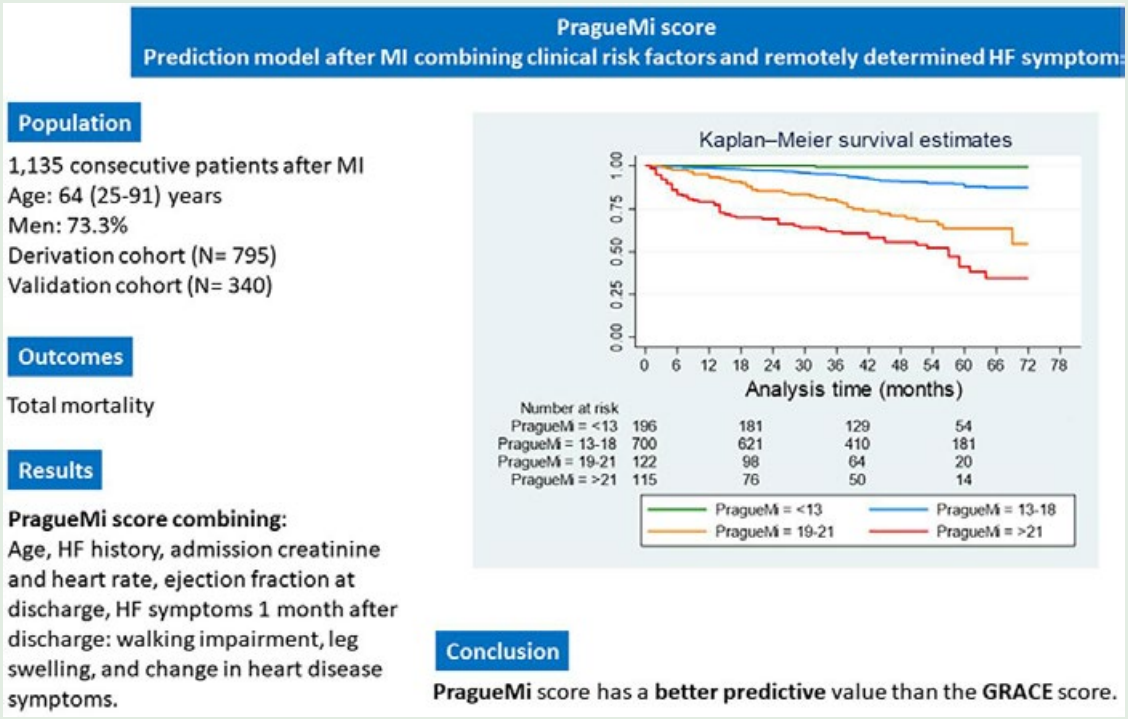

Keywords Myocardial infarction • Heart failure • Symptoms • Risk prediction • Questionnaire • Mortality

Introduction

For optimal management of patients recovering from a myocardial infarction (MI), identification of individuals at increased risk of adverse outcomes is essential. This allows targeted proactive interventions in at-risk patients to improve their symptoms, function, and survival. The Global Registry of Acute Coronary Events (GRACE) score has been recommended by the guidelines to stratify patients' risk after MI.[1] However, discrimination of the GRACE model for 1-year mortality evaluated by the area under the receiver operating curve (AUC) is within the 0.82–0.89 range.[2] Thus, a better performing model is of clinical need.

Heart failure (HF) is a common complication of MI, developing in up to 40% of patients and increasing total mortality risk by three-fold.[3] The GRACE score evaluates HF using the Killip class. However, the Killip classification evaluates only pulmonary congestion, neglecting other HF symptoms. Furthermore, many patients develop HF symptoms early after hospital discharge. Interestingly, HF developing later after MI is associated with higher mortality risk as compared with HF developing at MI presentation.[4] Thus, evaluation of HF symptoms and signs is an important goal of post-discharge visits.

For decades, clinicians have been using unstructured questions on HF symptoms. Nevertheless, unstructured questioning is time-consuming, influenced by the physician's subjective interpretation, and may not be consistently done in all patients, and as such limits actionability. Our previous research showed that structured HF symptom evaluation using the Kansas City Cardiomyopathy Questionnaire (KCCQ) identifies HF symptoms in two out of five patients after MI[5] and identifies patients at increased mortality risk.[6] We hypothesized that the integration of HF symptoms with clinical risk factors may provide superior risk prediction after MI beyond the GRACE score. This may better define a high-risk group that may benefit from a more proactive approach and pharmacological and non-pharmacological therapy of HF.

The objectives of this study were as follows: (i) to select KCCQ items and clinical factors associated with total mortality risk after MI, (ii) to create a prognostic score (PragueMI score) based on identified variables in the derivation cohort, and (iii) to compare the predictive value of the PragueMi score against the GRACE score in the validation cohort.

Methods

Population

In this cohort design study, we have used data from the prospective Institute for Clinical and Experimental Medicine Acute Myocardial Infarction Registry (AMBITION registry).[7] The registry collects clinical data and biospecimens from consecutive patients hospitalized for acute coronary syndrome since June 2017 at the Institute for Clinical and Experimental Medicine, Prague, Czech Republic, a tertiary heart centre with around-the-clock coronary intervention service. The Fourth Universal Definition of Myocardial Infarction has been used.[8] Patients underwent a detailed interview during their hospital stay, and additional information was obtained from medical record abstraction and laboratory studies. One month after discharge, patients were asked to complete the 23-item KCCQ. Because most patients did not have HF, in the questionnaire, we have replaced 'heart failure' with 'heart disease'. The patients had a choice of completing the KCCQ through an online application or on a paper form returned by regular mail.

The inclusion criterion was hospitalization for MI between June 2017 and September 2022. Patients with missing KCCQ were excluded from this analysis. Death was ascertained through June 2023. Mortality data were provided by the Institute of Health Information and Statistics of the

Czech Republic (UZIS), which keeps a list of all deceased persons and dates of death in the Czech Republic by law. This study was approved by a local ethics committee and complies with the Declaration of Helsinki.

Primary outcome

The primary outcome of the analysis was all-cause mortality.

Global Registry of Acute Coronary Events score

The Eagle model estimates for death within 6 months after discharge was used.[9] Variables included in the model were age, heart rate, systolic blood pressure, creatinine level, troponin elevation, ST segment depression on initial electrocardiogram **(**ECG), previous history of MI and HF, and percutaneous coronary intervention (PCI).

Statistical methods

Continuous variables are presented as mean and SDs or medians and interquartile range (IQR). Nominal variables are shown as counts and percentages.

All consecutive patients hospitalized for MI between June 2017 and September 2022 were included in this analysis. No formal power calculation was performed.

To identify factors associated with mortality risk after MI, we have used restricted cubic splines adjusted for age. This allowed us to detect non-linear associations and to categorize continuous variables. We have used Cox regression with both forward and backward selection to identify factors independently associated with the mortality risk. Potential variables selection was based on a literature search and included the following factors: age, admission heart rate, systolic blood pressure, creatinine level, fasting glycaemia, glycated haemoglobin, haemoglobin, maximal troponin level, ST segment depression on initial ECG, ST-elevation myocardial infarction (STEMI), previous history of MI, HF or PCI, ejection fraction at hospital discharge, and KCCQ items. Variables independently associated with the mortality risk in the derivation cohort were used for the PragueMi score creation. We have used regression coefficients to create relative weights for each category. To compare the performance of the PragueMi score as compared with the GRACE score, we have used the following methods: (i) assessment of the difference in the area under the receiver operating characteristic curve (AUC), (ii) the Brier score, and (iii) the continuous net reclassification improvement (NRI).

The AUC is an overall measure of model discrimination. It measures the model's ability to distinguish between patients with and without events. The AUC ranges from 0 to 1, where 0.5 indicates a random classification and 1 signifies a perfect classifier. To compare differences in AUC, we have used the Delong–Delong test using the R riskRegression package.[10]

The Brier score is a measure of model calibration. It is calculated as the mean squared difference between the predicted probability and the actual outcome. The Brier score for a perfectly calibrated model is 0.[11] The riskRegression package was also used to calculate the Brier score at different time points.[10]

The NRI quantifies how well a new model reclassifies subjects—either appropriately or inappropriately—as compared with an old model.[12] We have used the R nricens package for continuous NRI calculation.

Statistical analyses were conducted with R statistical software version 4.2.2 (R Foundation for Statistical Computing, Vienna, Austria), SPSS version 25.0 (IBM Corporation, Armonk, NY, USA), and STATA version 17 (StataCorp, College Station, TX, USA). All statistical tests and confidence intervals were two sided with a significance level of 0.05.

Results

Population

Between June 2017 and September 2022, 1769 patients were hospitalized for MI. Of these, 69 (3.9%) had missing KCCQ due to death within 1 month after hospital discharge. In total, 1135 (66.8% of eligible) patients had available both clinical data and KCCQ that patients filled 1 month after hospital discharge. A comparison of patients with available and missing KCCQ is shown in Supplementary material online, *Table S1*.

Table 1 Characteristics of the derivation and validation cohort

	Derivation cohort	Validation cohort
Total, No	795	340
Age, years	64.7 ± 11.5	63.7 ± 12.8
Female sex, *n* (%)	208 (26.2)	95 (27.9)
Risk factors		
Current smoking, *n* (%)	331 (41.6)	126 (37.1)
Arterial hypertension, *n* (%)	507 (63.8)	208 (61.2)
Diabetes, *n* (%)	153 (19.2)	72 (21.2)
CVD history		
Previous MI, *n* (%)	96 (12.1)	36 (10.6)
Heart failure history, *n* (%)	31 (3.9)	13 (3.8)
Previous PCI, *n* (%)	112 (14.1)	41 (12.1)
Previous CABG, *n* (%)	34 (4.3)	11 (3.2)
Previous stroke, *n* (%)	49 (6.2)	23 (6.8)
Clinical characteristics at MI presentation		
STEMI, *n* (%)	471 (59.2)	211 (62.2)
Heart rate, b.p.m.	76 ± 18	77 ± 19
Systolic BP, mmHg	144 ± 26	146 ± 25
Cardiac arrest, *n* (%)	23 (2.9)	11 (3.2)
Killip class		
I, *n* (%)	650 (81.8)	287 (84.4)
II, *n* (%)	115 (14.5)	42 (12.4)
III, *n* (%)	21 (2.6)	9 (2.6)
IV, *n* (%)	9 (1.1)	2 (0.6)
Creatinine, mmol/L	83.8 (71.5–100.5)	83.1 (70.5–100.6)
ST depression, *n* (%)	125 (15.7)	40 (11.8)
EF below 35%, *n* (%)	112 (14.1)	44 (12.9)
Outcomes		
Primary composite outcome, *n* (%)	105 (13.2)	43 (12.6)
Death, *n* (%)	103 (13.0)	43 (12.6)

CABG, Coronary artery bypass grafting; STEMI, ST-elevation myocardial infarction; BP, blood pressure; EF, ejection fraction.

Patients not included in this analysis due to missing KCCQ were slightly older and required more often cardiopulmonary resuscitation before hospital admission, while maximal troponin and mortality were similar in those included and not included in this analysis. The study CONSORT diagram is shown in Supplementary material online, *Figure S1*.

During a median follow-up of 46 months (IQR 29–61), 146 (12.9%) patients died. The study population was randomly split into derivation (70%, $n = 795$) and validation cohort (30%, $n = 340$).

Model development

Demographic characteristics of the 795 patients in the derivation cohort are shown in *Table 1*. Restricted cubic splines for age and age-adjusted continuous variables are shown in *Figure 1*. Based on cubic splines, categories of continuous variables were created and used in the multivariate Cox model. Forward and backward variable selection was used to create the final model. The final model included the following variables: age, HF history, admission creatinine and heart rate, ejection

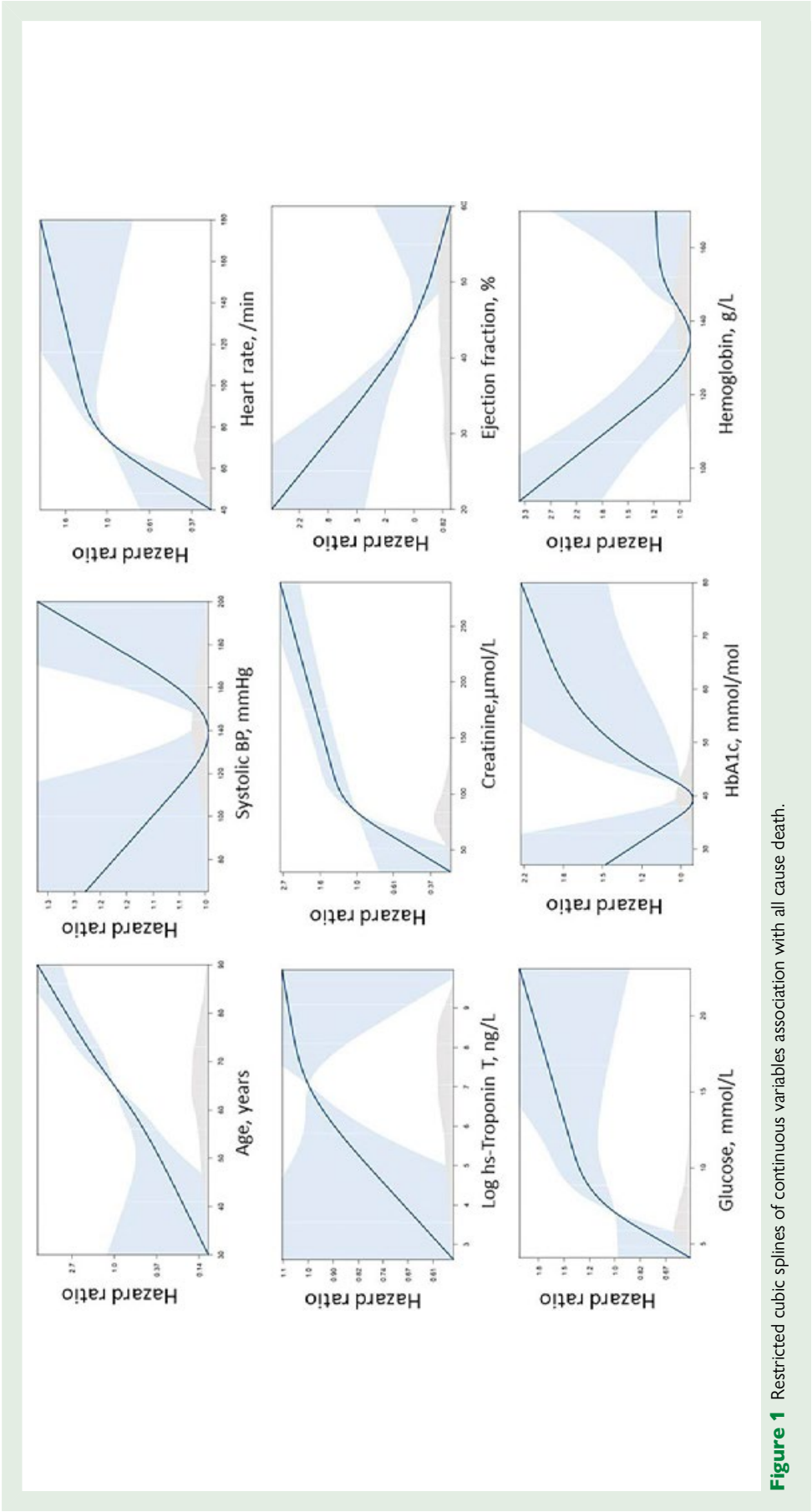

Figure 1 Restricted cubic splines of continuous variables association with all cause death.

Table 2 PragueMi score

No.	Variables	Levels	Score
1.	**Age, years**	≤45	1
		46–49	2
		50–69	4
		70–79	6
		≥80	10
2.	**Creatinine, μmol/L**	<100	1
		100–119	3
		120–159	4
		≥160	7
3.	**Heart rate, /min**	< 50	1
		50–69	3
		70–99	4
		≥100	7
4.	**Discharge EF, %**	≤35	3
		>35	1
5.	**Heart failure history**	No	1
		Yes	3
6.	**Walking 1 block on ground level**		
		Extremely limited	4
		Quite a bit limited	2
		Moderately limited	2
		Slightly limited	1
		Not at all limited	1
		Limited for other reasons	4
7.	**Compared with 2 weeks ago, have your symptoms of heart disease (shortness of breath, fatigue, or ankle swelling) changed? My symptoms have become**		
		Much worse	3
		Slightly worse	3
		Not changed	2
		Slightly better	2
		Much better	1
		I've had no symptoms	1
8.	**Over the past 2 weeks, how much has swelling in your feet, ankles, or legs bothered you? It has been**		
		Extremely bothersome	3
		Quite a bit bothersome	3
		Moderately bothersome	1
		Slightly bothersome	1
		Not at all bothersome	1
		I've had no swelling	1

Creatinine level and heart rate at hospital admission.
Walking impairment, change in symptoms, and leg oedema evaluated at 1 month after hospital discharge.

fraction at hospital discharge, and HF symptoms evaluated by the KCCQ 1 month after discharge, which included walking impairment, leg swelling, and the change in heart disease symptoms over the last 2 weeks. Based on the regression coefficients in the final model, the PragueMi score was developed (*Table 2*). In the derivation cohort, the PragueMi score showed superior discrimination and calibration as compared with the GRACE score (*Table 3*).

Table 3 Grace and PragueMi scores comparison in the derivation (Table A) and validation cohort (Panel B)

	Model discrimination			Model calibration		Reclassification		
Time (months)	Grace score AUC (95% CI)	PragueMi score AUC (95% CI)	*P*	Delta Brier score	*P*	NRI	NRI+	NRI−
Table A								
6	75.1 (64.7–85.4)	95.0 (91.5–98.4)	<0.0001	−0.4 (−0.7 to −0.1)	0.01	2.00 (1.98–2.00)	1.00 (1.00–1.00)	1.00 (0.98–1.00)
12	74.7 (66.7–82.7)	90.1 (84.5–95.7)	<0.0001	−0.8 (−1.3 to −0.2)	0.004	2.05 (1.97–2.23)	1.11 (1.00–1.27)	0.94 (0.93–1.00)
18	73.4 (66.0–80.8)	87.0 (81.1–92.9)	<0.0001	−1.3 (−2.0 to −0.6)	<0.001	2.47 (2.26–3.11)	1.60 (1.40–2.20)	0.87 (0.83–0.92)
24	72.2 (65.1–79.3)	86.4 (80.9–91.9)	<0.0001	−1.3 (−2.0 to −0.6)	<0.001	2.39 (2.08–2.54)	1.57 (1.28–1.71)	0.82 (0.80–0.85)
36	67.9 (61.4–74.4)	82.3 (76.4–88.1)	<0.0001	−1.7 (−2.6 to −0.8)	<0.001	1.85 (1.66–2.83)	1.45 (1.28–2.30)	0.39 (0.39–0.52)
Table B								
6	77.4 (62.2–92.5)	90.1 (81.8–98.4)	0.04	−0.5 (−1.1 to 0.1)	0.099	1.13 (0.42–1.34)	0.54 (0.16–0.80)	0.59 (0.25–0.72)
12	76.2 (64.7–87.7)	89.7 (83.5–96.0)	0.004	−0.7 (−1.4 to 0.0)	0.068	1.15 (0.85–1.72)	0.56 (0.20–1.00)	0.59 (0.51–0.78)
18	71.8 (60.7–82.8)	85.6 (76.5–94.6)	0.002	−1.4 (−2.3 to −0.4)	0.005	1.14 (0.88–1.40)	0.54 (0.30–0.88)	0.60 (0.38–0.65)
24	73.3 (64.0–82.5)	84.3 (76.5–92.1)	0.003	−1.4 (−2.4 to −0.4)	0.007	0.97 (0.64–1.38)	0.39 (0.08–0.74)	0.58 (0.54–0.65)
36	69.0 (59.7–78.2)	80.1 (72.1–88.2)	0.0009	−1.6 (−2.8 to −0.3)	0.016	0.85 (0.55–1.05)	0.27 (−0.02–0.49)	0.58 (0.52–0.68)

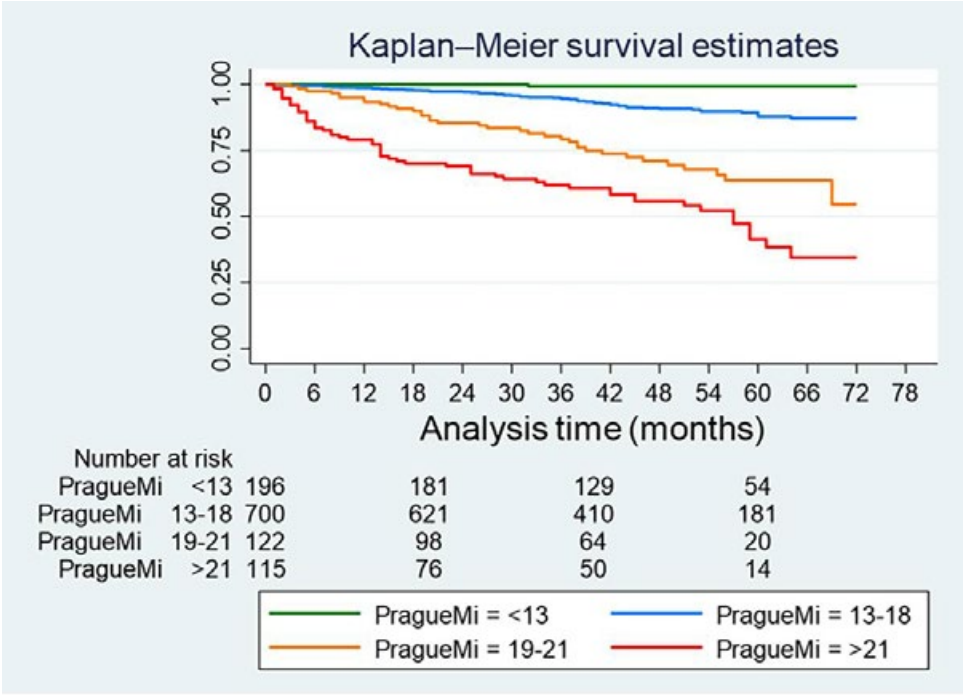

Figure 2 Kaplan–Meier survival curves by PragueMi categories.

Table 4 PragueMi score performance in different subgroups

Variables	AUC (95% CI)	P
Sex		
Male	0.87 (0.85–0.89)	0.41
Female	0.91 (0.87–0.94)	
Age, years		
≤60	0.94 (0.91–0.96)	0.19
>60	0.84 (0.81–0.87)	
eGFR, mL/min/1.73 m^2		
<60	0.83 (0.78–0.87)	0.87
≥60	0.84 (0.82–0.87)	
Diabetes		
No	0.89 (0.87–0.91)	0.63
Yes	0.86 (0.81–0.90)	
Ejection fraction, %		
>40	0.87 (0.84–0.89)	0.58
<40	0.89 (0.85–0.93)	
MI type		
Non-STEMI	0.86 (0.83–0.89)	0.41
STEMI	0.90 (0.88–0.92)	

eGFR, estimated glomerular filtration rate; STEMI, ST-elevation myocardial infarction.

Model validation

The validation cohort included 340 patients. The PragueMi score showed superior discrimination and calibration as compared with the GRACE score (*Table 3*). Over several study time points, PragueMi improved the continuous NRI, significantly improving both event and non-event NRI (*Table 3*). While the AUC and Brier scores were similar in the derivation and validation cohort, NRI was lower in the validation cohort probably due to lower statistical power in a smaller cohort.

Risk categories of the PragueMi score

Due to similar model performance in the derivation and validation cohort, we have combined them and created PragueMi risk categories based on observed risk. The Kaplan–Meier curves by PragueMi score categories are shown in *Figure 2*. The 196 patients (17.3% of the study cohort) with PragueMi score of <13 had excellent prognosis, with 100% event-free survival at 2 years. On the other hand, event-free survival in patients with PragueMi > 21 (10% of the study cohort) was 82.1% at 6 months and 77.8% at 1 year. The PragueMi score performance was consistent in different subgroups (*Table 4*).

Discussion

In this study, we show that HF symptoms evaluated remotely using a questionnaire possess an important prognostic value that adds to clinical risk factors. Our PragueMi score based on five clinical variables and three HF symptoms has superior discrimination, calibration, and risk reclassification properties as compared with the currently guideline-recommended GRACE score based only on clinical risk factors.

The prognosis of patients after MI is very heterogeneous.[13] Thus, the identification of patients at increased mortality risk is of clinical need. This allows a personalized approach to secondary prevention with intervention targeted at individuals that benefit the most.

Until now, the prediction models after MI have been only based on clinical risk factors, neglecting patients' symptoms. However, for

decades, clinicians have been searching for HF symptoms in patients after MI to identify at-risk individuals and to modify treatment accordingly.[14] Yet, this approach is time-consuming, influenced by provider skills and subjective interpretation.[15] Patient-reported outcomes coupled with modern telemedicine options allow the remote collection of patients' symptoms and empower patients to become a valuable source of clinically important data, without increasing the burden on the provider.[15]

Several previous studies have shown the utility of the KCCQ to predict prognosis in patients after MI.[6,16,17] No previous study evaluated the utility of combining patient-reported outcomes with clinical risk factors after MI. As KCCQ was developed for HF patients, not all items are relevant in patients after MI. In this study, we have identified that among the 23 KCCQ items, walking limitation, leg oedema, and change in heart disease symptoms over the last 2 weeks have the greatest predictive value among patients after MI.

In the present study, we have decided to evaluate HF symptoms 1 month after hospital discharge instead of evaluating them during the hospital stay. This decision was based on the fact that in many patients, HF symptoms develop later after discharge due to left ventricular remodelling. Furthermore, functional requirements for everyday living are higher outside of the hospital; thus, the patient may not recognize the newly developed limitations during the hospital stay.

In clinical settings, the PragueMi score may be particularly useful during post-discharge outpatient visits and also for remote monitoring of patients after discharge to identify high-risk patients who may benefit from closer follow-up and advanced therapies. As compared with other prediction scores that are based only on clinical variables, a potential barrier of the PragueMi score is that it also requires patients' symptoms evaluation. However, it includes only three easy-to-answer questions, which may also be answered remotely before the outpatient visit using an online questionnaire or dedicated app, thus decreasing the burden on providers. Furthermore, identifying HF symptoms before the outpatient visit may help to streamline the visit to this important issue.

Among discharged patients, the PragueMi score > 21 identified 10% of the population as very high risk, with 18% 6-month and 22% 12-month mortality rates, respectively. Timely identification of these patients followed by initiation or up-titration of HF pharmacotherapy and referral for advanced HF therapies such as heart transplant and left ventricular assist device has the potential to improve prognosis in these high-risk patients. Based on results of the STRONG-HF[18] study with rapid up-titration of HF pharmacotherapy, a meta-analysis of sodium-glucose transport protein 2 inhibitors use in HF,[19] and sacubitril–valsartan studies results,[20] we estimate that a multifactorial intervention targeted at these high-risk patients may decrease the mortality risk by at least 20–30%. Future randomized studies will be needed to test whether clinical decision-making based on the PragueMi score will lead to an improvement in clinical outcomes.

Study limitations

First, this is a single-centre study; thus, the model performance was only internally validated. Because no previous study systematically collected KCCQ 1 month after hospital discharge, we were unable to externally validate our model. This may limit the generalizability of our findings. However, the characteristics of our cohort are very similar to other recent cohorts of patients after MI.[21] In the future, the performance of our model needs to be tested in other cohorts. Second, due to missing KCCQ in some patients, our results may be the subject of a selection bias. However, while there were some statistically significant differences between patients with and without KCCQ available, clinically these differences are negligible. Thus, we assume that these missing data do not affect the generalizability of our results. Furthermore, in this study, we have identified the three most predictive items of the KCCQ. This reduction in the number of questions may improve the response rate in future studies. Third, data required for the PragueMi score were collected at different time points. Automated data collection of in-hospital data together with remote HF symptoms evaluation online or using an app may help to integrate PragueMi score into everyday practice without additional burden on clinicians.

The strengths of our study include a well-defined systematically collected cohort of consecutive MI patients with multiple clinical factors and remote HF symptoms evaluated as possible predictors of mortality risk.

Conclusion

Heart failure symptoms evaluated remotely using a questionnaire possess an important prognostic value that adds to clinical risk factors. The PragueMi risk score combines these predictors and has superior discrimination, calibration, and risk reclassification properties compared with the guideline-recommended GRACE score. Future studies will have to address whether clinical decision-making based on the PragueMi score can significantly improve the care of patients after MI.

Supplementary material

Supplementary material is available at *European Journal of Preventive Cardiology*.

Author contributions

P.W. conceived and designed the study and analysed the data. J.M., D.J., M.Ž., M.Š., and M.K collected the data. All authors were involved in writing and revising the manuscript and approved the final version. P.W. is the guarantor of this work and as such has full access to all the data and takes responsibility for the integrity of all data and the accuracy of the data analysis.

Funding

This study was supported by the Ministry of Health of the Czech Republic (grant number NV 19-09-00125) and by the project National Institute for Research of Metabolic and Cardiovascular Diseases (Programme EXCELES, Project No. LX22NPO5104)—funded by the European Union—Next Generation EU.

Conflict of interest: none declared.

Data availability

The data that support the findings of this study are available from the corresponding author (P.W.) upon reasonable request.

References

1. Byrne RA, Rossello X, Coughlan JJ, Barbato E, Berry C, Chieffo A, *et al.* 2023 ESC guidelines for the management of acute coronary syndromes: developed by the task force on the management of acute coronary syndromes of the European Society of Cardiology (ESC). *Eur Heart J* 2023;**44**:3720–3826.
2. Obradovic D, Loncar G, Zeymer U, Pöss J, Feistritzer H-J, Freund A, *et al.* Impact of anaemia and iron deficiency on outcomes in cardiogenic shock complicating acute myocardial infarction. *Eur J Heart Fail* 2023. Online ahead of print.
3. Jenča D, Melenovský V, Stehlik J, Staněk V, Kettner J, Kautzner J, *et al.* Heart failure after myocardial infarction: incidence and predictors. *ESC Heart Fail* 2021;**8**:222–237.
4. Gerber Y, Weston SA, Enriquez-Sarano M, Berardi C, Chamberlain AM, Manemann SM, *et al.* Mortality associated with heart failure after myocardial infarction: a contemporary community perspective. *Circ Heart Fail* 2016;**9**:e002460.
5. Wohlfahrt P, Jenča D, Stehlik J, Melenovský V, Mrázková J, Staněk V, *et al.* Heart failure-related quality-of-life impairment after myocardial infarction. *Clin Res Cardiol* 2023;**112**:39–48.

6. Wohlfahrt P, Jenča D, Melenovský V, Stehlik J, Spertus JA, Mrázková J, *et al.* Remote heart failure symptoms assessment after myocardial infarction identifies patients at risk for death. *J Am Heart Assoc* 2024;**13**:e032505.
7. Wohlfahrt P, Jenča D, Melenovský V, Šramko M, Kotrč M, Želízko M, *et al.* Trajectories and determinants of left ventricular ejection fraction after the first myocardial infarction in the current era of primary coronary interventions. *Front Cardiovasc Med* 2022;**9**: 1051995.
8. Thygesen K, Alpert JS, Jaffe AS, Chaitman BR, Bax JJ, Morrow DA, *et al.* Fourth universal definition of myocardial infarction (2018). *Circulation* 2018;**138**:e618–e651.
9. Eagle KA, Lim MJ, Dabbous OH, Pieper KS, Goldberg RJ, Van de Werf F, *et al.* A validated prediction model for all forms of acute coronary syndrome: estimating the risk of 6-month postdischarge death in an international registry. *JAMA* 2004;**291**: 2727–2733.
10. DeLong ER, DeLong DM, Clarke-Pearson DL. Comparing the areas under two or more correlated receiver operating characteristic curves: a nonparametric approach. *Biometrics* 1988;**44**:837–845.
11. Gerds TA, Schumacher M. Consistent estimation of the expected Brier score in general survival models with right-censored event times. *Biom J* 2006;**48**:1029–1040.
12. Uno H, Tian L, Cai T, Kohane IS, Wei LJ. A unified inference procedure for a class of measures to assess improvement in risk prediction systems with survival data. *Stat Med* 2013;**32**:2430–2442.
13. Spencer FA, Meyer TE, Gore JM, Goldberg RJ. Heterogeneity in the management and outcomes of patients with acute myocardial infarction complicated by heart failure. *Circulation* 2002;**105**:2605–2610.
14. Mohammad Rizwan A, Carolyn SPL, Anna S, Simon PPH, Sarah B, Francesco Z, *et al.* Symptoms and signs in patients with heart failure: association with 3-month hospitalisation and mortality. *Heart* 2024;**110**:578-585.
15. Wohlfahrt P, Stehlik J, Pan IZ, Ryan JJ. Empowering people living with heart failure. *Heart Fail Clin* 2020;**16**:409–420.
16. Kosiborod M, Soto GE, Jones PG, Krumholz HM, Weintraub WS, Deedwania P, *et al.* Identifying heart failure patients at high risk for near-term cardiovascular events with serial health status assessments. *Circulation* 2007;**115**:1975–1981.
17. Soto GE, Jones P, Weintraub WS, Krumholz HM, Spertus JA. Prognostic value of health status in patients with heart failure after acute myocardial infarction. *Circulation* 2004;**110**:546–551.
18. Mebazaa A, Davison B, Chioncel O, Cohen-Solal A, Diaz R, Filippatos G, *et al.* Safety, tolerability and efficacy of up-titration of guideline-directed medical therapies for acute heart failure (STRONG-HF): a multinational, open-label, randomised, trial. *Lancet* 2022; **400**:1938–1952.
19. Cardoso R, Graffunder FP, Ternes CMP, Fernandes A, Rocha AV, Fernandes G, *et al.* SGLT2 inhibitors decrease cardiovascular death and heart failure hospitalizations in patients with heart failure: a systematic review and meta-analysis. *eClinicalMedicine* 2021;**36**:100933.
20. Solomon SD, Vaduganathan ML, Claggett B, Packer M, Zile M, Swedberg K, *et al.* Sacubitril/valsartan across the spectrum of ejection fraction in heart failure. *Circulation* 2020;**141**:352–361.
21. Mohammad MA, Olesen KKW, Koul S, Gale CP, Rylance R, Jernberg T, *et al.* Development and validation of an artificial neural network algorithm to predict mortality and admission to hospital for heart failure after myocardial infarction: a nationwide population-based study. *Lancet Digit Health* 2022;**4**:e37–e45.

J. Hašková et al.

Efficacy and Safety of Stereotactic Radiotherapy in Patients With Recurrent Ventricular Tachycardias. The Czech Experience

JACC: CLINICAL ELECTROPHYSIOLOGY
Impact Factor: 8,0

rejstřík

JACC: CLINICAL ELECTROPHYSIOLOGY VOL. 10, NO. 4, 2024

ORIGINAL RESEARCH

VENTRICULAR ARRHYTHMIAS - RADIOTHERAPY

Efficacy and Safety of Stereotactic Radiotherapy in Patients With Recurrent Ventricular Tachycardias

The Czech Experience

Jana Hašková, MD,[a,b] Dan Wichterle, MD, PhD,[a,c] Josef Kautzner, MD, PhD,[a,b] Marek Šramko, MD, PhD,[a] Petr Peichl, MD, PhD,[a] Lukáš Knybel PEng, PhD,[d] Otakar Jiravský, MD,[e,f] Radek Neuwirth, MD,[e,f] Jakub Cvek, MD, PEng, PhD[d]

ABSTRACT

BACKGROUND Stereotactic arrhythmia radiotherapy (STAR) has been proposed recently in patients with refractory ventricular tachycardia (VT).

OBJECTIVES The purpose of this study was to describe the efficacy and safety of STAR in the Czech Republic.

METHODS VT patients were recruited in 2 expert centers after at least 1 previously failed catheter ablation (CA). A precise strategy of target volume determination and CA was used in 17 patients treated from December 2018 until June 2022 (EFFICACY cohort). This group, together with an earlier series of 19 patients with less-defined treatment strategies, composed the SAFETY cohort (n = 36). A dose of 25 Gy was delivered.

RESULTS In the EFFICACY cohort, the burden of implantable cardioverter-defibrillator therapies decreased, and this drop reached significance for direct current shocks (1.9 ± 3.2 vs 0.1 ± 0.2 per month; $P = 0.03$). Eight patients (47%) underwent repeated CA for recurrences of VT during 13.7 ± 11.6 months. In the SAFETY cohort (32 procedures, follow-up >6 months), 8 patients (25%) presented with a progression of mitral valve regurgitation, and 3 (9%) required intervention (median follow-up of 33.5 months). Two cases of esophagitis (6%) were seen with 1 death caused by the esophago-pericardial fistula (3%). A total of 18 patients (50%) died during the median follow-up of 26.9 months.

CONCLUSIONS Although STAR may not be very effective in preventing VT recurrences after failed CA in an expert center, it can still modify the arrhythmogenic substrate, and when used with additional CA, reduce the number of implantable cardioverter-defibrillator shocks. Potentially serious sides effects require close follow-up.

From the [a]Department of Cardiology, IKEM, Prague, Czech Republic; [b]Faculty of Medicine and Dentistry, Palacký University, Olomouc, Czech Republic; [c]Faculty of Medicine, Charles University, Prague, Czech Republic; [d]Department of Oncology, University Hospital Ostrava and Ostrava University Medical School, Ostrava, Czech Republic; [e]Department of Cardiology, Hospital AGEL Třinec-Podlesí, Třinec, Czech Republic; and the [f]Faculty of Medicine, Masaryk University, Brno, Czech Republic.
The authors attest they are in compliance with human studies committees and animal welfare regulations of the authors' institutions and Food and Drug Administration guidelines, including patient consent where appropriate. For more information, visit the Author Center.

Manuscript received May 3, 2023; revised manuscript received November 27, 2023, accepted December 4, 2023.

ISSN 2405-500X https://doi.org/10.1016/j.jacep.2023.12.002

Catheter ablation (CA) has become a strategy of choice for the management of electrical storm and/or recurrent ventricular tachycardias (VTs) in patients with structural heart disease of different etiology.[1-3] However, the efficacy of CA could be limited by the large size of the substrate and/or by the inability to reach its critical region for various reasons, such as deep intramyocardial location, the presence of old thrombus, or adhesions within the pericardial sac. Among alternative strategies, stereotactic body radiotherapy (SBRT) or more specifically, stereotactic arrhythmia radiotherapy (STAR), has been employed. The first case reports on the therapeutic use of STAR in cases of failed CA were published <10 years ago.[4,5] Since then, several groups published their initial experience with this strategy in relatively small clinical studies or case series.[6-10] Since our first case report,[4] the number of STAR procedures performed by our consortium increased. In the meantime, we have unified CA strategies and indicated to STAR only the patients who had VT recurrences despite repeated ablations in 1 of the 2 expert centers. We also developed a reproducible strategy of accurate image integration, ie, merging data on substrate extent and location from an electroanatomic mapping system with computed tomography (CT) scans.[11] This approach appeared important for precise targeting of the critical region of the substrate.[12]

The primary goal of this report is to describe the efficacy of STAR in a subgroup of patients with failed repeated CA in an expert center in whom the above-sophisticated planning strategy was used (EFFICACY cohort). The secondary goal is to evaluate the safety of STAR in the entire Czech patient population (SAFETY cohort).

METHODS

PATIENT POPULATION. In the EFFICACY cohort, before STAR, patients underwent 2 or more CAs for recurrent, scar-related VT in the 2 Czech expert centers, using the endocardial and/or epicardial approach, and had subsequent VT recurrences. In addition, the most accurate strategy of target volume determination was used. This cohort consisted of 17 patients treated from December 2018 until June 2022. The SAFETY cohort consisted of all cases from the EFFICACY cohort and the early series of 19 patients with a less stringent CA strategy and less exact method of STAR target determination from January 2014 through December 2018. With the 3 patients who had 2 STAR procedures, the total number of STAR procedures in the SAFETY cohort reached 39. Subjects with mechanical assist devices were excluded. All subjects were provided information about the potential benefits and risks of the treatment by a team of electrophysiologists who performed CA and radiation oncologists responsible for radiation therapy. The patients gave their written informed consent, and the Ethics Committees of all involved institutions approved the study protocol.

ARRHYTHMOGENIC SUBSTRATE DETERMINATION. In the EFFICACY cohort, regions of the substrate responsible for inducible or spontaneously occurring VTs were defined based on an integrated approach. An electroanatomic mapping system (CARTO 3, Biosense Webster, Inc) was used. In brief, 3-dimensional (3D) electroanatomic bipolar voltage maps of the left and/or right ventricles were constructed in sinus rhythm or during right ventricular pacing. The scar was defined by bipolar voltage <0.5 mV (normal tissue >1.5 mV). The dense scar was defined as areas of noncapture at an output of 10 mA and labeled in gray. Intracardiac echocardiography was used as a part of the ablation protocol to define the extent and location of the scar. All late and abnormal potentials were tagged in the maps. In addition, pace mapping during sinus rhythm was used to assess slow conduction channels and their exits. In tolerated VTs, entrainment mapping was also used to further specify the re-entrant circuit. Epicardial mapping was employed when a critical part of the substrate was suspected to be distant from the endocardium or when electrocardiography suggested epicardial origin. All the above information was used to identify critical components of re-entry VTs. In addition, the aortic arch was mapped with precise tagging of the orifice of the left main coronary artery as an anatomical landmark for CT image registration. The right ventricular implantable cardioverter-defibrillator (ICD) lead tip was annotated on the 3D map for the same reason. Patients from the earlier period had less uniform mapping and CA strategy and fewer ablations before STAR.

CATHETER ABLATION. CA was performed with an irrigated tip catheter (Thermocool or Thermocool SmartTouch, Biosense Webster, Inc) using a SmartAblate generator (Biosense Webster, Inc) and power-controlled mode (30-45 W and irrigation flow of 30 mL/min). The goal of CA was a complete modification of the substrate and non-inducibility of VTs. Eliminating late or fragmented potentials and

ABBREVIATIONS AND ACRONYMS

CA = catheter ablation
CT = computed tomography
CTV = clinical target volume
ICD = implantable cardioverter-defibrillator
LV = left ventricular
PTV = planning target volume
STAR = stereotactic arrhythmia radiotherapy
VT = ventricular tachycardia

achieving local noncapture and/or core isolation of the scar area were the main strategies of substrate modification.

CLINICAL TARGET VOLUME DETERMINATION. Since 2014, 3 different strategies of clinical target volume (CTV) determination have been used. In the initial series of 15 patients, CTV was marked by a side-by-side visual comparison of 3D electroanatomic maps of the arrhythmogenic substrate with CT scans. In the subsequent series of 6 patients, positron emission tomography/CT and body surface mapping (CardioInsight, Medtronic) during induced VTs were used to approximate the CTV. Finally, a novel strategy of co-registration of electroanatomic maps with preprocedural CT scans was used in 17 patients.[11,12]

STAR PLANNING. All patients underwent inspiratory breath-hold CT scanning with intravenous contrast enhancement before STAR. The internal target volume was calculated to account for heart contractions. The existing ICD lead was used as a fiducial marker to compensate for respiratory movements. No additional margin for planning target volume (PTV) delineation was added to reduce radiation toxicity in the initial series of 10 patients.[8] Later, we added an isometric margin of 3 mm in all patients. Since 2020 (last 10 patients), an additional 2 mm margin into the left ventricular (LV) cavity or patient-specific motion margin was employed.[13] We used the MultiPlan treatment planning system with sequential dose optimization and the CyberKnife radiosurgery system (both from Accuray, Inc). The metal deletion technique was used to evaluate how artifacts from leads influenced dose distribution. Monte Carlo dose calculation was applied to determine how proximity to lung tissues affected the dose distribution.

STAR PROCEDURE. Radiotherapy was performed in a single session without general anesthesia or sedation, as previously described.[8] The patient was placed on a robotic couch and monitored for respiratory activity. A correlation model was created between the spontaneous respiratory excursions and the movement of the lead. This enabled tracking the target volume without requiring the invasive placement of additional fiducial markers. During treatment, the manipulator synchronized its movement with the movement of the ICD lead and compensated for any deviation of the electrode position from the reference CT-scan position. In addition, x-rays were used at least once every 60 seconds to adapt to possible changes in respiratory movements. A dose of 25 Gy was optimized to cover at least 95% of the PTV. In case of conflict with dose-volume constraints for Organs at Risk, the dose and/or coverage were decreased. Irradiated ventricular segments were classified according to the recommendation of the American Heart Association.[14] The cardiologist supervised the entire procedure.

ASSESSMENT OF EFFICACY AND SAFETY. All patients were followed in the institutional outpatient clinics. The patients were evaluated every 6 months unless the clinical status changed. The follow-up visits included ICD interrogation and echocardiography. Chest x-ray was performed when clinically indicated.

Study endpoints included the first ICD therapy after STAR, assessed separately for episodes of antitachycardia pacing (ATP) and direct current (DC) shocks, repeated CA or STAR, and all-cause death. No blanking period was used. Arrhythmia burden (assessed as the average number of ATP and DC shocks per month) was investigated in 6-month periods starting 6 months before the index STAR. Acute and late radiation-induced events were evaluated using the Common Terminology Criteria for Adverse Events (CTCAE) 5.0 scale.

STATISTICAL ANALYSIS. Continuous variables were expressed as a mean ± SD or median (IQR) for non-normally distributed data, and compared by Wilcoxon signed rank test for dependent samples and Mann-Whitney *U* test for independent samples. Categorical variables were expressed as percentages and compared by Fisher exact test. In the EFFICACY cohort, Kaplan-Meier graphs were used to plot the event-free survival for individual endpoints. Arrhythmia burden was assessed in 6-month intervals before and after STAR. In a considerable proportion of patients, the duration of these periods was not exactly 6 months because of variations in the scheduling of outpatient visits (with device memory checkups) in the COVID-19 period and caused by other logistic or clinical reasons. Therefore, the rate of ICD therapies was always related to the true duration of a particular follow-up period. Analysis was performed "per patient" in the EFFICACY cohort and "per procedure" in the SAFETY cohort. The assessment of the risk for the progression of mitral valve disease associated with irradiation of basal compared with the remaining LV segments was logically the predefined analysis. It appeared subsequently that irradiation of basal inferior (and specifically basal inferolateral) segments is associated with even higher risk. Therefore, post hoc analysis was performed for the segments comprising the corresponding half and one-third of the perimitral area. A P value ≤0.05 was

considered significant. All analyses were performed using the STATISTICA Version 12 software (Statsoft Inc).

RESULTS

PATIENT POPULATION. The clinical characteristics of both patient cohorts are listed in Table 1. In the EFFICACY cohort, dilated cardiomyopathy was the underlying heart disease in 10 cases, followed by ischemic cardiomyopathy in 5. One patient had large cardiac fibroma, and another had burned-out hypertrophic cardiomyopathy. Before the STAR, patients underwent a median of 2 (Q1, Q3: 2, 3) endocardial ablations, and 10 of 17 had an epicardial approach. Two of them already had 1 prior STAR session and had VT recurrences. The SAFETY cohort consisted of 36 subjects with 3 repeated STAR procedures. The proportion of ischemic cardiomyopathy was higher in this group caused by their higher recruitment in the early phase of our experience. All patients with heart failure had optimized medical therapy before and after STAR.

TABLE 1 Baseline Characteristics of Patients

	EFFICACY Cohort (n = 17)	SAFETY Cohort (n = 36)
Men	88	92
Age, y	65 ± 11	66 ± 10
Ischemic cardiomyopathy	29	56
Coronary artery bypass grafting	24	38
Left ventricular ejection fraction, %	30 ± 10	31 ± 9
NYHA functional class	2.2 ± 0.5	2.4 ± 0.6
Brain natriuretic peptide, pg/mL	434 (204-820)	820 (390-2,540)
Diabetes mellitus	29	28
Chronic renal disease	47	28
Betablocker	94	97
Amiodarone	76	74
Sotalol	18	8
Number of prior endocardial ablations	2.2 ± 0.8	1.8 ± 0.9
Number of prior epicardial ablations	0.6 ± 0.5	0.4 ± 0.5

Values are %, mean ± SD, or median (IQR). Characteristics are calculated *"per patient"* in the EFFICACY cohort and *"per procedure"* in the SAFETY cohort.

STAR PROCEDURE. As assessed in the SAFETY cohort, the median procedure duration was 58 minutes (Q1, Q3: 50, 69 minutes; range 42-82 minutes). The median of PTV was 39.4 mL (Q1, Q3: 22.2, 62.1 mL, range 12.6-90.5 mL). The median of the isodose line with the prescribed radiation dose was 78% (Q1, Q3: 76%, 82%; range 66% to 84%), the median of the conformity index was 1.23 (Q1, Q3: 1.17, 1.31; range 1.11 to 1.78), and the median of homogeneity index was 1.28 (Q1, Q3: 1.22, 1.32; range 1.19 to 1.52).

EFFICACY OF STAR. Figure 1 provides an overview of all ablation procedures before or after the index STAR for the EFFICACY cohort and also indicates the follow-up duration until the last clinical visit or death. All patients had at least 1 CA before STAR (Figure 2). The mean follow-up period after STAR was 13.7 ± 11.6 months. During this period, 8 patients (47%) underwent at least 1 repeated CA for clinically relevant recurrences of VT (including repeated STAR in one) (Figure 3). At 1 year of follow-up, mortality reached 47%, with the rate of redo ablations 67% in surviving patients, and 50% when analyzing all subjects. Two patients (#3 and #7) died very early after STAR (within 3 months) without the indication for redo CA and 3 others died (#1, #2, and #5) without subsequent CA within 20 months (Figure 1). The lack of ICD data between the last outpatient visit and death in most deceased patients does not exclude VT recurrences treated by ICD. Virtually all surviving patients experienced some ICD therapies during the follow-up (Figure 4). The rates of DC shock and ATP at 1 year were 80% and 100%, respectively. Notably, the burden of ICD therapies decreased, and this drop reached statistical significance for ICD shocks during the follow-up (Figure 5, Table 2). However, only 10 patients survived beyond the onset of the efficacy evaluation period (6-18 months after STAR), 9 of them had analyzable data from ICD, and only 5 of them were free from re-do CA by the time of the last visit or death.

Substrate remapping and reablation were performed at a mean interval of 8 months (Q1, Q3: 2, 10 months) after STAR in 8 subjects. A total of 23 and 27 distinct VT morphologies were inducible before and after STAR, respectively. In total, 12 pairs of VTs (44%) were identified that had identical morphology before and after radiotherapy. The mean cycle length of these VT pairs decreased from 392 ± 98 ms to 456 ± 73 ms ($P = 0.03$) after STAR. The detailed analysis goes beyond the scope of this paper.

SAFETY OF STAR. Acute adverse effects (CTCAE version 5.0) were observed after 4 of 39 procedures (10%) and consisted of nausea (Grade 2 radiation-related toxicity). All of these patients responded well to setron-based antiemetic drugs administered for 3 days.

Long-term radiation-related side effects (CTCAE version 5.0) were evaluated after 32 of 39 procedures with a follow-up duration of at least 6 months. In this subgroup, the median duration of follow-up was

JACC: CLINICAL ELECTROPHYSIOLOGY VOL. 10, NO. 4, 2024
APRIL 2024:654–666

FIGURE 1 Time-Axis Plot With Historical and Follow-Up Ablation Procedures for 17 Consecutive Patients in the EFFICACY Cohort

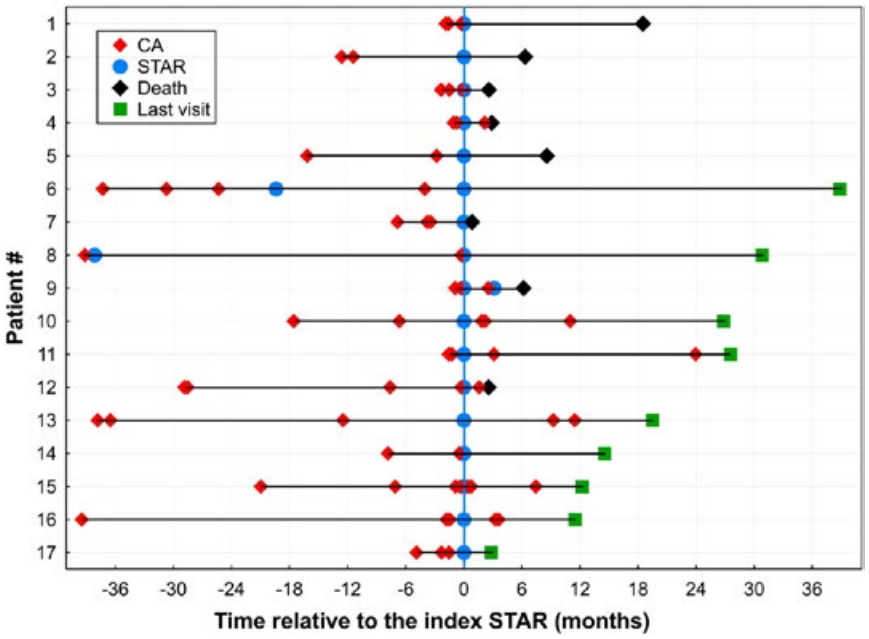

Individual axes are centered according to the index stereotactic arrhythmia radiotherapy (STAR) (time = 0). Red diamonds = catheter ablations (CAs); blue circles = STAR; black diamonds = death; green squares = last outpatient visit.

FIGURE 2 Flowchart of the EFFICACY Cohort

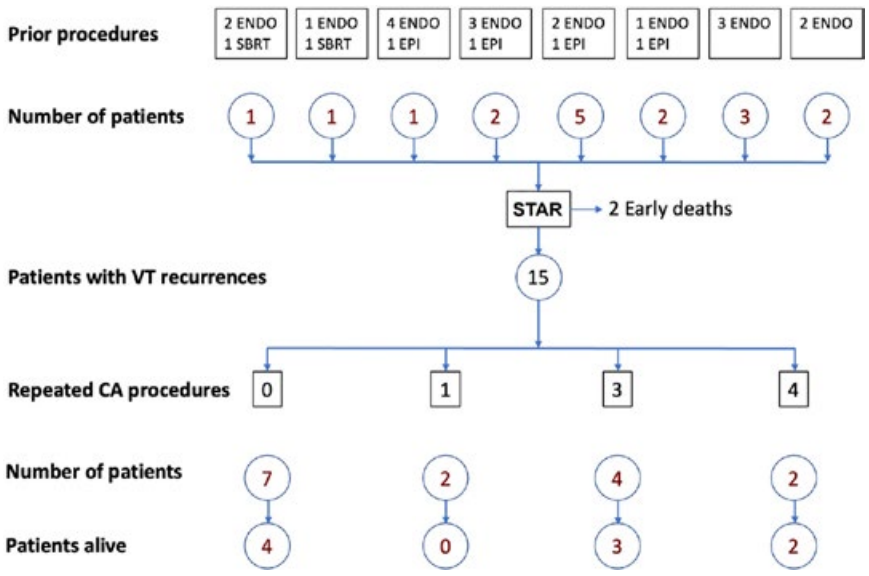

The diagram depicts the distribution of ablation procedures before and after the index stereotactic arrhythmia radiotherapy (STAR).

FIGURE 3 Kaplan-Meier Survival Curves After the Index STAR in the EFFICACY Cohort

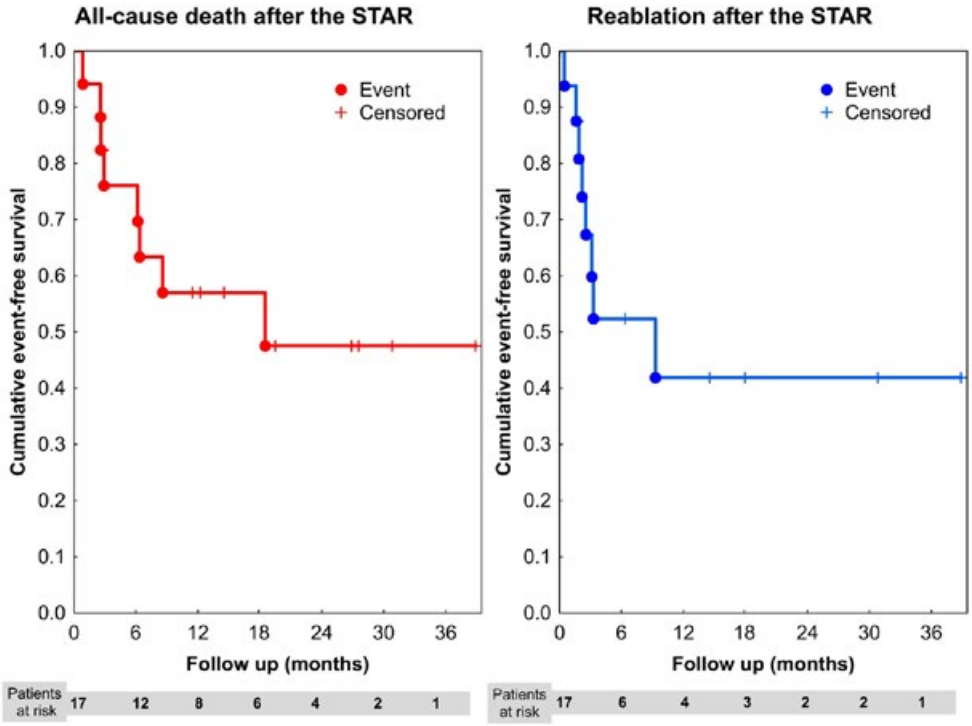

The left panel is for all-cause death; the right panel is for reablation caused by recurrent ventricular tachycardia (VT). Actuarial overall survival was 57% and 48% at 12 and 24 months, respectively. STAR = stereotactic arrhythmia radiotherapy.

33.5 months (Q1, Q3: 18.0, 44.6 months; range 6.2-71.9 months). No significant change was observed in LV ejection fraction within 6 months after STAR (31% ± 10% vs 31% ± 10%; $P = 0.75$).

Two patients had 2 STAR procedures and no long-term side effects. Four patients (12%) presented with radiological signs of lung fibrosis in a small area at a close distance from the PTV. Importantly, adverse effects potentially related to STAR occurred in 12% of cases. Eight patients (25%) gradually developed progression of known mitral valve regurgitation after STAR, and 3 (9%) of them had to undergo mitral valve intervention (Grade 4 toxicity). Two patients had transvenous edge-to-edge repair (22 and 49 months after STAR), and 1 subject had mitral valve replacement (33 months after STAR). Altogether, 7 patients had a progression of restrictive changes on the posterior leaflet; 1 had a progression of mitral annulus dilatation. The grade of mitral regurgitation changed from a pre-SBRT value of 1.6 ± 0.5 to 3.4 ± 0.5 at the last assessment. The risk of mitral valve disease progression significantly increased when 1 of 3 basal inferior LV segments was irradiated, and this risk was even higher when either the basal inferior or inferolateral LV segment was targeted (Table 3). Papillary muscles were part of the PTV in 14 of 32 patients with follow-up longer than 6 months and did not play a role in the progression of mitral regurgitation. Mitral valve disease progressed in 4 of 14 (29%) with papillary muscle in PTV which was comparable to 4 cases of mitral valve disease in 18 (22%) patients with papillary muscles outside the PTV ($P = 0.50$).

One significant tricuspid regurgitation (Grade 3 toxicity) was most probably unrelated to STAR. Two cases of esophagitis (6%) were seen with 1 (3%) radiation toxicity-related death (Grade 5 toxicity) caused by the unresectable esophago-pericardial fistula at 9 months after STAR.[15] This patient had previous bypass surgery using a gastroepiploic artery, which could increase the vulnerability of the esophagus.

Importantly, no ICD generator or lead malfunction was observed in our series of patients.

OVERALL MORTALITY. Of 36 patients who underwent STAR for recurrent VTs, 18 (50%) died during the median follow-up of 26.9 months (Q1, Q3: 8.6,

FIGURE 4 Kaplan-Meier Curves for ICD Therapy-Free Survival After the Index STAR in the EFFICACY Cohort

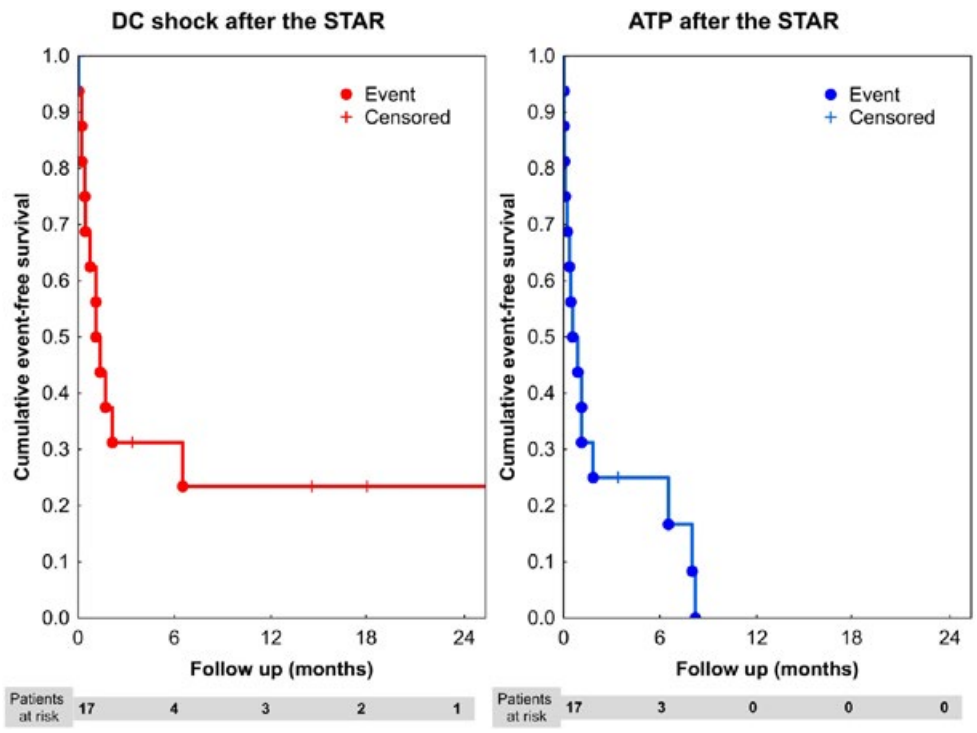

The left panel is for direct current (DC) shock; the right panel is for antitachycardia pacing (ATP). STAR = stereotactic arrhythmia radiotherapy.

43.1 months; range 0.9-71.9 months). The causes of death were as follows: progression of heart failure in 12 patients, and sudden death during recurrence of myocardial infarction, sudden unwitnessed death, COVID-19 pneumonia, pneumonia after stroke, carcinoma, and bleeding caused by esophago-pericardial fistula, each in 1 patient.

DISCUSSION

This observational study represents the third-largest published series on the efficacy of STAR in managing VT and the largest cohort on the long-term safety of the procedure. The results can be summarized as follows: 1) STAR by itself has uncertain efficacy in the prevention of VT recurrences when indicated as a bail-out procedure after previous CA procedures in an expert center despite the use of a high-accuracy method of CTV determination; 2) the net treatment effect of STAR together with subsequent CA consisted of a significant decrease of ICD shocks during the follow-up; 3) several adverse effects potentially linked to STAR were noted, including 3 mitral valve interventions for progression of mitral regurgitation and 1 STAR-related death caused by esophago-pericardial fistula; and 4) the mortality in the study population was relatively high and reflected mainly the severity of the underlying advanced heart disease (Central Illustration).

EFFICACY OF STAR. Several rather small clinical studies reported on the early experience with STAR in patients with VT who failed previous CA or who were considered high-risk for CA. Our early experience with 10 patients showed a significant reduction of VT burden after STAR by 88%.[8] However, during a median follow-up of 28 months, VT recurred in 8 of 10 patients. Patients in this early series had predominantly ischemic cardiomyopathy with less complex substrates. In addition, the strategy of CA before STAR was less comprehensive, and endpoints were variably defined. In contrast, the EFFICACY cohort in the current study had a higher proportion of patients with nonischemic cardiomyopathy, and the CA strategy was standardized in both centers, including the procedural endpoints. These factors may explain more optimistic results reported by our group earlier.[8]

FIGURE 5 Reduction in ICD Therapies Burden After the Index STAR in the EFFICACY Cohort

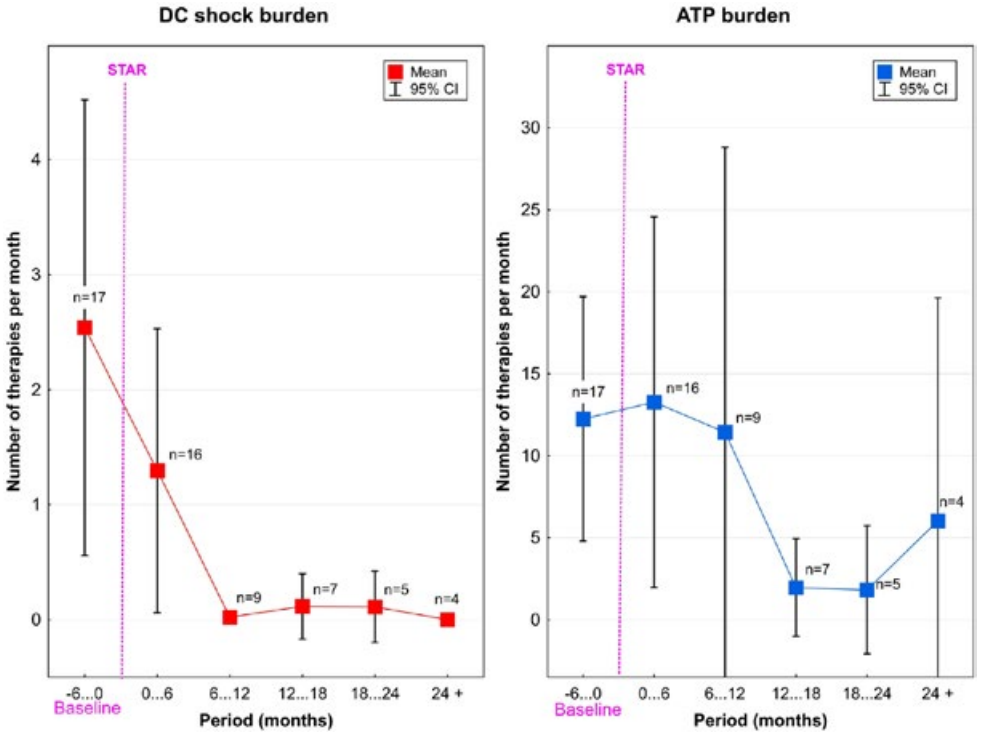

The dotted magenta line indicates the time of the STAR. The left panel is for direct current (DC) shock; the right panel is for antitachycardia pacing (ATP). Abbreviation as in Figures 1 and 2.

The largest prospective study on 19 patients with refractory VT and/or ventricular ectopy causing cardiomyopathy (ENCORE VT [Electrophysiology-Guided Noninvasive Cardiac Radioablation for Ventricular Tachycardia] study) was published by Robinson et al.[7] Importantly, patients with more than 3 distinct clinical VT morphologies or more than 5 induced VT morphologies were not included in the study. Three patients did not have previous CA for various reasons. The majority of patients were on more than 1 antiarrhythmic drug. High-dose amiodarone (>300 mg daily) was used in 8 patients. Imaging strategies combined with body surface mapping were used to define the STAR treatment volume. The aim was to target all areas of ventricular scar, approximating the VT exit site and harboring related circuits using the TrueBeam or Edge (Varian) delivery system. A significant reduction of VT episodes or ectopic burden was observed in 17 of 18 patients (94%) during the median follow-up of 13 months. In 16 VT patients, a 94% reduction of VT episodes was observed outside of the 6-week blanking period. This allowed a decrease in antiarrhythmic medication. Despite the significant decrease in VT burden, many patients (11 of 16, 69%) had recurrences of VT between the end of the 6-week blanking period and the 6-month visit. In contrast, all of our patients had at least 1 previous CA performed in 2 expert centers, and the antiarrhythmic medication consisted of amiodarone in a dose of 200 mg daily. Patients with multiple morphologies of clinical or inducible VTs were not excluded. We used a different delivery system: CyberKnife. No blanking period was employed in our study. All of these factors might contribute to the differences in efficacy and the need for additional CA. The threshold for redo CA in our centers is lower than elsewhere, and CA as an established therapy is preferred to the escalation of antiarrhythmic treatment or redo STAR. Remapping data suggested slowing of clinical VT after SBRT, which may explain better efficacy of ATP and subsequent CA.

Other authors also reported their early experience with STAR with variable results and usually short-term follow-up. Although most of them observed a significant reduction of VTs, the overall efficacy is not very high. Lloyd et al[9] found a significant reduction of

TABLE 2 Comparison of ICD Therapies in EFFICACY Cohort at Baseline and During the Follow-Up

	Baseline		Months 6-18		
	N	Mean ± SD	N	Mean ± SD	*P* Value
Unpaired comparison					
ATP/month	17	12.2 ± 14.5	9	10.2 ± 22.4	0.13
DC shock/month	17	2.5 ± 3.9	9	0.1 ± 0.2	0.005
ATP + DC shock/month	17	14.8 ± 16.2	9	10.3 ± 22.4	0.07
Paired comparison					
ATP/month	9	19.9 ± 16.6	9	10.2 ± 22.4	0.17
DC shock/month	9	1.9 ± 3.2	9	0.1 ± 0.2	0.03
ATP + DC shock/month	9	21.9 ± 19.2	9	10.3 ± 22.4	0.11

Analysis was performed for all available data (unpaired comparison) and in a pairwise fashion that included only patients who survived >6 months. *P*-values are either Mann-Whitney *U* test, or Wilcoxon signed rank test, as appropriate.

ATP = antitachycardia pacing; DC = direct current.

VT episodes in a cohort of 10 patients with advanced heart failure and VT over the mean follow-up of 176 days. However, 2 patients were placed in a hospice, and 3 other subjects underwent a heart transplant. Carbucicchio et al[10] reported a significant reduction of VT therapies after STAR in a group of 7 patients at 6 months of follow-up, although only 2 were free from recurrent VTs. Chin et al[16] described an apparent benefit of STAR (decrease of VT episodes or their absence) in 33% of their 8-patient series. However, even in patients who benefited from STAR, there was a variable temporal pattern in response, and most patients had recurrences of VT. Gianni et al[17] demonstrated VT recurrences in all 5 patients who underwent STAR after failed CA. The first Asian experience with 7 patients was published by Ho et al.[18] Again, 4 of 5 subjects with structural heart disease had recurrences of VT after STAR. Another report from Asia described STAR in 3 patients.[19] During 13.5 ± 2.8 months, patients had a significantly lower burden, but they all had recurrences of VT and died within this period. A study by Qian et al[20] described the results of STAR in treating 6 patients with VT and postinfarction cardiomyopathy. Besides a reduction in device shocks, device-treated or sustained VT episodes were not significantly decreased, and 50% of subjects died within a follow-up period of 231 days. A recent study by Ninni et al[21] reported on clinical outcomes associated with STAR using the CyberKnife system in 17 patients with refractory electrical storm. In 5 patients with incessant VT, the time to effectiveness ranged from 1 to 7 weeks after STAR. Among the 12 remaining patients, early VT recurrences occurred in 7. After a median of 12.5 months (Q1, Q3: 10.5, 17.8 months) of follow-up, a significant reduction of the VT burden was observed beyond 6 weeks. However, many patients had CA shortly before STAR or were sedated and treated by antiarrhythmic drugs.

Our data from the EFFICACY cohort with reasonably long follow-up correspond to the previously mentioned experience and suggest that the efficacy of STAR per se is rather low. Practically all studies showed that STAR does not suppress all VTs and that VT recurrences are common. However, reducing device shocks appears to be the most reproducible result

TABLE 3 Relationship Between Irradiated Myocardial Segments and the Progression of Mitral Valve Disease

	Segments	Risk (%)	Irradiated Region		
Irradiated Region	Risk of Significant Mitral Valve Regurgitation (n = 32)			Risk (%)	*P* Value
Basal segments	# 1-6	7/19 (37)	Rest of segments	1/13 (8)	0.07
Basal inferior segments	# 3-5	6/12 (50)	Rest of segments	2/20 (10)	0.02
Basal inferolateral segments	# 4-5	6/10 (60)	Rest of segments	2/22 (10)	0.005
	Risk of Significant Mitral Valve Regurgitation Requiring Valve Intervention (n = 32)				
Basal segments	# 1-6	3/19 (16)	Rest of segments	0/13 (0)	0.20
Basal inferior segments	# 3-5	3/12 (25)	Rest of segments	0/20 (0)	0.04
Basal inferolateral segments	# 4-5	3/10 (30)	Rest of segments	0/22 (0)	0.02

Left ventricular segments are numbered according to the recommendation of the American Heart Association expert document.[14] *P* values are single-sided Fisher exact test.

CENTRAL ILLUSTRATION The Main Results of the Study in the EFFICACY and SAFETY Cohorts

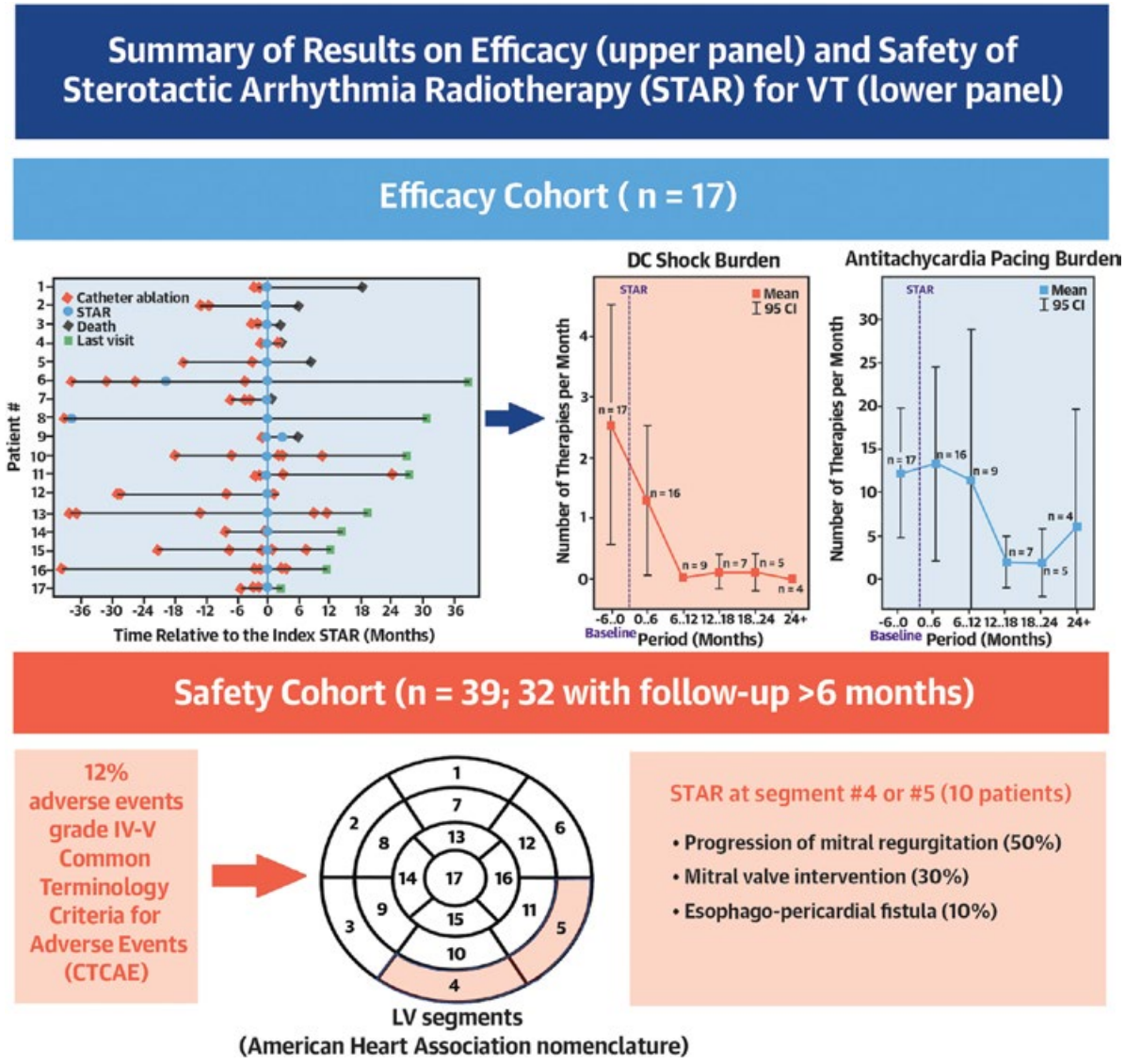

Hašková J, et al. J Am Coll Cardiol EP. 2024;10(4):654-666.

The upper panel shows a time-axis plot with historical and follow-up ablation procedures in the EFFICACY cohort and reduction in ICD therapies burden after the index STAR. The lower panel summarizes the rate of adverse events grade IV-V (Common Terminology Criteria for Adverse Events) and the relationship of STAR segments #4 and #5 to adverse events. ICD = implantable cardioverter-defibrillator; STAR = stereotactic arrhythmia radiotherapy; VT = ventricular tachycardia.

of STAR for recurrent VT after previous CA. In this context, it is important to emphasize that such an effect was obtained in almost all patients on top of previous CA procedures. Not only that, at the time when we observed a significant reduction of ICD shocks, a large proportion of patients had already received subsequent CA for clinically significant recurrences of VT, which precluded any meaningful statistical analysis of the effect of standalone STAR. This observation supports the view that STAR may rather have an adjuvant role to CA than become the first-line therapy managing VT in structural heart disease. Failure of repeated CA in an expert center appears to select patients who probably have more diffuse substrates or more advanced heart disease. Without a head-to-head randomized comparison of

both strategies, ideally in a less diseased population, it would be impossible to evaluate the true efficacy of standalone STAR.

SAFETY OF STAR. The main strength of our study is the analysis of the long-term side effects of STAR. The most frequently observed side effect in our series was a significant progression of mitral valve regurgitation. A detailed analysis of the relationship between the irradiated regions and the risk of mitral valve disease progression showed that STAR targeting the basal inferior and inferolateral segment of the LV significantly increased this risk. We revealed that further restriction of the posterior leaflet was primarily responsible for the progression of mitral regurgitation (Supplemental Table 1). The most serious complication in our series was death caused by esophagopericardial fistula.[15] The patient had irradiation of the basal LV segments, and previous coronary artery bypass grafting using a gastroepiploic artery could increase tissue vulnerability in this region. Interestingly, another case of gastro-pericardial fistula requiring surgical repair was reported (in abstract form only) 2.4 years after STAR.[22] Other groups reported rather less-severe cases of toxicity, such as pericardial effusions. However, the follow-up was relatively short.

Our observations open the question of the risks and benefits of STAR. Considering that none of the previously published series reports on a median follow-up longer than 12 months, we feel that the risk of late adverse effects could be significantly underreported. Longer vigilant follow-up is necessary to describe the actual safety profile of STAR for VT. Due to this uncertainty about safety, STAR should not be performed outside of clinical studies on the management of intractable VTs.

MORTALITY AFTER STAR. Because STAR is often indicated in a population of patients in the terminal phase of heart failure, long-term survival is limited. Robinson et al[22] presented preliminary follow-up data from the ENCORE study. The 1- and 2-year overall survival rates were 72% and 58%, with 8 deaths being recorded. Regarding their relation to STAR, 4 had a possible relationship (2 heart failure, 2 VT recurrences). Chin et al[16] reported 3 deaths out of 8 patients, and Gianni et al[17] reported 2 deaths from heart failure out of 5 patients. Carbucicchio et al[10] observed 3 deaths in a series of 7 patients; 1 of them was unexplained. In the Taiwanese experience with 3 cases of STAR, all patients died (within 14 months).[18] Another center from Taiwan reported on 3 patients, and all died during 13.5 ± 2.8 months.[19] Similarly, in a study by Qian et al,[20] 3 of 6 patients died.

Our data from the SAFETY cohort with a median follow-up of 26.9 months align with these reports. We report 50% mortality, mainly from nonarrhythmic causes. The fact that there was no significant difference in LV ejection fraction after STAR does not indicate the worsening of heart failure caused by radiotherapy. Rather, this implies that STAR could be employed as adjuvant therapy for patients with VTs and comorbidities when CA fails, is impossible because of access issues, or is considered technically demanding and associated with a substantial risk of failure or complications. In patients with less advanced heart failure or with fewer comorbidities, other treatment modalities such as LV assist device implant or heart transplant should be considered after failed repeated CA instead of STAR.

STUDY LIMITATIONS. The evaluation of STAR efficacy was limited not only by a relatively small sample size but also by a high mortality rate and shorter follow-up compared with the SAFETY cohort. The lack of a control group does not allow assessment of the causal effect of STAR (plus CA) on the decrease of ICD therapies. Because a substantial proportion of patients had another CA for VT recurrences after STAR, we can only speculate that the therapeutic effect is caused by the synergism of both modalities. The absence of data on ICD therapies between the last outpatient visit and death in most deceased patients might partly contribute to lower arrhythmic burden after STAR. Other bias-introducing factors that favor a decrease in arrhythmia burden may include selection bias caused by patient enrollment in the period of frequent ventricular arrhythmias, changes in antitachycardia function programming during the follow-up, and relatively high mortality of the sicker patient cohort. Furthermore, it is important to emphasize that the strategy of CA, as well as the technique of CTV determination, developed significantly between 2014 and 2020. A higher number of previous CA procedures and more nonischemic patients compared with the historical cohort of our first 10 cases suggest that our EFFICACY cohort consists of patients who are truly resistant to CA in the expert center with access to all contemporary technologies for CA. This was the reason why we separately analyzed efficacy in the most homogeneous cohort and safety in the entire patient population.

It is also important to mention that STAR in our cohort was not delivered by the C-arm technology, which differs from robotic linear accelerators. However, there is no data that either technology has different clinical efficacy or is more prone to toxicity.[23] We are also aware of some targeting inaccuracies when using the ICD lead to track respiratory

movements. Therefore, we use safety margins as published recently.[13]

CONCLUSIONS

STAR per se has limited efficacy in highly selected patients with structural heart disease and recurrent VT after previous CA in an expert center. Because many patients required another CA early during the follow-up after STAR to treat the VT recurrences, our study suggests that the decreased number of ICD shocks was caused by the synergistic effect of STAR and follow-up CA. The long-term safety of STAR is still unknown, and observed delayed side effects may limit its use. At present, STAR should be offered only as a bail-out strategy for patients with VTs and comorbidities when CA fails or is not feasible.

FUNDING SUPPORT AND AUTHOR DISCLOSURES

This work was supported by grant project AZV NU20-02-00244 from the Ministry of Health of the Czech Republic. This work was also supported by the project National Institute for Research of Metabolic and Cardiovascular Diseases (Programme EXCELES, Project No. LX22NPO5104), funded by the European Union-Next Generation EU. Dr Cvek has received personal fees from Accuray, and Roche for lectures. All other authors have reported that they have no relationships relevant to the contents of this paper to disclose.

ADDRESS FOR CORRESPONDENCE: Dr Jana Hašková, Department of Cardiology, Institute for Clinical and Experimental Medicine (IKEM), Vídeňská 1958/9, Prague 4, 140 21 Czech Republic. E-mail: hasj@ikem.cz.

PERSPECTIVES

COMPETENCY IN PATIENT CARE AND PROCEDURAL SKILLS: Patients with structural heart disease and VT recurrent after CA in an expert center may benefit from targeted STAR of the myocardial substrate and better quality of life because of fewer device shocks. However, the risk of adverse effects has to be considered.

TRANSLATIONAL OUTLOOK: More information is needed about the effects of STAR on the myocardial substrate and the optimal dose to improve efficacy and minimize the risk of serious side effects.

REFERENCES

1. Sapp JL, Wells GA, Parkash R, et al. Ventricular tachycardia ablation versus escalation of antiarrhythmic drugs. *N Engl J Med*. 2016;375:111–121.

2. Aldhoon B, Wichterle D, Peichl P, Cihak R, Kautzner J. Outcomes of ventricular tachycardia ablation in patients with structural heart disease: the impact of electrical storm. *PloS One*. 2017;12:e0171830.

3. Maskoun W, Saad M, Abualsuod A, et al. Outcome of catheter ablation for ventricular tachycardia in patients with ischemic cardiomyopathy: a systematic review and meta-analysis of randomized clinical trials. *Int J Cardiol*. 2018;267:107–113.

4. Cvek J, Neuwirth R, Knybel L, et al. Cardiac radiosurgery for malignant ventricular tachycardia. *Cureus*. 2014;6:e190. https://doi.org/10.7759/cureus.190

5. Loo BW Jr, Soltys SG, Wang L, et al. Stereotactic ablative radiotherapy for the treatment of refractory cardiac ventricular arrhythmia. *Circ Arrhythm Electrophysiol*. 2015;8:748–750.

6. Cuculich PS, Schill MR, Kashani R, et al. Noninvasive cardiac radiation for ablation of ventricular tachycardia. *N Engl J Med*. 2017;377:2325–2336.

7. Robinson CG, Samson PP, Moore KM, et al. Phase I/II trial of electrophysiology-guided noninvasive cardiac radioablation for ventricular tachycardia. *Circulation*. 2019;139:313–321.

8. Neuwirth R, Cvek J, Knybel L, et al. Stereotactic radiosurgery for ablation of ventricular tachycardia. *Europace*. 2019;21:1088–1095.

9. Lloyd MS, Wight J, Schneider F, et al. Clinical experience of stereotactic body radiation for refractory ventricular tachycardia in advanced heart failure patients. *Heart Rhythm*. 2020;17:415–422.

10. Carbucicchio C, Andreini D, Piperno G, et al. Stereotactic radioablation for the treatment of ventricular tachycardia: preliminary data and insights from the STRA-MI-VT phase Ib/II study. *J Interv Card Electrophysiol*. 2021;62:427–439.

11. Abdel-Kafi S, Sramko M, Omara S, et al. Accuracy of electroanatomical mapping-guided cardiac radiotherapy for ventricular tachycardia: pitfalls and solutions. *Europace*. 2021;23:1989–1997.

12. Peichl P, Sramko M, Cvek J, Kautzner J. A case report of successful elimination of recurrent ventricular tachycardia by repeated stereotactic radiotherapy: the importance of accurate target volume delineation. *Eur Heart J Case Rep*. 2020;5:ytaa516.

13. Dvorak P, Knybel L, Dudas D, Benyskova P, Cvek J. Stereotactic ablative radiotherapy of ventricular tachycardia using tracking: Optimized target definition workflow. *Front Cardiovasc Med*. 2022;9:870127.

14. Cerqueria MD, Weissman NJ, Dilsizian V, et al. Standardized myocardial segmentation and nomenclature for tomographic imaging of the heart: a statement for Healthcare Professionals from the Cardiac Imaging Committee of the Council on Clinical Cardiology of the American Heart Association. *Circulation*. 2002;105:539–542.

15. Haskova J, Jedlickova K, Cvek J, Knybel L, Neuwirth R, Kautzner J. Oesophagopericardial fistula as a late complication of stereotactic radiotherapy for recurrent ventricular tachycardia. *Europace*. 2022;24:969.

16. Chin R, Hayase J, Hu P, et al. Non-invasive stereotactic body radiation therapy for refractory ventricular arrhythmias: an institutional experience. *J Interv Card Electrophysiol*. 2021;61:535–543.

17. Gianni C, Rivera D, Burkhardt JD, et al. Stereotactic arrhythmia radioablation for refractory scar-related ventricular tachycardia. *Heart Rhythm*. 2020;17:1241–1248.

18. Ho LT, Chen JL, Chan HM, et al. First Asian population study of stereotactic body radiation therapy for ventricular arrhythmias. *Sci Rep*. 2021;11:10360.

19. Yugo D, Lo LW, Wu YH, et al. Case series on stereotactic body radiation therapy in non-ischemic cardiomyopathy patients with recurrent ventricular tachycardia. *Pacing Clin Electrophysiol*. 2021;44:1085–1093.

20. Qian PC, Quadros K, Aguilar M, et al. Substrate modification using stereotactic radioablation to treat refractory ventricular tachycardia in patients with ischemic cardiomyopathy. *J Am Coll Cardiol EP*. 2022;8:49–58.

JACC: CLINICAL ELECTROPHYSIOLOGY VOL. 10, NO. 4, 2024
APRIL 2024:654–666

21. Ninni S, Gallot-Lavallee T, Klein C, et al. Stereotactic radioablation for ventricular tachycardia in the setting of electrical storm. *Circ Arrhythm Electrophysiol*. 2022;15:e010955.

22. Robinson CG, Samson P, Moore KMS, et al. Longer term results from a Phase I/II study of EP-guided noninvasive cardiac radioablation for treatment of ventricular tachycardia (ENCORE-VT) (abstr). *Int J Radiat Oncol*. 2019;105:682.

23. Wei C, Qian PC, Boeck M, et al. Cardiac stereotactic body radiation therapy for ventricular tachycardia: current experience and technical gaps. *J Cardiovasc Electrophysiol*. 2021;32:2901–2914.

KEY WORDS catheter ablation, complications, stereotactic arrhythmia radiotherapy (STAR), ventricular tachycardia

APPENDIX For a supplemental table, please see the online version of this paper.

P. Peichl et al.

Efficacy and safety of focal pulsed-field ablation for ventricular arrhythmias: two-centre experience

Europace
Impact Factor: 7,9

rejstřík

ESC European Society of Cardiology

Europace (2024) **26**, euae192
https://doi.org/10.1093/europace/euae192

CLINICAL RESEARCH

Efficacy and safety of focal pulsed-field ablation for ventricular arrhythmias: two-centre experience

Petr Peichl [1]*, Alan Bulava [2], Dan Wichterle [1], Filip Schlosser [1], Predrag Stojadinović [1], Eva Borišincová [1], Peter Štiavnický [1], Jana Hašková [1], and Josef Kautzner [1]

[1]Department of Cardiology, IKEM, Vídeňská 1958/9, Praha 4, Prague 140 21, Czechia; and [2]České Budějovice Hospital and Faculty of Health and Social Sciences, University of South Bohemia in České Budějovice, České Budějovice, Czechia

Received 30 May 2024; accepted after revision 6 July 2024; online publish-ahead-of-print 11 July 2024

Aims A pulsed electric field (PF) energy source is a novel potential option for catheter ablation of ventricular arrhythmias (VAs) as it can create deeper lesions, particularly in scarred tissue. However, very limited data exist on its efficacy and safety. This prospective observational study reports the initial experience with VA ablation using focal PF.

Methods and results The study population consisted of 44 patients (16 women, aged 61 ± 14years) with either frequent ventricular premature complexes (VPCs, 48%) or scar-related ventricular tachycardia (VT, 52%). Ablation was performed using an irrigated 4 mm tip catheter and a commercially available PF generator. On average, 16 ± 15 PF applications (25 A) were delivered per patient. Acute success was achieved in 84% of patients as assessed by elimination of VPC or reaching non-inducibility of VT. In three cases (7%), a transient conduction system block was observed during PF applications remotely from the septum. Root analysis revealed that this event was caused by current leakage from the proximal shaft electrodes in contact with the basal interventricular septum. Acute elimination of VPC was achieved in 81% patients and non-inducibility of VT in 83% patients. At the 3-month follow-up, persistent suppression of the VPC was confirmed on Holter monitoring in 81% patients. In the VT group, the mean follow-up was 116 ± 75 days and a total of 52% patients remained free of any VA.

Conclusion Pulsed electric field catheter ablation of a broad spectrum of VA is feasible with acute high efficacy; however, the short-term follow-up is less satisfactory for patients with scar-related VT.

* Corresponding author. Tel: +420 26136 5006. *E-mail address*: petr.peichl@ikem.cz

Graphical Abstract

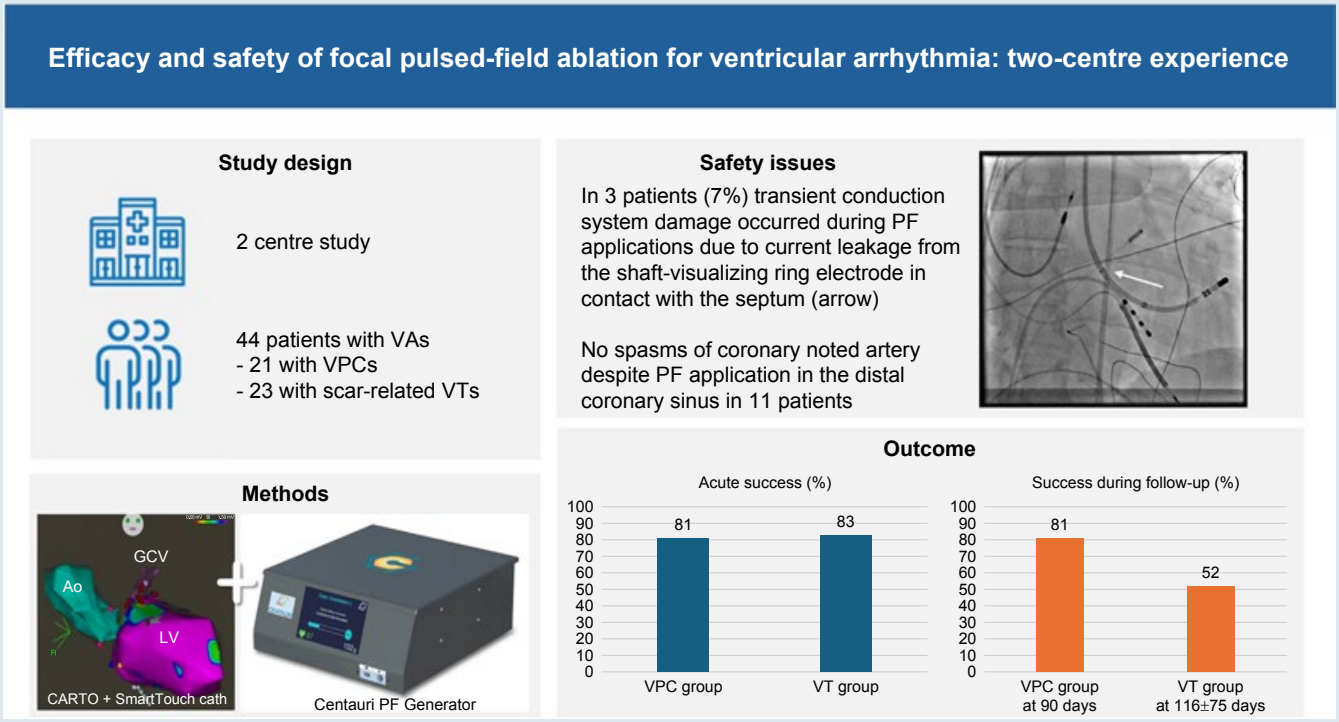

Keywords Catheter ablation • Ventricular premature complexes • Ventricular tachycardia • Pulsed-field energy

What's new?

- Ablation of ventricular arrhythmia using pulsed electric field (PF) delivered from a solid-tip 4 mm catheter is feasible with a high acute efficacy; however, despite favourable acute results, the recurrences are common in the ventricular tachycardia group and acute non-inducibility may not be the optimal endpoint.
- Compared to radiofrequency energy, focal PF ablation within the great cardiac vein was not limited by a high impedance or poor catheter-tip cooling and was not associated with coronary artery spasm.
- Unexpected conduction system block was observed during retrograde catheter ablation in the left ventricle due to current leakage from the proximal, shaft-visualizing electrodes of the ablation catheter.

Introduction

Catheter ablation (CA) is a well-established treatment of ventricular arrhythmias (VAs).[1] In patients with frequent ventricular premature complexes (VPCs), eliminating ectopic focus may improve symptoms or lead to normalization of left ventricular (LV) ejection fraction in case of arrhythmia-induced cardiomyopathy. In patients with sustained scar-related ventricular tachycardias (VTs), CA decreases the number of therapies from the implantable cardioverter-defibrillator (ICD) and VA-related hospitalizations[2] and may improve prognosis.[3] Until now, radiofrequency (RF) current has been the primary energy source employed for these procedures. However, the creation of deep lesions by RF ablation might be compromised in scar regions and associated with the risk of tissue overheating and steam pop.[4] A pulsed electric field (PF) is a novel energy source that enables fast creation of non-thermal lesions and may overcome some of the limitations of RF energy.

Currently, multiple systems allowing VA ablation by PF are in the phase of preclinical or early clinical evaluation.[5–7] The CENTAURI system (CardioFocus) is a novel PF generator that enables PF ablation using different commercially available catheters. The system delivers a biphasic, monopolar pulsed field at three selectable energy settings (19, 22, and 25 A) that is synchronized to the R-wave. Its safety and efficacy were evaluated for ablation of atrial fibrillation.[8] Anecdotally, this generator has been used for VA ablation, but so far, data on efficacy and safety are limited to the case reports and small case series.[9–11] Our study aimed to analyse the safety and efficacy of VA ablation using focal PF delivered by the CENTAURI generator coupled with a contact force-sensing ablation catheter and a 3D electroanatomical mapping system in a broad population of patients with frequent VPC or scar-related VT.

Methods

Study population and study design

This two-centre study included consecutive patients who underwent CA for VA between May 2023 and January 2024 using the CENTAURI generator. Initially, patients with VPC from the right ventricular (RV) outflow tract were included to assess the feasibility of PF ablation. However, after seven uneventful cases, the inclusion criteria expanded to patients with other VA that failed previous RF ablation (both during the same or the previous procedure). The patient was considered non-eligible for PF ablation if the VA originated from the vicinity of the AV node or proximal conduction

system. All patients signed informed consent with the procedure. The institutional Ethics Committee approved the study.

Catheter ablation procedure

The procedures were performed under conscious sedation with fentanyl and midazolam, or on propofol. After obtaining vascular access, unfractionated heparin was administered as an initial bolus, and further doses were adjusted to maintain the activated clotting time between 300 and 350 s. The LV was accessed either transseptally or retrogradely, depending on the VA origin, the actual INR level, the presence of peripheral arterial disease, and/or mechanical valve prosthesis. Procedures were navigated using a 3D electroanatomic mapping system (CARTO 3, Biosense Webster) and guided by intracardiac echocardiography (ICE; AcuNav, Siemens Medical Solutions). For mapping and ablation, a 3.5 mm irrigated-tip catheter (ThermoCool SmartTouch™, Biosense Webster) was used. Radiofrequency energy was delivered by SMARTABLATE (Biosense Webster) set to an output of 30–40 W for up to 60 s and titrated to reach an impedance drop of 10–15 Ohms. When PF was used, 25 A applications were delivered using the CENTAURI generator and repeated at each target site up to three times to maximize the lesion size. In the VPC group, these additional applications were delivered, only when the ectopy was eliminated by the initial pulse. In the VT group, repeated applications were delivered to each targeted site and inducibility was assessed only after delivering the planned lesion set.

For patients with frequent VPC, activation mapping was used as the primary mapping strategy, complemented by pacemapping. Catheter ablation targeted the site of the earliest activity during VPC. The procedure was considered acutely successful if the clinical VPC was eliminated despite the isoproterenol challenge.

For patients with scar-related VT, mapping and ablation strategy was described previously.[12] Briefly, one quadripolar catheter was inserted into the right ventricle for pacing. At baseline, programmed ventricular stimulation from the RV apex was performed at two drive trains (600 and 400 ms) and up to three extrastimuli. Substrate mapping was performed primarily during spontaneous rhythm or RV pacing using an integrated approach. Bipolar voltage maps (the lower threshold of 0.5 mV) were constructed and fragmented or late potentials were tagged. Zones of slow conduction were identified by the stimulus-to-QRS onset interval longer than 40 ms. The paced QRS morphology during sinus rhythm was used to match the exit sites of induced VTs. Activation and entrainment mapping were used for well-tolerated VT. The goal of subsequent CA was to abolish all abnormal signals or late potentials, often reaching isolation of the segment of the scar with no capture. In the case of tolerated VT, CA aimed to terminate the arrhythmia. The procedure was considered acutely successful when non-inducibility of any VT was achieved.

Whenever PF was applied within the great cardiac vein, coronary angiography was performed before and after the PF energy delivery to rule out spasms of the coronary arteries. The distance between the tip of ablation catheter and the coronary artery was measured (contour to contour) at the PF application site. No nitrates were applied prophylactically prior to PF applications.

In one of the centres, peripheral venous blood samples for the assessment of the serum levels of high-sensitivity troponin T (hsTnT) were obtained the next day (usually 18–24 h after the CA).

Clinical follow-up

Following CA, patients were evaluated in the outpatient clinic in 3-month intervals. Those with frequent VPC underwent 24-h Holter monitoring and CA were considered successful if the clinical VPC burden was significantly decreased (<20% of the pre-ablation level). Patients with scar-related VT were seen regularly in 3- or 6-month intervals, and the recurrence of VT was assessed by clinical history and ICD interrogation.

Statistical analysis

Continuous variables were expressed as means with standard deviations and compared with Student's *t*-test. Categorical variables were expressed as percentages and compared by Fisher's exact test. A $P < 0.05$ was considered significant.

Results

The population consists of 44 patients recruited in the two centres. A total of 57% of patients had previously failed RF ablation procedure(s) for VA. Twenty-one (48%) patients had frequent VPC with a mean burden of 27 ± 12% on a 24-h Holter monitoring. Twenty-three (52%) patients had scar-related VT. Baseline characteristics are displayed in *Table 1*.

In the VPC group, ectopy originated from the LV outflow tract, RV outflow tract, posteromedial LV papillary muscle, and posterobasal LV region in 52, 33, 10, and 5%, respectively. In the VT group, the ablation was performed in the lateral LV, LV outflow tract/great cardiac vein, anterior LV wall, lateral RV wall, inferior LV wall, LV papillary muscle, and RV outflow tract in 35, 26, 13, 9, 9, 4, and 4%, respectively.

The mean procedural duration was 113 ± 46 min, and the fluoroscopy time reached 6.9 ± 4.3 min with a radiation dose of 8521 ± 12 393 mGy/cm2 (*Table 2*). On average, 16 ± 15 PF applications (25 A) were delivered per patient. The PFs were well tolerated in analgosedation, and no generalized muscle contractions that would affect the alignment of electroanatomical maps were observed. Importantly, PF deliveries did not induce sustained VT or ventricular fibrillation in any of the patients. In nine patients (20%), RF delivery was attempted and failed prior PF applications (2 ± 7 applications per patient).

Table 1 Baseline characteristics

	All patients $n = 44$	Patients with VPCs $n = 21$	Patients with VT $n = 23$	*P*-value
Male sex (%)	64	47	78	0.06
Age (years)	61 ± 14	56 ± 13	63 ± 15	0.18
Body mass index (kg/m^2)	31 ± 5	30 ± 5	31 ± 5	0.62
Diabetes mellitus (%)	23	19	26	0.72
Arterial hypertension (%)	73	62	83	0.18
Structural heart disease (%)	55	4	96	<0.001
Mean LV ejection fraction (%)	45 ± 16	58 ± 9	33 ± 10	<0.001
Previous unsuccessful RF ablation (%)	57	38	74	<0.01

LV, left ventricular; RF, radio frequency ablation; VPC, ventricular premature contraction; VT, ventricular tachycardia.

Table 2 Procedural characteristics and outcome

	All patients $n = 44$	Patients with VPCs $n = 21$	Patients with VT $n = 23$	*P*-value
Procedural duration (min)	113 ± 46	84 ± 41	139 ± 33	<0.001
Fluoroscopy time (min)	6.9 ± 4.3	7 ± 4	7 ± 4	0.77
Fluoroscopy dose (mGy/cm^2)	8521 ± 12 393	8226 ± 10 657	8791 ± 14 030	0.88
PF applications per patient (*n*)	16 ± 15	7 ± 4	24 ± 16	<0.001
Acute success (%)	82	81	83	1.0
Absence of recurrences during follow-up (%)	66	81	52	0.06

PF, pulsed field; VPC, ventricular premature complex; VT, ventricular tachycardia.

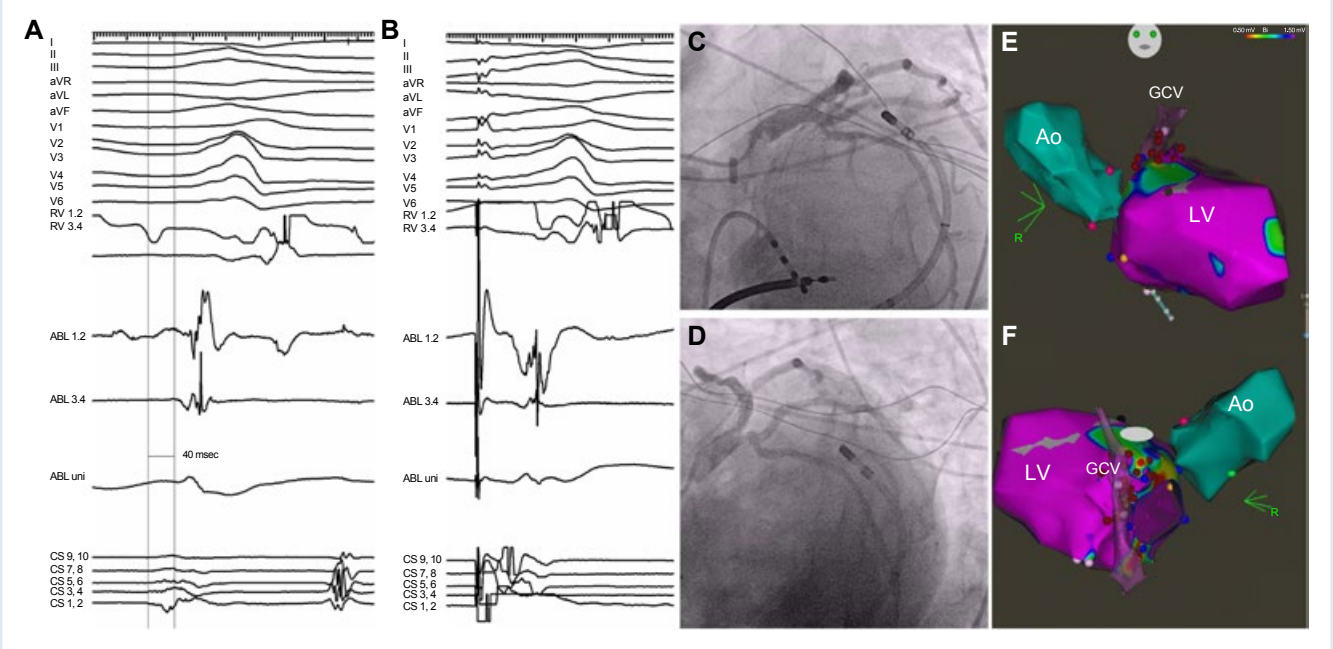

Figure 1 An illustrative case of ablation in the great cardiac vein in a patient with non-ischaemic cardiomyopathy and scar-related VT from the LV summit. (*A*) shows prematurity (−40 ms) and fragmentation during the VPC in the decapolar catheter positioned close to the substrate in the great cardiac vein (CS 3.4). Note relatively late activation in the ablation catheter positioned on the endocardium of the LV outflow tract. (*B*) shows the corresponding pace map with a long stimulus-to-QRS delay. (*C*) depicts angiography of the left coronary artery position prior to ablation. No spasm (*D*) was noted after four PF applications in the great cardiac vein. (*E* and *F*) display electroanatomical maps in anteroposterior (*E*) and modified cranial view (*F*). Ao, aorta; ABL, electrograms from ablation catheter; CS, coronary sinus; GCS, great cardiac vein; LV, left ventricular; PF, pulsed field; RV, right ventricle; VPC, ventricular premature complex.

Pulsed electric field ablation in the great cardiac vein

In 11 cases (8 and 3 in the VPC and VT groups, respectively), PF energy was applied in the great cardiac vein up to 2 mm from the coronary artery (mean distance of 5 ± 2 mm). No electrocardiogram changes attributable to ischaemia were noted after the PF applications, and subsequent coronary angiography did not reveal any abnormality/spasm in any of these patients (*Figure 1*). In 7 of 11 patients (63%), PF ablation led to acute suppression of VA. The mean prematurity during VPC/VT in patients was higher in those with acutely successful ablation compared to those where no acute effect was seen (31 ± 8 ms vs. 18 ± 5 ms, $P = 0.08$).

Conduction system block during pulsed electric field applications

Transient conduction system block occurred in three cases (7%) during PF application on the lateral LV wall remotely from the conduction system. It consisted of complete AV block in one and left bundle branch block in two patients. Conduction blocks resolved in all cases within 1 h. Root analysis revealed that these events occurred during the retrograde approach to the LV. In such cases, the proximal shaft-visualizing electrodes of the ablation catheter were located close to the proximal portion of the conduction system at the LV aspect of the interventricular septum (*Figure 2*). Intracardiac echocardiography monitoring revealed that these unexpected adverse events were accompanied by

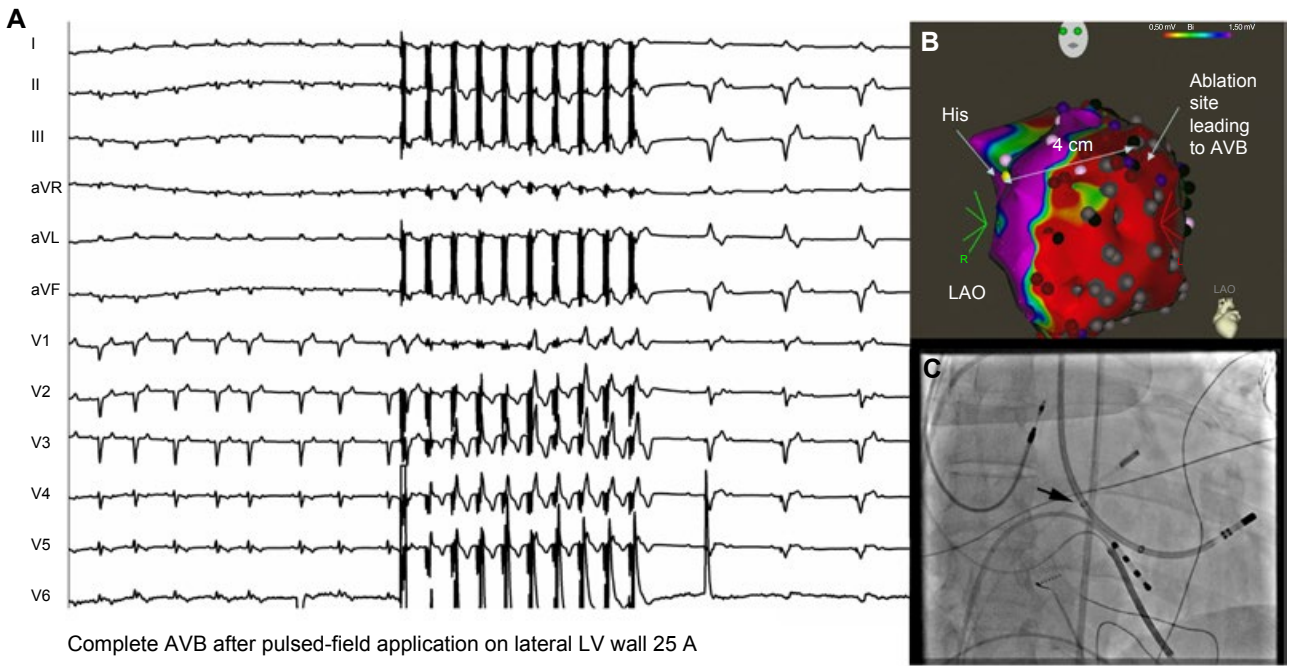

Figure 2 (*A*) shows the occurrence of complete AV block after PF ablation in a patient with non-ischaemic cardiomyopathy. (*B*) depicts an electroanatomical voltage map. The distance between the site of the application leading to the AV block and the location of His bundle recordings was 4 cm. (*C*) displays the fluoroscopic position of the ablation catheter. Note that the location of the proximal ring electrode on the catheter shaft is at the His bundle area (see text for further explanation). A, amper; AVB, AV block; His, his bundle recording site; LAO, left anterior oblique view; PF, pulsed field.

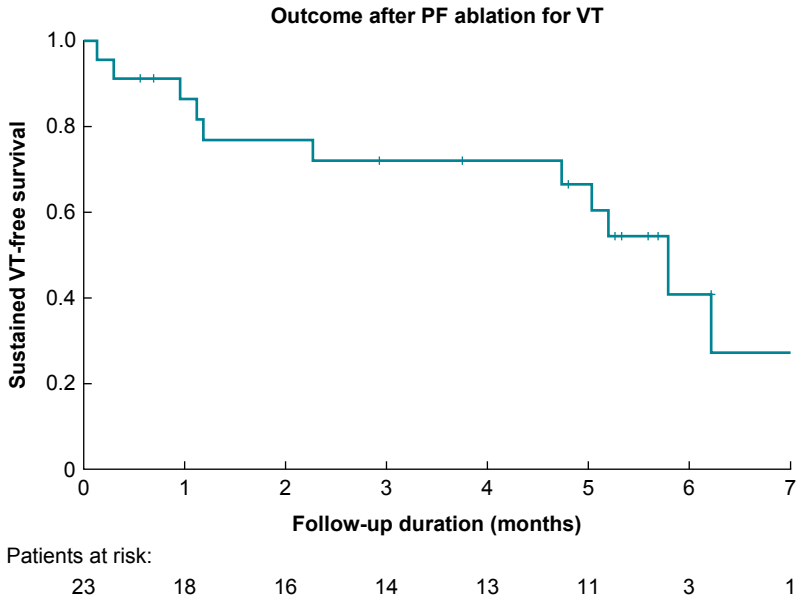

Figure 3 Kaplan–Meier curve of sustained VT-free survival after PF ablation. PF, pulsed field; VT, ventricular tachycardia.

the emission of microbubbles from these electrodes during PF energy delivery, suggesting the leakage of the current (see Supplementary material online, *Video S1*). Formation of the microbubbles could easily be prevented by covering the shaft electrodes with the sheath.

Acute elimination of VPC was achieved in 17/21 (81%) patients and non-inducibility in 19/23 (83%) patients with VT. At the 3-month follow-up, persistent suppression of the VPCs was confirmed on Holter monitoring in 17/21 (81%) patients. The mean VPC burden

decreased from 27 ± 12 to 7 ± 13% (reduction by 73 ± 51%, $P < 0.001$). In one patient with ectopy from posteromedial papillary muscle, acute suppression was achieved; however, the late recurrence of the same VPC morphology was observed at 3 months. On the other hand, in one patient who had acutely unsuccessful ablation, VPC disappeared during follow-up. In the group of patients with scar-related VT, the mean follow-up was 116 ± 75 days and 12/23 (52%) of patients remained free of any VT (*Figure 3*).

Myocardial lesion size

Levels of hsTnT were assessed in 43% of patients before and after ablation and increased from 19 ± 12 to 600 ± 425 ng/L ($P < 0.001$). The increase was higher in patients with VT compared to those with VPC, but the difference was not significant (623 ± 446 ng/L vs. 323 ± 238 ng/L, $P = 0.22$).

Discussion

The main findings of this study can be summarized as follows: (i) ablation of VA using PF delivered from a solid-tip 4 mm catheter is feasible with a high acute efficacy; (ii) despite favourable acute results, the recurrences are common in the VT group and acute non-inducibility may not be the optimal endpoint; (iii) compared to RF energy, focal PF ablation within the great cardiac vein was not limited by a high impedance or poor catheter-tip cooling and was not associated with coronary artery spasm; (iv) unexpected conduction system block was observed during retrograde CA in the LV due to current leakage from the proximal, shaft-visualizing electrodes of the ablation catheter; and (v) focal PF ablation was not associated with excessive myocardial damage as assessed by troponin levels post-ablation.

Compared to RF ablation of VA, PF energy offers several potential benefits. First, due to the non-thermal nature of PF, tissue overheating with a risk of steam pop is highly unlikely. Second, several preclinical studies suggested that PF can penetrate better into the scar tissue,[5,13,14] which is particularly important in patients with scar-related VT. Third, PF applications are much shorter compared to RF and, thus, might be advantageous in some locations, where the stability of the catheter is challenging (e.g. on papillary muscle).[15] This may also result in more favourable procedural times.

Acute and short-term follow-up

While the focal PF ablation was quite successful (as assessed by acute suppression of the VPC or VT inducibility) in both groups, the short-term outcome in patients with VT was far less satisfactory. This may not be surprising, since the nature of VA is quite different in these patient cohorts. In the case of VPC, localized PF ablation has a higher chance of abolishing the focal source. On the other hand, the ablation target is far more extensive in scar-related VT, potentially also located more in-depth of the myocardial wall. In such a scenario, the studied PF energy delivery might not be effective enough and more pulses and/or higher energy deliveries were needed. However, this study reports one of the first larger experiences with PF ablation of VPC/VT that aimed at patients who failed RF ablation and safety was the primary interest. In addition, the pulse configuration used by the studied generator might not be ideal for VA ablation and could be further studied and optimized. Unfortunately, once PF ablation is delivered, local electrograms are instantaneously abolished and there is not much left, how to learn about the quality and durability of the created lesion. Finally, the explanation for the different efficacy of PF ablation in both groups might be a selection bias with more patients in the VT group having already previously unsuccessful RF ablation.

Regarding the assessment of the acute effect of PF ablation in scar-related VT, a new paradigm shift can be observed. In contrast to RF ablation, where the abolition of local abnormal electrograms was considered a reasonable endpoint of the substrate modification, PF delivery results in acute disappearance of the local electrograms, which may not reflect the creation of durable lesions. Acute lesions by PF compared to RF are known to have a much larger zone of reversible injury.[16] This may also affect inducibility of VA at the end of the procedure. Thus, acute non-inducibility of VT after PF ablation might not be the optimal endpoint of the procedure. Whether the use of non-invasive programmed ventricular stimulation[17] performed remotely from the ablation procedure could better assess the acute effect of ablation is to be investigated.

Pulsed electric field delivery in the great cardiac vein

Application of RF energy in the great cardiac vein is often limited by the high impedance and temperature rise.[18] Thus, alternative approaches, including alcohol venous injection,[19] and bipolar ablation[20] have been proposed. Pulsed electric field may pose another option for VPC originating in the LV summit, and experimental data have shown that PF is feasible in this scenario.[21] Pulsed electric field ablation in the great cardiac vein has been also described in a clinical setting.[10] Our current experience supports these observations. Based on clinical observations of coronary spasms, obtained with multielectrode PF delivery in the vicinity of the right coronary artery,[22] the safety of PF ablation within the great cardiac vein is important. In this respect, we performed coronary angiography before and after PF delivery at a distance up to 2 mm (mean of 5 mm) to the coronary artery with no spasms noted. We can speculate that the lack of observed coronary spasms in our cohort could be due to the catheter design (4 mm tip vs. multispline catheter). Similarly to our experience, Brešković *et al.*[23] have used a focal PF catheter within the coronary sinus for left-sided accessory pathways, and no clinically relevant spasms were reported. Nevertheless, our patient cohort was very small and the ablation catheter did not touch directly the coronary artery during any PF application. Thus, more data on the safety of this approach are still needed.

Conduction system damage during pulsed electric field applications

The observations of transient conduction system blocks prompted us to evaluate the root cause of this phenomenon. Our explanation of these adverse events by leakage of the current through the proximal shaft-visualizing electrodes of the ablation catheter was confirmed by information obtained from the CENTAURI manufacturer. Because the high-voltage pulses are delivered to the tip of the ablation catheter during PF application, considerably high-voltage pulses are also synchronously delivered to proximal shaft-visualizing electrodes to prevent sparking and shortcutting between the wires within the catheter shaft. When these electrodes are in close proximity to the conduction system (such as during the retrograde access to the LV), the PF delivery may cause a transient conduction block. This explanation is supported by the preclinical studies that have described the high sensitivity of the conduction system to PF energy.[7] Of note, this mechanism is specific only to the use of the SmartTouch ThermoCool™ catheter. The other catheters approved for the CENTAURI generator (i.e. TactiCath SE, Abbott and STABLEPOINT, Boston Scientific) do not have such electrodes on the shaft. But even for the SmartTouch catheter, the inadvertent damage of the conduction system could be prevented by covering and isolating these electrodes with the long sheath or by preferring the transseptal access to LV, which makes this adverse event unlikely.

Myocardial damage

Pulsed electric field ablation leads to only moderate myocardial damage as assessed by troponin post-ablation increase. Studies assessing the

troponin T dynamics in patients undergoing PF ablation of atrial fibrillation with a multielectrode catheter have reported much higher values (up to three times).[24,25] Our observation is reassuring, since extensive myocardial damage in patients with scar-related VT and impaired LV ejection fraction may result in pump failure. On the other hand, PF may acutely affect a much larger area and this reversible zone of stunned ventricular myocardium may cause acute haemodynamic decompensation. Further studies are needed to clarify the haemodynamic risks associated with more extensive PF ablation in the ventricle.

Study limitations

This was a prospective observational study aiming to describe the efficacy and safety of VA ablation by focal PF delivery in a spectrum of different VA. Thus, the small sample size may limit the validity of our observations, and additional studies with larger patient cohorts are needed to further explore the specific aspects and risks of focal PF ablation of VA in various patient populations. In addition, patients with arrhythmias in the vicinity of the proximal conduction system were on purpose not included in this study and no statement regarding safety/efficacy can be made in this respect. Finally, the observations made with the studied combination of the specific PF generator and ablation catheter cannot be extrapolated to other PF ablation technologies.

Conclusions

Initial experience with the focal PF ablation of VA demonstrated high acute efficacy in ablation of both VPC and scar-related VT. However, the short-term success rate was more satisfactory in VPC patients, which reflects the size and complexity of the arrhythmogenic substrate and uncertainty about the endpoint of PF CA in scar-related VT. Pulsed electric field ablation was found particularly useful for ablation within the great cardiac vein.

Supplementary material

Supplementary material is available at *Europace* online.

Authors' contribution

Substantial contributions to the conception and design or the acquisition, analysis, or interpretation of the data: P.P. and A.B. Substantial contributions to the drafting of the articles or critical revision for important intellectual content: P.P., A.B., D.W., P.S., and J.K. Final approval of the version to be published: P.P., A.B., D.W., P.S., F.S., E.B., P.Š., J.H., and J.K. Agreement to be accountable for all aspects of the work in ensuring that questions related to the accuracy or integrity of any part of the article are appropriately investigated and resolved: P.P., A.B., and J.K.

Funding

This paper was supported by the National Institute for Metabolic and Cardiovascular Research 'CarDia' (Programme EXCELES, ID Project No. LX22NPO5104)—funded by the European Union—Next Generation EU (KC). This work was also funded by the project (Ministry of Health, Czech Republic) for development of research organization 00023001 (IKEM, Prague, Czech Republic)—institutional support.

Conflict of interest: P.P. reports personal fees from Biotronik, Biosense Webster, Boston Scientific, Medtronic, and St. Jude Medical (Abbott). A.B. reports personal fees from Biotronik for participation in the scientific advisory board and has received speaker honoraria from Biotronik, Boston Scientific, and St. Jude Medical (Abbott). J.K. reports personal fees from Biosense Webster, Boston Scientific, GE Healthcare, Medtronic, and St. Jude Medical (Abbott) for participation in scientific advisory boards and has received speaker honoraria from Biosense Webster, Biotronik, Boston Scientific, Medtronic, and St. Jude Medical (Abbott). The remaining authors have no disclosures.

Data availability

Data available upon request.

References

1. Zeppenfeld K, Tfelt-Hansen J, de Riva M, Winkel BG, Behr ER, Blom NA *et al.* 2022 ESC guidelines for the management of patients with ventricular arrhythmias and the prevention of sudden cardiac death. *Eur Heart J* 2022;**43**:3997–4126.
2. Ravi V, Poudyal A, Khanal S, Khalil C, Vij A, Sanders D *et al.* A systematic review and meta-analysis comparing radiofrequency catheter ablation with medical therapy for ventricular tachycardia in patients with ischemic and non-ischemic cardiomyopathies. *J Interv Card Electrophysiol* 2023;**66**:161–75.
3. Della Bella P, Baratto F, Vergara P, Bertocchi P, Santamaria M, Notarstefano P *et al.* Does timing of ventricular tachycardia ablation affect prognosis in patients with an implantable cardioverter defibrillator? Results from the multicenter randomized PARTITA trial. *Circulation* 2022;**145**:1829–38.
4. Leshem E, Zilberman I, Barkagan M, Shapira-Daniels A, Sroubek J, Govari A *et al.* Temperature-controlled radiofrequency ablation using irrigated catheters: maximizing ventricular lesion dimensions while reducing steam-pop formation. *JACC Clin Electrophysiol* 2020;**6**:83–93.
5. Younis A, Buck E, Santangeli P, Tabaja C, Garrott K, Lehn L *et al.* Efficacy of pulsed field vs radiofrequency for the reablation of chronic radiofrequency ablation substrate: redo pulsed field ablation. *JACC Clin Electrophysiol* 2024;**10**:222–34.
6. Koruth JS, Kuroki K, Iwasawa J, Viswanathan R, Brose R, Buck ED *et al.* Endocardial ventricular pulsed field ablation: a proof-of-concept preclinical evaluation. *Europace* 2020;**22**:434–9.
7. Zyl M van , Ladas TP, Tri JA, Yasin OZ, Ladejobi AO, Tan NY, Christopoulos G *et al.* Bipolar electroporation across the interventricular septum: electrophysiological, imaging, and histopathological characteristics. *JACC Clin Electrophysiol* 2022;**8**:1106–18.
8. Anić A, Phlips T, Brešković T, Koopman P, Girouard S, Mediratta V *et al.* Pulsed field ablation using focal contact force-sensing catheters for treatment of atrial fibrillation: acute and 90-day invasive remapping results. *Europace* 2023;**25**:euad147.
9. Hansen J, Haugdal MA, Johannessen A, Hansen ML, Worck R, Ruwald MH. Focal pulsed field electroporation of left ventricular premature contractions after failed radiofrequency ablation. *HeartRhythm Case Rep* 2023;**9**:581–5.
10. Mestrovic IP, Breskovic T, Markovic M, Kurtic E, Mestrovic T, Anic A. Ablation of epicardial ventricular focus through coronary sinus using pulsed-field ablation. A case report. *J Cardiovasc Electrophysiol* 2024;**35**:856–61.
11. Worck R, Haugdal MA, Johannessen A, Hansen ML, Ruwald MH, Hansen J. A case of safe and durable focal pulsed-field electroporation treatment of outflow tract premature ventricular contractions. *Heart Rhythm O2* 2023;**4**:463–5.
12. Peichl P, Wichterle D, Pavlu L, Cihak R, Aldhoon B, Kautzner J. Complications of catheter ablation of ventricular tachycardia: a single-center experience. *Circ Arrhythm Electrophysiol* 2014;**7**:684–90.
13. Im SI, Higuchi S, Lee A, Stillson C, Buck E, Morrow B *et al.* Pulsed field ablation of left ventricular myocardium in a swine infarct model. *JACC Clin Electrophysiol* 2022;**8**:722–31.
14. Sandhu U, Alkukhun L, Kheiri B, Hodovan J, Chiang K, Splanger T *et al.* In vivo pulsed-field ablation in healthy vs. chronically infarcted ventricular myocardium: biophysical and histologic characterization. *Europace* 2023;**25**:1503–9.
15. Qiu J, Dai M, Bai Y, Chen G. Potential application of pulsed field ablation in ventricular arrhythmias. *Medicina (Kaunas)* 2023;**59**:723.
16. Nakagawa H, Castellvi Q, Neal R, Girouard S, Laughner J, Ikeda A *et al.* Effects of contact force on lesion size during pulsed field catheter ablation: histochemical characterization of ventricular lesion boundaries. *Circ Arrhythm Electrophysiol* 2024;**17**:e012026.
17. Muser D, Hayashi T, Castro SA, Supple GE, Schaller RD, Santangeli P *et al.* Noninvasive programmed ventricular stimulation-guided management following ventricular tachycardia ablation. *JACC Clin Electrophysiol* 2019;**5**:719–27.
18. Yamada T, Doppalapudi H, Litovsky SH, McElderry HT, Kay GN. Challenging radiofrequency catheter ablation of idiopathic ventricular arrhythmias originating from the left ventricular summit near the left main coronary artery. *Circ Arrhythm Electrophysiol* 2016;**9**:e004202.
19. Tavares L, Lador A, Fuentes S, Da-Wariboko A, Blaszyk K, Malaczynska-Rajpold K *et al.* Intramural venous ethanol infusion for refractory ventricular arrhythmias: outcomes of a multicenter experience. *JACC Clin Electrophysiol* 2020;**6**:1420–31.
20. Futyma P, Sauer WH. Bipolar radiofrequency catheter ablation of left ventricular summit arrhythmias. *Card Electrophysiol Clin* 2023;**15**:57–62.
21. Buist TJ, Groen MHA, Wittkampf FHM, Loh P, Doevendans PAFM, van Es R *et al.* Feasibility of linear irreversible electroporation ablation in the coronary sinus. *Cardiovasc Eng Technol* 2023;**14**:60–6.

22. Reddy VY, Petru J, Funasako M, Kopriva K, Hala P, Chovanec M *et al.* Coronary arterial spasm during pulsed field ablation to treat atrial fibrillation. *Circulation* 2022;**146**: 1808–19.
23. Brešković T, Lisica L, Jurišić Z, Petrović D, Sikirić I, Metličić V *et al.* Ablation of accessory pathways in different anatomic locations using focal pulsed field ablation. *Heart Rhythm* 2024. doi:10.1016/j.hrthm.2024.03.030
24. Krisai P, Knecht S, Badertscher P, Mühl A, Osswald S, Roten L *et al.* Troponin release after pulmonary vein isolation using pulsed field ablation compared to radiofrequency and cryoballoon ablation. *Heart Rhythm* 2022;**19**:1471–2.
25. Popa MA, Bahlke F, Kottmaier M, Foerschner L, Bourier F, Lengauer S *et al.* Myocardial injury and inflammation following pulsed-field ablation and very high-power short-duration ablation for atrial fibrillation. *J Cardiovasc Electrophysiol* 2024;**35**:317–27.

P. Peichl et al.

Mapping and ablation of ventricular tachycardia using dual-energy lattice-tip focal catheter: early feasibility and safety study

Europace
Impact Factor: 7,9

‹ rejstřík

ESC European Society of Cardiology

Europace (2024) **26**, euae275
https://doi.org/10.1093/europace/euae275

CLINICAL RESEARCH

Mapping and ablation of ventricular tachycardia using dual-energy lattice-tip focal catheter: early feasibility and safety study

Petr Peichl [1]*, Dan Wichterle [1], Filip Schlosser [1], Predrag Stojadinović [1], Vojtěch Nejedlo[2], Eva Borišincová [1], Josef Marek [1], Peter Štiavnický [1], Jana Hašková [1], and Josef Kautzner [1]

[1]Department of Cardiology, IKEM, Vídeňská 1958/9, Prague 140 00, Czechia; and [2]Cardiac Ablation Solutions, Medtronic, Minneapolis, MN, USA

Received 1 September 2024; accepted after revision 22 October 2024; online publish-ahead-of-print 31 October 2024

Aims Catheter ablation is an effective treatment method for recurrent ventricular tachycardias (VTs). However, at least in part, procedural and clinical outcomes are limited by challenges in generating an adequate lesion size in the ventricular myocardium. We investigated procedural and clinical outcomes of VT ablation using a novel 'large-footprint' catheter that allows the creation of larger lesions either by radiofrequency (RF) or by pulsed field (PF) energy.

Methods and results In prospectively collected case series, we describe our initial experience with VT ablation using a lattice-tip, dual-energy catheter (Sphere-9, Medtronic), and a compatible proprietary electroanatomical mapping system (Affera, Medtronic). The study population consisted of 18 patients (aged 55 ± 15 years, one woman, structural heart disease: 94%, ischaemic heart disease: 56%, left ventricular ejection fraction: 34 ± 10%, electrical storm: 22%) with recurrent sustained VTs and ≥1 previously failed endocardial RF ablation with conventional irrigated-tip catheter in 66% of patients. On average, 12 ± 7 RF and 8 ± 9 PF applications were delivered per patient. In three-fourths of patients undergoing percutaneous epicardial ablation, spasms in coronary angiography were observed after PF applications. All resolved after intracoronary administration of nitrates. No acute phrenic nerve palsy was noted. One patient suffered from a stroke that resolved without sequelae. Post-ablation non-inducibility of VT was achieved in 89% of patients. Ventricular-arrhythmia-free survival at three months was 78%.

Conclusion VT ablation using a dual-energy lattice-tip catheter and a novel electroanatomical mapping system is feasible. It allows rapid mapping and effective substrate modification with good outcomes during short-term follow-up.

* Corresponding author. Tel: +420 261 365 006; fax: +420 236 052 985. *E-mail address:* pepi@ikem.cz

Graphical Abstract

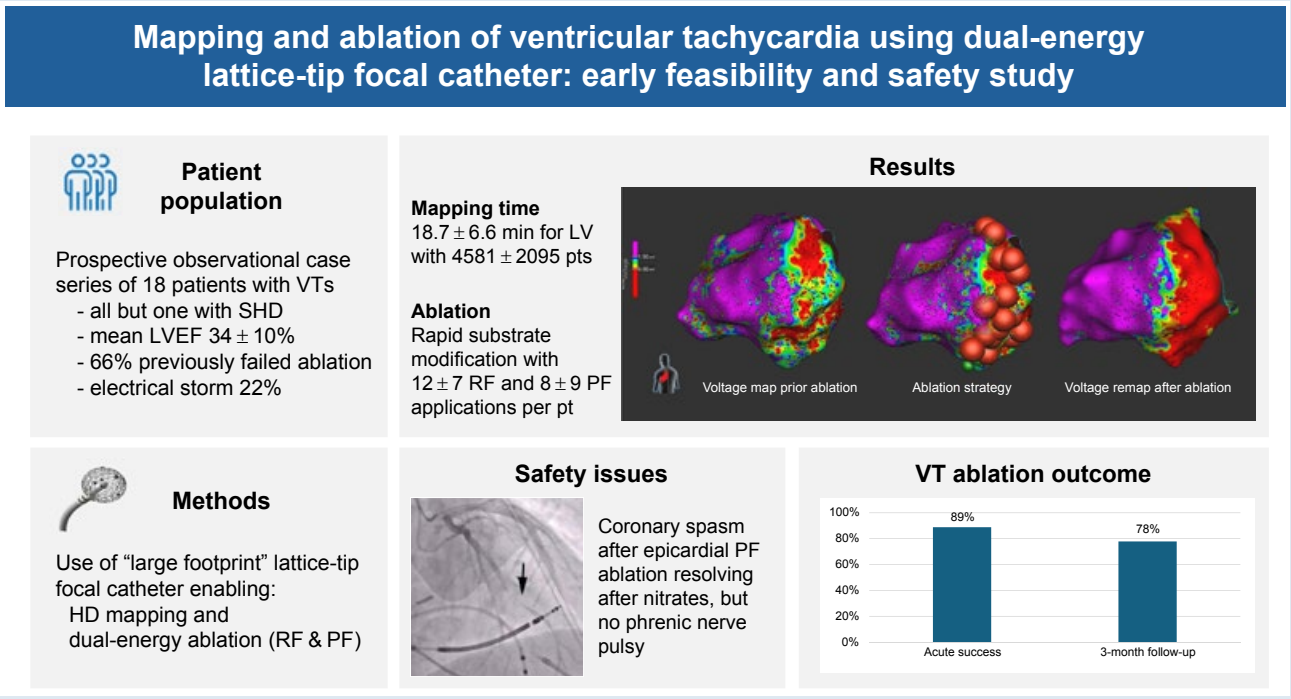

Keywords Catheter ablation • Ventricular tachycardia • Pulsed field • Radiofrequency ablation

What's new?

- Lattice-tip catheter in combination with electroanatomical mapping system allows rapid high-density mapping of VTs and arrhythmogenic substrate.
- Ablation results in effective substrate modification without excessive troponin release with good outcomes during short-term follow-up.
- Pulsed field applications in epicardial space were commonly associated with spasms of coronary arteries but not phrenic nerve palsy.

Introduction

Catheter ablation (CA) is a well-established treatment of ventricular arrhythmias.[1,2] In patients with structural heart disease (SHD) and sustained ventricular tachycardias (VTs), CA has been shown to decrease the risk of shocks of implantable cardioverter-defibrillator (ICD), ventricular-arrhythmia-related hospitalizations[3] and possibly to improve prognosis.[4] However, the creation of deep lesions by radiofrequency (RF) ablation might be compromised in regions of fat and pre-existing scar, and risk collateral damage to coronary arteries and phrenic nerve. A lattice-tip catheter is a novel large-footprint mapping/ablation catheter (Sphere-9, Medtronic, Minneapolis, MN) that allows the application of both high-energy RF and pulsed field (PF) energy, using a compatible proprietary electroanatomical mapping system and generator (Affera, Medtronic, Minneapolis, MN).

The effectiveness and safety of the above system have been previously clinically validated for the treatment of atrial fibrillation (AF).[5] The potential application of the system for lesion creation in ventricular myocardium has been studied extensively in experiment.[6–8] However, the clinical use of a lattice-tip catheter for VT ablation has been reported only in case reports and small case series.[9,10]

We aimed to analyse the early-experience safety and efficacy of VT ablation using a lattice-tip catheter in patients with different clinical types of VT.

Methods

Study population and study design

This series included consecutive patients who underwent CA for VT between January and June 2024 using the Affera system. Patients were included when presented either with (i) SHD VTs or (ii) had a history of previously failed CA for VT. Patients with idiopathic VTs originating from typical regions like outflow tracts were not considered. All patients provided informed consent with the procedure. The institutional review board approved the study.

Catheter ablation procedure

The procedures were performed under general anaesthesia in all cases. After obtaining vascular access, procedures were navigated using a three-dimensional electroanatomic mapping system (Affera, Medtronic) and guided by intracardiac echocardiography (AcuNav, Siemens Medical Solutions). A 9 mm lattice-tip catheter (Sphere-9, Medtronic) was used for mapping and ablation. If needed, epicardial access was obtained using the Sosa technique.[11]

The Affera mapping and ablation system has been described earlier.[6] Briefly, the lattice-tip catheter contains a magnetic sensor and nine microelectrodes on the surface of the collapsible frame that collect near-field unipolar electrograms against the central indifferent electrode. The electroanatomical map is acquired rapidly by simultaneous recordings from all microelectrodes. At the same time, a dedicated algorithm automatically annotates local electrograms from each microelectrode. The mapping

time was defined as the time interval between the first and last acquired point of the voltage map of the targeted chamber.

At the beginning of the procedure, unfractionated heparin was administered as an initial bolus, and further doses were adjusted to maintain the activated clotting time between 300 and 350 s. Depending on the substrate location and/or the presence of peripheral arterial disease, the left ventricle (LV) was accessed either transseptally or retrogradely.

Our mapping and ablation strategy was described previously.[12] Briefly, one quadripolar catheter was inserted into the right ventricle (RV) for pacing. At baseline, programmed ventricular stimulation from the ventricular apex was performed at two drive trains (600 and 400 ms) and up to three extrastimuli. Activation and entrainment mapping were used for well-tolerated VTs. Substrate mapping/ablation was performed primarily during spontaneous rhythm or RV pacing. Bipolar voltage maps (the lower threshold of 0.5 mV) were constructed and fragmented or late potentials were tagged. Zones of slow conduction were identified by stimulus-to-QRS onset intervals longer than 40 ms. The paced QRS morphology during sinus rhythm was used to match the exit sites of induced VTs. An increase in electrode temperature during RF/PF applications was used as a surrogate for tissue contact. The exact position and contact of the lattice-tip catheter with the tissue was confirmed by intracardiac echocardiography.

The primary strategy was high-energy RF ablation.[13] If RF ablation alone could not achieve VT suppression or adequate substrate modification, PF applications were added to consolidate the lesions further. Pulsed field was not used in close vicinity to the proximal ventricular conduction system. On the other hand, only PF energy was used in epicardial space. When RF energy was used for endocardial lesions, ablations were delivered for 30 s per lesion. For PF ablations, 5 s applications were delivered and repeated at each target site up to three times to maximize the lesion size.

The goal of CA was to abolish all abnormal signals or late potentials, often achieving electrical isolation of the scarred segment. The procedure was considered acutely successful in case of non-inducibility of any sustained VT using the same stimulation protocol as for induction.

Coronary angiography was performed before and after the epicardial PF energy delivery to identify the presence of potential coronary artery spasms. No nitrates were given prophylactically before PF applications. The phrenic nerve function after epicardial ablation was assessed by either (i) direct pacing of the phrenic nerve or (ii) observation of diaphragm motion on fluoroscopy.

Peripheral venous blood samples were obtained the next day (usually 18–24 h after the CA) to assess the serum levels of high-sensitivity troponin T (hsTnT).

Clinical follow-up

Following the CA, patients were seen in the outpatient clinic 3 months after the ablation. The recurrence of VT was assessed by clinical history and ICD interrogation. ICD programming was individualized according to the cycle lengths of clinical VTs.

Statistical analysis

Continuous variables were expressed as means with standard deviations and compared with the Student's *t*-test. Categorical variables were expressed as percentages and compared using the Wilcoxon paired test. A *P*-value of <0.05 was considered significant.

Results

The case series comprises 18 patients (aged 55 ± 15 years, one woman) with recurrent VTs. One patient had idiopathic focal VT from the crux of the heart; the others had SHD-related VT (94%). The underlying SHD was coronary artery disease (53%), non-ischaemic cardiomyopathy (35%), congenital heart disease (6%), and hypertrophic cardiomyopathy (6%). A total of 66% of patients were after ≥1 previously failed RF ablation procedure(s) (range 1–3), and 22% were in the electric storm at the time of ablation. Baseline characteristics are displayed in *Table 1*.

Table 1 Baseline characteristics

	***N* = 18**
Male sex (%)	94
Age (years)	55 ± 15
Body mass index (kg/m^2)	29 ± 4
Diabetes mellitus (%)	28
Arterial hypertension (%)	67
History of atrial fibrillation (%)	44
Structural heart disease (%)	94
Coronary artery disease (%)	56
Left ventricular ejection fraction (%)	34 ± 10
Previous unsuccessful ablation (%)	67
Electric storm at the time of ablation (%)	22
Implantable cardioverter-defibrillator (%)	94

Electroanatomic mapping

An average of 4452 ± 1724 and 4581 ± 2095 points was collected for the RV and LV voltage maps, respectively. The mean mapping time was 18.3 ± 9.6 min for RV and 18.7 ± 6.6 min for LV. The mapping was perceived as easy. However, in certain regions, such as perimitral or peritricuspid areas, navigation with intracardiac echocardiography had to be used to place the catheter correctly.

The arrhythmogenic substrate was identified on the anterior/anteroseptal LV wall (28%), inferior LV wall (28%), lateral LV wall (22%), within RV (17%), and in periaortic region (6%).

Radiofrequency or pulsed field delivery

Compared to our previous experience with a 4 mm-tip catheter, myocardial capture during pacemapping/entrainment was more difficult and sometimes impossible to achieve with the lattice-tip catheter. This could be explained by the smaller pacing electrodes on the surface of the catheter tip. Due to this limitation in pacemapping or entrainment mapping, we preferred to start ablation with high-energy RF to see changes in electrograms, which may promptly disappear when PF is used for the initial lesion. Pulsed field was delivered later to consolidate previous RF lesions.

On average, 12 ± 7 RF and 8 ± 9 PF applications were delivered per patient. In the presence of an extensive substrate, the ablation strategy most commonly comprised scar homogenization or core scar isolation (*Figure 1*). Epicardial PF ablations did not lead to transmural lesions as assessed by corresponding endocardial signals (*Figure 2*). The applications of PF energy did not induce ventricular fibrillation or sustained VT in any of the patients; however, myocardial capture was commonly observed during PF applications (*Figure 3*). This myocardial capture could result in non-specific VT termination when PF was applied during ongoing VT.

The mean procedural duration was 157 ± 31 min, with a fluoroscopy time of 5.2 ± 4.0 min (*Table 2*).

Acute ablation outcome

The ablation resulted in acute non-inducibility in 16/18 (89%) patients. In one case, the patient was after previous surgical repair of the postinfarction ventricular septal defect, and a pericardial patch covered a portion of the septum. Despite extensive RF and PF ablations close to the presumed

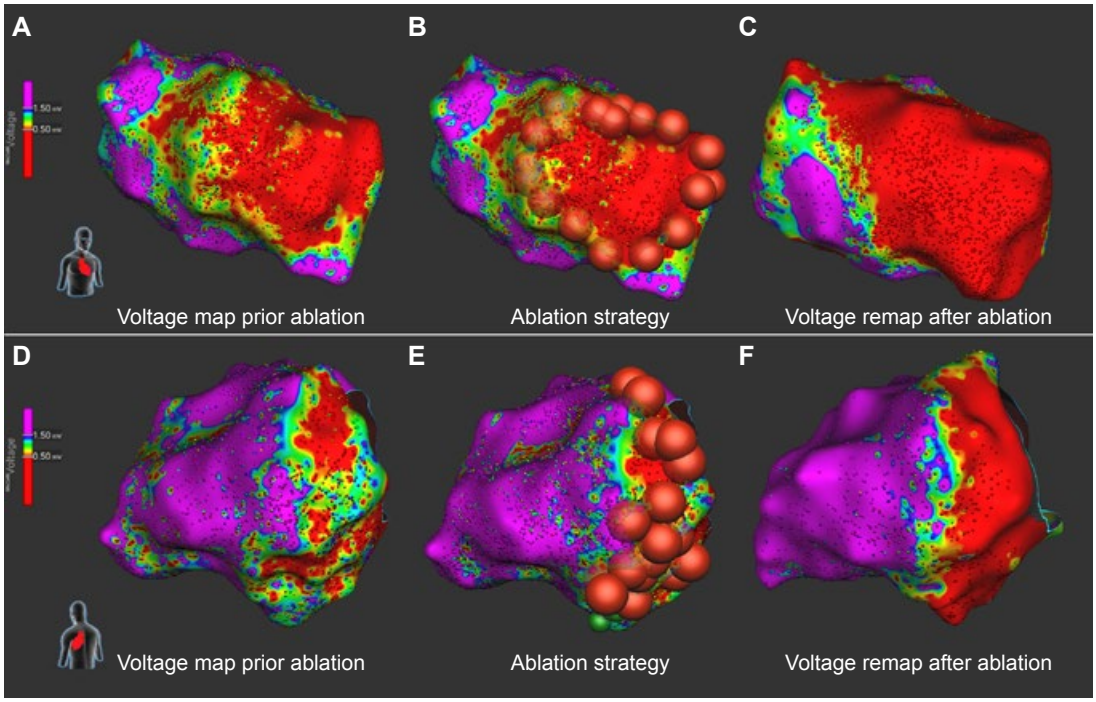

Figure 1 Examples of substrate modification in patients with VTs after previous myocardial infarction. Panels *A* to *C* show LV voltage maps in the right anterior oblique view in a patient with an extensive anteroseptal scar. Panels *D* to *F* depict LV voltage maps in posterior view in a patient after inferolateral myocardial infarction. Note the elimination of local voltage within the ablated zone after either core scar isolation (panel *B*) or substrate homogenization (panel *E*).

exit VT site, arrhythmia inducibility could not be suppressed. The patient subsequently underwent stereotactic radiotherapy. In the other patient, the ablation of the arrhythmogenic substrate on the lateral LV wall failed due to the inaccessible epicardial location of the VT circuit because of the presence of adhesions.

Complications

Coronary angiography performed after epicardial PF applications showed spasms of the adjacent coronary artery (*Figure 4*) in three out of four patients undergoing epicardial ablation. Interestingly, ECG changes attributable to ischaemia were noted only in one patient. When spasm was observed, intracoronary nitroglycerine was administered (starting at a dose of 0.5 mg and reaching up to 2–3 mg until resolution of spasm or systemic hypotension was seen). For cases with observed coronary spasm, the mean distance from the coronary artery and the centre of the lattice-tip catheter was 7 ± 3 mm. No spasm was seen in a patient, where the distance was 21 mm. In all cases, the spasm resolved after the intracoronary application of nitrates. On the other hand, no phrenic nerve palsy was observed in three patients, where PF applications were delivered in epicardial space in the vicinity of the phrenic nerve (in one case directly on site with phrenic nerve capture; in two cases within the distance of 1–2 cm). One patient suffered from a stroke, which resolved within one month without any sequelae. This was a patient with hypertrophic cardiomyopathy and a history of pre-existing thrombus in the LV aneurysm. Preprocedural imaging using transthoracic echocardiography with echocontrast revealed no thrombus, and the activated clotting time was maintained above 300 s. The source of the presumed embolism causing the stroke is, therefore, unknown.

The extent of myocardial damage

As a surrogate for myocardial damage, levels of hsTnT were assessed before and after ablation, and increased from 36 ± 26 ng/L to 995 ± 580 ng/L ($P < 0.01$).

Short-term follow-up

The VT recurred in two patients with procedural failure. In two additional patients, recurrences were seen during a short-term follow-up of 3 months. One patient had one episode of VT treated by antitachycardia pacing. The other case was a patient with non-ischaemic cardiomyopathy who had a recurrence of incessant slow VT from the RV inferior basal region despite previous endo-epicardial RF/PF ablation. This VT had been successfully treated with a 4 mm-tip catheter inserted underneath the inferior tricuspid leaflet. The most plausible interpretation is that with a large-tip catheter design, we failed to map/ablate the sharp angle between the myocardial wall and the posterior leaflet of the tricuspid valve (*Figure 5*).

Discussion

The main findings of this study can be summarized as follows: (i) electroanatomical mapping with the novel system was rapid and reliable; however, pacemapping or entrainment mapping was limited by frequent non-capture; (ii) ablation using a large-footprint catheter, enabling both RF and PF, is feasible and effective for rapid modification of the arrhythmogenic substrate; (iii) reachability of some narrow regions by the large tip might be limited compared to the 4 mm-tip, and intraprocedural imaging with intracardiac echocardiography might be

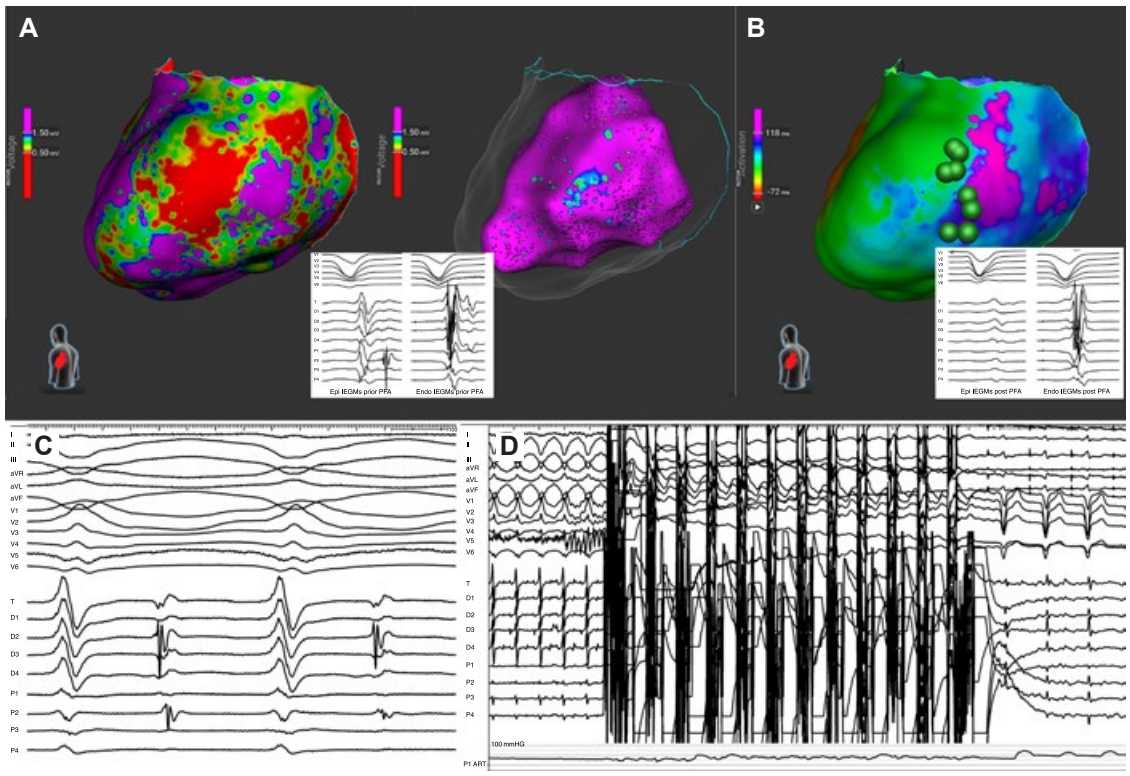

Figure 2 Panel *A* depicts epicardial (left) and endocardial (right) voltage map in the left lateral view in a patient with non-ischaemic cardiomyopathy. Panel *B* shows an epicardial activation map during sinus rhythm with delayed activation on the basal lateral wall (violet colour) with marked PF ablation tags (green). Note that the late potentials on both epicardial and endocardial local electrograms were eliminated by PF epicardial ablation. At the same time, the endocardial voltage was not affected. Panel *C* depicts mid-diastolic potentials in epicardium during inducible VT. Panel *D* shows the termination of VT during epicardial PF ablation. During PF application, note the myocardial capture (visible on ECG and arterial pressure tracing).

helpful; (iv) ablation did not result in excessive myocardial damage; (v) epicardial PF ablation adjacent to the phrenic nerve did not result in acute palsy; and (vi) PF ablation close to the coronary artery induced subclinical spasms.

Radiofrequency vs. pulsed field efficacy considerations

The current study used RF energy as the primary energy source for ablation. First, this decision was backed by historical experience with this energy source. Secondly, experimental studies have shown that RF current can create larger lesions than PF.[14] Thirdly, unlike PF, the change in local electrograms caused by ablation can be assessed after RF delivery. On the other hand, PF may provide several potential advantages over RF. Most importantly, several preclinical studies suggested that PF can penetrate better both healthy and scar/fatty tissue.[15–17] This is particularly important in patients with SHD or those undergoing repeated ablation procedures. However, acute lesions by PF compared to RF are known to have a much larger zone of reversible injury.[18] Our previous experience with PF ablation of SHD VTs using a solid-tip catheter[19] has shown that PF delivery resulted in more likely temporary suppression of VT inducibility with a higher recurrence during follow-up. Lastly, PF applications were commonly associated with local myocardial capture. Thus, when ongoing VT terminated during PF energy delivery, it was unclear whether it was due to the successful elimination of the culprit isthmus of slow conduction or due to overdrive pace termination by PF.

Radiofrequency vs. pulsed field safety considerations

Both energy sources differ concerning the risk of collateral damage. First, due to the non-thermal nature of PF, tissue overheating with a risk of steam pop is highly unlikely. Similarly, PF is known to spare ganglionic plexi and nerves.[20] In the recent analysis of 17 k patients undergoing AF ablation, the incidence of phrenic nerve injury by PF was 0.06%.[21] Our current experience with epicardial delivery of PF is in line with the above observations and suggests the relative safety of PF applications near the phrenic nerve.

In addition, Reddy *et al.*[22] have shown that using PF energy in the vicinity of the coronary arteries often resulted in their spasms, and pretreatment with nitrates could effectively prevent them. In this respect, coronary angiography in our study showed acute spasms in most of the patients with PF epicardial ablation. In some experimental studies,[23] PF application on the coronary artery led to acute spasm that was followed by chronic mild stenosis via neointimal neoplasia. On the other hand, RF application on the top of the coronary artery might lead to thrombotic occlusion. Thus, due to the non-thermal mechanism of action, it is reasonable to anticipate that the incidence of coronary artery stenosis will be lower for PF compared to the thermal alternatives. Due to this difference, PF may enable epicardial ablation of the substrate very close to the coronary artery. Nevertheless, before more data are available, it seems advisable to perform coronary angiography before and after epicardial PF delivery. Such a strategy will also allow immediate intracoronary administration of nitrates when spam is observed.

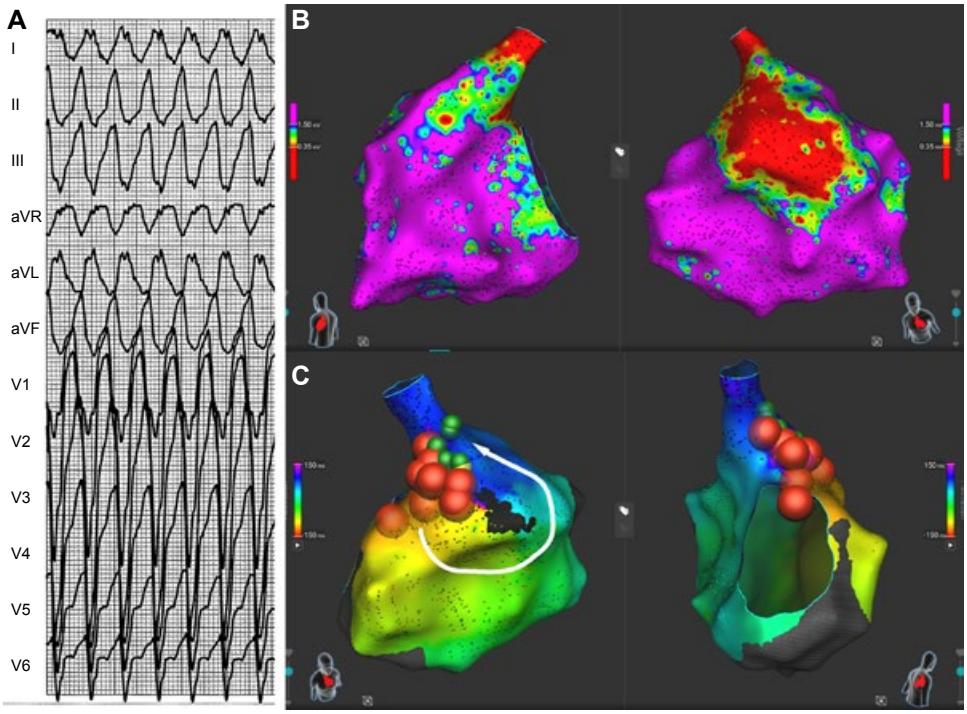

Figure 3 Panel *A* depicts a 12-lead ECG during VT in a patient with grown-up congenital heart disease after repeated surgical correction procedures and implantation of a balloon-expandable pulmonary stent valve. Panel *B* shows a voltage map of the RV with prominent scarring in the lateral RV outflow tract. Panel *C* shows the activation map during VT. The arrhythmia was successfully abolished by both radiofrequency (red tags) and pulsed field (green tags) ablation between the pulmonary valve stent and scarring on the RV lateral wall.

Table 2 Procedural characteristics and outcome

	***N* = 18**
Epicardial access (%)	22
Number of inducible ventricular tachycardia morphologies (*n*)	1.4 ± 1.3
Procedural duration (min)	157 ± 31
Fluoroscopy time (min)	5.2 ± 4.0
Fluoroscopy dose (μGy m^2)	4627 ± 9557
RF applications (*n*)	12 ± 7
PF applications (*n*)	8 ± 9
Post-ablation ventricular arrhythmia non-inducibility (%)	89
Ventricular-arrhythmia-free survival at 3 months (%)	78

Large-footprint-tip vs. 4 mm-tip focal catheter

Large-footprint lattice-tip catheter allowed rapid modification of extensive arrhythmogenic substrate either in the form of scar homogenization[24] or core scar isolation.[25] Although the concept of creating large lesions by the large-tip catheter is attractive for targeting the intramural substrate, different designs of ablation catheters might also have potential shortcomings. Some narrow areas (e.g. space between AV valves and myocardial wall, excavations within the endocardial surface, and base of the papillary muscles) might be more challenging to reach even with real-time imaging (*Figure 5*). This underscores the role of intracardiac echocardiography, which enables precise visualization of the lattice tip and its tailored placement. Theoretically, if prominent trabeculation is observed in the region of interest and ablation by the lattice-tip cannot eliminate the VT, complimentary use of a 4 mm-tip ablation catheter might be considered. Notably, scarring and remodelling after myocardial infarction lead mostly to thinning and smoothing of the myocardial wall and facilitate mapping and ablation with the lattice-tip catheter. Patients with non-ischaemic cardiomyopathy differ since their endocardial surface may have prominent trabeculations and variable thickness. The critical components of the substrate may be localized intramurally and may be more challenging to be recognized and ablated. However, it is yet to be determined, for which substrates this will be relevant and to what degree it will impact clinical outcomes.

The extent of myocardial damage

Studies assessing the troponin T dynamics in patients undergoing AF ablation have reported relatively high values of this biomarker.[26,27] Therefore, there was uncertainty about the extent of myocardial damage using PF on the ventricular level. Our data on the combined use of RF and PF for VT ablation suggest that myocardial damage was relatively moderate (about three times lower). This reflects a much lower number of PF deliveries compared to the average PF ablation for AF as well as targeting mainly scar tissue. The absence of excessive troponin is reassuring because, in patients with pre-existing SHD and impaired LV ejection fraction, extensive damage might lead to pump failure.

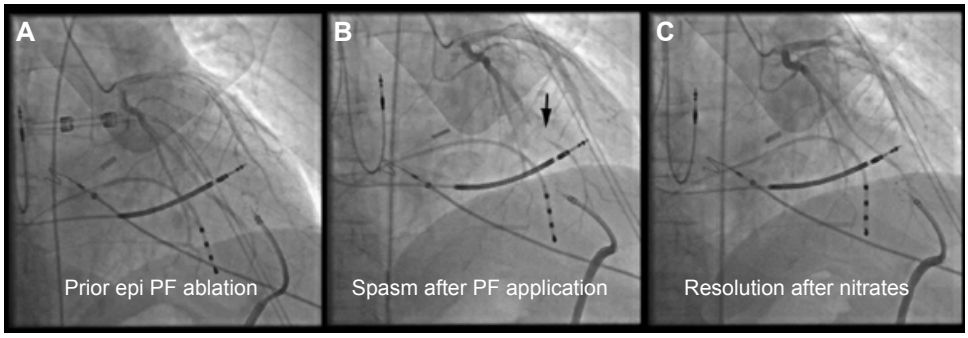

Figure 4 Example of coronary spasm induced by epicardial ablation on the lateral LV wall in vicinity of the marginal branch. Panel *A* shows preablation coronary angiography, panel *B* depicts the spasm of the marginal branch, and panel *C* shows the resolution of the spasm after intracoronary nitrate administration. Interestingly, no ECG changes were seen.

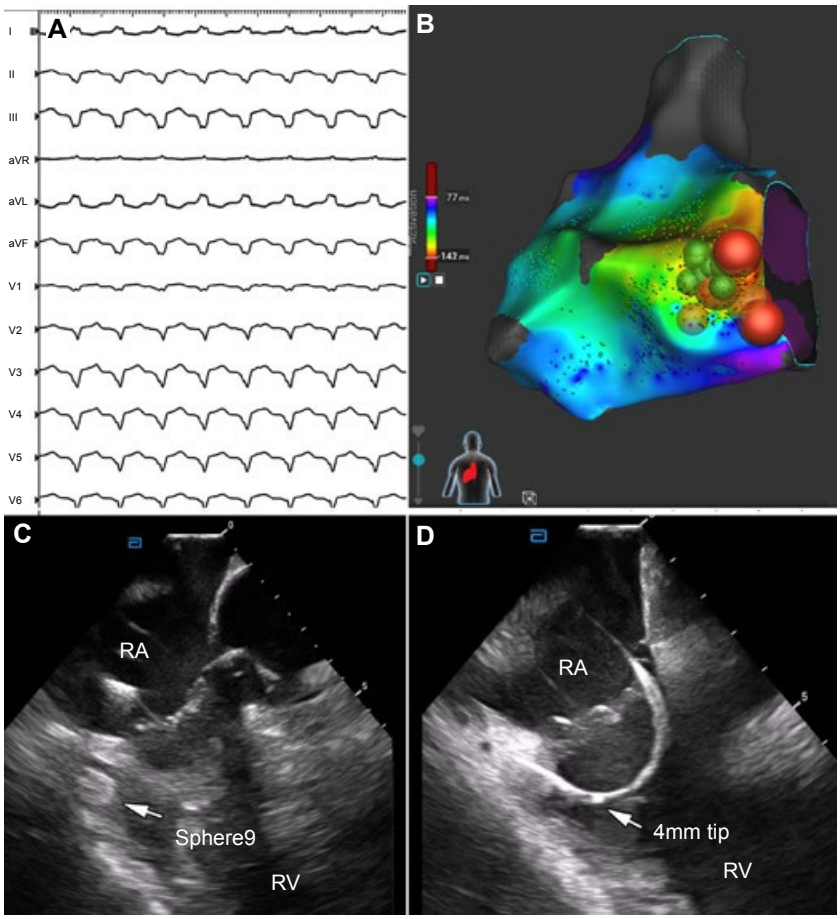

Figure 5 Panel *A* shows a 12-lead ECG of slow VT in a patient with non-ischaemic cardiomyopathy. Panel *B* shows an activation map during VT originating from RV inferoseptal processus. Despite extensive ablation, including the epicardial approach, VT recurred. During the re-ablation session, VT was successfully abolished by a conventional 4 mm irrigated-tip catheter inserted under the inferior leaflet of the tricuspid valve. Due to the larger size of the lattice tip, the catheter likely did not fit into the narrow space under the tricuspid valve, which could be then successfully cannulated and ablated with a 4 mm-tip catheter. Panels *C* and *D* show intracardiac echocardiography images with the position of the lattice-tip and 4 mm-tip close to the tricuspid annulus from the corresponding ablation sessions.

Study limitations

This prospective observational study described the initial experience with the novel electroanatomic mapping and ablation system in VT ablation. Therefore, we inherently investigated and ablated a broad spectrum of different VT substrates. Another limitation may be the combined use of high-energy RF and PF in most patients. A small number of patients may limit the validity of our observations. No nitrates were administered prophylactically before PF application in the epicardial space; thus, it is unknown whether such a strategy could prevent the occurrence of PF-induced spasms.

Conclusions

VT ablation using a dual-energy lattice-tip catheter and a novel electroanatomical mapping system is feasible and allows rapid mapping and effective substrate modification with good outcomes during short-term follow-up. Pulsed field applications in epicardial space were commonly associated with spasms of coronary arteries but not phrenic nerve palsy. Despite effective ablation, lesions did not result in excessive troponin release.

Authors contribution

Substantial contributions to the conception and design or the acquisition, analysis, or interpretation of the data: P.P., J.K. Substantial contributions to the drafting of the articles or critical revision for important intellectual content: P.P., D.W., P.S., J.K. Final approval of the version to be published: P.P., D.W., P.S., V.N., F.S., E.B., P.Š., J.M., J.H., J.K. Agreement to be accountable for all aspects of the work in ensuring that questions related to the accuracy or integrity of any part of the article are appropriately investigated and resolved: P.P., J.K.

Funding

This paper was supported by the National Institute for Metabolic and Cardiovascular Research 'CarDia' (Programme EXCELES, ID Project No. LX22NPO5104)—funded by the European Union—Next Generation EU (KC). This work was also funded by the project (Ministry of Health, Czech Republic) for development of research organization 00023001 (IKEM, Prague, Czech Republic)—institutional support.

Conflict of interest: J.K. reports personal fees from Biosense Webster, Boston Scientific, GE Healthcare, Medtronic, and St. Jude Medical (Abbott) for participation in scientific advisory boards and has received speaker honoraria from Biosense Webster, Biotronik, Boston Scientific, Medtronic, ProMed CS, St. Jude Medical (Abbott), and Viatris. P.P. has received speaker honoraria from St. Jude Medical (Abbott) and Medtronic and has served as a consultant for Biotronik and Boston Scientific. V.N. is an employee of Medtronic. The remaining authors have no disclosures to declare.

Data availability

Data available on request.

References

1. Zeppenfeld K, Tfelt-Hansen J, de Riva M, Winkel BG, Behr ER, Blom NA *et al.* 2022 ESC guidelines for the management of patients with ventricular arrhythmias and the prevention of sudden cardiac death. *Eur Heart J* 2022;**40**:3997–4126.
2. Natale A, Zeppenfeld K, Della Bella P, Liu X, Sabbag A, Santangeli P *et al.* Twenty-five years of catheter ablation of ventricular tachycardia: a look back and a look forward. *Europace* 2023;**25**:euad225.
3. Ravi V, Poudyal A, Khanal S, Khalil C, Vij A, Sanders D *et al.* A systematic review and meta-analysis comparing radiofrequency catheter ablation with medical therapy for ventricular tachycardia in patients with ischemic and non-ischemic cardiomyopathies. *J Interv Card Electrophysiol* 2023;**66**:161–75.
4. Della Bella P, Baratto F, Vergara P, Bertocchi P, Santamaria M, Notarstefano P *et al.* Does timing of ventricular tachycardia ablation affect prognosis in patients with an implantable cardioverter defibrillator? Results from the multicenter randomized PARTITA trial. *Circulation* 2022;**145**:1829–38.
5. Anter E, Mansour M, Nair DG, Sharma D, Taigen TL, Neuzil P *et al.* Dual-energy lattice-tip ablation system for persistent atrial fibrillation: a randomized trial. *Nat Med* 2024;**30**:2303–10.
6. Kitamura T, Hocini M, Bourier F, Martin R, Takigawa M, Frontera A *et al.* Larger and deeper ventricular lesions using a novel expandable spherical monopolar irrigated radiofrequency ablation catheter. *J Cardiovasc Electrophysiol* 2019;**30**:1644–51.
7. Shapira-Daniels A, Barkagan M, Yavin H, Sroubek J, Reddy VY, Neuzil P *et al.* Novel irrigated temperature-controlled lattice ablation catheter for ventricular ablation. *Circ Arrhythm Electrophysiol* 2019;**12**:e007661.
8. Nies M, Watanabe K, Kawamura I, Santos-Gallego CG, Reddy VY, Koruth JS. Preclinical study of pulsed field ablation of 'difficult' ventricular targets: intracavitary mobile structures, interventricular septum and left ventricular free wall. *Circ Arrhythm Electrophysiol* 2024;**17**:e012734.
9. Yokoyama M, Vlachos K, Duchateau J, Sacher F, Jaïs P, Tixier R. Pulsed field epicardial ablation for VT storm: a case report of bail-out therapy. *Heart Rhythm* 2024. doi:10.1016/j.hrthm.2024.08.021. Online ahead of print.
10. Pannone L, Doundoulakis I, Cespón-Fernández M, Eltsov I, Chierchia GB, de Asmundis C *et al.* A large footprint focal catheter toggling between pulsed field and radiofrequency energy: first clinical experience for ventricular tachycardia ablation. *Europace* 2024;**26**:euae193.
11. Sosa E, Scanavacca M, d'Avila A, Pilleggi F. A new technique to perform epicardial mapping in the electrophysiology laboratory. *J Cardiovasc Electrophysiol* 1996;**7**:531–6.
12. Peichl P, Wichterle D, Pavlu L, Cihak R, Aldhoon B, Kautzner J. Complications of catheter ablation of ventricular tachycardia: a single-center experience. *Circ Arrhythm Electrophysiol* 2014;**7**:684–90.
13. Barkagan M, Leshem E, Rottmann M, Sroubek J, Shapira-Daniels A, Anter E. Expandable lattice electrode ablation catheter: a novel radiofrequency platform allowing high current at low density for rapid, titratable, and durable lesions. *Circ Arrhythm Electrophysiol* 2019;**12**:e007090.
14. Yavin HD, Higuchi K, Sroubek J, Younis A, Zilberman I, Anter E. Pulsed-field ablation in ventricular myocardium using a focal catheter: the impact of application repetition on lesion dimensions. *Circ Arrhythm Electrophysiol* 2021;**14**:e010375.
15. Im SI, Higuchi S, Lee A, Stillson C, Buck E, Morrow B *et al.* Pulsed field ablation of left ventricular myocardium in a swine infarct model. *JACC Clin Electrophysiol* 2022;**8**:722–31.
16. Younis A, Buck E, Santangeli P, Tabaja C, Garrott K, Lehn L *et al.* Efficacy of pulsed field vs radiofrequency for the reablation of chronic radiofrequency ablation substrate: redo pulsed field ablation. *JACC Clin Electrophysiol* 2024;**10**:222–34.
17. Sandhu U, Alkukhun L, Kheiri B, Hodovan J, Chiang K, Splanger T *et al.* In vivo pulsed-field ablation in healthy vs. chronically infarcted ventricular myocardium: biophysical and histologic characterization. *Europace* 2023;**25**:1503–9.
18. Nakagawa H, Castellvi Q, Neal R, Girouard S, Laughner J, Ikeda A *et al.* Effects of contact force on lesion size during pulsed field catheter ablation: histochemical characterization of ventricular lesion boundaries. *Circ Arrhythm Electrophysiol* 2024;**17**:e012026.
19. Peichl P, Bulava A, Wichterle D, Schlosser F, Stojadinović P, Borišincová E *et al.* Efficacy and safety of focal pulsed-field ablation for ventricular arrhythmias: two-centre experience. *Europace* 2024;**26**:euae192.
20. Stojadinović P, Wichterle D, Peichl P, Nakagawa H, Čihák R, Hašková J *et al.* Autonomic changes are more durable after radiofrequency than pulsed electric field pulmonary vein ablation. *JACC Clin Electrophysiol* 2022;**8**:895–904.
21. Ekanem E, Neuzil P, Reichlin T, Kautzner J, van der Voort P, Jais P *et al.* Safety of pulsed field ablation in more than 17,000 patients with atrial fibrillation in the MANIFEST-17K study. *Nat Med* 2024;**30**:2020–9.
22. Reddy VY, Petru J, Funasako M, Kopriva K, Hala P, Chovanec M *et al.* Coronary arterial spasm during pulsed field ablation to treat atrial fibrillation. *Circulation* 2022;**146**:1808–19.
23. Higuchi S, Im SI, Stillson C, Buck ED, Jerrell S, Schneider CW *et al.* Effect of epicardial pulsed field ablation directly on coronary arteries. *JACC Clin Electrophysiol* 2022;**8**:1486–96.
24. Gökoğlan Y, Mohanty S, Gianni C, Santangeli P, Trivedi C, Güneş MF *et al.* Scar homogenization versus limited-substrate ablation in patients with nonischemic cardiomyopathy and ventricular tachycardia. *J Am Coll Cardiol* 2016;**68**:1990–8.
25. Tzou WS, Frankel DS, Hegeman T, Supple GE, Garcia FC, Santangeli P *et al.* Core isolation of critical arrhythmia elements for treatment of multiple scar-based ventricular tachycardias. *Circ Arrhythm Electrophysiol* 2015;**8**:353–61.
26. Krisai P, Knecht S, Badertscher P, Mühl A, Osswald S, Roten L *et al.* Troponin release after pulmonary vein isolation using pulsed field ablation compared to radiofrequency and cryoballoon ablation. *Heart Rhythm* 2022;**19**:1471–2.
27. Popa MA, Bahlke F, Kottmaier M, Foerschner L, Bourier F, Lengauer S *et al.* Myocardial injury and inflammation following pulsed-field ablation and very high-power short-duration ablation for atrial fibrillation. *J Cardiovasc Electrophysiol* 2024;**35**:317–27.

P. Stojadinović et al.

Periprocedural acute haemodynamic decompensation during substrate-based ablation of scar-related ventricular tachycardia: a rare and unpredictable event

Europace
Impact Factor: 7,9

‹ rejstřík

ESC European Society of Cardiology

Europace (2024) **00**, euae145
https://doi.org/10.1093/europace/euae145

CLINICAL RESEARCH

Periprocedural acute haemodynamic decompensation during substrate-based ablation of scar-related ventricular tachycardia: a rare and unpredictable event

Predrag Stojadinović [1,2], Dan Wichterle [1]*, Petr Peichl [1], Robert Čihák[1], Bashar Aldhoon [1], Eva Borišincová [1], Petr Štiavnický [1], Jana Hašková [1], Adam Ševčík [1], and Josef Kautzner [1]

[1]Institute for Clinical and Experimental Medicine, Vídeňská 1958/9 Prague 140 21, Czechia; and [2]First Faculty of Medicine, Institute of Physiology, Charles University, Prague, Czechia

Received 8 January 2024; accepted after revision 9 April 2024

Aims Patients with structural heart disease (SHD) undergoing catheter ablation (CA) for ventricular tachycardia (VT) are at considerable risk of periprocedural complications, including acute haemodynamic decompensation (AHD). The PAINESD score was proposed to predict the risk of AHD. The goal of this study was to validate the PAINESD score using the retrospective analysis of data from a large-volume heart centre.

Methods and results Patients who had their first radiofrequency CA for SHD-related VT between August 2006 and December 2020 were included in the study. Procedures were mainly performed under conscious sedation. Substrate mapping/ablation was performed primarily during spontaneous rhythm or right ventricular pacing. A purposely established institutional registry for complications of invasive procedures was used to collect all periprocedural complications that were subsequently adjudicated using the source medical records. Acute haemodynamic decompensation triggered by CA procedure was defined as intraprocedural or early post-procedural (<12 h) development of acute pulmonary oedema or refractory hypotension requiring urgent intervention. The study cohort consisted of 1124 patients (age, 63 ± 13 years; males, 87%; ischaemic cardiomyopathy, 67%; electrical storm, 25%; New York Heart Association Class, 2.0 ± 1.0; left ventricular ejection fraction, 34 ± 12%; diabetes mellitus, 31%; chronic obstructive pulmonary disease, 12%). Their PAINESD score was 11.4 ± 6.6 (median, 12; interquartile range, 6–17). Acute haemodynamic decompensation complicated the CA procedure in 13/1124 = 1.2% patients and was not predicted by PAINESD score with AHD rates of 0.3, 1.8, and 1.1% in subgroups by previously published PAINESD terciles (<9, 9–14, and >14). However, the PAINESD score strongly predicted mortality during the follow-up.

Conclusion Primarily substrate-based CA of SHD-related VT performed under conscious sedation is associated with a substantially lower rate of AHD than previously reported. The PAINESD score did not predict these events. The application of the PAINESD score to the selection of patients for pre-emptive mechanical circulatory support should be reconsidered.

* Corresponding author. Tel: +420 602 848 364; fax: +420 236 052 985. *E-mail address:* wichterle@hotmail.com

Graphical Abstract

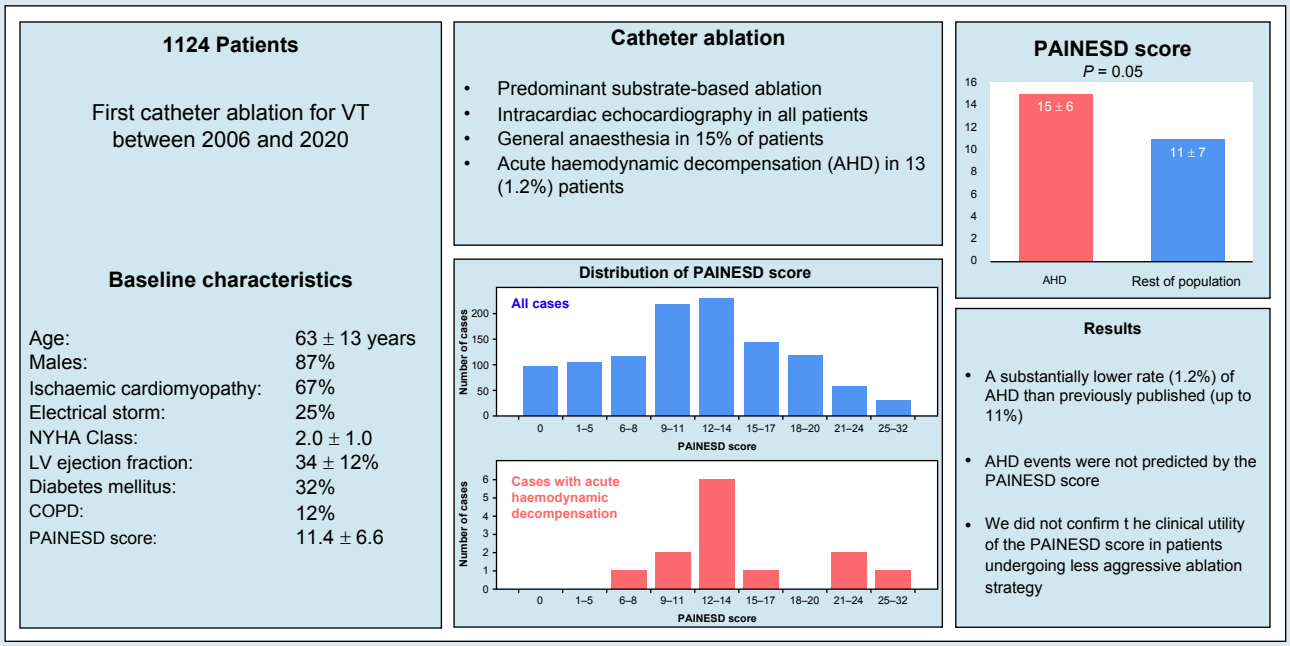

Keywords Catheter ablation • Ventricular tachycardia • Acute haemodynamic decompensation • Mechanical circulatory support • Risk assessment • PAINESD score

What's new?

- We observed a substantially lower rate (1.2%) of acute haemodynamic decompensation during catheter ablation (CA) of structural heart disease–related ventricular tachycardia (VT) than previously reported (up to 11%), and they were not predicted by the PAINESD score.
- This observation may be explained by predominant substrate-based CA under conscious sedation that prevents prolonged low cardiac output state related to general anaesthesia–induced hypotension and repeated VT induction and mapping during VT.
- The application of the PAINESD score to the selection of patients for pre-emptive mechanical circulatory support should be reconsidered.

Introduction

Radiofrequency catheter ablation (CA) is an established treatment method for the management of ventricular tachycardias (VTs) in patients with structural heart disease (SHD).[1,2] Previous studies demonstrated the superiority of CA, compared with conventional treatment in managing the electrical storm,[3–5] improving quality of life,[6] and reducing VT recurrences and related hospitalizations.[6,7] However, due to underlying SHD, concomitant heart failure, and a high burden of comorbidities, patients undergoing CA for VT are at considerable risk of periprocedural complications, including acute haemodynamic decompensation (AHD) with a reported rate of up to 11%.[8] The PAINESD score was proposed to predict the risk of AHD and identify the patients who may benefit from pre-emptive use of mechanical circulatory support (MCS) devices.[8–10] It is calculated as a sum of risk points for chronic obstructive pulmonary disease (5 points), age > 60 years (3 points), ischaemic cardiomyopathy (6 points), New York Heart Association (NYHA) Class > 2 (6 points), left ventricular (LV) ejection fraction < 25% (3 points), electrical storm (5 points), and diabetes mellitus (3 points). Other groups used the PAINESD score for this purpose with variable success.[11,12] There are no data on the role of PAINESD in predicting haemodynamic deterioration during predominant substrate-based ablation without general anaesthesia (GA) and multiple inductions of VT. Therefore, the goal of this study was to investigate the incidence of AHD and the predictive power of the PAINESD score in a cohort of patients with ablation of SHD-related VT, based primarily on substrate mapping and pace mapping in sinus rhythm or right ventricular pacing.

Methods

Study population and study design

This single-centre study included consecutive patients who underwent their first CA for SHD-related VT in a large tertiary hospital between August 2006 and December 2020. We excluded those who had already LV assist device implanted. All patients signed informed consent with the procedure. The study was approved by the institutional ethics committee. Data were collected prospectively. We calculated the PAINESD score for each patient and assessed the distribution of AHD according to the terciles of PAINESD. The association of PAINESD and its components with all-cause mortality was also investigated.

Catheter ablation procedure

The procedures were performed mainly under conscious sedation with fentanyl and midazolam. Propofol was not used. General anaesthesia was used in patients requiring the epicardial access or in those who were on artificial ventilation because of haemodynamical or electrical instability before the CA. After obtaining vascular access, unfractionated heparin was administered as an initial bolus and continuous infusion to maintain the

activated clotting time between 300 and 350 s. The LV was accessed either transseptally or retrogradely, depending on the substrate location, the actual INR level, the presence of peripheral arterial disease, and/or mechanical valve prosthesis. Procedures were navigated using a three-dimensional electroanatomic mapping system CARTO 3 (Biosense Webster) or Ensite (Abbott) and guided by intracardiac echocardiography (AcuNav, Siemens Medical Solutions). Radiofrequency energy was delivered using 30–40 W over a 3.5 mm irrigated-tip catheter (NaviStar ThermoCool, Biosense Webster, or Cool Flex, Abbott). One quadripolar catheter was inserted into the right ventricle for pacing. At baseline, programmed ventricular stimulation from the ventricular apex was performed at two drive trains (600 and 400 ms) and up to three extrastimuli except for incessant VT or focally triggered ventricular fibrillation (VF). Induced VTs that were not well-tolerated were immediately terminated by overdrive pacing or cardioverted. During the procedure, patients were carefully monitored, and mean arterial blood pressure was maintained at >65 mm Hg to reduce the risk of organ dysfunction. Activation and entrainment mapping were used only for well-tolerated VTs. Substrate mapping/ablation was performed primarily during spontaneous rhythm or right ventricular pacing using an integrated approach.[13] Regions of abnormal wall morphology and motion as assessed by intracardiac echocardiography were explored first. Bipolar voltage maps (the lower threshold of 0.5 mV) were constructed and fragmented, or late potentials were tagged. Zones of slow conduction were identified by stimulus-to-QRS onset interval longer than 40 ms. The paced QRS morphology during sinus rhythm was used to match the exit sites of induced VT. The goal of subsequent CA was to abolish all abnormal signals or late potentials, often reaching isolation of the segment of the scar with no capture. The second goal was to abolish the inducibility of clinical VT and all inducible VTs. However, programmed ventricular stimulation at the end of the CA procedure was not performed systematically, mainly because of safety concerns in patients with severe LV dysfunction and/or fragile haemodynamics.

Clinical follow-up

Following the CA, most patients were routinely evaluated in our outpatient clinic at 3, 6, and every 6–12 months afterwards. A purposely established institutional registry for complications of invasive procedures was used to collect all periprocedural complications that were subsequently adjudicated using the source medical records. Acute haemodynamic decompensation triggered by CA was defined as intraprocedural or early post-procedural (<12 h) development of acute pulmonary oedema or refractory hypotension requiring urgent intervention including (but not limited to) inotropic/vasoactive agents and/or artificial ventilation and/or MCS. Data on mortality were obtained/verified for all subjects from the national registry of citizens.

Statistical analysis

All statistical analyses were conducted in R (http://www.R-project.org). Continuous variables are presented as means with standard deviations. Survival is displayed using Kaplan–Meier curves, and the differences between subgroups were assessed by the log-rank test. The Cox proportional hazard models were used to calculate the corresponding hazard ratios (HR) with 95% confidence intervals (CI) and to investigate the independent predictive value of individual risk factors for all-cause death. A $P < 0.05$ was considered significant.

Results

The baseline and procedural characteristics are shown in *Tables 1* and 2. The study cohort consisted of 1124 patients (age, 63 ± 13 years; males, 87%; ischaemic cardiomyopathy, 67%; electrical storm, 25%; NYHA Class, 2.0 ± 1.0; LV ejection fraction, 34 ± 12%; diabetes mellitus, 32%; chronic obstructive pulmonary disease, 12%). The mean PAINESD score of the study cohort was 11.4 ± 6.6 [median, 12; interquartile range (IQR), 6–17].

Catheter ablation was performed in GA in 170 (15%) patients; 115 (10%) patients had elective GA for procedures with epicardial access; 55 (5%) patients had GA as part of the management of arrhythmic storm. Catheter ablation (total duration, 187 ± 79 min; radiofrequency

Table 1 Baseline characteristics of the study population

Baseline characteristics	*N* = 1124
Male (%)	87
Age (years)	63 ± 13
Age > 60 years (%)	70
Weight (kg)	89 ± 17
Height (cm)	175 ± 9
Body mass index (kg/m^2)	29 ± 5
Body surface area (m^2)	2.0 ± 0.2
Congestive heart failure (%)	93
CHA_2DS_2-VASc score	3.6 ± 1.7
Implantable cardioverter-defibrillator (%)	78
Cardiac resynchronisation therapy (%)	35
Arterial hypertension (%)	66
Diabetes mellitus (%)	31
Stroke/transient ischaemic attack (%)	12
Coronary (or peripheral) artery disease (%)	68
Chronic obstructive pulmonary disease (%)	12
NYHA Class	2.0 ± 1.0
NYHA Class ≥ III (%)	31
Left ventricular ejection fraction (%)	34 ± 12
Left ventricular ejection fraction < 25% (%)	25
Serum creatinine (μmol/L)	112 ± 48
Electrical storm (%)	25
PAINESD score	11.4 ± 6.6
Type of cardiomyopathy	
Ischaemic cardiomyopathy (%)	67
Dilated cardiomyopathy (%)	18
Arrhythmogenic cardiomyopathy (%)	5
Hypertrophic cardiomyopathy (%)	1
Valvular cardiomyopathy (%)	11
Other cardiomyopathy (%)	13

Data are provided as means ± SD or percentages.
NYHA, New York Heart Association.

Table 2 Procedural characteristics

Procedural characteristics	*N* = 1124
Radiofrequency time (min)	23 ± 16
Fluoroscopic dose (μGy m^2)	1114 ± 1803
Fluoroscopic time (min)	10.4 ± 8.1
Procedure time (min)	187 ± 79
Major complications (%)	7.7
Major vascular access complications (%)	4.4
General anaesthesia (%)	15.1
Acute haemodynamic decompensation (%)	1.2

Data are provided as means ± SD or percentages.

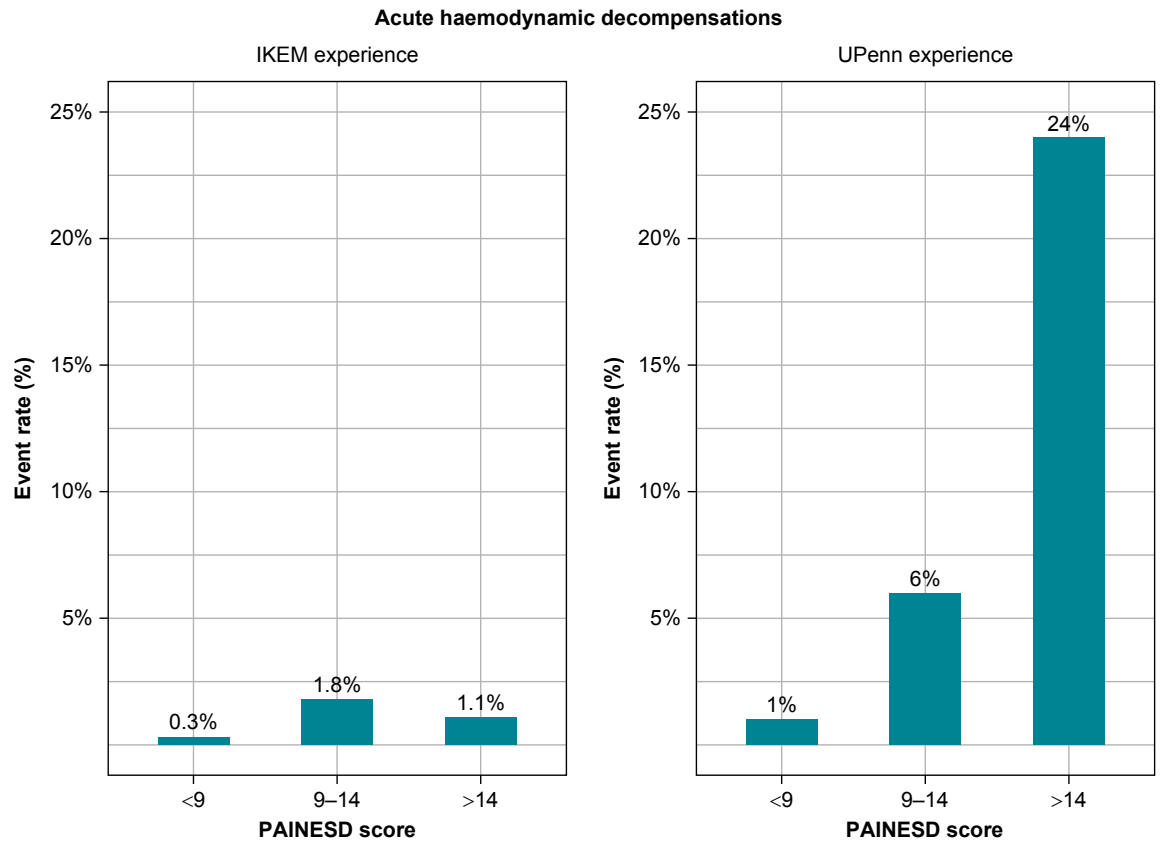

Figure 1 Acute haemodynamic decompensation according to the PAINESD score. Comparison between IKEM and UPenn experience.[8] IKEM, Institute for Clinical and Experimental Medicine; UPenn, University of Pennsylvania.

time, 23 ± 16 min) was complicated by AHD in 13 of 1124 (1.2%) patients, and these adverse events were not predicted by the PAINESD score. In subgroups by previously published PAINESD terciles [<9 ($n = 318$), 9–14 ($n = 451$), and >14 ($n = 355$)], a total of 1, 8, and 4 AHD events occurred with corresponding rates of 0.3, 1.8, and 1.1%, respectively (*Figure 1*). The clinical characteristics of the patients with AHD are summarized in *Table 3*. Four patients in the AHD group were intubated in the electrophysiology room due to incessant VT/VF; nine patients were treated with norepinephrine; three patients were treated with intravenous diuretics. Acute haemodynamic decompensation events did not accumulate in patients with PAINESD score in upper tercile in whom the highest AHD risk was reported up to 24% (*Figure 1*). Four of 1124 patients subsequently underwent MCS implantation early (>12 h, <5 days) after the procedure to treat pre-existing cardiogenic shock. None of them met the clinical criteria for acute cardiac decompensation during the procedure.

During a mean follow-up of 4.2 (IQR: 2.1–7.3) years, a total of 318 patients (28%) underwent repeated CA. Forty (3.6%) patients underwent implantation of a LV assist device [median 65 (IQR: 26–378) days after the CA], and 51 (4.5%) patients underwent heart transplant. A total of 539 (48%) patients died during the follow-up. Patients with periprocedural AHD were more likely to have electrical storms, chronic obstructive pulmonary disease, worse NYHA Class, and adverse outcomes including the need for MCS implantation (*Table 4*).

The impact of individual PAINESD risk factors on all-cause mortality in the univariate analysis is displayed in *Figure 2*. After multivariate adjustment, independent predictors of all-cause mortality were age > 60 years (HR 2.0, 95% CI 1.6–2.5, $P < 0.0001$), ischaemic cardiomyopathy (HR 1.6, 95% CI 1.2–2.0, $P < 0.0001$), NYHA Class ≥ III (HR 1.8, 95% CI 1.5–2.1, $P < 0.0001$), LV ejection fraction < 25% (HR 2.3, 95% CI 1.9–2.8, $P < 0.00001$), electrical storm (HR 1.4, 95% CI 1.2–1.7, $P < 0.001$), and diabetes mellitus (HR 1.4, 95% CI 1.1–1.6, $P < 0.001$). However, the presence of chronic pulmonary disease did not reach statistical significance after multivariate adjustment (HR 1.2, 95% CI 1.0–1.6, $P = 0.08$). The PAINESD score was a strong predictor of long-term mortality in this cohort (*Figure 3*).

Discussion

To the best of our knowledge, this study investigated the largest single-centre cohort of patients undergoing CA for SHD-related VT. We retrospectively evaluated the predictive power of the PAINESD score for the incidence of AHD after the predominant substrate-based strategy of ablation. The results can be summarized as follows: (i) A substantially lower rate (1.2%) of AHD was observed than previously published (up to 11%),[6] and (ii) AHD events did not accumulate in patients with upper-tercile PAINESD score in whom the highest AHD risk was reported (up to 24%). Therefore, we did not confirm the clinical utility of the PAINESD score in patients undergoing less aggressive ablation strategy.

In principle, strategies of CA for VT in SHD can be divided into two groups. The first utilizes predominant activation and entrainment mapping during ongoing VT. The second relies mostly on substrate mapping, in which abnormal signals are identified during sinus rhythm or ventricular pacing.[14,15] It may be complemented with imaging of the

Table 3 Acute heart decompensation during the ablation procedure

Procedure date	Age (years)	Chronic obstructive pulmonary disease	Ischaemic cardiomyopathy	NYHA	Left ventricular ejection fraction (%)	Electrical storm	Diabetes mellitus	PAINESD score	Type of haemodynamic deterioration
17/05/2007	54	No	Yes	III	25	Yes	No	17	Periprocedural pulmonary oedema
11/03/2009	40	No	No	III	15	Yes	No	14	Periprocedural hypotension, CPR
29/12/2011	69	No	Yes	II	40–45	No	Yes	12	Incessant VT, CPR
12/12/2013	73	No	Yes	IV	15–20	Yes	Yes	26	Incessant VF, CPR
14/09/2015	79	No	Yes	II	35–40	Yes	No	14	Incessant VT, CPR
04/07/2017	59	Yes	Yes	III	25–30	Yes	No	22	Post-procedural pulmonary oedema
14/09/2017	52	No	No	II–III	15–20	Yes	No	8	Refractory VF, CPR
06/10/2017	71	No	Yes	II–III	30–35	Yes	No	14	Post-procedural pulmonary oedema
18/12/2017	78	No	Yes	II–III	25–30	No	No	9	Post-procedural pulmonary oedema
24/01/2018	86	Yes	No	III–IV	35–40	No	No	14	Post-procedural pulmonary oedema
10/07/2019	67	No	Yes	NK	NK	No	Yes	12	Pulseless electrical activity, CPR
22/08/2019	69	No	Yes	III	20–25	Yes	No	23	Post-procedural cardiogenic shock
25/09/2019	68	No	Yes	II–III	NK	No	No	9	Post-procedural pulmonary oedema

Data are provided as means ± SD or counts (proportions).
CPR, cardiopulmonary resuscitation; NK, not known; NYHA, New York Heart Association; VT, ventricular tachycardia; VF, ventricular fibrillation.

scar using magnetic resonance imaging, computed tomography, or intracardiac echocardiography.[16–22] Unfortunately, a head-to-head comparison of the two strategies in large, randomized trials is not available. A meta-analysis of six studies (including two small randomized trials) comparing a strategy guided by activation and entrainment mapping with a substrate-based approach demonstrated comparable periprocedural efficacy, complications, VT recurrences, and mortality rates.[23]

The risk of acute haemodynamic decompensation during catheter ablation of ventricular tachycardia

Owing to the severity of underlying disease and comorbidities, patients undergoing CA for SHD-related VT are at a substantial risk of periprocedural complications including AHD, which is associated with increased short- and long-term mortality.[9,24–26] The haemodynamic instability may have different causes. One could be the use of GA with cardio- and vasodepressive effects that often necessitate inotropic/vasoactive support. This can promote the spontaneous occurrence of less-tolerated VTs. The other reason could reflect repeated inductions of VT leading to coronary, cerebral, and renal hypoperfusion. Moreover, the low cardiac output state may even persist after the restitution of the normal sinus rhythm and precipitate further deterioration of cardiac systolic function.[24]

The PAINESD score was proposed by a group at the University of Pennsylvania to predict the risk of AHD and identify the patients who may benefit from the pre-emptive use of MCS devices. They had reported a high incidence of AHD events (in 22 of 193 patients, 11%), which, interestingly, occurred in the majority of patients (63%) during substrate ablation (not during ongoing VT).[8,27] However, CA was performed under GA in a substantial proportion of cases (32%).

Table 4 Comparison between AHD and rest of population group

	AHD	Rest of population	*P*-value
Male	92.3%	87.1%	0.58
Age (years)	66.6 ± 12.4	63.4 ± 13	0.38
Ischaemic cardiomyopathy	76.9%	66.7%	0.44
Dilated cardiomyopathy	23.1%	17.8%	0.62
Arterial hypertension	69.2%	66.4%	0.83
Congestive heart failure	100%	92.7%	0.46
NYHA Class	2.8 ± 0.6	2.0 ± 1.0	0.01
Diabetes mellitus	23.1%	31,4%	0.52
Stroke/transient ischaemic attack	30.8%	11,3%	0.03
Coronary (or peripheral) artery disease	84.6%	68.2%	0.21
CHA_2DS_2-VASc score	4.3 ± 1.5	3.6 ± 1.7	0.28
Chronic obstructive pulmonary disease	15.4%	11.6%	0.67
Serum creatinine (μmol/L)	136.9 ± 56.3	112.2 ± 47.9	0.07
Left ventricular ejection fraction (%)	27.6 ± 9.3	34.2 ± 12.5	0.08
Electrical storm	61.5%	24.3%	0.002
PAINESD score	14.9 ± 5.6	11.4 ± 6.6	0.05
Procedure time (min)	171 ± 38	189 ± 60	0.34
General anaesthesia (%)	23.1%	15.0%	0.42
Radiofrequency time (min)	27.6 ± 15.8	22.7 ± 15.5	0.31
Re-ablation during follow-up	23.1%	28.4%	0.67
MCS during follow-up	23.1%	3.3%	0.0001
Heart transplant during follow-up	0.0%	4.6%	0.43
Death	76.9%	47.6%	0.04

Data are provided as means ± SD or counts (proportions).
AHD, acute haemodynamic decompensation; MCS, mechanical circulatory support; NYHA, New York Heart Association.

The authors concluded that substrate-based ablation *per se* cannot prevent AHD events. In contrast, the incidence of AHD in our cohort was substantially (10 times) lower and was not predicted by the PAINESD score (*Table 5* and *Figure 1*). Our population had fewer patients with electric storm (25 vs. 47%) and fewer patients with chronic obstructive pulmonary disease (12 vs. 16%). On the other hand, it had more patients with ischaemic cardiomyopathy (67 vs. 56%), more patients with NYHA Class ≥ 3 (31 vs. 20%), and more patients with diabetes (31 vs. 20%). The mean PAINESD score in the development cohort[6] was not presented, but its middle-tercile range of 9–14 indicates that it was close to our mean PAINESD of 11 ± 7. Two studies were published on patients undergoing CA of SHD-related VT with comparable results to ours. In the study by Martins *et al.*[28] involving 102 patients, the PAINESD score did not predict early mortality or haemodynamic decompensations. In another study by Della *et al.*,[29] intraprocedural AHD occurred in only 6 among 528 patients (1.1%).

Thus, it suggests that the risk of AHD highly varies between different centres and must be precipitated by other factors currently not included in the PAINESD score. Although we can only speculate, we believe that the crucial factors that can explain the lower risk of AHD observed in our patient population include careful intraprocedural haemodynamical monitoring (including monitoring of cardiac contractility with intracardiac echocardiography), preference for conscious sedation over GA, and use of substrate-based mapping as the dominant strategy.

The role of pre-emptive mechanical circulatory support in catheter ablation of ventricular tachycardia

The AHD is associated with a high risk of morbidity and mortality,[8] and the use of the rescue extracorporeal membrane oxygenation in patients in whom AHD already occurred was associated with a high mortality rate (76% at a median follow-up of 10 days after the procedure).[8] A propensity score–matched analysis by Muser *et al.*[10] reported a benefit of pre-emptive use of MCS (Impella in all cases) in reducing the AHD events (7 vs. 23%, in MCS and control group, respectively, $P < 0.01$). However, this approach was not associated with improved mortality or arrhythmia-related survival. Moreover, there was a substantially increased risk of complication in the MCS group requiring surgical intervention. Increased risk of periprocedural complications when MCS was used was also reported by another group.[30] In a study by Mathuria *et al.*,[12] 30-day mortality of patients undergoing VT ablation with pre-emptive MCS ($n = 24$, PAINESD 16.5) compared with those ablated without MCS ($n = 57$, PAINESD 13.4) was similar (4 vs. 3%). Of note, in our study, the 30-day mortality of patients with comparable PAINESD scores (15–18 vs. 12–15) who underwent CA without pre-emptive MCS was 7/218 (3%) vs. 15/297 (5%), respectively. In another study, Neuzner *et al.*[11] used pre-emptive micro-axial MCS to prevent AHD in 26 patients undergoing VT ablation with a high PAAINESD (variant of PAINESD) score (21 ± 3), and they were successful in

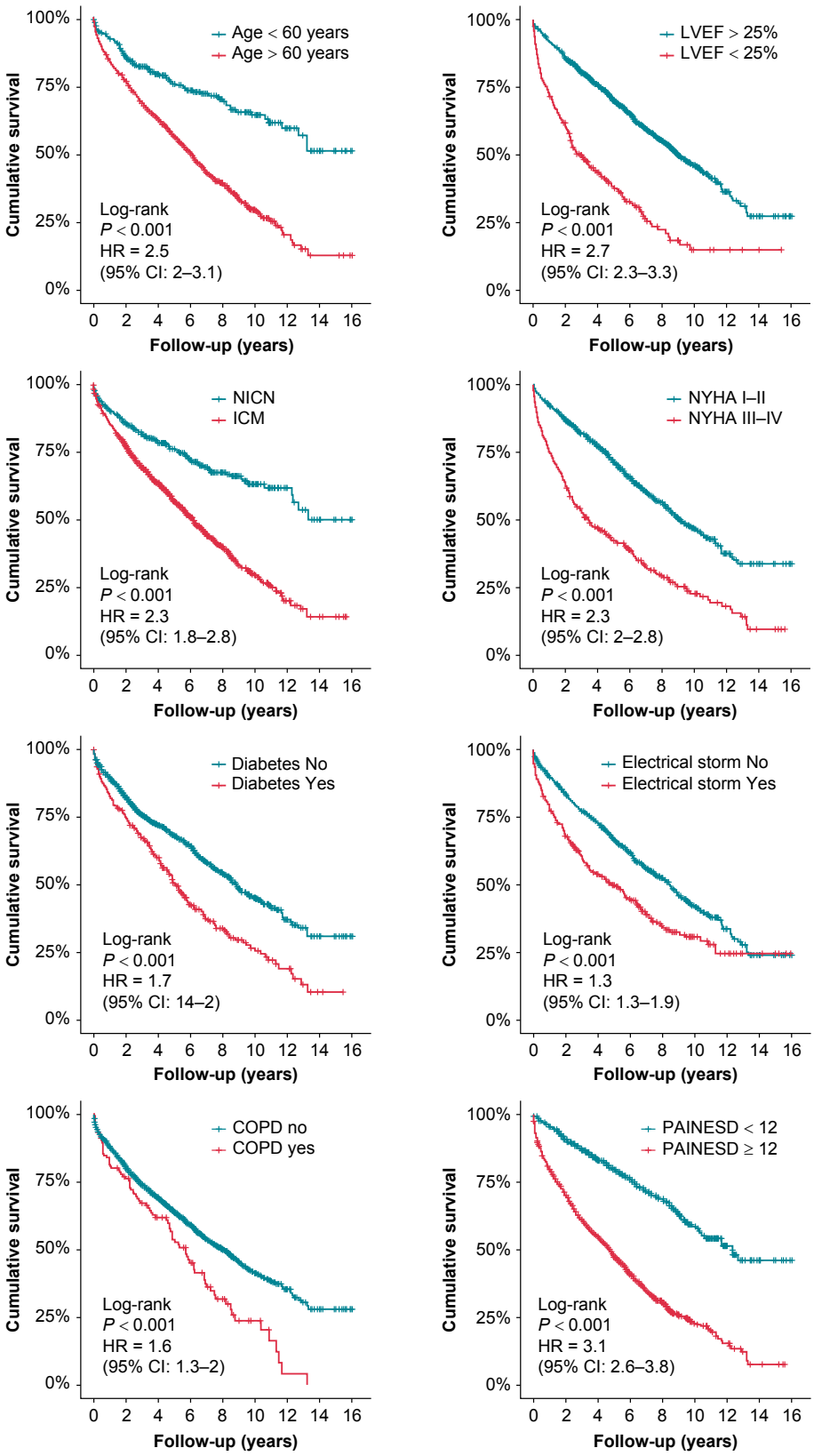

Figure 2 Dichotomized clinical factors associated with all-cause mortality (univariate Cox regression analysis). COPD, chronic obstructive pulmonary disease, LVEF, left ventricular ejection fraction; ICM, ischaemic cardiomyopathy; NICM, non-ischaemic cardiomyopathy; NYHA, New York Heart Association.

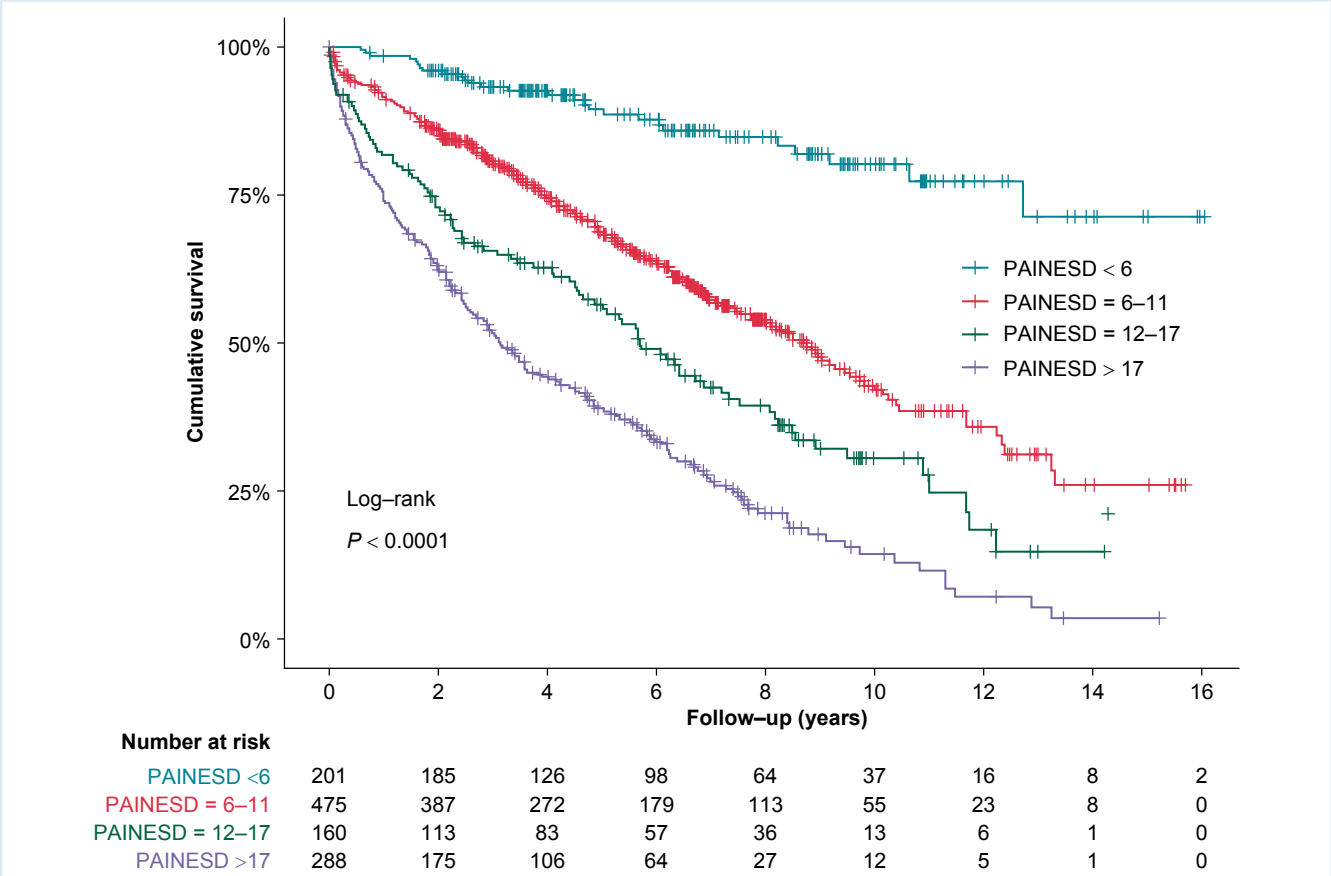

Figure 3 All-cause mortality: the impact of the PAINESD score. Kaplan–Meier survival curves for the population categorized by quartiles of PAINESD score.

Table 5 Comparisons between our experience and previously published data

	IKEM experience	UPenn experience[8]	International VT Ablation Center Collaborative group[27]
Number of patients	1124	193	2061
Age (years)	63 ± 13	62 ± 15	62 ± 13
Left ventricular EF (%)	34 ± 12	37 ± 16	34 ± 13
Follow-up duration	4.2 years	21 ± 7 months	1 year
Electrical storm (%)	25	47	35
PAINESD score	11 ± 7	*NA*	9.8[a]
Acute haemodynamic decompensation (%)	1.2	11	NA
Early (31 day) mortality (%)	2.9	*NA*	5
Late (21 month) mortality (%)	18	16	NA
Procedural time (min)	187 ± 79	480	284 ± 117

Data are provided as means ± SD or counts (proportions).
EF, ejection fraction; IKEM, Institute for Clinical and Experimental Medicine; NA, not available; UPenn, University of Pennsylvania; VT, ventricular tachycardia.
[a]Estimated based on a weighted average of three study groups (early mortality group, late mortality group, and the rest of the population group)

all but one case with bail-out use of MCS. However, such results are of limited relevance, since the control group is missing. Thus, the role of MCS and the selection of appropriate candidates during the CA of VT remain controversial.

PAINESD score as the predictor of mortality

In a large multicentre registry of 2061 patients[9] undergoing CA for SHD-related VT, the PAINESD score was a good predictor of early and long-term mortality. Our study confirmed these results. The key question remains whether the prognosis in such a high-risk group could be improved by more effective CA. Conversely, less aggressive CA aimed to prevent periprocedural AHD in high-risk patients may lead to a higher recurrence rate. In this regard, both early mortality, as an indicator of the safety and immediate risk associated with the procedure, and late mortality, which could reflect the efficacy of the procedure, were comparable in our cohort to those reported after more aggressive CA (*Table 5*). The outcome of the CA is always a balance between efficacy (i.e. the ability to abolish all inducible VTs resulting in lengthy procedures) and safety. In our hands, less aggressive CA aimed to avoid AHD was not associated with poorer outcomes. Overall, our results do not support the routine use of PAINESD score for the prediction of AHD and certainly not for the routine use of MCS devices based on a high PAINESD score.

Study limitations

This was a retrospective study. The enrolment period was very long so the ablation strategy could undergo some change. The study did not investigate all potential risk factors as we tried to be in line with the original definition of the PAINESD score. For example, creatinine level that is known as a strong risk predictor was not included although it was available. Similarly, VT inducibility was not considered as it was not tested consistently at the end of the procedure because of safety concerns.

Conclusions

In our large cohort of patients with CA of SHD-related VT, the incidence of AHD was substantially lower than previously reported. This observation may be explained by a strategy of predominant substrate-based CA under conscious sedation that prevents hypotension and prolonged low cardiac output state related to VT induction and activation mapping. In such a scenario, the PAINESD score may lead to unnecessary prophylactic use of MCS during the CA of VT.

Author's contributions

Substantial contributions to the conception and design or the acquisition, analysis, or interpretation of the data: P.S., D.W., P.P., R.C., B.A., P.S., J.H., E.B., and J.K. Substantial contributions to the drafting of the articles or critical revision for important intellectual content: P.S., D.W., P.P., and J.K. Final approval of the version to be published: J.K. Agreement to be accountable for all aspects of the work in ensuring that questions related to the accuracy or integrity of any part of the article are appropriately investigated and resolved: P.S. and D.W.

Funding

This study was supported by the project National Institute for Research of Metabolic and Cardiovascular Diseases (Programme EXCELES, Project No. LX22NPO5104)—Funded by the European Union, NextGenerationEU. This work was also funded by the project (Ministry of Health, Czech Republic) for development of research organization 00023001 (IKEM, Prague, Czech Republic)—institutional support.

Conflict of interest: J.K. reports personal fees from Biosense Webster, Boston Scientific, GE Healthcare, Medtronic, and St. Jude Medical (Abbott) for participation in scientific advisory boards and has received speaker honoraria from Biosense Webster, Biotronik, Boston Scientific, Medtronic, ProMed CS, St. Jude Medical (Abbott), and Viatris. P.P. has received speaker honoraria from St. Jude Medical (Abbott) and has served as a consultant for Biotronik and Boston Scientific. The remaining authors have no disclosures.

References

1. Zeppenfeld K, Tfelt-Hansen J, de Riva M, Winkel BG, Behr ER, Blom NA, *et al.* Esc guidelines for the management of V tachyarrhytmias and the prevention of sudden cardiac death of the European Society of Cardiology (ESC). *Eur Heart J* 2022;**43**:3997–4126.
2. Natale A, Zeppenfeld K, Della BP, Liu X, Sabbag A, Santangeli P, *et al.* Twenty-five years of catheter ablation of ventricular tachycardia: a look back and a look forward. *Europace* 2023;**25**:euad225.
3. Conti S, Pala S, Biagioli V, Del Giorno G, Zucchetti M, Russo E, *et al.* Electrical storm: a clinical and electrophysiological overview. *World J Cardiol* 2015;**7**:555.
4. Koželuhová M, Peichl P, Hlivák P, Čihák R, Wichterle D, Vančura V, *et al.* Spektrum idiopatických komorových tachykardií ve specializovaném centru. *Interv a akutní Kardiol* 2009;**8**:228–232.
5. Bennett RG, Turnbull S, Sood A, Aung M, Duncan E, Barman P, *et al.* Emergency out-of-hours catheter ablation for ventricular arrhythmia storm: a UK and Australian experience. *Europace* 2023;**25**:euad215.
6. Gula LJ, Doucette S, Leong-Sit P, Tang ASL, Parkash R, Sarrazin JF, *et al.* Quality of life with ablation or medical therapy for ventricular arrhythmias: a substudy of VANISH. *J Cardiovasc Electrophysiol* 2018;**29**:421–434.
7. Zeppenfeld K, Wijnmaalen AP, Ebert M, Baldinger SH, Berruezo A, Catto V, *et al.* Clinical outcomes in patients with dilated cardiomyopathy and ventricular tachycardia. *J Am Coll Cardiol* 2022;**80**:1045–1056.
8. Santangeli P, Muser D, Zado ES, Magnani S, Khetpal S, Hutchinson MD, *et al.* Acute hemodynamic decompensation during catheter ablation of scar-related ventricular tachycardia: incidence, predictors, and impact on mortality. *Circ Arrhythmia Electrophysiol* 2015;**8**:68–75.
9. Muser D, Castro SA, Liang JJ, Santangeli P. Identifying risk and management of acute haemodynamic decompensation during catheter ablation of ventricular tachycardia. *Arrhythmia Electrophysiol Rev* 2018;**7**:282–287.
10. Muser D, Liang JJ, Castro SA, Hayashi T, Enriquez A, Troutman GS, *et al.* Outcomes with prophylactic use of percutaneous left ventricular assist devices in high-risk patients undergoing catheter ablation of scar-related ventricular tachycardia: a propensity-score matched analysis. *Hear Rhythm* 2018;**15**:1500–1506.
11. Neuzner J, Dietze T, Paliege R, Gradaus R. Effectiveness of a percutaneous left ventricular assist device in preventing acute hemodynamic decompensation during catheter ablation of ventricular tachycardia in advanced heart failure patients: a retrospective single-center analysis. *J Cardiovasc Electrophysiol* 2019;**30**:2864–2868.
12. Mathuria N, Wu G, Rojas-Delgado F, Shuraih M, Razavi M, Civitello A, *et al.* Outcomes of pre-emptive and rescue use of percutaneous left ventricular assist device in patients with structural heart disease undergoing catheter ablation of ventricular tachycardia. *J Interv Card Electrophysiol* 2017;**48**:27–34.
13. Kautzner J, Čihák R, Peichl P, Vančura V, Bytešník J. Catheter ablation of ventricular tachycardia following myocardial infarction using three-dimensional electroanatomical mapping. *Pacing Clin Electrophysiol* 2003;**26**:342–347.
14. Kahle AK, Jungen C, Alken FA, Scherschel K, Willems S, Pürerfellner H, *et al.* Management of ventricular tachycardia in patients with ischaemic cardiomyopathy: contemporary armamentarium. *Europace* 2022;**24**:538–551.
15. Hanaki Y, Komatsu Y, Nogami A, Kowase S, Kurosaki K, Sekiguchi Y, *et al.* Combined endo- and epicardial pace-mapping to localize ventricular tachycardia isthmus in ischaemic and non-ischaemic cardiomyopathy. *Europace* 2022;**24**:587–597.
16. Yamashita S, Sacher F, Mahida S, Berte B, Lim HS, Komatsu Y, *et al.* Image integration to guide catheter ablation in scar-related ventricular tachycardia. *J Cardiovasc Electrophysiol* 2016;**27**:699–708.
17. Yamashita S, Sacher F, Hooks DA, Berte B, Sellal JM, Frontera A, *et al.* Myocardial wall thinning predicts transmural substrate in patients with scar-related ventricular tachycardia. *Hear Rhythm* 2017;**14**:155–163.
18. Bunch TJ, Weiss JP, Crandall BG, Day JD, Dimarco JP, Ferguson JD, *et al.* Image integration using intracardiac ultrasound and 3D reconstruction for scar mapping and ablation of ventricular tachycardia. *J Cardiovasc Electrophysiol* 2010;**21**:678–684.
19. Engert F, Bahlke F, Erhard N, Krafft H, Popa M-A, Risse E, *et al.* VT ablation based on CT imaging substrate visualization: results from a large cohort of ischemic and non-ischemic cardiomyopathy patients. *Clin Res Cardiol* 2023. doi:10.1007/s00392-023-02321-1
20. Esposito A, Palmisano A, Antunes S, Maccabelli G, Colantoni C, Rancoita PMV, *et al.* Cardiac CT with delayed enhancement in the characterization of ventricular tachycardia structural substrate: relationship between CT-segmented scar and electro-anatomic mapping. *JACC Cardiovasc Imaging* 2016;**9**:822–832.
21. Siontis KC, Kim HM, Dabbagh GS, Latchamsetty R, Stojanovska J, Jongnarangsin K, *et al.* Association of preprocedural cardiac magnetic resonance imaging with outcomes of

ventricular tachycardia ablation in patients with idiopathic dilated cardiomyopathy. *Hear Rhythm* 2017;**14**:1487–1493.
22. Komatsu Y, Cochet H, Jadidi A, Sacher F, Shah A, Derval N, *et al.* Regional myocardial wall thinning at multidetector computed tomography correlates to arrhythmogenic substrate in postinfarction ventricular tachycardia: assessment of structural and electrical substrate. *Circ Arrhythmia Electrophysiol* 2013;**6**:342–350.
23. Kumar S, Baldinger SH, Romero J, Fujii A, Mahida SN, Tedrow UB, *et al.* Substrate-based ablation versus ablation guided by activation and entrainment mapping for ventricular tachycardia: a systematic review and meta-analysis. *J Cardiovasc Electrophysiol* 2016;**27**:1437–1447.
24. Skhirtladze K, Mora B, Moritz A, Birkenberg B, Ankersmit HJ, Dworschak M. Impaired recovery of cardiac output and mean arterial pressure after successful defibrillation in patients with low left ventricular ejection fraction. *Resuscitation* 2010;**81**:1123–1127.
25. Eckardt L, Doldi F, Anwar O, Gessler N, Scherschel K, Kahle A-K, *et al.* Major in-hospital complications after catheter ablation of cardiac arrhythmias: individual case analysis of 43 031 procedures CLINICAL RESEARCH. *Europace* 2023;**26**:1–12.
26. Peichl P, Wichterle D, Pavlů L, ČihÁk R, Aldhoon B, Kautzner J. Complications of catheter ablation of ventricular tachycardia a single-center experience. *Circ Arrhythmia Electrophysiol* 2014;**7**:684–690.
27. Santangeli P, Frankel DS, Tung R, Vaseghi M, Sauer WH, Tzou WS, *et al.* Early mortality after catheter ablation of ventricular tachycardia in patients with structural heart disease. *J Am Coll Cardiol* 2017;**69**:2105–2115.
28. Martins A, Antonio PS, Pereira SC, Brito J, Silva BV, Da Silva PA, *et al.* Is it possible to predict mortality and recurrence of VT after ablation? PAINESD risk score applicability vs new predictors. *EP Eur* 2022;**24**:40695.
29. Della BP, Baratto F, Tsiachris D, Trevisi N, Vergara P, Bisceglia C, *et al.* Management of ventricular tachycardia in the setting of a dedicated unit for the treatment of complex ventricular arrhythmias: long-term outcome after ablation. *Circulation* 2013;**127**:1359–1368.
30. Kusa S, Miller MA, Whang W, Enomoto Y, Panizo JG, Iwasawa J, *et al.* Outcomes of ventricular tachycardia ablation using percutaneous left ventricular assist devices. *Circ Arrhythmia Electrophysiol* 2017;**10**:1–7.

M. Bébarová et al.

Aminophylline at clinically relevant concentrations affects inward rectifier potassium current in healthy porcine and failing human cardiomyocytes in a similar manner

Biomedicine & Pharmacotherapy
Impact Factor: 6,9

rejstřík

Biomedicine & Pharmacotherapy 181 (2024) 117733

Contents lists available at ScienceDirect

Biomedicine & Pharmacotherapy

journal homepage: www.elsevier.com/locate/biopha

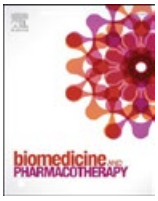

Aminophylline at clinically relevant concentrations affects inward rectifier potassium current in healthy porcine and failing human cardiomyocytes in a similar manner

Markéta Bébarová [a,b,*], Olga Švecová [a], Roman Kula [a], Michal Pásek [a,c], Edita Jeklová [d], Petr Fila [e,f], Martin Pešl [g,h]

[a] Department of Physiology, Faculty of Medicine, Masaryk University, Kamenice 5, Brno 625 00, Czech Republic
[b] Department of Internal Medicine and Cardiology, University Hospital Brno and Faculty of Medicine, Masaryk University, Jihlavská 20, Brno 625 00, Czech Republic
[c] Institute of Thermomechanics, Czech Academy of Sciences, Dolejškova 5, Prague 182 00, Czech Republic
[d] Veterinary Research Institute, Hudcova 70, Brno 621 00, Czech Republic
[e] Centre of Cardiovascular Surgery and Transplantation, Pekařská 53, Brno 602 00, Czech Republic
[f] Department of Cardiovascular Surgery and Transplantation, Faculty of Medicine, Masaryk University, Kamenice 5, Brno 625 00, Czech Republic
[g] ICRC, St. Anne's University Hospital, Pekařská 53, Brno 602 00, Czech Republic
[h] 1st Department of Internal Medicine, Cardio-Angiology, Faculty of Medicine, Masaryk University, Pekařská 53, Brno 602 00, Czech Republic

ARTICLE INFO

Keywords:
Aminophylline
Arrhythmia
Inward rectifier
Action potential
Pig
Human

ABSTRACT

Aminophylline, a bronchodilator mainly used to treat severe asthma attacks, may induce arrhythmias. Unfortunately, the underlying mechanism is not well understood. We have recently described a significant, on average inhibitory effect of aminophylline on inward rectifier potassium current I_{K1}, known to substantially contribute to arrhythmogenesis, in rat ventricular myocytes at room temperature. This study was aimed to examine whether a similar effect may be observed under clinically relevant conditions. Experiments were performed using the whole cell patch clamp technique at 37°C on enzymatically isolated healthy porcine and failing human ventricular myocytes. The effect of clinically relevant concentrations of aminophylline (10–100 μM) on I_{K1} did not significantly differ in healthy porcine and failing human ventricular myocytes. I_{K1} was reversibly inhibited by ~20 and 30 % in the presence of 30 and 100 μM aminophylline, respectively, at −110 mV; an analogical effect was observed at −50 mV. To separate the impact of I_{K1} changes on AP configuration, potentially interfering ionic currents were blocked (L-type calcium and delayed rectifier potassium currents). A significant prolongation of AP duration was observed in the presence of 100 μM aminophylline in porcine cardiomyocytes which well agreed with the effect of a specific I_{K1} inhibitor Ba^{2+} (10 μM) and with the result of simulations using a porcine ventricular cell model. We conclude that the observed effect of aminophylline on healthy porcine and failing human I_{K1} might be involved in its proarrhythmic action. To fully understand the underlying mechanism, potential aminophylline impact on other ionic currents should be explored.

1. Introduction

Aminophylline, a complex of bronchodilator theophylline and solubility-improving agent ethylenediamine (2:1), is used in clinical practice to treat namely severe asthma attacks [22,24,31,8]. It is also known to be abused by professional athletes who do not suffer from asthma [23]. The administration of aminophylline is associated with an increased risk of tachyarrhythmias, most often atrial fibrillation, even at therapeutic concentrations (*e.g.* [34,6]). Life-threatening ventricular arrhythmias have been described as well (*e.g.* [28,26,14]).

Mechanisms underlying the proarrhythmic aminophylline action are not well understood. As known, aminophylline is a non-specific phosphodiesterase (PDE) inhibitor and an adenosine receptor antagonist [37]. The proarrhythmic action of aminophylline in atria may be related to its positive chronotropic effect, a heterogenous shortening of the atrial effective refractory period (ERP), and a dispersion of recovery of atrial excitability (reviewed by [33]). In ventricles, a significant aminophylline-induced shortening of the ERP was documented in dogs

* Corresponding author at: Department of Physiology, Faculty of Medicine, Masaryk University, Kamenice 5, Brno 625 00, Czech Republic.
E-mail address: mbebar@med.muni.cz (M. Bébarová).

https://doi.org/10.1016/j.biopha.2024.117733
Received 1 November 2024; Received in revised form 29 November 2024; Accepted 3 December 2024
Available online 9 December 2024

[20]. Recently, Klimovic et al. [19] have demonstrated an increase in the frequency of rhythm irregularities in both therapeutic and overdose aminophylline concentrations using embryonic bodies formed by human pluripotent stem cell-derived cardiomyocytes. They have suggested a possible role for sarcoplasmic reticulum dysfunction in aminophylline-induced arrhythmogenesis.

Studies focused on the effect of aminophylline/theophylline on the pivotal ionic channels that may affect cardiac repolarization are mostly missing. The only existing study, to our knowledge, is our previous study showing a dual, on average inhibitory, aminophylline effect on inward rectifier potassium (Kir) current (I_{K1}) in rat ventricular myocytes at room temperature [30]. Since changes in Kir currents including I_{K1} may considerably contribute to arrhythmogenesis (*e.g.* [17,13]), this study aimed to explore whether an interaction between aminophylline and I_{K1} might occur in other species and conditions closer to the real clinical situation, namely at 37 °C in healthy porcine and failing human ventricular myocytes.

2. Materials and methods

2.1. Cell isolation

For the isolation of left ventricular cardiomyocytes, we used healthy hearts of 8 pigs (the average weight 50.0 ± 6.1 kg; 3 males and 5 females) and failing hearts of 5 patients (the average age 53.8 ± 6.2 years; for an overview of the basic patients´ data, see Table 1). The porcine hearts were explanted from the cadavers of healthy pigs immediately after their euthanasia in deep anesthesia induced by a combination of tiletamine, zolazepam, ketamine, and xylazine (2 mg/kg of the body weight for all substances; Veterinary Research Institute, Brno, Czech Republic). All experiments using human failing hearts were performed under the ethical standards of the Centre of Cardiovascular Surgery and Transplantation, Brno, Czech Republic, and approved by the Ethics Committee of the Centre. The informed consent of all patients, attachment number 18, from Mar 18, 2020, is archived.

The pig heart was quickly removed, a branch of the left coronary artery was immediately cannulated, and the respective region of the left ventricle was perfused with an ice-cold cardioplegic solution for approx. 5 min (composition in mM: NaCl 110, KCl 16, $NaHCO_3$ 10, $MgCl_2$, 16, $CaCl_2$ 0.6; pH was adjusted to 7.8 with NaOH). Then, the heart was placed into the same ice-cold cardioplegic solution and quickly transported to the laboratory. In the case of the explanted human heart, it was put into the ice-cold cardioplegic solution right in the operating room, transported quickly to the laboratory, and a branch of the left coronary artery was cannulated. Subsequently, the same procedure was applied to the pig and human hearts to obtain the isolated left ventricular myocytes. The cannulated heart was attached to a gravity-driven Langendorff apparatus. The region of interest was sequentially perfused with the following solutions (oxygenated with 100 % O_2 and warmed to 37 °C): (i.) a nominally Ca-free Tyrode solution (0.6 μM Ca^{2+}, ~10 min), (ii.) with the same solution supplemented with collagenase (Collagenase A, Roche Diagnostics GmbH, Mannheim, Germany; 1 mg/ml, 34.9 ± 1.7 min in the pig hearts and 33.4 ± 3.7 min in the human hearts), and (iii.) finally with the nominally Ca-free Tyrode solution again (~10 min). Then the heart was removed from the perfusion apparatus and gelatinous myocardial tissue in the perfused region was dissected and placed into the nominally Ca-free Tyrode solution (37 °C). The tissue was cut and filtered through a nylon mesh. The final cell suspension was left to sediment. After ~10 min, the supernatant was removed and replaced with a fresh nominally Ca-free Tyrode solution. The cells were washed in this way three times. During the final step, the spontaneous sedimentation of the cells was replaced with centrifugation of the suspension (400 rpm, 3 min). Then, the suspension of cells was exposed to an increased Ca^{2+} concentration of 1.8 mM, and the cells were left to adapt for an hour before the patch clamp measurements.

Table 1
Clinical characteristics of patients.

Patient No.	Sex	Age (years)	Main diagnosis	Ejection fraction (%)
Patient 1	male	51	restrictive cardiomyopathy	40
Patient 2	female	65	dilation cardiomyopathy	20
Patient 3	male	32	Becker's dystrophy	21
Patient 4	male	66	dilation cardiomyopathy	25
Patient 5	male	55	ischemic heart disease	19

The ejection fraction was determined according to the Teichholz formula (before the heart transplantation).

2.2. Solutions and chemicals

Tyrode solution of the composition below was used during both the dissociation procedure and perfusion of the cells during I_{K1} and AP measurements (in mM): NaCl 135, KCl 5.4, $MgCl_2$ 0.9, HEPES 10, NaH_2PO_4 0.33, and glucose 10 (pH was adjusted to 7.4 with NaOH). This solution was supplemented with 1.8 mM $CaCl_2$ during the patch clamp recordings. To keep the experimental conditions used in our previous study dealing with the effect of aminophylline on I_{K1} in rat ventricular myocytes [30], $CoCl_2$ (2 mM) and tetraethylammonium chloride (TEA, 50 mM), respectively, were applied to inhibit calcium current I_{Ca} and the delayed rectifier potassium current I_K in the course of the experiments. The patch electrode filling solution contained the following (in mM): L-aspartic acid 120, KCl 15, $MgCl_2$ 1, K_2ATP 5, EGTA 1, HEPES 5, GTP 0.1, Na_2-phosphocreatine 3 (pH 7.25 adjusted with KOH).

I_{K1} was evaluated as the current sensitive to 100 μM Ba^{2+} similarly as it was done in our previous papers (*e.g.* [4,30]). Although it is unlikely to activate ATP-sensitive potassium current $I_{K(ATP)}$ under the given experimental conditions (*i.e.* 5 mM ATP in the pipette solution, isolated cells), the inhibitor of $I_{K(ATP)}$ glibenclamide (10 μM) was present in all the performed experiments. Atropin (1 μM) was also added to avoid contamination of the measured I_{K1} by the acetylcholine-sensitive current $I_{K(ACH)}$.

$CoCl_2$, atropin, and $BaCl_2$ were prepared as 1 M, 1 mM, and 10 mM stock solutions, respectively, in the deionized water and held at 4° C. Glibenclamide was prepared as 100 mM stock solution in dimethyl sulfoxide (DMSO). The final concentration of DMSO was identical in the control and test solutions (0.01 %); this concentration seems to have no considerable effects on the cardiac I_{K1} [25,5]. To prepare the TEA-containing stock solution, NaCl in the used Tyrode solution (described above) was replaced equimolarly by TEACl. The stock solution of aminophylline was prepared as a fresh 100 mM solution before each measurement (dissolved in deionized water). Aminophylline was added to the Tyrode solution to obtain the final concentrations between 10 and 100 μM. The solutions were applied near the measured cell *via* an electronically operated perfusion system.

The chemicals were purchased from Sigma-Aldrich (Prague, Czech Republic) unless otherwise stated.

2.3. Electrophysiological measurements and evaluation

Single rod-shaped cells with well-visible striations were used for the current and voltage recordings applying the whole-cell patch-clamp technique in the voltage and current clamp modes, respectively. The patch pipettes were pulled from borosilicate glass capillary tubes and heat-polished on a programmable horizontal puller (Zeitz-Instrumente Vertriebs GmbH, Martinsried, Germany). The resistance of the filled glass electrodes was below 1.5 MΩ to keep the access resistance as low as possible. For the generation of experimental protocols and data acquisition, the Axopatch 200B equipment and pCLAMP 9.2 software (Molecular Devices, Sunnyvale, California, USA) were used. The series resistance was compensated up to 60 %. The capacitance was not

compensated because the contribution of capacity current to the measured current was regarded as negligible. The measured ionic currents were digitally sampled at 5 kHz and stored on the hard disc. The holding potential was −85 mV and the stimulation frequency was 0.2 Hz. I_{K1} was evaluated as the Ba^{2+}-sensitive current at the end of 500-ms pulses, either to −50 mV (the outward component) or to −110 mV (the inward component); the sodium current I_{Na} was inactivated during the first pulse to −50 mV. Action potentials (APs) were elicited using 0.5-ms suprathreshold current pulses at the stimulation frequency 1 Hz (sampling rate 10 kHz). The data were corrected for the estimated junction potential by shifting all voltage values by −10 mV. All measurements were performed at 37 °C.

2.4. Mathematical simulations

The simulations were performed using the CellML code of a recently published mathematical model of porcine ventricular cardiomyocyte [12] in the computational environment OpenCore v. 0.6. The code is available in the Supplementary Materials of the paper by Gaur et al. [12].

2.5. Statistical analysis

The normality of data distribution was tested using the Shapiro-Wilk test. Data are presented as mean ± S.E.M. from *n* cells/subjects (biological replicates in all cases). Parametric statistical tests (the paired *t*-test and one-way ANOVA with the Bonferroni post-test as individually specified in respective figure legends) were used to test the statistical significance of the observed differences; $P < 0.05$ was considered statistically significant. The software Origin 2022b (version 9.9.5.171; OriginLab Corporation) and GraphPad Prism 9 (version 9.5.1; GraphPad Software, Inc.) were used for the analysis.

3. Results

3.1. Effect of clinically relevant concentrations of aminophylline on I_{K1} in healthy porcine ventricular myocytes

As illustrated in Fig. 1A, I_{K1} was recorded at −50 and −110 mV which enabled the detection of the changes in its outward (repolarizing) and inward (depolarizing) components, respectively. The magnitude of I_{K1} was evaluated as the current sensitive to 100 μM Ba^{2+} at the end of 500-ms pulses (see the arrows in Fig. 1A) to avoid a contribution of any

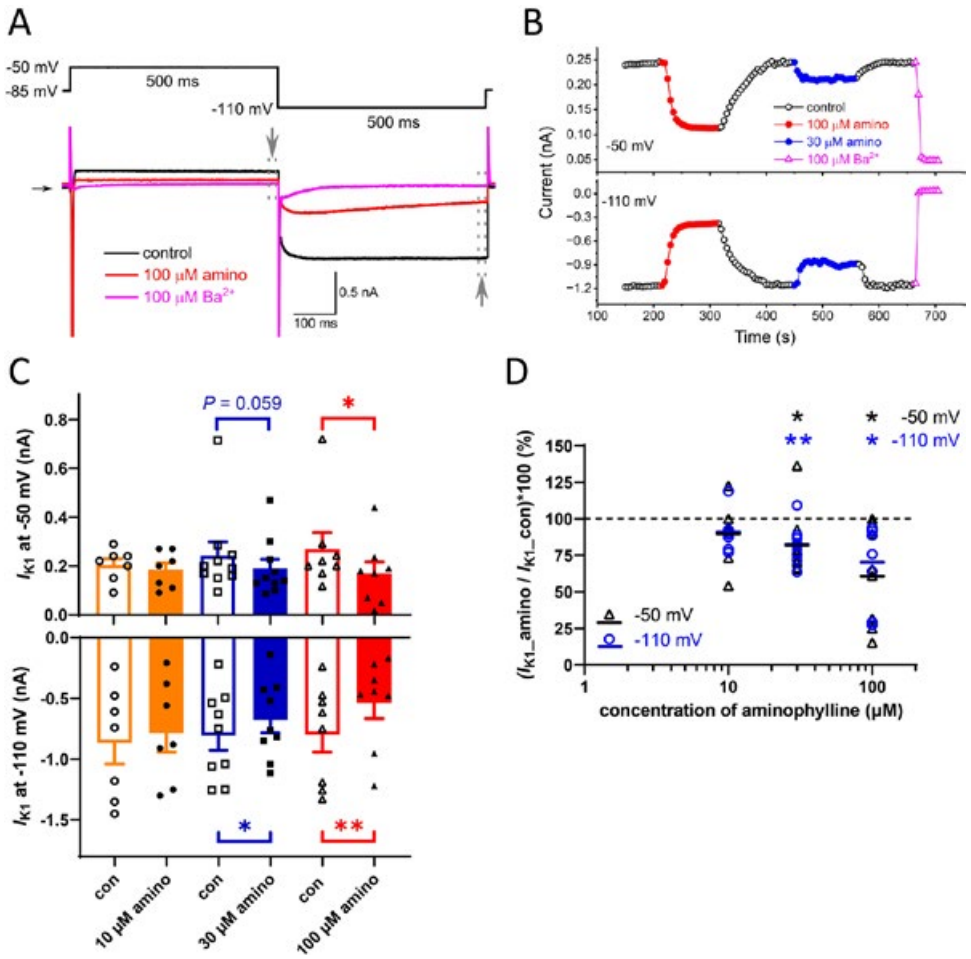

Fig. 1. Changes in inward rectifier potassium current I_{K1} at −50 and −110 mV in healthy porcine left ventricular cardiomyocytes in the presence of 10, 30, and 100 μM aminophylline (amino). A and B: An example of I_{K1} traces (A; I_{K1} was evaluated as the mean current sensitive to 100 μM Ba^{2+} at the end of the depolarizing pulse to −50 mV, *i.e.* the outward component of I_{K1}, and at the end of the repolarizing step to −110 mV, *i.e.* the inward component of I_{K1} – see the grey arrows) and time course of I_{K1} changes during application of 30 and 100 μM aminophylline (B). **C:** Average I_{K1} at −50 mV (upper panel) and −110 mV (lower panel) in 10, 30, and 100 μM aminophylline (amino) and respective controls ($n = 7/4$, 10/6, and 8/5 at −50 mV, and $n = 7/4$, 9/6, and 8/5 at −110 mV). **D:** Concentration dependence of the effect of aminophylline at clinically relevant concentrations between 10 and 100 μM on I_{K1}. To assess the statistical significance of the absolute (B) and relative (C) I_{K1} changes under aminophylline *vs.* the respective control, a paired *t*-test was used; * and * * - statistically significant differences at $P < 0.05$ and 0.01, respectively.

time-dependent currents that were not inhibited pharmacologically, *e.g.* sodium current I_{Na} which was activated and inactivated at the beginning of the pulse to −50 mV. In most examined healthy porcine ventricular myocytes, aminophylline caused an inhibition of I_{K1} which increased with the applied concentration between 10 and 100 μM (for a record during application of 30 and 100 μM aminophylline and 100 μM Ba^{2+}, see Fig. 1B). The average I_{K1} inhibition (Fig. 1C) was significant at 30 and 100 μM aminophylline reaching 17.4 ± 4.2 and 29.7 ± 9.8 %, respectively, at −110 mV (n = 9/6, $P < 0.05$, and n = 8/5, $P < 0.01$, respectively) and 18.2 ± 6.6 and 39.2 ± 11.9 %, respectively, at −50 mV (n = 10/6, $P = 0.059$, and n = 8/5, $P < 0.05$, respectively). At 10 μM aminophylline, the inhibition was insignificant at both tested voltages (9.0 ± 5.2 and 10.4 ± 8.1 % at −110 and −50 mV, respectively; n = 7/4 and $P > 0.05$ at both voltages). In a single cell, we observed an activation of I_{K1} (for an example of I_{K1} activation at 30 μM aminophylline, see Fig. 2C, middle and right lower panels) similarly as we did in our previously published study dealing with the effect of aminophylline on rat ventricular I_{K1} (for the data and detail explanation of the dual aminophylline effect, see [30]). Both activation and inhibition of I_{K1} by aminophylline were fully reversible during the following wash-out (as illustrated in Fig. 1B in the case of the inhibition). The effects did not significantly differ at −50 and −110 mV. The concentration dependence

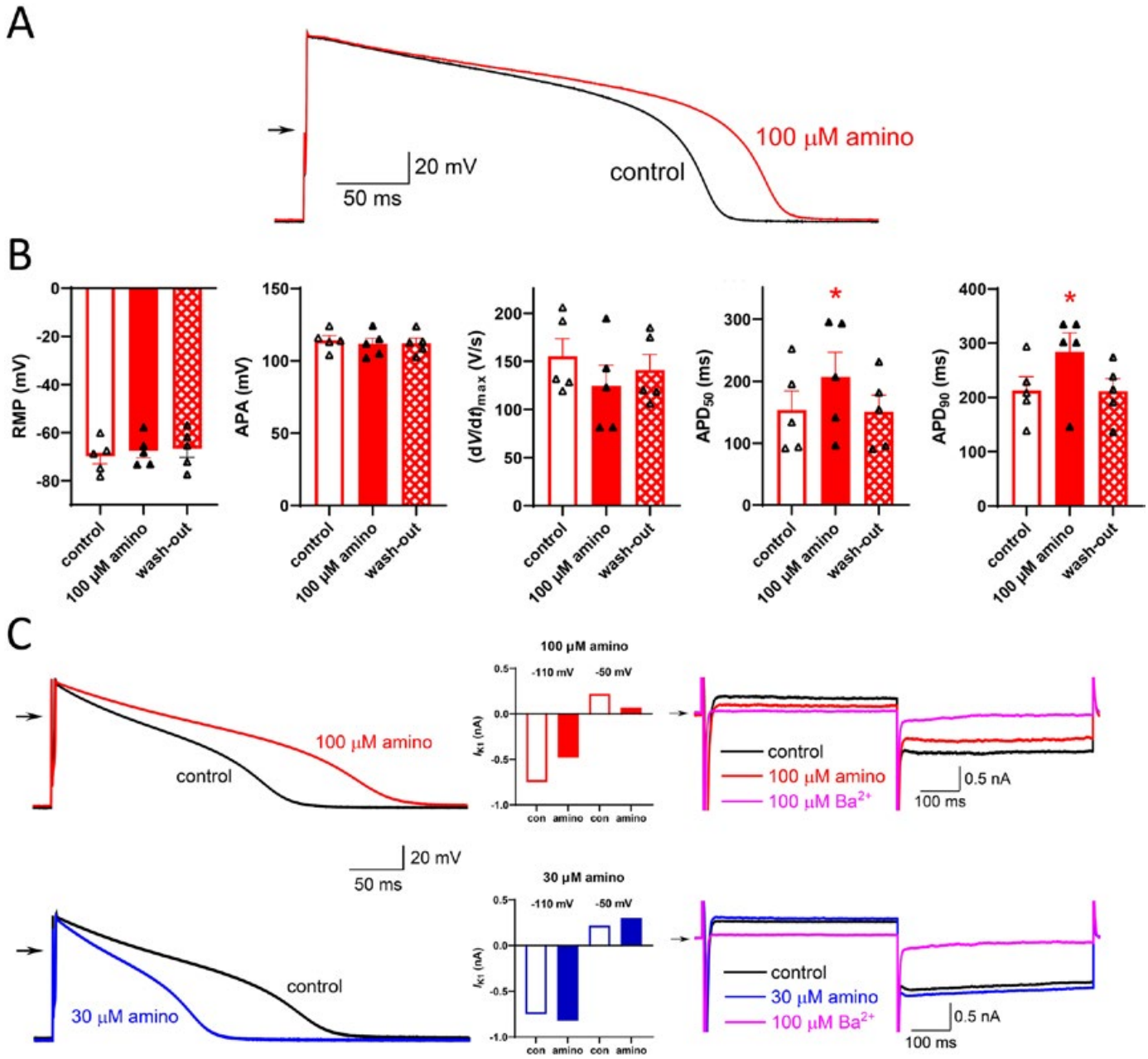

Fig. 2. Effect of 100 μM aminophylline (amino) on action potential (AP) configuration in healthy porcine left ventricular cardiomyocytes at 37°C (recorded in the presence of I_{Ca}, I_{Kr}, and I_{Ks} inhibitors to separate the impact of aminophylline-induced I_{K1} changes). A: An example of AP waveforms in control conditions (black line) and under the effect of 100 μM aminophylline (red line; for another example, please see Fig. 2C, left upper panel). B: Basic AP characteristics (n = 5/3); RMP – resting membrane potential, APA – AP amplitude, APD_{50} – AP duration at 50 %-repolarization, APD_{90} – AP duration at 90 %-repolarization; * - statistically significant differences at $P < 0.05$ (paired t-test *vs.* the respective control). **C:** An example of porcine cardiomyocyte showing a dual aminophylline effect on both AP duration (left panel) and I_{K1} (middle and right panels). Aminophylline at 100 μM induced an inhibition of I_{K1} (middle and right upper panels) and consequent AP prolongation (left upper panel) whereas 30 μM aminophylline resulted in opposite effects, *i.e.* I_{K1} activation (middle and right bottom panels) and AP shortening (left bottom panel).

of the aminophylline effect is shown in Fig. 1D.

3.2. Changes in action potential configuration in the presence of 100 μM aminophylline in healthy porcine ventricular myocytes

Subsequently, we tested if the effect of aminophylline on I_{K1} observed in healthy porcine ventricular myocytes (Fig. 1) may lead to any changes in action potential (AP) configuration in these cells (Fig. 2). To separate the impact of aminophylline-induced I_{K1} changes, we decided to analyze the effect of 100 μM aminophylline on APs under the absence of I_{Ca} and both rapid and slow components of I_K, I_{Kr}, and I_{Ks}, respectively, *i.e.* under the same experimental conditions used during I_{K1} measurements (see Materials and methods). No significant aminophylline-induced changes were apparent in the case of the maximal upstroke velocity ($(dV/dt)_{max}$), action potential amplitude (APA), and resting membrane potential (RMP; for all the parameters, $n = 5$, $P > 0.05$, Figs. 2A and 2B). In contrast, AP duration (APD) was significantly prolonged (Figs. 2A and 2B), both at 50 %- and 90 %-repolarization (APD_{50} and APD_{90}, respectively), APD_{50} from 153.5 ± 31.0 ms in control conditions to 206.9 ± 39.9 ms in the presence of 100 μM aminophylline (*i.e.* prolongation by ~35 %; $n = 5/3$, $P < 0.05$) and APD_{90} from 213.0 ± 25.2 ms in control conditions to 283.8 ± 35.2 ms in the presence of 100 μM aminophylline (*i.e.* prolongation by ~33 %; $n = 5/3$, $P < 0.05$). APD changes were fully reversible during the subsequent wash-out. These findings agreed well with simulations performed in a porcine ventricular cell model (Fig. 5; for details, see Discussion). Moreover, we observed similar changes in AP characteristics under the effect of 10 μM Ba^{2+} causing partial inhibition of I_{K1} (Fig. 3; recorded in the absence of I_{Ca}, I_{Kr}, and I_{Ks} inhibitors). In this case, a significant prolongation of both APD_{50} and APD_{90} by ~14 and 20 %, respectively ($n = 7/2$, $P < 0.05$ and 0.001, respectively) was accompanied by other tiny, but significant changes including an expected depolarizing shift of RMP by 2.03 mV ($n = 7/2$, $P < 0.05$).

As documented in Fig. 2C, we observed a dual impact of aminophylline-I_{K1} interaction in a single cell. When 100 μM aminophylline was applied, I_{K1} was inhibited and AP was prolonged in this cell (Fig. 2C, upper panels) in agreement with the average data from 5 measured cells (Fig. 2B). In contrast, 30 μM aminophylline induced an activation of I_{K1} and consequent AP shortening in the same cell (Fig. 2C, bottom panels). Therefore, heterogeneity in cardiac repolarization might be a potentially proarrhythmic consequence of aminophylline treatment (see Discussion).

3.3. Aminophylline-induced changes in I_{K1} investigated in porcine, human, and rat ventricular myocytes: an interspecies comparison

To approach even more clinically relevant conditions, we further analyzed the effect of 10 – 100 μM aminophylline in human ventricular myocytes freshly isolated from the failing hearts explanted during transplantation under the same experimental conditions. As in the case of I_{K1} in healthy porcine cardiomyocytes (Fig. 1), aminophylline showed an inhibitory action in failing human cardiomyocytes at both −110 and −50 mV (for example, an average inhibition by 23.3 ± 6.5 and 25.7 ± 3.4 % in the presence of 30 μM aminophylline at –110 and −50 mV, respectively; $n = 8/5$ and 6/5, respectively; $P < 0.01$ and $P < 0.05$, respectively, if the absolute values were compared, and $P < 0.01$ and $P < 0.001$, respectively, if the relative values were compared; Fig. 4B and Fig. 4C, upper panel). At 100 μM aminophylline and −50 mV (Fig. 4B, upper panel), the significance was missing if the absolute current values were compared (likely due to high variability of the data), but the effect was significant if the relative values were compared ($P < 0.01$; Fig. 4C, upper panel).

The relative effect observed in failing human cardiomyocytes at 37 °C (Fig. 4C, upper panel) was similar to that examined in healthy porcine ventricular cardiomyocytes at 37 °C in this study (Fig. 4C, middle panel) as well as to the effect investigated in healthy rat ventricular

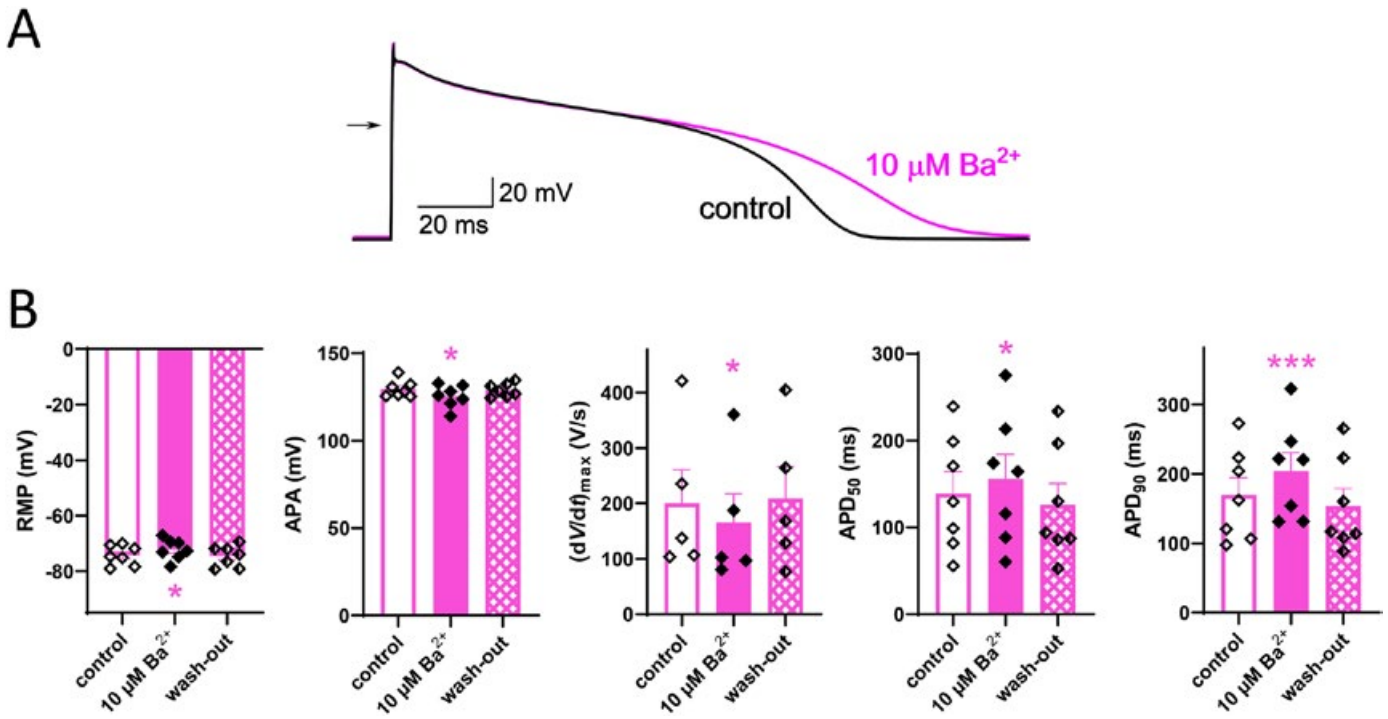

Fig. 3. Effect of a specific I_{K1} inhibitor Ba^{2+} in the concentration of 10 μM causing partial I_{K1} inhibition on action potential (AP) configuration in healthy porcine left ventricular cardiomyocytes at 37°C (without other ionic channel inhibitors). A: Representative AP waveforms in control conditions (the black line) and in the presence of 10 μM Ba^{2+} (the magenta line). B: Basic AP characteristics under the effect of a specific I_{K1} inhibitor 10 μM Ba^{2+} ($n = 7/2$); RMP – resting membrane potential, APA – AP amplitude, APD_{50} – AP duration at 50 %-repolarization, APD_{90} – AP duration at 90 %-repolarization; * and * ** - statistically significant difference at 10 μM Ba^{2+} *vs.* control at $P < 0.05$ and 0.001, respectively (paired *t*-test).

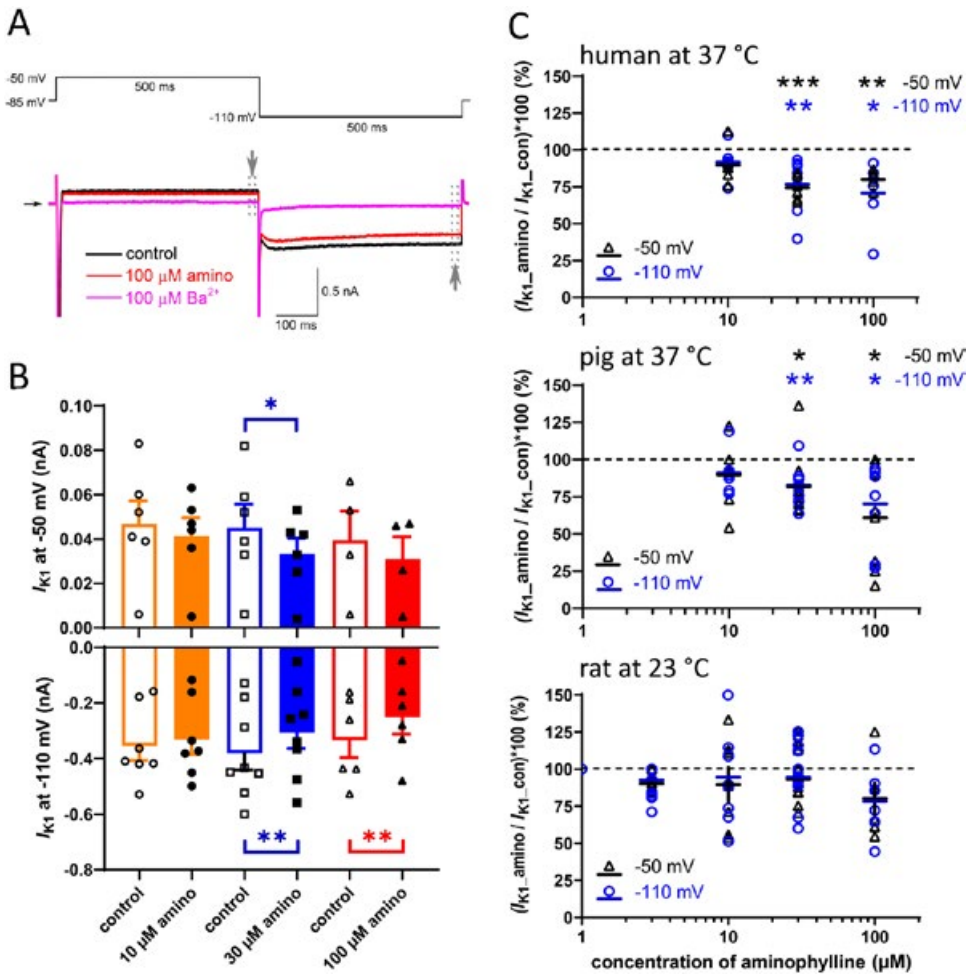

Fig. 4. Effect of aminophylline on I_{K1} in failing human cardiomyocytes. A: Scheme of the experimental protocol and representative I_{K1} traces in control, under 100 μM aminophylline, and specific I_{K1} inhibitor Ba^{2+} in the concentration of 100 μM. B: Average I_{K1} at −50 mV (upper panel) and at −110 mV (lower panel) in 10, 30, and 100 μM aminophylline (amino; dots, squares, and triangles, respectively, full symbols) and respective controls (dots, squares, and triangles, respectively, empty symbols; $n = 6/5$, 6/5, and 4/3 at −50 mV, and $n = 7/5$, 8/5, and 6/4 at −110 mV). **C:** Concentration dependence of the effect of 10–100 μM aminophylline on I_{K1} in human failing cardiomyocytes at 37 °C (for the respective n, see the legend A), in healthy porcine ventricular myocytes at 37 °C ($n = 7/4$, 10/6, and 8/5 at −50 mV, and $n = 7/4$, 9/6, and 8/5 at −110 mV), and in rat ventricular myocytes at 23 °C for comparison (the rat data were reused from our previously published paper, [30]; $n = 10/8$, 12/8, and 6/4 at −50 mV, and $n = 11/8$, 12/8, and 6/4 at −110 mV). To assess the statistical significance of the absolute (B) and relative (C) I_{K1} changes under aminophylline *vs.* the respective control, a paired *t*-test *vs.* the respective control was used; * , * *, and * ** - statistically significant differences at $P < 0.05$, 0.01, and 0.001, respectively. Except for the effect of 30 μM aminophylline at −50 mV in human and rat cardiomyocytes ($P < 0.05$), no statistically significant difference was observed in the relative effect of aminophylline at a given concentration between 10 and 100 μM in the investigated failing human and healthy pig and rat cardiomyocytes (one-way ANOVA with the Bonferroni post-test).

cardiomyocytes at 23 °C (Fig. 4C, lower panel; as published in our recent study [30]); the only significant difference was between the effect of 30 μM aminophylline in human and rat due to the dual effect present in rat, but not in human cardiomyocytes. The average changes were not significantly different at both tested voltages for any of the applied concentrations ($P > 0.05$).

4. Discussion

In this study, we first proved that aminophylline at clinically relevant concentrations of 30 and 100 μM exerted a comparable, on average inhibitory, effect on inward and outward components of I_{K1} in healthy porcine and failing human ventricular myocytes (Figs. 1 and 4). If other pivotal currents playing a role in AP plateau and repolarization, namely I_{Ca}, I_{Kr}, and I_{Ks}, were inhibited to separate the impact of I_{K1} changes on AP configuration, 100 μM aminophylline resulted in AP prolongation (Fig. 2) which well corresponded to the effect of a partial I_{K1} inhibition by 10 μM Ba^{2+} (Fig. 3). All these effects were fully reversible during the subsequent wash-out.

4.1. Dual aminophylline effect

A dual aminophylline effect on I_{K1} was observed in our previous study on rat ventricular myocytes (in 4 out of 12 rat cardiomyocytes, Fig. 4C, lower panel; [30]). The results presented here showed the activation effect less frequently - it was observed in only 1 out of 10 porcine cardiomyocytes (Figs. 1D and 2C, lower panel) and in none of 8 human cardiomyocytes at 30 μM aminophylline (Fig. 4C, upper panel). It might be a consequence of *e.g.* interspecies differences or differences in the used temperature (37 °C in porcine and human *vs.* 23 °C in rat cardiomyocytes). The origin of the dual aminophylline effect and its clinical significance have been thoroughly analyzed and discussed in our recently published paper [30].

4.2. Impact of separated aminophylline-induced I_{K1} inhibition on AP morphology

As shown in Fig. 5, the average inhibitory effect of 100 μM aminophylline on I_{K1} resulted in a substantial increase of APD_{50} as well

Fig. 5. Impact of I_{K1} inhibition on the action potential (AP) repolarization as simulated in a previously published porcine ventricular cell model ([12]; I_{Ca}, I_{Kr}, and I_{Ks} were suppressed during these simulations in agreement with their block within experiments). The control AP waveform (the black line) was substantially prolonged when the average I_{K1} inhibition by 34.5 % induced by 100 μM aminophylline in the experiments was introduced into the model (the red line). The simulated effect agreed well with the average effect observed during AP measurements in porcine ventricular myocytes (Fig. 2).

as APD_{90} (by ~30 and 34 %, respectively) in a mathematical model of porcine ventricular myocyte (previously published by [12]) under the same conditions that were used in our experiments (including a complete inhibition of I_{Ca}, I_{Kr}, and I_{Ks} to uncover AP changes resulting from the aminophylline-induced effect on I_{K1}). This result of mathematical modelling agrees well with the measured data (APD_{50} and APD_{90} were prolonged by ~35 and 33 %, respectively; Figs. 2A and 2B). Moreover, Ba^{2+} at the concentration of 10 μM, which causes partial inhibition of I_{K1} comparable to 100 μM aminophylline, resulted in similar AP changes (Fig. 3). This suggests that the experimentally observed delay in cardiac cell repolarization under complete inhibition of I_{Ca}, $I_{Kr,}$ and I_{Ks} might be a consequence of the inhibition of I_{K1} alone and that, except for I_{K1} and possibly I_{Ca}, I_{Kr}, and I_{Ks}, no other ionic membrane currents should be sensitive to 100 μM aminophylline. The surprisingly high impact of I_{K1} inhibition on APD appears to result from a different contribution of I_{K1} and I_{Kr} to AP repolarization in porcine ventricular myocytes *versus* that observed in human cardiomyocytes [12].

Considering the impact of aminophylline on I_{K1}, changes in RMP may be expected. However, no significant aminophylline-induced changes were apparent in the case of RMP (-69.8 ± 3.1 mV in control *vs.* −67.6 ± 2.8 mV under 100 μM aminophylline; $n = 5$, $P > 0.05$; Fig. 2B). Under the effect of 10 μM Ba^{2+} (Fig. 3), a significant depolarizing shift of RMP was observed, however, the change was tiny (by 2.7 %, from −74.2 ± 1.4 to −72.2 ± 1.4 mV, $n = 7$, $P < 0.05$), similar to that observed under 100 μM aminophylline (by 3.2 %), suggesting a consistent action of both drugs on I_{K1} in these concentrations.

4.3. Clinical relevance

Kir channels play an important role in various pathologies (*e.g.* [7,36, 32,39]) including arrhythmias (for a review, see [3]). Hence, drug-induced alterations in the function of Kir channels including those responsible for I_{K1} (*e.g.* [29,10,21,16]) may contribute to cardiac side effects of various primarily non-cardiac agents.

The average inhibitory effect of the bronchodilator aminophylline on I_{K1} increased with its increasing concentrations between 10 and 100 μM, reaching ~40 and ~20 % at 100 μM in healthy porcine and failing human ventricular myocytes, respectively, at −50 mV (Fig. 4). These concentrations cover well the common therapeutic plasma concentration of the drug [35]. In clinical practice, even a higher effect of aminophylline on I_{K1} might be observed because several times higher toxic levels of the drug have been reported in the case of overdose [15, 26].

The average inhibitory effect of aminophylline on I_{K1} and consequent delay in cardiac repolarization (Figs. 1 and 2, respectively) might result in a prolongation of QT interval and formation of early afterdepolarizations (EADs; [11,9,38]). The large scatter in the effects of aminophylline on individual cells in all tested species and even activation of I_{K1} that we observed in both porcine and rat ventricular myocytes (Fig. 4C, middle and lower panels) might increase the heterogeneity in the repolarization process (see Fig. 2C) and lead to the formation of premature ventricular complexes even in the absence of EADs [38]. However, as later discussed in the Limitations of the study, we examined the aminophylline effect on a single-cell level, and changes in AP waveform were investigated in the absence of several pivotal ionic currents, namely I_{Ca}, I_{Kr}, and I_{Ks}, which both limit considerations of the real effect of aminophylline on cardiac electrophysiology in the clinical setting, encouraging its further testing.

Since PDE inhibition is considered the main effect of aminophylline, an accumulation of cAMP, activation of protein kinase A (PKA), and associated changes in cardiac ionic currents, similar to those observed under β-adrenergic stimulation, might be expected, even in the absence of a direct interaction of aminophylline with the channels. These include the currents which were inhibited in the course of the majority of our experiments. Both I_{Ca} and I_{Ks} are well known to be activated by the cAMP-PKA pathway [18,2,27], thus, aminophylline might cause their increase which would have opposing effects on AP repolarization, leading to its delay in the case of I_{Ca} stimulation whereas in its acceleration in the case of I_{Ks} stimulation. In contrast, I_{Kr} was slightly decreased under β-adrenergic stimulation which diminished its role in cardiac cell repolarization in both guinea pig cardiomyocytes and the human heart [18,2]. Hence, in addition to the possible direct effects, an indirect effect of aminophylline, particularly on I_{Ca} and I_{Ks}, should be investigated in the future to resolve the apparent ambiguities.

4.4. Limitations of the study

Several potential limitations of this study should be considered. Here, we exclusively focused on the effect of aminophylline on I_{K1}. However, other ionic currents active during cardiac AP plateau and repolarization (*e.g.* I_{Ca}, I_{Kr}, and I_{Ks} or late sodium current $I_{Na,late}$) may be either directly or indirectly (through cAMP-PKA cascade) affected by the aminophylline action. Therefore, further investigation is needed to bring more insight into the complex effect of this clinically important agent.

The impact of aminophylline-induced I_{K1} changes on AP morphology very likely differs in porcine and human cardiomyocytes. As suggested by Gaur et al. [12] and as known from experimental studies (*e.g.* [1]), AP repolarization in human ventricular myocytes is not very sensitive to I_{K1} changes in comparison to that in porcine cardiomyocytes [12]. Hence, the real impact of aminophylline may differ in the human heart and should be further investigated, best in both healthy and diseased human cardiomyocytes where the contribution of individual ionic currents to AP repolarization is altered.

In this study, experiments were performed by the whole cell patch clamp technique in single, enzymatically isolated cells. To bring the data nearer to the clinical practice, recordings from multicellular specimens or even from the whole heart, at various pacing frequencies, and even during restitution pacing protocols might be beneficial and should be a part of future studies.

5. Conclusions

To sum up the main results of this study, we first tested the effect of clinically relevant concentrations of aminophylline on I_{K1} in healthy porcine and failing human ventricular myocytes at 37°C. A comparable average inhibitory effect was observed in both species resulting in a significant delay of repolarization in porcine ventricular myocytes under the same experimental conditions, *i.e.* during I_{Ca}, I_{Kr}, and I_{Ks} inhibition, which enabled separation of the impact of aminophylline-induced I_{K1}-changes on AP waveform. Moreover, a large scatter of the aminophylline effect on I_{K1} including even I_{K1} activation was apparent. The resulting heterogeneity in cardiac repolarization induced by aminophylline at clinically relevant concentrations might contribute to the arrhythmogenesis observed during the use of aminophylline in clinical practice. Since this study was specifically focused on the effect of aminophylline on I_{K1} channels, the effects of aminophylline on other ionic membrane currents and their proarrhythmic consequences should be addressed in

the future.

CRediT authorship contribution statement

Olga Švecová: Writing – review & editing, Writing – original draft, Methodology, Investigation. **Markéta Bébarová:** Writing – review & editing, Writing – original draft, Visualization, Supervision, Project administration, Investigation, Funding acquisition, Formal analysis, Data curation, Conceptualization. **Michal Pásek:** Writing – review & editing, Writing – original draft, Visualization, Methodology, Investigation. **Roman Kula:** Writing – review & editing, Writing – original draft, Investigation, Formal analysis. **Petr Fila:** Writing – review & editing, Writing – original draft, Methodology. **Edita Jeklová:** Writing – review & editing, Writing – original draft, Methodology, Funding acquisition. **Martin Pešl:** Writing – review & editing, Writing – original draft, Project administration, Methodology, Funding acquisition, Conceptualization.

Declaration of Competing Interest

The authors declare they have no conflict of interest.

Acknowledgments

This study was supported by the project MUNI/A/1547/2023 provided as the Specific University Research Grant by the Ministry of Education, Youth and Sports of the Czech Republic, by the grant projects NU20-06-00156 and NU22-02-00348 provided by the Ministry of Health of the Czech Republic, by the Ministry of Agriculture of the Czech Republic (RO0523), and with the support by MH CZ - DRO (FNBr, 65269705). The work of M. Pásek was carried out with the Institutional Support RVO: 61388998.

Data Availability

Data will be made available on request.

References

[1] T. Árpádffy-Lovas, A.S.A. Mohammed, M. Naveed, I. Koncz, B. Baláti, M. Bitay, N. Jost, N. Nagy, I. Baczkó, L. Virág, A. Varró, Species-dependent differences in the inhibition of various potassium currents and in their effects on repolarization in cardiac ventricular muscle, Can. J. Physiol. Pharmacol. 100 (2022) 880–889, https://doi.org/10.1139/cjpp-2022-0028.

[2] T. Banyasz, Z. Jian, B. Horvath, S. Khabbaz, L.T. Izu, Y. Chen-Izu, Beta-adrenergic stimulation reverses the I Kr-I Ks dominant pattern during cardiac action potential, Pflug. Arch. 466 (2014) 2067–2076, https://doi.org/10.1007/s00424-014-1465-7.

[3] M. Bébarová, Z. Horáková, R. Kula, Addictive drugs, arrhythmias, and cardiac inward rectifiers, Europace 19(3), 346-355 (2017), https://doi.org/10.1093/europace/euw071.

[4] M. Bébarová, P. Matejovič, M. Pásek, M. Šimurdová, J. Šimurda, Dual effect of ethanol on inward rectifier potassium current I_{K1} in rat ventricular myocytes, J. Physiol. Pharmacol. 65 (2014) 497–509.

[5] R.F. Bosch, G.R. Li, R. Gaspo, S. Nattel, Electrophysiologic effects of chronic amiodarone therapy and hypothyroidism, alone and in combination, on guinea pig ventricular myocytes, J. Pharmacol. Exp. Ther. 289 (1999) 156–165.

[6] R. Chazan, K. Karwat, K. Tyminska, W. Tadeusiak, W. Droszcz, Cardiac arrhythmias as a result of intravenous infusions of theophylline in patients with airway obstruction, Int. J. Clin. Pharmacol. Ther. 33 (1995) 170–175.

[7] Z.C. Chen, Y.Z. Cheng, L.J. Chen, K.C. Cheng, Y. Li, J. Cheng, Increase of ATP-sensitive potassium (K(ATP)) channels in the heart of type-1 diabetic rats, Cardiovasc. Diabetol. 11 (2012) 8, https://doi.org/10.1186/1475-2840-11-8.

[8] L. Cooney, I. Sinha, D. Hawcutt, Aminophylline dosage in asthma exacerbations in children: a systematic review, PloS. One 11 (2016) e0159965, https://doi.org/10.1371/journal.pone.0159965.

[9] L.X. Cubeddu, Drug-induced inhibition and trafficking disruption of ion channels: pathogenesis of qt abnormalities and drug-induced fatal arrhythmias, Curr. Cardiol. Rev. 12 (2016) 141–154, https://doi.org/10.2174/1573403x12666160301120217.

[10] M. Delgado-Ramírez, F.J. Rodriguez-Leal, A.A. Rodríguez-Menchaca, E.G. Moreno-Galindo, J.A. Sanchez-Chapula, T. Ferrer, Inhibitory effect of terfenadine on Kir2.1 and Kir2.3 channels, Acta Pharm. 71 (2) (2021) 317–324, https://doi.org/10.2478/acph-2021-0017.

[11] A.S. Dhamoon, J. Jalife, The inward rectifier current (IK1) controls cardiac excitability and is involved in arrhythmogenesis, Heart Rhythm 2 (2005) 316–324, https://doi.org/10.1016/j.hrthm.2004.11.012.

[12] N. Gaur, X.-Y. Qi, D. Benoist, O. Bernus, R. Coronel, S. Nattel, E.J. Vigmond, A computational model of pig ventricular cardiomyocyte electrophysiology and calcium handling: Translation from pig to human electrophysiology, PLoS Comput. Biol. 17 (6) (2021) e1009137, https://doi.org/10.1371/journal.pcbi.1009137.

[13] J. Heijman, J.B. Guichard, D. Dobrev, S. Nattel, Translational challenges in atrial fibrillation, Circ. Res. 122 (2018) 752–773, https://doi.org/10.1161/CIRCRESAHA.117.311081.

[14] L. Hendeles, L. Bighley, R.H. Richardson, C.D. Hepler, J. Carmichael, Frequent toxicity from IV aminophylline infusions in critically ill patients, Ann. Pharmacother. 40 (2006) 1417–1423, https://doi.org/10.1345/aph.140027.

[15] K. Ichikawa, T. Wada, T. Nishihara, M. Tsuji, A. Mori, F. Yokohama, D. Hasegawa, K. Kawamoto, M. Tanakaya, Y. Katyama, S. Sakuragi, H. Ito, A case of life-threatening supraventricular tachycardia storm associated with theophylline toxicity, J. Cardiol. Cases. 15 (2017) 125–128, https://doi.org/10.1016/j.jccase.2016.12.004.

[16] A. Iijima, O. Švecová, J. Hošek, R. Kula, M. Bébarová, Sildenafil affects the human Kir2.1 and Kir2.2 channels at clinically relevant concentrations: Inhibition potentiated by low Ba^2. Front. Pharmacol. 14 (2023) 1136272 https://doi.org/10.3389/fphar.2023.1136272.

[17] J. Jalife, Dynamics and molecular mechanisms of ventricular fibrillation in structurally normal hearts, Card. Electrophysiol. Clin. 8 (2016) 601–612, https://doi.org/10.1016/j.ccep.2016.04.009.

[18] C. Kang, A. Badiceanu, J.A. Brennan, C. Gloschat, Y. Qiao, N.A. Trayanova, I. R. Efimov, β-adrenergic stimulation augments transmural dispersion of repolarization via modulation of delayed rectifier currents I_{Ks} and I_{Kr} in the human ventricle, Sci. Rep. 7 (2017) 15922, https://doi.org/10.1038/s41598-017-16218-3.

[19] S. Klimovic, M. Scurek, M. Pesl, D. Beckerova, S. Jelinkova, T. Urban, D. Kabanov, Z. Starek, M. Bebarova, J. Pribyl, V. Rotrekl, K. Brat, Aminophylline induces two types of arrhythmic events in human pluripotent stem cell–derived cardiomyocytes, Front. Pharmacol. 12 (2022) 789730, https://doi.org/10.3389/fphar.2021.789730.

[20] K.H. Komadina, T.A. Carlson, P.J. Strollo, D.L. Navratil, Electrophysiologic study of the effects of aminophylline and metaproterenol on canine myocardium, Chest 101 (1992) 232–238, https://doi.org/10.1378/chest.101.1.232.

[21] M. Macháček, O. Švecová, M. Bébarová, Combination of sildenafil and Ba^{2+} at a low concentration show a significant synergistic inhibition of inward rectifier potassium current resulting in action potential prolongation, Front. Pharmacol. 13 (2022) 829952, https://doi.org/10.3389/fphar.2022.829952.

[22] G. Mahemuti, H. Zhang, J. Li, N. Tieliwaerdi, L. Ren, Efficacy and side effects of intravenous theophylline in acute asthma: a systematic review and meta-analysis, Drug. Des. Devel. Ther. 12 (2018) 99–120, https://doi.org/10.2147/DDDT.S156509.

[23] A.R. Morton, K.D. Fitch, Asthmatic drugs and competitive sport. An update, Sports Med 14 (4) (1992) 228–242, https://doi.org/10.2165/00007256-199214040-00002.

[24] M. Neame, O. Aragon, R.M. Fernandes, I. Sinha, Salbutamol or aminophylline for acute severe asthma: how to choose which one, when and why? Arch. Dis. Child. Educ. Pract. Ed. 100 (2015) 215–222, https://doi.org/10.1136/archdischild-2014-306186.

[25] T. Ogura, L.M. Shuba, T.F. McDonald, Action potentials, ionic currents and cell water in guinea pig ventricular preparations exposed to dimethyl sulfoxide, J. Pharmacol. Exp. Ther. 273 (1995) 1273–1286.

[26] F.P. Paloucek, K.A. Rodvold, Evaluation of theophylline overdoses and toxicities, Ann. Emerg. Med. 17 (1988) 135–144, https://doi.org/10.1016/s0196-0644(88)80299-3.

[27] A. Papa, J. Kushner, S.O. Marx, Adrenergic regulation of calcium channels in the heart, Annu. Rev. Physiol. 84 (2022) 285–306, https://doi.org/10.1146/annurev-physiol-060121-041653.

[28] A.K. Patel, J.B. Skatrud, J.H. Thomsen, Cardiac arrhythmias due to oral aminophylline in patients with chronic obstructive pulmonary disease, Chest 80 (1981) 661–665, https://doi.org/10.1378/chest.80.6.661.

[29] D. Ponce-Balbuena, A. López-Izquierdo, T. Ferrer, A.A. Rodríguez-Menchaca, I. A. Aréchiga-Figueroa, J.A. Sánchez-Chapula, Tamoxifen inhibits inward rectifier K + 2.x family of inward rectifier channels by interfering with phosphatidylinositol 4,5-bisphosphate-channel interactions, J. Pharmacol. Exp. Ther. 331 (2) (2009) 563–573, https://doi.org/10.1124/jpet.109.156075.

[30] N.J.D. Ramalho, O. Švecová, R. Kula, M. Šimurdová, J. Šimurda, M. Bébarová, Aminophylline at clinically relevant concentrations affects inward rectifier potassium current in a dual way, Pflug. Arch. – Eur. J. Physiol. 474 (2022) 303–313, https://doi.org/10.1007/s00424-021-02646-8.

[31] G.L. Saint, M.G. Semple, I. Sinha, D.B. Hawcutt, Optimizing the dosing of intravenous theophylline in acute severe asthma in children, Paediatr. Drugs 20 (2018) 209–214, https://doi.org/10.1007/s40272-017-0281-x.

[32] A. Staruschenko, M.R. Hodges, O. Palygin, Kir5.1 channels: potential role in epilepsy and seizure disorders, Am. J. Physiol. Cell. Physiol. 323 (3) (2022) C706–C717, https://doi.org/10.1152/ajpcell.00235.2022.

[33] J. Tamargo, R. Caballero, E. Delpón, Drug-induced atrial fibrillation, Expert. Opin. Drug. Saf. 11 (2012) 615–634, https://doi.org/10.1517/14740338.2012.698609.

[34] P. Varriale, S. Ramaprasad, Aminophylline induced atrial fibrillation, Pacing Clin. Electrophysiol. 16 (1993) 1953–1955, https://doi.org/10.1111/j.1540-8159.1993.tb00987.x.

[35] R.E. Vestal, C.E. Eiriksson Jr., B. Musser, L.K. Ozaki, J.B. Halter, Effect of intravenous aminophylline on plasma levels of catecholamines and related cardiovascular and metabolic responses in man, Circulation 67 (1983) 162–171, https://doi.org/10.1161/01.cir.67.1.162.
[36] Z.W. Yang, J.K. Chen, M. Ni, T. Zhao, Y.P. Deng, X. Tao, G.J. Jiang, F.M. Shen, Role of Kir6.2 subunits of ATP-sensitive potassium channels in endotoxemia-induced cardiac dysfunction, Cardiovasc. Diabetol. 12 (2013) 75, https://doi.org/10.1186/1475-2840-12-75.
[37] A. Zafar Gondal, H. Zulfiqar, Aminophylline. StatPearls, StatPearls Publishing, 2023.
[38] Z. Zhang, M.B. Liu, X. Huang, Z. Song, Z. Qu, Mechanisms of premature ventricular complexes caused by QT prolongation, Biophys. J. 120 (2021) 352–369, https://doi.org/10.1016/j.bpj.2020.12.001.
[39] D. Zuniga, A. Zoumpoulakis, R.F. Veloso, L. Peverini, S. Shi, A. Pozza, V. Kugler, F. Bonneté, T. Bouceba, R. Wagner, P.J. Corringer, C.A.H. Fernandes, C. Vénien-Bryan, Biochemical, biophysical, and structural investigations of two mutants (C154Y and R312H) of the human Kir2.1 channel involved in the Andersen-Tawil syndrome, FASEB J. 38 (21) (2024) e70146, https://doi.org/10.1096/fj.202401567R.

D. Rob et al.

Heart rhythm at hospital admission: A factor for survival and neurological outcome among ECPR recipients?

Resuscitation
Impact Factor: 6,5

Resuscitation 204 (2024) 110412

Contents lists available at ScienceDirect

Resuscitation

journal homepage: www.elsevier.com/locate/resuscitation

Short paper

Heart rhythm at hospital admission: A factor for survival and neurological outcome among ECPR recipients?

Daniel Rob [a], Klaudia Farkasovska [a], Petra Kavalkova [a], Milan Dusík [a], Stepan Havranek [a], Jan Pudil [a], Eliska Mockova [a], Jaromir Macoun [a,b], Jan Belohlavek [a,*]

[a] 2nd Department of Medicine – Department of Cardiovascular Medicine, First Faculty of Medicine, Charles University in Prague and General University Hospital in Prague, Czech Republic
[b] Department of Probability and Mathematical Statistics, Faculty of Mathematics and Physics, Charles University in Prague, Prague, Czech Republic

ARTICLE INFO

Keywords:
Heart arrest
Cardiac arrest
Cardiopulmonary resuscitation
Extracorporeal cardiopulmonary resuscitation
Extracorporeal membrane oxygenation
Heart rhythm
Cardiac rhythm
Rhythm conversion

ABSTRACT

Background: The initial rhythm is a known predictor of survival in extracorporeal cardiopulmonary resuscitation (ECPR) patients. However, the effect of the rhythm at hospital admission on outcomes in these patients is less clear.

Methods: This observational, single-center study assessed the influence of the rhythm at hospital admission on 30-day survival and neurological outcomes at discharge in patients who underwent ECPR for out-of-hospital cardiac arrest (OHCA).

Results: Between January 2012 and December 2023, 1,219 OHCA patients were admitted, and 210 received ECPR. Of these, 196 patients were analyzed. The average age was 52.9 years (±13), with 80.6 % male. The median time to ECPR initiation was 61 min (IQR 54–72). Patients with ventricular fibrillation as both the initial and admission rhythm had the highest 30-day survival rate (52 %: 35/67), while those with asystole in both instances had the lowest (6 %: 1/17, log-rank $p < 0.00001$). After adjusting for age, sex, initial rhythm, resuscitation time, location, bystander, and witnessed status, asystole at admission was linked to higher 30-day mortality (OR 4.03, 95 % CI 1.49–12.38, $p = 0.009$) and worse neurological outcomes (Cerebral Performance Category 3–5) at discharge (OR 4.61, 95 % CI 1.49–17.62, $p = 0.013$).

Conclusions: The rhythm at hospital admission affects ECPR outcomes. Patients presenting with and maintaining ventricular fibrillation have a higher chance of favorable neurological survival, whereas those presenting with or converting to asystole have poor outcomes. The rhythm at hospital admission appears to be a valuable criterion for deciding on ECPR initiation.

Background

Extracorporeal cardiopulmonary resuscitation (ECPR) is a complex intervention for selected cardiac arrest patients, but identifying appropriate candidates during cardiopulmonary resuscitation (CPR) is challenging due to time constraints and a lack of reliable predictors.[1–3] There is no consensus on inclusion or exclusion criteria, leading to significant variability between centers.[1–6]

Initial rhythm is an independent predictor of survival and neurological outcomes in out-of-hospital cardiac arrest (OHCA) patients, including those receiving ECPR.[7] Additionally, rhythm conversion from non-shockable to shockable rhythms has been linked to better outcomes, though evidence on the impact of admission rhythm on ECPR outcomes is limited.[8–10] This registry-based study analyzed the relationship between initial rhythm and rhythm at hospital admission on ECPR outcomes.

Abbreviations: CPC, cerebral performance category; CPR, cardiopulmonary resuscitation; ECG, Electrocardiogram; ECPR, extracorporeal cardiopulmonary resuscitation; EMS, emergency medical service; ERC, European Resuscitation Council; ESC, European Society of Cardiology; ICU, intensive care unit; OHCA, out-of-hospital cardiac arrest; OR, odds ratio; PEA, pulseless electrical activity; ROSC, return of spontaneous circulation; SD, standard deviation; VA ECMO, veno-arterial extracorporeal membrane oxygenation; VF, ventricular fibrillation.

* Corresponding author.
E-mail address: jan.belohlavek@vfn.cz (J. Belohlavek).

https://doi.org/10.1016/j.resuscitation.2024.110412
Received 7 September 2024; Received in revised form 7 October 2024; Accepted 10 October 2024
Available online 16 October 2024

Methods

Study setting and population

The prehospital CPR system and its outcomes in Prague, Czech Republic, have been described previously.[11] Since 2012, the emergency medical service (EMS) in Prague, Czech Republic, has collaborated closely with the General University Hospital's cardiac arrest center to transport patients without return of spontaneous circulation (ROSC) for ECPR. This study includes all patients aged ≥ 18 years with OHCA, resuscitated between January 2012 and December 2023, who were transported to our center and received ECPR. Patients from the Prague-OHCA trial (2013–2022) who received ECPR were also analyzed.[1]

Data acquisition

The Prague OHCA register prospectively collects detailed data on prehospital and hospital treatment and outcomes of OHCA. Initial electrocardiogram (ECG) rhythms are evaluated by EMS physicians, while intensive care unit (ICU) physicians assess rhythms at hospital arrival. All other cardiac arrest data are entered into the database according to Utstein recommendations.[12]

Procedures

All OHCA patients admitted to the hospital were treated according to the ERC (European Resuscitation Council) and ESC (European Society of Cardiology) guidelines at the time. Upon hospital admission, the ICU doctor checks the patient's status, including heart rhythm and ROSC. If eligible, veno-arterial extracorporeal membrane oxygenation (VA ECMO) cannulation is initiated by trained physicians.

Outcomes

The primary outcome was 30-day survival, and the secondary outcome was neurological status at discharge, assessed using the Cerebral Performance Category (CPC), where CPC 1–2 indicates a good outcome and CPC 3–5 indicates a poor outcome.

Statistical analysis

Numeric variables are expressed as medians with interquartile ranges, and categorical variables as counts with percentages. ANOVA was used for numeric variables, while categorical variables were compared using the $\chi 2$ or Fisher's exact test. The relationship between the time to ECMO initiation and the rhythm at hospital arrival was analyzed using Welch's test. Survival was analyzed with Kaplan-Meier and the log-rank test. Logistic regression assessed the association of hospital arrival rhythm with 30-day mortality and neurological outcomes, adjusting for baseline and resuscitation factors, with results expressed as odds ratios (ORs). $P < 0.05$ was considered significant. Analyses were performed using R software, version 4.2.3.

Results

Baseline and resuscitation characteristics

From January 2012 to December 2023, 1,219 adult OHCA patients were admitted, with 210 (17.2 %) receiving ECPR and 196 (16.1 %) included in the final analysis (Fig. 1). Baseline characteristics by initial rhythm are detailed in Supplementary Table 1.

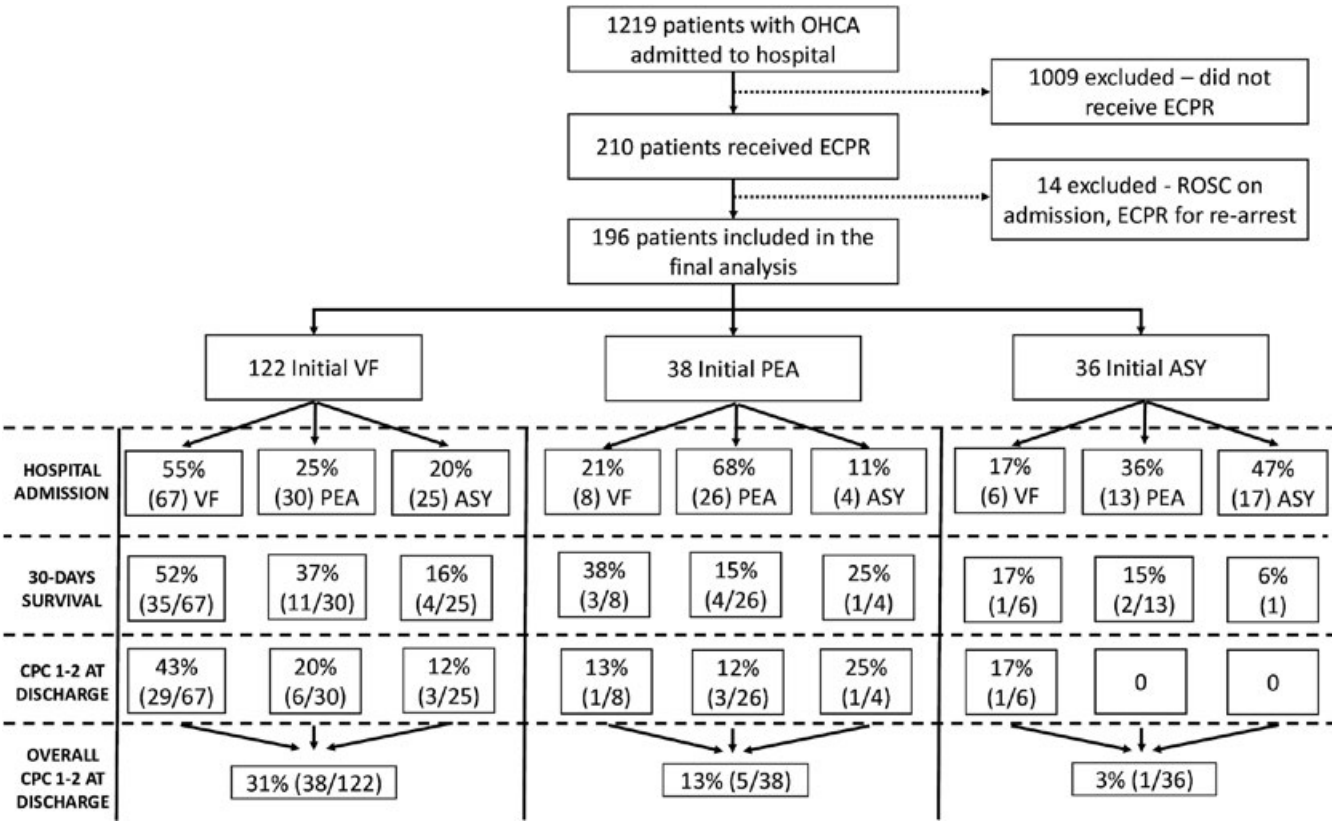

Fig. 1. Patient flow chart. ASY asystole, ECPR extracorporeal cardiopulmonary resuscitation, OHCA out-of-hospital cardiac arrest, PEA pulseless electrical activity, ROSC return of spontaneous circulation, VF ventricular fibrillation.

Relationship between time to ECMO initiation and rhythm at hospital arrival

The mean time to ECMO initiation was 61.3 min (standard deviation [SD] ± 16) for patients presenting with VF at hospital arrival, 61.8 min (SD ± 16.4) for those with PEA, and 70.7 min (SD ± 20.4) for the asystole group (p = 0.023).

Conversion between initial rhythm and rhythm at hospital arrival

Rhythm conversion proportions are shown in Fig. 1. Among initial ventricular fibrillation (VF) patients, 55 % sustained VF, 25 % converted to pulseless electrical activity (PEA), and 20 % converted to asystole. For initial PEA patients, 68 % remained in PEA, 21 % converted to VF, and 11 % to asystole. In the asystole group, 47 % remained in asystole, 36 % converted to PEA, and 17 % to VF.

30-day survival

For initial VF patients, the 30-day survival was 40.9 % (50/122), with the highest survival in those sustaining VF (52 %), followed by VF-to-PEA conversion (37 %) and VF-to-asystole conversion (16 %) (Fig. 2, log rank p < 0.0001). In the PEA group, survival was 21 % (8/38), with highest in PEA-to-VF (38 %), followed by sustained PEA (15 %) and PEA-to-asystole (25 %) (log rank p < 0.0001). Initial asystole patients had an 11.1 % (4/36) survival, with survival rates of 17 % for asystole-to-VF, 15 % for asystole-to-PEA, and 6 % for sustained asystole (log rank p < 0.0001).

Neurological outcomes at discharge

A favorable neurological outcome was observed in 31.1 % (38/122) of the VF cohort, with the best outcomes in sustained VF (43 %), followed by VF-to-PEA (20 %) and VF-to-asystole (12 %) (Fig. 1). In the PEA group, favorable outcomes were 13 % for PEA-to-VF, 11.5 % for sustained PEA, and 25 % for PEA-to-asystole. In the asystole group, the only favorable outcome (2.8 %, 1/36) was in a patient who converted to VF.

Multivariate logistic regression of 30-day mortality

Logistic regression showed that admission asystole was associated with significantly higher 30-day mortality (odds ratio (OR) 4.03, 95 % CI 1.49–12.38, p = 0.009) compared to VF. Admission PEA showed a non-significant trend towards higher mortality (OR 1.89, 95 % CI 0.86–4.23, p = 0.12) compared to VF (Table 1).

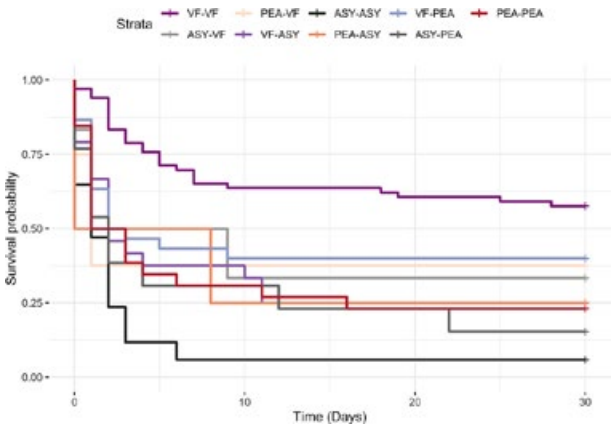

Fig. 2. Kaplan–Meier plot showing cumulative patient survival from index cardiac arrest to 30-days follow-up according to the initial rhythm and rhythm at hospital arrival. ASY asystole, PEA pulseless electrical activity, VF ventricular fibrillation.

Multivariate logistic regression of neurological outcome at discharge

Admission asystole was also associated with significantly higher odds of poor neurological outcomes (CPC 3–5) (OR 4.61, 95 % CI 1.49–17.62, p = 0.013) compared to VF. A significant trend was noted for admission PEA with poor neurological outcomes (OR 2.97, 95 % CI 1.23–7.64, p = 0.019) (Table 2).

Discussion

This prospective study highlights key differences in survival and neurological outcomes among ECPR recipients based on hospital arrival rhythms. Patients in VF had the best outcomes, while those in or converting to asystole had the worst. Despite extensive EMS efforts, many patients with initial VF and PEA converted to asystole, significantly worsening their prognosis. Admission asystole was associated with a fourfold increase in death and poor neurological outcomes, even after adjusting for covariates. The conversion to asystole may indicate prolonged hypoperfusion (e.g., no-flow time, low-flow time, CPR quality) and a stage where the heart and brain may have entered a metabolic phase leading to irreversible cell injury, at which point the benefit of ECPR may have already vanished.[8–9,13]

Our study also confirms that initial asystole is linked to poorer outcomes, whereas patients with initial VF benefit most from ECPR.[7] Given current and previous data, excluding patients with initial asystole from ECPR, especially those who remain in asystole after conventional CPR, seems reasonable, as no study has demonstrated a survival benefit justifying ECPR in this group.[1,7]

Despite the small sample size for initial non-shockable rhythms in our study, we analyzed asystole and PEA separately due to prior evidence showing worse outcomes with asystole compared to PEA in the OHCA population.[8] Our study also demonstrated differences in survival and neurological outcomes between PEA and asystole. However, larger studies are needed to clarify the role of PEA in the ECPR population.[1]

Previous data from non-ECPR OHCA populations partially support our findings, indicating that conversion from initial non-shockable rhythms to shockable rhythms is associated with better outcomes, still depending on the initial rhythm.[8] Unlike many prior studies, our analysis also included rhythm conversions from VF to non-shockable rhythms, which appear to be even more prognostically significant.

Our results are consistent with multicenter observational studies from Japan (JAAM-OHCA registry), which found poorer outcomes in OHCA patients who converted from a shockable to a non-shockable rhythm upon hospital arrival compared to those who maintained a shockable rhythm.[13] Unlike the JAAM-OHCA registry study, which focused on rhythm conversion in general OHCA patients, our research specifically analyzed all rhythm conversions, including those with initial non-shockable rhythms, and concentrated exclusively on ECPR

Table 1
Multivariate logistic regression analysis of 30-day mortality.

Factor	Odds Ratio	Confidence Interval	P value
Male gender	1.59	(0.65,3.90)	0.305
Age (years)	**1.03**	**(1.00,1.06)**	**0.047**
Witnessed arrest (yes)	2.27	(0.64,8.29)	0.200
Bystander CPR (yes)	2.34	(0.45,11.36)	0.298
Time of resuscitation (min)	**1.02**	**(1.00,1.05)**	**0.036**
Public place of cardiac arrest	0.71	(0.32,1.56)	0.401
Initial asystole rhythm	**7.36**	**(2.12,33.85)**	**0.004**
Initial PEA rhythm	2.51	(0.96,7.04)	0.066
Admission asystole rhythm	**4.03**	**(1.49,12.38)**	**0.009**
Admission PEA rhythm	1.89	(0.86,4.23)	0.117

Abbreviations: CPR: cardiopulmonary resuscitation, PEA: pulseless electrical activity.

Table 2
Multivariate logistic regression analysis of poor neurological outcome (CPC 3–5) at hospital discharge.

Factor	Odds Ratio	Confidence Interval	P value
Male gender	1.55	(0.58,4.02)	0.371
Age (years)	**1.04**	**(1.01,1.07)**	**0.018**
Witnessed arrest (yes)	2.54	(0.62,11.03)	0.196
Bystander CPR (yes)	1.31	(0.14,8.30)	0.786
Time of resuscitation (min)	1.02	(1.00,1.05)	0.097
Public place of cardiac arrest	0.76	(0.30,1.81)	0.541
Initial asystole rhythm	**22.25**	**(3.56,457.85)**	**0.006**
Initial PEA rhythm	1.51	(0.54,4.55)	0.438
Admission asystole rhythm	**4.61**	**(1.49,17.62)**	**0.013**
Admission PEA rhythm	**2.97**	**(1.23,7.64)**	**0.019**

Abbreviations: CPR: cardiopulmonary resuscitation, PEA: pulseless electrical activity.

recipients.

Another Japanese observational study, SAVE-J, focused on rhythm conversions among ECPR recipients with initial shockable rhythms but analyzed PEA and asystole conversions together.[13] Our study, however, found significantly worse outcomes for asystole compared to PEA, aligning with prior research in non-ECPR OHCA populations.[8,12] While SAVE-J reported minimal neurological benefit from ECPR in patients who converted from VF to PEA/asystole,[14] our data challenge this conclusion. We observed a 37 % survival rate and 20 % good neurological outcomes in patients who converted from VF to PEA, and a 16 % survival rate with 12 % good neurological outcomes in those who converted from VF to asystole, indicating that these patients can benefit from ECPR.[14].

Recently, a large single-center study from the University of Minnesota ECPR patient cohort was published, utilizing a machine learning model to predict favorable neurological outcomes following ECPR.[10] In this study, the rhythm at the time of cannulation was the most predictive variable among the 11 variables analyzed.[10] This finding aligns with our results and emphasizes the prognostic significance of rhythm prior to ECMO cannulation. However, in contrast to our study, the Minnesota ECPR cohort consisted solely of patients with an initial presentation of VF.[10]

Our findings suggest that both initial and admission rhythms, along with other key prognostic factors, can guide ECPR decision-making. Currently, no single criterion predicts survival with perfect accuracy, so ECPR decisions should involve a combination of criteria assessed by experienced, highly trained teams.[10,3–6] If larger studies confirm our results, they could impact routine clinical practice by making rhythm at hospital arrival a useful and easily recognizable parameter for ECPR teams, who often have limited information and time for decisions.[1,2]

The main limitations include the observational design, which may introduce selection bias, and the limited sample size for non-shockable rhythms, highlighting the need for larger studies. Our focus on initial and admission rhythms without analyzing the timing of conversions may limit patient stratification insights. Finally, as a single-center study from a specialized tertiary center, the generalizability of our findings may be limited.

Conclusions

This study highlights the rhythm at hospital arrival as a significant predictor of survival and neurological outcomes in ECPR for OHCA. Patients with sustained VF have the best outcomes, while those converting to asystole have poor prognoses. Initial asystole is strongly linked to unfavorable outcomes, challenging the benefit of ECPR over conventional CPR if asystole persists despite initial efforts. Combining the rhythm at hospital arrival with other prognostic factors could improve patient stratification and lead to more effective ECPR interventions.

Declarations

Ethics approval and consent to participate

The register and database used for clinical research were approved by the Institutional Review Board of the General University Hospital and First Faculty of Medicine, Charles University in Prague (14/20 VFN IGP). All ECPR patients who regained normal neurologic function, or their legal representatives if they did not regain consciousness, were asked to provide their written consent with registry enrollment and data use. Consent requirements were waived for participants without known legal representatives who died or had severe neurological deficits and were unable to provide informed consent.

CRediT authorship contribution statement

Daniel Rob: Writing – original draft, Visualization, Validation, Resources, Project administration, Methodology, Investigation, Funding acquisition, Formal analysis, Data curation, Conceptualization. **Klaudia Farkasovska:** Writing – review & editing, Visualization, Validation, Project administration, Methodology, Investigation, Formal analysis, Data curation. **Petra Kavalkova:** Writing – review & editing, Visualization, Validation, Project administration, Investigation, Formal analysis, Data curation, Conceptualization. **Milan Dusík:** Writing – review & editing, Visualization, Validation, Methodology, Investigation, Formal analysis, Data curation. **Stepan Havranek:** Writing – review & editing, Visualization, Supervision, Methodology, Investigation, Data curation, Conceptualization. **Jan Pudil:** Writing – original draft, Visualization, Validation, Supervision, Resources, Methodology, Investigation, Formal analysis, Conceptualization. **Eliska Mockova:** Writing – review & editing, Visualization, Validation, Project administration, Investigation, Formal analysis, Data curation, Conceptualization. **Jaromir Macoun:** Writing – original draft, Visualization, Validation, Software, Investigation, Formal analysis, Data curation, Conceptualization. **Jan Belohlavek:** Writing – original draft, Visualization, Validation, Supervision, Resources, Methodology, Investigation, Formal analysis, Conceptualization.

Funding

This study was supported by MH CZ–DRO-VFN00064165, General University Hospital in Prague and the Charles University Research program “Cooperatio – Intensive Care Medicine.”.

Declaration of competing interest

The corresponding author (JB) has received lecture honoraria from the Abiomed, Getinge, Xenios, Resuscitec, Novartis, Astra-Zeneca, Boegringer-Ingelheim.The remaining authors report no conflict of interest.

Acknowledgements

The authors express their gratitude to the Emergency Medical Service teams and the coronary care unit and catheterization laboratory teams of the 2nd Department of Internal Medicine, Cardiovascular Medicine, General University Hospital in Prague for their high-quality care.

References

1. Belohlavek J, Smalcova J, Rob D, et al. Effect of intra-arrest transport, extracorporeal cardiopulmonary resuscitation, and immediate invasive assessment and treatment on functional neurologic outcome in refractory out-of-hospital cardiac arrest: a randomized clinical trial. *JAMA*. 2022;327(8):737–747.
2. Yannopoulos D, Bartos J, Raveendran G, et al. Advanced reperfusion strategies for patients with out-of-hospital cardiac arrest and refractory ventricular fibrillation

(ARREST): a phase 2, single centre, open-label, randomised controlled trial. *Lancet*. 2020;396(10265):1807–1816.
3. Tran A, Rochwerg B, Fan E, et al. Prognostic factors associated with favourable functional outcome among adult patients requiring extracorporeal cardiopulmonary resuscitation for out-of-hospital cardiac arrest: A systematic review and meta-analysis. *Resuscitation*. 2023;110004.
4. Soar J, Böttiger BW, Carli P, et al. European resuscitation council guidelines 2021: adult advanced life support. *Resuscitation*. 2021;161:115–151.
5. Perman, S. M., Elmer, J., Maciel, C. B., et al. (2024). 2023 American Heart Association Focused Update on Adult Advanced Cardiovascular Life Support: An Update to the American Heart Association Guidelines for Cardiopulmonary Resuscitation and Emergency Cardiovascular Care. Circulation, 149(5), e254-e273.
6. Richardson ASC, Tonna JE, Nanjayya V, et al. Extracorporeal cardiopulmonary resuscitation in adults. Interim guideline consensus statement from the extracorporeal life support organization. *ASAIO J*. 2021;67(3):221–228.
7. Havranek S, Fingrova Z, Rob D, et al. Initial rhythm and survival in refractory out-of-hospital cardiac arrest. Post-hoc analysis of the Prague OHCA randomized trial. *Resuscitation*. 2022;181:289–296.
8. Luo S, Zhang Y, Zhang W, et al. Prognostic significance of spontaneous shockable rhythm conversion in adult out-of-hospital cardiac arrest patients with initial non-shockable heart rhythms: a systematic review and meta-analysis. *Resuscitation*. 2017; 121:1–8.
9. Cournoyer A, Cossette S, Potter BJ, et al. Prognostic impact of the conversion to a shockable rhythm from a non-shockable rhythm for patients suffering from out-of-hospital cardiac arrest. *Resuscitation*. 2019;140:43–49.
10. Crespo-Diaz R, Wolfson J, Yannopoulos D, et al. Machine learning identifies higher survival profile in extracorporeal cardiopulmonary resuscitation. *Crit Care Med*. 2024;52(7):1065–1076.
11. Franek O, Pokorna M, Sukupova P. Pre-hospital cardiac arrest in Prague, Czech Republic—The Utstein-style report. *Resuscitation*. 2010;81:831–835.
12. Nolan JP, Berg RA, Andersen LW, et al. Cardiac arrest and cardiopulmonary resuscitation outcome reports: update of the Utstein resuscitation registry template for in-hospital cardiac arrest: a consensus report from a task force of the international liaison committee on resuscitation (American heart association, European resuscitation Council, Australian and New Zealand Council on resuscitation, heart and stroke foundation of Canada, InterAmerican heart foundation, resuscitation Council of southern Africa, resuscitation Council of Asia). Circulation 2019;140:e746-e757.
13. Kandori K, Okada Y, Okada A, et al. Association between cardiac rhythm conversion and neurological outcome among cardiac arrest patients with initial shockable rhythm: a nationwide prospective study in Japan. *Eur Heart J Acute Cardiovasc Care*. 2021;10(2):119–126.
14. Nakashima T, Noguchi T, Tahara Y, et al. Patients with refractory out-of-cardiac arrest and sustained ventricular fibrillation as candidates for extracorporeal cardiopulmonary resuscitation-prospective multi-center observational study-. *Circ J*. 2019;83(5):1011–1018.

D. Jenča et al.

Iron deficiency and all-cause mortality after myocardial infarction

European Journal of Internal Medicine
Impact Factor: 5,9

rejstřík

European Journal of Internal Medicine xxx (xxxx) xxx

Contents lists available at ScienceDirect

European Journal of Internal Medicine

journal homepage: www.elsevier.com/locate/ejim

Original Article

Iron deficiency and all-cause mortality after myocardial infarction

Dominik Jenča [a,b], Vojtěch Melenovský [a], Jolana Mrázková [c], Marek Šramko [a,d], Martin Kotrč [a], Michael Želízko [a], Věra Adámková [e], Jan Piťha [a], Josef Kautzner [a,f], Peter Wohlfahrt [d,e,*]

[a] Department of Cardiology, Institute for Clinical and Experimental Medicine (IKEM), Prague, Czech Republic
[b] Third Medical School, Charles University, Prague, Czech Republic
[c] Experimental Medicine Centre, Institute for Clinical and Experimental Medicine (IKEM), Prague, Czech Republic
[d] First Medical School, Charles University, Prague, Czech Republic
[e] Department of Preventive Cardiology, Institute for Clinical and Experimental Medicine, Prague, Czech Republic
[f] Medical and Dentistry School, Palacký University, Olomouc, Czech Republic

ARTICLE INFO

Keywords:
Myocardial infarction
Iron deficiency
Outcomes
Mortality
Criteria

ABSTRACT

Background: Data on the clinical significance of iron deficiency (ID) in patients with myocardial infarction (MI) are conflicting. This may be related to the use of various ID criteria.
We aimed to compare the association of different ID criteria with all-cause mortality after MI.
Methods: Consecutive patients hospitalized for their first MI at a large tertiary heart center were included. We evaluated the association of different iron metabolism parameters measured on the first day after hospital admission with all-cause mortality.
Results: From the 1,156 patients included (aged 64±12 years, 25 % women), 194 (16.8 %) patients died during the median follow-up of 3.4 years. After multivariate adjustment, iron level ≤13 μmol/L (HR 1.67, 95 % CI 1.19–2.34) and the combination of iron level ≤12.8 μmol/L and soluble transferrin receptor (sTfR) ≥3 mg/L (HR 2.56, 95 % CI 1.64–3.99) termed as PragueID criteria were associated with increased mortality risk and had additional predictive value to the GRACE score. Compared to the model including iron level, the addition of sTfR improved risk stratification (net reclassification improvement 0.61, 95 % CI 0.52–0.69) by reclassifying patients into a higher-risk group. No association between ferritin level and mortality was found. 51 % of patients had low iron levels, and 58 % fulfilled the PragueID criteria.
Conclusion: Iron deficiency is common among patients with the first MI. The PragueID criteria based on iron and soluble transferrin receptor levels provide the best prediction of mortality and should be evaluated in future interventional studies for the identification of patients potentially benefiting from intravenous iron therapy.

1. Introduction

Iron is an essential element required for normal mitochondrial function [1,2] oxygen transport, synthesis of proteins and nucleic acids, and normal immune system function. Although iron is environmentally abundant, iron deficiency (ID) is one of the most common nutritional deficits worldwide affecting approximately two billion people [3].

In cardiovascular disease, the effect of ID has been best described in patients with heart failure (HF) [4]. ID affects approximately 50 % of HF patients and is associated with worse functional capacity, impaired quality of life, increased mortality, and hospitalization rate, irrespective of anemia presence [5]. Treatment with intravenous ferric carboxymaltose in patients with HF and ID improves symptoms, functional capacity, and quality of life, and reduces the risk of hospital admissions for HF and cardiovascular causes [6,7] Despite that, there is no consensus on ID definition in HF [8,9] The most commonly used are the guideline-recommended ID criteria based on ferritin and transferrin saturation [8,10] However, other criteria have been used as well [9,11]

Much less is known about ID effects in patients with myocardial infarction (MI). A systematic review and meta-analysis of 7 studies including a total of 2821 patients described worse long-term outcomes in the ID population, whereas short-term outcomes were heterogeneous across studies [12]. However, ID did not affect prognosis in MI patients with cardiogenic shock [13]. A small sample size and different criteria

* Corresponding author at: Department of Preventive Cardiology, Institute for Clinical and Experimental Medicine, Videnska 1958/9, 140 21 Prague 4, Czech Republic.
E-mail address: wohlfp@gmail.com (P. Wohlfahrt).

https://doi.org/10.1016/j.ejim.2024.04.020
Received 5 March 2024; Received in revised form 19 April 2024; Accepted 26 April 2024

Please cite this article as: Dominik Jenča et al., *European Journal of Internal Medicine*, https://doi.org/10.1016/j.ejim.2024.04.020

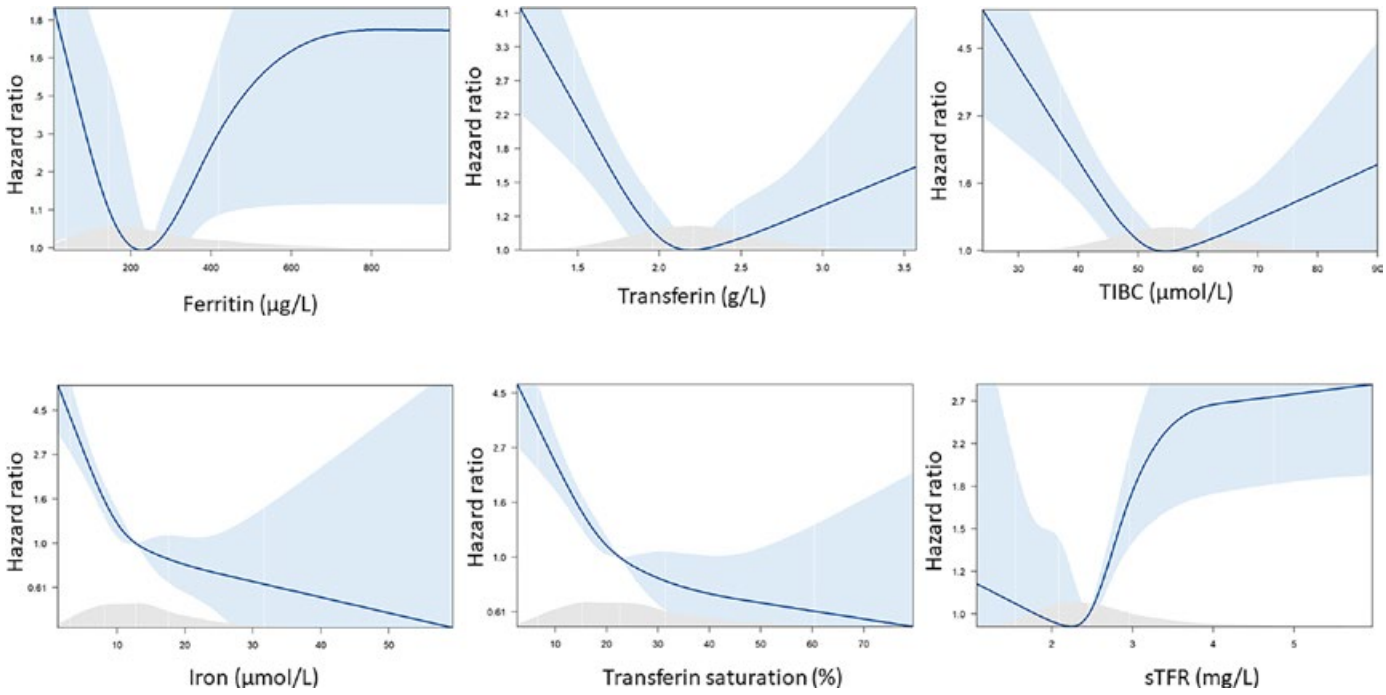

Fig. 1. Restricted cubic splines of different iron metabolism parameters and all-cause mortality after myocardial infarction.

for ID definitions may explain this heterogeneity in study outcomes. Furthermore, several criteria use ferritin to define ID. Nonetheless, ferritin is a positive acute phase reactant, thus the inflammatory reaction to MI may influence it [14]. Besides, ferritin has been suggested as a leakage product from damaged cells [15]. Therefore, ferritin may not be a good marker of ID in patients with MI.

For selecting patients potentially benefiting from intravenous iron therapy, the definition of ID is important. However, ID criteria currently used are based only on a consensus, while ID definition based on hard outcomes is missing. Misclassification of patients may dilute the therapy effect. This issue is further supported by an animal model of MI, which has shown no effect of iron supplementation in normal iron status [16]. Thus, the correct definition of ID is of great clinical importance. Until now, no previous study compared the association of different ID criteria with total mortality after MI.

To address this issue, the present study aimed to compare the prognostic significance of diverse criteria of iron deficiency measured on the first day after hospital admission in a large cohort of consecutive patients hospitalized for their first myocardial infarction at a large tertiary heart center.

2. Methods

2.1. Population

This study used data from the prospective Institute for Clinical and Experimental Medicine Acute Myocardial Infarction Registry (AMBITION registry) [17]. The registry collects clinical data and biospecimens from consecutive patients hospitalized for acute coronary syndrome since June 2017 at the Institute for Clinical and Experimental Medicine, Prague, Czech Republic, a tertiary heart center with around-the-clock coronary intervention service. The Fourth Universal Definition of Myocardial Infarction has been used [18]. Patients underwent a detailed interview during their hospital stay, and additional information was obtained from medical record abstraction and laboratory studies. For this analysis, we included consecutive patients enrolled between June 2017 and February 2023 with type I MI and no previous history of coronary artery disease. Iron metabolism was measured in the central laboratory from blood samples collected on the morning of the first day after hospital admission. Death was ascertained through December 1st, 2023. Mortality data were provided by the Institute of Health Information and Statistics of the Czech Republic (UZIS), which keeps a list of all deceased persons and dates of death in the Czech Republic by law. All patients signed informed consent. This study was approved by a local ethics committee and complies with the Declaration of Helsinki.

2.2. Primary outcome

The primary outcome of the analysis was all-cause mortality.

2.3. GRACE score

The Eagle model estimates for death within 6 months after discharge was used [19]. Variables included in the model were age, heart rate, systolic blood pressure, creatinine level, troponin elevation, ST segment depression on initial ECG, previous history of MI and heart failure, and PCI.

2.4. Statistical methods

Continuous variables are presented as mean and SDs or medians and IQRs. Hazard ratios (HR) are shown with a 95 % confidence interval (CI). Nominal variables are shown as counts and percentages.

We have used restricted cubic splines adjusted for age to detect a nonlinear association between different parameters of iron metabolism and the primary outcome. Furthermore, we have used decision tree analysis to set the cut points for ID definition. The Cox regression model was used to analyze the association of different ID criteria with the outcome.

The Global Registry of Acute Coronary Events (GRACE) score has been recommended by the guidelines to stratify patients' risk after MI [20]. To analyze the additional predictive value of different ID criteria to the GRACE score, we have used the difference in the area under the receiver operating characteristic curve (AUC), the Brier score, and the continuous net reclassification improvement (NRI).

Statistical analyses were conducted with R statistical software

Table 1
Population demographics.

Characteristics	Iron >12.8 & sTfR<3 (*n* = 490)	Iron ≤12.8 & sTfR<3 (*n* = 394)	Iron >12.8 & sTfR≥3(*n* = 83)	Iron ≤12.8 & sTfR≥3 (*n* = 189)	p
Age (years)	62.0 ± 11.9	64.3 ± 12.7*	66 ± 12.7*	67.6 ± 12.2*	< 0.001
Male sex, n (%)	376 (77 %)	292 (74 %)	60 (72 %)	139 (74 %)	0.68
STEMI, n (%)	304 (62 %)	279 (71 %)*	45 (54 %)	125 (66 %)	0.001
Anterior MI, n (%)	195 (40 %)	175 (44 %)	38 (46 %)	97 (51 %)	0.052
Subacute MI, n (%)	33 (7 %)	81 (21 %)*	8 (10 %)	41 (22 %)*	<0.0001
Multi-vessel disease, n (%)	138 (28 %)	121 (31 %)	26 (31 %)	74 (39 %)	0.052
CPR before admission, n (%)	14 (3 %)	31 (8 %)*	1 (1 %)	13 (7 %)	0.001
Admission HR, min^{-1}	74 ± 16	80 ± 20*	77 ± 17	82 ± 18*	<0.0001
Admission SBP, mmHg	145±26	138±29*	149±23	142±24	0.0002
Admission DBP, mmHg	80±13	78±15	82±14	79±14	0.10
Creatinine, $\mu mol.l^{-1}$	81 (70–93)	86 (72–102)*	86 (70–101)	91 (75–118)*	<0.0001
CKD-EPI, $ml/s/1.73m^2$	1.39 ± 0.30	1.28 ± 0.39*	1.26 ± 0.37*	1.16 ± 0.42*	<0.0001
Fasting glucose, mmol/L	7.93 ± 3.42	8.78 ± 3.81*	8.24 ± 3.19	9.72 ± 4.84*	<0.0001
HbA1c, $mmol.mol^{-1}$	41 (38–46)	42 (39–47)	41 (37–49)	44 (40–53)*	<0.0001
Maximal hsTroponin T, ng/L	1047 (314–3088)	2256 (825–5159)*	813 (255–2183)	2011 (685–4045)*	<0.0001
Total cholesterol	4.99 ± 1.16	4.57 ± 1.12*	5.09 ± 1.25	4.60 ± 1.26*	<0.0001
LDL cholesterol	3.34 ± 1.01	2.96 ± 1.03*	3.45 ± 1.23	2.97 ± 1.16*	<0.0001
Leukocyte count, $10^9.l^{-1}$	10.5 (8.4–15.2)	11.7 (9.5–15.0)*	10.0 (7.4–11.8)	11.8 (9.1–14.0)*	<0.0001
Hemoglobin, g/L	145 ± 13	141 ± 15*	144 ± 19	137 ± 21*	<0.0001
Hemoglobin <120, n (%)	12 (3 %)	38 (10 %)*	7 (9 %)*	38 (20 %)*	<0.0001
LV EF (%)	50 (40–55)	40 (35–50)*	50 (40–55)	40 (35–50)*	<0.0001
LV EF ≤ 40%, n (%)	69 (14 %)	125 (32 %)*	16 (19 %)	61 (32 %)*	< 0.0001
PCI or CABG, n(%)	479 (98 %)	355 (90 %)*	76 (92 %)*	165 (87 %)*	< 0.0001
Killip class I, n (%)	427 (87 %)	276 (70 %)*	75 (90 %)	114 (60 %)*	<0.0001
Risk factors					
Arterial hypertension, n (%)	270 (55 %)	228 (58 %)	54 (65 %)	135 (71 %)*	0.001
Diabetes mellitus, n (%)	88 (18 %)	82 (21 %)	19 (23 %)	82 (43 %)*	<0.0001
Current smoking, n (%)	247 (51 %)	184 (47 %)	32 (39 %)	66 (35 %)*	0.002
BMI, kg/m^2	28.6 ± 4.5	28.5 ± 4.8	30.3 ± 6.4*	29.3 ± 5.2	0.006
COPD, n (%)	28 (6 %)	24 (6 %)	5 (6 %)	11 (6 %)	0.996
Atrial fibrillation history, n (%)	17 (4 %)	18 (5 %)	7 (8)*	24 (13 %)*	<0.0001
Medications on admission					
ACE inhibitors or ARB, n (%)	212 (43 %)	168 (43 %)	36 (43 %)	95 (50%)	0.31
Statins, n (%)	85 (17 %)	76 (19 %)	15 (18%)	49 (26 %)	0.08
Antiplatelet therapy, n (%)	47 (10 %)	54 (14 %)	11 (13 %)	45 (24 %)*	0.002
Anticoagulants, n (%)	20 (4 %)	19 (5 %)	11 (13 %)*	21 (11 %)*	0.0002
Discharge medication[#]					
ACE inhibitors or ARB, n (%)	382 (78 %)	282 (74 %)	70 (84 %)	144 (79 %)	0.16
Beta blocker, n (%)	382 (78 %)	296 (78 %)	68 (82 %)	151 (83 %)	0.43
Statins, n (%)	480 (98 %)	365 (96 %)	79 (95 %)	168 (92 %)*	0.004
Aspirin, n (%)	474 (97 %)	349 (91 %)*	77 (93 %)	158 (86 %)*	<0.0001
Clopidogrel, n (%)	88 (18 %)	136 (36 %)*	34 (41 %)*	73 (40 %)*	<0.0001
Prasugrel, n (%)	19 (4 %)	5 (1 %)	3 (4 %)	2 (1 %)	0.05
Ticagrelor, n (%)	365 (75 %)	226 (59 %)*	44 (53 %)*	88 (48 %)*	<0.0001
Anticoagulation, n (%)	52 (11 %)	85 (22 %)*	15 (18 %)	55 (30 %)*	<0.0001
Tripple therapy, n (%)	33 (7 %)	48 (13 %)*	10 (12 %)	23 (13 %)*	0.02
Iron metabolism					
Iron, μmol/L	19.8 ± 7.0	8.4 ± 2.9*	17.6 ± 4.1*	7.5 ± 2.9*	<0.0001
Ferritin, μg/L	240 (138–391)	292 (180–490)*	189 (97–278)*	230 (103–412)	<0.0001
Transferrin, g/L	2.25 ± 0.35	2.1 ± 0.39*	2.4 ± 0.36*	2.31 ± 0.46*	<0.0001
TIBC, μmol/L	56.6 ± 8.9	53.0 ± 9.8*	60.6 ± 9.2*	58.1 ± 11.6	<0.0001
TSAT,%	35.9 ± 13.7	16.2 ± 5.6*	29.6 ± 7.1*	13.6 ± 5.3*	<0.0001
sTFR, mg/L	2.23 ± 0.40	2.33 ± 0.37	3.60 ± 0.85*	4.0 ± 1.62*	<0.0001
Scores					
GRACE	114 ± 23	122 ± 26*	121 ± 25	129 ± 26*	<0.0001
Outcome					
Death, n (%)	36 (7 %)	74 (19%)*	19 (23 %)*	65 (34 %)*	<0.0001

*$p < 0.05$ vs. Iron >12.8 & sTfR<3 group.
#missing in patients with in-hospital death.

version 4.2.2 (R Foundation for Statistical Computing, Vienna, Austria), JMP 17, SPSS version 25.0 (IBM Corporation, Armonk, NY), and STATA version 17 (StataCorp, College Station, TX). All statistical tests and confidence intervals were 2-sided with a significance level of 0.05.

3. Results

In total, 1156 patients (mean age 64 years, 75 % male) hospitalized for their first type I myocardial infarction between June 2017 and February 2023 were included in this analysis. During the median follow-up of 1224 days (IQR 626–1782), 194 (16.8 %) patients died.

Fig. 1 presents restricted cubic splines of the association between different parameters of iron metabolism and all-cause mortality risk. While there was no association between ferritin level and all-cause mortality, low iron, transferrin, TSAT, total iron binding capacity (TIBC), and high sTfR were associated with increased mortality risk.

3.1. Development of pragueid criteria

In the decision tree model, among the analyzed iron metabolism

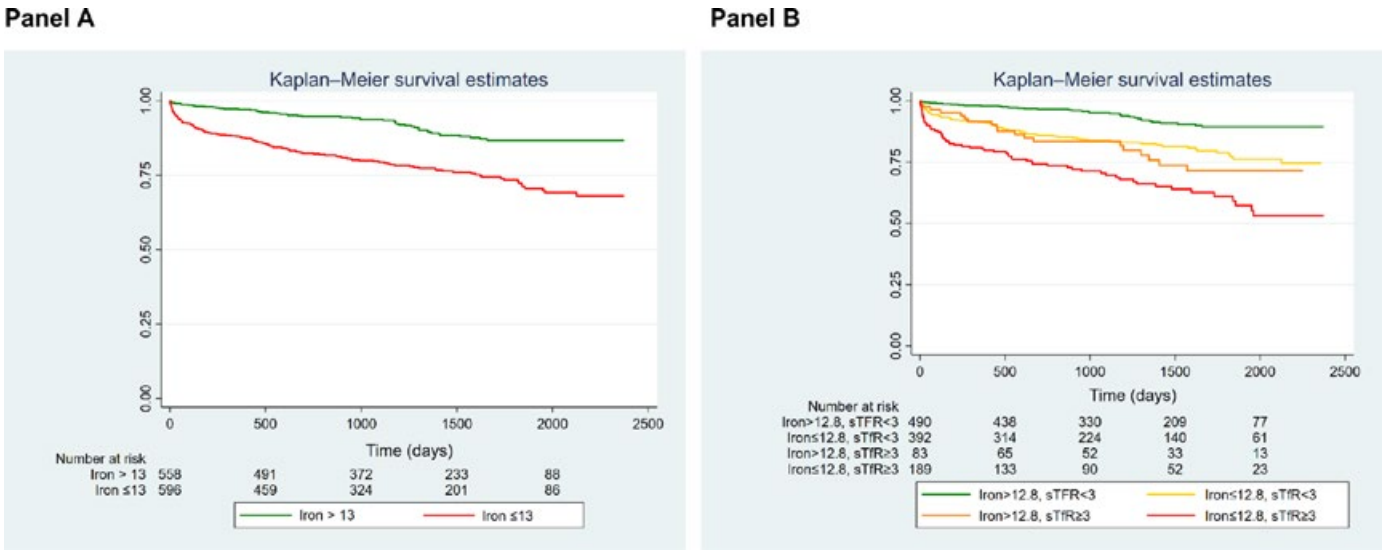

Fig. 2. Kaplan-Meier survival for iron (Panel A) and PragueID (Panel B) categories.

Table 2
Association of different iron deficiency criteria with all-cause mortality.

Iron deficiency criteria	Prevalence n(%)	Unadjusted HR (95 % CI)	Adjusted* HR (95 % CI)	Adjusted** HR (95 % CI)
Iron ≤13 μmol/L	598 (51.7)	2.78 (2.03–3.82)	2.06 (1.50–2.84)	1.67 (1.19–2.34)
TSAT <20 %	468 (40.5)	2.46 (1.85–3.28)	1.89 (1.41–2.53)	1.38 (1.01–1.90)
Ferritin <30 μg/L	20 (1.7)	1.44 (0.59–3.50]	1.58 (0.64–3.84)	1.55 (0.63–3.80)
Ferritin <100 μg/L	157 (13.6)	1.50 (1.05–2.13)	1.37 (0.96–1.95)	1.36 (0.93–1.98)
Guideline ID definition	357 (31.0)	1.69 (1.28–2.24)	1.57 (1.19–2.08)	1.34 (0.99–1.82)
Prague ID criteria				
2. Iron ≤12.8 μmol/L & sTfR<3 mg/L	394 (34.1)	2.79 (1.87–4.15)	2.07 (1.38–3.10)	1.75 (1.16–2.64)
3. Iron >12.8 μmol/L & sTfR≥3 mg/L	83 (7.2)	3.27 (1.88–5.70)	2.64 (1.51–4.61)	2.05 (1.15–3.64)
4. Iron ≤12.8 μmol/L & sTfR≥3 mg/L	189 (16.3)	5.76 (3.83–8.66)	3.72 (2.46–5.63)	2.56 (1.64–3.99)

* Adjusted for GRACE score.
** Adjusted for age, gender, HF history, CKD-EPI, admission systolic blood pressure and heart rate, absence of PCI, Killip class, ejection fraction <35 at discharge

A 95 % confidence interval is shown in bracelets. Guideline ID criteria were ferritin <100 μg/L or TSAT <20 % if ferritin was 100–299 μg/L.

parameters (iron, transferrin, TSAT, TIBC, TfR), the combination of iron ≤12.8 μmol/L and sTfR ≥ 3.0 mg/L showed the best association with total mortality risk. Based on these cut-points, we have created 4 groups – group 1 with normal iron and normal sTfR, group 2 with low iron and normal sTfR, group 3 with normal iron and high sTfR, and group 4 with low iron and high sTfR. We have termed this classification as PragueID criteria. Population demographics by PragueID criteria are shown in Table 1.

As shown in Fig. 2, the addition of sTfR to iron level can reclassify the risk associated with low iron to intermediate and high, while high sTfR in the presence of normal iron is associated with an intermediate risk.

3.2. Comparison of ID criteria

After adjustment for the GRACE score or other variables affecting mortality risk after MI, all ID criteria except for ferritin were independently associated with the total mortality (Table 2). The hazard ratio was highest for the Prague ID criteria and iron level. As assessed by the AUC and Brier score (Table 3), only the iron level and Prague ID criteria had additional prognostic value to the GRACE score. When the additional prognostic value of iron or PragueID was compared, there was no difference in AUC, but there was a borderline difference in the Brier score and an improvement in net reclassification improvement (NRI) in favor of the PragueID criteria. Beyond the iron level, PragueID correctly reclassified cases patients into the higher-risk group (Table 4).

4. Discussion

In the present study, we have analyzed the association of different ID criteria with all-cause mortality in patients hospitalized for their first MI. We show that ID is common among these patients, but the prevalence and prognostic implications differ by the criteria used. Among several criteria evaluated, only iron level and particularly the combination of iron level and soluble transferrin receptor were independently associated with the risk of all-cause mortality and improved risk prediction beyond the guidelines recommended GRACE score.

While ferritin is a guideline-recommended parameter for ID diagnosis in HF, we did not find any association between ferritin level and mortality risk. This finding among MI patients may be explained by the effect of cell necrosis and inflammatory response on ferritin levels. Thus, ferritin should not be used to define ID after MI.

Our observation is in line with previous studies. In patients with chronic HF, TSAT <20 % and serum iron ≤13 mmol/L were independently associated with death, but lower serum ferritin concentrations were paradoxically associated with better survival [9]. In a study of the prognostic value of temporal changes of iron metabolism parameter in patients with acute coronary syndrome, a decrease in TSAT and iron levels, but not changes in ferritin levels were associated with an increased risk of cardiovascular death and nonfatal ACS [21]. Among patients with coronary artery disease, sTfR was independently associated with an increased risk of cardiovascular death or MI [22]. We add to this evidence the observations that among several criteria of ID, the combination of low iron and high sTfR can identify patients at increased mortality risk, which may have the biggest benefit from iron supplementation.

To the best of our knowledge, this is the first large-scale study among consecutive MI patients evaluating the prevalence and prognostic significance of different ID criteria. We found that 51 % of patients after MI

Table 3
Additional predictive value of different iron deficiency criteria to the GRACE score 6 months (**Table A**) and 12 months (**Table B**) after hospital discharge.

Table A	6 months				
	AUC	Δ AUC	p	Δ Brier	p
Iron ≤13 μmol/L	82.6 (77.1—88.0)	2.5 (1.1—3.9)	0.001	−0.1(−0.2— −0.001)	0.01
TSAT <20 %	81.7 (76.2—87.2)	1.6 (0.1—3.2)	0.04	−0.1 (−0.2— −0.01)	0.047
Ferritin <30 μg/L	79.9 (74.3—85.6)	−0.2 (−0.3—0.001)	0.04	0.01 (−0.001—0.001)	0.74
Ferritin <100 μg/L	80.0 (74.3—85.8)	−0.1 (−0.6—0.5)	0.90	−0.001 (−0.1—0.01)	0.19
Guideline	80.5 (74.7—86.2)	0.4 (−0.7—1.5)	0.5	−0.1 (−0.2—−0.1)	0.02
Prague criteria	82.9 (77.5—88.2)	2.8 (0.9—4.7)	0.004	−0.3 (−0.4 — −0.1)	0.0003
		Table B			
	12 months				
	AUC	Δ AUC	p	Δ Brier	p
Iron ≤13 μmol/L	81.9 (77.0—86.9)	2.1 (0.7—3.6)	0.004	−0.2 (−0.3—−0.1)	0.005
TSAT <20 %	81.5 (76.6—86.4)	1.7 (0.2—3.2)	0.03	−0.1 (−0.3—0.1)	0.096
Ferritin <30 μg/L	79.8 (74.8—84.8)	−0.01 (−0.4—0.4)	0.96	0.01 (−0.001—0.001)	0.90
Ferritin <100 μg/L	79.8 (74.7—84.9)	0.001(−0.5—0.5)	1.0	−0.001 (−0.1—0.01)	0.19
Guideline	80.2 (75.1—85.3)	0.4 (−0.6—1.4)	0.4	−0.1 (−0.2 — −0.1)	0.044
Prague criteria	82.4 (77.6—87.2)	2.6 (0.7—4.5)	0.007	−0.3 (−0.6— −0.1)	0.001

A 95 % confidence interval is shown in bracelets.

Table 4
Comparison of model discrimination, calibration, and reclassification.

	Discrimination				Calibration		Reclassification		
Time	AUC Iron	AUC PragueID	AUC	p	Brier	p	NRI	NRI+	NRI-
6 months	82.6 (77.1–88.0)	82.9 (77.5–88.2)	0.3 (−1.1–1.7)	0.70	−0.1 (−0.3–0.01)	0.06	0.56 (0.34–0.87)	-10^{-15} (−0.20–0.28)	0.56 (0.52–0.59)
1 year	81.9 (77.0–86.9)	82.4 (77.6–87.2)	0.5 (−1.0–1.9)	0.50	−0.2 (−0.3–0.01)	0.06	0.66 (0.62–0.81)	0.64 (0.55–0.78)	0.01 (−0.004–0.08)
2 years	81.5 (77.3–85.6)	82.2 (78.1–86.3)	0.7 (−0.6–2.1)	0.30	−0.3 (−0.5–0.001)	0.04	0.60 (0.49–0.76)	0.57 (0.44–0.67)	0.03 (−0.01–0.09)
3 years	79.8 (75.6–84.0)	80.3 (76.0–84.6)	0.5 (−0.8–1.9)	0.40	−0.3 (−0.6–0.01)	0.06	0.61 (0.52–0.69)	0.56 (0.50–0.63)	0.04 (−0.009–0.08)

A model with Grace score and Iron class (Iron ≤13 μmol/L vs. Iron >13 μmol/L) was compared with a model including Grace score and PragueID class. A 95 % confidence interval is shown in brackets.
AUC – area under the curve, NRI – net reclassification improvement.

have iron ≤13 μmol/L and 58 % have ID if PragueID criteria are used. Thus, more than 50 % of patients with the first MI are affected by ID. This is similar to the ID prevalence in HF, among which 43 % of men and 54 % of women had iron ≤13 mmol/L [9]. After adjustment for other covariates, the mortality risk associated with low iron level in our study was increased by 67 %, and by 156 % in patients with low iron and high sTfR. Interestingly, this risk in MI patients is higher than the 37 % risk increase associated with iron ≤13 μmol/L among patients with HF [9]. This difference may be partially explained by the addition of antiplatelet therapy in MI patients, which may further worsen the pre-existing ID.

In previous studies, MI was associated with serum iron, TIBC, and TSAT decrease and ferritin increase, with MI severity affecting the magnitude of this change [23,24] Thus, low iron levels may be only a marker of MI severity. However, sTfR as a marker of iron demand is not affected by inflammation [22] and MI severity (**Supplementary Table 1**). This suggests that ID is not only a marker of MI severity but also a risk factor that may be intervened. Previous studies suggest the biological plausibility of this concept. In an animal model, the deleterious effect of ID was at least in part explained by increased oxidative/nitrosative stress and altered antioxidant defense caused by inhibition of the endothelial nitric oxide synthase (eNOS)/ soluble guanylate cyclase/protein kinase G pathway, leading to eNOS degradation via ubiquitin/proteasome system [25]. Altered energy metabolism is another possible explanation of the deleterious effect of ID in CAD [26,27] In a small study among STEMI patients, application of ultrasmall superparamagnetic iron-oxide within 4 days following an acute myocardial infarction led to smaller infarct size [28]. While our observational study is not able to answer the question of whether ID is a risk marker or a risk factor after MI, identifying ID criteria with the best predictive value sets the ground for future interventional studies with iron supplementation.

4.1. Strengths and limitations of the study

We must admit several limitations of our study. First, iron metabolism was measured at a single time point one day after hospital admission. Because iron parameters dynamically evolve after MI, we were unable to determine how measurements at different time points would affect the prognostic value of ID criteria.

Nevertheless, in a previous study using serial measurement in ACS patients, iron status patterns did not differ in those with and without events [21].

Second, we have used all-cause, rather than cardiovascular mortality, as we were unable to ascertain the cause of death. On the other hand, cardiovascular death is the leading cause of mortality in patients in the first four years after MI [29]. Based on previous studies analyzing the association of ID with total and cardiovascular mortality, we believe that changing the primary study objective would not affect our results [12, 30]

Third, due to the observational nature of our study, no causal inferences can be drawn from our results. Future interventional studies will be needed to evaluate the effects of iron supplementation in patients with ID defined by our criteria.

Fourth, we did not measure hepcidin level, which is considered a key regulator of iron homeostasis [31]. However, in a previous study hepcidine level was not independently associated with the outcome of patients with coronary heart disease [32].

Fifth, because we did not have data on iron supplementation during the study follow-up, we were unable to account for this effect.

The strengths of our study include analysis of various iron status parameters including sTfR and the large single-center cohort of consecutive MI patients with a relatively long follow.

5. Conclusion

The present study among consecutive patients hospitalized for their first myocardial infarction shows that iron deficiency is present in over 50 % of patients. Among several iron deficiency criteria, the combination of low iron level and high soluble transfer receptor were independently associated with mortality risk and improved risk stratification. The clinical benefit of iron supplementation decision-making based on our criteria will have to be addressed in future studies.

Declartion of competing interest

Dr. Jenča has received consulting fees from Swixx Biopharma. The remaining authors have nothing to disclose.

Data availability

The data that support the findings of this study are available from the corresponding author (PW) upon reasonable request.

Ethical approval information

The study was approved by a local ethics committee. All participants gave their written informed consent prior to data collection.

Funding

Supported by the Ministry of Health of the Czech Republic, grant nr. NV 19-09-00125, NU 22-02-00130 and by the project National Institute for Research of Metabolic and Cardiovascular Diseases (Programme EXCELES, Project No. LX22NPO5104) - Funded by the European Union - Next Generation EU. Funders did not determine the study design, conduct, or reporting.

Supplementary materials

Supplementary material associated with this article can be found, in the online version, at doi:10.1016/j.ejim.2024.04.020.

References

[1] Rensvold JW, Ong SE, Jeevananthan A, Carr SA, Mootha VK, Pagliarini DJ. Complementary RNA and protein profiling identifies iron as a key regulator of mitochondrial biogenesis. Cell Rep 2013;3(1):237–45.
[2] Rensvold JW, Krautkramer KA, Dowell JA, Denu JM, Pagliarini DJ. Iron deprivation induces transcriptional regulation of mitochondrial biogenesis. J Biol Chem 2016;291(40):20827–37.
[3] Gedfie S, Getawa S, Melku M. Prevalence and associated factors of iron deficiency and iron deficiency anemia among under-5 children: a systematic review and meta-analysis. Glob Pediatr Health 2022;9. 2333794×221110860.
[4] Savarese G, von Haehling S, Butler J, Cleland JGF, Ponikowski P, Anker SD. Iron deficiency and cardiovascular disease. Eur Heart J 2023;44(1):14–27.
[5] Beavers CJ, Ambrosy AP, Butler J, Davidson BT, Gale SE, PiÑA IL, Mastoris I, Reza N, Mentz RJ, Lewis GD. Iron deficiency in heart failure: a scientific statement from the heart failure society of America. J Card Fail 2023;29(7):1059–77.
[6] Anker SD, Comin Colet J, Filippatos G, Willenheimer R, Dickstein K, Drexler H, Lüscher TF, Bart B, Banasiak W, Niegowska J, Kirwan BA, Mori C, von Eisenhart Rothe B, Pocock SJ, Poole-Wilson PA, Ponikowski P. Ferric carboxymaltose in patients with heart failure and iron deficiency. N Engl J Med 2009;361(25):2436–48.
[7] Ponikowski P, Mentz RJ, Hernandez AF, Butler J, Khan MS, van Veldhuisen DJ, Roubert B, Blackman N, Friede T, Jankowska EA, Anker SD. Efficacy of ferric carboxymaltose in heart failure with iron deficiency: an individual patient data meta-analysis. Eur Heart J 2023;44(48):5077–91.
[8] McDonagh TA, Metra M, Adamo M, Gardner RS, Baumbach A, Böhm M, Burri H, Butler J, Čelutkienė J, Chioncel O, Cleland JGF, Coats AJS, Crespo-Leiro MG, Farmakis D, Gilard M, Heymans S, Hoes AW, Jaarsma T, Jankowska EA, Lainscak M, Lam CSP, Lyon AR, McMurray JJV, Mebazaa A, Mindham R, Muneretto C, Francesco Piepoli M, Price S, Rosano GMC, Ruschitzka F, Kathrine Skibelund A. 2021 ESC Guidelines for the diagnosis and treatment of acute and chronic heart failure. Eur Heart J 2021;42(36):3599–726.
[9] Masini G, Graham Fraser J, Pellicori P, Cleland John GF, Cuthbert Joseph J, Kazmi S, Inciardi Riccardo M, Clark Andrew L. Criteria for iron deficiency in patients with heart failure. J Am Coll Cardiol 2022;79(4):341–51.
[10] Yancy CW, Jessup M, Bozkurt B, Butler J, Casey DE, Colvin MM, Drazner MH, Filippatos GS, Fonarow GC, Givertz MM, Hollenberg SM, Lindenfeld J, Masoudi FA, McBride PE, Peterson PN, Stevenson LW, Westlake C. 2017 ACC/AHA/HFSA focused update of the 2013 ACCF/AHA guideline for the management of heart failure: a Report of the American College of Cardiology/American Heart Association Task Force on Clinical Practice Guidelines and the Heart Failure Society of America. Circulation 2017;136(6):e137–61.
[11] Kalra PR, Cleland JGF, Petrie MC, Thomson EA, Kalra PA, Squire IB, Ahmed FZ, Al-Mohammad A, Cowburn PJ, Foley PWX, Graham FJ, Japp AG, Lane RE, Lang NN, Ludman AJ, Macdougall IC, Pellicori P, Ray R, Robertson M, Seed A, Ford I, Kalra PR, Cleland JGF, Petrie MC, Thomson EA, Kalra PA, Squire IB, Ahmed FZ, Al-Mohammad A, Cowburn PJ, Foley PWX, Graham FJ, Japp AG, Lane RE, Lang NN, Ludman AJ, Macdougall IC, Pellicori P, Ray R, Robertson M, Seed A, Ford I, Boon N, Amoils S, Chapman C, Diness TG, McMurray J, Mindham R, Sandu P, Strom CC, Travers M, Wilcox R, Struthers A, Mark P, Weir C, Cowan E, Turner C, Austin R, Rogers P, Chandrasekaran B, Fraile E, Kyeremeh L, McGregor L, Osmanska J, Meyer B, Ahmad F, Fisher J, Summersgill C, Adeniji K, Chinnadurai R, Massimo L, Hardman C, Sykes D, Frank S, Smith S, Anwar M, Whittington B, Sookhoo V, Lyons S, Middle J, Housley K, Clark A, Bulemfu J, Critoph C, Chong V, Wood S, Szwejkowski B, Lang C, Duff J, MacDonald S, Schiff R, Donnelly P, Nageh T, Kunhunny S, Gardner R, McAdam M, McPherson E, Banerjee P, Sear E, Edwards N, Glover J, Murphy C, Cooke J, Spencer C, Francis M, Matthews I, McKie H, Marshall A, Large J, Stratford J, Clifford P, Boos C, Keeling P, Hughes D, Wong A, Jones D, James A, Williams R, Leslie S, Finlayson J, Hannah A, Campbell P, Walsh J, Quinn J, Piper S, Patale S, Gupta P, Sim V, Knibbs L, Lyons K, Dixon L, Petrie C, Wong Y-k, Labinjoh C, Duckett S, Massey I, Savage H, Matias S, Ramirez J, Manisty C, Hussain I, Sankaranarayanan R, Davis G, McClure S, Baxter J, Wicks E, Sobolewska J, Murphy J, Elzayat A, Cooke A, Wright J, Williams S, Muthumala A, Chaggar P, Webber S, Ellis G, Welch M, Bulugahapitiya S, Jackson T, Pakrashi T, Bakhai A, Krishnamurthy V, Gamma R, Ellery S, Jenkins G, Thomas G, Nightingale A, Greenlaw N, Wetherall K, Clarke R, Graham C, Kean S, Stevenson A, Wilson R, Boyle S, McHugh J, Hall L, Woollard J, Brunton C, Dinnett E, Reid A, Howe S, Nicholls J, Cunnington A, Douglas E, Fegen M, Jones M, McGowan S, Ross B, Surtees P, Stuart D. Intravenous ferric derisomaltose in patients with heart failure and iron deficiency in the UK (IRONMAN): an investigator-initiated, prospective, randomised, open-label, blinded-endpoint trial. Lancet North Am Ed 2022;400 (10369):2199–209.
[12] Reinhold J, Papadopoulou C, Baral R, Vassiliou VS. Iron deficiency for prognosis in acute coronary syndrome - A systematic review and meta-analysis. Int J Cardiol 2021;328:46–54.
[13] Obradovic D., Loncar G., Zeymer U., Pöss J., Feistritzer H.J., Freund A., Jobs A., Fuernau G., Desch S., Ceglarek U., Isermann B., von Haehling S., Anker S.D., Büttner P., Thiele H. Impact of anaemia and iron deficiency on outcomes in cardiogenic shock complicating acute myocardial infarction.n/a(n/a).
[14] Wang W, Knovich MA, Coffman LG, Torti FM, Torti SV. Serum ferritin: past, present and future. Biochim Biophys Acta 2010;1800(8):760–9.
[15] Kell DB, Pretorius E. Serum ferritin is an important inflammatory disease marker, as it is mainly a leakage product from damaged cells. Metallomics 2014;6(4): 748–73.
[16] Paterek A, Oknińska M, Leszek P, Mackiewicz U, Jankowska EA, Ponikowski P, Mączewski M. Intravenous ferric carboxymaltose does not provide benefits in reperfused acute myocardial infarction in the rat with normal iron status. Biomed Pharmacother 2021;141:111893.
[17] Wohlfahrt P, Jenča D, Melenovský V, Šramko M, Kotrč M, Želízko M, Mrázková J, Adámková V, Pitha J, Kautzner J. Trajectories and determinants of left ventricular ejection fraction after the first myocardial infarction in the current era of primary coronary interventions. Front Cardiovasc Med 2022;9:1051995.
[18] Thygesen K., Alpert J.S., Jaffe A.S., Chaitman B.R., Bax J.J., Morrow D.A., White H. D. Fourth Universal Definition of Myocardial Infarction (2018). 2018;138(20): e618–51.
[19] Eagle KA, Lim MJ, Dabbous OH, Pieper KS, Goldberg RJ, Van de Werf F, Goodman SG, Granger CB, Steg PG, Gore JM, Budaj A, Avezum A, Flather MD, Fox KA. A validated prediction model for all forms of acute coronary syndrome: estimating the risk of 6-month postdischarge death in an international registry. JAMA 2004;291(22):2727–33.
[20] Byrne RA, Rossello X, Coughlan JJ, Barbato E, Berry C, Chieffo A, Claeys MJ, Dan GA, Dweck MR, Galbraith M, Gilard M, Hinterbuchner L, Jankowska EA, Jüni P, Kimura T, Kunadian V, Leosdottir M, Lorusso R, Pedretti RFE, Rigopoulos AG, Rubini Gimenez M, Thiele H, Vranckx P, Wassmann S, Wenger NK, Ibanez B, Group ESCSD. 2023 ESC Guidelines for the management of acute coronary syndromes: developed by the task force on the management of acute coronary syndromes of the European Society of Cardiology (ESC). Eur. Heart J. 2023:ehad191.
[21] Gürgöze MT, Kardys I, Akkerhuis KM, Oemrawsingh RM, Groot HE, van der Harst P, Umans VA, Kietselaer B, Ronner E, Lenderink T, Asselbergs FW, Manintveld OC, Boersma E. Relation of iron status to prognosis after acute coronary syndrome. Am J Cardiol 2022;168:22–30.
[22] Weidmann H, Bannasch JH, Waldeyer C, Shrivastava A, Appelbaum S, Ojeda-Echevarria FM, Schnabel R, Lackner KJ, Blankenberg S, Zeller T, Karakas M. Iron metabolism contributes to prognosis in coronary artery disease: prognostic value of the soluble transferrin receptor within the atherogene study. J Am Heart Assoc 2020;9(9):e015480.

[23] Griffiths JD, Campbell LJ, Woodruff IW, Cruickshank D, Matthews JP, Hunt D, Campbell DG, Cowling DC. Acute changes in iron metabolism following myocardial infarction. Am J Clin Pathol 1985;84(5):649–54.
[24] Barash I, Djaldetti M. Ferrokinetic studies in acute myocardial infarction. Am Heart J 1975;90(2):159–64.
[25] Inserte J, Barrabés José A, Aluja D, Otaegui I, Bañeras J, Castellote L, Sánchez A, Rodríguez-Palomares José F, Pineda V, Miró-Casas E, Milà L, Lidón RM, Sambola A, Valente F, Rafecas A, Ruiz-Meana M, Rodríguez-Sinovas A, Benito B, Buera I, Delgado-Tomás S, Beneítez D, Ferreira-González I. Implications of iron deficiency in STEMI patients and in a murine model of myocardial infarction. JACC 2021;6 (7):567–80.
[26] Gill D, FDG M, Walker AP, Srai SKS, Laffan MA, Minelli C. The effect of iron status on risk of coronary artery disease. Arterioscler Thromb Vasc Biol 2017;37(9): 1788–92.
[27] Frise MC, Holdsworth DA, Johnson AW, Chung YJ, Curtis MK, Cox PJ, Clarke K, Tyler DJ, Roberts DJ, Ratcliffe PJ, Dorrington KL, Robbins PA. Publisher Correction: abnormal whole-body energy metabolism in iron-deficient humans despite preserved skeletal muscle oxidative phosphorylation. Sci Rep 2022;12(1): 3685.
[28] Florian A, Ludwig A, Rösch S, Yildiz H, Klumpp S, Sechtem U, Yilmaz A. Positive effect of intravenous iron-oxide administration on left ventricular remodelling in patients with acute ST-elevation myocardial infarction - a cardiovascular magnetic resonance (CMR) study. Int J Cardiol 2014;173(2):184–9.
[29] Fanaroff AC, Roe MT, Clare RM, Lokhnygina Y, Navar AM, Giugliano RP, Wiviott SD, Tershakovec AM, Braunwald E, Blazing MA. Competing risks of cardiovascular versus noncardiovascular death during long-term follow-up after acute coronary syndromes. J Am Heart Assoc 2017;6(9).
[30] Zeller T, Waldeyer C, Ojeda F, Schnabel RB, Schäfer S, Altay A, Lackner KJ, Anker SD, Westermann D, Blankenberg S, Karakas M. Adverse outcome prediction of iron deficiency in patients with acute coronary syndrome. Biomolecules 2018;8 (3).
[31] Ganz T. Hepcidin: looking back at two decades of progress. Nature Cardiovasc Res 2022;1(3):191–3.
[32] Zeller T, Altay A, Waldeyer C, Appelbaum S, Ojeda F, Ruhe J, Schnabel RB, Lackner KJ, Blankenberg S, Karakas M. Prognostic value of iron-homeostasis regulating peptide hepcidin in coronary heart disease-evidence from the large atherogene study. Biomolecules 2018;8(3).

R. Miklik et al.

Optimizing Energy Delivery in Cardioversion: A Randomized PROTOCOLENERGYTrial of 2 Different Algorithms in Patients With Atrial Fibrillation

Canadian Journal of Cardiology
Impact Factor: 5,8

Canadian Journal of Cardiology 40 (2024) 2130–2141

Clinical Research

Optimizing Energy Delivery in Cardioversion: A Randomized PROTOCOLENERGYTrial of 2 Different Algorithms in Patients With Atrial Fibrillation

Miklik Roman, MD, PhD,[a,‡] Rucki Lucjan, MD,[a,‡] Jiravsky Otakar, MD,[a,b] Spacek Radim, MD,[a,c] Chovancik Jan, MD, PhD,[a] Neuwirth Radek, MD,[a,b] Hudec Miroslav, MD,[a,b] Sknouril Libor, MD, PhD,[a] Jiravska Godula Bogna, MD,[a,d] Hecko Jan, Ing, PhD,[a,e] and Fiala Martin, MD, PhD[b,f]

[a] *Department of Cardiology, Nemocnice Agel Trinec-Podlesi, Trinec, Czechia*

[b] *Faculty of Medicine, Masaryk University, Brno, Czechia*

[c] *Third Faculty of Medicine, Charles University, Praha, Czechia*

[d] *Faculty of Medicine, Palacky University, Olomouc, Czechia*

[e] *Department of Cybernetics and Biomedical Engineering, Ostrava, Czechia*

[f] *Centre of Cardiovascular Care, Neuron Medical, Brno, Czechia*

See editorial by Dorian, et al., pages 2142-2144 of this issue.

Optimizing Energy Delivery in Cardioversion: A Randomised PROTOCOLENERGY Trial of Two Different Algorithms in Patients with Atrial Fibrillation

In AF cardioversion, both energy protocols (150J, 360J, 360J vs 3x360J) showed similar high cumulative efficacy.
An initial 150J shock proved beneficial in patients with BMI ≤ 29-34 kg/m² and women due to fewer skin complications.

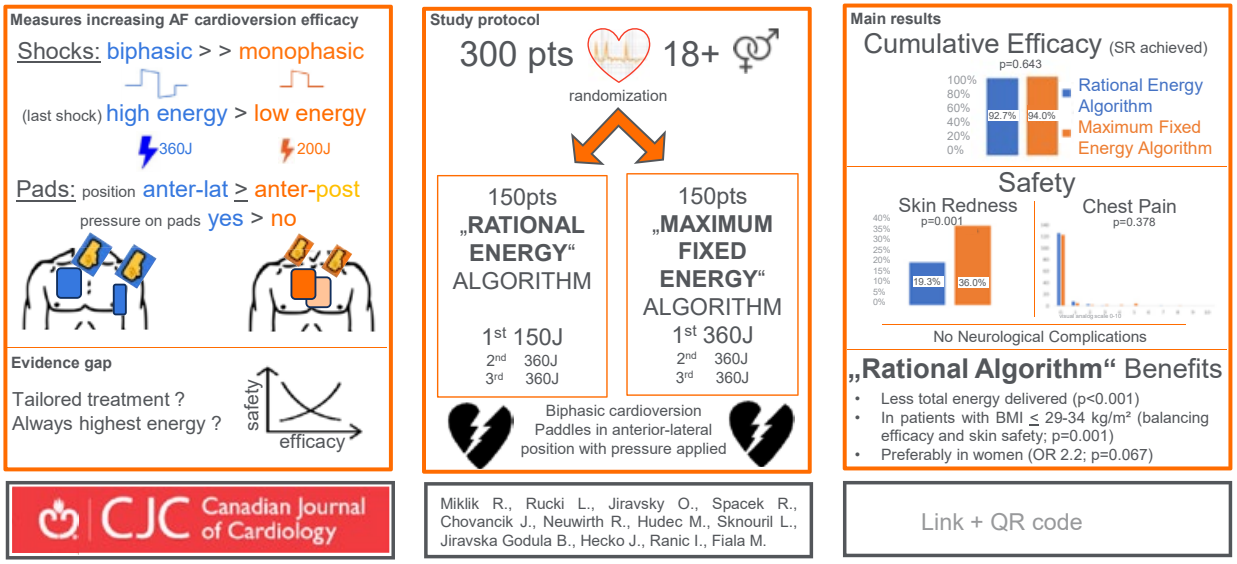

CJC Canadian Journal of Cardiology

Miklik R., Rucki L., Jiravsky O., Spacek R., Chovancik J., Neuwirth R., Hudec M., Sknouril L., Jiravska Godula B., Hecko J., Ranic I., Fiala M.

Link + QR code

https://doi.org/10.1016/j.cjca.2024.06.003

ABSTRACT

Background: The optimal energy protocol for direct current cardioversion of atrial fibrillation remains uncertain. The Rational vs Maximum Fixed Energy (PROTOCOLENERGY) randomized trial compared a stepwise escalating energy algorithm (RaA, 150 J, 360 J, and 360 J) with a maximum fixed energy algorithm (MfA, 3 x 360 J).

Methods: In a 1:1 randomized trial, 300 patients with atrial fibrillation received biphasic discharges via hand-held paddles in the anterolateral position. Primary endpoints were sinus rhythm at 1 minute and neurologic complications at 2 hours; secondary endpoints included sinus rhythm at 2 hours, skin changes and chest discomfort at 24 hours.

Results: Sinus rhythm at 1 minute was achieved in 92.7% of RaA and 94.0% of MfA patients ($P = 0.643$) and maintained at 2 hours in 91.3% of both groups. There were no neurologic complications. The protocols differed significantly after the first shock (72.7% in RaA vs 83.3% in MfA; $P = 0.026$) but equalized after subsequent maximum energy shocks. Fewer RaA patients experienced skin redness compared with MfA patients (19.3% vs 36.0%, $P = 0.001$), which was attributed to the lower initial 150-J shock and total energy delivered ($r = 0.243$, $P < 0.0001$). Chest discomfort at 24 hours was not different between groups ($P = 0.378$). In multivariate analysis, lower body mass index ($P < 0.001$, cutoff 29 to 34 kg/m^2) was associated with cardioversion success after the initial 150-J shock.

Conclusions: Both protocols showed similar high cumulative efficacy, but RaA with the initial 150-J shock proved to be beneficial in patients with body mass index less than 29 to 34 kg/m^2 because of fewer skin complications.

Clinical Trial Registration No: NCT05148923

RÉSUMÉ

Contexte : Le protocole énergétique optimal pour la cardioversion électrique de la fibrillation auriculaire reste incertain. L'essai randomisé «Rational vs Maximum Fixed Energy» (PROTOCOLENERGY) a comparé un algorithme d'énergie progressif par étape (APE, 150 J, 360 J et 360 J) à un algorithme d'énergie maximale fixe (AEMf, 3 x 360 J).

Méthodes : Dans un essai randomisé 1:1, 300 patients atteints de fibrillation auriculaire ont reçu des décharges biphasiques à l'aide de palettes tenues à la main en position antérolatérale. Les principaux critères d'évaluation étaient le rythme sinusal à 1 minute et les complications neurologiques à 2 heures; les critères d'évaluation secondaires étaient le rythme sinusal à 2 heures, les changements cutanés et l'inconfort thoracique à 24 heures.

Résultats : Le rythme sinusal à 1 minute a été atteint pour 92,7 % des patients avec APE et 94,0 % des patients avec AEMf ($p = 0,643$) et maintenu à 2 heures chez 91,3 % pour les deux groupes. Il n'y a pas eu de complications neurologiques. Les protocoles différaient de manière significative après le premier choc (72,7 % dans le groupe avec APE contre 83,3 % dans le groupe avec AEMf; $p = 0,026$) mais s'égalisaient après les chocs ultérieurs avec énergie maximale. Les patients APE ont été moins nombreux à présenter des rougeurs cutanées que les patients AEMf (19,3 % contre 36,0 %, $p = 0,001$), ce qui a été attribué au choc initial plus faible de 150-J et à l'énergie totale délivrée ($r = 0,243$, $p < 0,0001$). La gêne thoracique à 24 heures n'était pas différente entre les groupes ($p = 0,378$). Dans l'analyse multivariée, un indice de masse corporelle plus faible ($p < 0,001$, seuil de 29 à 34 kg/m^2) a été associé au succès de la cardioversion après le choc initial de 150-J.

Conclusions : Les deux protocoles ont montré une efficacité cumulative élevée similaire, mais le protocole APE avec un choc initial de 150-J s'est avéré bénéfique chez les patients dont l'indice de masse corporelle est inférieur à l'intervalle 29 à 34 kg/m^2 en raison d'un nombre moins important de complications cutanées.

Enregistrement de l'essai clinique : NCT05148923

Direct current cardioversion (DCCV) is an established procedure that is commonly used in the acute and elective management of patients with atrial fibrillation (AF). For years, many investigators have searched for the optimal strategy/protocol in studies using predominantly monophasic discharges, in terms of which type of waveform to use,[1,2] how and under what pressure to place the pads/handheld paddles,[3,4] which energy to choose for the first and subsequent discharges,[5-7] or whether to use periprocedural antiarrhythmic drug support.[8] In addition, many positive and negative clinical (eg, body mass index [BMI], age, sex, comorbidities) or structural (echocardiographic parameters) predictors of the short-term success of DCCV have been identified.[9-15] This suggests that the correct indication for DCCV and its optimal performance are essential for the restoration of sinus rhythm (SR).

The current standard for DCCV is the use of biphasic shock waves, which have been shown to be more effective and safer than monophasic shock waves.[2] A recent study by Schmidt et al.[16] showed—in a randomized fashion—that anterior-lateral electrode positioning was more effective than anterior-posterior electrode positioning for biphasic cardioversion. The study was published in 2021 and therefore could not have been included in the 2020 European Society of Cardiology guidelines, which still recommend anterior-posterior electrode positioning.[17]

With regard to the choice of self-adhesive electrodes vs hand-held electrodes with manual pressure and energy of the first and subsequent discharges, neither the aforementioned guidelines nor other international guidelines provide clear recommendations.[18-20] A study by Ramirez et al. demonstrated higher discharge efficiency using hand paddles with an applied external force of 80N. This approach was able to reduce the transthoracic impedance significantly compared with discharges performed with adhesive electrodes without pressure.[21] This conclusion suggests that the use of hand

Received for publication February 16, 2024. Accepted June 4, 2024.

‡These authors contributed equally to this work.
Corresponding author: Dr Otakar Jiravsky, Agel Trinec-Podlesi Hospital, Konska 453, 739 61, Trinec, Czechia. Tel.: +420602579193.
E-mail: otakar.jiravsky@npo.agel.cz
See page 2140 for disclosure information.

paddles with manual pressure may be more advantageous than the use of adhesive electrodes.

It has been repeatedly confirmed that even high-energy discharges above 200 to 300 J do not lead to an increase in cardiac troponins as a marker of myocardial damage.[22,23] This may indicate the routine use of high-energy discharges from the first discharge. On the other hand, elective cardioversions are—in most cases—outpatient procedures, and it is certainly desirable that the procedure is performed without complications: that is, without skin redness or burns after the discharges, without residual pain on the sternum, and especially without the need for hospitalization because of postdischarge arrhythmias. Previous experience at our cardiac centre suggests that physicians performing cardioversion often unnecessarily choose high-energy discharges, especially in patients with obesity and those on long-term amiodarone. The rationality of this approach was not confirmed in a multivariate analysis.[24]

Based on these facts and our experience, we designed and conducted a study to compare the efficacy and safety of 2 different cardioversion protocols using biphasic discharges delivered by manually controlled paddles in the anterior-lateral position. The aim of the study was to determine whether the use of a lower initial discharge energy is clinically justified in terms of patient safety and comfort, without compromising the overall clinical efficacy of subsequent energy escalation, compared with a protocol with a fixed maximum discharge energy.

Material and Methods

Study design

The Rational vs Maximum Fixed Energy (PROTOCOLENERGY) trial was an interventional, randomized, investigator-initiated, monocentric, parallel-assignment study conducted at the Agel Trinec-Podlesi Cardiocentre, Czech Republic. The study was registered on ClinicalTrials.gov (NCT05148923) and started on January 1, 2022, with the last patient randomized on December 22, 2022. Inclusion criteria were as follows: subjects older than 18 years with a diagnosis of AF, clinically indicated for elective outpatient DCCV; established therapeutic anticoagulation for at least 3 weeks before DCCV or performed esophageal echocardiography excluding the presence of intracardiac thrombus; and provided verbal and written informed consent to participate in the study. Exclusion criteria were identical to the known contraindications to elective cardioversion. Patients with implanted pacemakers or defibrillators were not excluded. When designing the study, we followed the Consolidated Standards of Reporting Trials (CONSORT) guidelines[25] (the CONSORT checklist is available in Supplemental Table S1).The study was conducted in accordance with the Declaration of Helsinki and approved by the local ethics committee.

Defibrillation waveform characteristics

In the PROTOCOLENERGY trial, we used biphasic truncated exponential shocks with impedance compensation delivered with the Mindray BeneHeart D3 defibrillator (Shenzhen Mindray Bio-Medical Electronics Co, Ltd, Shenzhen, China). This technology adjusts the peak current in response to the patient's chest impedance, thus customizing the shock to achieve an optimal current distribution across the myocardium without the need for manual adjustment by the operator. In short, the defibrillator charges to a high voltage level, which is then truncated at a predetermined time. The leading-edge voltage varies depending on the impedance of the chest cavity it encounters. For example, for a 360 J shock, the leading-edge voltage ranges from approximately 1500 V to 2000 V across the different impedances from 25 Ω to 175 Ω. The duration of each phase of the biphasic waveform is impedance dependent, with the first phase being longer than the second (5.1-12.5 ms and 3.2-8.6 ms, respectively, Supplemental Fig. S1). Finally, the defibrillator automatically adjusts the energy delivered based on real-time impedance measurements to maximize defibrillation success while minimizing potential tissue damage. As the transthoracic impedance increases, the actual energy delivered decreases slightly (ie, for a 360-J shock: 50 Ω-360 J, 75 Ω-349 J, 100 Ω-332 J).[26]

Randomization and treatment

Patients were admitted to a 1-day cardiology outpatient clinic. Study criteria were reviewed, and informed consent was obtained. Relevant demographic and clinical data were collected from patients and available medical records. Because of the large variability in echo data available at the time of cardioversion from referring physicians, only left atrial diameter and left ventricular ejection fraction (LVEF) were recorded. Randomization was performed in blocks of 20 using computer-generated sequences. Allocation concealment was ensured using sequentially numbered opaque sealed envelopes. Participants were assigned to 1 of 2 study protocols: rational energy algorithm (RaA), 150-J initial shock followed by maximum 360 J and 360 J or maximum fixed energy algorithm (MfA): maximum 360-J initial shock followed by 360 J and 360 J.

We used hand-held paddles with manual pressure placed in the anterior-lateral configuration. The setting was as follows: With the patient in the supine position on the bed, the attending physician leaned over the patient's chest and placed the lefthand paddle in the right inferoclavicular region and the righthand paddle in the left axial line near the suggested cardiac apex, avoiding the left breast nipple. When the device was charged, the physician applied a force equivalent to a "push-up" to the paddles[27] covered with echocardiographic gel, waited for maximum expiration, and fired the shock.

Subsequent second and possibly third shocks were applied in a smooth sequence after the previous one if AF was still present on the monitor, or AF recurred within 1 minute after the first or second shock if SR had been temporarily restored. The physician administering the shocks was not blinded to the allocated study arm, but the patients and a physician assessing skin changes were blinded. All subjects were sedated with 1 mg midazolam (2 mg for patients weighing more than 90 kg) and 0.15 mg/kg etomidate. After the procedure, patients were monitored for 2 hours and then discharged home if no complications occurred. All patients were contacted by telephone the following day for safety reasons and to collect secondary endpoints.

Endpoints and analyses

The primary efficacy endpoint was the presence of SR 1 minute after DCCV, and the primary safety endpoint was the incidence of neurologic adverse events 2 hours after DCCV.

The secondary efficacy endpoint was the presence of SR 2 hours after DCCV, and the secondary safety endpoints were the incidence of skin changes (no change, redness, burn) 2 hours after DCCV and the severity of skin discomfort or chest pain assessed using a visual analogue scale (VAS) 1 day after DCCV. The incidence of clinically relevant tachy/brady-arrhythmias was also assessed, as was the patient's self-reported rhythm status 1 day after DCCV.

With regard to the primary objective of the study, we performed a series of analyses to compare the efficacy and safety of the initial shocks of the 2 protocols: that is, 150 J vs 360 J, and to explore possible variables that, if present, would favour the use of one protocol over the other.

Statistical analysis

As we intended to compare 2 DCCV protocols that differed only in the energy of the initial shock, and then used maximum discharge energies in both protocols, we did not expect a significant difference in overall efficacy. To demonstrate a 3% significant difference in efficacy between the 2 protocols, approximately 3000 patients would need to be randomized. Therefore, we decided to perform an exploratory analysis with fewer patients, based on the expected differences in efficacy and safety of the first discharge: that is, 150 J vs 360 J. As a rationale for the sample calculation, we used the results of our recently published DCCV registry.[24] The success rate of the first low-energy shock to restore SR was 77.1%, and the cumulative success rate after the last high-energy shock was 89.6%. Therefore, we assumed a 12% difference in the success rate in favour of MfA (78% vs 90%). Based on 80% power and a significance level of 0.05, we estimated that approximately 145 patients would be needed in each arm. All randomized patients were included in the intention-to-treat (ITT) analysis.

Data were analyzed using IBM SPSS Statistics for Windows, version 29 (IBM Corp, Armonk, New York, USA). Nonparametric tests were used because of the non-normal distribution of the data, as confirmed by the Shapiro-Wilk test. Continuous variables are presented as median (interquartile range [IQR]) and categorical variables as number (percentage). Comparisons were made using the Mann-Whitney U test for continuous variables, the Pearson χ^2 test for categorical variables, and the Jonckheere-Terpstra test for ordinal variables.

Univariate analysis was performed to identify parameters associated with the effectiveness of the initial 150-J shock in achieving SR. Multivariate logistic regression was then performed, including parameters with a significance level of $P < 0.1$ in the univariate analysis, to further elucidate the independent predictors of 150 J DCCV efficacy. When appropriate, Spearman's correlation coefficient (r, 95% confidence interval [CI]) was determined to express the degree of association among parameters, receiver operating characteristic (ROC) curve analysis, and area under the curve (AUC) calculations were used to establish cutoff values and provide an overall measure of the discriminatory power of significant variables. In addition, Youden's J statistic was used to identify optimal cutoffs by maximizing the sum of sensitivity and specificity, providing a comprehensive visualization of ROC curve performance.

Results

Patients

During the study recruitment period, 579 patients were considered for DCCV procedures. Of these, 300 patients met the study criteria and were randomized 1:1, resulting in 150 subjects in the RaA and MfA protocols. Patients in both arms were well balanced (Table 1). During cardioversion, a total of 3 patients in the RaA arm and 4 patients in the MfA arm did not undergo a third discharge after 2 previous unsuccessful discharges. The reasons were problems with analgosedation in 5 patients, intermittent SR and AF in 1 patient (physician decided to discontinue DCCV), and junctional bradycardia in 1 patient. All these patients were considered DCCV failures and were included in the ITT analysis (Fig. 1).

Efficacy

The primary endpoint—that is, SR 1 minute after DCCV—was achieved in 139 (92.7%) patients in the RaA group and in 141 (94.0%) patients in the MfA group, $P = 0.643$. Similarly, no difference was found between the measured SR rates at 2 hours post-DCCV (both groups equal 137 [91.3%] patients, $P = 1.0$). In addition, the patient self-reported rhythm status on the following day did not differ between the groups (palpated or a device-detected regular rhythm considered as SR in 125 [90.6%] vs 127 [91.4%] cases, respectively, $P = 0.819$).

Safety

No cardioversion-related neurologic abnormalities or complications were observed. There were significant differences between the study arms in terms of skin changes 2 hours after DCCV ($P = 0.001$, Table 2), with the RaA group having fewer patients with skin redness. This difference was mainly because of the low vs high energy of the initial shock (Fig. 2). There were no cases of skin burns in either group.

The mean cumulative energy delivered per subject was 361.6 ± 232.2 J. There was a significant difference between the groups (RaA median 150 J, range 150 J to 870 J; MfA median 360 J, range 360 J to 1080 J; $P < 0.001$). A positive correlation was found between the total energy dose and the incidence of skin redness ($r = 0.243$, 95% CI, 0.130-0.350; $P < 0.0001$).

There were no significant differences in the severity of chest pain 1 day after DCCV between the 2 study arms ($P = 0.378$, Table 2). With regard to other safety measures, as mentioned earlier, 5 subjects experienced problems with analgesia leading to protocol deviations, but these did not have clinically relevant consequences. Three subjects in the RaA group experienced clinically relevant junctional bradycardia, 2 of whom required overnight monitoring without the need for pacemaker implantation.

Table 1. Baseline characteristics of the study participants

	Total	Study arm		*P*-value
		Rational energy algorithm (150, 360, 360 J)	Maximum fixed energy algorithm (360, 360, 360 J)	
Total	300	150	150	
Sex				
Male	199 (66%)	97 (65%)	102 (68%)	0.541
Female	101 (34%)	53 (35%)	48 (32%)	
Age (years)	68 [13]	68 [13]	69 [12]	0.425
BMI (kg/m^2)	31.8 [8.0]	31.8 [8.5]	31.9 [7.7]	0.986
CHA_2DS_2-VASC				
0	10 (3.3%)	5 (3.3%)	5 (3.3%)	0.429
1	39 (13.0%)	21 (14.0%)	18 (12.0%)	
2	85 (28.3%)	44 (29.3%)	41 (27.3%)	
3	90 (30.0%)	45 (30.0%)	45 (30.0%)	
4	38 (12.7%)	17 (11.3%)	21 (14.0%)	
5	24 (8.0%)	10 (6.7%)	14 (9.3%)	
6	7 (2.3%)	7 (4.7%)	0	
7	6 (2.0%)	0	6 (4.0%)	
8	1 (0.3%)	1 (0.7%)	0	
Anticoagulation type				
Warfarin	13 (4.3%)	7 (4.7 %)	6 (4.0%)	0.961
NOAC	285 (95.0%)	142 (94.7%)	143 (95.3%)	
LMVH	2 (0.7%)	1 (0.7%)	1 (0.7%)	
Antiarhythmic drugs				
No antiarrhythmics	83 (27.7%)	39 (26.0%)	44 (29.3%)	0.69
Propafenone	67 (22.3%)	36 (24.0%)	31 (20.7%)	
Sotalol	32 (10.7%)	18 (12.0%)	14 (9.3%)	
Amiodarone	117 (39.0%)	57 (38.0%)	60 (40.0%)	
Dronedarone	1 (0.3%)	0	1 (0.7%)	
Beta blockers				
On beta blockers	222 (74.0%)	114 (76.0%)	108 (72.0%)	0.43
RAAS				
No RAAS	88 (29.3%)	47 (31.3%)	41 (27.3%)	0.484
ACEI	139 (46.3%)	72 (48.0%)	67 (44.7%)	
Sacubitril/valsartan	8 (2.7%)	4 (2.7%)	4 (2.7%)	
Sartan	65 (21.7%)	27 (18.0%)	38 (25.3%)	
BP systole (mm Hg)	143 [28]	142 [27]	144 [28]	0.617
BP diastole (mm Hg)	83 [15]	83 [15]	83 [15]	0.847
Heart rate (per minute)	88 [25]	89 [26]	88 [23]	0.88
Left atrial diameter (mm)	47 [7]	47 [7]	48 [7]	0.701
LVEF (%)	54 [8]	54 [8]	55[8]	0.9

ACEI, angiotensin-converting enzyme inhibitor; BMI, body mass index; BP, blood pressure; LMWH, low molecular weight heparin; LVEF, left ventricular ejection fraction; NOAC, non-vitamin K antagonist oral anticoagulants; RAAS, renin-angiotensin-aldosterone system.

CHA_2DS_2-VASc: Congestive heart failure (1 point); Hypertension (1 point); Age ≥75 years (2 points); Diabetes mellitus (1 point); previous Stroke or transient ischemic attack (TIA) or thromboembolism (2 points); Vascular disease (1 point); Age 65 to 74 years (1 point); Sex category (female) (1 point).

Initial 150-J shock analysis

Regarding the initial success rates of the RaA and MfA protocols to restore SR, we found that the protocols differed significantly: that is, after 150 J vs 360 J (109 [72.7%] vs 125 [83.3%] patients, $P = 0.026$). After subsequent maximum energy shocks in both protocols, the success rates were similar (Fig. 3). In univariate analysis, we assessed differences in all recorded parameters between patients who achieved SR after the initial 150-J discharge and those who did not. Both weight (mean 104 [IQR: 20] kg in AF vs 91 [IQR: 29] kg in SR, $P < 0.001$) and BMI (mean 34.1 [IQR: 7.4] kg/m^2 in AF vs 30.5 [7.8] kg/m^2 in SR, $P < 0.001$) were statistically significant. In addition, female sex showed a notable trend toward restoration of SR ($P = 0.086$, Supplemental Table S2). Given the collinearity between weight and BMI, and the widespread use of BMI in clinical practice, we chose to include only BMI in the multivariate regression analysis. The results were consistent with the univariate analysis. In particular, for each unit increase in BMI, the odds of achieving SR decreased by 10.8% (odds ratio (OR), 0.892; 95% CI, 0.832-0.956; $P < 0.001$). In addition, being female was associated with 2.2-fold increased odds of achieving SR, although this was borderline significant ($P = 0.067$, Supplemental Table S3).

Association of BMI and initial 150-J shock success

While the cumulative DCCV success rate including all 300 patients did not show a pronounced variance based on low or high BMI ($P = 0.984$, Supplemental Fig. S2), in the RaA group BMI values seemed to play an important role ($P = 0.076$, Fig. 4A). To find an optimal cutoff value for BMI to justify the use of 150 J as the initial DCCV shock to reduce the risk of skin redness while maintaining a high rate of SR recovery, we performed an ROC analysis with BMI as the pivotal variable. This revealed an AUC of 0.675 (95% CI, 0.582-0.769) with a standard error of 0.048 ($P = 0.001$, Fig. 4B). Subsequent Youden's J statistics identified 2 zeniths, with the BMI range of 29 to 34 kg/m^2 as the most appropriate cutoff that harmonized both sensitivity and specificity (Fig. 4C).

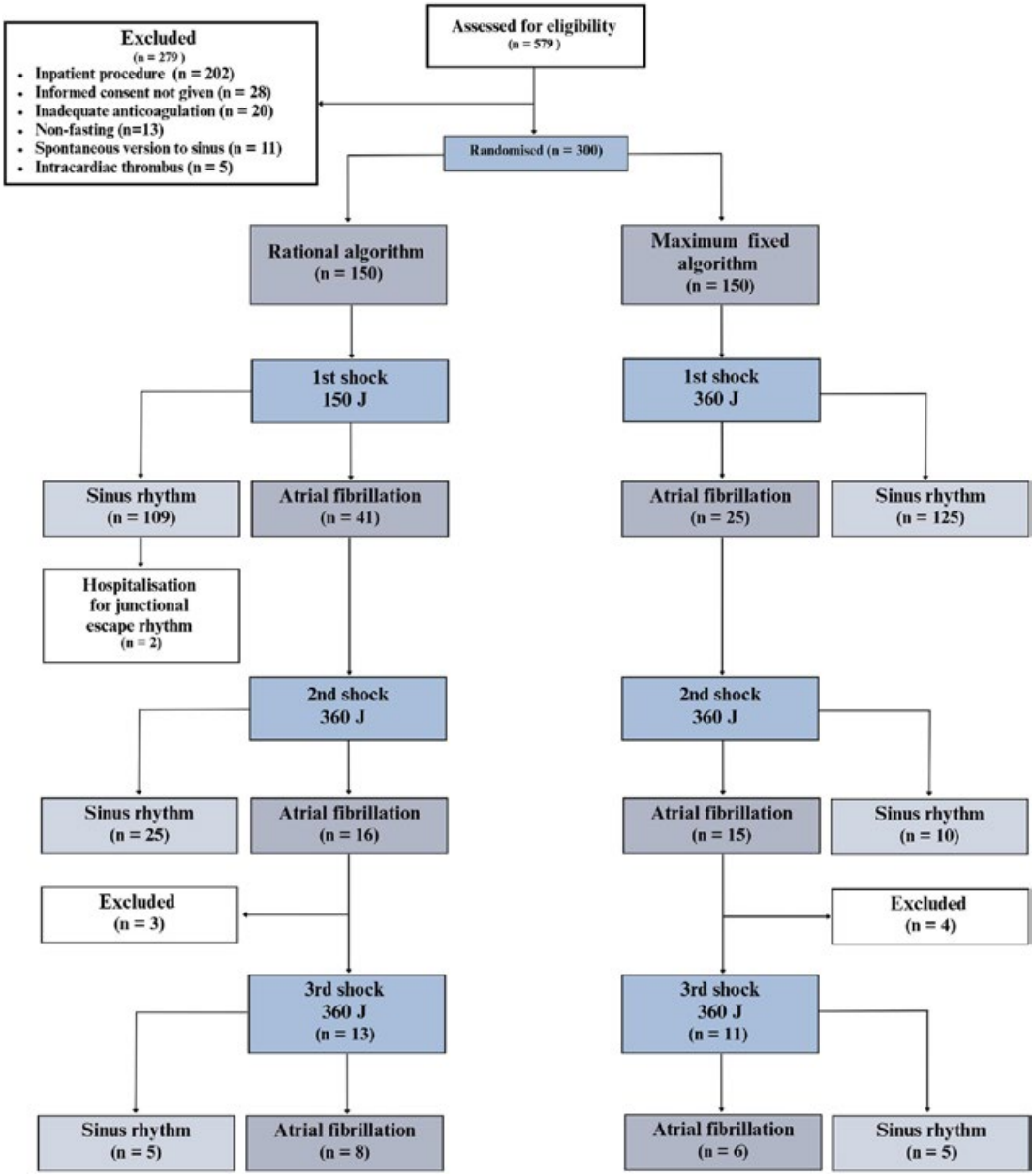

Figure 1. CONSORT flow diagram of the PROTOCOLENERGY study.

Discussion

Efficacy

This study compared 2 protocols for cardioverting AF, both using the maximum available 360-J energy shocks but differing in the energy of the initial shock. The main finding was that the cumulative success rates were similar, but patients who received the lower 150-J initial shock had less frequent skin irritation related to the cumulative energy dose delivered. The low escalating (rational) energy protocol was shown to be feasible for patients with lower BMI and for women in whom the initial 150-J shock was sufficient to restore SR.

The optimal DCCV algorithm is a daily dilemma in clinical practice. Despite a large number of previously published observational studies and reports,[28] there is a paucity of randomized data addressing the issue of energy selection or escalation. The first randomized trial using impedance-compensated biphasic shocks with pads in anterior-lateral position (self-adhesive, no manual pressure applied), the **B**iphasic **E**nergy **S**election for **T**ransthoracic Cardioversion of **A**trial **F**ibrillation (BEST-AF) trial,[29] compared a low escalation protocol (100-150-200-200 J) with a fixed energy protocol (200-200-200 J). The authors found no difference in the overall success rate, defined as the restoration of SR for at least 30 seconds (90% vs 88%, $P = 0.56$) and also demonstrated that a higher initial shock energy resulted in a higher initial success rate (48% vs 71%, $P < 0.01$), particularly in patients with obesity and BMI > 25 kg/m^2 (44% vs 75%, $P = 0.001$). The second study, the **C**omparison of **H**igh vs **E**scalating **S**hock**s** (CHESS) trial,[23] used biphasic shocks with self-adhesive pads (no manual pressure, no impedance compensation) in the anterior-posterior position, and compared an

Table 2. Secondary safety endpoints

	Total	Study arm		*P* value
		Rational energy algorithm (150, 360, 360 J)	Maximum fixed energy algorithm (360, 360, 360 J)	
Skin changes 2 hours post- DCCV				
No skin changes	217 (72.3%)	121 (80.7%)	96 (64.0%)	**0.001**
Skin redness	83 (27.7%)	29 (19.3%)	54 (36.0%)	
Skin burns	0	0	0	
Chest pain (VAS 1-10) 24 hours post DCCV				
0	249 (89.9%)	126 (91.3%)	123 (88.5%)	0.378
1	12 (4.3%)	7 (5.1%)	5 (3.6%)	
2	5 (1.8%)	3 (2.2%)	2 (1.4%)	
3	3 (1.1%)	1 (0.7%)	2 (1.4%)	
4	2 (0.7%)	0	2 (1.4%)	
5	4 (1.4%)	0	4 (2.9%)	
7	1 (0.4%)	1 (0.7%)	0	
8	1 (0.4%)	0	1 (0.7%)	

Bold values indicate statistical significance ($P < 0.05$).
DCCV, direct current cardioversion; VAS, visual analogue scale.

energy-escalating protocol with a maximum energy of 200 J of the last shock with a fixed-energy protocol using novel maximum energy shocks of 3 x 360 J. The authors found a profound difference between the protocols in terms of initial and cumulative efficacy in favour of the fixed maximum-energy protocol.

Compared with our study, subjects in both protocol groups of the PROTOCOLENERGY study had higher rates of successful cardioversion after both the first and last protocol-guided shock (comparison of studies in Table 3). In addition, high rates (> 90%) of restoration of SR at 2 hours were observed. This may be because the PROTOCOLENERGY trial incorporated the best of previous studies: in particular, the use of maximum high energy in cardioversion protocols, the use of impedance-compensated waveforms that automatically adjust the peak current to match patients with different chest impedances, and the use of manual pressure to increase shock effectiveness. Under these conditions, the cumulative efficacy of DCCV can be as high as 94%, regardless of the initial shock energy.

It is important to note that there are different definitions of DCCV success. In the aforementioned studies, 30 seconds to

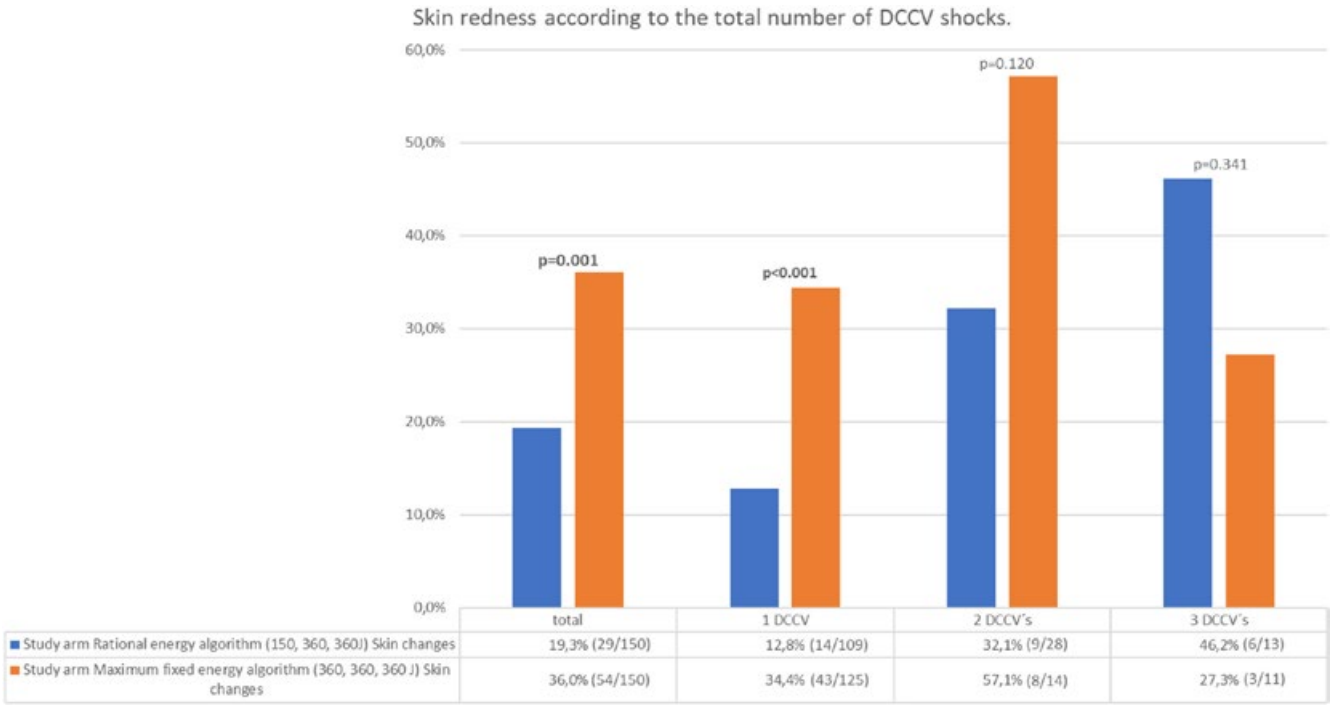

Figure 2. Incidence of skin redness postcardioversion by DCCV shock number and algorithm. Significant differences in the incidence of skin erythema were observed between the 2 algorithms overall (**left, total bars**) and between patients receiving only 1 (initial) DCCV shock, favouring RaA with 150-J shock. The differences in skin redness were not statistically significant in patients receiving 2 or 3 DCCV shocks, likely because of the uniform energy level (360 J) used in subsequent shocks in both protocols, underscoring the skin-protective effect of the low energy of the initial shock. DCCV, direct current cardioversion; RaA, rational energy algorithm.

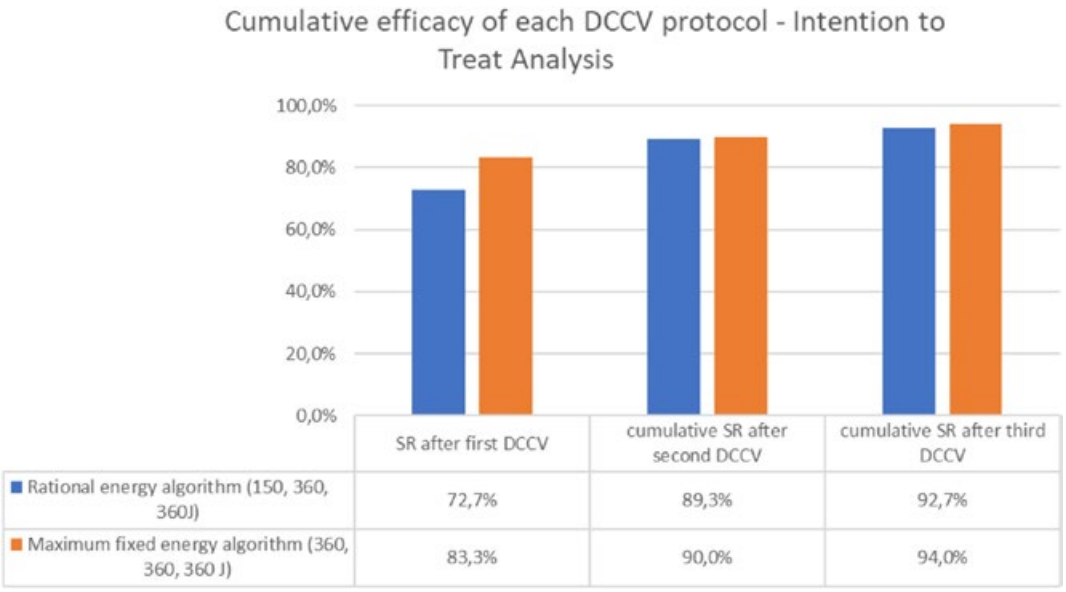

Figure 3. Efficacy of each DCCV protocol after first, second and third shock. The DCCV success rate after the first shock was significantly higher in the MfA protocol group using a maximum energy of 360 J. The cumulative success rates after subsequent shocks, delivered uniformly at 360 J for both algorithms, were not significantly different, highlighting similar efficacy in SR restoration beyond the first shock. DCCV, direct current cardioversion; MfA, maximum fixed-energy algorithm; SR, sinus rhythm.

1 minute of postshock SR preservation was considered successful DCCV. In the Ottawa AF Cardioversion Protocol published by Ramirez et al.,[27] implementing similar measures as in our study, the DCCV success reached 99.2%, but was defined as $\geq$ 2 consecutive sinus beats or atrial-paced beats in patients with implantable devices. As the CHESS trial used 3 x 360 J energy in the fixed-energy group but differed in the energy-escalating group, we chose to use the same endpoint definition as the CHESS trial to allow for better comparison among trials and protocols.

Safety

There was no evidence of an increased risk of clinically relevant arrhythmias or neurologic complications with either protocol or when comparing the incidence of adverse events

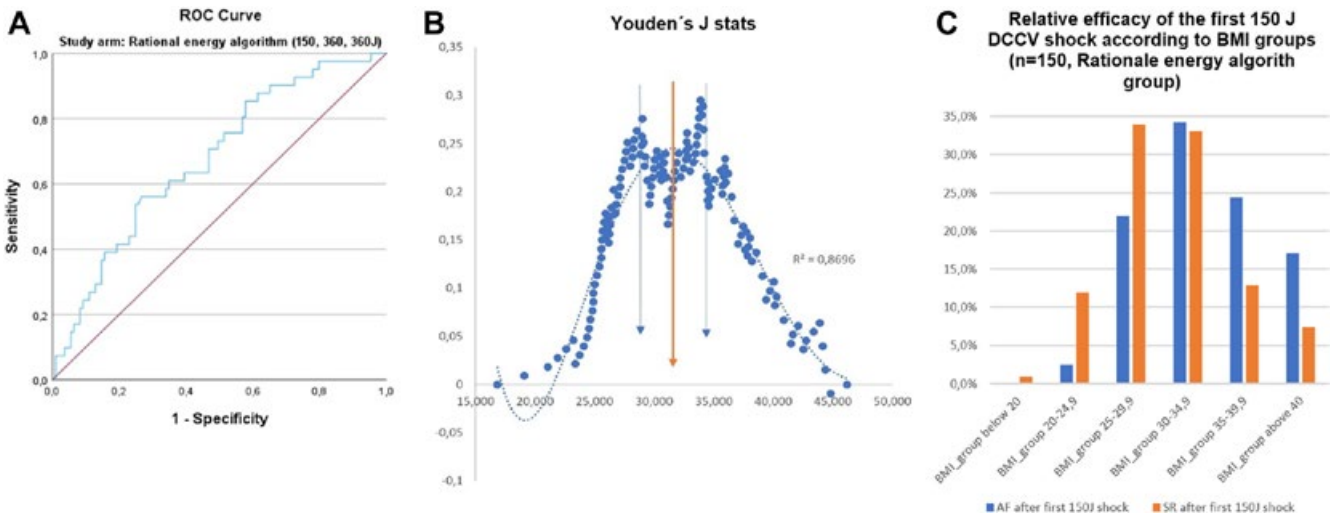

Figure 4. Analysis of association of BMI with success of initial 150J shock. (**A**) Relative efficacy of the initial 150-J DCCV shock across different BMI categories. The graph clearly shows that—despite the statistical insignificance—the percentage of successful cardioversions was much higher in the lower BMIs than in the higher BMIs. (**B**) The ROC curve analysis for BMI and DCCV success after the initial 150-J shock. The AUC value of 0.675 indicates a moderate predictive value of BMI for cardioversion success in patients with AF. (**C**)Visualization of 2 BMI peaks using Youden's J statistic. The peaks identify a BMI of 29 to 34 kg/m^2 as the most appropriate cutoff for predicting 150J shock success, combining both sensitivity and specificity. AF, atrial fibrillation; AUC, area under the curve; BMI, body mass index; DCCV, direct current cardioversion; ROC, receiver operating characteristic.

Table 3. Comparison of BEST-AF, CHESS and PROTOCOLENERGY randomized trials in patients undergoing biphasic elective cardioversion

	BEST-AF[29]		CHESS[23]		PROTOCOLENERGY	
Pads position	Anterior-lateral		Anterior-posterior		Anterior-lateral	
Manual pressure applied	No		No		Yes	
Waveform type	Truncated exponential, impedance compensated		Truncated exponential		Truncated exponential, impedance compensated	
Cardioversion success definition	Sinus rhythm 30 seconds after cardioversion		Sinus rhythm 1 minute after cardioversion		Sinus rhythm 1 minute after cardioversion	
Patients total	380		276		300	
	Energy escalating: 100,150,200,200 J	Fixed energy: 200,200,200 J	Energy escalating: 125,150,200 J	Fixed energy: 360,360,360 J	Energy escalating: 150,360,360 J	Fixed energy: 360,360,360J
Success rate: (1) Initial shock	48%	71%†	34%	75%‡	73%	83%*
(2) Cumulative	90%	88%	66%	88%‡	93%	94%*
Number of shocks (Average [± SD], median [IQR])	1.88 (± 1.04)	1.46 (± 0.76)†	2 [1-3]	1 [1-1]§	1.36 (± 0.64)	1.24 (± 0.58)*
Energy applied (Average [± SD], median [IQR])	202 J (± 135)	251 J (± 110)†	275 J (125-475)	360 J (360-360)§	150 J (150-870)	360J (360-1080) ***
Initial shock success predictors	BMI < 25 kg/m^2		N/A		BMI < 29-34 kg/m^2, female	
Cumulative success predictors	Short duration of AF		N/A		N/A	
Safety: (1) Arrhythmias	No difference		Low rates, no difference		Low rates, no difference	
(2) Skin changes	N/A		Redness/burns no difference		No burns, more redness in Fixed	

AF, atrial fibrillation; BMI, body mass index; IQR, interquartile range; SD, standard deviation.

* $P < 0.05$ between the protocols within the study.

† $P < 0.01$ between the protocols within the study.

‡ $P < 0.001$ between the protocols within the study.

§ P value unknown between the protocols within the study.

with previous studies. Although there was no difference in skin redness between the low-escalation (up to 200 J) and maximum-fixed (360 J) protocol groups in the CHESS trial using self-adhesive anterior-posterior pads, in our study using hand-held paddles in the anterior-lateral position and manual pressure, the incidence of skin redness was significantly higher in the maximum-fixed energy group, especially after the first shock. This may be because of the use of impedance-compensated shocks with different peak currents, independent of the total energy delivered, depending on chest impedance, which is generally higher in patients with obesity and women and lower in patients with heart failure and those with reduced hemoglobin levels.[30] Chest impedance is significantly influenced by pad size, pad position, and skin-to-pad contact and generally decreases with the number of shocks delivered. However, increased impedance has not been associated with cardioversion success.[12]

Relationship among BMI, sex, and initial 150-J shock success rate

In the post-hoc analysis, a BMI of 29-34 kg/m^2 was identified as a potential cutoff for initiating DCCV with a 150-J shock. In the BEST-AF trial, overweight patients (BMI $>$ 25 kg/m^2) were also significantly less likely to regain SR with the initial 150-J vs 200-J shock (44% vs 75%, $P <$ 0.001).[29] This may be explained by higher defibrillation thresholds in patients with obesity.[31] The current study confirms previous findings and recommends a BMI cutoff to be considered when choosing between low or high energy of the initial shock.

Although not statistically significant, women were more likely than men to restore SR after the initial 150 J. Our daily practice supports the clinical relevance of such an observation and is consistent with the results of previous studies.[32] With a concept of less skin irritation and maintained efficacy, initiating cardioversion with lower energy—especially in women rather than in men—seems to be a feasible approach.

Future directions

Recently, a meta-analysis comparing different approaches to DCCV was published after the trial was completed.[28] The results of this analysis demonstrated the superiority of biphasic waveforms, high energy shocks, and manual pressure. The PROTOCOLENERGY study has already used these approaches and added further data to support the use of a maximum energy of 360 J, which is feasible to start with but essential to end with during the course of DCCV.

There is growing evidence that the simultaneous use of 2 defibrillators, known as dual DCCV, further increases the overall success rate of electrical cardioversion, with no safety issues when 200-J shocks are used. Darrat et al.[33] incorporated dual DCCV into a step-up institutional protocol and achieved 99.3% success in restoring SR, and in a randomized trial in patients with obesity and AF (BMI $>$ 35 kg/m^2) the success rate of single vs dual DCCV was 86% vs 98%, with a higher likelihood of failure with single DCCV (adjusted OR, 12.6; 95% CI, 1.3-118.9).[34] Despite higher success rates compared with single DCCV studies including PROTOCOLENERGY, further studies are needed to elucidate the optimal output energy for dual DCCV and to justify its use in daily clinical practice. Potential indications for dual DCCV may include failure of single DCCV[34] or patients with known extensive cardiac fibrosis, which has recently been associated with endocardial damage, thrombus formation, conduction abnormalities, and atrial re-entry.[35]

Limitations

The study has several limitations. First, it is a single-centre study. However, the approach to patients with AF and DCCV is similar between complex cardiology centres in the Czech Republic. Second, not all patients indicated for DCCV were enrolled. For logistic reasons, we chose to randomize patients with stable AF who were indicated for an elective outpatient procedure, and excluded hospitalized patients, those with decompensated heart failure, and those indicated for acute DCCV. Therefore, it is questionable whether the results can be generalized to all patients with AF. Third, we did not record detailed information on biochemical variables (potassium, magnesium, renal function, N-terminal pro-B-type natriuretic peptide [NT-proBNP]), echocardiographic parameters other than LVEF and left atrial diameter (left/right atrial volume, valvular disease, ischemic heart disease, diastolic filling pressure calculations, left atrial and ventricular strain), or duration/type of AF, which are known to potentially influence the onset and course of AF and were therefore not included in our analyses. The aim was to keep the study as simple and real-world as possible, and this information was not available for patients referred for elective DCCV from different centres. Fourth, the cumulative energy delivered during DCCV may be slightly less than the output energy set on the defibrillator, depending on the individual patient's thoracic impedance values, pulse duration, and leading-edge voltage. These values were not recorded. Fifth, a total of 7 patients did not receive a third shock as per protocol and were included as failures in the ITT analysis. These protocol deviations did not change the overall results of the study, as an on-treatment analysis (not shown) excluding these patients produced the same results. Finally, the physician administering the shock was not blinded, but the patients and the physician assessing the skin changes and all outcome assessments were blinded.

Conclusions

Energy escalation (150 J-360 J-360 J) and maximum fixed energy (3 x 360 J) DCCV protocols showed similar high cumulative efficacy. Starting with 150 J, the initial shock appeared to be adequate for most patients with BMI less than 29 to 34 kg/m^2 and for women who benefited from less skin erythema compared with the initial 360-J shock. With its high efficacy but better tolerability, the energy escalation protocol should be preferred to the maximum fixed energy protocol in elective cardioversion patients.

Acknowledgements

We would like to thank the patients and the staff of the Agel Hospital Trinec-Podlesi for their contribution to the study.

Ethics Statement

This study was conducted in accordance with the Declaration of Helsinki and approved by the local ethics committee of Agel Hospital Trinec-Podlesi (approval number EK1/21). All participants provided written informed consent prior to their inclusion in the study. The researchers ensured that patient confidentiality and data protection measures were strictly adhered to throughout the research process. The study protocol and procedures were designed to minimize risks to participants while maximizing potential benefits to scientific knowledge and patient care in the field of cardiology.

Patient Consent

The authors confirm that patient consent forms have been obtained for this article.

Funding Sources

This work was supported by the Educational and Research Institute AGEL, grant number IGS202009. The funding agency had no role in the design, execution, interpretation, or writing of the study.

Disclosures

The authors have no conflicts of interest to disclose.

References

1. Ambler JJS, Deakin CD. A randomized controlled trial of efficacy and ST change following use of the Welch-Allyn MRL PIC biphasic waveform versus damped sine monophasic waveform for external DC cardioversion. Resuscitation 2006;71:146-51.
2. Page RL, Kerber RE, Russell JK, et al. Biphasic versus monophasic shock waveform for conversion of atrial fibrillation: the results of an international randomized, double-blind multicenter trial. J Am Coll Cardiol 2002;39:1956-63.
3. Zhang B, Li X, Shen D, Zhen Y, Tao A, Zhang G. Anterior-posterior versus anterior-lateral electrode position for external electrical cardioversion of atrial fibrillation: a meta-analysis of randomized controlled trials. Arch Cardiovasc Dis 2014;107:280-90.
4. Kirchhof P, Mönnig G, Wasmer K, et al. A trial of self-adhesive patch electrodes and hand-held paddle electrodes for external cardioversion of atrial fibrillation (MOBIPAPA). Eur Heart J 2005;26:1292-7.
5. Boodhoo L, Mitchell ARJ, Bordoli G, Lloyd G, Patel N, Sulke N. DC cardioversion of persistent atrial fibrillation: a comparison of two protocols. Int J Cardiol 2007;114:16-21.
6. Gallagher MM, Guo XH, Poloniecki JD, Guan Yap Y, Ward D, Camm AJ. Initial energy setting, outcome and efficiency in direct current cardioversion of atrial fibrillation and flutter. J Am Coll Cardiol 2001;38:1498-504.
7. Joglar JA, Hamdan MH, Ramaswamy K, et al. Initial energy for elective external cardioversion of persistent atrial fibrillation. Am J Cardiol 2000;86:348-50.
8. Singh SN, Tang XC, Reda D, Singh BN. Systematic electrocardioversion for atrial fibrillation and role of antiarrhythmic drugs: a substudy of the SAFE-T trial. Heart Rhythm 2009;6:152-5.
9. Döring C, Richter U, Ulbrich S, et al. The impact of right atrial size to predict success of direct current cardioversion in patients with persistent atrial fibrillation. Korean Circ J 2023;53:331-43.
10. Jaakkola S, Lip GYH, Biancari F, et al. Predicting unsuccessful electrical cardioversion for acute atrial fibrillation (from the AF-CVS score). Am J Cardiol 2017;119:749-52.
11. Hellman T, Kiviniemi T, Vasankari T, et al. Prediction of ineffective elective cardioversion of atrial fibrillation: a retrospective multi-center patient cohort study. BMC Cardiovasc Disord 2017;17:33.
12. Roh S-Y, Ahn J, Lee K-N, et al. The impact of personal thoracic impedance on electrical cardioversion in patients with atrial arrhythmias. Medicina (Kaunas) 2021;57:618.
13. Rochlani YM, Shah NN, Pothineni NV, Paydak H. Utilization and predictors of electrical cardioversion in patients hospitalized for atrial fibrillation. Cardiol Res Pract 2016;2016:8956020.
14. Wałek P, Gorczyca I, Sielski J, Wożakowska-Kapłon B. Left atrial emptying fraction determined during atrial fibrillation predicts maintenance of sinus rhythm after direct current cardioversion in patients with persistent atrial fibrillation. PLoS One 2020;15:e0238002.
15. Wałek P, Roskal-Wałek J, Dłubis P, Tracz J, Wożakowska-Kapłon B. Left atrial wall motion velocity assessed during atrial fibrillation predicts sinus rhythm maintenance after electrical cardioversion in patients with persistent atrial fibrillation. Int J Environ Res Public Health 2022;19:15508.
16. Schmidt AS, Lauridsen KG, Møller DS, et al. Anterior-lateral versus anterior−posterior electrode position for cardioverting atrial fibrillation. Circulation 2021;144:1995-2003.
17. Hindricks G, Potpara T, Dagres N, et al. 2020 ESC guidelines for the diagnosis and management of atrial fibrillation developed in collaboration with the European Association of Cardio-Thoracic Surgery (EACTS). Eur Heart J 2020;42(5):373-498.
18. Stiell IG, de Wit K, Scheuermeyer FX, et al. 2021 CAEP acute atrial fibrillation/flutter best practices checklist. CJEM 2021;23:604-10.
19. Soar J, Böttiger BW, Carli P, et al. European Resuscitation Council Guidelines 2021: adult advanced life support. Resuscitation 2021;161:115-51.
20. Cheung CC, Nattel S, Macle L, Andrade JG. Management of atrial fibrillation in 2021: an updated comparison of the current CCS/CHRS, ESC, and AHA/ACC/HRS guidelines. Can J Cardiol 2021;37:1607-18.
21. Ramirez FD, Fiset SL, Cleland MJ, et al. Effect of applying force to self-adhesive electrodes on transthoracic impedance: implications for electrical cardioversion. Pacing Clin Electrophysiol 2016;39:1141-7.
22. Lobo R, White RD, Donato LJ, et al. Absence of significant myocardial injury following elective direct current cardioversion for atrial fibrillation. Heart Rhythm O2 2023;4:180-6.
23. Schmidt AS, Lauridsen KG, Torp P, Bach LF, Rickers H, Løfgren B. Maximum-fixed energy shocks for cardioverting atrial fibrillation. Eur Heart J 2020;41:626-31.
24. Jiravsky O, Rucki L, Hudec M, et al. Identifying parameters associated with the use of higher discharge energy in electrical cardio version for persistent atrial fibrillation. J Atrial Fibrillation Electrophysiol 2023;16:6-11.
25. Schulz KF, Altman DG, Moher D; the CONSORT Group. CONSORT 2010 statement: updated guidelines for reporting parallel group randomised trials. BMC Med 2010;8:18.

26. BeneHeart D3/BeneHeart D2 Defibrillator/Monitor Operator's Manual. Available from, www.mindray.com.

27. Ramirez FD, Sadek MM, Boileau I, et al. Evaluation of a novel cardioversion intervention for atrial fibrillation: the Ottawa AF cardioversion protocol. Europace 2019;21:708-15.

28. Nguyen ST, Belley-Côté EP, Ibrahim O, et al. Techniques improving electrical cardioversion success for patients with atrial fibrillation: a systematic review and meta-analysis. Europace 2023;25:318-30.

29. Glover BM, Walsh SJ, McCann CJ, et al. Biphasic energy selection for transthoracic cardioversion of atrial fibrillation: the BEST AF trial. Heart 2008;94:884-7.

30. Fumagalli S, Boni N, Padeletti M, et al. Determinants of thoracic electrical impedance in external electrical cardioversion of atrial fibrillation. Am J Cardiol 2006;98:82-7.

31. Kistler PM, Sanders P, Morton JB, Vohra JK, Kalman JM, Sparks PB. Effect of body mass index on defibrillation thresholds for internal cardioversion in patients with atrial fibrillation. Am J Cardiol 2004;94:370-2.

32. Lip GYH, Merino JL, Banach M, et al. Clinical factors related to successful or unsuccessful cardioversion in the EdoxabaN versus warfarin in subjectS UndeRgoing cardiovErsion of Atrial Fibrillation (ENSURE-AF) randomized trial. J Arrhythm 2020;36:430-8.

33. Darrat Y, Leung S, Elayi L, et al. A stepwise external cardioversion protocol for atrial fibrillation to maximize acute success rate. Europace 2023;25:828-34.

34. Aymond JD, Gullatt T, Bernard ML, et al. EFficacy and safety of dual direct current cardioversion versus single direct current cardioversion as an initial treatment strategy in obese patients with atrial fibrillation. Heart Rhythm 2023;20:S69-70.

35. Nattel S. Atrial fibrosis, endocardial damage, and thrombosis in atrial fibrillation: association with underlying conditions or causal? JACC: Clin Electrophysiol 2023;9:1169-71.

Supplementary Material

To access the supplementary materiál accompanying this article, visit the online version of the *Canadian Journal of Cardiology* at www.onlinecjc.ca and at https://doi.org/10.1016/j.cjca.2024.06.003.

M. Miklovič et al.

Renal denervation improves cardiac function independently of afterload and restores myocardial norepinephrine levels in a rodent heart failure model

Hypertension Research
Impact Factor: 4,3

rejstřík

Hypertension Research (2024) 47:2718–2730
https://doi.org/10.1038/s41440-024-01580-3

ARTICLE

Special Features - Renal Denervation and Sympathetic Nerve System

Renal denervation improves cardiac function independently of afterload and restores myocardial norepinephrine levels in a rodent heart failure model

Matúš Miklovič[1,2] · Olga Gawryś[1] · Zuzana Honetschlägerová[1] · Petr Kala[1,3] · Zuzana Husková[1] · Soňa Kikerlová[1] · Zdeňka Vaňourková[1] · Šárka Jíchová[1] · Alena Kvasilová[4] · Misuzu Kitamoto[4] · Hana Maxová[1,2] · Guillermo Puertas-Frias[5] · Tomáš Mráček[5] · David Sedmera[4] · Vojtěch Melenovský[1,6]

Received: 30 June 2023 / Revised: 4 December 2023 / Accepted: 24 December 2023 / Published online: 2 February 2024

Abstract

Renal nerves play a critical role in cardiorenal interactions. Renal denervation (RDN) improved survival in some experimental heart failure (HF) models. It is not known whether these favorable effects are indirect, explainable by a decrease in vascular afterload, or diminished neurohumoral response in the kidneys, or whether RDN procedure per se has direct myocardial effects in the failing heart. To elucidate mechanisms how RDN affects failing heart, we studied load-independent indexes of ventricular function, gene markers of myocardial remodeling, and cardiac sympathetic signaling in HF, induced by chronic volume overload (aorto-caval fistula, ACF) of Ren2 transgenic rats. Volume overload by ACF led to left ventricular (LV) hypertrophy and dysfunction, myocardial remodeling (upregulated Nppa, MYH 7/6 genes), increased renal and circulating norepinephrine (NE), reduced myocardial NE content, increased monoaminoxidase A (MAO-A), ROS production and decreased tyrosine hydroxylase (+) nerve staining. RDN in HF animals decreased congestion in the lungs and the liver, improved load-independent cardiac function (Ees, PRSW, Ees/Ea ratio), without affecting arterial elastance or LV pressure, reduced adverse myocardial remodeling (Myh 7/6, collagen I/III ratio), decreased myocardial MAO-A and inhibited renal neprilysin activity. RDN increased myocardial expression of acetylcholinesterase (Ache) and muscarinic receptors (Chrm2), decreased circulating and renal NE, but increased myocardial NE content, restoring so autonomic control of the heart. These changes likely explain improvements in survival after RDN in this model. The results suggest that RDN has remote, load-independent and favorable intrinsic myocardial effects in the failing heart. RDN therefore could be a useful therapeutic strategy in HF.

Keywords Heart failure · Norepinephrine · Renal denervation · Volume overload · Sympathetic nervous system

Introduction

Renal sympathetic innervation plays an important role in cardiorenal interactions and in the pathophysiology of heart failure (HF) [1, 2]. The renal nerves contain both afferent and efferent sympathetic nerve fibers, establishing a

Supplementary information The online version contains supplementary material available at https://doi.org/10.1038/s41440-024-01580-3.

✉ Vojtěch Melenovský
vojtech.melenovsky@ikem.cz

[1] Center for Experimental Medicine, Institute for Clinical and Experimental Medicine—IKEM, Prague, Czech Republic

[2] Department of Pathophysiology, 2nd Faculty of Medicine, Charles University, Prague, Czech Republic

[3] Department of Cardiology, University Hospital Motol and 2nd Faculty of Medicine, Charles University, Prague, Czech Republic

[4] Institute of Anatomy, First Faculty of Medicine, Charles University, Prague, Czech Republic

[5] Institute of Physiology, Czech Academy of Sciences, Prague, Czech Republic

[6] Department of Cardiology, Institute for Clinical and Experimental Medicine—IKEM, Prague, Czech Republic

Graphical Abstract

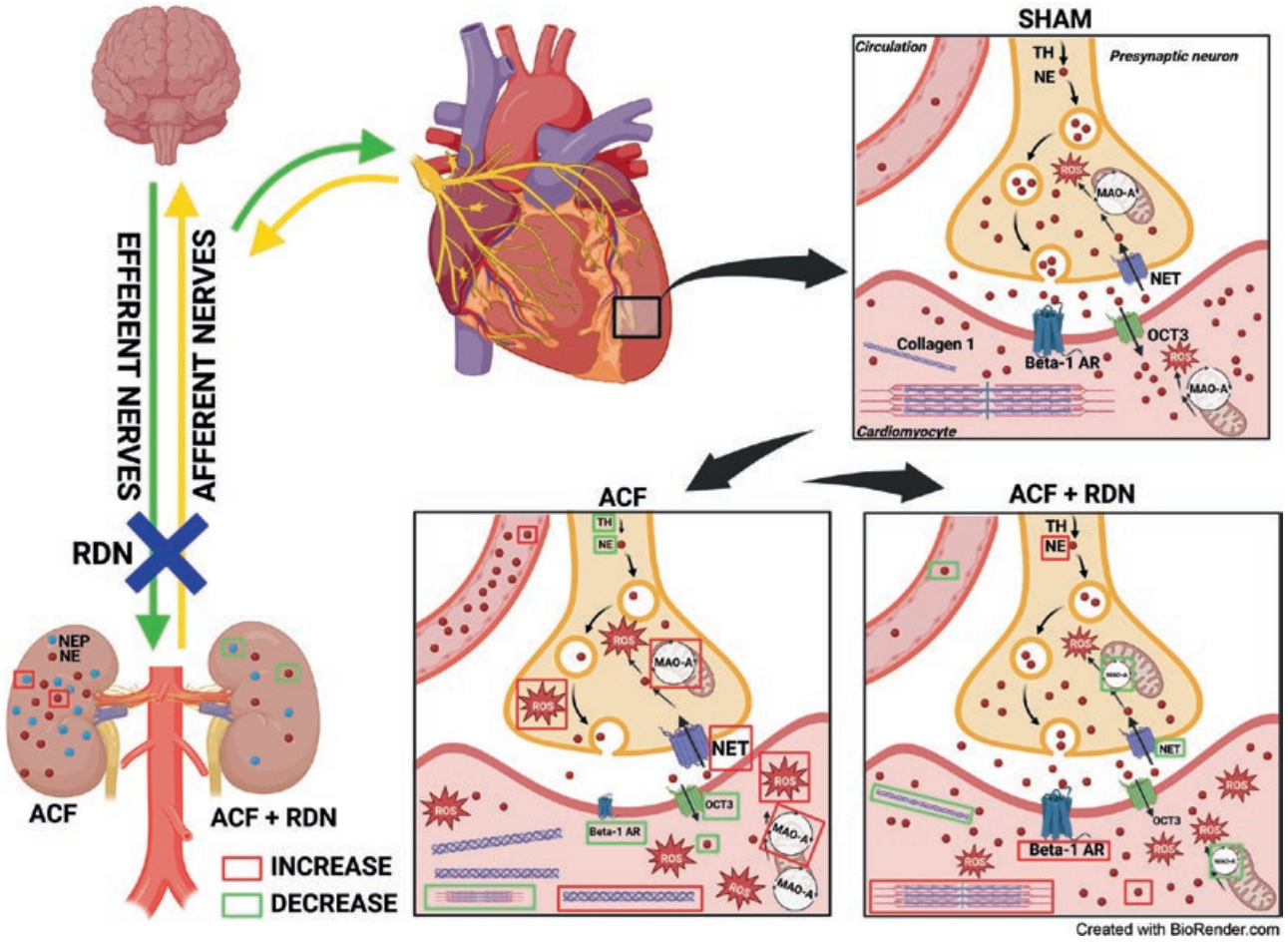

bidirectional link between the kidneys and the brain [3]. Through this connection, the brain centers, located in the hypothalamus and in the brain stem, collect renal and other sensory inputs and regulate sympathetic nerve output to peripheral organs, including the kidneys and the heart [1]. Chronic HF is accompanied by sympathetic overactivation, increased norepinephrine (NE) release from the heart and the kidneys into the plasma [4], depleted NE in the myocardium [5], increased production of reactive oxygen species (ROS) [6], and downregulated beta-1 adrenergic receptors (Adrb1), which all contribute to decreased contractility, fibrosis and further propagation of myocardial damage [7–9].

Renal denervation (RDN) is a non-pharmacological treatment method consisting of the targeted destruction of nerve fibers around the renal arteries by radiofrequency energy, ultrasound or by locally-applied chemical toxin [10–14], that eliminates both efferent and afferent sympathetic signals, reduces kidney NE and attenuates the central sympathetic drive [15, 16]. RDN demonstrated marked antihypertensive effects in experimental studies and also in clinical trials [17].

Intriguingly, RDN showed favorable effects not only in hypertension but more recently also in experimental models of HF, where it improved survival [10, 12, 18, 19]. This is somewhat surprising because pharmacological unselective central sympathetic inhibition in HF patients led to excessive mortality and was abandoned [20]. The mechanisms of favorable effects of RDN in HF have not yet been sufficiently elucidated. The key unresolved questions remain, whether RDN effects in HF are explainable by an attenuated neurohumoral response in the kidneys, by reduced vascular afterload, or whether RDN procedure per se has direct myocardial effects in the failing heart.

In this study, we investigated the effects of RDN on HF due to volume overload from aortocaval fistula (ACF)—well established HF model of high cardiac output with markedly expressed neurohumoral activation and congestion [5, 21, 22]. We used Ren-2 transgenic rat (TGR) [19, 23, 24], a strain that displays rapid and pronounced onset of HF symptoms after ACF induction [19]. It is known that in TGR rats, a hypotensive effect occurs in very early stages after ACF, due to the transfer of volume and

pressure from the aorta to the inferior vena cava [19, 25]. To separate the impact of RDN on vascular load from intrinsic myocardial effects, we utilized pressure-volume (PV) analysis, and we studied the effects on molecular markers of myocardial remodeling. We further analyzed in a greater detail changes in the myocardial sympathetic system, that are grossly deregulated in this HF model [5, 26].

Methods

Animals and the protocol

The study was performed in accordance with relevant regulations and was approved by the Animal Ethics Committee of IKEM and by the Ministry of Health of the Czech Republic (#12468/2021-5/OVZ). Heterozygous TGR were generated by breeding female homozygous HanSD rats with male homozygous TGR as described [27]. Eight-week-old TGR underwent ACF surgery to induce volume overload. After 1 week, animals underwent bilateral RDN (mechanical and chemical by topical phenol application) from laparotomy [28, 29]. Two weeks after RDN, the functions of the left ventricle (LV) were measured by PV analysis, and the animals were examined using echocardiography each week. Animals were killed by thiopental sodium i.p. overdose (in the case of in vivo measurements of echocardiography and PV analysis), or by decapitation (hormonal and molecular analyses).

Aortocaval fistula and renal denervation surgery

The animals were anaesthetized using ketamine and midazolam (Calypsol, Gedeon Richter, Hungary, 160 mg/kg and Midazolam, Kalcex, Latvia, 160 mg/kg, i.p.). The ACF was created as described previously and this procedure is routinely performed in our laboratory [19, 21, 30]. The sham-operated rats underwent opening and closing of the abdominal cavity, without the aortocaval fistula procedure. After the surgery, meloxicam analgesia (1–2 mg/kg/day, s.c.) was given for 2–3 days.

Bilateral RDN procedure was performed 1 week after ACF surgery. Animals were anaesthetized using ketamine/midazolam and bilateral RDN procedure was performed as described in previous studies [19, 31–33]. Intact animals underwent laparotomy and retraction of the abdominal organs.

Echocardiography

An echocardiographic examination was performed on the day of surgery before the creation of ACF/sham. The second examination was performed after 1 week, before RDN/intact surgery, and once per week during the next 2 weeks until the end of the experiment. Prior to the echocardiographic examination, the animals were anesthetized with 4% isoflurane (IsoVet®, Piramal Healthcare, UK). During the image acquisition, the rats were maintained under isoflurane anesthesia (1.5–2%, Combi-vet® system, Rothacher Medical GmbH, Heitenried, Switzerland). B-Mode and M-Mode images were recorded in parasternal long and short axis view and used for measurements of dimensions of LV internal diameter, and anterior and posterior walls. Echocardiographic examination was done by Vevo® 2100 Imaging System with the MS250S transducer (13–24 MHz), and evaluated in VevoLab (v3.2.0, FUJIFILM VisualSonics, Inc., Toronto, ON, Canada).

Pressure-volume analysis

Rats were anesthetized with thiopental (50 mg/kg, i.p., VAUB Pharma a.s., Roztoky, CZ) and echocardiography was performed as described above. Rats were intubated and artificially ventilated through the procedure (Ugo Basile, Gemonio, IT). The left jugular vein was cannulated with saline for securing central venous access. A balloon catheter (LeMaitre Single Lumen Embolectomy Catheter, 2F, Burlington, MA, USA) was inserted via the left femoral vein to the vena cava inferior, below the diaphragm to maintain the best position for preload reduction [34]. Functions of the LV were invasively assessed by a PV catheter (Millar, 2F, Houston, TX, USA) introduced into the LV via the right carotid artery as described in previous studies [35–37]. Volume signal was calibrated by cuvette calibration unit of known volumes fulfilled with heparinized warm blood taken from LV after the experiment. Data from PV loops were captured and analyzed in LabChart Pro software (ADInstruments, Bella Vista, NSW, Australia) as discussed in detail in our previous study [34].

Gene expression analysis

LV was homogenized in RNAzol® RT (#RN190; Molecular Research Center, Inc., Cincinnati, USA) and RNA free water was added to samples and mixed. After the precipitation the samples were centrifuged (12,000 × *g*, 15 min, 4 °C) and the supernatant was transferred. The RNA was precipitated with 75% ethanol and gently mixed, incubated for 15 min, room temperature (rt), centrifuged (12,000 × *g*, 20 min, 4 °C) and the supernatant was discarded. The pellet was washed twice with 75% ethanol, centrifuged (7500 × *g*, 5 min, 4 °C) and dried in a thermoblock at 55 °C. The pellet was dissolved in RNA free water, incubated in the thermoblock for 10 min and stored at −80 °C until analysis. The concentration and purity of the RNA were measured. Bio-Rad C1000 Thermal cycler (Bio-Rad s.r.o., Prague, Czech

Republic) was used with High Capacity cDNA Reverse Transcription Kit (#4368813; Applied Biosystems, Foster City, CA, USA). Transcribed cDNA samples were diluted with DEPC-treated water and mixed with TaqMan Fast Advanced Master Mix (#4444556; Applied Biosystems, Foster City, CA, USA). The solution was transferred to a TaqMan Array Card (384-well microfluidics TaqMan array cards; custom setting of selected genes), centrifuged twice (1200 RPM, 1 min, 4 °C) and sealed. The quantification was done on ViiA™ 7 Real-time PCR system (Applied Biosystems, Foster City, CA, USA) and the measurement of mRNA expressions was performed in accordance with the manufacturer's instructions.

Relative gene expression was calculated by the $2-\Delta\Delta Ct$ method, which is frequently used for such experiments [38–40]. Housekeeping gene GAPDH was used as the normalizer to calculate relative gene expression. Final results were expressed as the n-fold difference in gene expression of mRNA of target genes between experimental and control.

Immunohistochemistry

Dissected basal halves of free walls of the LV were whole-mount stained with anti-tyrosine hydroxylase primary antibody (1:500, rabbit AB152, Merck Millipore) visualized with Cy5 coupled goat-anti-rabbit secondary antibody (1:200, Jackson Immuno Research) as described [41]. Incubation times were prolonged (blocking 24 h in normal goat serum, 1:10, primary antibody 48 h, washing 12 h, secondary antibody 24 h, all at rt with continuous gentle rocking), and Triton-X concentration was increased at 0.1%.

After staining, the samples were pinned epicardial side up to the bottom of a deep Petri dish covered with Sylgard and cleared in Scale2 for at least 48 h [42]. The samples were then examined on a confocal Olympus BX61 system (FluoView 1000) using a 2x, 0.14 NA dry objective (overview picture) followed by 25x ScaleView objective (NA 1.0). Three confocal stacks spanning at least 50-micron depth were collected from different location at 1-micron z-step. For analysis, substacks of 10 µm thickness were selected from the subepicardial region, and maximum intensity projections of green channel (488 nm excitation, detecting tissue autofluorescence derived mostly from the myocytes) and far-red channel (635 nm excitation, specific fluorescence of anti-tyrosine hydroxylase immunostaining) were created in ImageJ. Percentage of red to red + green channel was then calculated after signal thresholding in ImageJ.

Myocardial ROS production by monoamine oxidase A

Myocardial hydrogen peroxide production by monoamine oxidase A (MAO-A) was determined fluorometrically measuring the oxidation of Amplex Red reagent (Thermo Fisher Scientific, Waltham, MA, USA) coupled to the enzymatic reduction of H_2O_2 by horseradish peroxidase. Briefly, 10% homogenates were prepared in ice-cold KCl-based media (120 mM KCl, 3 mM HEPES, 5 mM KH2PO4, 3 mM MgSO4, and 1 mM EGTA, pH 7.2) from frozen free wall of LV using zirconium oxide grinding balls (3 min, 30 Hz), Retsch MM 400 mixer mill (Retsch, Haan, Germany) and filtered through a fine mesh. Protein concentration was estimated by the BCA method. An aliquot of the homogenate was saved for SDS-PAGE analyses. The assay was performed using 0.15 mg/ml of protein in KCl-based media with or without the MAO-A substrate tyramine (50 µM) or its specific inhibitor clorgylin (1 µM), in the presence of 50 µM Amplex Red and 1 U/ml HPR. A standard curve of 1–10 µM H_2O_2 was established in every plate to calibrate the signal to nmol produced. The increase in the fluorescence was recorded for 30 min at 37 °C with an Infinite M200 plate reader (Tecan Group Ltd., Männedorf, Switzerland) at 544/590 nm.

Western blot analysis

LV tissue (free wall) was homogenized and protein concentration in the supernatant was measured using Pierce BCA protein assay (Thermo Fisher Scientific, Waltham, MA, USA). Protein was separated by sodium dodecyl sulfate polyacrylamide gel electrophoresis (SDS-PAGE) and transferred onto the polyvinyl difluoride membrane in transfer buffer at 100 V for 1.5 h. Membranes were blocked with 2.5% BSA/5% non-fat dry milk in TRIS buffered saline with Tween20 (TBS-T) and washed with TBS-T. The membranes were incubated with primary antibodies overnight at 4 °C (more antibody dilutions details in supplement). After incubation and washing, the membranes were incubated with horseradish peroxidase-conjugated secondary antibody for 1 h at rt. After last washing, the immunoblots were exposed to SuperSignal West Dura Substrate (Thermo Scientific, Rockford, IL, USA) for chemiluminescent detection. Relative densitometry was determined using ImageJ software (NIH, Bethesda, MD, USA). Protein data were normalized to the housekeeping protein GAPDH. Final results were expressed as the n-fold difference in target protein expression between experimental and control group.

Neprilysin activity in kidney tissue

Neprilysin activity was assessed in whole kidney samples as described before [43, 44]. Briefly, kidney tissue was homogenized in ice-cold neprilysin assay buffer supplemented with protease inhibitors aprotinin and phenylmethylsulfonyl fluoride using mixer mill MM400,

Table 1 Organ weights and principal hemodynamic parameters of the left ventricle

Strain	sham/intact	sham/RDN	ACF/intact	ACF/RDN
Organ weight (g)				
n	25	28	25	28
Body weight	438 ± 9.59	439 ± 8.25	425 ± 8.38	418 ± 7.2
Heart weight	1.62 ± 0.02	1.6 ± 0.03	2.24 ± 0.03*	1.95 ± 0.04*†
Left atrium	0.04 ± 0.001	0.041 ± 0.001	0.074 ± 0.002*	0.065 ± 0.002*†
Left ventricle (with IVS)	1.22 ± 0.02	1.19 ± 0.02	1.53 ± 0.02*	1.36 ± 0.03*†
Kidney weight	1.61 ± 0.03	1.65 ± 0.04	1.56 ± 0.04	1.51 ± 0.02
Lungs weight	1.81 ± 0.06	1.85 ± 0.04	2.47 ± 0.12*	2.1 ± 0.06*†
Liver weight	15.97 ± 0.43	15.49 ± 0.4	16.6 ± 0.39	14.83 ± 0.33†
Hemodynamics				
n	8	11	14	10
Stroke work (mmHg*μl)	6957 ± 784	7334 ± 646	10,757 ± 581*	7953 ± 841†
Cardiac output (μl/min)	17,305 ± 2052	20,426 ± 1193	32,205 ± 1843*	24,544 ± 2765†
Stroke volume (μl)	44.1 ± 4.8	49.1 ± 3.5	78.9 ± 3.6*	60.5 ± 6.6†
Mean ventricular pressure (mmHg)	75.4 ± 3.7	65 ± 2.2*	68.4 ± 2.3	67.1 ± 2.2
End-systolic pressure (mmHg)	169 ± 3.7	149 ± 3.8*	143 ± 3.1*	142 ± 2.2*
End-diastolic pressure (mmHg)	7 ± 0.78	5.5 ± 0.63	12.7 ± 1.63*	8.2 ± 0.69†
End-diastolic volume (μl)	230 ± 21.1	260 ± 13.3	356 ± 13.3*	264 ± 27†
End-systolic volume (μl)	175 ± 17.9	207 ± 6.7	260 ± 12.3*	191 ± 19.3†
Heart rate (bpm)	389 ± 8.5	392 ± 7.6	384 ± 6.5	403 ± 3.5

Values are means ± SEM

*$p < 0.05$ vs. sham/intact; †$p < 0.05$ vs. ACF/intact

centrifuged (12,000 × *g*, 10 min, 4 °C) and supernatant was collected. Neprilysin activity was measured by a fluorometric assay (K487-100; BioVision, Milpitas, CA, USA).

The measurement of norepinephrine in kidney and heart tissue

NE was measured in kidney cortex and LV heart samples. Briefly, wet tissue samples were weighted and homogenized in 0,05 M PB (pH 7.4) supplemented with protease inhibitor cocktail (Sigma-Aldrich, St. Louis, MO, USA) and ascorbic acid using mixer mill MM400, centrifuged twice (3000 × *g*, 10 min, 4 °C and 10,000 × *g*, 10 min, 4 °C) and supernatant was collected. NE concentration was measured by a solid phase enzyme-linked immunosorbent assay based on the sandwich principle, using commercially available ELISA kit (RE59261; IBL International, Hamburg, Germany). More methodological details are provided in Supplementary Information.

Statistical analysis

Statistical analysis of the data was performed using GraphPad Prism software v9.4.1 (Graph Pad Software, San Diego, CA, USA). All results are presented as the mean ± standard error of the mean. The data were analyzed using one-way ANOVA (organ weights, core hemodynamic parameters, gene and protein expressions) with Fisher's LSD post hoc test or two-way ANOVA (echocardiography results) followed by Tukey's post hoc multiple comparison test. The values of p below 0.05 were considered as statistically significant.

Results

Weights, cardiac dimensions and principal LV hemodynamics

Table 1 shows organ weights and hemodynamics in the sham-operated control group, in a group with HF induced by ACF, and in a group with ACF and RDN. The sham/RDN group compared to the sham/intact group displayed no significant changes in organ weight parameters but significantly decreased end-systolic pressure (149 ± 3.8 vs. 169 ± 3.7 mmHg, $p < 0.05$) and mean LV pressure (65 ± 2.2 vs. 75.4 ± 3.7 mmHg, $p < 0.05$).

ACF had an impact on multiple organ weight parameters that are typically changed in HF, with no effect on the body weight or tibia length (not shown). ACF/intact rats had increased heart weight and LV weight. Similarly, compared to the sham group, ACF/intact rats had significantly increased weight of the left atrium (LA) and weight of the lungs, reflecting HF-related congestion. Compared to the

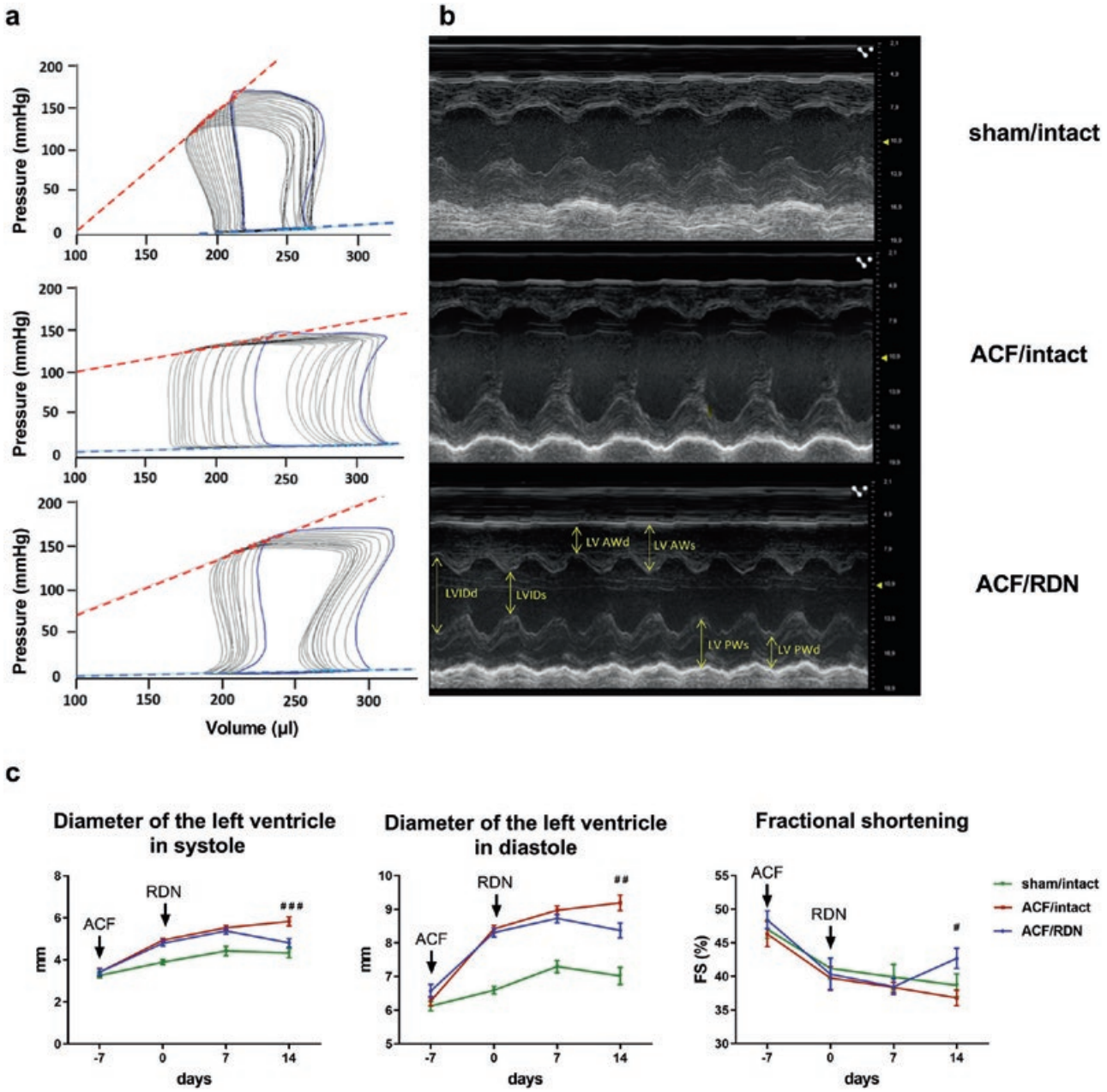

Fig. 1 In vivo measurement of LV contractility and dimensions. **a** Representative pressure-volume loops from invasive pressure-volume analysis. Red line—end-systolic elastance (Ees), blue line—end-diastolic pressure-volume relationship (EDPVR). **b** Echocardiographic M mode images of parasternal long axis view. LV AWd left ventricular anterior wall thickness in diastole, LV AWs left ventricular anterior wall thickness in systole, LVIDd left ventricular internal diameter in diastole, LVIDs left ventricular internal diameter in systole, LV PWd left ventricular posterior wall thickness in diastole, LV PWs left ventricular posterior wall thickness in systole. **c** Diameter of left ventricle in systole (LVIDs) and diastole (LVIDd) measured during each week of experiment (3 weeks); FS fractional shortening. $N = 10$ in sham/intact, $N = 19$ in ACF/intact, $N = 13$ in ACF/RDN. $^{\#\#\#}p < 0.001$; $^{\#\#}p < 0.01$; $^{\#}p < 0.05$, ACF/intact vs. ACF/RDN group, compared to the day 14

sham/intact group, ACF/intact rats had significantly increased stroke volume, stroke work, and cardiac output. End-systolic and end-diastolic pressure (EDP) measured by PV analysis were increased in ACF/intact group compared to the sham/intact group, similar to echocardiographic measurements (Fig. 1b, c). Moreover, ACF rats had also a significant decrease in end-systolic pressure (143 ± 3.1 vs. 169 ± 3.7 mmHg, $p < 0.05$) compared to sham rats.

Compared to intact ACF, RDN significantly decreased heart weight, LA, LV weight, and congestion of the lungs and liver. RDN in ACF rats significantly decreased stroke work and normalized stroke volume and cardiac output. RDN in

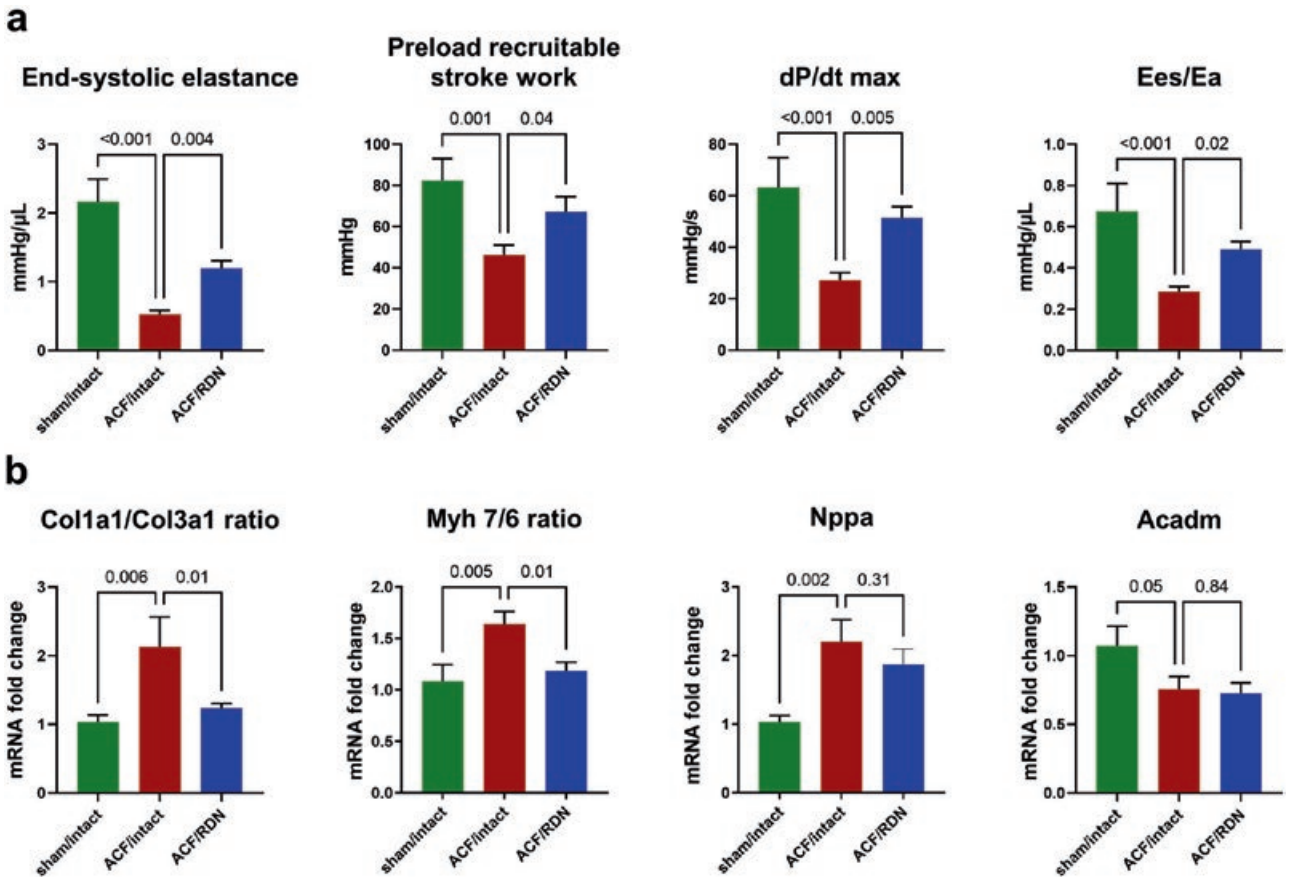

Fig. 2 LV function and gene expression of selected HF markers and the impact of RDN. **a** Systolic function parameters measured by invasive PV analysis, Ees/Ea, ventricular-arterial coupling ratio. **b** Gene expression of markers of fibrosis—collagen I/III (Col1a1/Col3a1) ratio, myocardial stress—Myosin heavy chain 7/6 (Myh 7/6) ratio, natriuretic peptide A (Nppa) and mitochondrial fatty acid beta-oxidation pathway, acyl-CoA dehydrogenase medium chain (Acadm). $N = 9$ in sham/intact, $N = 9$ in ACF/intact, $N = 10$ in ACF/RDN

ACF rats also decreased dilatation of LV (Fig. 1b, c), which was shown as reduced LV end-systolic and end-diastolic volumes. We observed that ACF/RDN group had also reduced EDP (8.2 ± 0.69 vs. 12.7 ± 1.63 mmHg, $p < 0.05$) compared to ACF intact group. Heart rate was not affected by ACF or RDN in any groups.

LV function and HF markers: the impact of ACF

ACF/intact group had significantly decreased systolic function compared to the sham/intact group. ACF/intact group had also decreased end-systolic elastance (Ees) and preload recruitable stroke work (PRSW) compared to the sham/intact group. ACF/intact had also decreased ventricular-arterial coupling compared to sham/intact (Ees/Ea ratio, Fig. 2a).

ACF/intact group had extensive upregulation of markers of myocardial damage/remodeling compared to the sham/intact group. ACF/intact group had increased fibrotic marker collagen I/III (Col1a1/Col3a1) gene expression ratio. Similarly, maladaptive hypertrophy markers myosin heavy chain isotype ratio (Myh 7/6) and myocardial stress gene natriuretic peptide A (Nppa) were increased in ACF/intact group compared to the sham/intact group. ACF/intact group had a significantly decreased ($p = 0.05$) medium-chain acyl-Coa dehydrogenase (Acadm, Fig. 2b).

Cardiac autonomic nervous system: the impact of ACF

ACF rats had significantly increased NE levels in plasma and kidney (Fig. 3a, b), but depleted LV content of NE compared to the sham group (Fig. 3c). Correspondingly, we observed decreased LV protein expression of the key NE-synthetizing enzyme tyrosine hydroxylase (TH) in the LV (Fig. 3d) and diminished LV myocardial density of TH-positive sympathetic nerves (Fig. 4a, c, d). From proteins involved in the myocardial fate of NE, we observed an increased expression ($p = 0.03$) of presynaptic norepinephrine transporter (NET, responsible for synaptic NE reuptake, Fig. 3e) and significant decrease of organic cation transporter (OCT3, responsible for myocardial uptake of NE) in ACF compared to the sham/

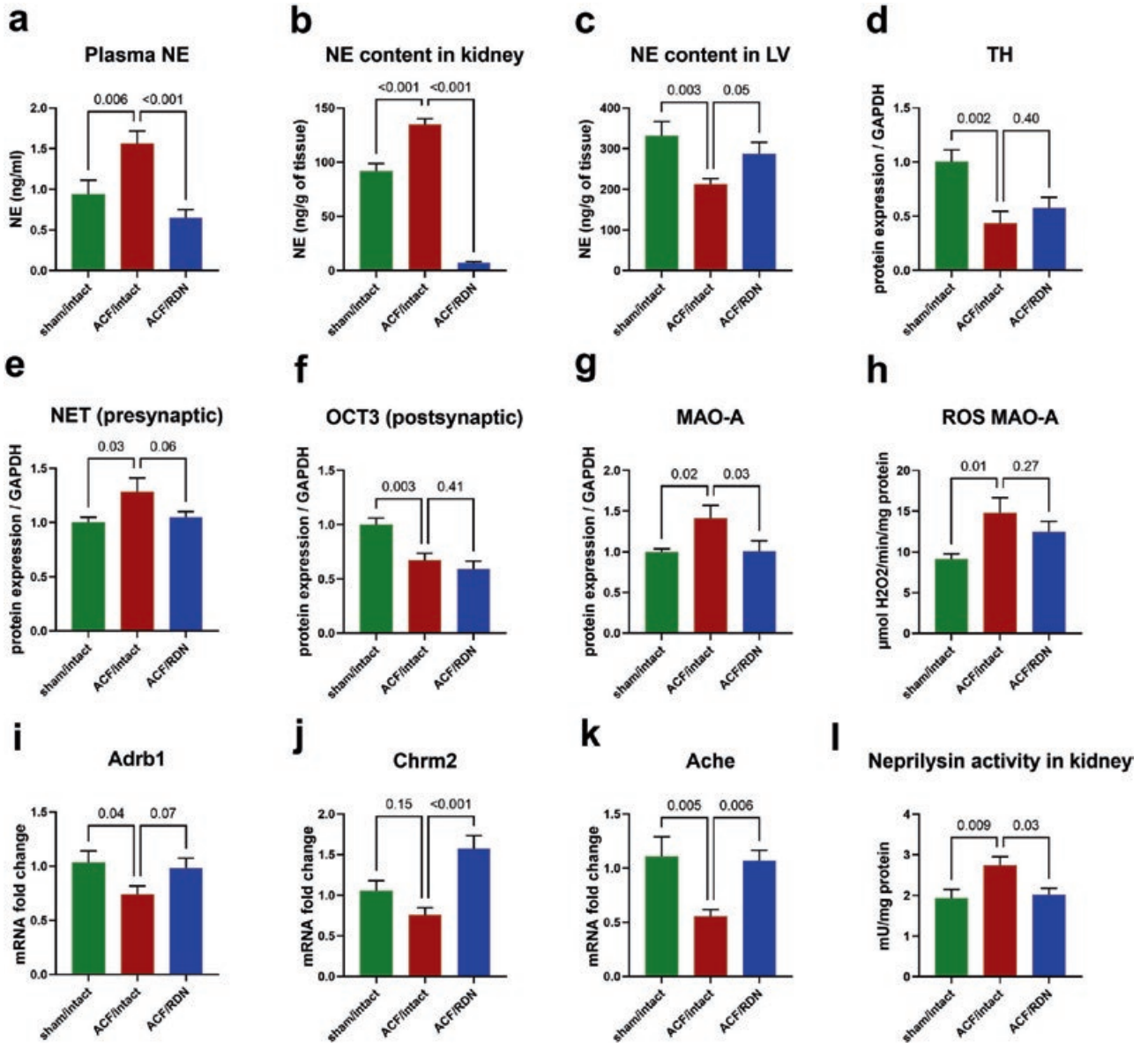

Fig. 3 Impact of ACF and effects of RDN on selected parameters of sympathetic nervous system in left ventricle. **a** Plasma norepinephrine (NE). **b** NE content in kidney. **c** NE content in left ventricle (LV). **d** Biosynthesis of NE—protein expression of tyrosine hydroxylase (TH). **e** Preganglionic NE transport—protein expression of NE transporter (NET). **f** NE transport to cardiomyocyte—protein expression of organic cation transporter 3 (OCT3). **g** Degradation of NE—protein expression of monoamine oxidase A (MAO-A). **h** Production of reactive oxygen species (ROS) by MAO-A. **i** Gene expression of beta-1 adrenergic receptor (Adrb1). **j** Gene expression of choline muscarinic receptor type 2 (Chrm2). **k** Gene expression of acetylcholinesterase (Ache). **l** Neprilysin activity measured in kidney. $N = 8$ in sham/intact, $N = 8$ in ACF/intact, $N = 8$ in ACF/RDN

control group (Fig. 3f). MAO-A, NE-degrading enzyme was upregulated (Fig. 3g) and correspondingly, ROS generated by MAO-A (Fig. 3h) were increased in ACF LV, while gene expression of Adrb1 was downregulated compared to sham/intact group (Fig. 3i).

In parasympathetic cardiac signalization, ACF/intact rats had decreased acetylcholinesterase (Ache) and an unsignificant trend to decreased choline muscarinic receptor type 2 (Chrm2, Fig. 3j, k) in the LV compared to sham/intact.

ACF/intact rats displayed increased neprilysin activity in the kidney, compared to the sham/intact group (Fig. 3l).

LV function and HF markers: the impact of RDN

RDN procedure significantly improved LV systolic function in ACF/RDN animals compared to the ACF/intact group. ACF/RDN group had increased Ees, PRSW, and Ees/Ea ratio compared to ACF/intact group (Fig. 2a). Peak LV

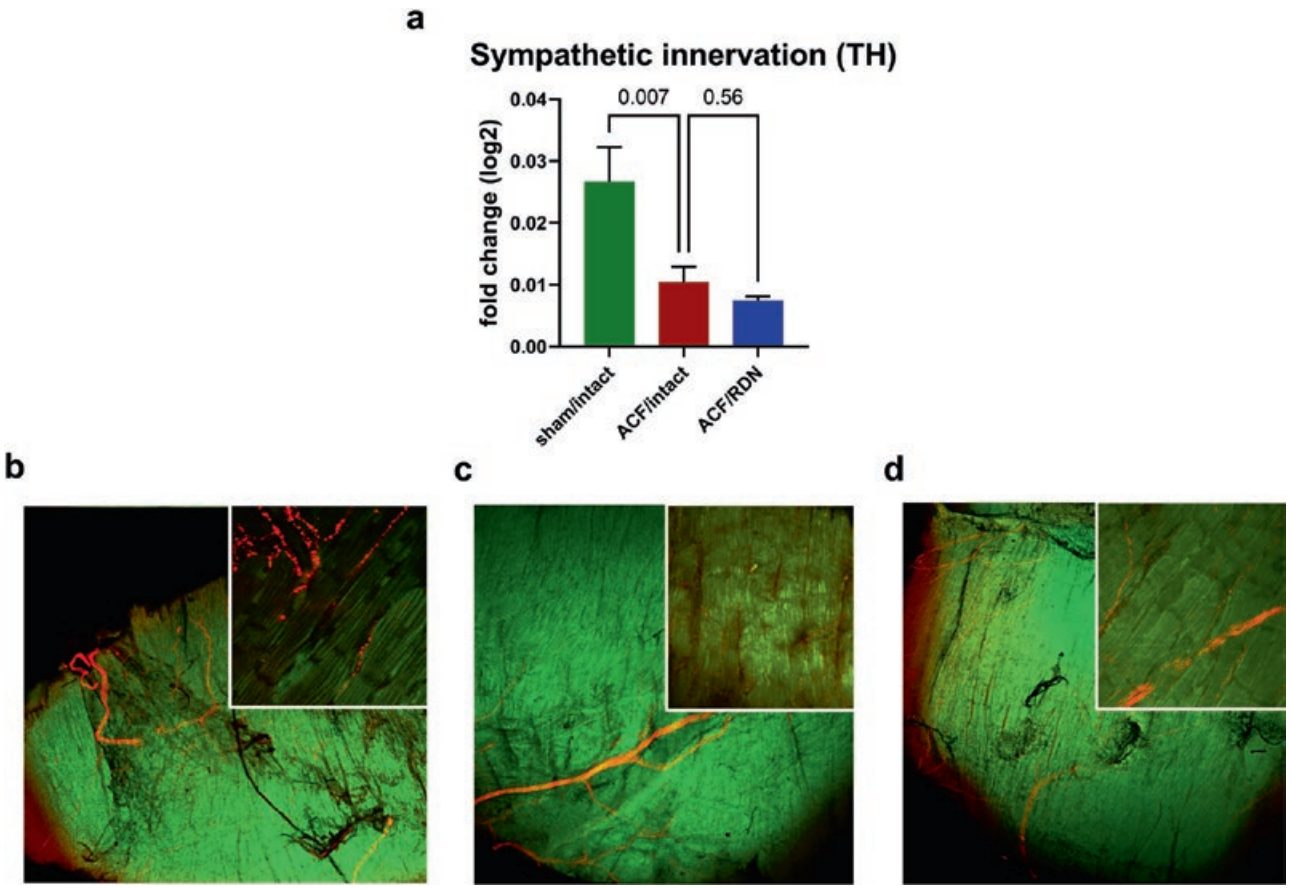

Fig. 4 Results of immunohistochemical staining of tyrosine hydroxylase (TH, red color) in left ventricle. Zoom 25x in a smaller square embedded in an illustrative zoom 2x in a larger square. **a** Ratio of sympathetic nerves immunostained with TH antibody to the total area. **b** sham/intact. **c** ACF/intact. **d** ACF/RDN. $N = 4$ in sham/intact, $N = 5$ in ACF/intact, $N = 4$ in ACF/RDN

pressure or effective arterial elastance (Ea) was not affected by RDN (2 ± 0.23 vs. 2.2 ± 0.22, $p = 0.5$, see Supplementary Information).

ACF/RDN group had less elevated markers of adverse myocardial remodeling compared to ACF/intact group—reduced gene expression of fibrotic markers (Col1a1/Col3a1 ratio), decreased the Myh 7/6 ratio compared to ACF/intact group, while Nppa gene expression was not significantly reduced. After RDN in the ACF group, we did not observe any changes in medium-chain fatty acids in gene expression of Acadm compared to ACF/intact rats (Fig. 2b).

Cardiac autonomic nervous system in HF: the impact of RDN

RDN in ACF rats significantly reduced NE in the plasma and in the kidney (Fig. 3a, b). Despite we targeted the sympathetic nervous system in the kidney, we observed profound changes of sympathetic nerves in the heart—RDN led to increased NE levels in LV compared to ACF/intact rats (Fig. 3c).

In ACF/RDN group, we observed a numerically higher, but not significant increase in protein expression of TH (Fig. 3d). Sympathetic nerve density measured by TH staining was not significantly changed in ACF/RDN compared to ACF/intact (Fig. 4a, d). There was no difference in OCT3 (Fig. 3f), but strong trend to reduce protein expression of NET (presynaptic NE reuptake, $p = 0.06$, Fig. 3e) and significantly reduced MAO-A in ACF/RDN group, compared to ACF/intact rats (Fig. 3g). RDN/ACF rats displayed a trend to ($p = 0.07$) to higher gene expression of Adrb1 (Fig. 3i), and significantly increased gene expression of Chrm2 and Ache (Fig. 3j, k). We observed a significant positive correlation between gene expression of Adrb1 and TH among all groups (see Supplementary Information). RDN in ACF rats significantly reduced the activity of neprilysin in the kidney, compared to ACF/intact rats (Fig. 3l).

Discussion

The principal findings of our study were that volume overload due to ACF leads to overt HF with congestion,

accompanied by cardiac dysfunction, myocardial remodeling, reduced NE content and sympathetic nerve density in the heart, and enhanced sympathetic activation in the kidney. RDN procedure in our HF model reduced congestion and improved cardiac function, independently of changes in afterload, improved markers of cardiac remodeling, and partly restored cardiac NE levels and autonomic signaling. The study indicates that RDN has remote favorable intrinsic effects within the heart and it suggests that RDN could be a therapeutic approach not only for hypertension but also for HF.

Impact of ACF on cardiac function

First, we confirmed that volume overload due to ACF leads to changes in the heart and in other organs consistent with overt HF, which was associated with intrinsic impairment of cardiac function by load-independent PV analysis [22, 35, 36, 45]. We validated our previous observation that the main NE-degrading enzyme—MAO-A is massively upregulated in failing ACF heart, which raised the question of how is cardiac sympathetic system disarranged in ACF [26]. Despite renal and circulating NE levels were massively increased in our HF model, NE levels were reduced in the failing myocardium, in agreement with other HF models, and in humans with advanced HF [5, 6, 46, 47]. Myocardial NE depletion occurred probably due to a combination of increased spillover from the sympathetic endings in the heart due to increased central sympathetic drive, and due to enhanced NE degradation by MAO-A.

Despite altered NE signaling in the failing heart cannot per se explain full cardiac dysfunction [48], it may contribute to abnormal cardiac performance. Increased cardiac NE spillover from sympathetic nerve endings leads to myocardial beta-1 adrenergic downregulation [7–9], diminished heart rate response, and cardiac performance during stress [49]. Increased myocardial NE catabolism by MAO-A, a major ROS-generating enzyme, may promote ROS-driven adverse cardiac remodeling [6]. We found evidence for all these mechanisms in our HF model, indicating that an intact cardiac sympathetic system is relevant for normal cardiac function.

In contrast with some [6, 50] but not all authors [5, 51], we did not find evidence for reduced synaptic NE reuptake in the failing myocardium as the cause of NE depletion. However, we did observe reduced sympathetic nerve density, which has also been found in other experimental HF models [5, 52, 53]. This reduction could result from inadequate sympathetic nerve growth, not paralleling extensive cardiomyocyte hypertrophy (a "dilution" effect), or from nerve damage, caused by high levels of ROS generated by MAO-A [7]. Additionally, the failing ACF hearts exhibited evidence of diminished parasympathetic signaling, suggesting that a vagal withdrawal also contributed to an autonomic imbalance in the failing heart.

Impact of RDN on HF

Using load-independent PV analysis, our data convincingly demonstrate, for the first time, that RDN improves intrinsic myocardial indexes of contractility, such as Ees, PRSW, and Ees/Ea ratio, that were impaired by volume overload. This suggests that favorable myocardial effects of RDN in our HF model occurred beyond simple reduction of cardiac afterload. Reduction in cardiac output and stroke volume in ACF by RDN is considered beneficial and reflects the reduction of hypertrophy and dilation. The restitution of load-independent contractility was also accompanied by direct evidence of more favorable myocardial remodeling, as indicated by less abnormal gene expression of Myh 7/6 ratio and collagen I/III ratio in the ACF heart after RDN. The improvements in cardiac function and remodeling were complemented by the marked effects of RDN on the cardiac autonomic nervous system.

Notably, RDN in ACF animals reduced circulating NE, but it increased abnormally low NE levels in the LV. The increase of myocardial NE content was not explainable by increased growth of sympathetic nerves (as TH gene expression and nerve densities were similar), or presynaptic or postsynaptic transport by NET or OCT3. Increased myocardial NE content may be due to attenuated central sympathetic drive by RDN, with less NE being released from nerve endings. It is known from previous studies, that RDN eliminates not only efferent sympathetic nerves but also afferent, centrally projecting nerve fibers, which regulate the central sympathetic drive toward the heart [1, 3, 54], and these central effects of RDN may be actually dominant. Experimental denervation of the stellate ganglion and renal afferent denervation had a similar cardiorenal protective effect [55]. Based on the observed effects of RDN on NE plasmatic and cardiac levels in the ACF model, we propose that the mechanism leading to increased myocardial NE content may be in reduced cardiac spillover due to diminished central sympathetic drive toward the heart, which was not measured in our study but was confirmed by direct neural recordings in a sheep HF model [56]. Myocardial MAO-A expression, which was also reduced after RDN, may be responsive to diminished NE exposure and this decrease in MAO-A may further beget less NE degradation [6]. Follow-up studies with measurements of myocardial NE kinetics and with measurements of systemic sympathetic nerve activity would be necessary to confirm our assumptions.

Besides the strong effect of RDN on the cardiac sympathetic system, RDN may influence parasympathetic signaling, as evidenced by increased gene expression of

Chrm2 and Ache in ACF. A catheter-based RDN in ovine HF supports this suggestion that RDN is increasing cardiac parasympathetic nerve activity and controls heart rate, however, further comprehensive investigations are required to fully understand the effect of RDN on the cardiac parasympathetic nervous system [56, 57].

The improvements in cardiac structure and function induced by RDN are more likely to explain improved survival in the ACF model, than the direct effects of RDN on renal hemodynamics. This was shown by our previous study, where RDN improved survival rate, but had no effect on reduced renal blood flow or exaggerated renal vascular responsiveness to angiotensin II [19]. Yet, the kidneys can participate in the beneficial effect of RDN by less pronounced neurohumoral activation in ACF after RDN. Besides reducing renal NE content and spillover, RDN reduces renal neprilysin activity, thus leading to less degradation of cardioprotective natriuretic peptides [2, 43]. RDN has therefore similar, or even greater, effects as neprilysin inhibitor sacubitril [43].

Effect of RDN in other HF models and clinical implications

Experimental studies of RDN in other HF models, using less accurate methodology, also indicated, that cardioprotective effects of RDN may be mediated beyond pressure reduction [19, 24]. Besides the effects of RDN on cardiac hypertrophy and congestion, RDN improved myocardial function, ventricular and atrial fibrosis in the ischemia-reperfusion swine model [58], and in rabbits with rapid ventricular pacing [16]. RDN also improved survival, decreased sympathetic nerve activity and catecholamine spillover, reduced fibrosis, and improved LV function (assessed by LV ejection fraction) in myocardial infarction-induced HF in dogs, or in rats [2, 32, 43, 59]. None of these studies used precise load-independent LV function assessment, in contrast to our study.

The specific clinical implication of RDN lies in its potential to modulate the sympathetic nervous system [12, 60, 61]. Sympathetic overactivity is associated with conditions such as HF, resistant hypertension, and chronic kidney disease. RDN aims to disrupt the excessive sympathetic nerve activity by selectively ablating or modulating the renal sympathetic nerves, potentially leading to a reduction in sympathetic outflow and restoration of NE signaling in the heart [18, 62], attenuation of neurohumoral activation, and normalization of cardiac autonomic control. This modulation of sympathetic activity by RDN may help manage HF, improve cardiac function, and potentially improve outcomes [3, 10, 56]. Despite RDN affects multiple targets in HF, it is likely still relatively organ-selective, not causing systemic hypotension, in contrast to an unselective drug-induced central inhibition of sympathetic outflow, that was associated with worse outcomes in HF [20]. The absence of the hypotensive effect of RDN in HF models is also an important aspect, because hypotension complicates the management of more advanced phases of HF and often represents a critical limit for more aggressive pharmacotherapy.

Our study has some limitations. To accelerate the onset of cardiac dysfunction, which in normotensive strains may take 15–20 weeks [30, 63], we utilized the hypertensive TGR strain, where HF develops earlier and myocardial changes may be more pronounced than in normotensive strains. Due to high pressure and volume overload in ACF, an increased volume is ejected into the arteries, and consequently, there is a decrease in vascular resistance, elasticity, and peripheral vascular resistance [64]. Thus, Ea is already significantly reduced in the early stages of the ACF model (Supplementary Fig. 1), and RDN probably did not have the capacity to reduce it even lower. We used unselective chemical and mechanical ablation of the renal nerves which may differ from RDN by radiofrequency energy. The durability of RDN effects and potential reinnervation was not studied. We did not directly measure the central sympathetic nerve drive or NE spillover. Based on RDN-induced changes in the cardiac autonomic nervous system it could be suggested that systemic sympathetic nerve activity was decreased after RDN, however, we did not evaluate any other markers of systemic sympathetic nerve activity. Because we used NE kidney levels as a marker of success of RDN, we cannot use them as a marker of reduced systemic sympathetic nerve activity in denervated rats. Unfortunately, we cannot quantify and localize which part of myocardial MAO-A came from sympathetic neurons or from cardiomyocytes.

In conclusion, our results showed that RDN improved LV contractility and function independently of cardiac loading, attenuated abnormal cardiac remodeling, restored cardiac NE levels and cardiac autonomic signaling in HF, induced by chronic volume overload. These changes likely explain previously observed improvement of survival after RDN in this model [19]. The results suggest that RDN has remote favorable intrinsic effects within the heart and RDN could be a useful therapeutic strategy in HF.

Acknowledgements We express our gratitude to all the individuals who took part in this study and the personnel at the Experimental Medicine Center—IKEM, particularly Prof. Ludek Cervenka.

Funding This work has been supported by Ministry of Health of the Czech Republic, grant nos. NU22-02-00161, NV19-02-00130, NU-20-02-00052. All rights reserved. Project National Institute for Research of Metabolic and Cardiovascular Diseases (Programme EXCELES, Project no. LX22NPO5104)—Funded by the European Union—Next Generation EU, and Grant Agency of Charles University (GAUK), grant number 304121. Open access publishing supported by the National Technical Library in Prague.

Compliance with ethical standards

Conflict of interest The authors declare no competing interests.

Publisher's note Springer Nature remains neutral with regard to jurisdictional claims in published maps and institutional affiliations.

References

1. Katsurada K, Ogoyama Y, Imai Y, Patel KP, Kario K. Renal denervation based on experimental rationale. Hypertens Res. 2021;44:1385–94.
2. Polhemus DJ, Gao J, Scarborough AL, Trivedi R, McDonough KH, Goodchild TT, et al. Radiofrequency renal denervation protects the ischemic heart via inhibition of GRK2 and increased nitric oxide signaling. Circ Res. 2016;119:470–80.
3. Sharp TE, Lefer DJ. Renal denervation to treat heart failure. Annu Rev Physiol. 2021;83:39–58.
4. Thomas JA, Marks BH. Plasma norepinephrine in congestive heart failure. Am J Cardiol. 1978;41:233–43.
5. Kristen AV, Kreusser MM, Lehmann L, Kinscherf R, Katus HA, Haass M, et al. Preserved norepinephrine reuptake but reduced sympathetic nerve endings in hypertrophic volume-overloaded rat hearts. J Card Fail. 2006;12:577–83.
6. Kaludercic N, Takimoto E, Nagayama T, Feng N, Lai EW, Bedja D, et al. Monoamine oxidase A-mediated enhanced catabolism of norepinephrine contributes to adverse remodeling and pump failure in hearts with pressure overload. Circ Res. 2010;106:193–202.
7. Liang CS, Rounds NK, Dong E, Stevens SY, Shite J, Qin F. Alterations by norepinephrine of cardiac sympathetic nerve terminal function and myocardial β-adrenergic receptor sensitivity in the ferret: normalization by antioxidant vitamins. Circulation. 2000;102:96–103.
8. Liggett SB. Desensitization of the β-adrenergic recepton: distinct molecular determinants of phosphorylation by specific kinases. Pharm Res. 1991;24:29–41.
9. Schwinn DA, Leone BJ, Spahn DR, Chesnut LC, Page SO, McRae RL, et al. Desensitization of myocardial beta-adrenergic receptors during cardiopulmonary bypass. Evidence for early uncoupling and late downregulation. Circulation. 1991;84:2559–67.
10. Krum H, Schlaich M, Whitbourn R, Sobotka PA, Sadowski J, Bartus K, et al. Catheter-based renal sympathetic denervation for resistant hypertension: a multicentre safety and proof-of-principle cohort study. Lancet. 2009;373:1275–81.
11. Mahfoud F, Tunev S, Ewen S, Cremers B, Ruwart J, Schulz-Jander D, et al. Impact of lesion placement on efficacy and safety of catheter-based radiofrequency renal denervation. J Am Coll Cardiol. 2015;66:1766–75.
12. Townsend RR, Mahfoud F, Kandzari DE, Kario K, Pocock S, Weber MA, et al. Catheter-based renal denervation in patients with uncontrolled hypertension in the absence of antihypertensive medications (SPYRAL HTN-OFF MED): a randomised, sham-controlled, proof-of-concept trial. Lancet. 2017;390:2160–70.
13. Felix M, Jean R, Horst S, Stefan B, Sebastian E, Michael B, et al. Alcohol-mediated renal denervation using the peregrine system infusion catheter for treatment of hypertension. JACC Cardiovasc Inter. 2020;13:471–84.
14. Azizi M, Schmieder RE, Mahfoud F, Weber MA, Daemen J, Davies J, et al. Endovascular ultrasound renal denervation to treat hypertension (RADIANCE-HTN SOLO): a multicentre, international, single-blind, randomised, sham-controlled trial. Lancet. 2018;391:2335–45.
15. Mahfoud F, Böhm M, Schmieder R, Narkiewicz K, Ewen S, Ruilope L, et al. Effects of renal denervation on kidney function and long-term outcomes: 3-year follow-up from the Global SYMPLICITY Registry. Eur Heart J. 2019;40:3474–82.
16. Yamada S, Lo LW, Chou YH, Lin WL, Chang SL, Lin YJ, et al. Renal denervation ameliorates the risk of ventricular fibrillation in overweight and heart failure. Europace. 2020;22:657–66.
17. Mahfoud F, Kandzari DE, Kario K, Townsend RR, Weber MA, Schmieder RE, et al. Long-term efficacy and safety of renal denervation in the presence of antihypertensive drugs (SPYRAL HTN-ON MED): a randomised, sham-controlled trial. Lancet. 2022;399:1401–10.
18. Katsurada K, Shinohara K, Aoki J, Nanto S, Kario K. Renal denervation: basic and clinical evidence. Hypertens Res. 2022;45:198–209.
19. Honetschlagerová Z, Gawrys O, Jíchová Š, Škaroupková P, Kikerlová S, Vaňourková Z, et al. Renal sympathetic denervation attenuates congestive heart failure in angiotensin II-dependent hypertension: studies with Ren-2 transgenic hypertensive rats with aortocaval fistula. Kidney Blood Press Res. 2021;46:95–113.
20. Cohn JN, Pfeffer MA, Rouleau J, Sharpe N, Swedberg K, Straub M, et al. Adverse mortality effect of central sympathetic inhibition with sustained-release moxonidine in patients with heart failure (MOXCON). Eur J Heart Fail. 2003;5:659–67.
21. Garcia R, Diebold S. Simple, rapid, and effective method of producing aortocaval shunts in the rat. Cardiovasc Res. 1990;24:430–2.
22. Jarkovská D, Miklovič M, Švíglerová J, Červenka L, Škaroupková P, Melenovský V, et al. Effects of trandolapril on structural, contractile and electrophysiological remodeling in experimental volume overload heart failure. Front Pharm. 2021;12:729568.
23. Sharkovska Y, Kalk P, Lawrenz B, Godes M, Hoffmann LS, Wellkisch K, et al. Nitric oxide-independent stimulation of soluble guanylate cyclase reduces organ damage in experimental low-renin and high-renin models. J Hypertens. 2010;28:1666–75.
24. Honetschlägerová Z, Hejnová L, Novotný J, Marek A, Červenka L. Effects of renal denervation on the enhanced renal vascular responsiveness to angiotensin II in high-output heart failure: angiotensin II receptor binding assessment and functional studies in ren-2 transgenic hypertensive rats. Biomedicines. 2021;9:1803.
25. Abassi Z, Goltsman I, Karram T, Winaver J, Hoffman A. Aortocaval fistula in rat: a unique model of volume-overload congestive heart failure and cardiac hypertrophy. 2011;2011:729497.
26. Petrak J, Pospisilova J, Sedinova M, Jedelsky P, Lorkova L, Vit O, et al. Proteomic and transcriptomic analysis of heart failure due to volume overload in a rat aorto-caval fistula model provides support for new potential therapeutic targets—monoamine oxidase A and transglutaminase 2. Proteome Sci. 2011;9:69.
27. Mullins JJ, Peters J, Ganten D. Fulminant hypertension in transgenic rats harbouring the mouse Ren-2 gene. Nature. 1990;344:541–4.
28. Bello Reuss E, Colindres RE, Pastoriza Munoz E, Pastoriza-Muñoz E, Mueller RA, Gottschalk CW. Effects of acute unilateral renal denervation in the rat. J Clin Invest. 1975;56:208–17.
29. Eriguchi M, Tsuruya K. Renal sympathetic denervation in rats. Methods Mol Biol. 2016;1397:45–52.

30. Kratky V, Vanourkova Z, Sykora M, Bacova BS, Hruskova Z, Kikerlova S, et al. AT1 receptor blocker, but not an ACE inhibitor, prevents kidneys from hypoperfusion during congestive heart failure in normotensive and hypertensive rats. Sci Rep. 2021;11:4271.
31. Ikeda S, Shinohara K, Kashihara S, Matsumoto S, Yoshida D, Nakashima R, et al. Contribution of afferent renal nerve signals to acute and chronic blood pressure regulation in stroke-prone spontaneously hypertensive rats. Hypertens Res. 2022;46:268–79.
32. Pinkham MI, Loftus MT, Amirapu S, Guild SJ, Quill G, Woodward WR, et al. Renal denervation in male rats with heart failure improves ventricular sympathetic nerve innervation and function. Am J Physiol Regul Integr Comp Physiol. 2017;312:R368–79.
33. Osborn JW, Foss JD. Renal nerves and long-term control of arterial pressure. Compr Physiol. 2017;7:263–320.
34. Miklovič M, Kala P, Melenovský V. Simultaneous biventricular pressure-volume analysis in rats. J Physiol Pharmacol. 2023;74:131–147.
35. Kala P, Miklovič M, Jíchová Š, Škaroupková P, Vaňourková Z, Maxová H, et al. Effects of epoxyeicosatrienoic acid-enhancing therapy on the course of congestive heart failure in angiotensin II-dependent rat hypertension: from mrna analysis towards functional in vivo evaluation. Biomedicines. 2021;9:1053.
36. Havlenova T, Skaroupkova P, Miklovic M, Behounek M, Chmel M, Jarkovska D, et al. Right versus left ventricular remodeling in heart failure due to chronic volume overload. Sci Rep. 2021;11:1–17.
37. Kala P, Bartušková H, Pit'ha J, Vaňourková Z, Kikerlová S, Jíchová Š, et al. Deleterious effects of hyperactivity of the renin-angiotensin system and hypertension on the course of chemotherapy-induced heart failure after doxorubicin administration: a study in ren-2 transgenic rat. Int J Mol Sci. 2020;21:1–20.
38. Livak KJ, Schmittgen TD. Analysis of relative gene expression data using real-time quantitative PCR and the $2-\Delta\Delta CT$ method. Methods. 2001;25:402–8.
39. Schmittgen TD, Zakrajsek BA, Mills AG, Gorn V, Singer MJ, Reed MW. Quantitative reverse transcription-polymerase chain reaction to study mRNA decay: comparison of endpoint and real-time methods. Anal Biochem. 2000;285:194–204.
40. Winer J, Jung CKS, Shackel I, Williams PM. Development and validation of real-time quantitative reverse transcriptase–polymerase chain reaction for monitoring gene expression in cardiac myocytesin vitro. Anal Biochem. 1999;270:41–9.
41. Bohuslavova R, Cerychova R, Papousek F, Olejnickova V, Bartos M, Görlach A, et al. HIF-1α is required for development of the sympathetic nervous system. Proc Natl Acad Sci USA. 2019;116:13414–23.
42. Kolesová H, Čapek M, Radochová B, Janáček J, Sedmera D. Comparison of different tissue clearing methods and 3D imaging techniques for visualization of GFP-expressing mouse embryos and embryonic hearts. Histochem Cell Biol. 2016;146:141–52.
43. Polhemus DJ, Trivedi RK, Gao J, Li Z, Scarborough AL, Goodchild TT, et al. Renal sympathetic denervation protects the failing heart via inhibition of neprilysin activity in the kidney. J Am Coll Cardiol. 2017;70:2139–53.
44. Carpenter TC, Stenmark KR. Hypoxia decreases lung neprilysin expression and increases pulmonary vascular leak. Am J Physiol Cell Mol Physiol. 2001;281:L941–8.
45. Kala P, Sedláková L, Škaroupková P, Kopkan L, Vaňourková Z, Táborský M, et al. Effect of angiotensin-converting enzyme blockade, alone or combined with blockade of soluble epoxide hydrolase, on the course of congestive heart failure and occurrence of renal dysfunction in Ren-2 transgenic hypertensive rats with aorto-caval fistula. Physiol Res. 2018;67:401–15.
46. Eisenhofer G, Kopin IJ, Goldstein DS. Leaky catecholamine stores: undue waste or a stress response coping mechanism? Ann N Y Acad Sci. 2004;1018:224–30.
47. Dequattro V, Nagatsu T, Mendez A, Verska J. Determinants of cardiac noradrenaline depletion in human congestive failure. Cardiovasc Res. 1973;7:344–50.
48. Spann JF, Sonnenblick EH, Cooper T, Chidsey CA, Willman VL, Braunwald E. Cardiac norepinephrine stores and the contractile state of heart muscle. Circ Res. 1966;19:317–25.
49. Lakatta EG, Gerstenblith G, Angell CS, Shock NW, Weisfeldt ML. Diminished inotropic response of aged myocardium to catecholamines. Circ Res. 1975;36:262–9.
50. Backs J, Haunstetter A, Gerber SH, Metz J, Borst MM, Strasser RH, et al. The neuronal norepinephrine transporter in experimental heart failure: evidence for a posttranscriptional down-regulation. J Mol Cell Cardiol. 2001;33:461–72.
51. Hu B, Zhang J, Wang J, He B, Wang D, Zhang W, et al. Responses of PKCε to cardiac overloads on myocardial sympathetic innervation and NET expression. Auton Neurosci Basic Clin. 2018;210:24–33.
52. Himura Y, Felten SY, Kashiki M, Lewandowski TJ, Delehanty JM, Liang CS. Cardiac noradrenergic nerve terminal abnormalities in dogs with experimental congestive heart failure. Circulation. 1993;88:1299–309.
53. Kaye DM, Vaddadi G, Gruskin SL, Du XJ, Esler MD. Reduced myocardial nerve growth factor expression in human and experimental heart failure. Circ Res. 2000;86:e80–4.
54. Tsai WC, Chan YH, Chinda K, Chen Z, Patel J, Shen C, et al. Effects of renal sympathetic denervation on the stellate ganglion and brain stem in dogs. Hear Rhythm. 2017;14:255–62.
55. Zhiqiu X, Nanoth VN, Li H, Lie G, Boesen EI, Schiller AM, et al. Cardiac spinal afferent denervation attenuates renal dysfunction in rats with cardiorenal syndrome type 2. JACC Basic Transl Sci. 2022;7:582–96.
56. Booth LC, De Silva RAU, Pontes RB, Yao ST, Hood SG, Lankadeva YR, et al. Renal, cardiac, and autonomic effects of catheter-based renal denervation in ovine heart failure. Hypertension. 2021;78:706–15.
57. Van Amsterdam WAC, Blankestijn PJ, Goldschmeding R, Bleys RLAW. The morphological substrate for renal denervation: nerve distribution patterns and parasympathetic nerves. A post-mortem histological study. Ann Anat. 2016;204:71–9.
58. Sharp TE, Polhemus DJ, Li Z, Spaletra P, Jenkins JS, Reilly JP, et al. Renal denervation prevents heart failure progression via inhibition of the renin-angiotensin system. J Am Coll Cardiol. 2018;72:2609–21.
59. Zhang W, Zhou Q, Lu Y, Li Y, Zhang L, Zhang J, et al. Renal denervation reduced ventricular arrhythmia after myocardial infarction by inhibiting sympathetic activity and remodeling. J Am Heart Assoc. 2018;7:e009938.
60. Schroeder C, Jordan J. Norepinephrine transporter function and human cardiovascular disease. Am J Physiol Circ Physiol. 2012;303:H1273–82.
61. Brandt MC, Mahfoud F, Reda S, Schirmer SH, Erdmann E, Böhm M, et al. Renal sympathetic denervation reduces left ventricular hypertrophy and improves cardiac function in patients with resistant hypertension. J Am Coll Cardiol. 2012;59:901–9.
62. Kario K, Wang TD. Perspectives of renal denervation from hypertension to heart failure in Asia. Hypertens Res. 2022;45:193–7.
63. Kala P, Červenka L, Škaroupková P, Táborský M, Kompanowska-Jezierska E, Sadowski J. Sex-linked differences in the mortality in Ren-2 transgenic hypertensive rats with aorto-caval fistula: effects of treatment with angiotensin converting enzyme alone and combined with inhibitor of soluble epoxide hydrolase. Physiol Res. 2019;68:589–601.
64. Valerianova A, Mlcek M, Grus T, Malik J, Kittnar O. New porcine model of arteriovenous fistula documents increased coronary blood flow at the cost of brain perfusion. Front Physiol. 2022;13:1–8.

P. Kuchynka et al.

Long-term outcomes and reverse remodelling in recently diagnosed unexplained left ventricular systolic dysfunction

ESC Heart Failure
Impact Factor: 3,8

‹ rejstřík

ESC HEART FAILURE
ESC Heart Failure 2024; **11**: 859–870
Published online 10 January 2024 in Wiley Online Library (wileyonlinelibrary.com) **DOI:** 10.1002/ehf2.14643

ORIGINAL ARTICLE

Long-term outcomes and reverse remodelling in recently diagnosed unexplained left ventricular systolic dysfunction

Petr Kuchynka[1], Jana Podzimkova[1], Josef Marek[1], Barbara Anna Danek[2], Ivana Vitkova[3], Miluse Kreidlova[4], Lenka Roblova[1], Tomas Kovarnik[1], Stanislav Simek[1], Jan Horak[1], Jan Habasko[1], Ales Linhart[1] and Tomas Palecek[1]*

[1]*2nd Department of Medicine, Department of Cardiovascular Medicine, First Faculty of Medicine, Charles University in Prague and General University Hospital in Prague, Prague, Czech Republic;* [2]*Division of Cardiology, University of Washington Medical Center, Seattle, WA, USA;* [3]*Institute of Pathology, First Faculty of Medicine, Charles University and General University Hospital in Prague, Prague, Czech Republic; and* [4]*Institute of Medical Biochemistry and Laboratory Diagnostics, First Faculty of Medicine, Charles University and General University Hospital in Prague, Prague, Czech Republic*

Abstract

Aims In patients with recently diagnosed non-ischaemic LV systolic dysfunction, left ventricular reverse remodelling (LVRR) and favourable prognosis has been documented in studies with short-term follow-up. The aim of our study was to assess the long-term clinical course and stability of LVRR in these patients.

Methods and results We prospectively studied 133 patients (37 women; 55 [interquartile range 46, 61] years) with recently diagnosed unexplained LV systolic dysfunction, with heart failure symptoms lasting <6 months and LV ejection fraction <40% persisting after at least 1 week of therapy. All patients underwent endomyocardial biopsy (EMB) at the time of diagnosis and serial echocardiographic and clinical follow-up over 5 years. LVRR was defined as the combined presence of (1) LVEF ≥ 50% or increase in LVEF ≥ 10% points and (2) decrease in LV end-diastolic diameter index (LVEDDi) ≥ 10% *or* (3) LVEDDi ≤ 33 mm/m^2. LVRR was observed in 46% patients at 1 year, in 60% at 2 years and 50% at 5 years. Additionally, 2% of patients underwent heart transplantation and 12% experienced heart failure hospitalization. During 5-year follow-up, 23 (17%) of the study cohort died. In multivariate analysis, independent predictors of mortality were baseline right atrial size (OR 1.097, CI 1.007–1.196), logBNP level (OR 2.02, CI 1.14–3.56), and PR interval (OR 1.02, CI 1.006–1.035) ($P < 0.05$ for all). The number of macrophages on EMB was associated with overall survival in univariate analysis only. LVRR at 1 year of follow-up was associated with a lower rate of mortality and heart failure hospitalization ($P = 0.025$). In multivariate analysis, independent predictors of LVRR were left ventricular end-diastolic volume index (OR 0.97, CI 0.946–0.988), LVEF (OR 0.89, CI 0.83–0.96), and diastolic blood pressure (OR 1.04, CI 1.01–1.08) ($P < 0.05$ for all).

Conclusions LVRR occurs in over half of patients with recent onset unexplained LV systolic dysfunction during first 2 years of optimally guided heart failure therapy and then remains relatively stable during 5-year follow-up. Normalization of adverse LV remodelling corresponds to a low rate of mortality and heart failure hospitalizations during long-term follow-up.

Keywords Dilated cardiomyopathy; Endomyocardial biopsy; Left ventricular systolic dysfunction; Mortality; Reverse remodelling

Received: 15 March 2023; Revised: 7 November 2023; Accepted: 5 December 2023
**Correspondence to: Tomas Palecek, 2nd Department of Medicine, Department of Cardiovascular Medicine, General University Hospital in Prague, First Faculty of Medicine, Charles University in Prague, U Nemocnice 2, 128 08 Prague 2, Czech Republic. Email: tomas.palecek@vfn.cz*
[Correction added on 30 January 2024, after first online publication: Article title has been corrected in this version.]

Introduction

Dilated cardiomyopathy (DCM) is defined by the presence of left ventricular (LV) or biventricular dilatation and LV systolic dysfunction in the absence of abnormal loading conditions or coronary artery disease sufficient to cause global systolic impairment.[1] It still represents the third most common cause of heart failure with reduced ejection fraction, and the most frequent reason for heart transplantation.[2] Nevertheless, the prognosis of patients with DCM has markedly

improved due to advances in pharmacological as well as non-pharmacological heart failure therapy. In many patients, left ventricular reverse remodelling (LVRR) occurs because of medications including ACE inhibitors/ARBs, beta-blockers and mineralocorticoid receptor antagonists (MRA) and, when indicated, cardiac resynchronization therapy (CRT-D or CRT-P).[3]

In the last decade, many studies have shown that LVRR occurs in at least one third of patients, especially in those with recently diagnosed non-ischaemic LV systolic dysfunction.[4–8] Several clinical and echocardiographic predictors of LVRR have been suggested. However, a majority of these studies had only short or mid-term clinical or echocardiographic follow-up and endomyocardial biopsy (EMB) was used to characterize the presence of inflammatory cardiomyopathy in only a few of these cohorts. Therefore, the aim of our study was to assess long-term clinical course and predictors of mortality and LVRR in regularly followed patients with recently diagnosed unexplained LV systolic dysfunction undergoing EMB.

Methods

We prospectively studied 133 consecutive patients with recently diagnosed unexplained LV systolic dysfunction who were referred to our institution between April 2007 and November 2013 for further diagnostic evaluation. All individuals had a history of heart failure symptoms <6 months, LV ejection fraction (EF) < 40% persisting after at least 1 week of conventional heart failure therapy according to current guidelines.[9] The criteria of unexplained LV systolic dysfunction were based on exclusion of the following: significant coronary artery disease as assessed by invasive coronary angiography, the development of symptoms during pregnancy or in postpartum period, Takotsubo syndrome, presence of moderate or severe primary valvulopathy, haemodynamically significant congenital heart disease, atrial fibrillation or any other supraventricular arrhythmia with ventricular rate >100/min, frequent ventricular ectopy, any uncorrected metabolic or endocrine disorder, systemic autoimmune disease, history of alcohol or drug abuse, history of cardiotoxic oncological treatment, and family history of DCM.[10] Signed informed consent was obtained from all patients in a format standardized by our institution. This investigation conforms to the principles outlined in the Declaration of Helsinki.

The baseline diagnostic evaluation included physical examination, assessment of heart failure symptoms according to the New York Heart Association (NYHA) classification, 12-lead electrocardiogram (ECG), transthoracic echocardiography, EMB, and blood tests including complete biochemical analysis and blood count.

All echocardiographic measurements were performed as recommended by the current guidelines of the European Association of Cardiovascular Imaging and the American Society of Echocardiography, respectively.[11,12] Namely, LV diameters were measured by 2D echocardiography in the parasternal long-axis view. LV volumes and LVEF were calculated from the apical 2-chamber and 4-chamber view using the biplane method of disks. Left atrial volume (LAV), right atrial area (RA area), right ventricular end-diastolic diameter (RVEDD) and tricuspid annular plane systolic excursion (TAPSE) were all assessed in the apical 4-chamber view. Doppler indices of LV diastolic function including peak early diastolic mitral inflow velocity (E) and early mitral annular velocities averaged together (e') were measured in the apical 4-chamber view. Pulmonary artery systolic pressure (PASP) was estimated as the sum of the measured peak tricuspid regurgitation gradient and the estimated RA pressure based on inferior vena cava respiratory variability. The severity of mitral as well as tricuspid regurgitation was classified semi-quantitatively with a four-grade scale.

EMB was performed with a flexible bioptome (Cordis, USA), from the interventricular septum accessed via the right internal jugular vein. At least six EMB specimens were obtained from each patient. At least two samples were placed in 10% formalin solution and subsequently underwent histopathological and immunohistochemical analysis. Four EMB specimens were placed in saline and immediately transported to a specialized laboratory for detection of the presence of viruses using PCR analysis and electron microscopy. PCR and reverse transcription PCR analysis was focused on detection of herpetic viruses (herpesvirus type 1 and 2, human cytomegalovirus, Epstein–Barr virus and human herpesvirus type 6), enteroviruses (including coxsackievirus and echovirus), adenoviruses and parvovirus B19. Histological analysis was performed using the Dallas criteria for acute myocarditis.[13] Immunohistochemical analysis consisted of staining for LCA +, CD3+ and CD68+ immunocompetent cells. Myocardial inflammation was defined as the presence of ≥14 leucocytes/mm^2 including ≥7 lymphocytes/mm^2.[14]

During the 5-year follow-up period, patients underwent comprehensive clinical evaluation and transthoracic echocardiography at least once a year. The data obtained in the 1st, 2nd, and 5th year of follow-up are presented. For the purpose of the current study, LVRR was defined as the combined presence of (1) LVEF ≥50% or increase in LVEF ≥10% points and (2) decrease in LV end-diastolic diameter index (LVEDDi) ≥10% *or* (3) LVEDDi ≤33 mm/m^2 (4). LVEF recovery was defined by LVEF ≥ 50% documented at least at once during the above-described follow-up visits. Sustained LVEF recovery was defined as LVEF ≥50% that persisted until the last follow-up. Placement of an implantable cardioverter-defibrillator (ICD) or cardiac resynchronization therapy device with the added capability for defibrillation (CRT-D) was recommended to all patients who fulfilled valid criteria according to dedicated guidelines.[15]

Statistics

Continuous variables were summarized using mean ± standard deviation or median [25th, 75th percentile], as appropriate. The Shapiro-Wilks test for normality was used. Discrete variables were summarized using proportions. Survival analysis was performed using the Kaplan–Meier method and the Cox proportional hazards model was used for multivariate survival modelling. Variables with statistically significant associations with the outcomes of interest in univariate models were used in multivariate modelling. Predictors of LVRR were analysed using logistic regression. In the multivariate model, to avoid redundancy we chose only one baseline LV geometry parameter: LV end-diastolic volume index (LVEDVi) and selection was done using fast backward elimination algorithm.[16] Numeric changes in LVEF and LVEDDi during follow-up were analysed using a linear mixed model for repeated measures. NYHA class at follow-up was compared using the chi-square test. A *P*-value <0.05 was considered significant. R software version 4.1.2 (The R Foundation for statistical computing, Vienna, Austria) was used for statistical analysis.

Table 1 Demographic, clinical, and laboratory characteristics

Number of subjects	133
Age (years)	55 [46, 61]
Gender (women)	37 (27.8%)
Height (cm)	175 ± 10
Weight (kg)	89 ± 20
SBP (mmHg)	116 ± 17
DBP (mmHg)	70 ± 12
Heart rate (b.p.m.)	81 ± 14
HF symptoms duration (days)	56 [28, 123]
NYHA class I/II/III/IV (class)	4/25/45/57
Arterial hypertension	52 (39.1%)
Diabetes mellitus	17 (12.7%)
eGFR (mL/min/1.73 m^2)	78 ± 18
CKD (1/2/3/4/5)	38/72/21/2/0
Sinus rhythm	124 (93.2%)
Atrial fibrillation	9 (7%)
LBBB	25 (18.7%)
BNP (pg/mL)	405 [198, 789]
TnI (μg/L)	0.05 [0.03, 0.16]
CRP (mg/L)	5 [2, 9]

Variables are expressed as means and standard deviations, median [25th, 75th percentile] or as a count and percentage of subjects.
BNP, B-type natriuretic peptide; CKD, chronic kidney disease with grading based on estimation of glomerular filtration rate; CRP, C-reactive protein; DBP, diastolic blood pressure; eGFR, estimation of glomerular filtration rate; HF, heart failure; LBBB, left bundle branch block; NYHA, New York Heart Association; SBP, systolic blood pressure; TnI, troponin I.

Results

The baseline demographic, clinical, laboratory, and echocardiographic characteristics of the study population are summarized in *Tables 1 and 2*, respectively. The majority (77%) of patients had advanced symptoms of heart failure (NYHA class III or IV). BNP levels were significantly elevated (>100 pg/mL) in all study subjects. Twenty-five (19%) study subjects had left bundle branch block. Severely decreased LVEF (<30%) was documented in 107 (80%) individuals.

Endomyocardial biopsy findings are presented in *Table 3*. Histological signs of active or borderline myocarditis according to the Dallas criteria were found in three (2%) patients. Immunohistochemical analysis revealed myocardial inflammation in 22 (17%) patients. In all these patients, the inflammatory infiltrate was lymphocytic. The presence of a viral genome by PCR was detected in 69 (52%) patients. Specifically, PCR was positive for the genome of herpetic viruses in 35 patients, enteroviruses in seven patients, adenoviruses in three patients, and parvovirus B19 in 33 patients. Electron microscopy revealed viral particles in 82 (62%) cases, including viruses belonging to the Herpesviridae family in 50 subjects, to the Picornaviridae family in 34 patients, and to the Parvoviridae family in 30 individuals.

Heart failure medication is summarized in *Table 4*. At 1 year, 120 (100%) patients were treated with ACE inhibitors/ARBs; 118 (98%) patients were treated with beta-blockers; and 80 (67%) patients were treated with mineralocorticoid receptor antagonists. At 2 years, 108 (99%), 109 (100%), and 56 (51%) patients were treated with ACE inhibitors/ARBs, beta-

Table 2 Baseline echocardiographic parameters

Number of subjects	133
LVEDD (mm)	68 ± 7
LVEDDi (mm/m^2)	34 [31, 37]
LVESD (mm)	59 ± 8
LVESDi (mm/m^2)	29 [27, 32]
LVEDV (mL)	199 [159, 239]
LVEDVi (mL/m^2)	96 [83, 114]
LVESV (mL)	143 [113, 176]
LVESVi (mL/m^2)	70 [57, 85]
LVEF (%)	28 ± 7
E (m/s)	0.77 ± 0.26
e' (cm/s)	7 [5, 8]
E/e' ratio	12 [9, 14]
Mitral regurgitation (grade)	2 [1, 2.5]
LAV (mL)	97 [73,122]
LAVi (mL/m^2)	47 [37, 61]
RVEDD (mm)	36 [32, 41]
TAPSE (mm)	18 [15, 21]
Tricuspid regurgitation (grade)	1 [1, 1.5]
RA area (cm^2)	18 [15, 22]
RAP (mmHg)	3 [3, 8]
PASP (mmHg)	36 [27, 47]

Variables are expressed as means and standard deviations or median [25th, 75th percentile].
E, peak early diastolic velocity; e', peak early diastolic mitral annular velocity; LAV, left atrial volume; LAVi indexed, left atrial volume; LVEDD, left ventricular end-diastolic diameter; LVEDDi, indexed left ventricular end-diastolic diameter; LVEDV, left ventricular end-diastolic volume; LVEDVi, indexed left ventricular end-diastolic volume; LVESD, left ventricular end-systolic diameter; LVESDi, indexed left ventricular end-systolic diameter; LVESV, left ventricular end-systolic volume; LVESVi, indexed left ventricular end-systolic volume; LVEF, left ventricular ejection fraction; PASP, pulmonary artery systolic pressure; RA area, right atrial area; RAP, right atrial pressure; RVEDD, right ventricular end-diastolic diameter; TAPSE, tricuspid annular plane systolic excursion.

blockers, and mineralocorticoid receptor antagonists, respectively. At 5 years, 88 (99%), 87 (99%), and 45 (51%) patients were treated with ACE inhibitors/ARBs, beta-blockers, and mineralocorticoid receptor antagonists, respectively. Neither angiotensin receptor-neprilysin inhibitors nor sodium-glucose cotransporter 2 inhibitors were available for heart failure treatment during the study period.

Clinical outcomes

During a median follow-up of 5 years, 23 subjects died (17% of total initial study population). Kaplan–Meier estimates of overall survival are presented in *Figure 1*. One subject underwent heart transplantation at the first year of follow-up, two patients at 2 years, and three patients at 5 years of follow-up, cumulatively. Furthermore, totally 16 subjects experienced hospitalizations for heart failure during the follow-up period. Kaplan–Meier estimates of survival without heart failure hospitalization or transplantation are shown in *Figure 2*. Cumulatively, five patients underwent primary preventive ICD implantation during the first year of follow-up, seven patients at 2 years, and 12 patients at 5 years of follow-up, respectively (total 9% of the initial study population). CRT-D implantation for primary prevention was performed in 10 patients at 1 year, 19 patients at 2 years, and 22 patients at 5 years (total 17% of the initial study population). Only one subject underwent CRT-P implantation. During the follow-up period, 9 out of 34 patients with ICD/CRT-D experienced an appropriate ICD shock. The cumulative rate of appropriate shock in patients with CRT-D or ICD was 13% (2/15) at 1 year, 15% (4/26) at 2 years and 26% (9/34) at 5 years of follow-up, respectively. Inappropriate shocks occurred in three (9%) individuals with ICD/CRT-D during the follow-up period.

Table 3 Endomyocardial biopsy findings

PCR focused on viruses (NAS)	133
- positive endomyocardial biopsy	69 (52%)
EM focused on viruses (NAS)	133
- positive endomyocardial biopsy	82 (62%)
Dallas criteria (NAS)	133
- active or borderline myocarditis +	3 (2%)
IH criteria for myocarditis (NAS)	128
- positive	22 (17%)
HLA DR (NAS)	109
- grade 0/1/2/3	35/35/19/20
LCA (NAS)	86
- positive cells (counts)	5 [2, 8]
CD3 (NAS)	122
- positive cells (counts)	3 [1, 5]
CD 68 (NAS)	85
- positive cells (counts)	1 [0, 3]

Variables are expressed as means and standard deviations or median [25th, 75th percentile] or as a count and percentage of subjects.
CD, cluster of differentiation; EM, electron microscopy; HLA, Human Leucocyte Antigen DR isotype; IH criteria for myocarditis, immunohistochemical criteria defined as ≥14 leucocytes/mm^2 and ≥7 CD 3 positive T-lymphocytes/mm^2; LCA, leucocyte common antigen; NAS, number of subjects available for analysis; PCR, polymerase chain reaction.

The incidence of left ventricular reverse remodelling and its predictors

LVRR was documented in 46% individuals at 1 year, in 60% at 2 years and 50% at 5 years of follow-up, respectively. At last follow-up, patients with LVRR required significantly less diuretics (P = 0.0008) and mineralocorticoid receptor antagonists (P = 0.0033) than patients without LVRR. The NYHA class was better in subjects who experienced LVRR than in those without LVRR ($P < 0.001$).

Baseline echocardiographic, ECG, and clinical variables significantly associated with LVRR at last follow-up in univariate analysis and the multivariate model are listed in *Table 5*. Changes in LVEF and LVEDDi stratified by gender during the

Table 4 Heart failure treatment

	Baseline	1 year	2 years	5 years
Number of subjects	133	120	109	89
ACE-I/ARBs	133 (100%)	120 (100%)	108 (99%)	88 (99%)
SUBMAXD/MAXD/TD	110/0/23	60/9/51	41/13/54	24/6/58
Beta-blockers	133 (100%)	118 (98%)	109 (100%)	87 (98%)
SUBMAXD/MAXD/TD	123/0/10	58/17/43	37/20/52	25/12/50
Loop diuretics	123 (92%)	84 (70%)	66 (61%)	51 (57%)
MAXD	0	2	0	0
MRAs	111 (83%)	80 (67%)	56 (51%)	45 (51%)
SUBMAXD/MAXD/TD	7/0/104	10/0/70	8/0/48	6/0/39
Ivabradine	1 (1%)	4 (3%)	8 (7%)	9 (10%)
SUBMAXD/MAXD/TD	0/1/0	0/3/1	0/2/6	0/1/8
CRT-D or CRT-P	0 (0%)	11 (9%)	20 (18%)	23 (26%)

Variables are expressed as a count and percentage of subjects.
ACE-I, angiotensin-converting enzyme inhibitor; ARB, angiotensin receptor blocker; CRT-D, cardiac resynchronization therapy with defibrillator; CRT-P, cardiac resynchronization therapy without defibrillator; MAXD, maximal tolerated dose; MRA, mineralocorticoid receptor antagonist; TD, target dose; SUBMAXD, submaximal dose.

Figure 1 Kaplan–Meier estimates of overall survival.

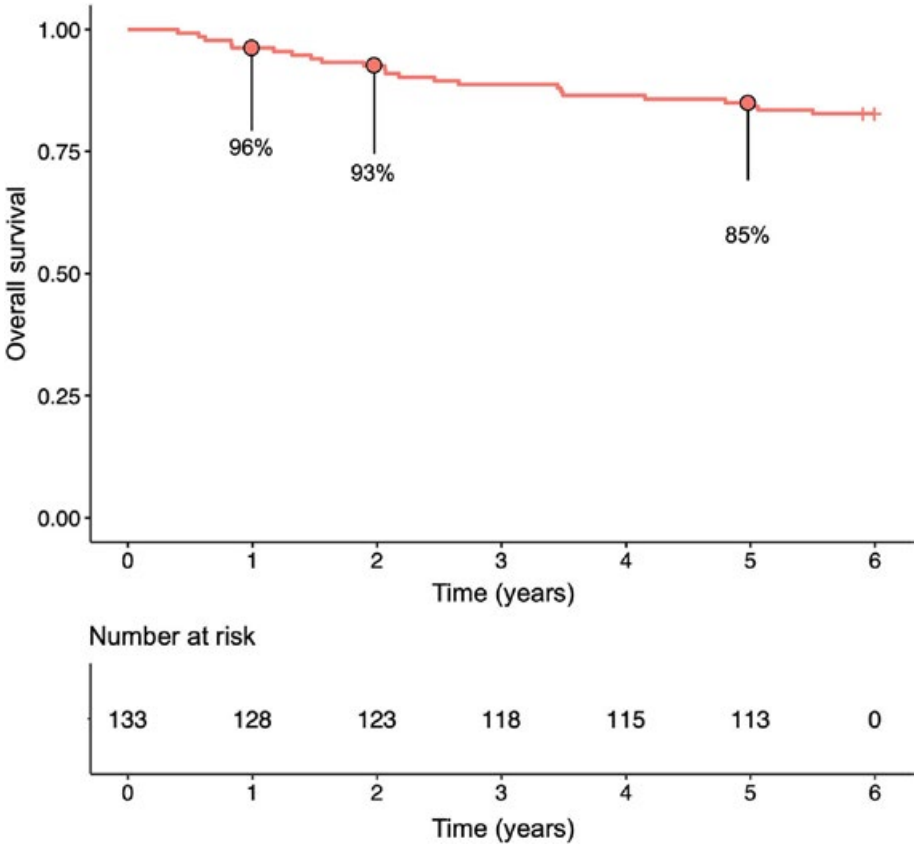

follow-up are depicted in *Figures 3 and 4*. The median LVEF was improved at 1 year (baseline 27% [23–33%] vs. at 1 year 40% [33–52%]) and then remained relatively stable during the rest of the follow-up period (44% [38–56%] at 2 years, 45% [34%–54%] at 5 years; $P < 0.001$ overall). The median LVEDDi decreased at 1 year (baseline 34 mm/m^2 [31–37 mm/m^2] vs. at 1 year 31 mm/m^2 [28–35 mm/m^2]) and then remained stable during the rest of the follow-up period (31 mm/m^2 [28–34 mm/m^2] at 2 years, 31 mm/m^2 [27–33 mm/m^2] at 5 years; $P < 0.001$ overall).

Overall, LVEF recovery was present in 25% of subjects at 1 year, in 28% at 2 years and 22% at 5 years of follow-up. Transient LV recovery was documented in 15 (11%) subjects during the follow-up period. Compared to the patients with sustained LV recovery, these individuals had larger LVEDD (71 ± 4.6 vs. 68 ± 6 mm, $P = 0.048$), LVESD (64 ± 4.9 vs. 58 ± 7.9 mm, P = 0.008), LVEDV (225 [202, 250] vs. 190 [166, 225] mL, $P = 0.017$) and LVEDVi (112 ± 21 vs. 98 ± 23 mL/m^2, $P = 0.036$), respectively. To further analyse the EMB results, we have added EMB characteristics divided by the presence or absence of LVRR in *Table S1*. However, there were no significant differences in the EMB parameters between these two subgroups.

Predictors of mortality

In univariate analysis, overall survival was associated with baseline RA area, RAP, tricuspid regurgitation grade, E/e', PR interval duration, BNP level, and number of macrophages in EMB, as depicted in *Table 6*. Furthermore, the presence of acute myocarditis on EMB by Dallas criteria was marginally associated with mortality ($P = 0.02$), but because only three out of 133 patients met these criteria, we could not derive reliable conclusions about this variable and therefore it was not included in survival modelling. In multivariate analysis of echocardiographic parameters, only RA area was found to be independently associated with mortality. In a multivariate model of clinical and laboratory variables (PR interval, BNP level, number of macrophages in EMB), only PR interval duration and BNP level remained significant predictors of mortality. When a combined model consisting of PR interval, BNP level, and RA area was created, all of these variables remained independently associated with mortality of the study population (*Table 7*). When changes in echocardiographic parameters at 1 year of follow-up were analysed, only increase in RVEDD was a significant univariate predictor of subsequent mortality [HR

Figure 2 Kaplan–Meier estimates of survival without heart failure (HF) hospitalization or transplantation.

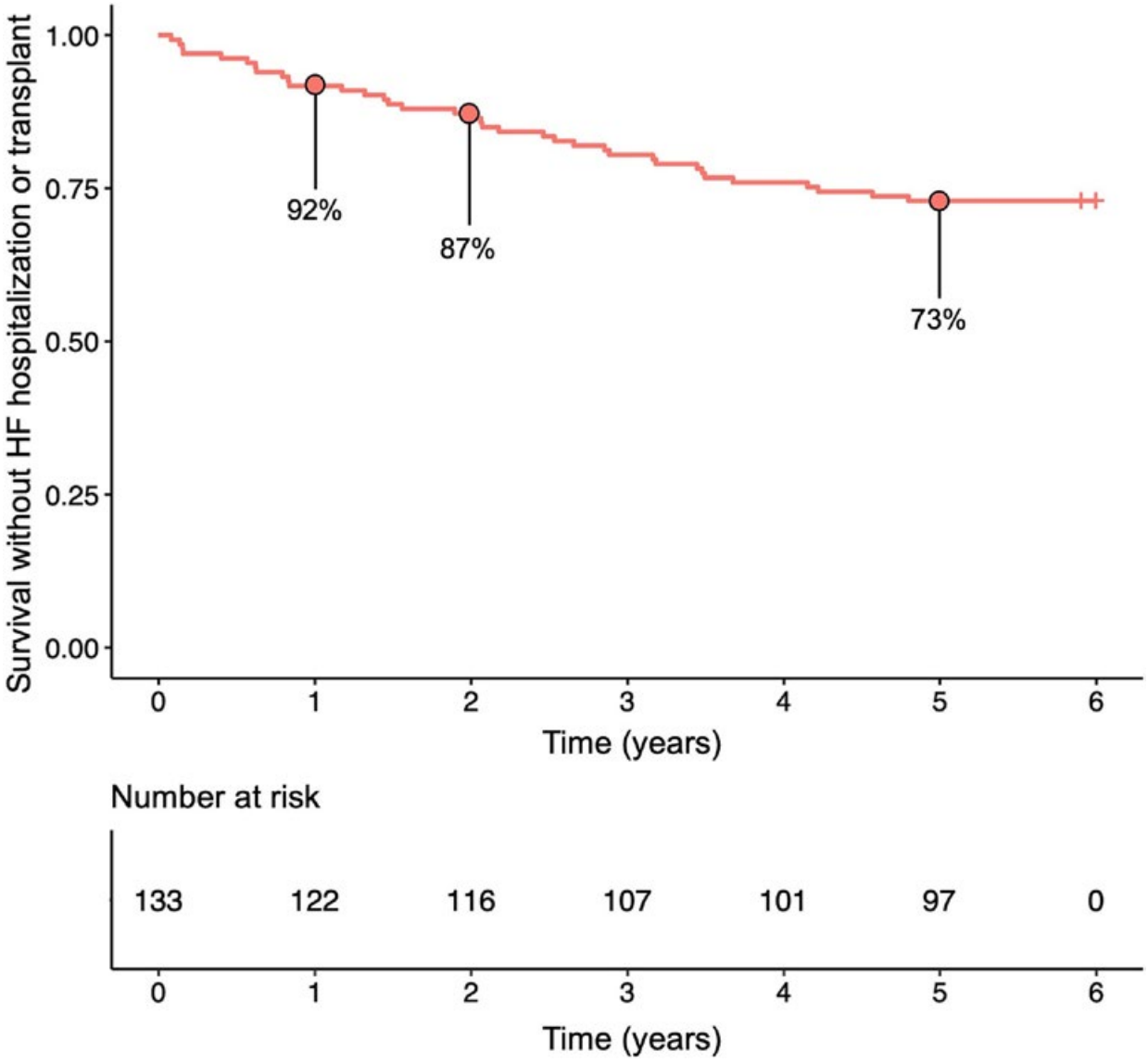

1.1 (CI 1.0–1.2); P = 0.048]. However, LVRR at 1 year of follow-up was shown to be a significant predictor of the combination of mortality and heart failure hospitalization (P = 0.025) (*Figure 5*).

Discussion

To our best knowledge, the present study is the first to report long-term prospective clinical and echocardiographic follow-up of patients who underwent EMB in the setting of recently diagnosed unexplained LV systolic dysfunction. A similar study with 59 ± 40 months of clinical follow-up was published by Ikeda et al.[8]; however, this was a retrospective analysis with echocardiographic follow-up of only 36 months and without EMB data. Other studies describing the course of patients with recently diagnosed unexplained LV systolic dysfunction had shorter duration of follow-up of clinical or echocardiographic data.[4–7]

Our study demonstrates several important findings. First, LVRR occurred in over half of our patients during first 2 years of follow-up, in the majority of whom LVRR occurred during the first year, and then remained almost stable until the end of the entire 5-year follow-up period. LVRR was accompanied by improvement in functional NYHA class and de-

Table 5 Predictors of LVRR

	Univariate			Multivariate*		
	OR	95% CI	*P*	OR	95% CI	*P*
LVEDV (mL)	0.991	[0.984–0.998]	0.0103			
LVEDVi (mL/m^2)	0.98	[0.964–0.997]	0.0184	0.97	[0.946–0.988]	0.0039
LVEDD (mm)	0.927	[0.873–0.984]	0.0129			
LVESD (mm)	0.951	[0.905–0.999]	0.0452			
EF (%)	0.941	[0.887–0.998]	0.0425	0.89	[0.83–0.96]	0.0045
e′ (m/s)	0.786	[0.631–0.979]	0.0316			
Diastolic BP (mmHg)	1.04	[1.01–1.08]	0.0138	1.04	[1.01–1.08]	0.0279
Symptom duration (days)	0.996	[0.992–1]	0.0472			

*Fast backward elimination algorithm.
BP, blood pressure; e′, peak early diastolic mitral annular velocity; EF, left ventricular ejection fraction; LVEDD, left ventricular end-diastolic diameter; LVEDV, left ventricular end-diastolic volume; LVEDVi, indexed left ventricular end-diastolic volume; LVESD, left ventricular end-systolic diameter; LVRR, left ventricular reverse remodelling.

Figure 3 Changes in left ventricular ejection fraction (LVEF) stratified by gender during follow-up.

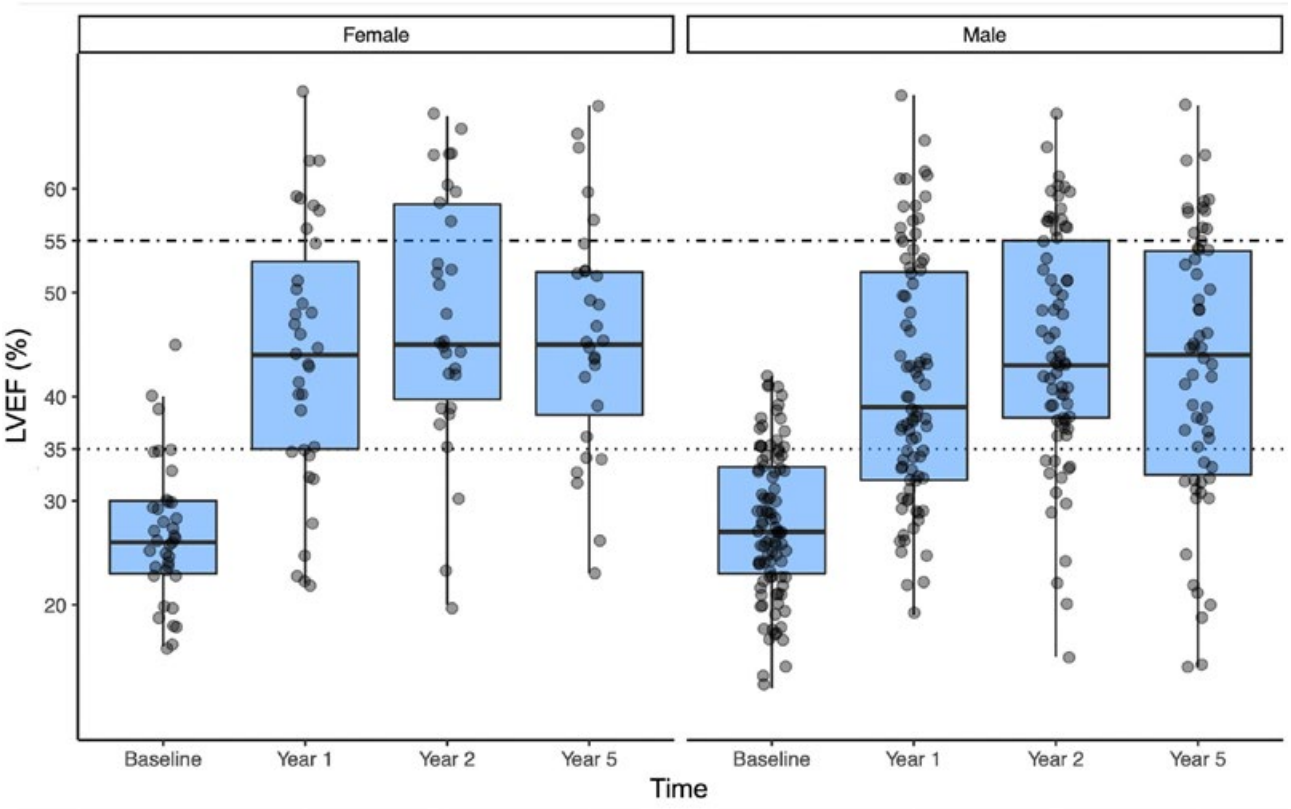

creased diuretic use. Moreover, sustained recovery of LVEF ≥50% was seen in almost one fourth of individuals during the whole follow-up. Second, the incidence of major adverse clinical outcomes was rather low in our cohort including mortality (17% during 5-year follow-up), heart transplantation (2%) and hospitalization for heart failure (12%), respectively. Third, RA size, BNP level, and PR interval appear to be significantly associated with mortality, while LVRR was a significant predictor of the combination of mortality and heart failure hospitalization.

The reported incidence of LVRR in cohorts of patients with recently diagnosed LV systolic dysfunction varies because of differences in its definition. In IMAC-2 trial, 70% individuals had an increase in LVEF at 6 months of at least 10 percentage points, and LV EF normalized (≥50%) in 25% of patients.[17] Ikeda et al. defined LVRR as an increase in LV EF from ≥10%

Figure 4 Changes in indexed left ventricular end-diastolic diameter (LVEDDi) stratified by gender during follow-up.

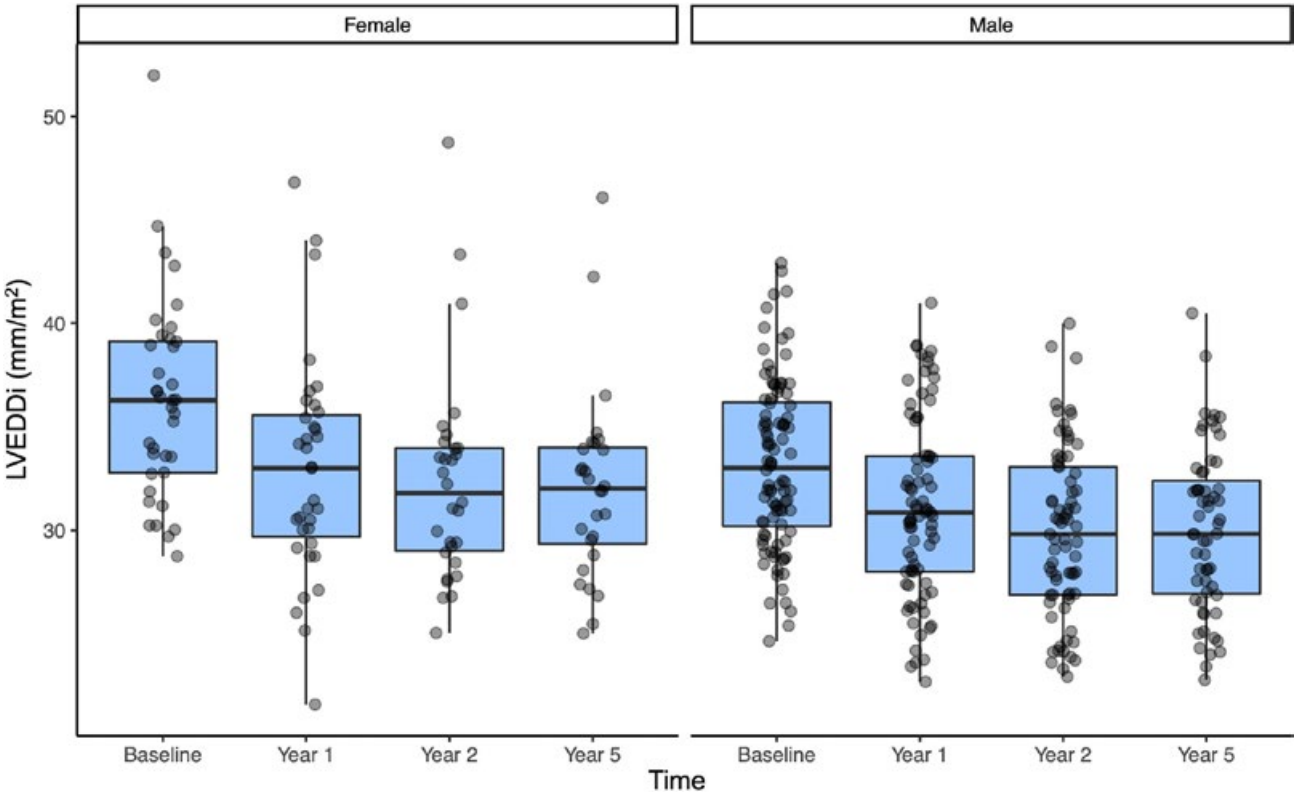

Table 6 Univariate predictors of mortality

	HR	95% CI	*P*
RA area (cm^2)	1.09	1.02–1.17	0.008
RAP (mmHg)	1.1	1.003–1.205	0.043
TR severity	1.79	1.11–2.9	0.017
E/e′	1.08	1.01–1.17	0.036
PR interval (per 10 ms)	1.18	1.04–1.34	0.009
logBNP	1.58	1.01–2.46	0.043
CD68+ cells in EMB	1.15	1.03–1.3	0.016

BNP, B-type natriuretic peptide; CD68+, cells in EMB macrophages in endomyocardial biopsy; E, peak early diastolic velocity; e′ peak early diastolic mitral annular velocity; RA area, right atrial area; RAP, right atrial pressure; TR, tricuspid regurgitation.

Table 7 Predictors of mortality in multivariate analysis

	OR	95% CI	*P*
PR interval	1.02	1.006–1.035	0.00575
logBNP	2.02	1.14–3.56	0.01557
RA area	1.097	1.007–1.196	0.03499

BNP, B-type natriuretic peptide; RA area, right atrial area.

to a final value of ≥35% together with ≥10% decrease in LVEDDi.[8] In their cohort of patients with idiopathic DCM, LVRR within 24 months occurred in 40% of patients and delayed LVRR occurred in 12% of patients during the remainder of the 36 months echocardiographic follow-up period. In our study we used the definition of LVRR which was first applied by Merlo et al.[4] In their cohort, 54% of patients had LVRR during 20 months follow-up. Our results are in agreement with these studies, demonstrating that early LVRR occurs in more than half of patients and remains stable over a 5-year period in the majority of cases. Importantly, sustained recovery of LVEF was found in 22% subjects at 5 years of follow-up. Again, in most patients who experienced sustained recovery of LVEF, its normalization occurred during the first year.

In the present study, the occurrence of LVRR was significantly predicted by baseline LVEDVi, LVEF and baseline diastolic blood pressure. Similar to our results, initial end-diastolic size of the LV and LVEF were identified as significant predictors of LVRR in other cohorts of patients with recently diagnosed non-ischaemic LV systolic dysfunction.[4–6] Initial LV dilatation and systolic function impairment, that is, baseline degree of adverse LV remodelling, thus represent important factors associated with the probability of LVRR.

Our study also shows that current long-term mortality and heart failure morbidity of patients with recently diagnosed unexplained LV systolic dysfunction is lower than few decades ago.[18] During 5 years of follow-up, 17% of total initial study population died, three patients underwent heart transplantation, and the cumulative rate of hospitalization for

Figure 5 Kaplan–Meier estimates of survival without heart failure (HF) hospitalization for patients with and without left ventricular reverse remodelling (LVRR).

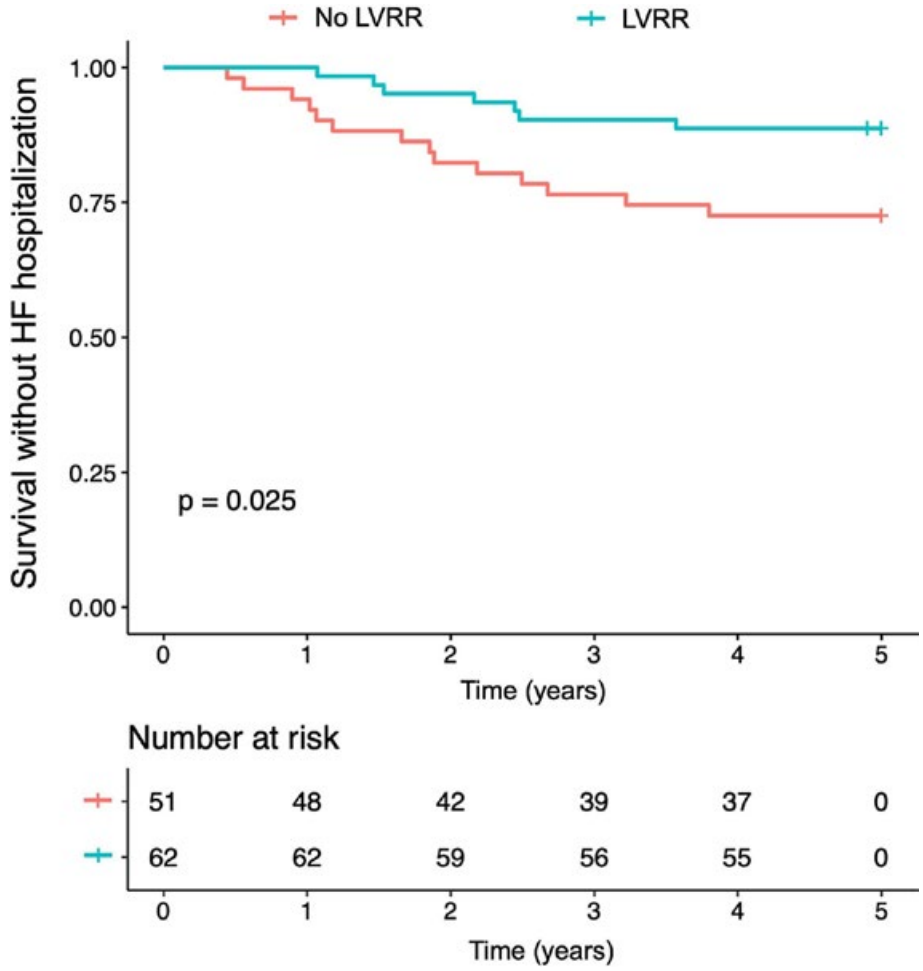

heart failure exacerbation was 12% of the initial population. This improvement in prognosis is clearly associated with the phenomenon of early LVRR which is attributable to the significant effect of heart failure therapy including CRT and potent anti-remodelling medications. Indeed, LVRR at the 1st year was shown to be a significant negative predictor of composite endpoint of mortality and heart failure hospitalizations. This finding is in agreement with previously published studies. Hoshikawa et al. and Ikeda et al. have shown that early LVRR is significantly related to a favourable prognosis in patients with idiopathic DCM.[8,19]

In the present study, RA area, BNP level, and PR interval were independently associated with mortality. Furthermore, increase in RVEDD at 1 year of follow-up was a significant predictor of mortality. It is well known that RA enlargement has a negative prognostic impact in patients with chronic systolic heart failure as it is primarily determined by chronically elevated RA pressure.[20] Importantly, elevated RA pressure is a negative prognostic factor associated with increased mortality in patients with DCM.[21] Our findings on the prognostic impact of the RA area and the degree of RV size reduction demonstrate the importance of structural right heart involvement in the prognosis of patients with recently diagnosed unexplained LV systolic dysfunction. The prognostic value of natriuretic peptides (BNP or NT-proBNP) has been repeatedly demonstrated in heart failure with reduced LVEF including patients with DCM,[22,23] and this was confirmed in our cohort. For the first time we demonstrate that PR interval prolongation seems to be significantly associated with mortality in individuals with recently diagnosed non-ischaemic LV systolic dysfunction. We did not find other ECG parameters, including the presence of LBBB, to be associated with mortality in our patients. This is probably related to the fact that 23 subjects with LBBB underwent CRT-D or CRT-P implantation, which improved their overall prognosis. We believe the PR interval prolongation found at the time of diagnosis of non-ischaemic LV systolic dysfunction may represent conduction system impairment which has an impact on prognosis.

All our patients with recently diagnosed unexplained LV systolic dysfunction underwent EMB. Myocardial inflammation as assessed by immunohistochemical analysis was detected in 17% of our cohort, while conventional histological analyses based on Dallas criteria revealed active or borderline myocarditis only in 2% of patients. On the other hand, viral genome was found in 52% using PCR and viral particles even in 62% based on EM assessment of our patients, respectively. These findings correspond to the results of other studies using EMB diagnostics in individuals with unexplained non-ischaemic LV systolic dysfunction. Kühl et al.[24] reported the presence of viral genome in 67% of 245 patients with 'idiopathic' LV systolic dysfunction, while active or borderline myocarditis according to the Dallas criteria were not found in any case. In the study published by Kuethe et al.,[25] 19% of 351 patients with chronic LV systolic dysfunction showed positive Dallas criteria and 39% immunohistochemical signs of inflammation; viral genome was detected in 58%. Recently, Kažukauskienė et al. found myocardial inflammation in 54% and cardiotropic viruses in 52% of their 57 patients with non-ischaemic DCM, respectively.[26]

Interestingly, the number of macrophages and not the presence of any viral genome in EMB specimens were associated with overall survival in univariate, but not in multivariate analysis. Gilotra et al. also reported that immunohistochemical signs of myocarditis were an independent predictor of the composite endpoint of death, LV assist device placement, and/or transplant at 1 year in their cohort of patients with acute-onset cardiomyopathy.[6] Similarly, Kindermann et al. demonstrated that immunohistological evidence of myocarditis, but not the presence of viral genome, was predictive of time to cardiac death or heart transplantation in patients with clinically suspected myocarditis.[27] The association between inflammation by a high number of T-cells and poor prognosis of patients with non-ischaemic DCM was also reported by Kažukauskienė et al.; however, the presence of viral genome did not predict adverse outcome during a 5-year follow-up in their study.[26] Our results thus support current view on performing EMB in patients with non-ischaemic LV systolic dysfunction only in high-risk clinical scenarios listed in recent Position statement of the Heart Failure Association of the European Society of Cardiology, the Heart Failure Society of America, and the Japanese Heart Failure Society.[28]

From a clinical point of view, the results of the present study clearly support the necessity of early initiation of optimal guideline-directed therapy with the aim of achieving LVRR and improvement of long-term clinical outcome in patients with recently diagnosed unexplained LV systolic dysfunction. Moreover, our data underscore the necessity of long-term regular echocardiographic and clinical follow-up of these individuals, because in some of them, LVRR is only temporary (11% in our study).

Study limitations

There are several limitations of our study. First, this is a single-centre study with relatively small sample size with potential impact on statistical power and generalizability of our findings. Second, cardiac magnetic resonance imaging as well as genetic testing were not available at our centre during the study period and therefore we were not able to incorporate their results into our analyses. The presence of late gadolinium enhancement or certain genetic mutations have been shown to be related to LVRR and the prognosis of patients with DCM.[7,29] Third, medical therapy of heart failure has evolved since the beginning of the study period. Angiotensin receptor-neprilysin inhibitors and sodium-glucose cotransporter 2 inhibitors, which currently represent essential heart failure therapy with significant effect on LVRR and prognosis, were still being tested in clinical trials during our study period and were not available for routine practice. We believe their use would very likely have a significant additive positive effect on echocardiographic as well as clinical outcomes of our patients with recent onset unexplained LV systolic dysfunction.

Conclusions

Left ventricular reverse remodelling occurs in over half of patients with recent onset unexplained LV systolic dysfunction during the first 2 years of optimal heart failure therapy and then remains stable in the majority of patients during long-term follow-up. This is reflected by relatively low mortality as well as low rate of hospitalization for heart failure at 5-year follow-up. The stage of initial adverse LV remodelling is significantly associated with subsequent LVRR.

Conflict of interest

The authors have no conflict of interest.

Funding

The study was supported by the Charles University Research Program Cooperatio Cardiovascular Science.

Supporting information

Additional supporting information may be found online in the Supporting Information section at the end of the article.

Table S1. Endomyocardial biopsy findings according to the left ventricular reverse remodelling.

References

1. Elliott P, Andersson B, Arbustini E, Bilinska Z, Cecchi F, Charron P, *et al*. Classification of the cardiomyopathies: A position statement from the European society of cardiology working group on myocardial and pericardial diseases. *Eur Heart J* 2008;**29**:270-276. doi:10.1093/eurheartj/ehm342
2. Maron BJ, Towbin JA, Thiene G, Antzelevitch C, Corrado D, Arnett D, *et al*. Contemporary definitions and classification of cardiomyopathies. *Circulation* 2006;**113**:1807-1816. doi:10.1161/CIRCULATIONAHA.106.174287
3. Nijst P, Martens P, Mullens W. Heart failure with myocardial recovery - The patient whose heart failure has improved: what next? *Prog Cardiovasc Dis* 2017;**60**:226-236. doi:10.1016/j.pcad.2017.05.009
4. Merlo M, Pyxaras SA, Pinamonti B, Barbati G, Di Lenarda A, Sinagra G. Prevalence and prognostic significance of left ventricular reverse remodeling in dilated cardiomyopathy receiving tailored medical treatment. *J Am Coll Cardiol* 2011;**57**:1468-1476. doi:10.1016/j.jacc.2010.11.030
5. Zou CH, Zhang J, Zhang YH, Wei BQ, Wu XF, Zhou Q, *et al*. Frequency and predictors of normalization of left ventricular ejection fraction in recent-onset nonischemic cardiomyopathy. *Am J Cardiol* 2014;**113**:1705-1710. doi:10.1016/j.amjcard.2014.02.028
6. Gilotra NA, Bennett MK, Shpigel A, Ahmed HM, Rao S, Dunn JM, *et al*. Outcomes and predictors of recovery in acute-onset cardiomyopathy: A single-center experience of patients undergoing endomyocardial biopsy for new heart failure. *Am Heart J* 2016;**179**:116-126. doi:10.1016/j.ahj.2016.06.019
7. Merlo M, Masè M, Vitrella G, Belgrano M, Faganello G, Di Giusto F, *et al*. Usefulness of addition of magnetic resonance imaging to echocardiographic imaging to predict left ventricular reverse remodeling in patients with nonischemic cardiomyopathy. *Am J Cardiol* 2018;**122**:490-497. doi:10.1016/j.amjcard.2018.04.017
8. Ikeda Y, Inomata T, Iida Y, Iwamoto-Ishida M, Nabeta T, Ishii S, *et al*. Time course of left ventricular reverse remodeling in response to pharmacotherapy: Clinical implication for heart failure prognosis in patients with idiopathic dilated cardiomyopathy. *Heart Vessels* 2016;**31**:545-554. doi:10.1007/s00380-015-0648-2
9. McMurray JJ, Adamopoulos S, Anker SD, Auricchio A, Böhm M, Dickstein K, *et al*. ESC Guidelines for the diagnosis and treatment of acute and chronic heart failure 2012: The Task Force for the Diagnosis and Treatment of Acute and Chronic Heart Failure 2012 of the European Society of Cardiology. Developed in collaboration with the Heart Failure Association (HFA) of the ESC. *Eur Heart J* 2012;**33**:1787-1847. doi:10.1093/eurheartj/ehs104
10. Palecek T, Kuchynka P, Hulinska D, Schramlova J, Hrbackova H, Vitkova I, *et al*. Presence of *Borrelia burgdorferi* in endomyocardial biopsies in patients with new-onset unexplained dilated cardiomyopathy. *Med Microbiol Immunol* 2010;**199**:139-143. doi:10.1007/s00430-009-0141-6
11. Nagueh SF, Appleton CP, Gillebert TC, Marino PN, Oh JK, Smiseth OA, *et al*. Recommendations for the evaluation of left ventricular diastolic function by echocardiography. *J Am Soc Echocardiogr* 2009;**22**:107-133. doi:10.1093/ejechocard/jep007
12. Lang RM, Bierig M, Devereux RB, Flachskampf FA, Foster E, Pellikka PA, *et al*. Recommendations for chamber quantification: a report from the American Society of Echocardiography's Guidelines and Standards Committee and the Chamber Quantification Writing Group, developed in conjunction with the European Association of Echocardiography, a branch of the European Society of Cardiology. *J Am Soc Echocardiogr* 2005;**18**:1440-1463. doi:10.1016/j.echo.2005.10.005
13. Aretz HT. Myocarditis: The Dallas criteria. *Hum Pathol* 1987;**18**:619-624. doi:10.1016/S0046-8177(87)80363-5
14. Caforio AL, Pankuweit S, Arbustini E, Basso C, Gimeno-Blanes J, Felix SB, *et al*. Current state of knowledge on aetiology, diagnosis, management, and therapy of myocarditis: A position statement of the European Society of Cardiology Working Group on myocardial and pericardial diseases. *Eur Heart J* 2013;**34**:2636-2648. doi:10.1093/eurheartj/eht210
15. Vardas PE, Auricchio A, Blanc JJ, Daubert JC, Drexler H, Ector H, *et al*. Guidelines for cardiac pacing and cardiac resynchronization therapy: The Task Force for Cardiac Pacing and Cardiac Resynchronization Therapy of the European Society of Cardiology. Developed in collaboration with the European Heart Rhythm Association. *Eur Heart J* 2007;**28**:2256-2295. doi:10.1093/eurheartj/ehm305
16. Lawless JF, Singhal K. Efficient screening of nonnormal regression models. *Biometrics* 1978;**34**:318-327. doi:10.2307/2530022
17. McNamara DM, Starling RC, Cooper LT, Boehmer JP, Mather PJ, Janosko KM, *et al*. Clinical and demographic predictors of outcomes in recent onset dilated cardiomyopathy: Results of the IMAC (intervention in myocarditis and acute cardiomyopathy)-2 study. *J Am Coll Cardiol* 2011;**58**:1112-1118. doi:10.1016/j.jacc.2011.05.033
18. Seferović PM, Polovina M, Bauersachs J, Arad M, Gal TB, Lund LH, *et al*. Heart failure in cardiomyopathies: A position paper from the Heart Failure Association of the European Society of Cardiology. *Eur J Heart Fail* 2019;**21**:553-576. doi:10.1002/ejhf.1461
19. Hoshikawa E, Matsumura Y, Kubo T, Okawa M, Yamasaki N, Kitaoka H, *et al*. Effect of left ventricular reverse remodeling on long-term prognosis after therapy with angiotensin-converting enzyme inhibitors or angiotensin II receptor blockers and β blockers in patients with idiopathic dilated cardiomyopathy. *Am J Cardiol* 2011;**107**:1065-1070. doi:10.1016/j.amjcard.2010.11.033
20. Sallach JA, Tang WH, Borowski AG, Tong W, Porter T, Martin MG, *et al*. Right atrial volume index in chronic systolic heart failure and prognosis. *JACC Cardiovasc Imaging* 2009;**2**:527-534. doi:10.1016/j.jcmg.2009.01.012
21. Unverferth DV, Magorien RD, Moeschberger ML, Baker PB, Fetters JK, Leier CV. Factors influencing the one-year mortality of dilated cardiomyopathy. *Am J Cardiol* 1984;**54**:147-152. doi:10.1016/0002-9149(84)90320-5
22. Li X, Chen C, Gan F, Wang Y, Ding L, Hua W. Plasma NT pro-BNP, hs-CRP and big-ET levels at admission as prognostic markers of survival in hospitalized patients with dilated cardiomyopathy: A single-center cohort study. *BMC Cardiovasc Disord* 2014;**14**:67. doi:10.1186/1471-2261-14-67
23. Fonarow GC, Peacock WF, Phillips CO, Givertz MM, Lopatin M, ADHERE Scientific Advisory Committee and Investigators. Admission B-type natriuretic peptide levels and in-hospital mortality in acute decompensated heart failure. *J Am Coll Cardiol* 2007;**49**:1943-1950. doi:10.1016/j.jacc.2007.02.037

24. Kühl U, Pauschinger M, Noutsias M, Seeberg B, Bock T, Lassner D, *et al*. High prevalence of viral genomes and multiple viral infections in the myocardium of adults with 'idiopathic' left ventricular dysfunction. *Circulation* 2005;**111**: 887-893. doi:10.1161/01.CIR.0000155616.07901.35
25. Kuethe F, Franz M, Jung C, Porrmann C, Reinbothe F, Schlattmann P, *et al*. Outcome predictors in dilated cardiomyopathy or myocarditis. *Eur J Clin Invest* 2017;**47**:513-523. doi:10.1111/eci.12772
26. Kažukauskienė I, Baltrūnienė V, Jakubauskas A, Žurauskas E, Maneikienė VV, Daunoravičius D, *et al*. Prevalence and prognostic relevance of myocardial inflammation and cardiotropic viruses in non-ischemic dilated cardiomyopathy. *Cardiol J* 2022;**29**:441-453. doi:10.5603/CJ.a2020.0088
27. Kindermann I, Kindermann M, Kandolf R, Klingel K, Bültmann B, Müller T, *et al*. Predictors of outcome in patients with suspected myocarditis. *Circulation* 2008;**118**:639-648. doi:10.1161/CIRCULATIONAHA.108.769489
28. Seferović PM, Tsutsui H, McNamara DM, Ristić AD, Basso C, Bozkurt B, *et al*. Heart Failure Society of America and Japanese Heart Failure Society Position statement on endomyocardial biopsy. *Eur J Heart Fail* 2021;**23**:854-871. doi:10.1002/ejhf.2190
29. Akhtar MM, Lorenzini M, Cicerchia M, Ochoa JP, Hey TM, Sabater Molina M, *et al*. Clinical phenotypes and prognosis of dilated cardiomyopathy caused by truncating variants in the TTN gene. *Circ Heart Fail* 2020;**13**:e006832. doi:10.1161/CIRCHEARTFAILURE.119.006832

L. Juříková et al.

Decreased quality of life in Duchenne muscular disease patients related to functional neurological and cardiac impairment

Frontiers in Neurology
Impact Factor: 3,5

rejstřík

frontiers | Frontiers in Neurology

TYPE Original Research
PUBLISHED 08 February 2024
DOI 10.3389/fneur.2024.1360385

OPEN ACCESS

EDITED BY
Liang Wang,
Sun Yat-sen University, China

REVIEWED BY
Hoi Shan Sophelia Chan,
The University of Hong Kong, Hong Kong SAR, China
Carlos Vera,
Stanford University, United States

*CORRESPONDENCE
Lucia Masárová
✉ lucia.masarova@fnusa.cz

RECEIVED 22 December 2023
ACCEPTED 24 January 2024
PUBLISHED 08 February 2024

CITATION
Juříková L, Masárová L, Panovský R, Pešl M, Revendová KŽ, Volný O, Feitová V, Holeček T, Kincl V, Danhofer P, Voháňka S, Haberlová J and Podolská K (2024) Decreased quality of life in Duchenne muscular disease patients related to functional neurological and cardiac impairment. *Front. Neurol.* 15:1360385. doi: 10.3389/fneur.2024.1360385

Decreased quality of life in Duchenne muscular disease patients related to functional neurological and cardiac impairment

Lenka Juříková[1], Lucia Masárová[2]*, Roman Panovský[2,3], Martin Pešl[2,3,4], Kamila Žondra Revendová[5,6], Ondřej Volný[2,5,6], Věra Feitová[2,7], Tomaš Holeček[2,7,8], Vladimír Kincl[2,3], Pavlína Danhofer[1], Stanislav Voháňka[9], Jana Haberlová[10] and Karolína Podolská[10]

[1]Department of Paediatric Neurology, Faculty of Medicine of Masaryk University, University Hospital Brno, Brno, Czechia, [2]International Clinical Research Center, St. Anne's University Hospital, Faculty of Medicine, Masaryk University, Brno, Czechia, [3]1st Department of Internal Medicine-Cardio-angiology, Faculty of Medicine, St. Anne's University Hospital, Brno, Czechia, [4]Department of Biology, Faculty of Medicine, Masaryk University, Brno, Czechia, [5]Department of Neurology, University Hospital Ostrava, Brno, Czechia, [6]Centre for Clinical Neurosciences, Faculty of Medicine, University Ostrava, Ostrava, Czechia, [7]Department of Medical Imaging, St. Anne's University Hospital, Brno, Czechia, [8]Department of Biomedical Engineering, University of Technology, Brno, Czechia, [9]Department of Neurology, Faculty of Medicine, University Hospital Brno, Masaryk University, Brno, Czechia, [10]Department of Paediatric Neurology, 2nd Faculty of Medicine, Charles University and Motol University Hospital, Prague, Czechia

In this prospective study involving 37 Duchenne muscular dystrophy (DMD) patients aged 8–18 years and older, we examined the impact of neurological and cardiac factors on quality of life (QoL). Our findings revealed a negative correlation between upper limb movement and overall mobility, self-service, and usual activities. Ambulatory and non-ambulatory DMD patients showed significant differences in mobility-related parameters. Cardiac evaluations demonstrated associations between mitral annular plane systolic excursion (MAPSE) and mobility-related aspects. The PEDSQL 3.0 neuromuscular model questionnaire further highlighted age-related and movement-related correlations with QoL. The loss of ambulatory status and reduced upper limb movement were negatively associated with QoL, while upper limb movement positively correlated with septal MAPSE. However, no significant associations were found between MAPSE and anxiety/depression. These findings underscore the multifaceted impact of DMD on QoL and emphasize the importance of considering both neurological and cardiac factors in comprehensive patient care.

KEYWORDS

quality of life, Duchenne muscular dystrophy, cardiac magnetic resonance, neurological status, cardiac impairment

Introduction

The most common X-recessive inherited progressive muscular disease is Duchenne muscular dystrophy (DMD). It affects approximately 1:5000 living boys (1). The first symptoms of DMD manifest at the age of two years because of the absence of dystrophin protein, leading to gradual weakness and muscle injury (2).

DMD is still causally incurable (3). Due to the advances in medical care and symptomatic therapy, the life expectancy of DMD patients has been prolonged and their quality of life (QoL) has been improving (4, 5). Today, DMD patients live up to 30 or 40 years (6). It is well-known that DMD influences the QoL not only for patients, but also for their families (7–11).

According to the World Health Organization, QoL is defined as a person's perception of their position in life including the culture and values in the system in which the person lives, correlating to a person's goals, expectations, standards, and concerns. It is a complex of physical health, psychological status, level of independence, social relationships, personal beliefs, and a person's relationship with various features of the environment (12). Published reports about the QoL in DMD patients are not uniform. Some of the previous studies reported a decline only in physical functions compared to healthy controls, while the others show that a whole spectrum of QoL parameters were decreased to age-matched controls (7, 13–15). The results may also have been influenced by self/proxy reports (by the parents/caregivers) (16–22) or by the help of pediatricians (14).

The Pediatric Quality of Life (PEDSQL) 3.0 Neuromuscular Module questionnaire among children/adolescents, EQ-5D, and Individualized Neuromuscular QoL questionnaire for adults are the most commonly used questionnaires in the published studies (23–26).

To date, only one study describing the QoL in DMD patients related to respiratory and cardiac functions including left ventricular ejection fraction (LVEF) evaluated by echocardiography and the presence or absence of electrocardiogram (ECG) abnormalities or cardiomyopathy has been published (27).

To our knowledge, there has been no prospective study describing the QoL of all-aged DMD patients in correlation with a complex evaluation firstly of neurological clinical status and cardiac impairment using cardiac magnetic resonance (CMR), and secondly of the influence of cardiac therapy or corticosteroid therapy, body mass index (BMI), and anxiety/sadness.

Objectives

The main purpose of this prospective study was to investigate the QoL concerning neurological clinical status and cardiac impairment using CMR, and the influence of actual therapy, BMI, and anxiety/sadness in DMD patients based on a completed questionnaire.

Methods

Participants

DMD patients 8–18 years and older born in the Czech Republic were consecutively included between 01/2022 to 09/2023 in close cooperation with EndDuchenne (a patient advocacy group). All DMD patients were diagnosed based on their clinical symptoms and/or elevated creatine kinase, and confirmed by genetic testing. The most common genetic mutation was the deletion of 44–63 exons in 65% of our cohort.

This study was performed in accordance with the Declaration of Helsinki (2000) of the World Medical Association and was approved by the Institutional Ethics Committee (University Hospital Brno, reference number 20130410–03). All DMD patients or their parents (for patients younger than 18 years) signed the informed consent.

Every patient was examined by an experienced pediatric neurologist and also an experienced cardiologist including ECG and ECG Holter, and the following pieces of information were collected: demographic data (age, weight, height), current pharmacotherapy (corticosteroid therapy, beta-blockers, angiotensin converting enzyme inhibitors (ACEI), sartan-losartan (generic name of sartan), diuretics), comorbidities (hypertension, diabetes mellitus, chronic renal insufficiency), an actual feeling of dyspnoea and palpitations.

All DMD patients were monitored for respiratory status such as a need of nocturnal non-invasive positive pressure ventilation (NIPPV). Six DMD patients of our cohort use nocturnal NIPPV. Neurological clinical status included the following information - ambulatory/non-ambulatory, self-sitting or sitting requiring help, and the presence of scoliosis including a history of scoliosis surgery. Upper limb movement was assessed in 5 various degrees: preserved mobility, moderately limited mobility, limited mobility, very limited mobility, and work with touchpad/mouse.

DMD patients were divided into three groups based on age: 8–12 years, 13–18 years, and adult patients. All of them were asked to complete questionnaires for muscular dystrophy. The younger patients completed the PEDSQL 3.0 neuromuscular model questionnaire, and the older ones EQ-5D. Due to possible differences between self and proxy reports, we employed a PEDSQL 3.0 neuromuscular model questionnaire completed by DMD patients and their parents. All DMD patients and parents were instructed by an experienced pediatric neurologist how to complete the questionnaire in electronic version. None of the DMD patients were taking any psychotropic medications or opioids when the questionnaire was administered.

Questionnaires

PEDSQL 3.0 neuromuscular model questionnaire

PEDSQL is an instrument used to assess Health-Related QoL (HRQoL) in children and adolescents aged 2 to 18. It consists of both generic core and disease-specific modules. The PEDSQL 3.0 Neuromuscular Module questionnaire is a disease-specific module for measuring children's QoL assessing their neuromuscular disease, communication difficulties, and family resources. This instrument is acknowledged as a validated health outcome measure for patients with neuromuscular diseases (28). It was validated for the Czech Republic (29) for the DMD patient cohort and was translated into the Czech language. Its electronic version can be requested through this web page ePROVIDE™ - Online Support for Clinical Outcome Assessments.[1]

1 mapi-trust.org

EQ-5D questionnaire

EQ-5D questionnaire is a standardized measure of HRQoL developed by the EuroQol Group to provide a simple, generic questionnaire for use in clinical and economic appraisal and population health surveys. EQ-5D assesses health status in terms of five dimensions of health and is considered a 'generic' questionnaire because these dimensions are not specific to a specific patient group or health condition. EQ-5D can also be referred to as a patient-reported outcome measure (PROM) because patients can complete the questionnaire themselves to provide information about their current health status and how this changes over time (30). It was validated for the Czech population for patients with chronic pain (31) and can be found on the following web page: Available versions – EQ-5D (euroqol.org).

After a baseline clinical check-up and collection of all patient information, the DMD patients underwent a neurological examination. On the same day the patients were examined, the questionnaire in the electronic version was completed. After completing the questionnaire, DMD patients were examined by CMR within one week after their clinical examination by a neurologist.

Inclusion criteria for CMR: the absence of CMR contraindications such as an implanted pacemaker/defibrillator, cochlear implant, other ferromagnetic metal parts in the patient's body, claustrophobia, etc.; the absence of contraindications for using contrast media such as severe renal insufficiency; the patient's ability to co-operate during CMR examination; no known cardiovascular pathology apart from dystrophin cardiomyopathies.

All DMD patients underwent the CMR according to our previously published protocol (32) using a 1.5 T scanner (Ingenia, Philips Medical Systems, Best, The Netherlands) equipped with 5- and 32-element phased array receiver coils allowing for the use of parallel acquisition techniques in the supine position in repeated breath-hold. Four DMD patients underwent CMR examination without application of contrast agent.

CMR protocol

Functional imaging using balanced steady-state free precession cine sequences included four-chamber, two-chamber, and LV outflow tract long axis views, and a short axis stack from the cardiac base to the apex in the perpendicular plane to the LV long axis.

Late gadolinium enhancement (LGE) images in all long-axis views and the short-axis views were acquired 10 min after an intravenous bolus of 0.2 mmol/kg of the gadolinium-based contrast agent gadobutrol (Gadovist, Bayer-Schering Pharma, Germany) using an inversion-recovery turbo field echo sequence and, in case of doubt, also by phase-sensitive inversion recovery turbo field echo. Both 2-dimensional and 3-dimensional data acquisitions were performed in mid-diastole.

CMR analysis

The following parameters were evaluated: LVEF, end-diastolic/end-systolic volume (EDV/ESV), septal/lateral/average m*itral annular plane systolic excursion (MAPSE),* presence/absence of LGE. LV functional and morphological parameters were calculated from the short axis view stack using the summation-of-disc methods in accordance with recommendations for post-processing evaluation from the Society for Cardiovascular Magnetic Resonance (33). Septal and lateral MAPSE was measured as previously described (34, 35) by defining end-diastolic and end-systolic mitral annular planes on a long-axis four-chamber view. The average MAPSE was calculated as the mean of septal and lateral MAPSE.

LGE was defined as an area of visually identified contrast enhancement greater than the mean signal intensity of an adjacent area of the reference myocardium. LGE was not evaluated in four DMD patients who underwent the examination without application of contrast agent.

Statistical analysis

The data were analyzed using Stata Statistical Software Release 17 (StataCorp, College Station, TX). The continuous variables were reported as means and standard deviations (SDs) or medians and interquartile ranges (IQRs) according to the data distribution. The normality of data was evaluated by the Shapiro–Wilk test. Categorical variables were reported as counts and percentages. The Spearman correlation was used to assess the relationship between the components of the PEDSQL 3.0 neuromuscular model questionnaire and EQ-5D, age, BMI, upper limb movement, and CMR parameters. Similarly, the relationship between upper limb movement and CMR parameters was evaluated using the Spearman correlation. The Spearman's rank correlation coefficient was interpreted according to Prion and Haerling (36). The Wilcoxon rank-sum (Mann–Whitney) test was used to assess differences in the components of the PEDSQL 3.0 neuromuscular model questionnaire and EQ-5D between the predefined subgroups (heart failure treatment, current corticosteroid therapy, the ability to walk, the ability to sit, the presence of scoliosis, the presence of LGE). The difference between the categories of the PEDSQL 3.0 neuromuscular model questionnaire filled in by the parent or by the patient was evaluated using the Wilcoxon signed-rank test. All tests were two-tailed, and p values <0.05 were considered statistically significant.

Results

A total of 37 DMD patients (median age 16.8 years) were enrolled in the final analysis. The basic demographic data are shown in Table 1. The detailed information about current corticosteroid therapy is shown in Table 2. Results from both questionnaires are shown in Table 3.

EQ-5D questionnaire

DMD patients taking ACEI/sartans had better total mobility than DMD patients without therapy ($p = 0.048$).

There was a negative correlation between the movement of the upper limbs and total mobility ($r_s = -0.619$, $p = 0.0001$), self-service ($r_s = -0.863$, $p < 0.001$), and usual activities ($r_s = -0.765$, $p < 0.001$). On the contrary, movement of the upper limbs positively correlated with good/bad days ($r_s = 0.515$, $p = 0.001$). No correlation was found between the movement of the upper limbs, anxiety, and pain.

There was a statistically significant difference in total mobility ($p < 0.001$), self-service ($p < 0.001$), usual activities ($p = 0.0001$), and good and bad days ($p = 0.0095$) when comparing the ambulatory/non-ambulatory DMD patients ($p < 0.001$).

Similar results were found when comparing sitting/non-sitting DMD patients. There was a significant difference in total mobility ($p < 0.001$), self-service ($p < 0.001$), usual activities ($p < 0.001$), and good/bad days ($p = 0.039$) (see Table 4). No difference was found for

TABLE 1 Basic demographic data.

Variable	
Age, median (IQR)	16.8 (13.9–20.7)
Weight, median (IQR)	50 (40–76)
Height, mean (SD)	1.55 (0.19)
Ambulatory patients (*n*, %)	19 (51.4%)
Self-sitting patients (*n*, %)	24 (64.9%)
Upper limbs movement, median (IQR)	4 (2–5)
Scoliosis (*n*, %)	19 (51.4%)
Surgery of scoliosis (*n*, %)	2 (5.4%)
Actual feeling of dyspnea (*n*, %)	2 (5.4%)
Actual feeling of palpitations (*n*, %)	0 (0%)
Arrhythmia (*n*, %)	0 (0%)
NIPPV (*n*, %)	6 (16,2%)
Diabetes mellitus (*n*, %)	0 (0%)
Chronic renal insufficiency (*n*, %)	0 (0%)
Corticosteroid therapy (*n*, %)	20 (54.1%)
ACEI/Sartans (*n*, %)	28 (75.7%)
LVEF, median (IQR)	64 (53–68)
EDV, median (IQR)	91 (70–119)
MAPSE septal	10.5 (9–12)
MAPSE lateral	11 (10–13)
MAPSE average	11 (10–11.5)
Presence of LGE	22 (66.7%)*

ACEI, angiotensin converting enzyme inhibitors; EDV, end-systolic volume; IQR, interquartil range; LGE, late gadolinium enhancement; LVEF, left ventricular ejection fraction; MAPSE, mitral annular plane systolic excursion; NIPPV, Non-invasive positive pressure ventilation; *n*, number, *p*, *p*-value, SD, standard deviation. *Data only for 33 patients.

TABLE 2 Detailed information of corticosteroid therapy.

Corticosteroid therapy	DMD patients (*n*, %)
Currently	20 (54,1%)*
Never	14 (37%)
Previously	3 (8,1%)

DMD, Duchenne muscular dystrophy; *n*, number. *One patient takes deflazacort.

anxiety and pain. DMD patients with or without scoliosis showed a statistical difference only on good/bad days ($p = 0.011$).

When evaluating cardiac parameters, the following statistically significant correlations were found: a weak positive correlation between EDV and anxiety ($r_s = 0.330$, $p = 0.046$), a weak negative correlation between average MAPSE and total mobility ($r_s = -0.386$, $p = 0.020$), lateral MAPSE and total mobility ($r_s = -0.344$, $p = 0.040$), septal MAPSE and total mobility ($r_s = -0.355$, $p = 0.034$), and septal MAPSE and usual activities ($r_s = -0.342$, $p = 0.039$) (Table 5).

PEDSQL 3.0 neuromuscular model questionnaire

DMD patients aged 8–18 (median 13.9 years, IQR 11.6–15.6) and their parents completed the PEDSQL 3.0 neuromuscular model questionnaire. A statistically significant differences in disease category was found between the PEDSQL 3.0 neuromuscular model questionnaires completed by the DMD patients and their parents ($p = 0.008$) (see Figure 1).

TABLE 3 PEDSQL 3.0 neuromuscular model and EQ-5D results.

Scale	*N*	Median (IQR)
PEDSQL3.0 neuromuscular model questionnaire		
Child self-report		
Disease	19	19 (15–30)
Communication	19	6 (3–8)
Family	19	8 (6–11)
Parent report		
Disease	18	23.5 (17–34)
Communication	18	6.5 (4–9)
Family	18	8 (6–13)
EQ-5D		
Total mobility	36	3 (2–3)
Self-service	37	2 (2–3)
Usual activities	37	2 (2–3)
Pain	36	2 (1–2)
Anxiety	37	1 (1–2)
Good/bad days	37	7 (5–8)

IQR, interquartile range; *n*, number; PEDSQL, Pediatric quality of life questionnaire.

There was no significant difference in the PEDSQL 3.0 neuromuscular model questionnaire for DMD patients taking or not taking ACEI/sartans, nor for those taking or not taking corticosteroids.

BMI did not correlate with any of the evaluated parameters in the PEDSQL 3.0 neuromuscular model questionnaire.

QoL negatively correlated with movement of the upper limbs using PEDSQL 3.0 neuromuscular model questionnaire in the disease category completed by the DMD patients ($r_s = -0.748$, $p = 0.0002$) and by the parents ($r_s = -0.742$, $p = 0.0004$).

Movement of upper limbs positively correlated with septal MAPSE ($r_s = 0.3422$, $p = 0.038$).

Discussion

This was the first prospective study describing a detailed evaluation of the QoL in DMD patients of various ages and degrees of disability in relation to functional neurological and cardiac impairment. The most important results of our prospective study were the relation/association between:

1. Better movement of the upper limbs and total mobility, self-service, and good/bad days, but not usual activities.
2. Decreased QoL and movement of the upper limbs using the PEDSQL 3.0 neuromuscular model questionnaire in disease category completed both by DMD patients and their parents.
3. Movement of the upper limbs and septal MAPSE also trended toward average MAPSE.
4. Scoliosis and good/bad days.
5. EDV and anxiety/depression, but not average MAPSE and overall mobility or lateral MAPSE and total mobility.

TABLE 4 QoL and neurological impairment in our DMD cohort.

Scale	*n*	Sitting	Non-sitting	*p*	Ambulatory	Non-ambulatory	*p*
PEDSQL 3.0 neuromuscular model							
Child self-report							
Disease	19	18.5 (14.5–28)	30 (28–36)	0.114	17 (14.5–23.5)	28 (28–31)	0.113
Communication	19	4 (3–8)	7 (6–9)	0.258	3.5 (2–7.5)	7 (4–8)	0.223
Family	19	8 (4–10.5)	7 (6–16)	0.935	7.5 (1–10)	8 (7–15)	0.392
Parent report							
Disease	18	18 (17–30)	35 (31–39)	0.071	17 (14–30)	31 (24–35)	0.097
Communication	18	6 (3–8)	9 (6–12)	0.201	7 (3–8)	6 (5–12)	0.425
Family	18	7 (6–16)	7 (6–16)	1.000	8 (7–15)	8 (2–10)	0.385
EQ-5D							
Total mobility	36	2 (2–3)	3 (3–3)	<0.001	2 (1–2)	3 (3–3)	<0.001
Self-service	37	2 (1–2)	3 (3–3)	<0.001	2 (1–2)	3 (2–3)	<0.001
Usual activities	37	2 (1–2)	3 (3–3)	<0.001	2 (1–2)	3 (2–3)	<0.001
Pain	36	2 (1.5–2)	2 (1–2)	0.517	2 (1–2)	2 (1–2)	1.000
Anxiety	37	1 (1–2)	1 (1–2)	0.578	1 (1–2)	1 (1–2)	0.864
Good/bad days	37	7 (5–8)	5 (4–7)	0.039	7.5 (6–8)	5 (4–7)	<0.001

DMD, Duchenne muscular dystrophy; QoL, quality of life; *n*, number; *p*, *p*-value; PEDSQL, Pediatric quality of life. Scales are reported as medians and IQRs.

6. Septal MAPSE and total mobility or usual activities.
7. DMD patients taking ACEI/sartans had better overall mobility than DMD patients without therapy for heart failure.

Compared to the previously published studies focused on QoL in DMD patients (7, 8, 10, 11, 13–25, 27, 29, 37–39), we included all-aged DMD patients, we used the common questionnaires such as EQ-5D and PEDSQL 3.0 neuromuscular model questionnaire, and the results were not under/overestimated due to proxy reports as the PEDSQL 3.0 neuromuscular model questionnaire was completed both by DMD patients and their parents in our study. Possible reasons why DMD patients perceive their QoL as higher compared to their parents include fears about their child's disorder, the adaptation of DMD patients to their disease, an inexact perception of a child's status by their parents, limitations of the child, and the influence of environmental factors (13–15, 40). The results of our study were consistent with the previous studies, as the PEDSQL 3.0 neuromuscular model questionnaire completed by the parents showed more decreased QoL of DMD patients in the disease category compared to those who self-reported.

According to Powell et al., a comprehensive and reliable PROM of QoL including physical and social domain (41, 42) that is typically used for DMD patients (43–47) has a significant positive correlation with the PEDSQL 3.0 neuromuscular model questionnaire and the EQ-5D questionnaires used in our study (46). Moreover, we analyzed the most functional parameters related to the QoL for DMD patients that have ever been published.

Respiratory and cardiac impairments

When assessing the respiratory functions and QoL, the aspects of daily living and disability were highlighted in DMD patients on NIPPV compared to DMD patients without NIPPV. Regardless of the reduction in pulmonary function and daily living activities, DMD patients on NIPPV showed similar HRQoL to patients without NIPPV (27). The relationship between the physical and mental domains contrary to forced vital capacity did not show any statistically significant results (27). It is consistent with cardiomyopathy where DMD patients with or without cardiomyopathy reported similar disability scores (27). In our investigation, a minority of DMD patients necessitated nocturnal NIPPV; hence, we refrained from correlating its influence with the evaluated parameters.

In our study, we focused on cardiac function using CMR and QoL in DMD patients. Based on our previous study, Panovský et al. (48), DMD patients had impaired LV systolic function measured by MAPSE and global LV strain regardless of normal LVEF and the absence of LGE (48). The higher the EDV the higher anxiety/depression in DMD patients, whereas average MAPSE and total mobility or lateral MAPSE and total mobility were associated negatively. Similarly, decreasing septal MAPSE introduced reduced total mobility and usual activities. The better movement of the upper limbs the higher the septal MAPSE value. No arrhythmia was detected based on ECG Holter monitoring in our cohort. When evaluating the presence or absence of LGE and LVEF, there were no statistically significant differences observed in relation to any of the assessed parameters.

According to Porcher et al., DMD patients who take ACEI therapy prophylactically had significantly higher overall survival and lower rates of hospitalization for heart failure (49). This correlates with the results of our study that found DMD patients on ACEI/sartans had better overall mobility than DMD patients without therapy. Contrary to it, there was no significant difference for those taking ACEI/sartans according to the PEDSQL 3.0 neuromuscular model questionnaire.

Corticosteroid therapy

It is well-known that corticosteroid therapy can improve physical functioning and prolong estimated life expectancy and HRQoL in muscular dystrophy patients (11, 39, 50). We concentrated on influence

10.3389/fneur.2024.1360385

TABLE 5 Correlation between QoL and cardiac impairment using CMR.

Variable	*n*		LVEF	EDV	ESV	MAPSE average	MAPSE lateral	MAPSE septal
PEDSQL 3.0 neuromuscular model								
Child self-report								
Disease	19	r_s	0.106	−0.044	0.047	0.041	0.102	0.002
		P	0.665	0.859	0.849	0.867	0.677	0.994
Communication	19	r_s	0.257	−0.196	0.140	−0.115	−0.063	−0.040
		P	0.288	0.422	0.569	0.641	0.799	0.873
Family	19	r_s	0.088	−0.256	−0.117	0.027	0.001	0.017
		P	0.721	0.290	0.634	0.913	0.999	0.945
Parent report								
Disease	18	r_s	0.156	0.010	0.086	0.061	0.060	0.065
		P	0.535	0.969	0.734	0.811	0.815	0.797
Communication	18	r_s	0.307	−0.351	−0.247	0.078	0.013	0.148
		P	0.216	0.153	0.324	0.760	0.960	0.559
Family	18	r_s	−0.058	−0.087	0.061	0.004	0.015	−0.028
		P	0.819	0.731	0.811	0.988	0.953	0.913
EQ-5D								
Total mobility	36	r_s	0.168	−0.150	−0.139	−0.386	−0.344	−0.355
		P	0.328	0.382	0.421	0.020	0.040	0.034
Self-service	37	r_s	0.092	−0.131	−0.081	−0.219	−0.094	−0.320
		P	0.589	0.439	0.635	0.192	0.580	0.054
Usual activities	37	r_s	0.135	−0.196	−0.146	−0.278	−0.173	−0.342
		P	0.427	0.245	0.390	0.096	0.305	0.038
Pain	36	r_s	−0.003	0.238	0.041	0.064	0.233	−0.018
		P	0.987	0.162	0.814	0.709	0.172	0.919
Anxiety	37	r_s	−0.318	0.330	0.309	−0.235	−0.195	−0.202
		P	0.055	0.046	0.063	0.162	0.248	0.231
Good/bad days	37	r_s	−0.034	−0.147	−0.026	0.216	0.117	0.221
		P	0.841	0.386	0.878	0.199	0.492	0.188

CMR, cardiac magnetic resonance; EDV, end-diastolic volume; ESV, end-systolic volume; QoL, quality of life; LVEF, left ventricular ejection fraction; MAPSE, mitral annular plane systolic excursion; *p*, *p*-value; PEDSQoL, pediatric quality of life questionnaire.

of current corticosteroid therapy in our cohort. The average age at which corticosteroid therapy was initiated in our cohort is 5 years. All patients receive prednisone at a dose of 0.75 mg/kg/day, with the exception of one patient who takes deflazacort at a dose of 0.9 mg/kg/day. Some patients chose not to undergo corticosteroid therapy due to the gradual progression of the disease or concerns about potential side effects. Additionally, DMD patients discontinued corticosteroid therapy when they were no longer ambulatory, despite some guidelines recommending its use for preventing heart or respiratory failure.

Concerning the QoL, DMD patients taking or not taking corticosteroid therapy did not show any differences in their PEDSQL 3.0 neuromuscular model questionnaire.

BMI

It was well-recognized that the administration of steroids can result in weight gain and short stature (51). In the case of our study, BMI did not correlate with any of the evaluated parameters in the PEDSQL 3.0 neuromuscular model questionnaire.

Pain

DMD patients usually do not complain of pain although their ability to manage pain is limited (52, 53). It was not the subject of our study.

Movement of upper limbs + total mobility + tiredness

Overall mobility in DMD is a crucial item of QoL (46). Younger DMD patients are usually more tired due to the extra work/effort required for movement, whereas older DMD patients move less (46). Focusing on the movement of the upper limbs, we found a positive

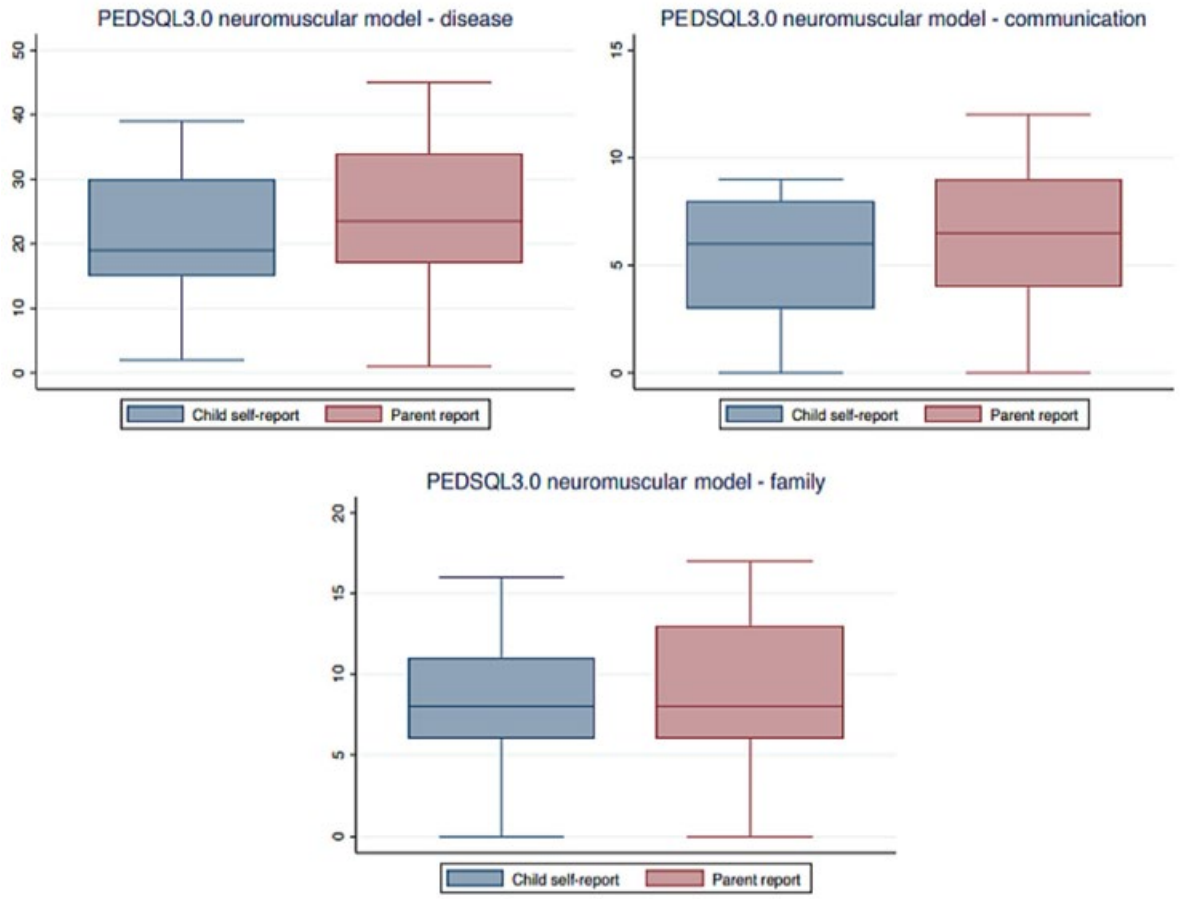

FIGURE 1
PEDSQL 3.0 neuromuscular model questionnaire completed by DMD patients and their parents. DMD, Duchenne muscular dystrophy; PEDSQL, pediatric quality of life questionnaire.

association with total mobility, self-service, and good/bad days in DMD patients, but it correlated negatively with usual activities. QoL negatively correlated with movement of the upper limbs using the PEDSQL 3.0 neuromuscular model questionnaire in disease category completed both by the DMD patients and their parents. Moreover, movement of the upper limbs positively correlated with septal MAPSE.

When assessing the ambulatory/non-ambulatory and sitting/non-sitting DMD patients, statistically significant difference in total mobility was found. Ambulatory/non-ambulatory and sitting/non-sitting DMD patients showed significant differences in self-service, usual activities, and good/bad days.

DMD patients with/without scoliosis showed a statistically significant difference in good/bad days.

Anxiety/sadness/mood/good or bad days

The QoL focused on physical activities, health, and friends in DMD patients was reduced (13). Pangalila et al. reported that social issues of QoL were affected/impaired in DMD patients compared to the control group (54). Based on previous studies, it is known that the general mood and feelings assessed for parents were decreased than that for DMD patients (11, 55). From the children's perspective, physical activities and health and friends were lower (13).

This is consistent with the results in our study in which EDV was positively associated with anxiety/depression, but was negatively associated with average MAPSE and total mobility, as were lateral MAPSE and total mobility.

Limitations of the study

It was a small sample because of the rare occurrence of DMD and it was a single-centre study. The questionnaire was completed in electronic version. The results of our study cannot be generalized to the worldwide population due to various levels of health care and social possibilities (56–58). In our study, our emphasis was on categorizing DMD patients into two primary groups: ambulatory and non-ambulatory. Specifically, detailed information on five subcategories of upper limb movement was collected exclusively from the "non-ambulatory DMD patients," with the corresponding data absent for ambulatory DMD patients. Regarding the evaluation of

corticosteroid therapy's influence, our focus was solely on the ongoing pharmacotherapy. Future studies focused on QoL in DMD are needed to confirm our results.

Conclusion

This study delved into various dimensions of QoL in DMD patients, considering neurological, cardiac, therapeutic, and emotional aspects. Key findings revealed significant correlations: improved upper limb movement positively related to overall mobility and emotional well-being, while QoL displayed negative associations with upper limb movement. Cardiac parameters, especially septal MAPSE, were interlinked with motor function. QoL distinctions were apparent among ambulatory/non-ambulatory and sitting/non-sitting DMD patients. Anxiety/depression correlated with cardiac parameters, highlighting the intricate connection between emotional and cardiac well-being. Treatment with ACEI/sartans positively impacted overall mobility. Despite study limitations, these insights underscore the imperative for personalized care strategies in DMD patient management.

Data availability statement

The original contributions presented in the study are included in the article/supplementary material, further inquiries can be directed to the corresponding author.

Ethics statement

The studies involving humans were approved by Institutional Ethics Committee (University Hospital Brno, reference number 20130410-03). The studies were conducted in accordance with the local legislation and institutional requirements. Written informed consent for participation in this study was provided by the participants' legal guardians/next of kin.

Author contributions

LJ: Writing – original draft, Writing – review & editing, Conceptualization, Data curation, Formal analysis, Funding acquisition, Investigation, Methodology, Project administration, Resources, Software, Supervision, Validation, Visualization. LM: Writing – original draft, Writing – review & editing, Conceptualization, Data curation, Formal analysis, Funding acquisition, Investigation, Methodology, Project administration, Resources, Software, Supervision, Validation, Visualization. RP: Conceptualization, Data curation, Formal analysis, Funding acquisition, Investigation, Methodology, Project administration, Resources, Software, Supervision, Validation, Visualization, Writing – review & editing. MP: Conceptualization, Data curation, Formal analysis, Funding acquisition, Investigation, Methodology, Project administration, Resources, Software, Supervision, Validation, Visualization, Writing – review & editing. KR: Conceptualization, Data curation, Formal analysis, Funding acquisition, Investigation, Methodology, Project administration, Resources, Software, Supervision, Validation, Visualization, Writing – review & editing. OV: Conceptualization, Data curation, Formal analysis, Funding acquisition, Investigation, Methodology, Project administration, Resources, Software, Supervision, Validation, Visualization, Writing – review & editing. VF: Conceptualization, Data curation, Formal analysis, Funding acquisition, Investigation, Methodology, Project administration, Resources, Software, Supervision, Validation, Visualization, Writing – review & editing. TH: Conceptualization, Data curation, Formal analysis, Funding acquisition, Investigation, Methodology, Project administration, Resources, Software, Supervision, Validation, Visualization, Writing – review & editing. VK: Conceptualization, Data curation, Formal analysis, Funding acquisition, Investigation, Methodology, Project administration, Resources, Software, Supervision, Validation, Visualization, Writing – review & editing. PD: Conceptualization, Data curation, Formal analysis, Funding acquisition, Investigation, Methodology, Project administration, Resources, Software, Supervision, Validation, Visualization, Writing – review & editing. SV: Conceptualization, Data curation, Formal analysis, Funding acquisition, Investigation, Methodology, Project administration, Resources, Software, Supervision, Validation, Visualization, Writing – review & editing. JH: Conceptualization, Data curation, Formal analysis, Funding acquisition, Investigation, Methodology, Project administration, Resources, Software, Supervision, Validation, Visualization, Writing – review & editing. KP: Conceptualization, Data curation, Formal analysis, Funding acquisition, Investigation, Methodology, Project administration, Resources, Software, Supervision, Validation, Visualization, Writing – review & editing.

Funding

The author(s) declare financial support was received for the research, authorship, and/or publication of this article. The five of the authors of this publication are members of the European Reference Network for Neuromuscular Diseases – Project ID N°870177. This publication was supported by specific research grant of Masaryk university (MUNI/A/1624/2023).

Conflict of interest

The authors declare that the research was conducted in the absence of any commercial or financial relationships that could be construed as a potential conflict of interest.

Publisher's note

References

1. Stark AE. Determinants of the incidence of Duchenne muscular dystrophy. *Ann Transl Med*. (2015) 3:287. doi: 10.3978/j.issn.2305-5839.2015.10.45

2. Wong SH, McClaren BJ, Archibald AD, Weeks A, Langmaid T, Ryan MM, et al. A mixed methods study of age at diagnosis and diagnostic odyssey for Duchenne muscular dystrophy. *Eur J Hum Genet EJHG*. (2015) 23:1294–300. doi: 10.1038/ejhg.2014.301

3. Birnkrant DJ, Bushby K, Bann CM, Apkon SD, Blackwell A, Brumbaugh D, et al. Diagnosis and management of Duchenne muscular dystrophy, part 1: diagnosis, and neuromuscular, rehabilitation, endocrine, and gastrointestinal and nutritional management. *Lancet Neurol*. (2018) 17:251–67. doi: 10.1016/S1474-4422(18)30024-3

4. Eagle M, Baudouin SV, Chandler C, Giddings DR, Bullock R, Bushby K. Survival in Duchenne muscular dystrophy: improvements in life expectancy since 1967 and the impact of home nocturnal ventilation. *Neuromuscul Disord NMD*. (2002) 12:926–9. doi: 10.1016/S0960-8966(02)00140-2

5. Passamano L, Taglia A, Palladino A, Viggiano E, D'Ambrosio P, Scutifero M, et al. Improvement of survival in Duchenne muscular dystrophy: retrospective analysis of 835 patients. *Acta Myol*. (2012) 31:121–5.

6. Landfeldt E, Thompson R, Sejersen T, McMillan HJ, Kirschner J, Lochmüller H. Life expectancy at birth in Duchenne muscular dystrophy: a systematic review and meta-analysis. *Eur J Epidemiol*. (2020) 35:643–53. doi: 10.1007/s10654-020-00613-8

7. Baiardini I, Minetti C, Bonifacino S, Porcu A, Klersy C, Petralia P, et al. Quality of life in Duchenne muscular dystrophy: the subjective impact on children and parents. *J Child Neurol*. (2011) 26:707–13. doi: 10.1177/0883073810389043

8. Witte RA. The psychosocial impact of a progressive physical handicap and terminal illness (Duchenne muscular dystrophy) on adolescents and their families. *Br J Med Psychol*. (1985) 58:179–87. doi: 10.1111/j.2044-8341.1985.tb02632.x

9. Gagliardi BA. The impact of Duchenne muscular dystrophy on families. *Orthop Nurs*. (1991) 10:41–9. doi: 10.1097/00006416-199109000-00009

10. Grootenhuis MA, de Boone J, van der Kooi AJ. Living with muscular dystrophy: health related quality of life consequences for children and adults. *Health Qual Life Outcomes*. (2007) 5:31. doi: 10.1186/1477-7525-5-31

11. Bray P, Bundy AC, Ryan MM, North KN, Everett A. Health-related quality of life in boys with Duchenne muscular dystrophy: agreement between parents and their sons. *J Child Neurol*. (2010) 25:1188–94. doi: 10.1177/0883073809357624

12. Vahedi S. World Health Organization quality-of-life scale (WHOQOL-BREF): analyses of their item response theory properties based on the graded responses model. *Iran J Psychiatry*. (2010) 5:140–53.

13. Zamani G, Heidari M, Azizi Malamiri R, Ashrafi MR, Mohammadi M, Shervin Badv R, et al. The quality of life in boys with Duchenne muscular dystrophy. *Neuromuscul Disord NMD*. (2016) 26:423–7. doi: 10.1016/j.nmd.2016.05.004

14. Elsenbruch S, Schmid J, Lutz S, Geers B, Schara U. Self-reported quality of life and depressive symptoms in children, adolescents, and adults with Duchenne muscular dystrophy: a cross-sectional survey study. *Neuropediatrics*. (2013) 44:257–64. doi: 10.1055/s-0033-1347935

15. Bendixen RM, Senesac C, Lott DJ, Vandenborne K. Participation and quality of life in children with Duchenne muscular dystrophy using the international classification of functioning, disability, and health. *Health Qual Life Outcomes*. (2012) 10:43. doi: 10.1186/1477-7525-10-43

16. Riley AW. Evidence that school-age children can self-report on their health. *Ambul Pediatr*. (2004) 4:371–6. doi: 10.1367/A03-178R.1

17. Raat H, Bonsel GJ, Essink-Bot ML, Landgraf JM, Gemke RJBJ. Reliability and validity of comprehensive health status measures in children: the child health questionnaire in relation to the health utilities index. *J Clin Epidemiol*. (2002) 55:67–76. doi: 10.1016/S0895-4356(01)00411-5

18. Ravens-Sieberer U, Gosch A, Abel T, Auquier P, Bellach BM, Bruil J, et al. Quality of life in children and adolescents: a European public health perspective. *Soz Praventivmed*. (2001) 46:294–302. doi: 10.1007/BF01321080

19. McPhail S, Beller E, Haines T. Two perspectives of proxy reporting of health-related quality of life using the Euroqol-5D, an investigation of agreement. *Med Care*. (2008) 46:1140–8. doi: 10.1097/MLR.0b013e31817d69a6

20. Marques JCB, Oliveira JA, Goulardins JB, Nascimento RO, Lima AMV, Casella EB. Comparison of child self-reports and parent proxy-reports on quality of life of children with attention deficit hyperactivity disorder. *Health Qual Life Outcomes*. (2013) 11:186. doi: 10.1186/1477-7525-11-186

21. Grimaldi Capitello T, Fiorilli C, Placidi S, Vallone R, Drago F, Gentile S. What factors influence parents' perception of the quality of life of children and adolescents with neurocardiogenic syncope? *Health Qual Life Outcomes*. (2016) 14:79. doi: 10.1186/s12955-016-0476-9

22. Nolan LB. An exploration of proxy- and self-reported adolescent health in low-resource settings. *Surv Res Methods*. (2016) 10:65–83. doi: 10.18148/srm/2016.v10i2.6711

23. Connolly MA, Johnson JA. Measuring quality of life in paediatric patients. *PharmacoEconomics*. (1999) 16:605–25. doi: 10.2165/00019053-199916060-00002

24. Hullmann SE, Ryan JL, Ramsey RR, Chaney JM, Mullins LL. Measures of general pediatric quality of life: child health questionnaire (CHQ), DISABKIDS chronic generic measure (DCGM), KINDL-R, pediatric quality of life inventory (PedsQL) 4.0 generic Core scales, and quality of my life questionnaire (QoML). *Arthritis Care Res*. (2011) 63:S420–30. doi: 10.1002/acr.20637

25. Vincent KA, Carr AJ, Walburn J, Scott DL, Rose MR. Construction and validation of a quality of life questionnaire for neuromuscular disease (INQoL). *Neurology*. (2007) 68:1051–7. doi: 10.1212/01.wnl.0000257819.47628.41

26. Crossnohere NL, Fischer R, Lloyd A, Prosser LA, Bridges JFP. Assessing the appropriateness of the EQ-5D for Duchenne muscular dystrophy: a patient-centered study. *Med Decis Mak Int J Soc Med Decis Mak*. (2021) 41:209–21. doi: 10.1177/0272989X20978390

27. Kohler M, Clarenbach CF, Böni L, Brack T, Russi EW, Bloch KE. Quality of life, physical disability, and respiratory impairment in Duchenne muscular dystrophy. *Am J Respir Crit Care Med*. (2005) 172:1032–6. doi: 10.1164/rccm.200503-322OC

28. Wiwaha G, Sari DM, Biben V, Sunjaya DK, Hilmanto D. Translation and validation of Indonesian version of pediatric quality of life inventory™ (PedsQL™) neuromuscular module. *Health Qual Life Outcomes*. (2022) 20:33. doi: 10.1186/s12955-022-01933-x

29. Landfeldt E, Lindgren P, Bell CF, Guglieri M, Straub V, Lochmüller H, et al. Health-related quality of life in patients with Duchenne muscular dystrophy: a multinational, cross-sectional study. *Dev Med Child Neurol*. (2016) 58:508–15. doi: 10.1111/dmcn.12938

30. Devlin N, Parkin D, Janssen B. *Methods for Analysing and reporting EQ-5D data*. Cham: Springer Nature (2020).

31. Obradovic M, Lal A, Liedgens H. Validity and responsiveness of EuroQol-5 dimension (EQ-5D) versus short Form-6 dimension (SF-6D) questionnaire in chronic pain. *Health Qual Life Outcomes*. (2013) 11:110. doi: 10.1186/1477-7525-11-110

32. Panovský R, Pešl M, Holeček T, Máchal J, Feitová V, Mrázová L, et al. Cardiac profile of the Czech population of Duchenne muscular dystrophy patients: a cardiovascular magnetic resonance study with T1 mapping. *Orphanet J Rare Dis*. (2019) 14:10. doi: 10.1186/s13023-018-0986-0

33. Schulz-Menger J, Bluemke DA, Bremerich J, Flamm SD, Fogel MA, Friedrich MG, et al. Standardized image interpretation and post processing in cardiovascular magnetic resonance: Society for Cardiovascular Magnetic Resonance (SCMR) board of trustees task force on standardized post processing. *J Cardiovasc Magn Reson*. (2013) 15:35. doi: 10.1186/1532-429X-15-35

34. Puchalski MD, Williams RV, Askovich B, Sower CT, Hor KH, Su JT, et al. Late gadolinium enhancement: precursor to cardiomyopathy in Duchenne muscular dystrophy? *Int J Cardiovasc Imaging*. (2009) 25:57–63. doi: 10.1007/s10554-008-9352-y

35. Florian A, Ludwig A, Engelen M, Waltenberger J, Rösch S, Sechtem U, et al. Left ventricular systolic function and the pattern of late-gadolinium-enhancement independently and additively predict adverse cardiac events in muscular dystrophy patients. *J Cardiovasc Magn Reson*. (2014) 16:81. doi: 10.1186/s12968-014-0081-1

36. Prion SK, Haerling KA. Making sense of methods and measurement: spearman-rho ranked-order correlation coefficient. *Clin Simul Nurs*. (2014) 10:535–6. doi: 10.1016/j.ecns.2014.07.005

37. Wei Y, Speechley KN, Zou G, Campbell C. Factors associated with health-related quality of life in children with Duchenne muscular dystrophy. *J Child Neurol*. (2016) 31:879–86. doi: 10.1177/0883073815627879

38. Houwen-van Opstal SLS, Jansen M, van Alfen N, de Groot IJM. Health-related quality of life and its relation to disease severity in boys with Duchenne muscular dystrophy: satisfied boys, worrying parents--a case-control study. *J Child Neurol*. (2014) 29:1486–95. doi: 10.1177/0883073813506490

39. Uzark K, King E, Cripe L, Spicer R, Sage J, Kinnett K, et al. Health-related quality of life in children and adolescents with Duchenne muscular dystrophy. *Pediatrics*. (2012) 130:e1559–66. doi: 10.1542/peds.2012-0858

40. Liang R, Chan SHS, Ho FKW, Tang OC, Cherk SWW, Ip P, et al. Health-related quality of life in Chinese boys with Duchenne muscular dystrophy and their families. *J Child Health Care*. (2019) 23:495–506. doi: 10.1177/1367493519857423

41. Uttley L, Carlton J, Woods HB, Brazier J. A review of quality of life themes in Duchenne muscular dystrophy for patients and carers. *Health Qual Life Outcomes*. (2018) 16:237. doi: 10.1186/s12955-018-1062-0

42. Lue YJ, Chen SS, Lu YM. Quality of life of patients with Duchenne muscular dystrophy: from adolescence to young men. *Disabil Rehabil*. (2017) 39:1408–13. doi: 10.1080/09638288.2016.1196398

43. Bann CM, Abresch RT, Biesecker B, Conway KC, Heatwole C, Peay H, et al. Measuring quality of life in muscular dystrophy. *Neurology*. (2015) 84:1034–42. doi: 10.1212/WNL.0000000000001336

44. Straub V, Mercuri E. Report on the workshop: meaningful outcome measures for Duchenne muscular dystrophy, London, UK, 30-31 January 2017. *Neuromuscul Disord NMD*. (2018) 28:690–701. doi: 10.1016/j.nmd.2018.05.013

45. Mokkink LB, Terwee CB, Patrick DL, Alonso J, Stratford PW, Knol DL, et al. The COSMIN checklist for assessing the methodological quality of studies on measurement properties of health status measurement instruments: an international Delphi study. *Qual Life Res Int J Qual Life Asp Treat Care Rehabil*. (2010) 19:539–49. doi: 10.1007/s11136-010-9606-8

46. Powell PA, Carlton J, Rowen D, Chandler F, Guglieri M, Brazier JE. Development of a new quality of life measure for Duchenne muscular dystrophy using mixed methods: the DMD-QoL. *Neurology*. (2021) 96:e2438–50. doi: 10.1212/WNL.0000000000011896

47. Rowen D, Powell P, Mukuria C, Carlton J, Norman R, Brazier J. Deriving a preference-based measure for people with Duchenne muscular dystrophy from the DMD-QoL. *Value Health J Int Soc Pharmacoeconomics Outcomes Res*. (2021) 24:1499–510. doi: 10.1016/j.jval.2021.03.007

48. Panovský R, Pešl M, Máchal J, Holeček T, Feitová V, Juříková L, et al. Quantitative assessment of left ventricular longitudinal function and myocardial deformation in Duchenne muscular dystrophy patients. *Orphanet J Rare Dis*. (2021) 16:57. doi: 10.1186/s13023-021-01704-9

49. Porcher R, Desguerre I, Amthor H, Chabrol B, Audic F, Rivier F, et al. Association between prophylactic angiotensin-converting enzyme inhibitors and overall survival in Duchenne muscular dystrophy—analysis of registry data. *Eur Heart J*. (2021) 42:1976–84. doi: 10.1093/eurheartj/ehab054

50. Hendriksen JGM, Poysky JT, Schrans DGM, Schouten EGW, Aldenkamp AP, Vles JSH. Psychosocial adjustment in males with Duchenne muscular dystrophy: psychometric properties and clinical utility of a parent-report questionnaire. *J Pediatr Psychol*. (2009) 34:69–78. doi: 10.1093/jpepsy/jsn067

51. Lamb MM, West NA, Ouyang L, Yang M, Weitzenkamp D, James K, et al. Corticosteroid treatment and growth patterns in ambulatory males with Duchenne muscular dystrophy. *J Pediatr*. (2016) 173:207–213.e3. doi: 10.1016/j.jpeds.2016.02.067

52. Pangalila RF, van den Bos GA, Bartels B, Bergen M, Stam HJ, Roebroeck ME. Prevalence of fatigue, pain, and affective disorders in adults with duchenne muscular dystrophy and their associations with quality of life. *Arch Phys Med Rehabil*. (2015) 96:1242–7. doi: 10.1016/j.apmr.2015.02.012

53. Hunt A, Carter B, Abbott J, Parker A, Spinty S, deGoede C. Pain experience, expression and coping in boys and young men with Duchenne muscular dystrophy - a pilot study using mixed methods. *Eur J Paediatr Neurol EJPN*. (2016) 20:630–8. doi: 10.1016/j.ejpn.2016.03.002

54. Pangalila RF, van den Bos GAM, Bartels B, Bergen MP, Kampelmacher MJ, Stam HJ, et al. Quality of life of adult men with Duchenne muscular dystrophy in the Netherlands: implications for care. *J Rehabil Med*. (2015) 47:161–6. doi: 10.2340/16501977-1898

55. Davis SE, Hynan LS, Limbers CA, Andersen CM, Greene MC, Varni JW, et al. The PedsQL in pediatric patients with Duchenne muscular dystrophy: feasibility, reliability, and validity of the pediatric quality of life inventory neuromuscular module and generic Core scales. *J Clin Neuromuscul Dis*. (2010) 11:97–109. doi: 10.1097/CND.0b013e3181c5053b

56. Cavazza M, Kodra Y, Armeni P, De Santis M, López-Bastida J, Linertová R, et al. Social/economic costs and health-related quality of life in patients with Duchenne muscular dystrophy in Europe. *Eur J Health Econ HEPAC*. (2016) 17:19–29. doi: 10.1007/s10198-016-0782-5

57. Steffensen B, Otto C, Werlauff U, Rahbek J, Hoejberg A, Kirschner J, et al. G.P.388 - health related quality of life in European adults with DMD: results from the care-NMD-project. *Neuromuscul Disord*. (2015) 25:S302. doi: 10.1016/j.nmd.2015.06.412

58. Thomas PT, Rajaram P, Nalini A. Psychosocial challenges in family caregiving with children suffering from Duchenne muscular dystrophy. *Health Soc Work*. (2014) 39:144–52. doi: 10.1093/hsw/hlu027

Glossary

ACEI	Angiotensin converting enzyme inhibitors
BMI	Body mass index
CMR	Cardiac magnetic resonance
DMD	Duchenne muscular dystrophy
ECG	Electrocardiogram
EDV	End-diastolic volume
EF	Ejection fraction
ESV	End-systolic volume
HRQoL	Health-related quality of life
IQRs	Interquartile ranges
LGE	Late gadolium enhancement
LV	Left ventricular
LVEF	Left ventricular ejection fraction
MAPSE	Mitral annular plane systolic excursion
NIPPV	Non-invasive positive pressure ventilation
PEDSQL	Pediatric quality of life questionnaire
PROM	Patient-reported outcome measure
QoL	Quality of life
SDs	Standard deviation

A. Kvasnička et al.

Long-chain polyunsaturated fatty acid-containing phosphatidylcholines predict survival rate in patients after heart failure

Heliyon
Impact Factor: 3,4

rejstřík

Heliyon 10 (2024) e39979

Contents lists available at ScienceDirect

Heliyon

journal homepage: www.cell.com/heliyon

Research article

Long-chain polyunsaturated fatty acid-containing phosphatidylcholines predict survival rate in patients after heart failure

Aleš Kvasnička [a,b,1], Karel Kotaška [c,1], David Friedecký [a,b,*], Karolína Ježdíková [c], Radana Brumarová [b], Tomáš Hnát [d], Petr Kala [d,e,**]

[a] Laboratory for Inherited Metabolic Disorders, Department of Clinical Biochemistry, University Hospital, Olomouc, Czech Republic
[b] Faculty of Medicine and Dentistry, Palacký University in Olomouc, Czech Republic
[c] Department of Medical Chemistry and Clinical Biochemistry, 2nd Medical Faculty, University Hospital Motol, Prague, Czech Republic
[d] Department of Cardiology, University Hospital Motol and 2nd Faculty of Medicine, Charles University, Prague, Czech Republic
[e] Center of Experimental Medicine, Institute of Clinical and Experimental Medicine, Prague, Czech Republic

ARTICLE INFO

Keywords:
Lipidomics
Eicosanoids
Survival rate
Heart failure
PUFA
PC
HF survival
Atherosclerosis
Phosphatidylcholine

ABSTRACT

Background: Heart failure (HF) is becoming an increasingly prevalent issue, particularly among the elderly population. Lipids are closely associated with cardiovascular disease (CVD) pathology. Lipidomics as a comprehensive profiling tool is showing to be promising in the prediction of events and mortality due to CVD as well as identifying novel biomarkers.

Materials and methods: In this study, eicosanoids and lipid profiles were measured in order to predict survival in patients with de novo or acute decompensated HF. Our study included 50 patients (16 females, mean age 73 years and 34 males, mean age 71 years) with de novo or acute decompensated chronic HF with a median follow-up of 7 months. Lipids were semiquantified using targeted lipidomic liquid chromatography-mass spectrometry (LC-MS/MS) analysis. Eicosanoid concentrations were determined using a commercially available sandwich ELISA assay.

Results: From 736 lipids and 3 eicosanoids, 39 significant lipids were selected (by using the Mann-Whitney *U* test after Benjamini-Hochberg correction) with the highest number of representatives belonging to the polyunsaturated (PUFA) phosphatidylcholines (PC). PC 42:10 ($p = 1.44 \times 10^{-4}$) was found to be the most statistically significantly elevated in the surviving group with receiver operating characteristics of AUC = 0.84 ($p = 3.24 \times 10^{-7}$). A multivariate supervised discriminant analysis based on the aforementioned lipid panel enabled the classification of the groups of surviving and non-surviving patients with 90 % accuracy.

Conclusions: In the present study we describe a trend in PUFA esterified in PC that were systematically increased in surviving patients with HF. This trend in low-abundant and rarely identified PUFA PC (mainly very long chain PUFA containing PC such as PC 42:10 or PC 40:9 containing FA 22:6, FA 20:5 and FA 20:4) suggests candidate biomarkers.

* Corresponding author. Department of Clinical Biochemistry, University Hospital Olomouc, Zdravotniků 7, Olomouc, Czech Republic.
** Corresponding author. Department of Cardiology, University Hospital Motol, V Úvalu 84, 150 00, Prague, Czech Republic.
E-mail addresses: david.friedecky@upol.cz (D. Friedecký), Petr.Kala@fnmotol.cz (P. Kala).
[1] These authors contributed equally to this work and should be considered shared first authors.

https://doi.org/10.1016/j.heliyon.2024.e39979
Received 11 August 2023; Received in revised form 19 October 2024; Accepted 29 October 2024
Available online 30 October 2024

1. Introduction

Heart failure (HF) is becoming a significant public health concern, largely due to the ageing population and the associated mortality from de novo or acute decompensated HF. Although the age-adjusted incidence of HF is decreasing in developed countries, probably due to improved management of cardiovascular disease (CVD), the overall incidence is increasing as the population ages [1]. The current prevalence of heart failure is estimated to be 1–2% in all adults and up to 10 % in those over the age of 70 [2,3]. It is likely that the true prevalence of heart failure is higher than that indicated by studies, which usually include only cases that have been recognised and diagnosed. It is therefore beneficial to investigate the diagnosis and progression monitoring of CVD and de novo or acute decompensated HF using novel approaches such as lipidomics, with the objective of gaining insight into the underlying biochemical processes behind and stratifying risk groups.

Lipidomics is a field of study that focuses on the analysis of lipids, including their quantification, as well as the study of their catabolic or anabolic biochemical pathways. The association of changes in the plasma lipidome with the progression of CVD in patients or the prediction of its acute complications has already been well described in the literature. Promising results from recent lipidomics studies have defined several CVD-related lipid classes (mainly ceramides) and individual plasma lipids that are attracting the attention of clinicians, given that they are already part of the Mayo Clinic test catalogue (CERAM test) [4–6]. Ceramides are bioactive sphingolipids with a pivotal role in cell signalling, proliferation, senescence, adhesion, migration, and angiogenesis. They have recently been shown also to influence CVD-related processes, including LDL aggregation and uptake, endothelial dysfunction, and inflammation [7,8]. A ceramide- and phospholipid-based risk score, CERT2, has been developed and validated on multi-cohort samples to effectively predict the risk of cardiovascular events and death in patients with coronary artery disease [6]. Similarly, the CERAM test, which is based on the analysis of plasma ceramides (16:0; 18:0; 24:1 and their ratios to 24:0), can predict the risk of major adverse cardiovascular events (such as myocardial infarction, coronary revascularisation, acute coronary syndrome hospitalization and mortality) within the next 1–5 years [9]. Nevertheless, it would be advantageous to test these findings in a clinical setting with the potential to identify new lipids that could be used to predict the survival of patients with de novo or acute decompensated HF.

Eicosanoids are bioactive lipid mediators which are derived from the catalysis of n-3 and n-6 polyunsaturated fatty acid (PUFA) substrates by lipoxygenases (LOXs), cyclooxygenases (COXs), or cytochrome P450s (CYPs). Epoxyeicosatrienoic acids (EETs) and 20-hydroxyeicosatetraenoic acid (20-HETE) are the products of CYPs epoxygenases (EETs) and ω-hydroxylases (20-HETE), respectively. The subsequent rapid conversion of EETs to the less active dihydroxyeicosatrienoic acids (DHETs) is catalysed by soluble epoxide hydrolases (sEH). EETs exert a variety of physiological functions, including cell proliferation, inflammation modulation, vascular function (vasodilation) and natriuresis. Chronic vascular inflammation may contribute to the development and progression of atherosclerotic cardiovascular disease, including coronary artery disease (CAD) and acute myocardial infarction (AMI). Anti-inflammatory drugs (such as interleukin-6 receptor antagonists) have demonstrated their efficacy as a novel therapeutic approach in CAD [10]. The vasoactive and natriuretic effects of eicosanoids suggesting their potential beneficial role in heart failure have been tested in preclinical studies in various animal models, leading to the development of orally active EET analogues and sEH inhibitors [11]. Both, EET analogues and sEH inhibitors, showed positive morphological, hemodynamic and mortality effects in animal HF models in our recent studies [12,13]. However, the potential role of eicosanoids in clinical cardiovascular disease particularly in HF, is not fully understood [14,15].

The aim of the study was to investigate the eicosanoids and lipid profiles as a biomarker panel for predicting survival in patients with de novo or acute decompensated chronic HF.

2. Materials and methods

2.1. Chemicals and reagents

Acetonitrile (ACN), isopropanol (IPA), water, and ammonium acetate (AmAc), all in liquid chromatography-mass spectrometry (LC-MS/MS) grade, were purchased from Sigma-Aldrich (St. Louis, MO, USA). As internal standards, the SPLASH® LIPIDOMIX® Mass Spec Standard mixture and ceramide (d18:1-d7/15:0) were used and purchased from Avanti Polar Lipids (Alabaster, AL, USA). Arachidonic acid-d8 was purchased from the Cayman Chemical Company (Ann Arbor, MI, USA). As the standard reference material for plasma, we used the NIST® SRM® 1950 - "Metabolites in frozen human plasma" (SRM 1950) which was purchased from Sigma-Aldrich (St. Louis, MO, USA).

2.2. Patient groups

The study included 50 patients (16 females, aged from 30 to 96 years, mean age 73 years and 34 males, aged from 46 to 86 years, mean age 71 years) with de novo or acute decompensated chronic HF admitted to our tertiary cardiovascular centre. This study was approved by the Ethics Committee of University Hospital Motol (number EK-739/21, approved on 16.6. 2021). Written informed consent was obtained from all participants enrolled in the study. During the prospective median follow-up of 7 months, 13 patients died (hereafter referred to as the non-surviving group). The patients were characterised by cardiological assessments, including the left ventricular ejection fraction (LVEF). Biochemical parameters (CRP, NT-proBNP, LDL, creatinine) were determined using commercially available biochemical and immunochemical assays. Furthermore, eGFR was calculated using the CKD-EPI equation. Clinical data and risk factors were analysed. A summary of the patient's characteristics is provided in Table 1 and provided in detail in Table S1.

2.3. Serum preparation and eicosanoid analysis

Sample collection, preparation and storage were carried out with a consideration to minimize preanalytical effects [16]. Blood samples were collected the next day (after admission) in the morning before breakfast in tubes coated with microscopic silica particles as a coagulation activator. After centrifugation (10 min, 4000 rpm, 8 °C), the serum was separated, aliquoted, directly analysed (eicosanoid analysis) and the rest was stored at −80 °C (for lipidomic analysis). The concentration of eicosanoids (14,15-EET, 14, 15-DHET and 20-HETE) was determined using commercially available sandwich ELISA assays (MyBioSource, USA). The ELISA assays were performed according to the manufacturer's instructions and previously published protocol [17], and the semiquantitative data are presented in Table S1.

2.4. Lipidomic analysis

2.4.1. Sample preparation for lipidomic analysis

Serum samples for lipidomic analysis were firstly placed from −80 °C to −20 °C overnight and thawed on ice the next day. After freeze-thawing and mixing for 10s on a vortex mixer, the extraction was performed using a protocol described in Ref. [18] by mixing 50 μL of serum with 150 μL of IPA containing internal standards (specified in Table S4). Samples were stored in the freezer (-20 °C) overnight for deproteinization and on the following day, the mixture was centrifuged (10 min, 14 000 g, 4 °C). The supernatant above the protein pellet was transferred (approximately 150 μL) into a glass LC-MS vial. A 10 μL aliquot was taken from each sample and pooled as a quality control (QC) sample. The samples were then immediately subjected to LC-MS analysis. Samples were double randomized, firstly during the sample preparation and secondly with respect to the order of the analytical runs. The QC sample was analysed as every 6th injection and was used for the instrument stability monitoring. Five independently prepared replicates of the SRM 1950 were measured during the analysis.

2.4.2. Liquid chromatography

The method for pseudotargeted lipidomic analysis, using liquid chromatography coupled to mass spectrometry, was used in the same settings as in previous studies [19]. The LC separation was performed by an ExionLC™ system (Sciex, Foster City, CA, USA), the data were acquired using QTRAP® 6500+ mass spectrometer (Sciex, Foster City, CA, USA) and the system was controlled by the Analyst software (version 1.6.2, Sciex, Foster City, CA, USA). For the chromatographic separation, the reversed-phase BEH C8 column (2.1 mm, 100 mm, 1.7 μm, Waters, Milford, MA, U.S.A.) was employed. The mobile phase A was ACN: H_2O (3:2, v/v), and the mobile phase B was IPA: ACN (9:1, v/v), and both contained 10 mM AmAc. The flow rate was set at 0.35 ml/min and the column temperature was 55 °C. The elution gradient started at 32 % B up to 1.5 min, then increased linearly to 85 % B at 15.5 min, then it increased again to 97 % B at 15.6 min, was held for 2.4 min. The gradient then reached its initial composition of 32 % B at 18.1 min and it was held for 1.9 min for equilibration of the column.

Table 1
Patient characteristics. Data are presented as median (interquartile range, Q1/Q3) or number (%) and p-values correspond to the two-tailed Mann-Whitney test (continuous variables) or Fisher's exact test (categorical variables).

Description of the patient cohort	Surviving group (n = 37)	Non-surviving group (n = 13)	p-value
Age (years)	76 (68/80)	81 (71/86)	0.0698
Female (%)	37.8	15.4	0.1792
BMI (kg/m^2)	28 (25.1/31.1)	29.4 (27.4/31.9)	0.3265
Weight (kg)	82 (75/94)	85 (75/90)	0.4395
HFrEF (%)	51.4	76.9	0.1906
HFmrEF (%)	13.5	0	0.3087
HFpEF (%)	35.1	23.1	0.5075
LVEF (median %)	40 (27/55)	25 (20/40)	0.1221
Statin (%)	59.5	46.2	0.5204
Hypertension (%)	81.1	69.2	0.4446
Type 2 diabetes mellitus (%)	48.7	46.2	>0.9999
Coronary artery disease (%)	78.4	69.2	0.7069
COPD (%)	24.3	23.1	>0.9999
Chronic kidney disease (eGFR <1 ml/s/1.73m^2) (%)	48.7	76.9	0.1084
Biochemical characteristics			
NT-proBNP (ng/l)	3785 (2458/8541)	11263 (7185/26269)	**0.0155**
eGFR (ml/s/1.73m^2)	1.0 (0.7/1.3)	0.5 (0.4/0.6)	**0.0019**
CRP (mg/l)	6.8 (1.9/13.3)	23.5 (17/47.1)	**0.0030**
LDL cholesterol (mmol/l)	2.4 (1.7/3.1)	1.7 (1.3/2.5)	0.1149
Total cholesterol (mmol/l)	4.1 (3.3/4.9)	3.1 (2.9/3.9)	0.0994

Abbreviations: HFrEF - heart failure with reduced ejection fraction (LVEF ≤40 %), HFmrEF - heart failure with mildly reduced ejection fraction (LVEF 41–49 %), HFpEF - heart failure with preserved ejection fraction (LVEF ≥50 %), LVEF - left ventricular ejection fraction, NT-proBNP - N-terminal-prohormone brain natriuretic peptide, COPD - chronic obstructive pulmonary disease, eGFR - estimated glomerular filtration rate, CRP - C-reactive protein, LDL - low-density lipoprotein, SD - standard deviation, BMI - body mass index.

2.4.3. Mass spectrometry

The parameters of the ion source and gasses of the mass spectrometer were set accordingly: ion spray voltage, +4500 V and −4500 V; curtain gas, 40 psi; both ion source gases 1 and 2, 60 and 50 psi respectively, and source temperature, 400 °C. Scheduled multiple reaction monitoring (MRM) with a 2-min window was used for the data acquisition. Positive and negative ionization of compounds was performed in one analysis using the polarity switching function of the used mass spectrometer used. Specific acyl-defining MRM transitions in negative mode were calculated using LipidCreator software [20]. These MRM were added to the method for identification of lipid molecular species (acyl-specific identification) where all adducts and fragment types are provided in detail in Table S2. Due to instrumentation capabilities, it was not possible to perform acyl-specific fragmentations for all lipids (limitation of the number of MRM transitions to achieve sufficient sensitivity), but after the identification of statistically significant lipids, these lipids were further fragmented using a QC sample to elucidate their structural composition (Fig. S1). Declustering potentials and collision energies were optimized using deuterated standards as well as the linearity and other analytical parameters, these have been already provided in detail in our previous work using the same lipidomic approach [21]. Lipid elution curves plotted using the R script [22] (Fig. S2) were used to ensure correct lipid annotation.

2.5. Data treatment and statistical analysis

Raw data from the lipidomic analysis were processed in SCIEX OS software (Sciex, version 1.6.1) using semiautomatic peak integration algorithm. Peak areas were divided by areas of their internal standards (always one internal standard per lipid (sub)class, listed in Table S4). The concentration calculated in this way (for which Type I correction was applied) [23] should be considered semiquantitative (level 3) according to the guidelines of the Lipidomics Standards Initiative [24]. The concentrations of lipids are shown in Table S5 and the calculation of the concentration is described in our previously published work [19]. A comparison of the concentration of lipids in SRM NIST 1950 with the reference values is shown in Fig. S3 (and in detail in Table S6). Pareto scaling, and mean centering were applied to the final dataset (Table S3). Statistical evaluation of the data was performed in GraphPad (version 9.0, San Diego, California, USA), SIMCA software (version 15.0, Umetrics, Umeå, Sweden), R program (4.0.3) [25] using the Metabol package [26] and IBM SPSS Statistics (28.0.1.1). Data were analysed using both multivariate (principal component analysis, PCA; orthogonal partial least squares discriminant analysis, OPLS-DA) and univariate (box plots, Mann-Whitney *U* test, fold change) methods. The Cytoscape program (https://cytoscape.org/) was used for global visualization of changes occurring in lipid profiles [27]. In the Cytoscape visualization (Fig. 2), each of the detected compounds was represented by a circle (node). The size of the nodes represented the -log p-value and the colour was based on fold-change (shades of red/blue represented an increase/decrease between two tested groups). The p-value from the Mann-Whitney *U* test was corrected by the Benjamini-Hochberg approach (Table S7) [28]. The ROC analysis and Kaplan-Meier survival analysis were performed to evaluate the diagnostic and predictive power of lipids and eicosanoids in the patient's cohort where a p-value <0.05 was considered statistically significant (Table S7). The raw data and Tables S1–7 have been uploaded to the MassIVE database and are publicly available under the provided link: https://doi.org/10.25345/C5J960F34. To evaluate the associations of selected lipids with biochemical and physiological parameters, we have applied Spearman correlation analysis (where correlations of 0–0.19, 0.20–0.39, 0.40–0.59, 0.60–0.79, and 0.80–1.00 were considered as negligible, weak, moderate, strong and very strong, respectively) (Fig. S4). A Cox regression model was fitted using GraphPad Prism (version 10.0, San Diego, CA, USA) to calculate hazard ratios (HR) associated with HF death occurring during 7 months follow-up using days from admission to death or end of follow-up as the time scale (Table S10).

The power of the study was evaluated and an effect size >0.84 (Cohen's D) was calculated for the comparison of the non-surviving (N = 13) and surviving (N = 37) groups to be statistically significant for the two-tailed *t*-test under the conditions of type I error (alpha = 0.05) and required power (1 – beta = 0.8).

3. Results

3.1. Serum lipidomics, map of lipid classes and univariate statistics

A total of 736 lipids and 3 eicosanoids were measured and semiquantified in serum using our analytical setup. The following lipid classes were identified (the abbreviation of the lipid class is given in parentheses followed by the number of lipids in this class): cholesteryl esters (CE, 11), ceramides (Cer, 29), diacylglycerols (DG, 20), free fatty acids (FA, 16), dihexosylceramides (Hex2Cer, 5), monohexosylceramides (HexCer, 16), lysophosphatidylcholines and their plasmanyl/plasmenyl variants (LPC, LPC-O, LPC-P 40), lysophosphatidylethanolamines and their plasmanyl variant (LPE, LPE-O, 16), phosphatidylcholines and their plasmanyl/plasmenyl variants (PC, PC-O, PC-P, 157), phosphatidylethanolamines and their plasmanyl/plasmenyl variants (PE, PE-O, PE-P, 132), phosphatidylinositols (PI, 45), phosphatidylserines (PS, 5), sphingomyelins (SM, 89), triacylglycerols (TG, 154), eicosanoids (3 + 2 ratios) and cholesterol. The high number of lipids for some lipid classes (e.g. TG, PC, PE) is due to the fact that both the total sum and specific acyl variants of these lipids were measured in our analysis and were retained in the dataset for further processing in the subsequent statistical analysis.

The Mann-Whitney *U* test was used to differentiate between the groups of surviving patients from non-surviving patients during the observation period of our study. After applying the Benjamini-Hochberg correction, 39 altered lipids consisting of 16 PC, 15 SM, 3 TG, 2 LPC-P, LPC, Cer and HexCer were considered statistically significant. A volcano plot was used to visualize a general overview of the changes in lipid concentrations (Fig. 1). The significant PC were mainly polyunsaturated species (more than 5 double bonds on average) such as PC 42:10, PC 36:6, and PC 40:9. Using an additional fragmentation analysis (Fig. S1), to elucidate the structure (acyl-

chain composition) of these low abundant long PUFA PC, it was found that PC 42:10, PC 40:9, and PC 40:7 are dominantly represented by PC 20:4_22:6, PC 20:4_20:5, and PC 18:1_22:6, respectively. On the other hand, the significantly increased SM in the surviving group were mono- or diunsaturated (SM d16:1/18:0, SM d18:2/20:0, SM d16:1/24:0), but also polyunsaturated species with 40 and more carbon atoms such as SM d40:5, and SM d42:6. Significant TG contained 50–51 carbons and 1–2 double bonds, namely TG 50:1, TG 50:2 and TG 51:1. A map of all lipids grouped by lipid class was generated to provide details of all identified and semiquantified lipids (Fig. 2). To investigate the associations of individual parameters with the levels of our proposed lipid markers, we performed a Spearman correlation analysis (Fig. S4) of physiological (age, BMI) and biochemical parameters (LDL, total cholesterol, eGFR, CRP), the CVD biomarker NT-proBNP and all significant (mostly PUFA) PC. Correlation analysis revealed moderate to strong positive correlations between all the PUFA PC but only a moderate positive or negative correlations between the above-mentioned parameters and PUFA PC. For example, the most significantly altered lipid PC 42:10 showed a moderate negative correlation with NT-proBNP (−0.56) and CRP (−0.41), a moderate positive correlation with total cholesterol (0.54) and a strong positive correlation with PC 40:9 (0.86) and PC 40:7 (0.71). The average correlation between significant PUFA PC and age and BMI was close to 0 (−0.05 and −0.04, respectively), which is considered a negligible correlation. In addition, we performed a comparative ROC analysis which showed that the significantly altered PUFA PC had a better clinical performance (higher AUC) as classifiers of surviving vs. non-surviving patients compared to NT-proBNP, CRP and eGFR (Fig. S5). To account for the limited sample size of our study, we randomly (using the Excel function "RANDARRAY") divided the samples into the training set (approximately $^{2}/_{3}$ of the samples) and the validation set (approximately $^{1}/_{3}$ of the samples). We performed supervised OPLS-DA analysis (Fig. S7 A, B, C, D) and ROC analysis (Fig. S7 E, F) to compare the results of the training and validation sets.

3.2. *Detailed lipid analysis based on acyl chain lengths and saturation reveals systematic alterations*

To visualize trends in acyl chain length (number of carbons) and number of double bonds, the comparative plots were generated for each lipid (sub)class (Fig. 3). The PC lipid class exhibited the highest number of elevated lipids (in surviving patients) with the highest degree of unsaturation within a given acyl chain length. In the case of LPC, which are biochemically closely related to PC, this trend appears to be less pronounced but still partially present. Conversely, for the SM and TG classes, the most significant changes were

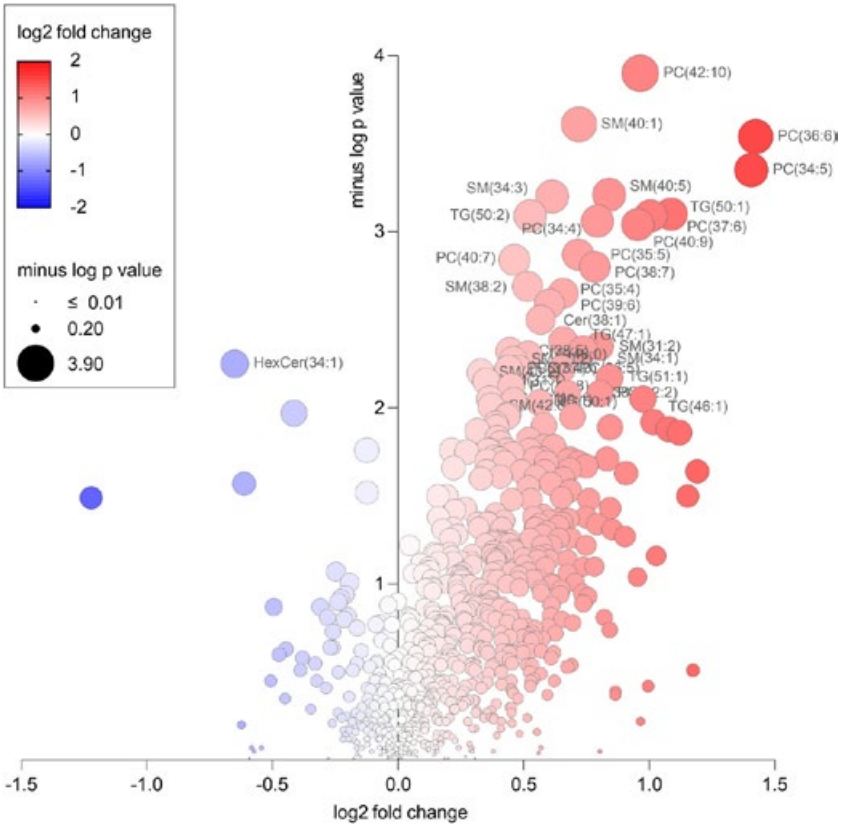

Fig. 1. Volcano plot of all 736 lipids. The y-axis and the size of the circles represent the -log p-value (Mann-Whitney *U* test) between surviving vs. non-surviving patients. The colour of the circles and the x-axis represent a log2 fold change of medians between surviving vs. non-surviving patients. Circles with labels correspond to lipids that remained significant after Benjamini-Hochberg correction of the p-value. (For interpretation of the references to colour in this figure legend, the reader is referred to the Web version of this article.)

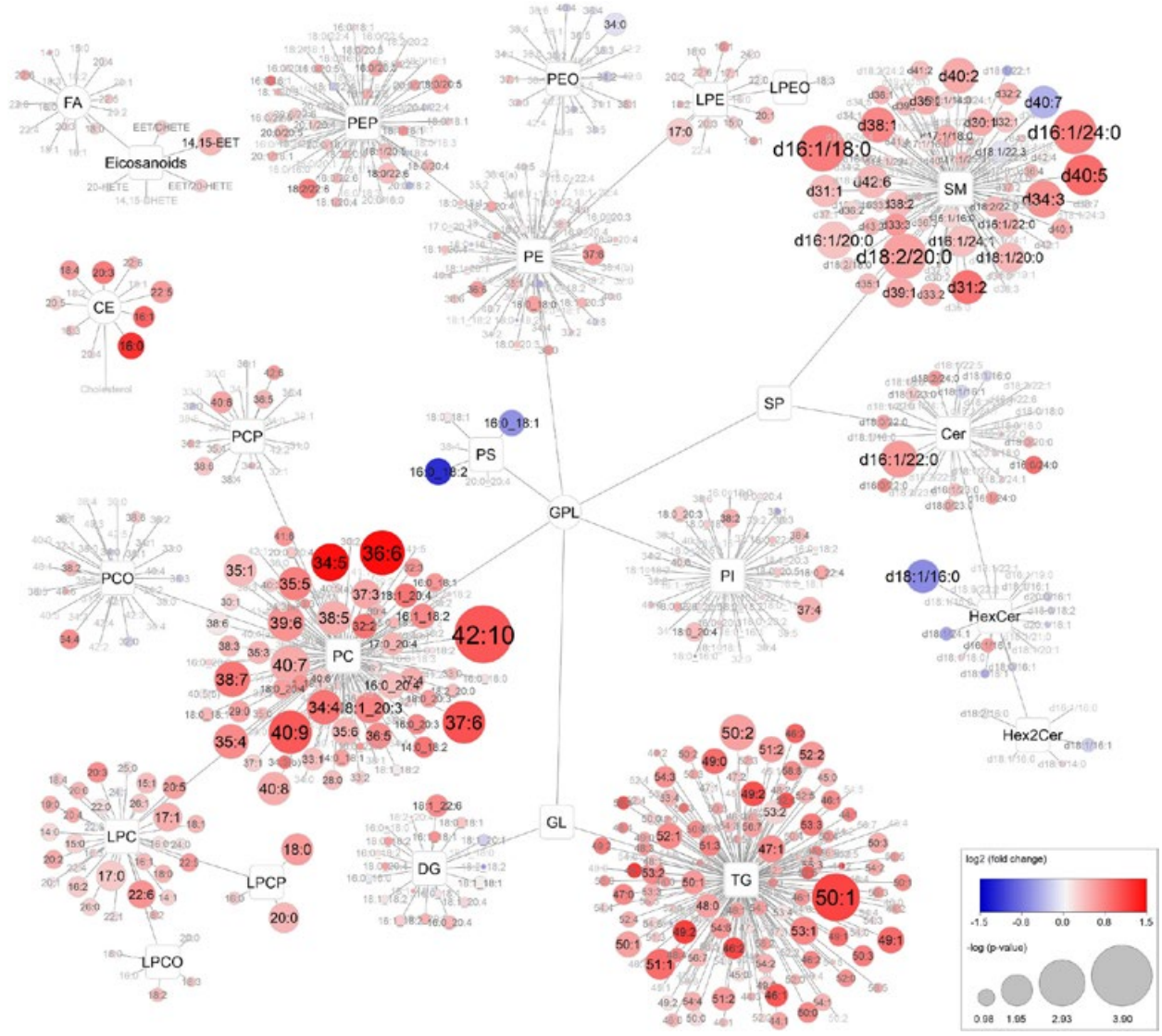

Fig. 2. Map of lipids and eicosanoids showing the entire lipidome divided into individual lipid classes and subclasses. The size of the circles represents the -log p-value (Mann-Whitney *U* test) between surviving and non-surviving patients. The colour of the circles represents a log2 fold change of medians between surviving and non-surviving patients. (For interpretation of the references to colour in this figure legend, the reader is referred to the Web version of this article.)

observed for mono- and di-unsaturated lipids with longer acyl chains.

3.3. ROC and survival analysis based on selected biomarkers

The clinical performance of the identified lipid markers was evaluated by ROC analysis (details in Table S7), where a significant result (p-value<0.05) was obtained for 155 lipids and 1 eicosanoid. The ROC analysis of eicosanoids showed a significant prognostic power of 14,15-EET (AUC = 0.72) with respect to the alive-to-death ratio in the patient cohort during the 7-month follow-up study. Similarly, prognostic power was found for multiple lipids across 17 lipid classes listed in Table S8. These lipid classes were (with the number of significant lipids in parentheses): TG (48), PC (37), SM (31), LPC (13), CE (5), LPC-P (2), LPE (2), PC-P (3), PE-P (3), PI (2), PS (2), Cer (2), HexCer (1), DG (1), PC-O (1), PE (1), PE-O (1). The top 10 lipids with the lowest p-value (as determined by ROC analysis) were 6 polyunsaturated PC species with more than 5 double bonds, 3 mono or di-unsaturated SM species and one mono-unsaturated TG, and their average AUC value was 0.80. The overall average AUC of all significant lipids was 0.71. For each of these lipid classes, one lipid with the lowest p-value of the ROC curve was selected and presented in Table S8. Parameters from the ROC analyses were used to define cut-off values (Table 2 and Table S8), which were subsequently utilised to construct Kaplan-Meier survival curves (Fig. 4 and Fig. S6). We further focused on the systematically altered lipids from the PC class (selected as those

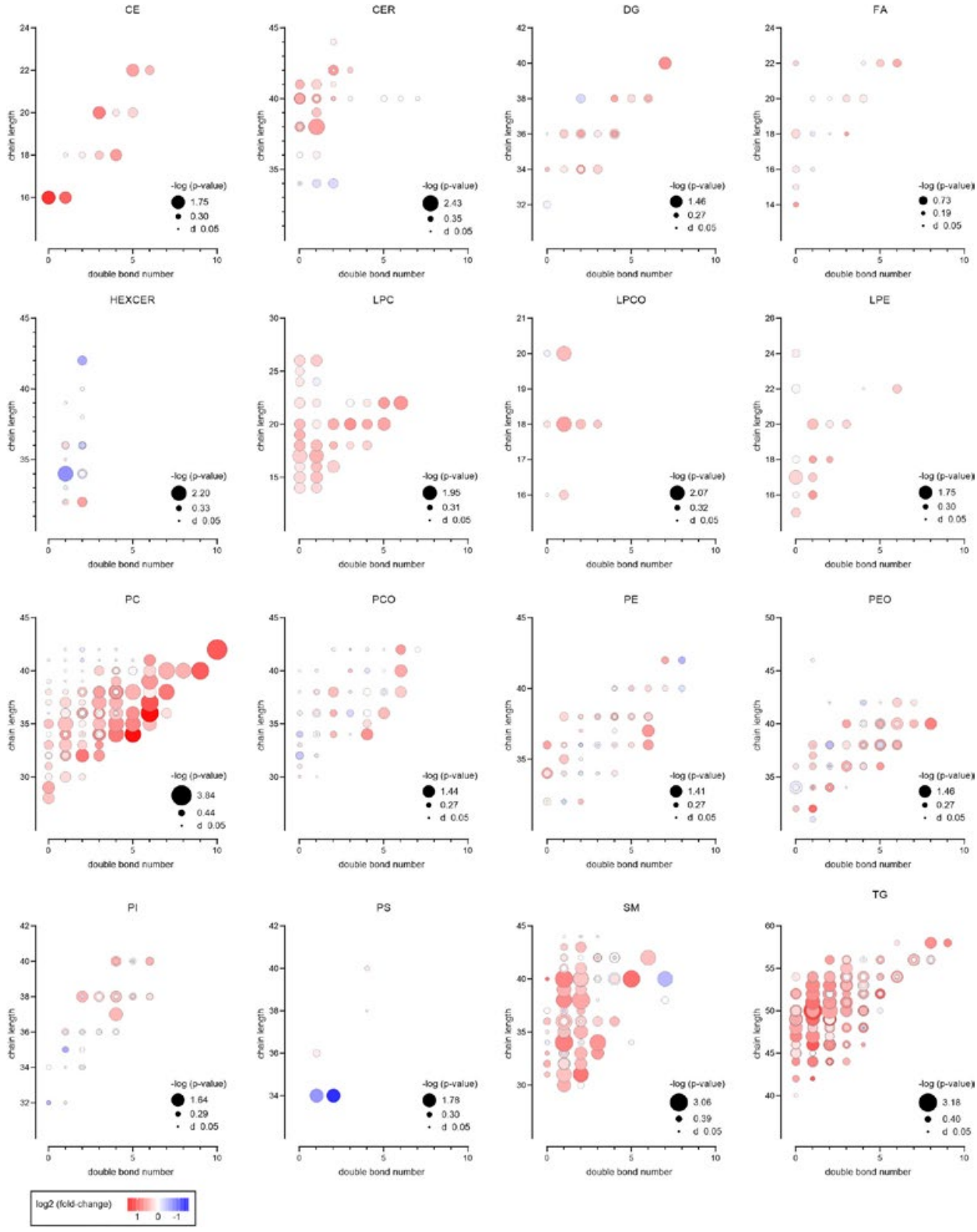

(caption on next page)

Fig. 3. Detailed view into trends of double bonds and acyl chain length of lipids divided into lipid classes and subclasses. The y-axis corresponds to the number of carbons and the x-axis represents the number of double bonds of a total lipid composition. The size of the circles represents the -log p-value (Mann-Whitney *U* test) between surviving and non-surviving patients. The colour of the circles represents the log2 fold change of the medians between surviving and non-surviving patients. (For interpretation of the references to colour in this figure legend, the reader is referred to the Web version of this article.)

with the significant change according to the Mann-Whitney *U* test), specifically PC 42:10, PC 36:6, PC 40:9, PC 37:6, PC 40:7 and PC 34:5, which were used to construct ROC curves (Table 2) and Kaplan-Meier survival curves (Fig. 4, and additionally the log-rank value and p-value in Table S9).

The patients were closely monitored by the clinic and data on exact survival time in days were available for statistical analysis. These data were used to construct Kaplan-Meier survival curves using the cut-off estimates from the ROC analyses (shown in Table 2 and detailed in Table S7). The representative Kaplan-Meier survival curves for the most significantly altered PUFA PC (as listed in Table 2) are shown in Fig. 4.

3.4. Multivariate discriminant analysis predicts survival of CVD patients

To verify how the defined lipid panel (39 significant lipids, selected by Mann-Whitney *U* test after BH correction) discriminates the group of surviving from non-surviving patients, the data were subjected to unsupervised and supervised multivariate analyses (Fig. 5). A partial grouping of surviving and non-surviving patients (48.6 % explained variance on the first component) was observed in the unsupervised principal component analysis (PCA). The contributions of lipids to the construction of the PCA score plot are shown in the loading plot (Fig. 5, B). Furthermore, supervised orthogonal partial least squares discriminant analysis (OPLS-DA) showed an almost complete separation of the studied groups (Fig. 5, C). Although the OPLS-DA model R2Y value of 0.535 and Q2 value of 0.245 is not considered to be a model with good predictability (threshold >0.5 for both values), the permutation test (Fig. 5, D) showed that the original model yielded higher R2Y and Q2 values than the permutated models. The results of these analyses provide evidence that the combination of selected lipid markers is capable of discriminating between surviving and non-surviving patients. The model achieved an accuracy of 95 % and 77 % was achieved for survival and non-survival patients, respectively (Table 3). The OPLS-DA model correctly classified 35 out of 37 surviving patients and 10 out of 13 non-surviving patients.

3.5. Validation of results and analysis of covariates

In order to validate the results, the samples were divided into the training set (approximately two-thirds of the samples) and the validation set (approximately one-third of the samples). The results demonstrated that both the training and validation sets showed complete separation of samples from the surviving and non-surviving groups in the OPLS-DA (Fig. S7 A, B). Furthermore, both the training and validation OPLS-DA models demonstrated the ability to correctly classify samples from these two groups with 96.88 % and 100 % model accuracy, respectively (Fig. S7 C, D). Finally, an ROC analysis was performed to compare the clinical performance of the first six most significantly altered PUFA PC which showed, that PUFA PC as markers were able to discriminate between surviving and non-surviving patients in both the training and validation sets, with a mean AUC of 0.76 and 0.83, respectively (Fig. S7 E, F). A Cox regression analysis was conducted to assess whether serum CRP, NT-proBNP, eGFR and PC 42:10 were associated with death after HF. The PC 42:10 was identified as the only significant covariate (HR: 0.058, 95 % CI: 0.008–0.367; p = 0.003), while no significant associations were observed for the remaining covariates (Table S10).

4. Discussion

The present study was conducted on patients with de novo or acute decompensated chronic HF who were accepted and treated at our tertiary cardiovascular centre. The study focused on a cohort of patients from a purely clinical setting. Furthermore, this study did not focus on the prediction of events or death in the general population or in those at risk of developing the disease, but rather on patients at an advanced stage of the disease (de novo or acute decompensated HF). The potential of lipids and eicosanoids to distinguish between the surviving and non-surviving groups of patients was evaluated. Our findings indicate that peripheral levels of lipids (mainly PUFA PC) and eicosanoids (especially 14,15-EET) offer significant prognostic power with respect to the alive-to-death ratio in HF patients during 7-month follow-up. These findings suggest that it is possible to stratify this susceptible group from those

Table 2
Results of the ROC analysis of the six most significantly altered PUFA PC showing AUC, Gini index, Max K-S and cut-off values.

Lipid	AUC	Std. Error	Asymptotic significance (p-value)	Gini Index	Max K-S	Cut-off (nmol/ml)
PC 42:10	0.84	0.07	3.235E-07	0.68	0.63	0.19
PC 36:6	0.80	0.06	2.183E-06	0.60	0.58	0.35
PC 40:9	0.79	0.07	2.072E-05	0.58	0.49	0.04
PC 37:6	0.79	0.07	1.633E-05	0.58	0.54	0.72
PC 40:7	0.78	0.06	2.094E-05	0.55	0.55	6.21
PC 34:5	0.77	0.06	2.795E-05	0.54	0.59	0.23

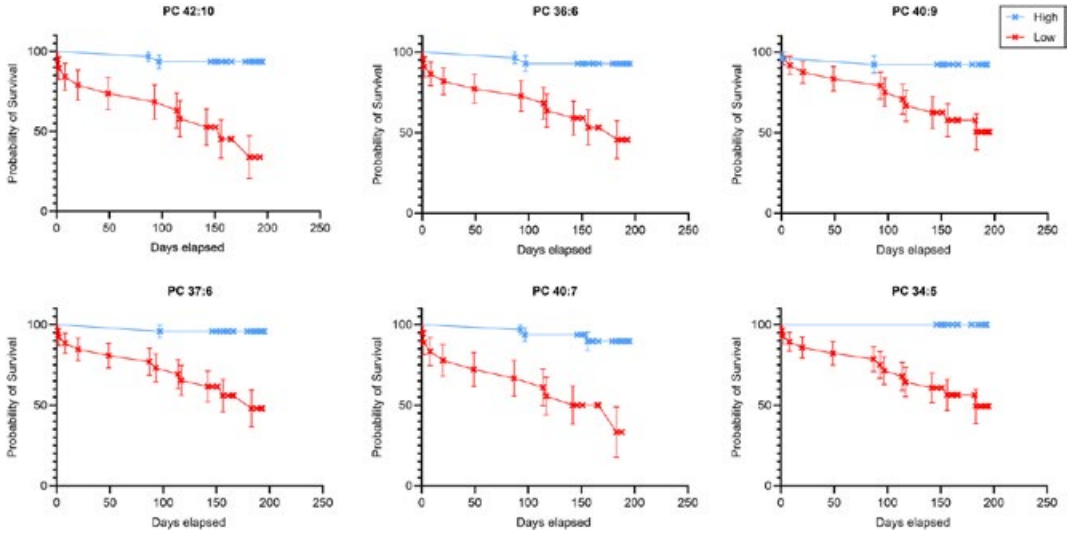

Fig. 4. Kaplan-Meier survival curves of the six most significantly decreased PUFA PC in the non-surviving group compared to the surviving group (detailed in Table 2).

with a higher chance of survival using our lipid panel.

In terms of lipidomics, we identified numerous significant lipids across lipid classes and subclasses, which belonged primarily to PC, SM, TG, LPC-P, LPC, Cer, and HexCer. Significantly altered lipids (n = 39) were selected using univariate statistics to construct multivariate models. The classification performance of the selected lipids was evaluated using a validated supervised OPLS-DA model which demonstrated an overall 90 % accuracy in classifying patients at risk of death. To provide a more detailed description of the common structural features of these significant lipids, we constructed plots according to the number of carbons and double bonds for each lipid by lipid (sub)class. A clear trend was identified in the PC class, namely that as the number of double bonds increases (towards polyunsaturated species), the significance and clinical performance to distinguish the surviving group from the non-surviving group of patients increases regardless of the number of carbons. Although several individual polyunsaturated PC species such as PC 36:6 or PC 34:4 have been identified as significant both in our and also previous studies [29], our study highlights a yet undescribed systematic phenomenon across this whole lipid class. Upon closer examination, we also found significant changes in long (>40 carbons) and highly polyunsaturated (>7 double bonds) phosphatidylcholines such as PC 40:9, PC 40:7 and especially PC 42:10, which was the most significantly elevated lipid in the surviving patients. Some of these low-abundant long-chain PUFA PC have not yet been identified and even detected in previous studies (due to their unexpected occurrence in plasma) and consequently they are not included in predictive models such as CERT2 and others [6]. Furthermore, the results from the correlation analysis indicated that PUFA PC are moderately correlated with CVD markers associated with cardiac complications and prognosis such as NT-proBNP and CRP, however, in comparison, PUFA PC show better clinical performance as classifiers of non-surviving patients after a heart attack and that PUFA PC are not correlated with BMI nor age. On the basis of the Cox regression analysis, the common HF-related biochemical parameters (NT-proBNP, CRP and eGFR) were not significantly associated with the risk of death after HF. PC 42:10 as the most discriminating PUFA PC (based on univariate statistical analysis) was significantly associated with death after HF, independent of the aforementioned parameters.

These findings are consistent with several studies showing a cardioprotective effect of PUFA (especially linoleic acid) in direct association with all-cause mortality [30]. Many studies are based on the analysis of total free and total esterified fatty acids (usually determined by GC-MS). It has been shown that esterified PUFA in serum are even more strongly associated with CVD mortality than free dietary PUFA [30]. However, GC-MS analysis of esterified fatty acids is performed in a destructive manner, i.e. we only observe the sum of the fatty acids but do not know their origin (which lipids they are derived from). Our work takes this knowledge a step further by measuring the individual lipids in which the fatty acids are esterified thus allowing us to identify which lipid class is most important in relation to the cardioprotective function of esterified PUFA during HF. The structural composition of these low abundant lipids at the molecular species level was confirmed by fragmentation experiments. According to our results, the PUFA with the most significant cardioprotective role with respect to survival after HF are mainly FA 22:6, FA 20:4 and FA 20:5 esterified in PC.

Moreover, myocardial phospholipid remodelling has been observed in association with various forms of heart failure, often manifesting as lower levels of linoleic acid and a reciprocal elevation of long-chain unsaturated fatty acids, such as FA 22:6 and FA 20:4 [31,32]. In contrast to the myocardial tissue, in plasma and serum, the levels of free and esterified PUFA (mainly ω-3 species) are elevated in both patients with low CVD risk and lower risk of CAD [6,33,34]. This observation may be related to the increased activity of δ-6 desaturase (D6D), the rate-limiting enzyme in PUFA biosynthesis [32]. Although D6D inhibition reversed the pathological manifestation of HF in an animal model [32], in our study elevated serum PUFA esterified in PC are associated with surviving HF patients. Several studies have investigated the beneficial effects of PUFA on cardiac function. Omega-3 FA have been shown to suppress the expression of pro-inflammatory cytokines and the infiltration of inflammatory cells into the heart. In subjects with stable ischemic

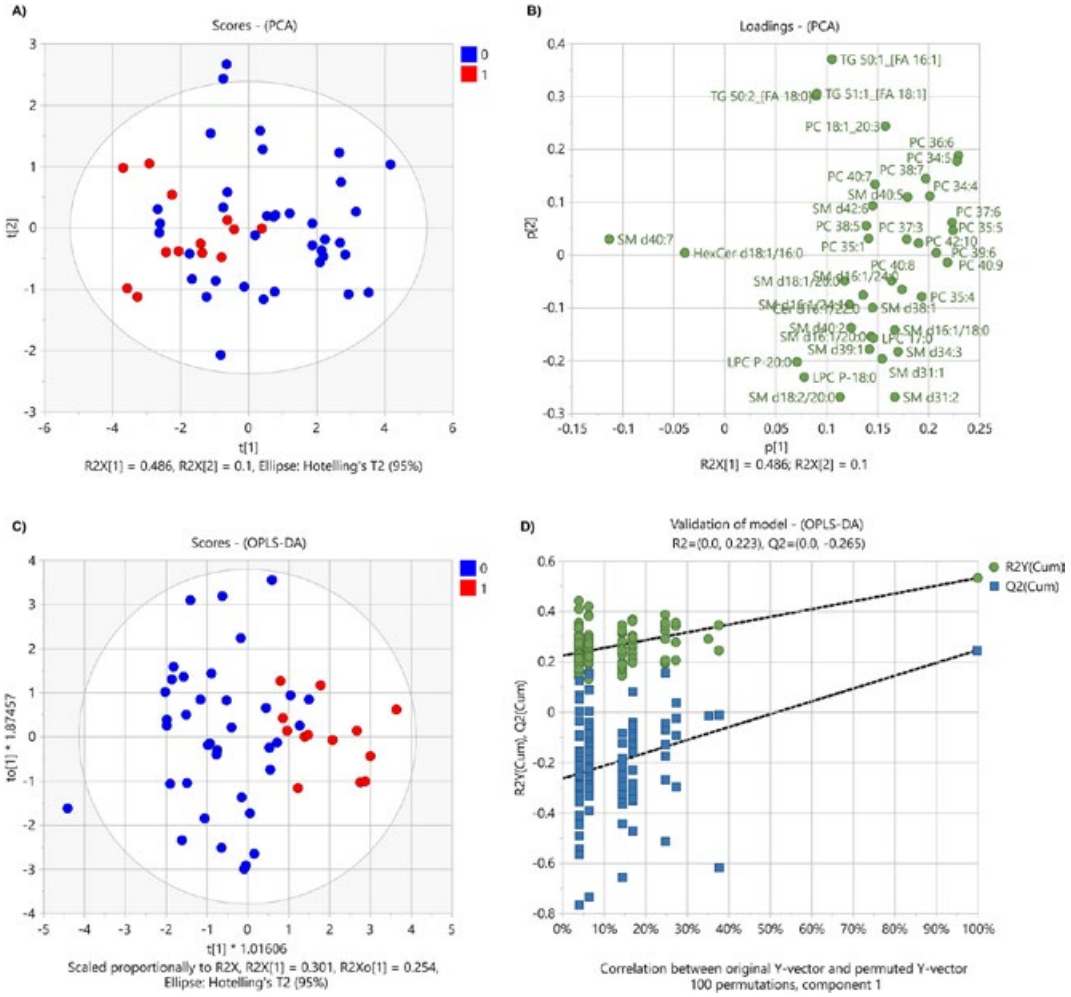

Fig. 5. Multivariate statistical analysis. The score plot (A) and loading plot (B) represent the results of an unsupervised principal component analysis. Discriminant analysis (OPLS-DA) score plot (C) and permutation analysis (D) are based on the lipids selected by p-value below the BH-corrected critical value (39 lipids). The red colour in (A) and (C) represents the non-surviving group and the blue colour represents the surviving group of patients. (For interpretation of the references to colour in this figure legend, the reader is referred to the Web version of this article.)

Table 3
Classification performance of the supervised statistical model (OPLS-DA) from Fig. 5C.

	n	Correct	0	1
Surviving group (0)	37	94.59 %	35	2
Non-surviving group (1)	13	76.92 %	3	10
Total	50	90.00 %	38	12
Fisher's prob.	1.6e-06			

heart failure), supplementation with omega-3 PUFAs has been shown to improve endothelial function, inflammatory and fibrotic status [35,36]. Further research is needed to elucidate the role of PUFAs in the pathobiochemistry of HF.

In addition, particular attention was paid to eicosanoids. The reduced availability of biologically active epoxygenase products expressed as the EET/DHET ratio is commonly used to assess the bioavailability of these metabolites [37–39] as was also validated in our preclinical study, where this ratio was reduced by approximately 65 % in the kidney and left ventricle (LV) of the animal CHF model as compared to controls [12,13]. There were no significant differences in the protein expression of the enzymes responsible for EETs production in the kidney and LV. However, the expression of sEH protein, an enzyme responsible for converting EETs to DHETs, was significantly increased in the animal HF model in LV tissue [13]. In this human pilot study, we did not measure the direct tissue concentrations of eicosanoids in the heart or kidney, where we would expect a deficiency of active EETs based on our previous preclinical data. In addition, we investigated the serum levels of 14,15-EET, 14,15-DHET and 20-HETE in our patient cohort. We

demonstrated significant diagnostic power of 14,15-EET in patients with a significant cut-off of 0.24 nmol/mL (78.18 ng/mL).

The increased peripheral concentration of eicosanoids may be a compensatory mechanism for decreased availability in cardiac and renal tissues and to counterbalance the activated renin-angiotensin system [40–42]. Several body compartments contribute to peripheral plasma levels of eicosanoids, as different cell types produce eicosanoids that act in a paracrine and autocrine manner [40]. Low peripheral eicosanoid levels may indicate more advanced heart failure with a worse prognosis [38,39].

Our study has several limitations. First, we enrolled de novo or acutely decompensated chronic HF patients because they are at higher risk of CVD events and lipidomics including eicosanoid levels of stable HF patients remain to be elucidated in the next part of our project. Second, the study size is relatively small, with a median age of 74 years and therefore follow-up is short (median of 7 months), thus our exploratory results should be validated in a broader spectrum of HF patients with bigger cohorts and longer follow-up. As our work is a pilot study with a limited number of samples our results should be validated on a larger set of samples where an extended analysis of confounding factors should be performed and evaluated using logistic regression and Cox proportional hazard models. Additionally, a more complex and sensitive analysis of eicosanoids (and possibly also other oxylipins) using LC-MS may provide a deeper insight into the pathobiochemical mechanism of heart failure and risk of death and should be the focus of further studies.

5. Conclusions

Lipidomics is an important tool for predicting complications in CVD and HF. The results of our lipidomic and eicosanoid analysis show that the largest changes related to survival after HF occur at the level of long-chain polyunsaturated PC (namely PC 42:10, PC 40:9 and PC 36:6), where a strong systematic trend is observed. A further focus should be placed on low-abundant lipid markers, which have been omitted in many publications and predictive models.

CRediT authorship contribution statement

Aleš Kvasnička: Writing – original draft, Visualization, Validation, Software, Methodology, Investigation, Formal analysis, Data curation. **Karel Kotaška:** Writing – review & editing, Visualization, Supervision, Resources, Project administration, Investigation, Funding acquisition, Formal analysis, Data curation, Conceptualization. **David Friedecký:** Writing – original draft, Visualization, Validation, Supervision, Software, Resources, Project administration, Methodology, Investigation, Funding acquisition, Formal analysis, Data curation, Conceptualization. **Karolína Ježdíková:** Writing – review & editing, Resources, Methodology, Investigation, Conceptualization. **Radana Brumarová:** Writing – review & editing, Methodology, Investigation. **Tomáš Hnát:** Writing – review & editing, Resources, Methodology, Investigation. **Petr Kala:** Writing – review & editing, Visualization, Resources, Project administration, Methodology, Investigation, Funding acquisition, Formal analysis, Data curation, Conceptualization.

Ethics and consent

This study was approved by the Ethics Committee of the University Hospital Motol (number EK-739/21, approved on 16.6. 2021). Written informed consent was obtained from all participants enrolled in the study.

Data availability statement

The datasets generated and/or analysed during the current study including all the raw data, additional files (containing Figs. S1–S7 and Tables S1–S10) are available in the MassIVE repository, https://doi.org/10.25345/C5J960F34.

Declaration of competing interest

The authors declare that they have no known competing financial interests or personal relationships that could have appeared to influence the work reported in this paper.

Acknowledgements

The work was supported by the Project of the Ministry of Health (MH), Czech Republic (CZ) for the conceptual development of research organization 00064203 (University Hospital Motol, Charles University), Grant Agency of Charles University (GAUK, grant number 68121) and MH CZ - DRO (FNOl, 00098892).

Appendix A. Supplementary data

Supplementary data to this article can be found online at https://doi.org/10.1016/j.heliyon.2024.e39979.

References

[1] N. Conrad, A. Judge, J. Tran, H. Mohseni, D. Hedgecott, A.P. Crespillo, M. Allison, H. Hemingway, J.G. Cleland, J.J.V. McMurray, K. Rahimi, Temporal trends and patterns in heart failure incidence: a population-based study of 4 million individuals, Lancet 391 (2018) 572–580, https://doi.org/10.1016/S0140-6736(17)32520-5.

[2] V.L. Roger, Epidemiology of heart failure, Circ. Res. 113 (2013) 646–659, https://doi.org/10.1161/CIRCRESAHA.113.300268.

[3] T.A. McDonagh, M. Metra, M. Adamo, R.S. Gardner, A. Baumbach, M. Böhm, H. Burri, J. Butler, J. Čelutkienė, O. Chioncel, J.G.F. Cleland, A.J.S. Coats, M. G. Crespo-Leiro, D. Farmakis, M. Gilard, S. Heymans, A.W. Hoes, T. Jaarsma, E.A. Jankowska, M. Lainscak, C.S.P. Lam, A.R. Lyon, J.J.V. McMurray, A. Mebazaa, R. Mindham, C. Muneretto, F. Piepoli, S. Price, G.M.C. Rosano, F. Ruschitzka, K. Skibelund, ESC Guidelines for the diagnosis and treatment of acute and chronic heart failure: developed by the Task Force for the diagnosis and treatment of acute and chronic heart failure of the European Society of Cardiology (ESC) with the special contribution of the Heart Failure Association (HFA) of the ESC, Eur. Heart J. 42 (2021) (2021) 3599–3726, https://doi.org/10.1093/eurheartj/ehab368.

[4] D.D. Wang, E. Toledo, A. Hruby, B.A. Rosner, W.C. Willett, Q. Sun, C. Razquin, Y. Zheng, M. Ruiz-Canela, M. Guasch-Ferré, D. Corella, E. Gómez-Gracia, M. Fiol, R. Estruch, E. Ros, J. Lapetra, M. Fito, F. Aros, L. Serra-Majem, C.-H. Lee, C.B. Clish, L. Liang, J. Salas-Salvadó, M.A. Martínez-González, F.B. Hu, Plasma Ceramides, Mediterranean Diet, and Incident Cardiovascular Disease in the PREDIMED Trial (Prevención con Dieta Mediterránea), Circulation 135 (2017) 2028–2040, https://doi.org/10.1161/circulationaha.116.024261.

[5] L.R. Peterson, V. Xanthakis, M.S. Duncan, S. Gross, N. Friedrich, H. Völzke, S.B. Felix, H. Jiang, R. Sidhu, M. Nauck, X. Jiang, D.S. Ory, M. Dörr, R.S. Vasan, J. E. Schaffer, Ceramide remodeling and risk of cardiovascular events and mortality, J. Am. Heart Assoc. 7 (2018), https://doi.org/10.1161/JAHA.117.007931.

[6] M. Hilvo, P.J. Meikle, E.R. Pedersen, G.S. Tell, I. Dhar, H. Brenner, B. Schöttker, M. Lääperi, D. Kauhanen, K.M. Koistinen, A. Jylhä, K. Huynh, N.A. Mellett, A. M. Tonkin, D.R. Sullivan, J. Simes, P. Nestel, W. Koenig, D. Rothenbacher, O. Nygård, R. Laaksonen, Development and validation of a ceramide- and phospholipid-based cardiovascular risk estimation score for coronary artery disease patients, Eur. Heart J. 41 (2020) 371–380, https://doi.org/10.1093/eurheartj/ehz387.

[7] R. Laaksonen, K. Ekroos, M. Sysi-Aho, M. Hilvo, T. Vihervaara, D. Kauhanen, M. Suoniemi, R. Hurme, W. März, H. Scharnagl, T. Stojakovic, E. Vlachopoulou, M.-L. Lokki, M.S. Nieminen, R. Klingenberg, C.M. Matter, T. Hornemann, P. Jüni, N. Rodondi, L. Räber, S. Windecker, B. Gencer, E.R. Pedersen, G.S. Tell, O. Nygård, F. Mach, J. Sinisalo, T.F. Lüscher, Plasma ceramides predict cardiovascular death in patients with stable coronary artery disease and acute coronary syndromes beyond LDL-cholesterol, Eur. Heart J. 37 (2016) 1967–1976, https://doi.org/10.1093/eurheartj/ehw148.

[8] K.A. McGurk, B.D. Keavney, A. Nicolaou, Circulating ceramides as biomarkers of cardiovascular disease: evidence from phenotypic and genomic studies, Atherosclerosis 327 (2021) 18–30, https://doi.org/10.1016/j.atherosclerosis.2021.04.021.

[9] CERAM - Overview, MI-heart ceramides, plasma, n.d. https://www.mayocliniclabs.com/test-catalog/overview/606777. (Accessed 9 August 2023).

[10] P.M. Ridker, B.M. Everett, T. Thuren, J.G. MacFadyen, W.H. Chang, C. Ballantyne, F. Fonseca, J. Nicolau, W. Koenig, S.D. Anker, J.J.P. Kastelein, J.H. Cornel, P. Pais, D. Pella, J. Genest, R. Cifkova, A. Lorenzatti, T. Forster, Z. Kobalava, L. Vida-Simiti, M. Flather, H. Shimokawa, H. Ogawa, M. Dellborg, P.R.F. Rossi, R.P. T. Troquay, P. Libby, R.J. Glynn, CANTOS trial group, antiinflammatory therapy with canakinumab for atherosclerotic disease, N. Engl. J. Med. 377 (2017) 1119–1131. https://www.nejm.org/doi/full/10.1056/nejmoa1707914.

[11] J.D. Imig, L. Cervenka, J. Neckar, Epoxylipids and soluble epoxide hydrolase in heart diseases, Biochem. Pharmacol. 195 (2022) 114866, https://doi.org/10.1016/j.bcp.2021.114866.

[12] P. Kala, L. Sedláková, P. Škaroupková, L. Kopkan, Z. Vaňourková, M. Táborský, A. Nishiyama, S.H. Hwang, B.D. Hammock, J. Sadowski, V. Melenovský, J. D. Imig, L. Červenka, Effect of angiotensin-converting enzyme blockade, alone or combined with blockade of soluble epoxide hydrolase, on the course of congestive heart failure and occurrence of renal dysfunction in Ren-2 transgenic hypertensive rats with aorto-caval fistula, Physiol. Res. 67 (2018) 401–415, https://doi.org/10.33549/physiolres.933757.

[13] P. Kala, M. Miklovič, Š. Jíchová, P. Škaroupková, Z. Vaňourková, H. Maxová, O. Gawrys, E. Kompanowska-Jezierska, J. Sadowski, J.D. Imig, J.R. Falck, J. Veselka, L. Červenka, R. Aiglová, M. Vícha, V. Gloger, M. Táborský, Effects of epoxyeicosatrienoic acid-enhancing therapy on the course of congestive heart failure in angiotensin II-dependent rat hypertension: from mRNA analysis towards functional in vivo evaluation, Biomedicines 9 (2021), https://doi.org/10.3390/biomedicines9081053.

[14] C.-C. Huang, M.-T. Chang, H.-B. Leu, W.-H. Yin, W.-K. Tseng, Y.-W. Wu, T.-H. Lin, H.-I. Yeh, K.-C. Chang, J.-H. Wang, C.-C. Wu, L.-F. Shyur, J.-W. Chen, Association of arachidonic acid-derived lipid mediators with subsequent onset of acute myocardial infarction in patients with coronary artery disease, Sci. Rep. 10 (2020) 8105, https://doi.org/10.1038/s41598-020-65014-z.

[15] K.L. Jamieson, T. Endo, A.M. Darwesh, V. Samokhvalov, J.M. Seubert, Cytochrome P450-derived eicosanoids and heart function, Pharmacol. Ther. 179 (2017) 47–83, https://doi.org/10.1016/j.pharmthera.2017.05.005.

[16] R. Lehmann, From bedside to bench-practical considerations to avoid pre-analytical pitfalls and assess sample quality for high-resolution metabolomics and lipidomics analyses of body fluids, Anal. Bioanal. Chem. 413 (2021) 5567–5585, https://doi.org/10.1007/s00216-021-03450-0.

[17] P. Kala, T. Hnat, K. Padrova, K. Kotaška, J. Veselka, Eicosanoids in human heart failure: pilot study of plasma epoxyeicosatrienoic and dihydroxyeicosatrienoic acid levels, Arch. Med. Sci. 19 (2023) 513–517, https://doi.org/10.5114/aoms/159313.

[18] M.H. Sarafian, M. Gaudin, M.R. Lewis, F.-P. Martin, E. Holmes, J.K. Nicholson, M.-E. Dumas, Objective set of criteria for optimization of sample preparation procedures for ultra-high throughput untargeted blood plasma lipid profiling by ultra performance liquid chromatography-mass spectrometry, Anal. Chem. 86 (2014) 5766–5774, https://doi.org/10.1021/ac500317c.

[19] A. Kvasnička, D. Friedecký, R. Brumarová, M. Pavlíková, K. Pavelcová, J. Mašínová, L. Hasíková, J. Závada, K. Pavelka, P. Ješina, B. Stibůrková, Alterations in lipidome profiles distinguish early-onset hyperuricemia, gout, and the effect of urate-lowering treatment, Arthritis Res. Ther. 25 (2023) 234, https://doi.org/10.1186/s13075-023-03204-6.

[20] B. Peng, D. Kopczynski, B.S. Pratt, C.S. Ejsing, B. Burla, M. Hermansson, P.I. Benke, S.H. Tan, M.Y. Chan, F. Torta, D. Schwudke, S.W. Meckelmann, C. Coman, O. J. Schmitz, B. MacLean, M.-C. Manke, O. Borst, M.R. Wenk, N. Hoffmann, R. Ahrends, LipidCreator workbench to probe the lipidomic landscape, Nat. Commun. 11 (2020) 2057, https://doi.org/10.1038/s41467-020-15960-z.

[21] A. Kvasnička, D. Friedecký, A. Tichá, R. Hyšpler, H. Janečková, R. Brumarová, L. Najdekr, Z. Zadák, SLIDE-novel approach to apocrine sweat sampling for lipid profiling in healthy individuals, Int. J. Mol. Sci. 22 (2021), https://doi.org/10.3390/ijms22158054.

[22] B. Drotleff, S.R. Roth, K. Henkel, C. Calderón, J. Schlotterbeck, M.A. Neukamm, M. Lämmerhofer, Lipidomic profiling of non-mineralized dental plaque and biofilm by untargeted UHPLC-QTOF-MS/MS and SWATH acquisition, Anal. Bioanal. Chem. 412 (2020) 2303–2314, https://doi.org/10.1007/s00216-019-02364-2.

[23] M. Wang, C. Wang, X. Han, Selection of internal standards for accurate quantification of complex lipid species in biological extracts by electrospray ionization mass spectrometry-What, how and why? Mass Spectrom. Rev. 36 (2017) 693–714, https://doi.org/10.1002/mas.21492.

[24] H.C. Köfeler, R. Ahrends, E.S. Baker, K. Ekroos, X. Han, N. Hoffmann, M. Holčapek, M.R. Wenk, G. Liebisch, Recommendations for good practice in MS-based lipidomics, J. Lipid Res. 62 (2021) 100138, https://doi.org/10.1016/j.jlr.2021.100138.

[25] R. The, Project for statistical computing, n.d. https://www.R-project.org/. (Accessed 9 August 2023).

[26] AlzbetaG, AlzbetaG/Metabol, First version, Zenodo, 2019, https://doi.org/10.5281/ZENODO.3235775. (Accessed 9 August 2023).

[27] P. Shannon, A. Markiel, O. Ozier, N.S. Baliga, J.T. Wang, D. Ramage, N. Amin, B. Schwikowski, T. Ideker, Cytoscape: a software environment for integrated models of biomolecular interaction networks, Genome Res. 13 (2003) 2498–2504, https://doi.org/10.1101/gr.1239303.

[28] Y. Benjamini, Y. Hochberg, Controlling the false discovery rate: a practical and powerful approach to multiple testing, J. R. Stat. Soc. 57 (1995) 289–300, https://doi.org/10.1111/j.2517-6161.1995.tb02031.x.

[29] P.A. Mundra, C.K. Barlow, P.J. Nestel, E.H. Barnes, A. Kirby, P. Thompson, D.R. Sullivan, Z.H. Alshehry, N.A. Mellett, K. Huynh, K.S. Jayawardana, C. Giles, M. J. McConville, S. Zoungas, G.S. Hillis, J. Chalmers, M. Woodward, G. Wong, B.A. Kingwell, J. Simes, A.M. Tonkin, P.J. Meikle, LIPID Study Investigators, Large-

scale plasma lipidomic profiling identifies lipids that predict cardiovascular events in secondary prevention, JCI Insight 3 (2018), https://doi.org/10.1172/jci.insight.121326.
[30] D.E. Laaksonen, K. Nyyssönen, L. Niskanen, T.H. Rissanen, J.T. Salonen, Prediction of cardiovascular mortality in middle-aged men by dietary and serum linoleic and polyunsaturated fatty acids, Arch. Intern. Med. 165 (2005) 193–199, https://doi.org/10.1001/archinte.165.2.193.
[31] D.K. Reibel, B. O'Rourke, K.A. Foster, H. Hutchinson, C.E. Uboh, R.L. Kent, Altered phospholipid metabolism in pressure-overload hypertrophied hearts, Am. J. Physiol. 250 (1986) H1–H6, https://doi.org/10.1152/ajpheart.1986.250.1.h1.
[32] C.H. Le, C.M. Mulligan, M.A. Routh, G.J. Bouma, M.A. Frye, K.M. Jeckel, G.C. Sparagna, J.M. Lynch, R.L. Moore, S.A. McCune, M. Bristow, S. Zarini, R. C. Murphy, A.J. Chicco, Delta-6-desaturase links polyunsaturated fatty acid metabolism with phospholipid remodeling and disease progression in heart failure, Circ. Heart Fail. 7 (2014) 172–183, https://doi.org/10.1161/circheartfailure.113.000744.
[33] W. Liu, X. Xie, M. Liu, J. Zhang, W. Liang, X. Chen, Serum ω-3 polyunsaturated fatty acids and potential influence factors in elderly patients with multiple cardiovascular risk factors, Sci. Rep. 8 (2018) 1102, https://doi.org/10.1038/s41598-018-19193-5.
[34] K. Tarasov, K. Ekroos, M. Suoniemi, D. Kauhanen, T. Sylvänne, R. Hurme, I. Gouni-Berthold, H.K. Berthold, M.E. Kleber, R. Laaksonen, W. März, Molecular lipids identify cardiovascular risk and are efficiently lowered by simvastatin and PCSK9 deficiency, J. Clin. Endocrinol. Metab. 99 (2014) E45–E52, https://doi.org/10.1210/jc.2013-2559.
[35] H. Toko, H. Morita, M. Katakura, M. Hashimoto, T. Ko, S. Bujo, Y. Adachi, K. Ueda, H. Murakami, M. Ishizuka, J. Guo, C. Zhao, T. Fujiwara, H. Hara, N. Takeda, E. Takimoto, O. Shido, M. Harada, I. Komuro, Omega-3 fatty acid prevents the development of heart failure by changing fatty acid composition in the heart, Sci. Rep. 10 (2020) 15553, https://doi.org/10.1038/s41598-020-72686-0.
[36] E. Oikonomou, G. Vogiatzi, D. Karlis, G. Siasos, C. Chrysohoou, T. Zografos, G. Lazaros, S. Tsalamandris, K. Mourouzis, G. Georgiopoulos, M. Toutouza, D. Tousoulis, Effects of omega-3 polyunsaturated fatty acids on fibrosis, endothelial function and myocardial performance, in ischemic heart failure patients, Clin. Nutr. 38 (2019) 1188–1197, https://doi.org/10.1016/j.clnu.2018.04.017.
[37] K.N. Theken, R.N. Schuck, M.L. Edin, B. Tran, K. Ellis, A. Bass, F.B. Lih, K.B. Tomer, S.M. Poloyac, M.C. Wu, A.L. Hinderliter, D.C. Zeldin, G.A. Stouffer, C.R. Lee, Evaluation of cytochrome P450-derived eicosanoids in humans with stable atherosclerotic cardiovascular disease, Atherosclerosis 222 (2012) 530–536, https://doi.org/10.1016/j.atherosclerosis.2012.03.022.
[38] S. Tacconelli, P. Patrignani, Inside epoxyeicosatrienoic acids and cardiovascular disease, Front. Pharmacol. 5 (2014) 239, https://doi.org/10.3389/fphar.2014.00239.
[39] K. Ma, J. Yang, Y. Shao, P. Li, H. Guo, J. Wu, Y. Zhu, H. Zhang, X. Zhang, J. Du, Y. Li, Therapeutic and prognostic significance of arachidonic acid in heart failure, Circ. Res. 130 (2022) 1056–1071, https://doi.org/10.1161/CIRCRESAHA.121.320548.
[40] J.D. Imig, Epoxides and soluble epoxide hydrolase in cardiovascular physiology, Physiol. Rev. 92 (2012) 101–130, https://doi.org/10.1152/physrev.00021.2011.
[41] J. Lai, C. Chen, The role of epoxyeicosatrienoic acids in cardiac remodeling, Front. Physiol. 12 (2021) 642470, https://doi.org/10.3389/fphys.2021.642470.
[42] X.-X. Guan, D.-N. Rao, Y.-Z. Liu, Y. Zhou, H.-H. Yang, Epoxyeicosatrienoic acids and fibrosis: recent insights for the novel therapeutic strategies, Int. J. Mol. Sci. 22 (2021), https://doi.org/10.3390/ijms221910714.

L. Monzo et al.

Pressure overload is associated with right ventricular dyssynchrony in heart failure with reduced ejection fraction

ESC Heart Failure
Impact Factor: 3,2

ESC HEART FAILURE
ESC Heart Failure 2024; **11**: 1097–1109
Published online 23 January 2024 in Wiley Online Library (wileyonlinelibrary.com) **DOI:** 10.1002/ehf2.14682

ORIGINAL ARTICLE

Pressure overload is associated with right ventricular dyssynchrony in heart failure with reduced ejection fraction

Luca Monzo[1,2], Marek Tupy[1], Barry A. Borlaug[3], Adrian Reichenbach[1], Ivana Jurcova[1], Jan Benes[1], Lenka Mlateckova[1], Jiri Ters[1], Josef Kautzner[1] and Vojtech Melenovsky[1]*

[1]*Institute for Clinical and Experimental Medicine (IKEM), Prague, Czech Republic;* [2]*Université de Lorraine INSERM, Centre, d'Investigations Cliniques Plurithématique, Nancy, France; and* [3]*Cardiovascular Division, Mayo Clinic, Rochester, MN, USA*

Abstract

Aims The determinants and relevance of right ventricular (RV) mechanical dyssynchrony in heart failure with reduced ejection fraction (HFrEF) are poorly understood. We hypothesized that increased afterload may adversely affect the synchrony of RV contraction.

Methods and results A total of 148 patients with HFrEF and 36 controls underwent echocardiography, right heart catheterization, and gated single-photon emission computed tomography to measure RV chamber volumes and mechanical dyssynchrony (phase standard deviation of systolic displacement timing). Exams were repeated after preload (N = 135) and afterload (N = 15) modulation. Patients with HFrEF showed higher RV dyssynchrony compared with controls (40.6 ± 17.5° vs. 27.8 ± 9.1°, $P < 0.001$). The magnitude of RV dyssynchrony in HFrEF correlated with larger RV and left ventricular (LV) volumes, lower RV ejection fraction (RVEF) and LV ejection fraction, reduced intrinsic contractility, increased heart rate, higher pulmonary artery (PA) load, and impaired RV–PA coupling (all $P \leq 0.01$). Low RVEF was the strongest predictor of RV dyssynchrony. Left bundle branch block (BBB) was associated with greater RV dyssynchrony than right BBB, regardless of QRS duration. RV afterload reduction by sildenafil improved RV dyssynchrony (P = 0.004), whereas preload change with passive leg raise had modest effect. Patients in the highest tertiles of RV dyssynchrony had an increased risk of adverse clinical events compared with those in the lower tertile [T2/T3 vs. T1: hazard ratio 1.98 (95% confidence interval 1.20–3.24), P = 0.007].

Conclusions RV dyssynchrony is associated with RV remodelling, dysfunction, adverse haemodynamics, and greater risk for adverse clinical events. RV dyssynchrony is mitigated by acute RV afterload reduction and could be a potential therapeutic target to improve RV performance in HFrEF.

Keywords Heart failure with reduced ejection fraction; Right ventricular dyssynchrony; Right ventricular failure; Pulmonary hypertension; SPECT

Received: 9 August 2023; Revised: 19 November 2023; Accepted: 27 December 2023
**Correspondence to: Vojtech Melenovsky, Department of Cardiology, Institute for Clinical and Experimental Medicine (IKEM), Prague 140 21, Czech Republic. Tel: +420-739528029; Fax: +420-261362986. Email: vojtech.melenovsky@ikem.cz*

Introduction

Left ventricular (LV) mechanical dyssynchrony has been extensively studied in patients with heart failure and reduced ejection fraction (HFrEF) due to its detrimental impact on LV performance and its implications for clinical outcomes.[1] The mechanisms and the relevance of right ventricular (RV) mechanical dyssynchrony in HFrEF are not well understood. Mechanical dyssynchrony is an independent predictor of clinical worsening in primary diseases affecting the right ventricle, such as pulmonary arterial hypertension (PAH) or arrhythmogenic right ventricular cardiomyopathy,[2,3] but studies in HFrEF are scarce.[4,5]

Evaluation of RV function and mechanical synchrony is most often performed by echocardiography, but advanced echo-based techniques such as three-dimensional (3D) tissue

Doppler imaging or speckle tracking require highly standardized post-processing and are limited by geometric features of the right ventricle, angle dependency, intraoperator and inter-operator variability, acoustic windows, and image quality.[6] In contrast, nuclear techniques for RV imaging, such as equilibrium gated single-photon emission computed tomography (GSPECT), are less hampered by the complex geometry of the right ventricle, are less operator dependent, and provide strong signal-to-noise ratio with isotropic 3D spatial information, allowing accurate quantification of RV volumes and function compared with echocardiography.[7,8] Automated phase analysis of GSPECT data has been suggested as a promising and reproducible option for the evaluation of RV dyssynchrony.[9,10]

The aim of this study was to investigate the correlates of RV dyssynchrony along with its prognostic significance in patients with advanced HFrEF using combined invasive–noninvasive pressure–volume analyses with acute load modulation. We hypothesized that increased RV load may adversely affect synchrony of RV contraction and as such contributing to worse RV chamber performance and prognosis.

Methods

Patient population

This prospective study enrolled patients with chronic (>6 months) symptomatic HFrEF [LV ejection fraction (LVEF) ≤40%] electively hospitalized for consideration of advanced therapies at the Institute for Clinical and Experimental Medicine (IKEM) in Prague, Czech Republic, from June 2016 to December 2020. All patients were followed up at IKEM (in the outpatient clinic or by planned elective hospitalization) at intervals dictated by the severity of their medical condition. Clinical events occurrence was ascertained by querying the hospital electronic records system and the national death registry. Patients with acute ischaemia, uncontrolled cardiac arrhythmia, haemodynamic instability needing inotropes or mechanical circulatory support, reversible cardiac dysfunction, active malignancy, endocrine disease, pre-existing treatment with a phosphodiesterase-5 (PDE5) inhibitor, and chronic or acute infection were excluded. To eliminate the confounding effect of pacing on RV dyssynchrony, only patients with native ventricular conduction were studied. In patients with an implanted cardiac device [implantable cardioverter defibrillator (ICD)/cardiac resynchronization therapy (CRT)], we ensured that the ventricle was not paced at the time of basal electrocardiogram (ECG), GSPECT, and right heart catheterization (RHC). Patients admitted with hypervolaemia were enrolled upon achieving normovolaemia, as determined by clinical judgement following the use of intravenous diuretics.

The control group consisted of individuals without HF (no clinical signs and symptoms typical of HF, no history of HF or HF-related hospitalizations, and normal natriuretic peptide levels) scheduled to undergo diagnostic or therapeutic procedures, including patients with unexplained shortness of breath of non-cardiac origin (11%) or patients undergoing closure of patent foramen ovale (89%).

The protocol was approved by the local ethics committee on 8 June 2016 (G-16-06-28, No. 986/16), and it was not considered as a clinical trial. All patients provided their informed consent for the procedures and for participating in this research study.

Study protocol

After signing informed consent, HF patients underwent history review, physical examination, echocardiography, ECG, Kansas City Cardiomyopathy Questionnaire, blood sampling, GSPECT, and RHC, as part of clinical work-up or for research purposes.

For the RHC procedure, to ensure uniformity of the pressure transducer setting, with the patient in the supine position, the zero level was established at the mid-thoracic line as recommended.[11] During shallow respiration, a 10 s strip of ectopy-free, high-quality signal was used to record and annotate pressure waveforms (Mac-Lab, GE Healthcare, Chicago, IL). Using a 7 Fr balloon-tipped triple-lumen Swan–Ganz catheter (Braun Melsungen AG, Melsungen, Germany) inserted via the right internal jugular vein, invasive pressures were measured in the right atrium and right ventricle. Then the catheter was advanced to the pulmonary artery (PA), and its position was verified by identifying the signature pressure curves. Systolic (sPAP), diastolic (dPAP), and mean (mPAP) PA pressure, as well as the mean values of respiratory-averaged PA wedge pressure (PAWP), were measured as previously described.[11] Cardiac output (CO) was measured by thermodilution as the average of at least three measurements [five in patients with atrial fibrillation (AF)] with a variance of <10%.[12] In patients with AF, pressure waveforms were recorded during ectopy-free periods with the smallest R-R interval variability and averaged over several cardiac cycles.[11] The systemic blood pressure (SBP) was measured after 10 min of rest in the supine position using an automated oscillometric monitor.

After RHC, patients underwent ECG-gated 3D equilibrium ^{99m}Tc-labelled blood pool GSPECT. All patients received an injection of stannous pyrophosphate (Technescan PYP, Curium, The Netherlands), and 30 min later, erythrocytes were *in vivo* labelled by intravenous injection of 740 MBq ^{99m}Tc isotope. The heart chambers were imaged using a D-SPECT camera (Spectrum Dynamics, Israel) equipped with collimated, pixilated cadmium zinc telluride crystal detectors allowing rapid (7 min) data acquisition with high spatial resolution (mean ef-

fective dose ~5 mSv).[13] Medications and conditions for examinations at both RHC and GSPECT were identical.

In a subgroup of HF patients, we explored the impact of afterload reduction (n = 15) and preload increase (n = 135) on RV dyssynchrony. Afterload reduction (achieved by administration of 20 mg intravenous sildenafil) was attempted in all euvolaemic subjects [right atrial (RA) pressure <10 mmHg] with a significant pre-capillary component of pulmonary hypertension [i.e. pulmonary vascular resistance >3 Wood units (WU) or transpulmonary gradient >15 mmHg] and without systemic hypotension (SBP > 90 mmHg), as part of the standard protocol for pre-transplant evaluation in our centre.[14] Haemodynamic assessment was performed before and 10 min after administering intravenous sildenafil, as part of the clinical evaluation protocol for HF patients. Patients who were administered sildenafil during RHC, underwent GSPECT imaging at least 35 h later (five times the elimination half-time of sildenafil), following which the sildenafil administration was repeated.

Preload increase was attempted in all patients unless technical or logistical issues occurred and was achieved by raising the legs of the patient by a 60° angle foam wedge for 7 min. Data acquisition for both GSPECT and RHC procedures started 30–60 s following the leg rise manoeuvre.

Haemodynamic and right ventricular pressure–volume analysis

The raw GSPECT data were post-processed by a single experienced nuclear physician (M.T.) using a semiautomatic commercially available plug-in software (QBS Cedars-Sinai, Los Angeles, CA) to obtain assessment of 3D volumes and systolic function in the time domain (*Figure 1* and Supporting Information, *Figure S1* and *Videos S1–S3*). Intraoperator reproducibility for GSPECT measures was assessed on 15 random subjects from the entire population. The Bland–Altman analysis showed a satisfying intraoperator reproducibility for both

Figure 1 Schematic illustration of the processing steps involved in the assessment of right ventricular (RV) dyssynchrony and volumes using gated myocardial perfusion single-photon emission computed tomography (SPECT) studies. After acquisition of electrocardiogram (ECG)-gated raw radionuclide angiocardiography (A), left and right ventricles were delineated by automatic processing on planar projections (B). For each temporal frame, a regional maximal count detection was performed. Consecutively, the first Fourier harmonic function was used to approximate the discrete sample points into a continuous wall-thickening curve (C). Based on the partial volume effect, this time–activity curve represents the thickening curve of this particular myocardial sample during a cardiac cycle. The point at which the continuous thickening curve intersects with the average count density of this voxel (horizontal line) is considered the onset of mechanical contraction (OMC) for this region (red circle). The software computes the OMC for all RV myocardial samples collected and then displays the composite result as a phase histogram. The surfaces resulting from ventricular delineation (Step B) are used to compute endocardial volumes at each interval of the gated data set and presented in a 3D reconstruction (D). The phase histogram was used to obtain the RV dyssynchrony indices, such as the phase mean and standard deviation (i.e. the standard deviation of the OMC phase distribution).

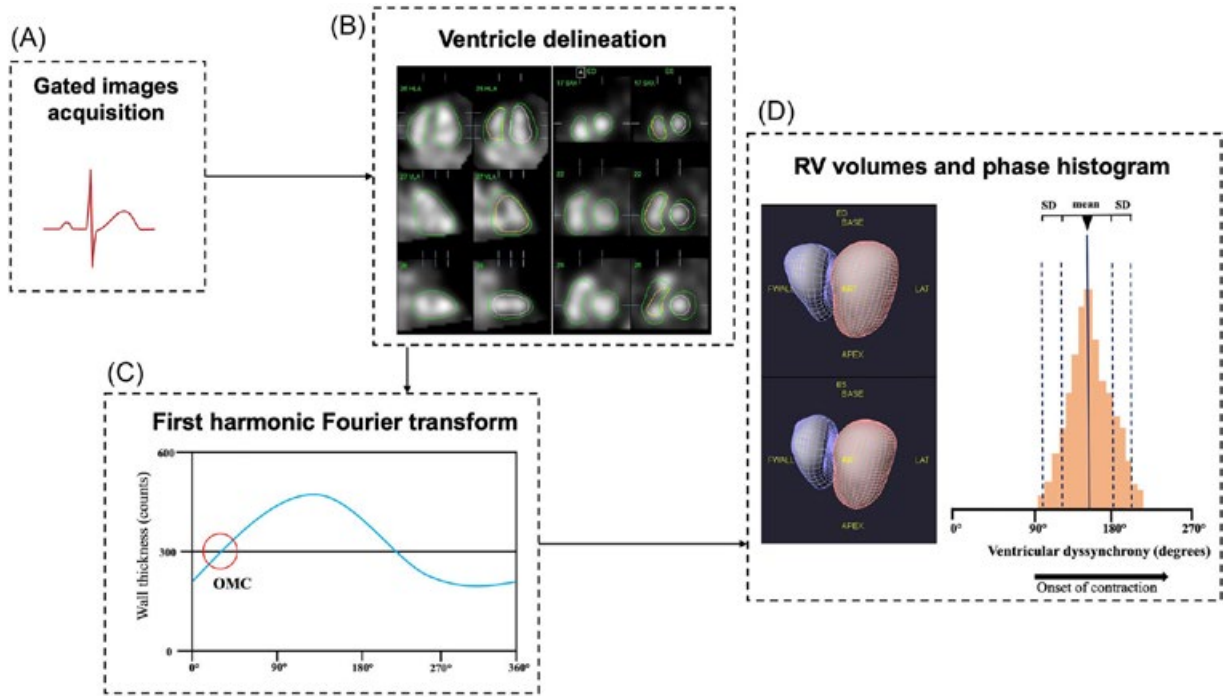

RV end-diastolic (mean bias 8.9 mL) and end-systolic (mean bias −4.3 mL) volumes (Supporting Information, *Figure S2*). GSPECT-derived ventricular volumes and RHC-derived pressures data were combined to calculate RV loading and contractility. Lumped RV afterload [PA elastance (Ea_{PA})] was estimated as the sPAP divided by the stroke volume (derived from thermodilution CO). The choice to utilize sPAP instead of mPAP for Ea_{PA} assessment stems from the observation that when pulmonary vascular impedance is elevated, sPAP provides a closer approximation of end-systolic pressure, whereas mPAP tends to underestimate it.[15,16] RV contractility was estimated using the simplified formula for end-systolic elastance (Ees) calculated as the RV maximal pressure/end-systolic volume (derived from GSPECT).[17] From these measurements, we derived ventricular–arterial coupling, calculated as RV Ees/Ea_{PA}. PA compliance was calculated as the RHC-derived stroke volume/PA pulse pressure, and the pulmonary vascular resistance (PVR) was calculated as transpulmonary gradient (mPAP − PAWP)/CO.[18] RV diastolic compliance was determined by the ratio of end-diastolic pressure (EDP) to end-diastolic volume (EDV), a measurement that has been shown to agree with the more rigorous diastolic elastance coefficient β calculated from a curvilinear adjustment of end-systolic and EDP/EDV ratios.[19] Pulmonary hypertension was defined as mPAP > 20 mmHg.[20]

Right ventricular dyssynchrony analysis

Phase analysis of GSPECT data was performed by a semiautomatic software (QBS Cedars-Sinai, Los Angeles, CA) as previously described.[21,22] The program performed Fourier transformation on the 16-frame time–activity curve of each myocardial sample to derive the first harmonic function. The temporal onset of ventricular mechanical contraction during the cardiac cycle of each myocardial sample was considered to be the phase of the inflection point of the thickening curve on a horizontal line representing the average myocardial count over a cardiac cycle.[23] The onset of ventricular mechanical phase information from the RV myocardial samples collected was used to generate a phase distribution, which is displayed in histogram. Phase standard deviation [PSD, i.e. the standard deviation (SD) of the phase distributions during cardiac cycle in degrees] was used to express dyssynchrony as previously described (*Figure 1*).[22,24] In unselected patients and control subjects, the repeatability of phase analysis approach is high and mainly attributable to automated generation of dyssynchrony parameters.[22,25]

Data analysis

Data are shown as mean ± SD or median and [25th–75th inter-quartile range (IQR)] for continuous variables (according to distribution) and total count (*n*) with proportion (%) for categorical variables. One-way ANOVA and Kruskal–Wallis tests were used to compare continuous variables between groups depending on the normality of the distribution, and the χ^2 test was used for categorical variables. Normality was assessed using the Shapiro–Wilk test. Trend tests were performed by using the Cochran–Armitage or Cuzick's trend test for categorical variables, and the Jonckheere–Terpstra test or linear regression for continuous variables, as appropriate. To assess the association of each variable with the severity of RV dyssynchrony (PSD), separate multiple logistic regression analyses were conducted. Variables not normally distributed had been log-transformed before the analysis. Pearson *r* or Spearman's coefficient (for abnormally distributed variables) was calculated for correlations. Highly significant univariate variables (*P* value <0.001) were included in the multivariate model. Cox proportional hazard regression was used to analyse the factors associated with the adverse outcome, defined as combined endpoint of death, urgent transplantation, or left ventricular assist device (LVAD) implantation without heart transplantation, as done before.[26–28] Kaplan–Meier curves with the log-rank statistics were used to illustrate the outcome. The effect of preload and afterload modulation on haemodynamic and GSPECT parameters was tested using paired *t*-test or the Wilcoxon signed-rank test as appropriate. A *P* value <0.05 was considered significant. All analyses were performed using JMP Pro 17.0 statistical software (SAS Institute, Inc., Cary, NC).

Results

Baseline characteristics: heart failure with reduced ejection fraction vs. controls

Patients with HFrEF (*n* = 148) were mostly middle-aged men with severe symptoms [77% in New York Heart Association (NYHA) Class III/IV] treated with optimized medical therapy (Supporting Information, *Table S1*). The median duration of HF was 3.6 [1.4; 7.5] years. As expected, patients with HFrEF displayed dilatation and impaired function of both ventricles compared with controls (*n* = 36), wider QRS duration, and higher natriuretic peptides. Nearly half (42%) of patients with HFrEF displayed RV dysfunction [RV ejection fraction (RVEF) ≤ 35%]. The median time between RHC and GSPECT was 1 day (IQR, 0–1 day). At baseline, the majority of patients with HFrEF had combined post-capillary and pre-capillary pulmonary hypertension [mPAP 34.3 ± 10.8 mmHg, PAWP 22.8 ± 8.5 mmHg, PVR 2.9 (1.9; 4.2) WU], with low CO (3.8 ± 0.9 L/min) (Supporting Information, *Table S2*). A total of 128 patients (87%) with HFrEF had pulmonary hypertension, and 110 (74%) had PVR > 2 WU.

Table 1 Baseline characteristics by RV dyssynchrony tertiles

	Tertile 1 (RV phase SD ≤ 30°) *N* = 49	Tertile 2 (RV phase SD 31–49°) *N* = 54	Tertile 3 (RV phase SD ≥ 50°) *N* = 45	*P* value[a]
Clinical characteristics				
Age (years)	55 ± 8	55 ± 10	52 ± 11	0.105
Male, *n* (%)	44 (90)	45 (83)	36 (80)	0.188
NYHA class, *n* (%): I–II; III–IV	10 (20); 39 (80)	14 (26); 40 (74)	10 (22); 35 (78)	0.822
Ischaemic HF aetiology, *n* (%)	29 (59)	22 (41)	14 (31)	0.006
Haemoglobin (mg/L)	136.9 ± 19.8	136.3 ± 16.5	137.6 ± 19.3	0.881
BNP (ng/L)	906 [390; 1796]	969 [524; 1930]	1,146 [665; 1835]	0.128
Echocardiography[b]				
Mitral regurgitation, *n* (%): 0–2 grade; 3–4 grade	27 (56); 21 (44)	23 (43); 30 (57)	18 (41); 26 (59)	0.136
Tricuspid regurgitation, *n* (%): 0–2 grade; 3–4 grade	32 (65); 17 (35)	35 (66); 18 (34)	27 (63); 16 (37)	0.808
Electrocardiography				
Heart rate (b.p.m.)	77 ± 16	79 ± 13	85 ± 16	0.012
QRS morphology, *n* (%): LBBB; RBBB; normal; other alterations[c]	4 (8); 7 (14); 17 (35); 21 (43)	16 (30); 5 (9); 11 (20); 22 (41)	11 (24); 1 (2); 8 (18); 25 (56)	0.191
QRS duration (ms)	116.4 ± 25.2	123.3 ± 24.7	118.7 ± 24.4	0.639
Therapy				
ACE, ARB, or ARNI, *n* (%)	37 (76)	35 (65)	31 (69)	0.470
ACE, ARB, or ARNI ≥50% target dose, *n* (%)	17 (46)	17 (49)	15 (48)	0.835
MRA, *n* (%)	45 (92)	46 (85)	37 (82)	0.170
MRA ≥50% target dose, *n* (%)	40 (91)	44 (96)	33 (89)	0.819
Beta-blocker, *n* (%)	41 (84)	47 (87)	36 (80)	0.644
Beta-blocker >≥50% target dose, *n* (%)	16 (40)	12 (26)	13 (36)	0.684
Devices, *n* (%): ICD; CRT; none	40 (82); 3 (6); 6 (12)	40 (74); 7 (13); 7 (13)	31 (69); 2 (4); 12 (27)	0.117
Haemodynamic				
RA mean pressure (mmHg)	8.7 ± 6.0	9.9 ± 5.6	10.2 ± 5.8	0.222
RV systolic elastance (Ees) (mmHg/mL)	0.36 [0.24; 0.62]	0.32 [0.22; 0.47]	0.25 [0.21; 0.43]	0.010
RV diastolic compliance (mL/mmHg)	13.8 [9.9; 25.3]	12.6 [8.0; 17.4]	8.8 [6.3; 13.4]	<0.001
Cardiac output (L/min)	4.1 ± 0.8	3.6 ± 0.9	3.6 ± 1.0	0.007
Stroke volume (mL)	55.1 ± 14.1	47.2 ± 12.9	43.8 ± 15.3	<0.001
PA mean pressure (mmHg)	31.1 ± 12.1	35.2 ± 9.0	36.6 ± 10.5	0.014
PA wedge pressure (mmHg)	20.5 ± 9.4	23.3 ± 7.2	24.9 ± 8.1	0.012
PA compliance (mL/mmHg)	2.2 [1.7; 3.3]	1.7 [1.2; 2.4]	1.7 [1.2; 2.4]	0.010
PA elastance (Ea_{PA}) (mmHg/mL)	0.91 [0.56; 1.22]	1.11 [0.80; 1.58]	1.27 [0.95; 1.76]	<0.001
PVR (WU)	2.3 [1.6; 3.1]	3.1 [2.4; 4.4]	3.1 [2.2; 4.7]	0.015
RV–PA coupling ratio	0.40 [0.26; 0.97]	0.28 [0.19; 0.41]	0.26 [0.14; 0.38]	<0.001
Systolic blood pressure (mmHg)	109.8 ± 14.6	109.9 ± 14.5	108.8 ± 19.9	0.765
Diastolic blood pressure (mmHg)	74.2 ± 8.5	76.4 ± 8.1	74.9 ± 13.2	0.719
GSPECT				
RV end-diastolic volume (mL)	256.9 ± 106.7	283.4 ± 90.9	287.9 ± 88.3	0.113
RV end-systolic volume (mL)	135.7 ± 82.6	180.1 ± 77.8	201.3 ± 81.7	<0.001

(*Continues*)

Table 1 (continued)

	Tertile 1 (RV phase SD ≤ 30°) *N* = 49	Tertile 2 (RV phase SD 31–49°) *N* = 54	Tertile 3 (RV phase SD ≥ 50°) *N* = 45	*P* value[a]
RV ejection fraction (%)	50.9 ± 14.2	38.2 ± 11.1	32.2 ± 12.0	<0.001
LV end-diastolic volume (mL)	342.0 ± 104.7	388.4 ± 110.1	406.9 ± 112.7	0.005
LV end-systolic volume (mL)	246.2 ± 92.9	296.6 ± 98.2	314.9 ± 103.9	0.001
LV ejection fraction (%)	29.2 ± 9.4	23.9 ± 7.3	23.2 ± 7.9	<0.001

ACE, angiotensin-converting enzyme; ARB, angiotensin receptor blocker; ARNI, angiotensin receptor–neprilysin inhibitor; BNP, brain natriuretic peptide; CRT, cardiac resynchronization therapy; GSPECT, gated single-photon emission computed tomography; ICD, implantable cardioverter defibrillator; LBBB, left bundle branch block; LV, left ventricular; MRA, mineralocorticoid receptor antagonist; NYHA, New York Heart Association; PA, pulmonary artery; PVR, pulmonary vascular resistance; RA, right atrial; RBBB, right bundle branch block; RV, right ventricular; SD, standard deviation; WU, Wood units.

[a]*P* value for trend.

[b]Mitral regurgitation and tricuspid regurgitation were assessed semi-quantitatively and reported using a four-stage grading (i.e. 0 = none-trace, 1 = mild, 2 = moderate, and 3 = severe).

[c]Other alterations include left anterior fascicular block, left posterior fascicular block, incomplete LBBB, and nonspecific intraventricular conduction delay.

Right ventricular dyssynchrony

Patients with HFrEF showed higher degree of RV dyssynchrony compared with controls (Supporting Information, *Table S2*). Based on the distribution in HF patients, RV dyssynchrony tertiles were created with cut-offs ≤30° (*N* = 49), 31–49° (*N* = 54), and ≥50° (*N* = 45). Patients with HFrEF falling in the lowest tertile of RV synchrony had lower heart rate and higher prevalence of ischaemic HF aetiology compared with patients in the highest tertile. In haemodynamic examination, patients with lower degree of RV dyssynchrony showed more favourable afterload (lower Ea_{PA}) and intracardiac pressures (lower PAWP), a better systolic function (higher CO and RVEF/LVEF and more preserved RV ventricular–arterial coupling ratio), and lower RV/LV volumes compared with higher tertiles (*Table 1*).

The degree of RV dyssynchrony was directly correlated with RV volumes (end-diastolic: $r = 0.172$, $P = 0.036$; end-systolic: $r = 0.353$, $P < 0.001$) and inversely correlated with RVEF ($r = -0.525$, $P < 0.001$) (*Figure 2A–C* and *Table 2*). From a haemodynamic perspective, increased RV afterload (expressed by the lumped RV afterload parameter PA elastance) and decreased RV end-systolic elastance were correlated with greater RV dyssynchrony (Supporting Information, *Figure S3A,B*). In addition, worse ventricular–arterial coupling ratio, larger LV volumes, and lower LVEF (Supporting Information, *Figure S3C–F* and *Table 2*), as well as higher PAWP and lower CO, were correlated with RV dyssynchrony. Patients with native left bundle branch block (LBBB) had more RV dyssynchrony than those with native right bundle branch block (RBBB) (45.7 ± 13.9° vs. 30.9 ± 11.1°, $P < 0.001$), regardless of QRS duration (*Figure 2D,E*). Those with non-ischaemic HF aetiology showed worse RV dyssynchrony (44.3 ± 17.8° vs. 35.8 ± 15.8°, $P = 0.003$), larger RV volumes (end-diastolic: 302 ± 98 vs. 243 ± 83 mL, $P < 0.001$; end-systolic: 199 ± 86 vs. 138 ± 69 mL, $P < 0.001$), and lower RVEF (36 ± 13% vs. 46 ± 15%, $P < 0.001$) compared with ischaemic patients (Supporting Information, *Figure S4*). No significant differences in terms of RV dyssynchrony were found among patients with and without AF (37 ± 19° vs. 41 ± 17°, $P = 0.414$). Among clinical parameters, a faster heart rate was correlated with a higher degree of RV dyssynchrony (*Table 2*).

In multivariable regression analysis, baseline low RVEF remained the only independent predictor of RV dyssynchrony. Excluding RVEF from the multivariate model, ventricular–arterial coupling and LVEF emerged as significant predictors of RV dyssynchrony (*Table 2*).

Preload and afterload modulation

The median time between RHC and GSPECT in this subgroup of patients was 2 days (IQR, 1–4 days). Compared with base-

Figure 2 Correlation between right ventricular (RV) dyssynchrony and (A) RV end-diastolic volume, (B) RV end-systolic volume, and (C) RV ejection fraction [all in heart failure with reduced ejection fraction (HFrEF) patients]. (D) RV dyssynchrony in HFrEF patients with left bundle branch block (LBBB), right bundle branch block (RBBB), and normal conduction. (E) Correlation between RV dyssynchrony and QRS duration in HFrEF patients. Asterisk stands for $P < 0.05$.

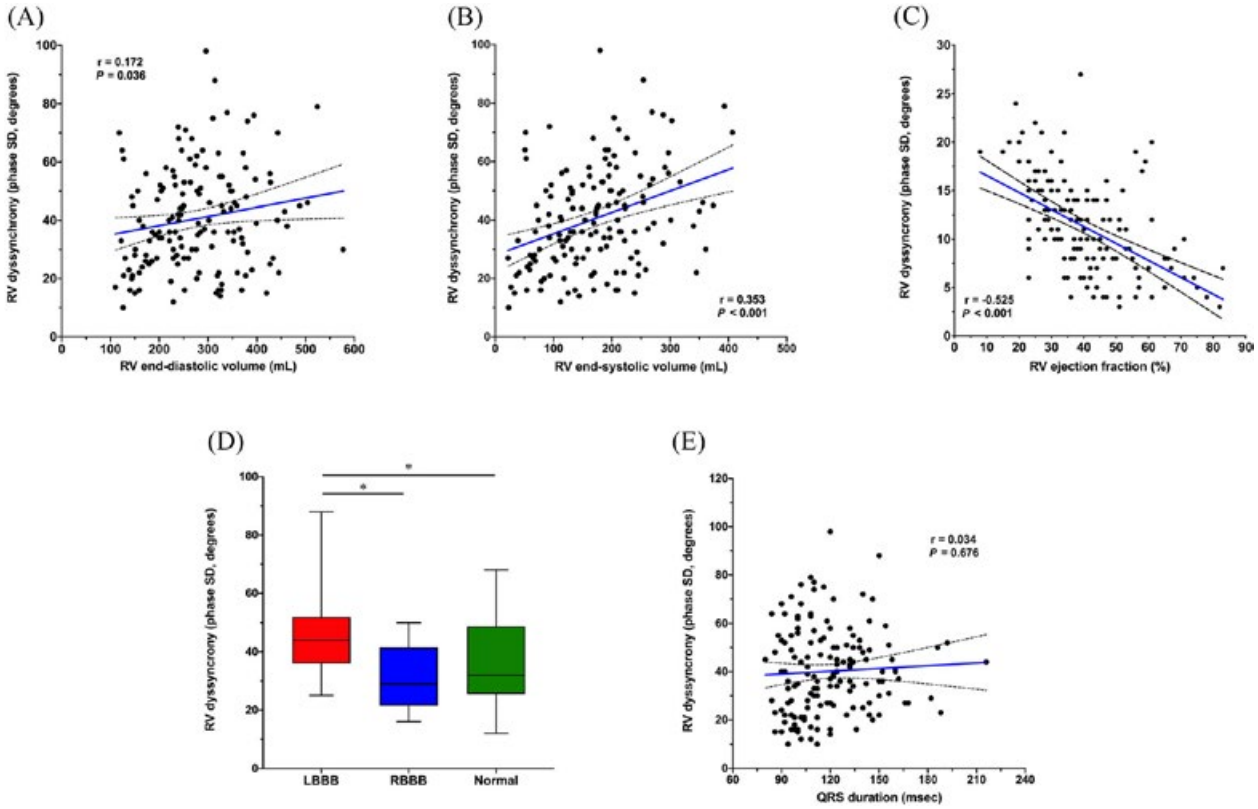

line, intravenous sildenafil (N = 15) decreased RA [−52 (−60; −37) %] and RV [RV EDP: −50 (−69; −25) %] pressure, RV afterload [Ea_{PA} −43 (−54; −26) %], and PAWP [−20 (−43; 0) %] (*Figure 3A*) while increased CO [14 (2; 30) %] (all $P < 0.01$). It also reduced RV volumes [end-diastolic: −16 (−28; −8) %; end-systolic: −39 (−48; −16) %] and increased RVEF [+23 (20; 52) %] (*Figure 3B*) (all $P < 0.01$), without significantly affecting RV Ees [0.01 (−0.11; 0.12) mmHg/mL] (Supporting Information, *Table S3*). On the left side, sildenafil infusion significantly reduced systolic blood pressure [−6.1 (−11.6; −0.5) mmHg] and systemic vascular resistance [−376 (−564; −188) dyn/s/cm^{-5}]. RV dyssynchrony decreased following sildenafil administration [−15.0° (−22.0°; 5.0°), P = 0.004] (*Figure 3C*).

Preload increase with passive leg raise (N = 135) significantly increased RA pressure [+26 (10; 46) %], RV EDP [27 (11; 56) %], RV afterload [Ea_{PA} +11 (−3; 29) %), and PAWP [15 (3; 36) %] (all $P < 0.05$), without a relevant impact on CO [+1 (−9; 5) %]. A slight albeit significant increase was noted in RV volumes [end-diastolic: +5 (−4; 16) %; end-systolic: +5 (−8; 18) %, all $P < 0.05$], without significant changes in RVEF [0 (−12; 13) %] and RV Ees [−0.01 (−0.04; 0.02) mmHg/mL] (Supporting Information, *Table S3*). Preload modulation had a modest influence on RV dyssynchrony in the overall population (P = 0.080) (Supporting Information, *Table S3*) but resulted in a significant RV dyssynchrony improvement in the subgroup of patients who underwent PDE5 inhibitors administration to test afterload reduction (Supporting Information, *Figure S5*). The effect of preload modulation was not significantly different between patients with and without AF [−1.9° (−11.7°; 7.9°) vs. −2.7° (−5.9°; 0.4°), P = 0.373].

Outcome

During a median follow-up of 206 days (IQR, 58–439 days), there were 83 composite events including 44 deaths, 33 assist device implantations, and 16 urgent cardiac transplantations. In univariable Cox regression analysis, the risk of composite outcome increased with higher RV dyssynchrony (*Figure 4*). In particular, patients in the highest tertiles of RV dyssynchrony (i.e. >30°) had an increased risk of adverse clinical events compared with those in the lower tertile {T2/T3 vs.

Table 2 Variables associated with RV dyssynchrony by univariate and multivariate linear regression models

	Univariate		Multivariate (Model 1)		Multivariate (Model 2)	
	Correlation coefficient (95% CI)	*P* value	Correlation coefficient (95% CI)	*P* value	Correlation coefficient (95% CI)	*P* value
Clinical characteristics						
Body mass index (kg/m^2)	−0.136 (−0.292 to 0.026)	0.098				
Age (years)	−0.147 (−0.301 to 0.014)	0.074				
QRS duration (ms)	0.035 (−0.127 to 0.195)	0.676				
BNP (pg/mL)	0.078 (−0.085 to 0.237)	0.347				
Haemoglobin (mg/L)	0.037 (−0.125 to 0.197)	0.657				
Heart rate (b.p.m.)	0.224 (0.065–0.372)	0.006	0.160 (−0.021 to 0.341)	0.082	0.100 (−0.094 to 0.294)	0.310
Tricuspid regurgitation (0–4 grade)	−0.028 (−0.190 to 0.135)	0.736				
Haemodynamics						
PA mean pressure (mmHg)	0.168 (0.007–0.321)	0.041	0.157 (−1.265 to 1.580)	0.826	−0.088 (−1.453 to 1.630)	0.909
PA wedge pressure (mmHg)	0.163 (0.001–0.316)	0.048	−0.353 (−1.825 to 1.118)	0.635	−0.319 (−1.915 to 1.275)	0.693
Cardiac output (L/min)	−0.211 (−0.360 to −0.051)	0.010	−2.680 (−7.524 to 2.164)	0.276	−0.638 (−5.817 to 4.539)	0.807
Systolic blood pressure (mmHg)	0.009 (−0.153 to 0.169)	0.917				
Pulmonary vascular resistance (WU)	0.208 (0.047–0.358)	0.011	3.724 (−10.430 to 17.880)	0.603	3.330 (−12.010 to 18.672)	0.668
PA compliance (mL/mmHg)	−0.131 (−0.285 to 0.031)	0.114				
PA elastance (Ea) (mmHg/mL)	0.247 (0.089–0.392)	0.003	—	—	—	—
RV systolic elastance (Ees) (mmHg/mL)	−0.272 (−0.415 to −0.116)	<0.001	—	—	—	—
RV ventricular–arterial coupling ratio	−0.402 (−0.529 to −0.258)	<0.001	6.548 (−0.593 to 13.691)	0.072	−7.905 (−12.597 to −3.213)	0.001
RV diastolic compliance (mL/mmHg)	0.016 (−0.146 to 0.177)	0.847				
GSPECT						
RV end-diastolic volume (mL)	0.172 (0.011–0.325)	0.036	—	—	—	—
RV end-systolic volume (mL)	0.353 (0.203–0.486)	<0.001	—	—	—	—
RV ejection fraction (%)	−0.525 (−0.632 to −0.397)	<0.001	−0.800 (−1.148 to −0.486)	<0.001	—	—
LV end-diastolic volume (mL)	0.182 (0.021–0.333)	0.027	—	—	—	—
LV end-systolic volume (mL)	0.215 (0.055–0.364)	0.009	—	—	—	—
LV ejection fraction (%)	−0.258 (−0.403 to −0.102)	0.002	−0.190 (−0.506 to 0.125)	0.234	−0.388 (−0.719 to −0.057)	0.022

BNP, brain natriuretic peptide; CI, confidence interval; GSPECT, gated single-photon emission computed tomography; LV, left ventricular; PA, pulmonary artery; RV, right ventricular; RVEF, right ventricular ejection fraction; WU, Wood units.
In the multivariable models, em dashes stand for variables not tested because of possible collinearity; meanwhile, empty rows mean that variables were not tested because of non-statistical significance in the univariate analysis. In multivariable Model 2, RVEF was excluded.

Figure 3 Change in (A) pulmonary artery (PA) wedge pressure, (B) right ventricular (RV) ejection fraction, and (C) RV dyssynchrony after sildenafil infusion (N = 15). Median values before and after sildenafil are reported on the relative sides of the chart. In (C), different colours represent changes in RV dyssynchrony tertiles of individual patients before and after sildenafil. Asterisk stands for $P < 0.05$.

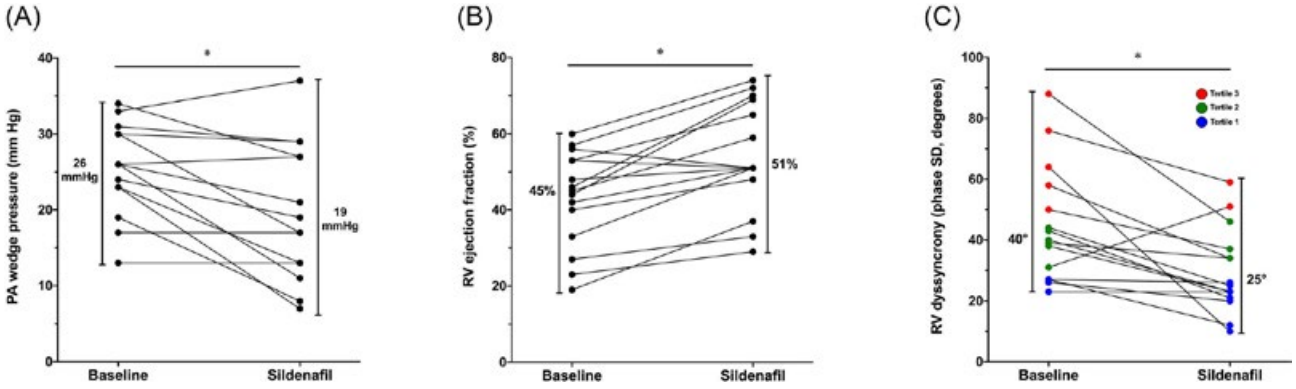

Figure 4 Kaplan–Meier curves for the composite outcome of death, urgent transplantation, or assist device implantation without heart transplantation stratified by right ventricular (RV) dyssynchrony tertiles.

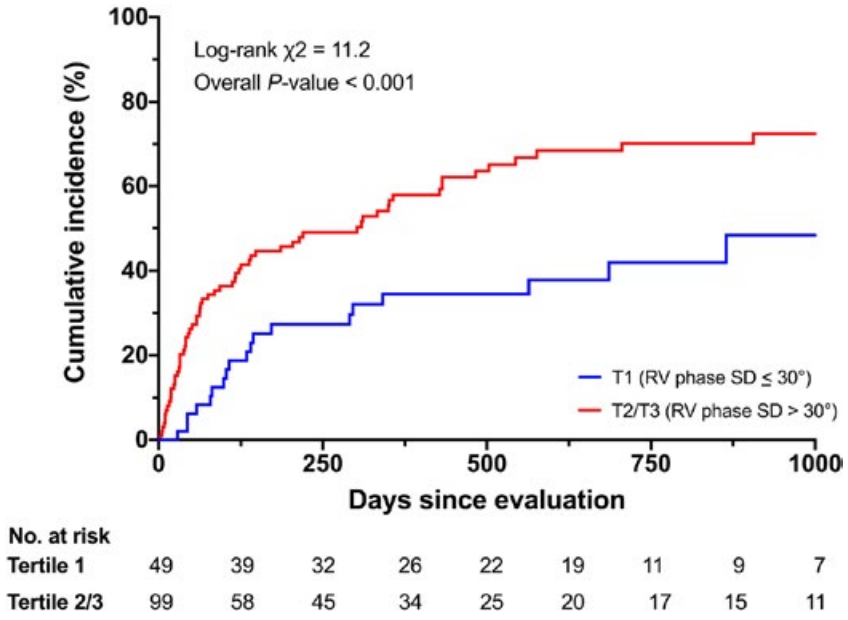

T1: hazard ratio [HR] 1.98 [95% confidence interval (CI) 1.20–3.24], P = 0.007}. Even after adjusting Cox analysis for the variables independently associated with RV dyssynchrony at multivariable analysis (i.e. RVEF, LVEF, and right ventricular–arterial coupling), a higher degree of dyssynchrony remained associated with worse outcomes [T2/T3 vs. T1: HR 1.81 (95% CI 1.02–3.19), P = 0.041]. A sensitivity analysis using as primary endpoint the composite of death or urgent cardiac transplantation (i.e. excluding LVAD implantation, being this event possibly influenced by referral bias to our tertiary centre) showed similar results [T2/T3 vs. T1: HR 1.96 (95% CI 1.18–3.26), P = 0.009].

Discussion

Our findings show that among patients with advanced HFrEF and native ventricular conduction, increases in RV dyssynchrony correlated with impaired RV structure and function and were predictive of greater risk of adverse outcomes. Patients with more dyssynchronous RV shortening had greater impairments in ventricular chambers contractility by combined pressure–volume analysis and larger ventricular volumes. Higher RV dyssynchrony was associated with more adverse haemodynamics—such as increased RV afterload—and conversely, afterload reduction with sildenafil improved

RV synchrony. These data point to an important, previously unrecognized role for RV dyssynchrony as an adverse finding in HFrEF and suggest that therapies to improve RV synchrony, including RV afterload reduction, may be helpful to improve clinical outcomes in patients with advanced HFrEF.

Prior studies on RV dyssynchrony have focused almost exclusively on patients with PAH, where it constitutes an established and independent prognostic factor.[2,29] In PAH, a combination of increased afterload and morphological RV remodelling was the major determinant of RV dyssynchrony.[2] As a novel observation, our study shows that the same parameters likely play a role in patients with HFrEF and RV dyssynchrony. Moreover, previous studies mainly focused on single imaging methods, meanwhile, our approach involved the simultaneous collection and combination of both dyssynchrony and pressure/volume data using GSPECT and RHC.

Increased afterload may induce RV dyssynchrony in HFrEF through several mechanisms. Due to the complex shape of the right ventricle, pulmonary hypertension causes inhomogeneity of RV's regional wall stress, leading to a non-uniform duration of contraction.[30,31] Non-synchronous patterns of regional ventricular contraction impair overall RV systolic function, the strongest correlate of RV dyssynchrony in our study, meanwhile have less an impact on RV remodelling. Primary alterations of the LV[32] or loading conditions[33] might further reduce the RV mechanical efficiency and consequently increase RV dyssynchrony in patients with HFrEF.[34] In this regard, previous experimental observations showed that LV contraction accounts for up to 40% of RV work, with septal contraction being the most important contributor to ventricular interdependence.[32] In our study, we found that patients with LBBB had more RV dyssynchrony than patients with RBBB, regardless of QRS duration. This is not surprising, because LBBB induces a typically abnormal contraction of the interventricular septum with marked early systolic shortening and leftward motion,[24] reducing in turn RV systolic efficiency and intraventricular synchrony.[4] On the contrary, RBBB-type delay shows modest effects on interventricular septum activation,[35] thus inducing a lower degree of dyssynchrony. Correcting LV dyssynchrony by CRT has been demonstrated to ameliorate RV dyssynchrony improving septum delay.[4] In contrast to LV dyssynchrony, QRS duration was poorly correlated with RV dyssynchrony in HFrEF patients, as also demonstrated in previous studies among patients with PAH and in healthy volunteers.[31,36]

Patients with non-ischaemic HF aetiology had a higher degree of RV dyssynchrony compared with patients with ischaemic HF. The most likely reason could be that the former group had a larger prevalence of primary myocardial tissue disease also affecting the right ventricle. In line, our finding that non-ischaemic HF patients showed larger RV volumes and lower RVEF compared with ischaemic patients seems to corroborate this hypothesis.

In our study, we observed a correlation between higher heart rate and the severity of RV dyssynchrony. Although causality cannot be clearly discerned from our data, it is worth to be noted that a higher heart rate might occur in sicker ventricles and/or in case of insufficient neurohormonal blockade, underlying the importance of the optimization of beta-blocker therapy in patients with HFrEF.

Increased afterload is also a major determinant of impaired RV systolic function. Indeed, afterload increase is the primum movens for the development of RV–PA uncoupling (i.e. the increase in RV contractility in response to increased afterload is not sufficient to support normal systolic function), leading in turn to a reduction in RV systolic (RVEF, RV Ees) and diastolic function, as well as to RV dilation,[37] all parameters strictly correlated with RV dyssynchrony in our study.

We show for the first time in patients with HFrEF that RV dyssynchrony can be acutely improved by afterload reduction. As previously demonstrated by our group, the acute infusion of a PDE5 inhibitor has RV afterload-reducing effects, decreasing PAWP predominantly through relief of pericardial restraint, and improves right ventricular–arterial coupling, RV volumes, and RVEF.[38,39] This improved haemodynamic profile causes a relief in intraventricular systolic pressure, and consequently in wall stress in the basal segments, resulting in a reduction of dyssynchrony because of shortening of the time to the contraction onset in the RV free wall.[40] In agreement with our data, previous studies showed that acute hypoxia-induced raise in afterload induces a robust increase in RV dyssynchrony.[33,36] These data support the importance of therapies to reduce PA pressures for improving RV shortening and synchrony in HFrEF. However, it should be emphasized that there is a lack of robust evidence from randomized clinical trials to substantiate the utilization of PAH-specific drugs in the management of pulmonary hypertension due to left heart disease in advanced and pre-transplant HFrEF patients.

We found only a marginal effect of preload modulation on RV dyssynchrony improvement. As cited above, elevated afterload can cause heterogeneity in RV regional wall stress, resulting in inhomogeneous duration of contraction.[30,31] In particular, the time to reach peak contraction in the RV free wall is generally more delayed compared with the interventricular-septal wall.[31] A recent healthy volunteers study showed that enhanced venous return may mitigate hypoxia-induced increases in RV dyssynchrony lengthening the time to peak contraction in the septum, aligning it with the RV free wall, and consequently reducing overall dyssynchrony.[33] The considerable duration of the leg rise manoeuvre (7 min) required for obtaining GSPECT volumetric data could potentially have caused significant volume redistribution, affecting to some extent the effect of preload increase on RV dyssynchrony. Differences in the studied populations and in the method of preload manipulation (lower body positive pressure vs. leg raise) may also account for the discrepancies between our study and previous literature. Interest-

ingly, we found that the effect of preload increases on RV dyssynchrony improvement became significant when tested in the subgroup of patients who underwent afterload reduction. This finding could be attributed to the higher RV afterload observed in the sildenafil group compared with the rest of the population, indicating a potentially enhanced role for preload modulation in this specific subset.

In our study, we showed that a higher degree of RV dyssynchrony was associated with worse outcomes, supporting clinical relevance of RV dyssynchrony in HFrEF patients. Although interesting, these findings should be interpreted in the context of the demonstrated strong associations between RV dyssynchrony, RV dysfunction, and RV afterload. RV pressure overload would cause RV dilatation and increased RV wall stress, leading to altered cell-to-cell electric coupling, non-uniform ventricular depolarization, and RV dyssynchrony. LBBB may further worsen the degree of RV dyssynchrony.[34]

Limitations

The current study has inherent limitations. Patients were referred to our tertiary centre leading to selection bias. We did not study patients with mild HFrEF or patients with HF with preserved ejection fraction (HFpEF), so our findings cannot be extended to all spectra of HF. We report data on a sample consisting predominantly of males. However, we did not find any gender difference in RV dyssynchrony at baseline (data not shown), and previous observations failed to show any influence of sex on RV dyssynchrony response to alterations in preload and afterload.[33] RV Ees was determined using a simplified formula that did not take V0 (theoretical volume of the unloaded ventricle) into account during the computation. Consequently, the accuracy of RV Ees estimation may have been influenced by the residual dependence of RV contractility on EDV, particularly when dealing with a dilated right ventricle. For the afterload reduction studies with sildenafil, each patient served as their own control, and there was no placebo arm, but this was not a clinical trial as sildenafil was administered as part of clinical practice to evaluate reversibility of pulmonary vascular disease in HFrEF. Some subjects in the control group showed borderline or mildly increased mPAP/PAWP. Similarly, controls showed, on average, an RV–PA coupling value at the lower limit of normality. These values were likely secondary to coexistent comorbidities such as hypertension, coronary artery disease, or mild pulmonary disease. Nevertheless, the differences in haemodynamics between the control and HFrEF group were wide and highly significant; in addition, all control subjects showed no relevant symptoms or signs of HF, ventricular dysfunction, or significantly elevated BNP levels. Therefore, it is likely that these findings had minimal impact on the validity of our control group. We conducted all measurements during spontaneous, uncontrolled breathing without breath-holding or respiratory gating, as we assumed that the respiration patterns were not significantly different between GSPECT and RHC. As a consequence, the combination of pressure and volume data might have increased data variability, compared with simultaneous approach. Preload increase was performed with a 7 min leg rise manoeuvre. A shorter passive leg raise, boosted with intravenous saline challenge, could have potentially resulted in more pronounced haemodynamic and dyssynchrony alterations. Owing to a technical limitation of the GSPECT machine, individuals with a heart rate exceeding 100 b.p.m. might experience a slight reduction in the accuracy of ventricular dyssynchrony evaluation. Likely due to the small sample size, we were able to show significant differences in the primary composite outcome only when categorizing the population based on a single threshold (e.g. PSD 30°). Nevertheless, this allowed us to define a subgroup with an increased risk of clinical events. It is theoretically possible that the decrease in LV afterload resulting from sildenafil administration could have potentially improved LV dyssynchrony and consequently participated to ameliorate RV dyssynchrony by reducing septum delay. Anyway, we cannot draw definite conclusions on this topic from current data. Furthermore, our study is primarily mechanistic, lacking direct or evident clinical implications. Finally, we cannot evaluate causality whether RV dyssynchrony is a cause or a consequence of RV dysfunction based upon the cross-sectional study design.

Conclusions

In this multimodality pressure–volume analysis in patients with advanced HFrEF, increased RV dyssynchrony was associated with higher RV afterload, lower contractility, and worse long-term outcome. Modulation of RV afterload attenuated the severity of RV mechanical dyssynchrony, identifying a possible therapeutic target. Further studies are warranted to determine whether amelioration of RV dyssynchrony by RV afterload reduction may help to improve RV performance in HFrEF.

Conflict of interest

None declared.

Funding

This work was supported by the Ministry of Health of the Czech Republic (Ministerstvo Zdravotnictví Ceské Republiky), Agency for Healthcare Research (AZV), Grants NU22-02-

00161, NU21-02-00402, and NV19-02-00130, and by the project of the National Institute for Research of Metabolic and Cardiovascular Diseases (Program EXCELES, ID Project No. LX22NPO5104)—funded by the European Union—Next Generation EU.

Supporting information

Additional supporting information may be found online in the Supporting Information section at the end of the article.

Table S1. Baseline characteristics of patients with HFrEF and controls.
Table S2. Imaging and hemodynamic data in patients with HFrEF and controls.
Table S3. Effect of afterload reduction (sildenafil) and preload increase (leg rise) on right ventricular dyssynchrony, hemodynamics and cardiac volumes derived from SPECT.
Figure S1. Three-dimensional reconstruction of ventricular end-diastolic (top row) and end-systolic (middle row) volumes and histograms of right ventricular (RV) phase standard deviation of systolic displacements (PSD) (bottom row) in controls and heart failure patients with low and high RV dyssynchrony. Abbreviations: Fwall, Right Ventricular Free Wall; Lat, Lateral Wall.
Figure S2. Bland–Altman plot for the intraoperator reproducibility of right ventricular (RV) A) end-diastolic volume (EDV) and B) end-systolic volume (ESV) measurements. The dashed line stands for the mean bias, the dotted lines represent the 95% limits of agreement.
Figure S3. Correlation between right ventricular (RV) dyssynchrony and A) pulmonary artery elastance; B) RV systolic elastance; C) right ventricular-arterial (RV-PA) coupling ratio; D) left ventricular (LV) end-diastolic volume; E) LV end-systolic volume; F) LV ejection fraction, all in HF patients.
Figure S4. Difference in A) right ventricular (RV) dyssynchrony; B) RV ejection fraction; C) RV end-diastolic volume and D) RV end-systolic volume among patient with ischemic and non-ischemic heart failure aetiology. Asterisk stands for $P < 0.05$.
Figure S5. Change in right ventricular (RV) dyssynchrony after leg rise (preload modulation) in the A) overall population (N = 135) and B) in the subgroup of patients underwent PDE5i administration to test afterload reduction (N = 15). Median values before and after sildenafil are reported on the relative sides of the chart. Different colours represent changes in RV dyssynchrony tertiles of individual patients before and after leg rise. Asterisk stands for $P < 0.05$.
Video S1. Control patient.
Video S2. Low RV dyssynchrony patient.
Video S3. High RV dyssynchrony patient.

References

1. Bleeker GB, Bax JJ, Steendijk P, Schalij MJ, van der Wall EE. Left ventricular dyssynchrony in patients with heart failure: Pathophysiology, diagnosis and treatment. *Nat Clin Pract Cardiovasc Med* 2006;**3**:213-219. doi:10.1038/ncpcardio0505
2. Badagliacca R, Reali M, Poscia R, Pezzuto B, Papa S, Mezzapesa M, *et al*. Right intraventricular dyssynchrony in idiopathic, heritable, and anorexigen-induced pulmonary arterial hypertension: Clinical impact and reversibility. *JACC Cardiovasc Imaging* 2015;**8**:642-652. doi:10.1016/j.jcmg.2015.02.009
3. Tops LF, Prakasa K, Tandri H, Dalal D, Jain R, Dimaano VL, *et al*. Prevalence and pathophysiologic attributes of ventricular dyssynchrony in arrhythmogenic right ventricular dysplasia/cardiomyopathy. *J Am Coll Cardiol* 2009;**54**:445-451. doi:10.1016/j.jacc.2009.04.038
4. Storsten P, Aalen JM, Boe E, Remme EW, Gjesdal O, Larsen CK, *et al*. Mechanical effects on right ventricular function from left bundle branch block and cardiac resynchronization therapy. *JACC Cardiovasc Imaging* 2020;**13**:1475-1484. doi:10.1016/j.jcmg.2019.11.016
5. Fauchier L, Marie O, Casset-Senon D, Babuty D, Cosnay P, Fauchier JP. Interventricular and intraventricular dyssynchrony in idiopathic dilated cardiomyopathy: A prognostic study with Fourier phase analysis of radionuclide angioscintigraphy. *J Am Coll Cardiol* 2002;**40**:2022-2030. doi:10.1016/S0735-1097(02)02569-X
6. Boogers MJ, Chen J, Veltman CE, van Bommel RJ, Mooyaart EA, Al Younis I, *et al*. Left ventricular diastolic dyssynchrony assessed with phase analysis of gated myocardial perfusion SPECT: A comparison with tissue Doppler imaging. *Eur J Nucl Med Mol Imaging* 2011;**38**:2031-2039. doi:10.1007/s00259-011-1870-5
7. Rich JD, Ward RP. Right-ventricular function by nuclear cardiology. *Curr Opin Cardiol* 2010;**25**:445-450. doi:10.1097/HCO.0b013e32833cb252
8. Fudim M, Fathallah M, Shaw LK, Liu PR, James O, Samad Z, *et al*. The prognostic value of diastolic and systolic mechanical left ventricular dyssynchrony among patients with coronary heart disease. *JACC Cardiovasc Imaging* 2019;**12**:1215-1226. doi:10.1016/j.jcmg.2018.05.018
9. Singh H, Singhal A, Sharma P, Patel CD, Seth S, Malhotra A. Quantitative assessment of cardiac mechanical synchrony using equilibrium radionuclide angiography. *J Nucl Cardiol* 2013;**20**:415-425. doi:10.1007/s12350-013-9705-3
10. Vallejo E, Jimenez L, Rodriguez G, Roffe F, Bialostozky D. Evaluation of ventricular synchrony with equilibrium radionuclide angiography: Assessment of variability and accuracy. *Arch Med Res* 2010;**41**:83-91. doi:10.1016/j.arcmed.2010.02.003
11. Rosenkranz S, Preston IR. Right heart catheterisation: Best practice and pitfalls in pulmonary hypertension. *Eur Respir Rev* 2015;**24**:642-652. doi:10.1183/16000617.0062-2015
12. Lavdaniti M. Invasive and non-invasive methods for cardiac output measurement. *Int J Caring Sci* 2008;**1**:6.
13. Hesse B, Lindhardt TB, Acampa W, Anagnostopoulos C, Ballinger J, Bax JJ,

et al. EANM/ESC guidelines for radionuclide imaging of cardiac function. *Eur J Nucl Med Mol Imaging* 2008;**35**:851-885. doi:10.1007/s00259-007-0694-9
14. Velleca A, Shullo MA, Dhital K, Azeka E, Colvin M, DePasquale E, *et al*. The International Society for Heart and Lung Transplantation (ISHLT) guidelines for the care of heart transplant recipients. *J Heart Lung Transplant* 2023;**42**:e1-e141. doi:10.1016/j.healun.2022.10.015
15. Wright SP, Groves L, Vishram-Nielsen JKK, Karvasarski E, Valle FH, Alba AC, *et al*. Elevated pulmonary arterial elastance and right ventricular uncoupling are associated with greater mortality in advanced heart failure. *J Heart Lung Transplant* 2020;**39**:657-665. doi:10.1016/j.healun.2020.02.013
16. Tello K, Richter MJ, Axmann J, Buhmann M, Seeger W, Naeije R, *et al*. More on single-beat estimation of right ventriculoarterial coupling in pulmonary arterial hypertension. *Am J Respir Crit Care Med* 2018;**198**:816-818. doi:10.1164/rccm.201802-0283LE
17. Sanz J, Garcia-Alvarez A, Fernandez-Friera L, Nair A, Mirelis JG, Sawit ST, *et al*. Right ventriculo-arterial coupling in pulmonary hypertension: A magnetic resonance study. *Heart* 2012;**98**:238-243. doi:10.1136/heartjnl-2011-300462
18. Vonk Noordegraaf A, Chin KM, Haddad F, Hassoun PM, Hemnes AR, Hopkins SR, *et al*. Pathophysiology of the right ventricle and of the pulmonary circulation in pulmonary hypertension: An update. *Eur Respir J* 2019 Jan;**53**:1801900. doi:10.1183/13993003.01900-2018
19. Tello K, Dalmer A, Axmann J, Vanderpool R, Ghofrani HA, Naeije R, *et al*. Reserve of right ventricular-arterial coupling in the setting of chronic overload. *Circ Heart Fail* 2019;**12**:e005512. doi:10.1161/CIRCHEARTFAILURE.118.005512
20. Simonneau G, Montani D, Celermajer DS, Denton CP, Gatzoulis MA, Krowka M, *et al*. Haemodynamic definitions and updated clinical classification of pulmonary hypertension. *Eur Respir J* 2019;**53**:1801913. doi:10.1183/13993003.01913-2018
21. Fudim M, Dalgaard F, Fathallah M, Iskandrian AE, Borges-Neto S. Mechanical dyssynchrony: How do we measure it, what it means, and what we can do about it. *J Nucl Cardiol* 2021;**28**:2174-2184. doi:10.1007/s12350-019-01758-0
22. Friehling M, Chen J, Saba S, Bazaz R, Schwartzman D, Adelstein EC, *et al*. A prospective pilot study to evaluate the relationship between acute change in left ventricular synchrony after cardiac resynchronization therapy and patient outcome using a single-injection gated SPECT protocol. *Circ Cardiovasc Imaging* 2011;**4**:532-539. doi:10.1161/CIRCIMAGING.111.965459
23. Chen J, Garcia EV, Folks RD, Cooke CD, Faber TL, Tauxe EL, *et al*. Onset of left ventricular mechanical contraction as determined by phase analysis of ECG-gated myocardial perfusion SPECT imaging: Development of a diagnostic tool for assessment of cardiac mechanical dyssynchrony. *J Nucl Cardiol* 2005;**12**:687-695. doi:10.1016/j.nuclcard.2005.06.088
24. Van Kriekinge SD, Nishina H, Ohba M, Berman DS, Germano G. Automatic global and regional phase analysis from gated myocardial perfusion SPECT imaging: Application to the characterization of ventricular contraction in patients with left bundle branch block. *J Nucl Med* 2008;**49**:1790-1797. doi:10.2967/jnumed.108.055160
25. Trimble MA, Velazquez EJ, Adams GL, Honeycutt EF, Pagnanelli RA, Barnhart HX, *et al*. Repeatability and reproducibility of phase analysis of gated single-photon emission computed tomography myocardial perfusion imaging used to quantify cardiac dyssynchrony. *Nucl Med Commun* 2008;**29**:374-381. doi:10.1097/MNM.0b013e3282f81380
26. Melenovsky V, Kotrc M, Borlaug BA, Marek T, Kovar J, Malek I, *et al*. Relationships between right ventricular function, body composition, and prognosis in advanced heart failure. *J Am Coll Cardiol* 2013;**62**:1660-1670.
27. Monzo L, Kotrc M, Benes J, Sedlacek K, Jurcova I, Franekova J, *et al*. Clinical and humoral determinants of congestion in heart failure: Potential role of adiponectin. *Kidney Blood Press Res* 2019;**44**:1271-1284. doi:10.1159/000502975
28. Aaronson KD, Schwartz JS, Chen TM, Wong KL, Goin JE, Mancini DM. Development and prospective validation of a clinical index to predict survival in ambulatory patients referred for cardiac transplant evaluation. *Circulation* 1997;**95**:2660-2667. doi:10.1161/01.CIR.95.12.2660
29. Murata M, Tsugu T, Kawakami T, Kataoka M, Minakata Y, Endo J, *et al*. Right ventricular dyssynchrony predicts clinical outcomes in patients with pulmonary hypertension. *Int J Cardiol* 2017;**1**:912-918. doi:10.1016/j.ijcard.2016.11.244
30. Calcutteea A, Chung R, Lindqvist P, Hodson M, Henein MY. Differential right ventricular regional function and the effect of pulmonary hypertension: Three-dimensional echo study. *Heart* 2011;**97**:1004-1011. doi:10.1136/hrt.2010.208900
31. Marcus JT, Gan CT, Zwanenburg JJ, Boonstra A, Allaart CP, Gotte MJ, *et al*. Interventricular mechanical asynchrony in pulmonary arterial hypertension: Left-to-right delay in peak shortening is related to right ventricular overload and left ventricular underfilling. *J Am Coll Cardiol* 2008;**51**:750-757. doi:10.1016/j.jacc.2007.10.041
32. Buckberg G, Hoffman JI. Right ventricular architecture responsible for mechanical performance: Unifying role of ventricular septum. *J Thorac Cardiovasc Surg* 2014;**148**:3166-3171. doi:10.1016/j.jtcvs.2014.05.044
33. Ewalts M, Dawkins T, Boulet LM, Thijssen D, Stembridge M. The influence of increased venous return on right ventricular dyssynchrony during acute and sustained hypoxaemia. *Exp Physiol* 2021;**106**:925-937. doi:10.1113/EP088657
34. Mashali MA, Saad NS, Peczkowski KK, Fanning T, Hare AN, Whitson BA, *et al*. Mechanical dyssynchrony of isolated left and right ventricular human myocardium in end-stage heart failure. *Circ Heart Fail* 2023;e009871. doi:10.1161/CIRCHEARTFAILURE.122.009871
35. Byrne MJ, Helm RH, Daya S, Osman NF, Halperin HR, Berger RD, *et al*. Diminished left ventricular dyssynchrony and impact of resynchronization in failing hearts with right versus left bundle branch block. *J Am Coll Cardiol* 2007;**50**:1484-1490. doi:10.1016/j.jacc.2007.07.011
36. Pezzuto B, Forton K, Badagliacca R, Motoji Y, Faoro V, Naeije R. Right ventricular dyssynchrony during hypoxic breathing but not during exercise in healthy subjects: A speckle tracking echocardiography study. *Exp Physiol* 2018;**103**:1338-1346. doi:10.1113/EP087027
37. Vonk Noordegraaf A, Westerhof BE, Westerhof N. The relationship between the right ventricle and its load in pulmonary hypertension. *J Am Coll Cardiol* 2017;**69**:236-243. doi:10.1016/j.jacc.2016.10.047
38. Monzo L, Reichenbach A, Al-Hiti H, Borlaug BA, Havlenova T, Solar N, *et al*. Acute unloading effects of sildenafil enhance right ventricular-pulmonary artery coupling in heart failure. *J Card Fail* 2021;**27**:224-232. doi:10.1016/j.cardfail.2020.11.007
39. Monzo L, Reichenbach A, Al-Hiti H, Jurcova I, Huskova Z, Kautzner J, *et al*. Pulmonary vasculature responsiveness to phosphodiesterase-5A inhibition in heart failure with reduced ejection fraction: Possible role of plasma potassium. *Front Cardiovasc Med* 2022;**9**:883911. doi:10.3389/fcvm.2022.883911
40. Palau-Caballero G, Walmsley J, Van Empel V, Lumens J, Delhaas T. Why septal motion is a marker of right ventricular failure in pulmonary arterial hypertension: Mechanistic analysis using a computer model. *Am J Physiol Heart Circ Physiol* 2017;**312**:H691-H700. doi:10.1152/ajpheart.00596.2016

T. Tykvartová et al.

The impact of phosphodiesterase-5 inhibition or angiotensin-converting enzyme inhibition on right and left ventricular remodeling in heart failure due to chronic volume overload

Pharmacol Res Perspect
Impact Factor: 2,9

rejstřík

Received: 18 October 2023 | Accepted: 20 December 2023

DOI: 10.1002/prp2.1172

ORIGINAL ARTICLE

The impact of phosphodiesterase-5 inhibition or angiotensin-converting enzyme inhibition on right and left ventricular remodeling in heart failure due to chronic volume overload

Tereza Tykvartova[1,2] | Matus Miklovic[1,2] | Martin Kotrc[1] | Petra Skaroupkova[1] | Ludmila Kazdova[1] | Jaroslava Trnovska[1] | Vojtech Skop[1,3] | Michal Kolar[4] | Jiri Novotny[4] | Vojtech Melenovsky[1]

[1]Institute for Clinical and Experimental Medicine—IKEM, Prague, Czech Republic

[2]Department of Pathophysiology, Second Faculty of Medicine, Charles University, Prague, Czech Republic

[3]Department of Biochemistry and Microbiology, University of Chemistry and Technology, Prague, Czech Republic

[4]Laboratory of Genomics and Bioinformatics, Institute of Molecular Genetics of the Czech Academy of Sciences, Prague, Czech Republic

Correspondence
Vojtech Melenovsky, Department of Cardiology, IKEM, Videnska 1958/9, Prague 4 140 21, Czech Republic.
Email: vojtech.melenovsky@ikem.cz

Funding information
Grant Agency of Charles University (GAUK), Grant/Award Number: 304121; Ministry of Health of the Czech Republic, Grant/Award Number: NU20-02-00052 and NU22-02-00161; Project National Institute for Research of Metabolic and Cardiovascular Diseases (Programme EXCELES), funded by the European Union—Next Generation EU, Grant/Award Number: LX22NPO5104

Abstract

While phosphodiesterase-5 inhibition (PED5i) may prevent hypertrophy and failure in pressure-overloaded heart in an experimental model, the impact of PDE5i on volume-overload (VO)-induced hypertrophy is unknown. It is also unclear whether the hypertrophied right ventricle (RV) and left ventricle (LV) differ in their responsiveness to long-term PDE5i and if this therapy affects renal function. The goal of this study was to elucidate the effect of PDE5i treatment in VO due to aorto-caval fistula (ACF) and to compare PDE5i treatment with standard heart failure (HF) therapy with angiotensin-converting enzyme inhibitor (ACEi). ACF/sham procedure was performed on male HanSD rats aged 8 weeks. ACF animals were randomized for PDE5i sildenafil, ACEi trandolapril, or placebo treatments. After 20 weeks, RV and LV function (echocardiography, pressure-volume analysis), myocardial gene expression, and renal function were studied. Separate rat cohorts served for survival analysis. ACF led to biventricular eccentric hypertrophy (LV: +68%, RV: +145%), increased stroke work (LV: 3.6-fold, RV: 6.7-fold), and reduced load-independent systolic function (PRSW, LV: −54%, RV: −51%). Both ACF ventricles exhibited upregulation of the genes of myocardial stress and glucose metabolism. ACEi but not PDE5i attenuated pulmonary congestion, LV remodeling, albuminuria, and improved survival (median survival in ACF/ACEi was 41 weeks vs. 35 weeks in ACF/placebo, $p = .02$). PDE5i increased cyclic guanosine monophosphate levels in the lungs, but not in the RV, LV, or kidney. PDE5i did not improve survival rate and cardiac and renal function in ACF rats, in contrast to ACEi. VO-induced HF is not responsive to PDE5i therapy.

Abbreviations: ACEi, angiotensin-converting enzyme inhibitor; ACF, aorto-caval fistula; DBP, diastolic blood pressure; dP/dt max, maximum ventricular pressure over time; dP/dt min, minimum ventricular pressure over time; EDP, ventricular end-diastolic pressure; EDV, end-diastolic volume; ESV, end-systolic volume; FAC, fractional area change; HF, heart failure; HanSD, Hannover Sprague Dawley rats; LV, left ventricle; MBP, mean blood pressure; PDE5, phosphodiesterase 5; PDE9, phosphodiesterase 9; PED5i, phosphodiesterase-5 inhibition; PP, pulse pressure; PRSW, preload recruitable stroke work; RAAS, renin-angiotensin-aldosterone system; RV, right ventricle; SBP, systolic blood pressure; SVR, systemic vascular resistance; TAPSE, tricuspid annular plane systolic excursion; Tau, ventricular diastolic time constant; VO, volume-overload.

KEYWORDS
heart failure, phosphodiesterase-5 inhibition, rats, right ventricle, volume overload

1 | INTRODUCTION

Heart failure (HF) is a progressive clinical syndrome with high morbidity, mortality, and constantly increasing prevalence that imposes a great burden on healthcare systems worldwide. It is crucial to develop novel therapeutic strategies to prevent or stabilize the course of the disease. Right ventricular (RV) dysfunction and renal dysfunction accelerate HF progression and are associated with increased HF mortality. However, detailed pathogenic mechanisms of both these conditions and their role in HF remain incompletely understood.

The aorto-caval fistula (ACF) represents a well-defined model to study advanced HF, characterized by eccentric cardiac hypertrophy and dysfunction, neurohormonal alterations including activation of the renin-angiotensin-aldosterone system (RAAS), congestion, and renal function impairment.[1–4] Blood recirculation via ACF imposes the same volume overload (VO) on the left and right heart, which makes the model useful for studying biventricular differences in response to experimental therapies.[5,6]

RAAS activation is antagonized by nitric oxide and natriuretic peptides signaling, two systems that stimulate guanylate cyclase to produce cyclic guanosine monophosphate (cGMP). The concentration of cGMP is strictly regulated and catalyzed by phosphodiesterases including phosphodiesterase 5 (PDE5) and 9 (PDE9), which represent potential pharmacological targets for the treatment of chronic HF.[7]

Although it is not significantly expressed in healthy heart, PDE5 overexpression was demonstrated in hypertrophied or failing myocardium of both RV and left ventricle (LV).[8–10] Apart from its vasodilatory properties, used in clinical practice to treat pulmonary hypertension or erectile dysfunction, PDE5 inhibitor (PDE5i) sildenafil was shown to have anti-hypertrophic and anti-apoptotic effects on isolated cardiac myocytes.[11,12] In experimental studies, sildenafil prevented and reversed hypertrophy and dysfunction of pressure-overloaded LV,[13] attenuated fibrosis, decreased pulmonary pressure, and enhanced both systolic and diastolic function of pressure-overloaded RV.[14–16] Whether these findings are applicable to hypertrophy induced by VO is uncertain. Signaling pathways involved in the pressure versus VO-induced hypertrophy differ considerably, and these pathological states may therefore require different pharmacotherapeutic interventions.[17,18] The impact of these interventions may vary between RV and LV,[19] but biventricular differences are rarely addressed.

In experimental HF, there is a notable upregulation of PDE5 in the kidney,[20] suggesting that PDE5i may have beneficial renal effects in HF.[21,22] The aim of this study was to evaluate the effect of long-term PDE5i on cardiac and renal function and survival in the rat ACF model and to identify potential differences in PDE5i effects on volume-overloaded LV or RV.

This task was addressed using load-independent biventricular pressure-volume analysis, echocardiography, assessment of renal hemodynamics and excretory function, and myocardial gene expression analysis of selected genes associated with HF development,[23,24] including the genes of the cGMP-dependent signaling pathway.[25,26] The effect of PDE5i on VO-induced HF was compared to an angiotensin-converting enzyme inhibitor (ACEi), which represents a current therapeutic standard of HF.[27,28]

2 | MATERIALS AND METHODS

2.1 | HF model

Male Hannover Sprague Dawley rats (HanSD) aged 8 weeks weighing 280–320 g and derived from an on-site certified breeding colony at IKEM were randomly assigned to two groups and underwent needle ACF or sham operation as described before.[4,29] Briefly, the rats were anesthetized with the ketamine/midazolam mixture (Calypsol, Gedeon Richter, Hungary, 160 mg/kg and Midazolam, Kalcex, Latvia, 160 mg/kg, i.p.) and a shunt was created between the infrarenal aorta and inferior vena cava using an 18-gauge needle (outer diameter 1.2 mm). The puncture site in the aorta was closed with acrylamide tissue glue (Histoacryl, B. Braun AG, Germany). The rats were housed in an air-conditioned animal facility on a 12/12-h light/dark cycle and were fed a standard salt/protein chow (0.45% NaCl, 19%–21% protein, SEMED, Czech Republic) with free access to tap water. Rats were weighed every week and the development of HF was assessed by the scoring procedure as described before.[3] At the end of the protocol, the creation of ACF was confirmed by laparotomy and was found successful in each case. The rats were exsanguinated, and the coronary arteries of the explanted heart were rapidly infused with a cardioplegic solution. The organs were weighed, and the weight values were factored by body weight. The investigation was performed in accordance with the NIH Guide for the Care and Use of Laboratory Animals (NIH Publication No. 85-23, 1996) and Animal protection laws of the Czech Republic (311/1997) and was approved by the Ethic Committee of IKEM.

2.2 | Study design

Four weeks after ACF creation, ACF animals were randomly assigned to treatment groups with PDE5i sildenafil (Vizarsin, Krka, Slovenia, 80 mg/kg/day dissolved in drinking water, $N = 76$), ACEi trandolapril (Gopten, Mylan, Ireland, 6 mg/L dissolved in drinking water, $N = 84$), or placebo ($N = 87$). After 20 weeks, echocardiography and biventricular pressure-volume analysis ($N = 19$–30/group),

myocardial gene expression analysis (qPCR, $N = 12–13$/group), renal hemodynamic studies ($N = 13–16$/group), and cGMP tissue level measurements ($N = 8$/group) were performed as described below. A separate rat cohort ($N = 22$-43/group) served for survival analysis and assessment of albuminuria.

2.3 | Echocardiography and hemodynamics

Echocardiography was performed under general anesthesia (ketamine/midazolam mixture given intraperitoneally as described above) using a 10 MHz transducer (Vivid System 7 Dimension; GE HealthCare, IL, USA). RV fractional area change (FAC) was defined as a difference between end-diastolic and end-systolic RV area, divided by end-diastolic area. RV volumes were calculated by the monoplane ellipsoid approximation method.[30] Subsequently, ventricular function was invasively assessed with 2F Pressure–Volume micromanometer-tip catheters (Millar, Houston, TX, USA) simultaneously introduced into the LV via the right carotid artery and into the RV via the internal jugular vein,[6] which is considered "gold standard" in the evaluation of systolic and diastolic function of the LV and RV.[31] The volume signals were adjusted by end-diastolic (EDV) and end-systolic volumes (ESV) gained by echocardiography shortly before invasive recordings as described previously.[29] The data were obtained using an 8-channel Power Lab recorder and analyzed by Labchart Pro software (ADInstruments, Bella Vista, NSW, Australia).

2.4 | Myocardial gene expression analysis

Samples of RV and LV free wall were placed into RNA later, total RNA was isolated, and genomic DNA was removed. RNA quantity and integrity were measured. The RNA was reverse transcribed and qPCR was performed employing RealTime ready Custom Panel 384–32 (Roche, p.n. 05582962001) containing function tested pre-plated qPCR assays for 29 target genes (*Acadm*, *Acta1*, *Angpt1*, *Angpt2*, *Apln*, *Aplnr*, *Atp2a2*, *Cs*, *Gucy1a3*, *Hif1a*, *Hk1*, *Il6*, *Maoa*, *Myh6*, *Myh7*, *Nos1*, *Nos2*, *Nos3*, *Nppa*, *Npr1*, *Npr2*, *Pde5a*, *Pde9a*, *Pkg*, *Slc2a1*, *Slc2a4*, *Tgm2*, *Tnfrsf1a*, *Vegfa*) and 3 reference genes average (*Hprt1*, *Sdha*, *Tbp*). The analysis was done on a LightCycler LC480 (Roche) according to the manufacturer's protocol. The acquired data were analyzed by the ΔCp method within the R/Bioconductor statistical environment.[32–34] The expression of mRNA of selected genes was related to a control group. The final results were expressed as the fold change difference of mRNA of the target gene between the experimental and control group.

2.5 | Renal hemodynamics and excretory function

Renal hemodynamic studies were performed according to the previously described protocol.[29,35] Briefly, the animals were anesthetized with thiopental sodium (50 mg/kg, i.p., VAUB Pharma a.s., Roztoky, CZ), and the left femoral artery was cannulated to measure arterial blood pressure. The left kidney was surgically isolated from the surrounding tissues and put in a lucite cup. The left ureter was catheterized to collect urine, and an ultrasonic transient-time flow probe (1RBF, Transonic Systems, Altron Medical Electronic GmbH, Germany) was installed on the left renal artery for continuous measurement of renal blood flow. A 0.5 mL bolus of 5% sinistrin (Inutest, Fresenius Kabi Austria GmbH, Austria) was administered to measure the glomerular filtration rate. Urine was gathered in three 30-min periods and blood samples were obtained after each collection. Urine volume was measured by gravimetry; sodium and potassium concentrations were determined photometrically. Values were expressed per gram of wet kidney weight. The fractional sodium and potassium excretion were calculated by standard formulas.

2.6 | Albuminuria

For albumin excretion measurement, the rats were placed in individual metabolic cages and (after appropriate habituation training) the urine was collected for 24 h in week 1, 4, 12, 20, 24, 28, 32, and 44 after initiation of treatment. Urinary albumin was measured using the quantitative sandwich enzyme immunoassay technique with the commercially available ELISA kit (ERA3201-1, AssayPro, MO, USA).

2.7 | cGMP tissue concentrations

All analyses were performed with the acetylation protocol to achieve maximal sensitivity. Briefly, tissue samples frozen in liquid nitrogen were crushed to a fine powder and homogenized in 0.1 M HCl. Precipitated proteins were separated by centrifugation at 20 000 *g* at 4°C. cGMP levels were measured in acetylated supernatants using a radioimmunoassay kit (cGMP-RIA) from IBL International (GmbH, Hamburg, Germany) according to the manufacturer's protocol. Results are shown as fmol cGMP per milligram of wet tissue weight.

2.8 | Statistical analysis

Statistical analysis was performed using Graph-Pad Prism software v9.4.1 (Graph Pad Software, San Diego, CA, USA). The groups were compared by one-way ANOVA and Tukey post hoc tests. The comparison of survival curves was performed using the log-rank (Mantel-Cox) test followed by Gehan-Breslow-Wilcoxon test. Results are presented as means ± SD, if not stated otherwise. A p-value lower than .05 was considered significant.

2.9 | Nomenclature of targets and ligands

Key protein targets and ligands in this article are hyperlinked to corresponding entries in http://www.guidetopharmacology.

org, the common portal for data from the IUPHAR/BPS Guide to Pharmacology[36] and are permanently archived in the Concise Guide to Pharmacology 2019/20.[37]

3 | RESULTS

3.1 | Organ weights and signs of HF

Twenty-four weeks after ACF creation, 70% of ACF rats exhibited clinical signs of HF. ACF animals had similar tibial length but the body weight was increased (+10%, $p<.01$), likely due to congestion (Table 1; Supporting Information 1). ACF led to significant biventricular hypertrophy, more pronounced for the RV than for the LV (+145%, $p<.001$ and +68%, $p<.001$), to increased lung weight (+41%, $p<.001$) due to congestion, and to reduced kidney weight (−17%, $p<.001$), probably related to hypoperfusion. ACEi treatment lowered body weight (−9%, $p<.01$) and lung weight (−14%, $p<.05$), indicating reduced congestion. PDE5i treatment did not alter the body and organ weight values (Table 1).

3.2 | Echocardiography

Echocardiography (Table 1; Figure 1A) revealed LV dilatation, eccentric remodeling with relative wall thinning (relative wall

TABLE 1 Baseline characteristics and echocardiography.

	Sham/placebo	ACF/placebo	ACF/PDE5i	ACF/ACEi	*p* (ANOVA)
Body weight (BW), g	550 ± 47	607 ± 71**	584 ± 45	550 ± 50##	.0006
Tibial length, mm	43.1 ± 1.08	43.5 ± 1.42	43 ± 1.77	43.2 ± 1.09	.6
Heart weight/BW, g kg^{-1}	2.97 ± 0.24	5.92 ± 0.77***	6 ± 0.69***	5.53 ± 0.86***	<.0001
LV weight/BW, g kg^{-1}	2.03 ± 0.17	3.42 ± 0.45***	3.54 ± 0.39***	3.15 ± 0.38***§§	<.0001
RV weight/BW, g kg^{-1}	0.53 ± 0.05	1.3 ± 0.23***	1.33 ± 0.21***	1.22 ± 0.18***	<.0001
Atrial weight/BW, g kg^{-1}	0.33 ± 0.06	0.99 ± 0.22***	0.99 ± 0.19***	0.89 ± 0.26***	<.0001
Lung weight/BW, g kg^{-1}	3.51 ± 0.37	4.96 ± 1.18***	5.01 ± 0.88***	4.28 ± 0.71*#§	<.0001
Liver weight/BW, g kg^{-1}	34.2 ± 5.02	31.4 ± 5.55	32.6 ± 4.71	30.5 ± 6.96	.2
Kidney weight/BW, g kg^{-1}	6.67 ± 0.64	5.52 ± 0.11***	5.8 ± 0.54***	5.78 ± 0.6***	<.0001
Heart failure score (0–7)	0.03	1.6***	1.5**	1.15*	.0008
Echocardiography: Left ventricle					
End-diastolic dimension, mm	6.68 ± 0.64	12.52 ± 1.16***	12.81 ± 1.01***	11.5 ± 0.92***###§§§	<.0001
Posterior wall thickness, mm	2.65 ± 0.29	2.12 ± 0.25***	2.14 ± 0.2***	2 ± 0.33***	<.0001
Relative wall thickness	0.76 ± 0.12	0.33 ± 0.05***	0.32 ± 0.05***	0.34 ± 0.05***	<.0001
Fractional shortening, %	58.2 ± 4.8	38.3 ± 5.93***	38.8 ± 5.46***	42.7 ± 5.06***#	<.0001
Heart rate, min^{-1}	457 ± 30.4	367 ± 36.9***	358 ± 45.3***	392 ± 39.2***§	<.0001
Stroke volume, mL	0.29 ± 0.08	1.47 ± 0.33***	1.63 ± 0.37***	1.27 ± 0.31***§§§	<.0001
Cardiac output, mL min^{-1}	130 ± 31.1	534 ± 103***	570 ± 90.4***	493 ± 120***§	<.0001
Mitral regurgitation grade (1–4)	0.29	1.31**	1.22*	1.21*	.006
Echocardiography: Right ventricle					
RVD1, mm	3.61 ± 0.34	6.89 ± 1.27***	6.55 ± 0.71***	6.54 ± 1.31***	<.0001
RVD2, mm	3.49 ± 0.25	6.8 ± 1.23***	6.56 ± 0.81***	6.92 ± 1.43***	<.0001
RVD3, mm	9.7 ± 0.72	13.7 ± 1.45***	13.4 ± 0.98***	12.9 ± 1.4***	<.0001
RV diastolic area, mm^2	31.8 ± 1.96	90.1 ± 21.2***	84.8 ± 12.9***	86.3 ± 21.1***	<.0001
Fractional area change, %	49.4 ± 4.1	41.8 ± 10.3**	42.2 ± 6.5*	43.9 ± 6.6	.006
TAPSE, mm	3.05 ± 0.21	3.94 ± 0.74***	4.29 ± 0.75***	3.96 ± 0.58***	<.0001
RV global strain, %	−9.3 ± 2.39	−13.2 ± 3.41**	−13.8 ± 4.43**	−12.6 ± 3.81*	.004
RV global strain rate, s^{-1}	1.4 ± 0.31	1.97 ± 0.44***	2.11 ± 0.46***	1.89 ± 0.27**	<.0001
Tricuspid regurgitation grade (1–4)	0.43	1.25**	1.11	0.95	.01

Note: Values are expressed as means ± SD. $N=19$ in sham/placebo group, $N=30$ in ACF/placebo group, $N=20$ in ACF/PDE5i group and $N=26$ in ACF/ACEi group. Tukey post hoc test: *$p<.05$, **$p<.01$, ***$p<.001$ versus sham/placebo, #$p<.05$, ##$p<.01$, ###$p<.001$ versus ACF/placebo, §$p<.05$, §§$p<.01$, §§§$p<.001$ versus ACF/PDE5i.

Abbreviations: ACEi, angiotensin-converting enzyme inhibitor; ACF, Rat model of aorto-caval fistula; LV, left ventricle; PDE5i, phosphodiesterase-5 inhibitor; RV, right ventricle; RVD1, right ventricular basal diameter at end-diastole; RVD2, right ventricular mid diameter at end-diastole; RVD3, right ventricular longitudinal diameter at end-diastole; TAPSE, tricuspid annular plane systolic excursion.

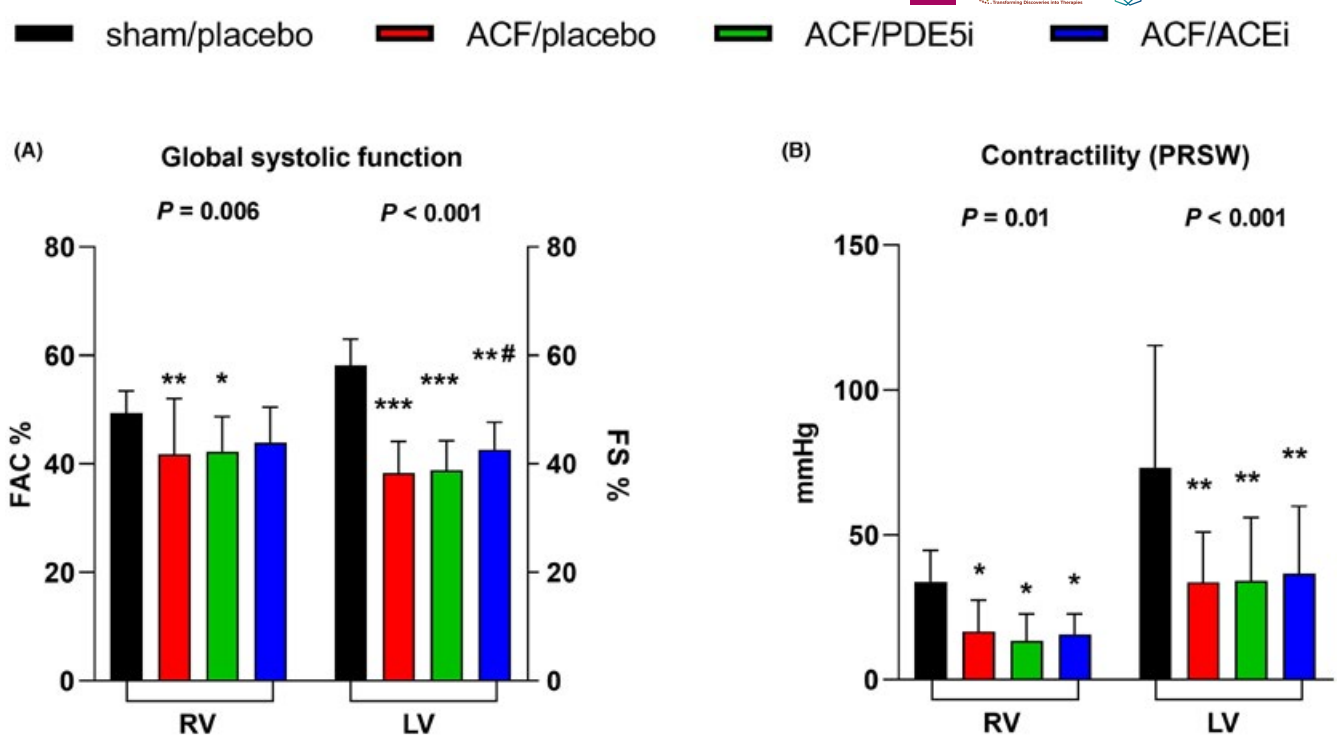

FIGURE 1 Effects of ACF, PDE5i, and ACEi on selected parameters of ventricular systolic function. (A) Global systolic function measured by echocardiography. (B) Contractility (PRSW) measured by pressure-volume analysis. ACEi, angiotensin-converting enzyme inhibitor; ACF, rat model of aorto-caval fistula; LV, left ventricle; PDE5i, phosphodiesterase-5 inhibitor; PRSW, preload recruitable stroke work; RV, right ventricle. $N = 19–26$ in each group. Data are presented as means ± SD. $^{*}p < .05$, $^{**}p < .01$, $^{***}p < .001$ versus sham/placebo, $^{\#}$versus ACF/placebo.

thickness reduced by−57%, $p < .001$), and LV systolic dysfunction (LV fractional shortening [FS] reduced by−34%, $p < .001$) in ACF rats. Due to blood recirculation via the systemic shunt, cardiac output was increased 4.1-fold ($p < .001$). The RV was also dilated and had depressed global systolic function (RV FAC reduced by−15%, $p < .01$). Regional echocardiographic parameters of RV function (TAPSE, global longitudinal strain) were affected by pronounced ventricular remodeling/dilatation and falsely augmented RV systolic function. ACEi limited LV remodeling and enhanced global LV systolic function (FS, +10%, $p < .05$) but PDE5i treatment did not show any beneficial effects.

3.3 | Invasive hemodynamics and pressure-volume analysis

In ACF, invasive hemodynamics (Table 2; Figure 1B) disclosed reduced systemic mean (−21 mmHg, $p < .01$) and diastolic blood pressure (−29 mmHg, $p < .001$), elevated end-diastolic filling pressures (more in the LV, +5.6 mmHg, $p < .001$) and volumes (identically in both ventricles, LV 6.4-fold, RV 5.9-fold, $p < .001$), and increased ventricular wall stress (2.7-fold, $p < .001$), as discussed previously.[5] Maximal LV pressure was reduced (−33 mmHg, $p < .001$), but maximal RV pressure was raised (+11.8 mmHg, $p < .001$), and RV stroke work was increased relatively more (6.7-fold, $p < .001$) compared to the LV (3.6-fold, $p < .001$), due to additional pulmonary hypertension. RV load-independent systolic function was similarly reduced compared to the LV (preload-recruitable stroke work, LV: −54%, $p < .01$, RV: −51%, $p < .05$). ACEi lowered systemic blood pressure (−25 mmHg, $p < .001$), and reduced LV volumes (EDV −20%, ESV −39%, $p < .01$), wall stress (−19%, $p < .05$), and filling pressure (−2.4 mmHg, $p < .05$). PDE5i tended to reduce transpulmonary pressure gradient (probably due to vasodilatation in the pulmonary vascular bed), but it had a neutral effect on LV and RV parameters. Neither treatment affected the load-independent systolic ventricular function of RV or LV (Figure 1B).

3.4 | Myocardial gene expression analysis

mRNA expression analysis of selected genes by qPCR (Figure 2; Supporting Information 2, for a full list see materials and methods section) revealed ACF-induced upregulation of several genes associated with myocardial stress, especially natriuretic peptide A (*Nppa*, RV 549-fold, LV 21-fold, $p < .05$). ACF rats exhibited elevated myosin heavy chain isotype 7 to 6 ratio (*Myh7/Myh6*, RV 8.4-fold, LV 4.9-fold, $p < .05$), angiopoietin 2 to 1 ratio (*Angpt2/1*, LV 19.8-fold, $p < .05$), downregulated apelin (*Apln*, RV 0.7-fold, LV 0.6-fold, $p < .05$) and citrate synthase (*Cs*, LV 0.5-fold, $p < .05$), and upregulated monoamine oxidase-A (*Maoa*, LV 9.2-fold, $p < .05$) and transglutaminase-2 (*Tgm2*, LV 2.2-fold, $p < .05$), genes that were previously linked to ACF.[38] There was an apparent metabolic shift from fatty

TABLE 2 Hemodynamic data from pressure-volume analysis.

	Sham/placebo	ACF/placebo	ACF/PDE5i	ACF/ACEi	*p* (ANOVA)
Systemic circulation					
SBP, mmHg	143 ± 28.3	131 ± 21.2	124 ± 21.6*	106 ± 14***###§	<.0001
DBP, mmHg	113 ± 25.3	84 ± 14***	82 ± 15.9***	71 ± 12.9***#	<.0001
MBP, mmHg	128 ± 26.8	107 ± 16.7**	103 ± 18***	87 ± 13.4***##	<.0001
PP, mmHg	29.3 ± 5.6	47 ± 8.4***	42.7 ± 8.6***	35.2 ± 6.6###§§	<.0001
SVR, mmHg min mL^{-1}	1.04 ± 0.26	0.21 ± 0.05***	0.19 ± 0.06***	0.19 ± 0.04***	<.0001
Left ventricle					
LV EDP, mmHg	6.35 ± 2.25	11.9 ± 4.14***	11.1 ± 3***	9.51 ± 2.16*#	<.0001
LV EDV, mL	0.31 ± 0.09	1.97 ± 0.54***	2.14 ± 0.54***	1.58 ± 0.39***##§§§	<.0001
LV mass/EDV, g mL^{-1}	3.8 ± 0.91	1.1 ± 0.25***	1.01 ± 0.23***	1.17 ± 0.28***	<.0001
LV ESV, mL	0.02 ± 0.01	0.5 ± 0.28***	0.51 ± 0.21***	0.31 ± 0.12***##§§	<.0001
LV max pressure, mmHg	153 ± 26.8	120 ± 17.4***	120 ± 18.7***	105 ± 12.6***#	<.0001
LV max wall stress, mmHg mL g^{-1}	43 ± 13.1	117 ± 34.5***	118 ± 24.1***	95 ± 20.2***#§	<.0001
Stroke work, mmHg mL	20.3 ± 6.17	73.1 ± 21.9***	83.9 ± 29.1***	70.3 ± 26.1***	<.0001
dP/dt max, mmHg s^{-1}	10405 ± 3965	8812 ± 3042	9800 ± 2445	8782 ± 2606	.3
PRSW, mmHg	73.2 ± 42.2	33.6 ± 17.4**	34.2 ± 21.8**	36.6 ± 23.3**	.0003
dP/dt min, mmHg s^{-1}	−10591 ± 3139	−5363 ± 1606***	−5939 ± 1651***	−5353 ± 1858***	<.0001
Tau, ms	11.2 ± 2.48	16.7 ± 3.8***	14.2 ± 3.43	13.4 ± 3.5##	<.0001
Right ventricle					
RV EDP, mmHg	4.04 ± 1.38	6.2 ± 1.95*	5.7 ± 2.59	5.03 ± 1.51	.03
RV EDV, mL	0.12 ± 0.01	0.71 ± 0.28***	0.64 ± 0.16***	0.7 ± 0.3***	<.0001
RV mass/EDV, g mL^{-1}	2.37 ± 0.35	1.22 ± 0.31***	1.26 ± 0.27***	1.03 ± 0.24***	<.0001
RV ESV, mL	0.038 ± 0.005	0.033 ± 0.2***	0.274 ± 0.09***	0.287 ± 0.168***	<.0001
RV max pressure, mmHg	34.1 ± 4.9	45.9 ± 6.39***	44.5 ± 3.44***	42.6 ± 6.16***	<.0001
RV max pressure—LVEDP gradient, mmHg	27.9 ± 6.2	35.1 ± 5.31**	33.3 ± 2.72	33.9 ± 6.83*	.01
RV max wall stress, mmHg mL g^{-1}	15.2 ± 3.15	35.8 ± 9.24***	35.8 ± 8.26***	43.8 ± 16***	<.0001
Stroke work, mmHg mL	1.09 ± 0.14	7.33 ± 2.46***	7.65 ± 2.29***	7.09 ± 2.88***	.0004
dP/dt max, mmHg s^{-1}	2222 ± 788	2908 ± 767	2700 ± 446	2689 ± 1079	.2
PRSW, mmHg	33.9 ± 10.77	16.7 ± 10.79*	13.4 ± 9.32*	15.6 ± 7.02*	.01
dP/dt min, mmHg s^{-1}	−1621 ± 297	−1610 ± 442	−1709 ± 245	−1603 ± 493	.9
Tau, ms	20.7 ± 12.79	20.7 ± 9.54	16.3 ± 4.65	20.7 ± 14.8	.7

Note: Values are expressed as means ± SD. $N = 19$ in sham/placebo group, $N = 30$ in ACF/placebo group, $N = 20$ in ACF/PDE5i group and $N = 26$ in ACF/ACEi group. Tukey post hoc test: $^{*}p < .05$, $^{**}p < .01$, $^{***}p < .001$ versus sham/placebo, $^{\#}p < .05$, $^{\#\#}p < .01$, $^{\#\#\#}p < .001$ versus ACF/placebo, $^{\S}p < .05$, $^{\S\S}p < .01$, $^{\S\S\S}p < .001$ versus ACF/PDE5i.

Abbreviations: ACEi, angiotensin-converting enzyme inhibitor; ACF, rat model of aorto-caval fistula; DBP, diastolic blood pressure; dP/dt max, maximum ventricular pressure over time; dP/dt min, minimum ventricular pressure over time; EDP, ventricular end-diastolic pressure; EDV, ventricular end-diastolic volume; ESV, ventricular end-systolic volume; LV, left ventricle; MBP, mean blood pressure; PDE5i, phosphodiesterase-5 inhibitor; PP, pulse pressure; PRSW, preload recruitable stroke work; RV, right ventricle; SBP, systolic blood pressure; SVR, systemic vascular resistance; Tau, ventricular diastolic time constant.

acid oxidation to glycolysis reflected by an elevated ratio (RV 3.2-fold, LV 2.8-fold, $p < .05$) of glycolytic enzyme hexokinase 1 (*Hk1*) to medium-chain acyl-CoA dehydrogenase (*Mcad*) and an increased ratio of glucose transporters *Glut1/Glut4* (LV 2-fold, $p < .05$). Gene expression changes caused by ACF-induced VO were similar in both ventricles and were partially reversed by ACEi treatment. ACEi downregulated *Nppa* (RV 0.6-fold, $p < .05$) and *Myh7/Myh6* ratio (RV 0.5-fold, LV 0.6-fold, $p < .05$). There was also a trend to downregulated *Maoa* (RV 0.2-fold, LV 0.4-fold) and reduced *Hk1/Mcad* ratio (LV 0.4-fold). ACEi downregulated *Tgm2* (LV 0.6-fold, $p < .05$) and reduced *Glut1/Glut4* (LV 0.5-fold, $p < .05$) ratio in ACF LV. PDE5i had no beneficial effects. ACF or the treatments did not alter the expression of genes of cGMP-dependent signaling pathway, that is, NO synthase 1–3 (*Nos 1–3*), natriuretic peptide receptor 1 and

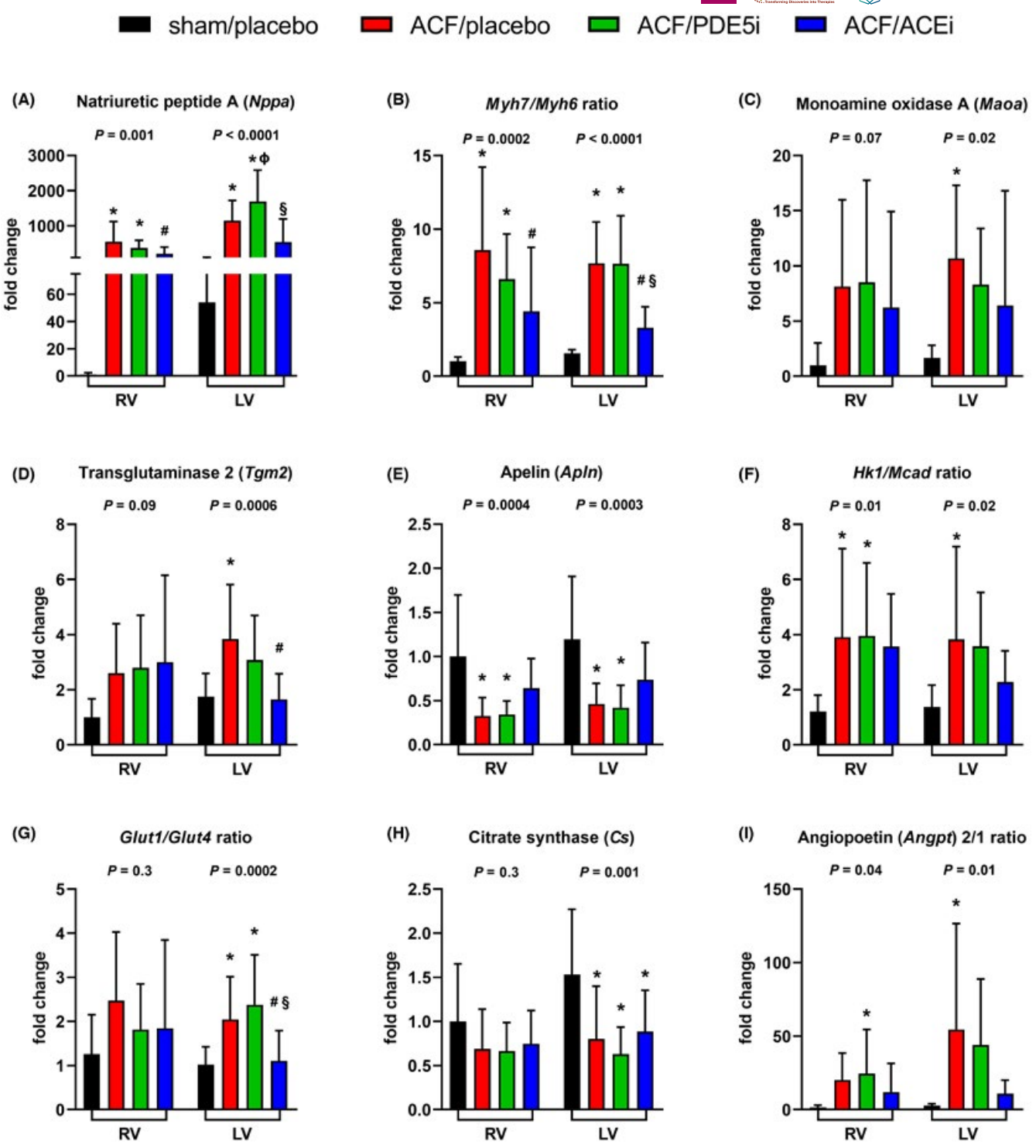

FIGURE 2 Effects of ACF, PDE5i, and ACEi on gene expression of selected cardiac markers of stress and metabolism. mRNA expression analysis of selected genes that reflect myocardial stress, substrate metabolism, and bioenergetics. (A) Natriuretic peptide A (*Nppa*). (B) *Myh7/Myh6* ratio. (C) Monoamine oxidase A (*Maoa*). (D) Transglutaminase 2 (*Tgm2*). (E) Apelin (*Apln*). (F) *Hk1/Mcad* ratio. (G) *Glut1/Glut4* ratio. (H) Citrate synthase (*Cs*). (I) Angiopoetin (*Angpt*) 2/1 ratio. Data are presented as means ± SD. The changes are normalized to sham/placebo RV. $N = 12–13$ in each group. ACF, rat model of aorto-caval fistula; PDE5i, phosphodiesterase-5 inhibitor; ACEi, angiotensin-converting enzyme inhibitor; RV, right ventricle; LV, left ventricle; *Myh7/Myh6* ratio, myosin heavy chain isotype 7 to 6 ratio; *Hk1/Mcad* ratio, ratio of glycolytic enzyme hexokinase to medium-chain acyl-CoA dehydrogenase; *Glut1/Glut4* ratio, glucose transporter 1/4 ratio. $^{*}p < .05$ versus sham/placebo, $^{\#}$versus ACF/placebo, §versus ACF/PDE5i, $^{\phi}$versus RV of the same group.

2 (*Npr1* and *Npr2*), soluble guanylate cyclase (*Gucy1a3*), cGMP-dependent protein kinase (*Pkg*), phosphodiesterase 5 (*Pde5a*), and phosphodiesterase 9 (*Pde9a*, Supporting Information 2).

3.5 | Renal hemodynamics and excretory function

In comparison with healthy controls, ACF animals exhibited significantly lower renal blood flow (Figure 3A, 4.19±1.65 vs. 7.18±1.69, $p<.001$), decreased diuresis (Figure 3B, urine flow 3.94±3.33 vs. 6.83±2.2, $p<.05$), and decreased fractional sodium excretion (Figure 3C, 0.09±0.19 vs. 0.36±0.32, $p<.05$). There was a trend toward higher fractional potassium excretion (32.8±4.9 vs. 16.4±10.1), probably due to secondary hyperaldosteronism (Figure 3D). ACEi tended to raise renal blood flow (5.49±1.48 vs. 4.19±1.65), urine flow (4.27±2.36 vs. 3.94±3.33), and fractional sodium excretion (0.24±0.24 vs. 0.09±0.19) and to decrease fractional potassium excretion (24.8±3.9 vs. 32.8±4.9); however, the differences were not statistically significant. PDE5i did not cause any beneficial effects. Glomerular filtration rate was not significantly different among groups, though it tended to be lower in ACF animals compared to sham-operated rats (Figure 3E, 0.75±0.97 vs. 0.91±0.65).

3.6 | Albuminuria

Aging of both ACF and sham-operated animals was accompanied by gradually increasing albuminuria, which was effectively suppressed with ACEi (Figure 3F). At the end of the study, albuminuria of ACEi-treated ACF animals was even lower than in healthy controls (3000±2000 μg/24 h vs. 8000±3000 μg/24 h, $p=.001$). PDE5i had no beneficial effect.

3.7 | Survival

At the end of the study (55 weeks after induction of ACF), all untreated ACF animals were dead. Median survival in ACF/placebo group was 35 weeks, identical to that in PDE5i-treated rats (Figure 4A). On the contrary, ACEi significantly improved the survival

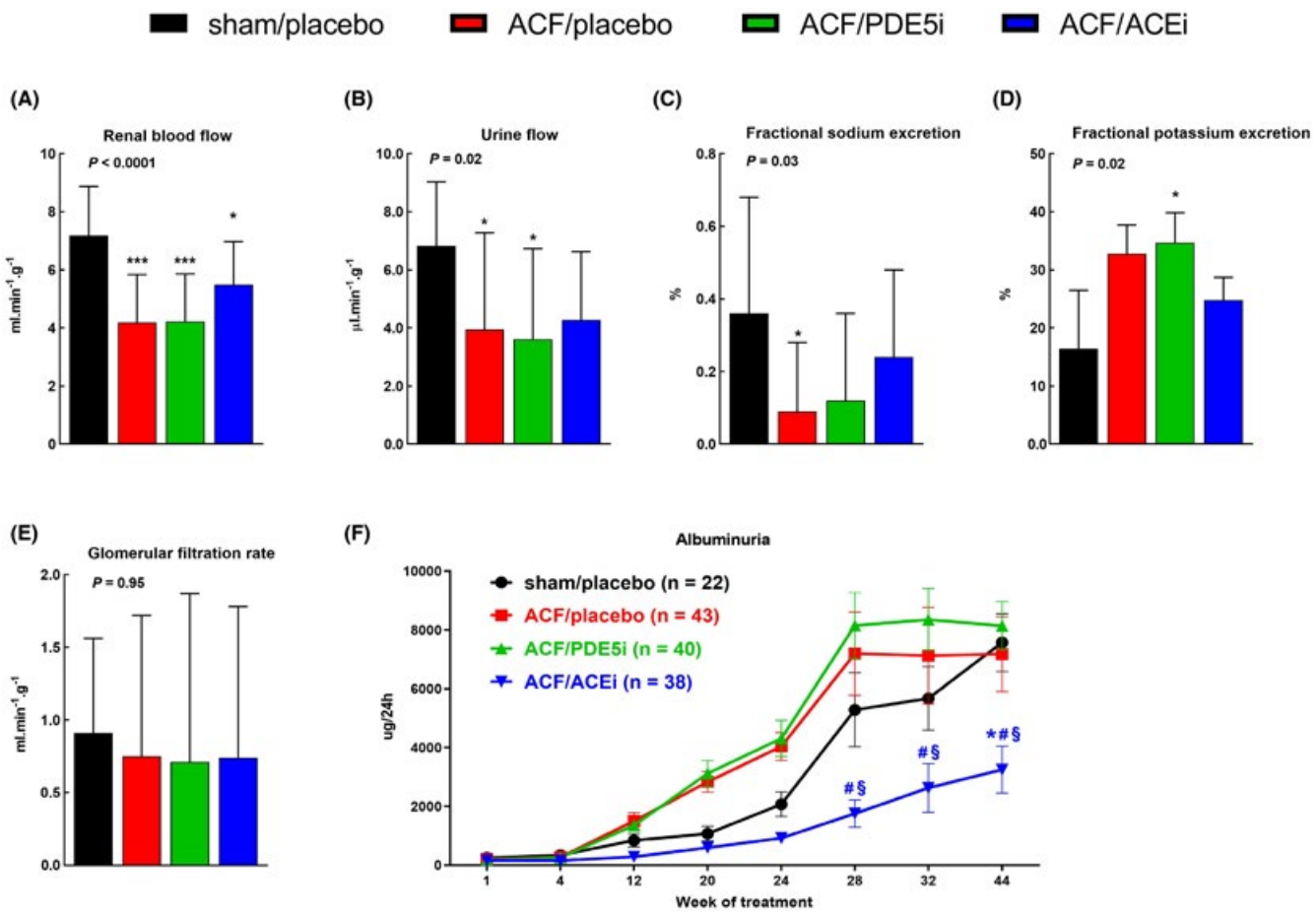

FIGURE 3 Effects of ACF, PDE5i, and ACEi on renal hemodynamics, excretory function, and albuminuria. (A) Renal blood flow. (B) Urine flow. (C) Fractional sodium excretion. (D) Fractional potassium excretion. (E) Glomerular filtration rate. (F) Albuminuria. Data in A–E are expressed per gram of wet kidney weight and presented as means±SD. ACEi, angiotensin-converting enzyme inhibitor; ACF, rat model of aorto-caval fistula; PDE5i, phosphodiesterase-5 inhibitor. $N=13–16$ in each group. $^{*}p<.05$, $^{***}p<.001$ versus sham/placebo, $^{\#}$versus ACF/placebo, §versus ACF/PDE5i.

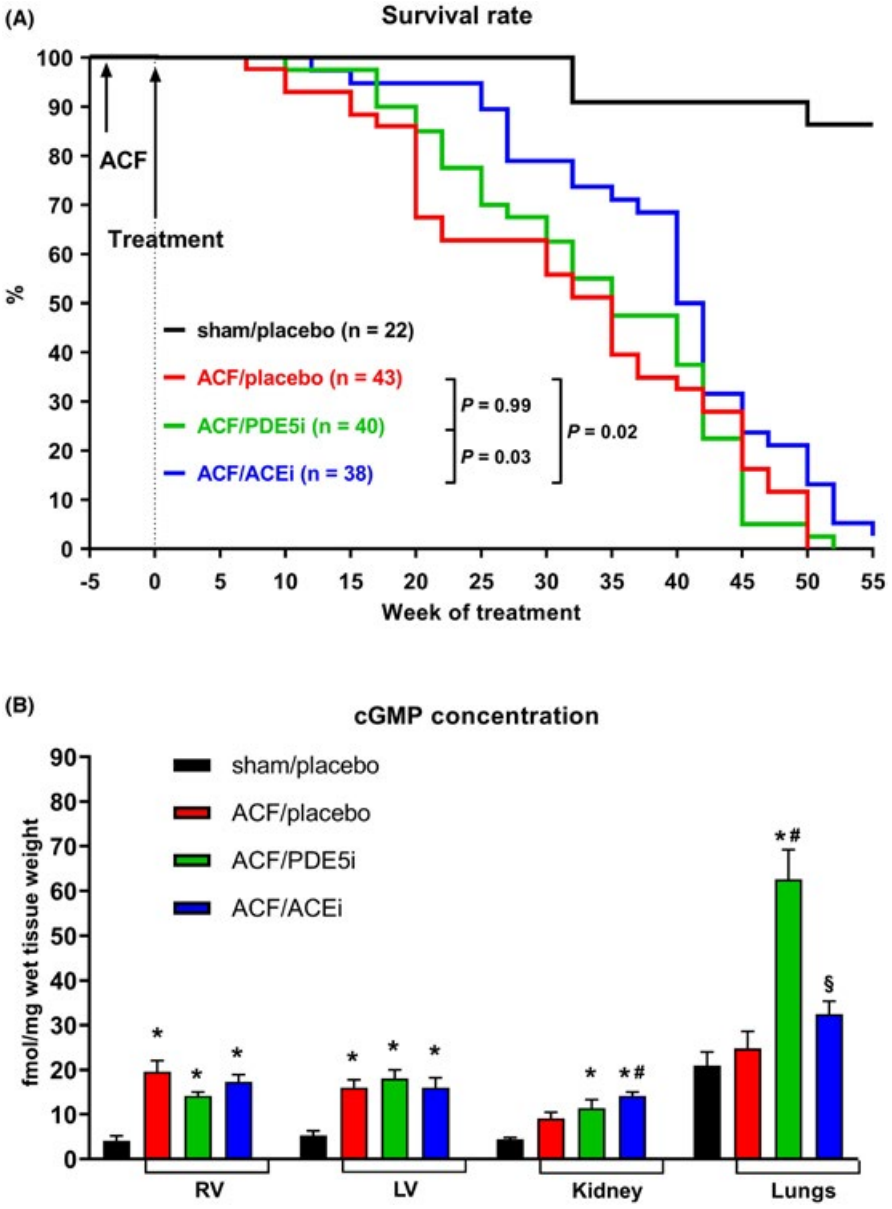

FIGURE 4 Effects of ACF, PDE5i, and ACEi on survival rate and cGMP tissue levels. (A) Survival rates. (B) cGMP tissue levels in the right and left ventricle, kidney, and lungs. Data in (B) are expressed as fmol cGMP per milligram of wet tissue weight and presented as means ± SD. $N = 8$ in each group. ACEi, angiotensin-converting enzyme inhibitor; ACF, rat model of aorto-caval fistula; cGMP, cyclic guanosine monophosphate; LV, left ventricle; PDE5i, phosphodiesterase-5 inhibitor; RV, right ventricle. *$p < .05$ versus sham/placebo, #versus ACF/placebo, §versus ACF/PDE5i.

rate (median survival in ACF/ACEi group was 41 weeks, $p = .02$ compared to untreated ACF rats). The beneficial influence of ACEi was most apparent in the first weeks after initiation of treatment; however, ACEi-treated ACF rats started to die rapidly after week 40 and only 2 of them survived till the end of the study (the survival rate at 55 weeks after induction of ACF was 5%). We observed 3 deaths (14%) in the sham-operated control group, probably due to old age.

3.8 | cGMP tissue levels

Myocardial cGMP levels were increased in ACF RV (19.6 ± 7 vs. 4.1 ± 3.1, $p < .05$) and LV (16 ± 5 vs. 5.3 ± 3, $p < .05$), probably due to stimulation of NP-receptor-associated particulate guanylate cyclases by elevated levels of natriuretic peptides. PDE5i raised cGMP concentration in the lungs (63 ± 19 vs. 21 ± 8.6, $p < .05$), however, not in the myocardium and the kidney (Figure 4B).

4 | DISCUSSION

The study describes the impact of long-term PDE5i and ACEi treatments in a rat HF model due to chronic VO induced by ACF. The main finding is that long-term therapy with PDE5i sildenafil does not improve the survival rate, and cardiac and renal function of animals with ACF. There were no relevant differences in the LV and RV responses to long-term PDE5i treatment. Finally, long-term ACEi therapy improved survival of ACF rats despite relatively small effects on cardiac remodeling, myocardial gene expression, and renal hemodynamics. The results indicate that cGMP-dependent signaling pathway does not play a major role in response to ACF, while supporting the role of ACEi in treating HF due to VO.

While the effects of PDE5i on hypertrophy and cardiac dysfunction were repeatedly studied in pressure overloaded heart,[13–15] there is a paucity of studies that examined the effects on volume overloaded heart. To our knowledge, this is the first such a complex

evaluation of long-term PDE5i treatment in VO that leads to overt HF. In the present study, employing comprehensive analysis of both RV and LV structure and load-independent function, myocardial gene expression, renal function assessment, and survival, we have not demonstrated any benefit of PDE5i after 20 weeks of treatment. A lack of protective effect of PDE5i treatment on ACF RV was described previously,[14] however, that study was limited to RV assessment and sildenafil was administered for 4 weeks only.

In another experimental VO model, Kim et al. demonstrated a significant attenuation of adverse LV remodeling and improvement of exercise capacity following a 4-month sildenafil treatment.[39] However, the rats in that study exhibited only a compensated LV hypertrophy rather than true HF, without increased chamber filing pressures. Endothelial NO synthase (NO synthase 3) was downregulated in untreated mitral regurgitation and it was increased by sildenafil. In our study, the expression of NO synthase 3 had a trend to decrease in ACF, with no effect of PDE5i treatment, which may explain the discrepant results between the two different models. Eskesen et al. observed improved LV function and less LV remodeling after PDE5i in a rat HF model of aortic regurgitation, which is however a model of combined pressure and VO, so the beneficial effects of PDE5i could be explainable by the reduction of pressure component.[40]

There may be several possible explanations for the lack of efficacy of PDE5i treatment in preventing hypertrophy and failure of VO heart. First, the administered dose of sildenafil could be insufficient to suppress PDE5 activity. However, this is improbable, as this dose is well above that previously shown to raise plasma cGMP levels in rats,[16] and we measured elevated cGMP levels in the lungs of sildenafil-treated rats, which confirmed the effectiveness of treatment. Second, cGMP synthesis in ACF myocardium could be insufficient. We observed increased cGMP concentrations both in ACF RV and LV, likely due to stimulation of particulate guanylate cyclase by elevated levels of natriuretic peptides. However, subcellular cGMP pool compartmentalization may also play a role, because PDE5i was demonstrated to exclusively increase the cGMP generated by soluble guanylate cyclase in response to NO, while the cGMP pool derived from natriuretic peptides-stimulated particulate guanylate cyclase was not affected in rat cardiomyocytes.[41] The third possible explanation could be the cGMP degradation by phosphodiesterases other than PDE5, particularly PDE9.[42] However, we did not observe *Pde9a* gene upregulation in ACF hearts. Finally, the cGMP-dependent signaling pathway may not be involved in the myocardial response to ACF-induced VO, and our gene expression data support this mechanism. ACF did not alter the expression of genes of the cGMP-dependent signaling pathway, arguing against a substantial role of this pathway in response to VO, at least in the ACF model of advanced HF. In addition, both ACF LV and RV exhibited eccentric hypertrophy, decreased contractility, and upregulation of genes connected with myocardial stress (*Nppa*, *Myh7/Myh6 ratio*), and metabolic switch from fatty acid oxidation to glycolysis (increased *Glut1/Glut4* and *Hk1/Mcad ratio*). The presented data provide no evidence for the heart chamber-specific responsiveness to long-term PDE5i.

Among other phosphodiesterases, PDE5 is also highly expressed in the kidney and was proposed to contribute to the blunted renal response to elevated levels of endogenous natriuretic peptides in advanced HF.[43,44] In the present study, we have not seen any beneficial effect of PDE5i treatment on renal hemodynamics and excretory function. Several experimental studies in dogs with overt HF induced by rapid ventricular pacing demonstrated improvement of renal function following administration of PDE5i either alone[43,45] or in combination with exogenous brain natriuretic peptide[46] or with PDE9 inhibition.[47] In all the above studies, phosphodiesterase inhibition was associated with increased renal cGMP concentrations. However, in our study, sildenafil failed to significantly raise renal cGMP level, although it tended to be higher in sildenafil-treated compared to placebo-treated rats. Based on our results, it is likely that renal PDE5 activity is not upregulated by ACF-induced VO.

A significant amount of PDE5 is present in the lung tissue, and inhibiting PDE5 leads to a decrease in pulmonary vascular resistance both in experimental models and also in patients with HF and pulmonary hypertension.[48–50] Based on our cGMP data, upregulation of PDE5 is likely to occur in the lungs of ACF rats, as PDE5i-treated animals have highly increased lung cGMP concentration.[50]

Finally, our study demonstrated that long-term ACEi improves the survival of ACF rats despite relatively small effects on cardiac remodeling, myocardial gene expression, and renal hemodynamics. ACEi treatment decreased systemic blood pressure, lowered LV maximal and filling pressures, reduced LV wall stress and LV volumes, attenuated albuminuria, diminished pulmonary congestion, and reduced body weight of ACF animals, likely due to alleviating congestion. However, treatment with ACEi had no effect on RV parameters, did not enhance load-independent LV systolic function, and did not significantly raise renal blood flow, urine flow, and fractional sodium excretion, confirming our previous observations.[51,52] The exact mechanisms of how ACEi protects against increased HF mortality due to ACF-induced VO, despite modest effects on cardiorenal function, deserve further investigation. Jarkovska et al. suggested the anti-arrhythmic effect of ACEi in ACF rats.[53]

The present study has several limitations. Only the resting hemodynamics was tested, because of technical reasons we did not perform preload changing maneuvers (vena cava balloon inflation), and therefore we cannot report arterial and ventricular elastance values. We tested the changes in myocardial gene expression only, but we did not perform proteomic analysis. We also did not measure protein kinase G activity and plasma and renal angiotensin levels as markers of PDE5i and ACEi efficacy, respectively. This study does not include a sham/control group treated with PDE5i or ACEi, which could add to a deeper understanding of individual treatments, but our question was narrowed down to the effect of treatment in rats with HF, and thus the primary focus was on translational research. Despite the known differences between sexes in various HF models, our current study has deliberately focused on only one gender. This approach stems from our previous investigation, in which no distinctions between sexes were observed in relation to the ACF model within the HanSD strain.[54]

In conclusion, the study shows that PDE5i does not improve survival rate and does not change the cardiac and renal function of ACF rats with advanced HF. The cGMP-dependent signaling pathway does

not seem to play a major role in response to ACF-induced VO. In contrast, mortality in the ACF model was reduced by ACEi treatment.

AUTHOR CONTRIBUTIONS

Participated in research design: T.T. and V.M. Conducted experiments: T.T., M.K., P.S., L.K., J.T., V.S., M.K., and J.N. Performed data analysis: T.T., M.M., M.K., P.S., and J.N. Wrote or contributed to the writing of the manuscript: T.T., M.M., M.K., P.S., L.K., J.T., V.S., M.K., J.N., and V.M.

ACKNOWLEDGMENTS

We express our gratitude to the individuals who took part in this study and to the staff at the Experimental Medicine Center—IKEM, particularly Prof. Ludek Cervenka.

FUNDING INFORMATION

Supported by Ministry of Health of the Czech Republic, grant no. NU22-02-00161, NU20-02-00052; Grant Agency of Charles University (GAUK), grant no. 304121; All rights reserved. Project National Institute for Research of Metabolic and Cardiovascular Diseases (Programme EXCELES, Project no. LX22NPO5104), Funded by the European Union—Next Generation EU.

CONFLICT OF INTEREST STATEMENT

The authors declare that they have no competing interests.

DATA AVAILABILITY STATEMENT

The data that support the findings of this study are available on request from the corresponding author.

ETHICS STATEMENT

This study was performed in accordance with the NIH Guide for the Care and Use of Laboratory Animals (NIH Publication No. 85-23, 1996) and Animal protection laws of the Czech Republic (311/1997) and was approved by the Ethic Committee of IKEM.

ORCID

Tereza Tykvartova https://orcid.org/0000-0001-8434-0165
Matus Miklovic https://orcid.org/0000-0003-0427-2583
Martin Kotrc https://orcid.org/0000-0002-2068-0379
Ludmila Kazdova https://orcid.org/0000-0003-1649-3391
Jaroslava Trnovska https://orcid.org/0000-0001-6468-8244
Vojtech Skop https://orcid.org/0000-0002-4685-4429
Jiri Novotny https://orcid.org/0000-0003-1338-638X
Vojtech Melenovsky https://orcid.org/0000-0001-8921-7078

REFERENCES

1. Abassi Z, Goltsman I, Karram T, Winaver J, Hoffman A. Aortocaval fistula in rat: a unique model of volume-overload congestive heart failure and cardiac hypertrophy. *J Biomed Biotechnol*. 2011;2011:e729497.
2. Benes J, Kazdova L, Drahota Z, et al. Effect of metformin therapy on cardiac function and survival in a volume-overload model of heart failure in rats. *Clin Sci*. 2011;121(1):29-41.
3. Melenovsky V, Benes J, Skaroupkova P, et al. Metabolic characterization of volume overload heart failure due to aorto-caval fistula in rats. *Mol Cell Biochem*. 2011;354(1):83-96.
4. Melenovsky V, Skaroupkova P, Benes J, Torresova V, Kopkan L, Cervenka L. The course of heart failure development and mortality in rats with volume overload due to aorto-caval fistula. *Kidney Blood Press Res*. 2012;35(3):167-173.
5. Havlenova T, Skaroupkova P, Miklovic M, et al. Right versus left ventricular remodeling in heart failure due to chronic volume overload. *Sci Rep*. 2021;11(1):1-17.
6. Miklovic M, Kala P, Melenovsky V. Simultaneous biventricular pressure-volume analysis in rats. *J Physiol Pharmacol*. 2023;74(2):131-147.
7. Dunkerly-Eyring B, Kass DA. Myocardial phosphodiesterases and their role in cGMP regulation. *J Cardiovasc Pharmacol*. 2020;75(6):483-493.
8. Nagendran J, Archer SL, Soliman D, et al. Phosphodiesterase type 5 is highly expressed in the hypertrophied human right ventricle, and acute inhibition of phosphodiesterase type 5 improves contractility. *Circulation*. 2007;116(3):238-248.
9. Pokreisz P, Vandenwijngaert S, Bito V, et al. Ventricular phosphodiesterase-5 expression is increased in patients with advanced heart failure and contributes to adverse ventricular remodeling after myocardial infarction in mice. *Circulation*. 2009;119(3):408-416.
10. Lu Z, Xu X, Hu X, et al. Oxidative stress regulates left ventricular PDE5 expression in the failing heart. *Circulation*. 2010;121(13):1474-1483.
11. Kishimoto I, Rossi K, Garbers DL. A genetic model provides evidence that the receptor for atrial natriuretic peptide (guanylyl cyclase-A) inhibits cardiac ventricular myocyte hypertrophy. *Proc Natl Acad Sci U S A*. 2001;98(5):2703-2706.
12. Das A, Xi L, Kukreja RC. Phosphodiesterase-5 inhibitor sildenafil preconditions adult cardiac myocytes against necrosis and apoptosis. Essential role of nitric oxide signaling. *J Biol Chem*. 2005;280(13):12944-12955.
13. Takimoto E, Champion HC, Li M, et al. Chronic inhibition of cyclic GMP phosphodiesterase 5A prevents and reverses cardiac hypertrophy. *Nat Med*. 2005;11(2):214-222.
14. Borgdorff MAJ, Bartelds B, Dickinson MG, et al. Sildenafil enhances systolic adaptation, but does not prevent diastolic dysfunction, in the pressure-loaded right ventricle. *Eur J Heart Fail*. 2012;14(9):1067-1074.
15. Borgdorff MA, Bartelds B, Dickinson MG, et al. Sildenafil treatment in established right ventricular dysfunction improves diastolic function and attenuates interstitial fibrosis independent from afterload. *Am J Physiol Heart Circ Physiol*. 2014;307(3):H361-H369.
16. Schäfer S, Ellinghaus P, Janssen W, et al. Chronic inhibition of phosphodiesterase 5 does not prevent pressure-overload-induced right-ventricular remodelling. *Cardiovasc Res*. 2009;82(1):30-39.
17. Toischer K, Rokita AG, Unsöld B, et al. Differential cardiac remodeling in preload versus afterload. *Circulation*. 2010;122(10):993-1003.
18. Dai W, Kloner RA, Dai W, Kloner RA. Is inhibition of phosphodiesterase type 5 by sildenafil a promising therapy for volume-overload heart failure? *Circulation*. 2012;125:1341-1343.
19. Friedberg MK, Redington AN. Right versus left ventricular failure: differences, similarities, and interactions. *Circulation*. 2014;129(9):1033-1044.
20. Forfia PR, Lee M, Tunin RS, Mahmud M, Champion HC, Kass DA. Acute phosphodiesterase 5 inhibition mimics hemodynamic effects of B-type natriuretic peptide and potentiates B-type natriuretic peptide effects in failing but not Normal canine heart. *J Am Coll Cardiol*. 2007;49(10):1079-1088.
21. Ghali-Ghoul R, Tahseldar-Roumieh R, Sabra R. Effect of chronic administration of sildenafil on sodium retention and on the hemodynamic complications associated with liver cirrhosis in the rat. *Eur J Pharmacol*. 2007;572(1):49-56.

22. Melenovsky V, Cervenka L, Viklicky O, et al. Kidney response to heart failure: proteomic analysis of cardiorenal syndrome. *Kidney Blood Press Res*. 2018;43(5):1437-1450.
23. Asakura M, Kitakaze M. Global gene expression profiling in the failing myocardium. *Circ J*. 2009;73(9):1568-1576.
24. Drake JI, Bogaard HJ, Mizuno S, et al. Molecular signature of a right heart failure program in chronic severe pulmonary hypertension. *Am J Respir Cell Mol Biol*. 2011;45(6):1239-1247.
25. Kong Q, Blanton RM. Protein kinase G I and heart failure: shifting focus from vascular unloading to direct myocardial antiremodeling effects. *Circ Heart Fail*. 2013;6(6):1268-1283.
26. Takimoto E. Cyclic GMP-dependent signaling in cardiac myocytes. *Circ J*. 2012;76(8):1819-1825.
27. Weinberg EO, Schoen FJ, George D, et al. Angiotensin-converting enzyme inhibition prolongs survival and modifies the transition to heart failure in rats with pressure overload hypertrophy due to ascending aortic stenosis. *Circulation*. 1994;90(3):1410-1422.
28. Lapointe N, Blais C, Adam A, et al. Comparison of the effects of an angiotensin-converting enzyme inhibitor and a vasopeptidase inhibitor after myocardial infarction in the rat. *J Am Coll Cardiol*. 2002;39(10):1692-1698.
29. Červenka L, Melenovský V, Husková Z, Škaroupková P, Nishiyama A, Sadowski J. Inhibition of soluble epoxide hydrolase counteracts the development of renal dysfunction and progression of congestive heart failure in Ren-2 transgenic hypertensive rats with aorto-caval fistula. *Clin Exp Pharmacol Physiol*. 2015;42(7):795-807.
30. Lange PE, Seiffert PA, Pries F, et al. Value of image enhancement and injection of contrast medium for right ventricular volume determination by two-dimensional echocardiography in congenital heart disease. *Am J Cardiol*. 1985;55(1):152-157.
31. Abraham D, Mao L. Cardiac pressure-volume loop analysis using conductance catheters in mice. *J Vis Exp*. 2015;2015(103):1-10.
32. Huber W, Carey VJ, Gentleman R, et al. Orchestrating high-throughput genomic analysis with Bioconductor. *Nat Methods*. 2015;12(2):115-121.
33. Livak KJ, Schmittgen TD. Analysis of relative gene expression data using real-time quantitative PCR and the $2^{-\Delta\Delta CT}$ method. *Methods*. 2001;25(4):402-408.
34. McCall MN, McMurray HR, Land H, Almudevar A. On non-detects in qPCR data. *Bioinformatics*. 2014;30(16):2310-2316.
35. Sporková A, Kopkan L, Varcabová S, et al. Role of cytochrome P-450 metabolites in the regulation of renal function and blood pressure in 2-kidney 1-clip hypertensive rats. *Am J Physiol Regul Integr Comp Physiol*. 2011;300(6):R1468-R1475.
36. Harding SD, Sharman JL, Faccenda E, et al. The IUPHAR/BPS guide to PHARMACOLOGY in 2018: updates and expansion to encompass the new guide to IMMUNOPHARMACOLOGY. *Nucleic Acids Res*. 2018;46(D1):D1091-D1106.
37. Alexander SPH, Fabbro D, Kelly E, et al. THE CONCISE GUIDE TO PHARMACOLOGY 2021/22: catalytic receptors. *Br J Pharmacol*. 2021;178(S1):S264-S312.
38. Petrak J, Pospisilova J, Sedinova M, et al. Proteomic and transcriptomic analysis of heart failure due to volume overload in a rat aorto-caval fistula model provides support for new potential therapeutic targets—monoamine oxidase a and transglutaminase 2. *Proteome Sci*. 2011;9(1):69.
39. Kim KH, Kim YJ, Ohn JH, et al. Long-term effects of sildenafil in a rat model of chronic mitral regurgitation: benefits of ventricular remodeling and exercise capacity. *Circulation*. 2012;125(11):1390-1401.
40. Eskesen K, Olsen NT, Dimaano VL, et al. Sildenafil treatment attenuates ventricular remodeling in an experimental model of aortic regurgitation. *SpringerPlus*. 2015;4(1):592.
41. Castro LRV, Verde I, Cooper DMF, Fischmeister R. Cyclic guanosine monophosphate compartmentation in rat cardiac myocytes. *Circulation*. 2006;113(18):2221-2228.
42. Lee DI, Zhu G, Sasaki T, et al. Phosphodiesterase 9A controls nitric-oxide-independent cGMP and hypertrophic heart disease. *Nature*. 2015;519(7544):472-476.
43. Margulies KB, Burnett JC. Inhibition of cyclic GMP phosphodiesterases augments renal responses to atrial natriuretic factor in congestive heart failure. *J Card Fail*. 1994;1(1):71-80.
44. Charloux A, Piquard F, Doutreleau S, Brandenberger G, Geny B. Mechanisms of renal hyporesponsiveness to ANP in heart failure. *Eur J Clin Invest*. 2003;33(9):769-778.
45. Yamamoto T, Wada A, Ohnishi M, et al. Chronic administration of phosphodiesterase type 5 inhibitor suppresses renal production of endothelin-1 in dogs with congestive heart failure. *Clin Sci Lond Engl*. 2002;103(suppl 48):258S-262S.
46. Chen HH, Huntley BK, Schirger JA, Cataliotti A, Burnett JC. Maximizing the renal cyclic 3′-5′-guanosine monophosphate system with type V phosphodiesterase inhibition and exogenous natriuretic peptide: a novel strategy to improve renal function in experimental overt heart failure. *J Am Soc Nephrol*. 2006;17(10):2742-2747.
47. Scott NJA, Rademaker MT, Charles CJ, Espiner EA, Richards AM. Hemodynamic, hormonal, and renal actions of phosphodiesterase-9 inhibition in experimental heart failure. *J Am Coll Cardiol*. 2019;74(7):889-901.
48. Lewis GD, Lachmann J, Camuso J, et al. Sildenafil improves exercise hemodynamics and oxygen uptake in patients with systolic heart failure. *Circulation*. 2007;115(1):59-66.
49. Barnes H, Brown Z, Burns A, Williams T. Phosphodiesterase 5 inhibitors for pulmonary hypertension. *Cochrane Database Syst Rev*. 2019;1(1):1-131.
50. Melenovsky V, Kotrc M, Borlaug BA, et al. Relationships between right ventricular function, body composition, and prognosis in advanced heart failure. *J Am Coll Cardiol*. 2013;62(18):1660-1670.
51. Kala P, Sedláková L, Škaroupková P, et al. Effect of angiotensin-converting enzyme blockade, alone or combined with blockade of soluble epoxide hydrolase, on the course of congestive heart failure and occurrence of renal dysfunction in Ren-2 transgenic hypertensive rats with aorto-caval fistula. *Physiol Res*. 2018;67(3):401-415.
52. Kratky V, Vanourkova Z, Sykora M, et al. AT1 receptor blocker, but not an ACE inhibitor, prevents kidneys from hypoperfusion during congestive heart failure in normotensive and hypertensive rats. *Sci Rep*. 2021;11(1):4271.
53. Jarkovská D, Miklovič M, Švíglerová J, et al. Effects of Trandolapril on structural, contractile and electrophysiological remodeling in experimental volume overload heart failure. *Front Pharmacol*. 2021;12:1-13.
54. Červenka L, Škaroupková P, Kompanowska-Jezierska E, Sadowski J. Sex-linked differences in the course of chronic kidney disease and congestive heart failure: a study in 5/6 nephrectomized Ren-2 transgenic hypertensive rats with volume overload induced using aorto-caval fistula. *Clin Exp Pharmacol Physiol*. 2016;43(10):883-895.

SUPPORTING INFORMATION

Additional supporting information can be found online in the Supporting Information section at the end of this article.

How to cite this article: Tykvartova T, Miklovic M, Kotrc M, et al. The impact of phosphodiesterase-5 inhibition or angiotensin-converting enzyme inhibition on right and left ventricular remodeling in heart failure due to chronic volume overload. *Pharmacol Res Perspect*. 2024;12:e1172. doi:10.1002/prp2.1172